• EDITORIAL •

Blossoming of gastroenterology during the twentieth century

Joseph B. Kirsner

Joseph B. Kirsner, The Louis Block Distinguished Service Professor of Medicine, Department of Medicine - Section of Gastroenterology, The University of Chicago, IL 60637, USA
Based in part on Kirsner, J.B. "100 Years of American Gastroenterology (1900-2000). *Medscape Gastroenterology*. (Available on the world wide web at: http://www.medscape.com/viewarticle/407942_4) and Kirsner, J.B. "The Scientification of Gastroenterology During the Twentieth Century." Foreword in Colonic Diseases. Koch, T.R., (Ed.) (With Permission)
Correspondence to: Joseph B Kirsner, M.D., Louis Block Distinguished Service, Professor of Medicine, The University of Chicago, 5841 South Maryland, MC 4076, Chicago, IL 60637, USA. jkirsner@medicine.bsd.uchicago.edu
Telephone: +1-773-702-6101   **Fax:** +1-773-752-4876
Received: 2004-03-20   **Accepted:** 2004-04-10

INTRODUCTION

Awareness of the digestive system began with the dawn of civilization, when man observing the feeding habits of animals in the surrounding environment, experimented with foods, edible and inedible. Identity came with discoveries of the digestive organs during the 16th and 17th centuries. Function was revealed by physiologic studies of digestion, absorption and secretion, metabolism, and motility during the 18th and 19th centuries. Diagnostic access improved with the technological advances of the 20th century. Understanding of gastrointestinal (GI) disease followed growth of the basic sciences and gastroenterology's increased involvement in scientific research during the 20th century.

The scientification of medicine and gastroenterology began during the latter part of the 19th century when the discovery of bacterial causes of disease revealed the potential of research in the discovery of new knowledge, and when the dogma of the past began to yield to clinical and basic investigation. Additional impetus came from A. Flexner's 1910 report on medical education, documenting the importance of a scientific foundation in medicine. Funds for gastroenterologic investigation were small, but research was in progress in the physiology laboratories of academic medical centers. Early in the 20th century, gastroenterology was yet an incompletely defined activity; but during the 1920s, outstanding clinicians established gastroenterology programs at university academic centers and major clinics. The entry of scientifically trained young physiccians into gastroenterology during the 1930s and 1940s increased research interest.

Specialization in medicine was underway and, in the United States in 1940, gastroenterology was certified as an academic specialty, important to the attraction of students and support for education and research. Similar recognition occurred elsewhere, but further progress was interrupted by World War II (1939-1945).

Post-World War II was a highly productive period for the basic and biomedical sciences. Wartime discoveries had documented the remarkable success of research and had motivated public and governmental support of basic investigation.

This trend accelerated in the United States, when the office of Scientific Research and Development (U.S. War Department) transferred 44 research contracts with universities and with industry to the then fledging National Institutes of Health (NIH) at the end of World War II. The General Medicine Study Section of the National Institute of Arthritis and Metabolic Diseases (NIH) became a major support of GI research and training. During the 1960s, 1970s and 1980s, academic medical center faculties enlarged and research training programs increased, creating new technologies and new disciplines. Important advances occasionally developed from insightful clinical observations. A classic example concerns the "epidemic" of pellagra, considered an infection early in the 20th century and accounting annually for 250 000 cases and 7 000 deaths in 15 Southern cotton-growing U.S. states. In 1914, at age 40, Dr. Joseph G. Goldberger of the Public Health Service, through shrewd clinical observations of patients, hospital staff, and patient diets, implicated a dietary deficiency (confirmed later as a nicotinic acid deficiency) as the cause of pellagra. However, scientific activity was associated with much prestige, and gastroenterology sought to become more "scientific".

Gastroenterology essentially incorporates basic concepts and technology, from multiple scientific disciplines, into its own investigation. The early 1900s' view of swallowing, as the forceful "bolting" of food from the throat directly into the stomach, was replaced by the recognition of pharyngeal and esophageal neuromuscular function, facilitating the physiological management of swallowing disorders. Histologic and microbiologic examination of endoscopically obtained gastric biopsies replaced the subjective diagnosis of "chronic gastritis". Not until the 1980s, however, was the role of *Helicobacter pylori* in gastritis and peptic ulcer identified. Multidisciplinary research clarified the process of gastric secretion and led to the development of H_2 blockers and proton pump inhibitors. Metabolic studies identified the specific L-glutamine requirement for the intestinal epithelium and the short-chain fatty acid, n-butyrate, for the colonic epithelium. Research into the nature of inflammation led to more effective strategies for the treatment of inflammatory bowel disease. Cellular biology identified the intracellular heat shock proteins, trefoil peptides, and stem cell growth factors, with therapeutic potential. The important role of genetic influence, in the development of colorectal cancer, celiac disease, and inflammatory bowel disease, was extended to other GI diseases.

Gastroenterology's 20th-century technological progress was equally impressive. The study of esophageal motility progressed from balloon kymography to intraluminal catheter manometry, transducers, and neuropharmacologic methodology. Fiberoptic endoscopy expanded diagnostic access to virtually all areas of the gastrointestinal tract. Safer polyethylene tubing eased transintestinal intubation and perfusion studies, and with small bowel biopsy and radioimmuno-assays, clarified intestinal absorption mechanisms. Microbiological and chromatographic tech-nologies, including hydrogen and carbon-14 breath tests, increased knowledge of the enteric flora, enabling the diagnosis of bacterial overgrowth responsive to antibacterial therapy. Needle biopsy of the liver established the morphological basis of hepatic disease and provided guidelines for the treatment of hepatitis and the monitoring of

liver transplantation. Discovery of the Australia antigen stimulated research, identifying seven types of hepatitis viruses (A, B, C, D, E, F, G), a major impetus in the growth of knowledge of liver disease. Biochemical and chromatographic technology determined the composition of bile and the process of formation, as well as the chemical dissolution of cholesterol gallstones. Enzyme and protein chemistry established the synthesis and trafficking of intracellular proteins and intracellular enzyme activation as the cause of acute pancreatitis. Transmission, electron microscopy and laser-scanning confocal micros-copy facilitated the study of intestinal epithelial cells, intracellular protein processing, and epi-thelial barrier function. Molecular biological techniques made possible the cloning of genes for cystic fibrosis, sodium, calcium, glucose, and amino acid transport. Advances in radiologic image intensification, ultrasonography, computed x-ray tomography of the abdomen, and magnetic resonance imaging among other achievements, increased access to the gastrointestinal tract.

Neuro-humoral and neuro-immune interactions of the GI tract, mediating colonic motility and visceral sensitivity, replaced psychogenic hypotheses of the irritable bowel. Studies of gastrointestinal immunology, including the gut mucosal immune system and the molecular mechanisms of inflammation, generated new pathogenic concepts and therapeutic resources in inflammatory bowel disease (IBD). Measurements of gastrointestinal blood flow, including laser Doppler velocimetry, facili-tated recognition of abdominal vascular impairment. Neurogastroenterology introduced methods of electrophysiology and cellular neurophysiology, identified the enteric nervous system as a "minibrain with intelligent circuits", and provided new understanding of "physiologic" GI disorders. Transgenic methodology created innovative animal models, enabling multidisciplinary studies of intestinal inflammation.

Expanded access to the gastrointestinal tract, including fiberoptic endoscopy, biopsies of the esophagus, stomach, small intestine, and colon, X-ray (CT scan)-guided biopsy of the liver and the pancreas, tests of hepatic and pancreatic functions, breath tests, quality X-rays, ultrasonography, computerized abdominal tomography, magnetic resonance imaging, and assessment of gastrointestinal motility improved the diagnosis of digestive disorders. Gastrointestinal therapy advanced with the discovery of sulfonamides, antibiotics, adrenocortical steroids, immune modifiers, H_2 receptor blockers, proton pump inhibitors, anti-inflammatory compounds, nutritional supports, vaccines, cancer chemotherapy, organ transplantation, and increasingly skilled abdominal surgery.

Many favorable circumstances converged to bring gastroenterology into the mainstream of advancing scientific thought, including an enlarging body of scientific knowledge, technological innovations permitting safer, more precise human studies, increased support of research and training, controlled clinical studies, establishment of research and scientific training programs, by the NIH and private philanthropy, and the enlarging global scientific communication network (journals, databases, electronic and computer systems).

The major accomplishment of gastroenterology during the 20th century has been the successful application of new scientific knowledge and technology to the investigation of gastrointestinal disorders. Digestive diseases involving multiple disciplines and innovative technology today are recognized as exciting and challenging problems. Now that gastroenterologic research frontiers are at the cutting edge of modern science, including such "new" sciences as biotechnology, structural biology, and pharmacogenetics, together with the ongoing molecular disciplines (microbiology, immunology, genetics). They will establish the 21st century as the gastroenterologic century.

Edited by Xu XQ and Wang XL **Proofread by** Xu FM

• GASTRIC CANCER •

Survival of patients with stomach cancer in Changle city of China

Jun Tian, Xiao-Dong Wang, Zhen-Chun Chen

Jun Tian, Department of Epidemiology and Health Statistics, Fujian Medical University, Fuzhou 350004, Fujian Province, China
Xiao-Dong Wang, College of Mathematics and Computer science, Fuzhou University, Fuzhou 350002, Fujian Province, China
Zhen-Chun Chen, Fujian Cancer Hospital, Fuzhou 350014, Fujian Province, China
Supported by the Natural Science Foundation of Fujian, No. A0210012
Correspondence to: Jun Tian, Department of Epidemiology and Health Statistics, Fujian Medical University, Fuzhou 350004, Fujian Province, China. tianjun@mail.fjmu.edu.cn
Telephone: +86-591-3569264
Received: 2004-02-02   **Accepted:** 2004-02-21

Abstract

AIM: The survival rate of patients with stomach cancer is used to evaluate the effects of treatments. The short- and mid-term survival of patients on the present level of treatments can be described by calculating 1- to 5-year survival rates. The aims of this study were to document patterns of survival after treatments for stomach cancer in Changle city and analyze whether the stage of cancer and the way of treatment impacted on survival of patients or not.

METHODS: A total number of 745 patients with stomach cancer reported in the Changle Cancer Registry from 1993 to 1998 were investigated with respect to the disease condition, the way of treatment and survival time. 1- to 5-year survival rates were estimated by using life-table method.

RESULTS: The 1- to 5-year survival rates in the patients with stomach cancer in Changle city were 54.23%, 41.77%, 37.95%, 33.98% and 30.47%, respectively. The 1- to 5-year survival rates in stageI or II group were 3, 6.1, 7.4, 8.9 and 9.8 times as high as those in stage III or IV group, respectively. The 1- to 5-year survival rates in operation group were 3.5, 8.7, 11.2, 11.7 and 19 times as high as those in no operation group, respectively. For the patients with stage III or IV stomach cancer the 1-year survival rate in operation group was 3 times as high as that in no operation group and 2-year survival rate in operation group was 11.9 times as high as that in no operation group. For the patients with stage III or IV stomach cancer, the differences of the survival rates average survival times between total gastrectomy and partial gastrectomy were not significant and the median survival times in these 2 groups were 8 mo and 9 mo, respectively.

CONCLUSION: Mid-term survival rates of patients with stomach cancer in Changle city are low. Stage of cancer is an important factor influencing survival of patients with stomach cancer. Surgery is an effective treatment for the patients with stage IV cancer and can raise short- and mid-term survival rates. Total gastrectomy should not be encouraged for the patients with late stage of cancer.

INTRODUCTION

The survival time is used to evaluate the effects of treatments for stomach cancer. The survival rates are calculated in the analysis for the survival time[1]. Many studies have been conducted on the survival analysis of stomach cancer in recent several decades[2-8]. The survival of patients with stomach cancer was influenced by the stage of cancer and the way of treatment[8,9]. Since stomach cancer often was not detected until an advanced state,survival rate was rather low. Only a few patients diagnosed with stomach cancer survive five years or more after diagnosis. There is a higher incidence rate of stomach cancer in Changle city of Fujian Province. To study the survival rates of the patients with stomach cancer and the prognostic factors in Changle city, we investigated the survival time of the patients with stomach cancer diagnosed from 1993 to 1998 and registered in the Changle Cancer Registry. The contents of our research were: (1) to estimate the survival rates of the patients with different stages of cancer and to compare these survival rates; (2) to estimate the survival rates of the patients with different ways of treatments and to compare these survival rates; (3) to analyze the survival benefit of the operation on the patients with stage IV stomach cancer; and (4) To make a comparison of survival between the patients with total gastrectomy and partial gastrectomy of stage IV stomach cancer.

MATERIALS AND METHODS

Materials

There were 747 patients with stomach cancer reported in Changle Cancer Registry from 1993 to 1998. Since two patients had no information of survival, the study sample consisted of 745 patients aged from 28 to 85 at registration. There were 593 male with age (60.1±10.1) years and 152 female with age (62.1±11.4) years in our sample. There were 473 dead patients and 272 patients were still alive during the term of investigation with the age (58.4±9.9).

Methods

The survival times of the 745 patients were obtained by visiting their home. After informed consent was obtained from each patient's family, the stage of cancer at diagnosis and way of treatment for the patient were obtained from the patient's medical record. The cause of death for each dead patient with stomach cancer was identified in the Hospital of Changle. The survival times of the patients who were not died of gastric cancer were not included in the data.

The proportion of stomach cancer patients surviving for one, two, three and five years can be a measure of the effect of treatments. The total survival rates by the stage of cancer and surgery were calculated and analyzed by Chi-square (χ^2 test) statistics. Survival analyses were performed by the life-table method[1]. The data were analyzed using the SAS 8.2 software.

RESULTS

The 1-, 2-, 3-, 4- and 5-year survival rates and their 95% confidence intervals (*CI*) were estimated using life-table method (Table 1). Table 1 shows that the 1-year survival rate is 54.2% and the 5-year survival rate is 30.5%.

Table 1 Survival rates using life-table method

Time(yr)	Survival rate	95% confidence interval
1	0.542	0.506-0.578
2	0.418	0.382-0.454
3	0.379	0.343-0.416
4	0.340	0.302-0.377
5	0.305	0.265-0.345

The survival rates by the stage of cancer

The stages of cancer and survival status of 745 patients are shown in Table 2. The patients with stage III or IV cancer had 66.67% total survival rate. There were significance differences between these four total survival rates (χ^2=353.76, P<0.0001).

A total number of 745 patients were grouped according to their stages of cancer. One group consisted of the patients with stage I or stage II stomach cancer and the other group consisted of the patients with stage III or stage IV stomach caner. The survival rates using life-table method in two groups are shown in Table 3. The 1-, 2-, 3-, 4- and 5-year survival rates in stage I or stage II group were 3, 6.1, 7.4, 8.9 and 9.8 times higher than those in stage III or IV group, respectively. The difference of the distributions of survival times between the two groups was significant since the two 95% confidence intervals at each year did not overlap.

Table 2 Total survival rates by stage of cancer

Stage of cancer	Number of patients	Patients alive (n)	Death patients (n)	Total survival rate(%)
I	120	115	5	95.83
II	120	80	40	66.67
III	121	42	79	34.71
IV	384	35	349	9.11

Table 3 Survival rates using life-table method by stage of cancer

Time (yr)	Stage I or II		Stage III or IV	
	Survival rate	95% confidence interval	Survival rate	95% confidence interval
1	1.000	-	0.324	0.283-0.365
2	0.955	0.929-0.982	0.156	0.124-0.189
3	0.899	0.857-0.940	0.122	0.090-0.154
4	0.820	0.763-0.877	0.092	0.057-0.127
5	0.739	0.665-0.813	0.075	0.034-0.117

Table 4 Survival rates of surgical and non-surgical patients using life-table method by surgery

Time (yr)	Operation		No operation	
	Survival rate	95% confidence interval	Survival rate	95% confidence interval
1	0.753	0.713-0.793	0.217	0.170-0.265
2	0.639	0.594-0.684	0.074	0.043-0.105
3	0.589	0.541-0.636	0.053	0.024-0.081
4	0.528	0.477-0.580	0.045	0.017-0.073
5	0.478	0.420-0.535	0.025	0.013-0.051

The survival rates of patients with and without surgery

A total number of 745 patients were divided into 2 groups according to the way of treatments. One group consisted of 453 patients who underwent operation with total survival rate 55.63% (252/453) and the other group consisted of 292 patients who had no operation with total survival rate 6.85% (20/292). The

difference of the total survival rates between the two groups was significant (χ^2=182.26, P<0.0001). The survival rates using life-table method in 2 groups are shown in Table 4. The 1-, 2-, 3-, 4- and 5-year survival rates in operation group were 3.5, 8.7, 11.2, 11.7 and 19 times as high as those in no operation group, respectively. The difference of the distributions of survival times between these two groups was significant.

The survival of the patients with late stage of cancer with and without surgery

A total number of 505 patients with stage III or IV stomach cancer were divided into two groups according to the way of treatments. One group consisted of 230 patients who underwent the gastrectomy operations and the other group consisted of 275 patients who had no operation. The survival rates using life-table method in the two groups are shown in Table 5. The 1-year and 2-year survival rates in operation group were 3 times and 11.9 times as high as those in no operation group, respectively. It was obvious that the survival times of the patients undergone the operation were longer than those of the patients not operated.

A total number of 145 (37.76%) patients with stage IV stomach cancer had gastric resection and 239 (62.24%) were not subjected to surgery. The 1-year survival rates in the 2 groups of patients with stage IV stomach cancer were 0.244 (95% CI 0.173-0.315) and 0.063 (95% CI 0.032-0.094), respectively. The averages of survival times in the two groups of the patients were 13.3 mo (95% CI 11.03-15.57) and 6.1 mo (95% CI 5.64-6.56), respectively. Median survival times in these 2 groups of the patients were 8 mo and 6 mo, respectively. The 1- and 2-year survival rates were significantly higher in operated patients than no operated patients. However, the average of survival time in operated patients prolonged only for 7.2 mo.

Table 5 Survival rates of surgical and non-surgical patients with stage III or IV stomach cancer using life-table method by surgery for patients

Time(yr)	Operation		No Operation	
	Survival rate	95% confidence interval	Survival rate	95% confidence interval
1	0.511	0.446-0.576	0.168	0.124-0.213
2	0.314	0.251-0.376	0.026	0.007-0.046
3	0.252	0.189-0.315	0.000	-
4	0.202	0.130-0.274	0.000	-
5	0.165	0.078-0.253	0.000	-

The survival of the patients with late stage of cancer by way of operation

Of 230 operated patients with late stage of cancer, 85 (36.96%) patients were with stage III cancer. There were 106 (46.09%) patients had total gastrectomy, 89 (38.70%) had partial gastrectomy and 20 (8.70%) had nonresectional surgery. The survival rates using life-table method in both total gastrectomy and partial gastrectomy are shown in Table 6. The averages of survival times and their 95% confidence intervals are shown in Table 7.

Table 6 Survival rates using life-table method by the way of operation for patients with stage III or IV stomach cancer

Time(yr)	Total gastrectomy		Partial gastrectomy	
	Survival rate	95% CI	Survival rate	95% CI
1	0.536	0.451-0.627	0.571	0.466-0.677
2	0.289	0.207-0.370	0.416	0.306-0.526

The 95% confidence interval for both the 1-year survival rate and 2-year survival rate in total gastrectomy group and those in partial gastrectomy group overlapped. These indicated that all the differences of the survival rates (both 1- and 2-year survival rates) between total gastrectomy group and partial gastrectomy group were not significant. Also, the 95% confidence interval for average of survival time in total gastrectomy group and that in partial gastrectomy group overlapped. This indicated that the difference of survival times between total gastrectomy group and partial gastrectomy group was not significant.

Table 7 Average of survival time by the way of operation in the patients with stage III or IV stomach cancer

Way of operation	Number of patients	Average of survival time (mo)	95% confidence interval
Total Gastrectomy	106	19.56	16.408-22.712
Partial Gastrectomy	89	16.42	14.300-18.540
Nonresectional Surgery	20	5.22	3.84-6.60

Of 145 operated patients with stage IV stomach cancer, 89(61.38%) were subjected to total gastrectomy and 41(28.28%) had partial gastrectomy. The 1-year survival rates in total gastrectomy and in partial gastrectomy were 0.1846(95% *CI* 0.0903-0.2789) and 0.2911(95% *CI* 0.1478-0.4344), respectively. The averages of survival times in total gastrectomy and in partial gastrectomy were 12.36 mo (95% *CI* 9.37-15.350) and 9.28 mo (95% *CI* 8.10-10.46), respectively. Median survival times in total gastrectomy and in partial gastrectomy were 8 mo and 9 mo, respectively. The result showed that prognosis of the patients with total gastrectomy was not better than that with partial gastrectomy.

DISCUSSION

Compared to other tumors, stomach cancer has a dismal prognosis and a low 5-year survival rate. In our research, 5-year survival rate of patients with stomach cancer in Changle city is 30.47%, which close to the results of some previous researches[7,8,14].

The stage of cancer is the most important independent prognostic factor[5,8-11]. The results using COX model in some researches showed that the death hazard of the patients with stage III cancer was 2.82 time as high as that of the patients with stage II cancer, and that with stage IV was 3.29 times as high as that with stage II cancer[5]. The 1- and 2-year survival rates in stage IV stomach cancer were 1.65 and 10 times as high as those in stage III cancer respectively[12]. The 5-year survival rate in stage I-stage IV were 81.2%, 50.4%, 24.4% and 5.2%, respectively[7]. Our research also showed that stage of cancer might make a notable impact on survival rate of stomach cancer and 1- to 5- year survival rates in stage I or II of cancer were higher than those in stage III or IV. Among the patients in our study, 94% of the patients visited the doctors after they had had the symptoms of stomach cancer, so 51.54% of the patients had late stage of cancer (stage IV). Only 1.6% of the patients were discovered tumor by the general check up, and they had long survival times since they were diagnosed at early stage. So, researching on how to discover stomach cancer at early stage must play an important role in preventing and curing of tumors.

Surgery provides the only possibility of cure in stomach cancer patients. The 1- and 2-year survival rates of operated patients were much higher than those of not operated patients[12-16]. Our results also confirmed this. However, whether resection should be performed in patients with the stage IV stomach cancer is still a question[12,17,18]. Some researchers suggested that surgery could raise 3-year survival rate of patients with stage IV cancer only if tumors were not diffusely infiltrative type, while short-term survival rates could not be raised even though resections were conducted for the patients with diffusely infiltrative type of cancer[19]. However, surgery did not prolong survival time in patients with peritoneal dissemination, hepatic metastasis, lymph node involvement and invasion to adjacent organs or with 3 of these 4 factors[12,20]. Some other researchers suggested that short-term improvement in survival for resected patients with distant metastases could be obtained and resectional surgery should be undertaken whenever possible in patients with stage IV stomach cancer as both short-term and long-term survival advantages had been demonstrated[12,21-23]. We suggest that surgery not only can raise 1-year survival rate for the patients with stage IV cancer, but also can make them have the possibility of survival for more than 2 years, however, the average of survival time in operated patients with stage IV cancer does not prolong much.

Some researchers suggested that total gastrectomy had a lower relapsing rate than partial gastrectomy, so it could raise long-term survival[12,14,24]. To improve long-term therapeutic effects, total gastrectomy should be recommended for stage III patients with cancer of the cardia and stomach fundus when tumor size is bigger than 3.0 cm or lymph node metastasis occur[22]. Some researches also showed that subtotal and total gastrectomies had a similar postoperative complication rate and surgical outcome, and total gastrectomies had benefits of survival prolongation and symptomatic palliation[23,25,26]. However, other researchers suggested that total gastrectomy could not get a higher survival rate than partial gastrectomy, but carried a higher postoperative complications rate and poorer quality of life than partial resections[8,27-33]. We suggest that although surgery can raise 1-year survival rate of patients with stage IV cancer, total gastrectomy does not get a better survival than partial gastrectomy for the patients with stage IV stomach cancer. Besides, result obtained from earlier stage research also showed that the quality of life in the patients with total gastrectomy was worse than those with partial gastrectomy.

In summary, our data obtained by epidemiological survey have shown that mid-term survival rates of patients with stomach cancer in Changle city are low. Stage of cancer is an important factor influencing survival of patients with stomach cancer. Surgery is an effective treatment for the patients with stage IV cancer and can raise short- and mid-term survival rates. Total gastrectomy should not be encouraged for the patients with late stage of cancer.

REFERENCES

1   **Lee ET**. Statistical Methods For Survival Data Analysis. Second Edition. New York: *John Wiley Sons Inc* **1992**: 9-117

2   **Jimeno-Aranda A**, Sainz Samitier R, Aragues GM. Gastric cancer in the province of Zaragoza: a survival study. *Neoplasma* 1996; **43**: 199-203

3   **Janer G**, Sala M, Kogevinas M. Health promotion trials at worksites and risk factors for cancer. *Scand J Work Environ Health* 2002; **28**: 141-157

4   **Lundegardh G**, Adami HO, Malker B. Gastric cancer survival in Sweden: lack of improvement in 19 years. *Ann Surg* 1986; **204**: 546-551

5   **Barchielli A**, Amorosi A, Balzi D, Crocetti E, Nesi G. Long-term prognosis of gastric cancer in a European country: a population-based study in Florence. 10-year survival of cases diagnosed in 1985-1987. *Eur J Cancer* 2001; **37**: 1674-1680

6   **Pinheiro PS**, van der Heijden LH, Coebergh JW. Unchanged survival of gastric cancer in the southeastern Netherlands since 1982: result of differential trends in incidence according to Lauren type and subsite. *Int J Cancer* 1999; **84**: 28-32

7   **Msika S**, Benhamiche AM, Jouve JL, Rat P, Faivre J. Prognostic factors after curative resection for gastric cancer. A population-based study. *Eur J Cancer* 2000; **36**: 390-396

8   **Msika S**, Benhamiche AM, Rat P, Faivre J. Long-term prognosis of gastric cancer in the population of Cote-d' Or. *Gastroenterol Clin Biol* 2000; **24**: 649-655

9   **Monnet E**, Faivre J, Raymond L, Garau I. Influence of stage at diagnosis on survival differences for rectal cancer in three European populations. *Br J Cance* 1999; **81**: 463-468

10   **Casariego Vales E**, Pita Fernandez S, Rigueiro Veloso MT, Pertega Diaz S, Rabunal Rey R, Garcia-Rodeja ME, Alvarez Cervela L. Survival and prognostic factors for gastric cancer. Analysis of 2334 patients. *Med Clin* 2001; **117**: 361-365

11   **Faivre J**, Forman D, Esteve J, Gatta G. Survival of patients with oesophageal and gastric cancers in Europe. EUROCARE Working Group. *Eur J Cance* 1998; **34**: 2167-2175

12   **Haugstvedt T**, Viste A, Eide GE, Soreide O. The survival benefit of resection in patients with advanced stomach cancer: the norwegian multicenter experience. Norwegian stomach cancer Trial. *Word J Surg* 1989; **13**: 617-621

13   **Pointner R**, Wetscher GJ, Gadenstatter M, Bodner E, Hinder RA. Gastric remnant cancer has a better prognosis than primary gastric cancer. *Arch Surg* 1994; **129**: 615-619

14   **Doglietto GB**, Pacelli F, Caprino P, Sgadari A, Crucitti F. Surgery: independent prognostic factor in curable and far advanced gastric cancer. *World J Surg* 2000; **24**: 459-464

15   **Tuech JJ**, Cervi C, Pessaux P, Villapadierna F, Bergamaschi R, Ronceray J, Arnaud JP. Early gastric cancer: univariate and multivariate analysis for survival. *Hepatogastroenterology* 1999; **46**: 3276-3280

16   **Maetani S**, Tobe T, Hirakawa A, Kashiwara S, Kuramoto S. Parametric survival analysis of gastric cancer patients. *Cancer* 1980; **46**: 2709-2716

17   **Valen B**, Viste A, Haugstvedt T, Eide GE, Soreide O. Treatment of stomach cancer. A national experience. *Br J Surg* 1988; **75**: 708-714

18   **Bonenkamp JJ**, Sasako M, Hermans J, van de Velde CJ. Tumor load and surgical palliation in gastric cancer. *Hepatogastroenterology* 2001; **48**: 1219-1221

19   **Murata S**, Terata N, Eguchi Y, Tani T, Shibata J, Kodama M. Prognosis of patients with resection of stage IV gastric cancer. *Int Surg* 1998; **83**: 283-286

20   **Maekawa S**, Saku M, Maehara Y, Sadanaga N, Ikejiri K, Anai H, Kuwano H, Sugimachi K. Surgical treatment for advanced gastric cancer. *Hepatogastroenterology* 1996; **43**: 178-186

21   **Kunisaki C**, Shimada H, Akiyama H, Nomura M, Matsuda G, Ono H. Survival benefit of palliative gastrectomy in advanced incurable gastric cancer. *Anticancer Res* 2003; **23**: 1853-1858

22   **Huang CM**, Zhang XF, Lu HS, Zhang JZ, Wu XY, Guan GX, Wang C. Long-term therapeutic effects of total gastrectomy in cancer of the cardia and stomach fundus. *Zhonghua Waike Zazhi* 2003; **41**: 729-732

23   **Wan YL**, Liu YC, Tang JQ, Wang X, Wu T, Pan YS, Huang SJ, Huang YT. Clinical analysis of combined resection for T4 gastric cancer: report of 69 cases. *Zhonghua Waike Zazhi* 2003; **41**: 594-596

24   **Wang CS**, Chao TC, Jan YY, Jeng LB, Hwang TL, Chen MF. Benefits of palliative surgery for far-advanced gastric cancer. *Chang Gung Med J* 2002; **25**: 792-802

25   **Bozzetti F**, Marubini E, Bonfanti G, Miceli R, Piano C, Crose N, Gennari L. Total versus subtotal gastrectomy: surgical morbidity and mortality rates in a multicenter Italian randomized trial. The Italian Gastrointestinal Tumor Study Group. *Ann Surg* 1997; **226**: 613-620

26   **Meriggi F**, Forni E. Radical surgical treatment of gastric cancer. Personal experience. *G Chir* 2002; **23**: 361-367

27   **Sjostedt S**, Pieper R. Gastric cancer. Factors influencing longterm survival and postoperative mortality. *Acta Chir Scand Suppl* 1986; **530**: 25-29

28   **Viste A**, Haugstvedt T, Eide GE, Soreide O**.** Postoperative complications and mortality after surgery for gastric cancer. *Ann Surg* 1988; **207**: 7-13

29   **Hansson LE**, Sparen P, Nyren O. Survival in stomach cnacer is improving: results of a nationwide population-based Swedish study. *Ann Surg* 1999; **230**: 162-169

30   **Harrison LE**, Karpeh MS, Brennan MF. Total gastrectomy is not necessary for proximal gastric cancer. *Surgery* 1998; **123**: 127-130

31   **Bozzetti F**, Marubini E, Bonfanti G, Miceli R, Piano C, Gennari L. Subtotal versus total gastrectomy for gastric cancer: five-year survival rates in a multicenter randomized Italian trial. Italian Gastrointestinal Tumor Study Group. *Ann Surg* 1999; **230**: 170-178

32   **De Manzoni G**, Verlato G, Roviello F, Di Leo A, Marrelli D, Morgagni P, Pasini F, Saragoni L, Tomezzoli A. Italian Research Group for Gastric Cancer. Subtotal versus total gastrectomy for T3 adenocarcinoma of the antrum. *Gastric Cancer* 2003; **6**: 237-242

33   **Yamamoto M**, Baba H, Kakeji Y, Endo K, Ikeda Y, Toh Y, Kohnoe S, Okamura T, Maehara Y. Postoperative morbidity/mortality and survival rates after total gastrectomy, with splenectomy/pancreaticosplenectomy for patients with advanced gastric cancer. *Hepatogastroenterology* 2004; **51**: 298-302

Edited by Kumar M **Proofread by** Xu FM

• LIVER CANCER •

Gender difference in clinicopathologic features and survival of patients with hepatocellular carcinoma

Pisit Tangkijvanich, Varocha Mahachai, Pongspeera Suwangool, Yong Poovorawan

Pisit Tangkijvanich, Department of Biochemistry, Faculty of Medicine, Chulalongkorn University, Bangkok 10330, Thailand
Varocha Mahachai, Department of Medicine, Faculty of Medicine, Chulalongkorn University, Bangkok 10330, Thailand
Pongspeera Suwangool, Department of Pathology, Faculty of Medicine, Chulalongkorn University, Bangkok 10330, Thailand
Yong Poovorawan, Viral Hepatitis Research Unit, Department of Pediatrics, Faculty of Medicine, Chulalongkorn University, Bangkok 10330, Thailand
Correspondence to: Professor Yong Poovorawan, Viral Hepatitis Research Unit, Department of Pediatrics, Faculty of Medicine, Chulalongkorn University, Bangkok 10330, Thailand. yong.p@chula.ac.th
Telephone: +662-256-4909   **Fax:** +662-256-4929
Received: 2003-11-18   **Accepted:** 2004-01-29

Abstract

AIM: To determine the influence of gender on the clinicopathologic characteristics and survival of patients with hepatocellular carcinoma (HCC).

METHODS: A retrospective analysis of medical records was performed in 299 patients with HCC and their clinicopathologic features and survival were compared in relation to gender.

RESULTS: There were 260 male (87%) and 39 female patients (13%), with a male-to-female ratio of 6.7:1. Female patients had lower mean serum bilirubin levels (P=0.03), lower proportion of alcohol abuse (P=0.002), smaller mean tumor size (P=0.02), more frequent nodular type but less frequent massive and diffuse types of HCC (P=0.01), were less advanced in Okuda's staging (P=0.04), and less frequently associated with venous invasion (P=0.03). The median survivals in females (14 mo) were significantly longer than that of male patients (4 mo) (P=0.004, log-rank test). Multivariate analysis demonstrated that high serum alpha-fetoprotein levels, venous invasion, extrahepatic metastasis and lack of therapy were independent factors related to unfavorable prognosis. However, gender did not constitute a predictive variable associated with patient survival.

CONCLUSION: Female patients tend to have higher survival rates than males. These differences were probably due to more favorable pathologic features of HCC at initial diagnosis and greater likelihood to undergo curative therapy in female patients.

INTRODUCTION

Hepatocellular carcinoma (HCC) is one of the most common cancers worldwide with a particularly high incidence in areas where chronic hepatitis B virus (HBV) and hepatitis C virus (HCV) are common[1,2]. These regions include sub-Saharan Africa, Far East and Southeast Asia where the annual rate is more than 30 cases per 100 000 persons. In contrast, in low-incidence areas such as Europe and North America, the annual rate is less than 5 cases per 100 000 persons[3]. In Thailand, where chronic HBV is endemic, it is estimated that more than 10 000 new cases of HCC are diagnosed each year. Indeed, HCC represents the most common malignancy in Thai males and the third most common malignancy in females[4].

Previously, we demonstrated that HCC in Thailand had an indisputable male predominance, with a male-to-female ratio of approximately 6:1[5]. In fact, HCC is notably more prevalent in males worldwide, with reported male-to-female ratios ranging from 2:1 to 8:1 in most series. Until now, however, only a few studies have specifically compared the clinicopathologic characteristics of patients with HCC in relation to gender. In addition, the contribution of sex difference to patient survival and prognosis is controversial[6-13]. The aim of the present study was, therefore, to determine the influence of gender on clinicopathologic features and patient survival. In this respect, we analyzed the medical records on individuals in whom HCC was diagnosed during a four-year period at King Chulalongkorn Memorial Hospital (Bangkok, Thailand).

MATERIALS AND METHODS

A total of 299 patients with HCC who were admitted to King Chulalongkorn Memorial Hospital between January 1996 and September 1999 were retrospectively analyzed and included in this study. All patients were diagnosed based on liver tumor characteristics detected by ultrasound/CT scan and confirmed by histology or serum alpha-fetoprotein (AFP) levels above 400 IU/mL. Of those, there were 260 male (87%) and 39 female patients (13%), making a male-to-female ratio of 6.7:1. We compared the difference and the clinicopathologic features, including age, biochemical liver function test, presence or absence of associated cirrhosis, etiologic factors predisposing towards HCC (alcohol abuse, hepatitis B or C), degree of tumor differentiation, gross pathology of tumor, tumor size, presence of vascular invasion, stage of HCC according to Okuda's criteria, evidence of distant metastasis and modalities of therapy of HCC. In addition, the patients' survival time for each group was also calculated, starting with the time of cancer diagnosis (including any incidence of perioperative mortality).

Gross pathology, tumor size, and localization of HCC as well as presence of portal or hepatic venous involvement, were obtained by abdominal ultrasound or computerized tomography (CT). In this study, the gross pathologic types of HCC were categorized according to Trevisani *et al.*[14] as follows: nodular, multinodular, infiltrative, diffuse (the mass was not clearly defined and the boundary was indistinct) or massive type (a huge mass >10 cm with the boundary not well defined).

Biochemical liver function tests were determined by automated chemical analyzer (Hitachi 911) at the central laboratory of Chulalongkorn Hospital. The normal levels obtained with healthy adults are within the range of 0-38 IU/L for serum aspartate aminotransferase (AST) and alanine aminotransferase (ALT) and 98-279 IU/L for serum alkaline

phosphatase (AP). Enzyme-linked immunosorbent assays (ELISA) were used for the detection of HBsAg (Auszyme II, Abbott Laboratories, North Chicago, IL), anti-HCV (ELISA II; Ortho Diagnostic Systems, Chiron Corp., Emeryville, CA) and AFP (Cobus Core, Roche Diagnostics, Basel, Switzerland).

Statistical analysis

Data were presented as percentage, mean and standard deviation. The Chi-square test and unpaired *t* test were used to assess the statistical significance of the difference between groups as appropriate. Survival curves were established using the Kaplan-Meier method and differences between curves were demonstrated using the log-rank test. The Cox regression analysis was performed to identify which independent factors have a significant influence on the overall survival. *P* values below 0.05 were considered statistically significant.

RESULTS

As shown in Table 1, the mean age of female patients (56.4±15.2 years) was slightly higher, but not significantly different from that of male patients (52.6±13.2 years). There was a significantly lower proportion of heavy alcohol consumption among females than males (*P*=0.002). However, there were no significant differences in positive rates of serum HBsAg and anti-HCV, nor in the frequency of associated liver cirrhosis between the two groups. Similarly, no significant differences between groups were observed regarding mean serum AFP levels and biochemical abnormalities, with the exception that female patients had significantly lower serum bilirubin levels than male patients (*P*=0.03).

Table 1 Demographic and clinical data of female and male patients with HCC at initial diagnosis

Characteristics	Female(n=39)	Male (n=260)	P
Age (yr)	56.4±15.2	52.6±13.2	NS
Underlying cirrhosis (+:-)	36:3	251:9	NS
Viral hepatitis marker			
HBsAg (+:-)	18:21	147:113	NS
Anti-HCV (+:-)	5:34	23:237	NS
Heavy alcohol consumption (+:-)	3:36	83:177	0.002
Mean AFP (IU/mL)	48 435.4±105 231.6	40 221.9±89 147.9	NS
Biochemical liver function tests			
Total bilirubin (mg/dL)	1.5±1.2	3.1±2.3	0.03
Alkaline phosphatase (IU/L)	451.6±277.3	529.3±375.0	NS
AST (IU/L)	128.4±133.2	154.3±135.2	NS
ALT (IU/L)	62.7±52.6	87.6±97.5	NS
Albumin (g/dL)	3.6±0.7	3.4±0.7	NS
Prothrombin time (sec)	14.5±2.8	15.1±9.3	NS

Quantitative variables were expressed as mean±SD; (+:-) indicates positive:negative. NS=not significant.

Table 2 demonstrates the clinicopathologic data of the patients at the time of the diagnosis of HCC. Female patients in this study tended to have less aggressive tumor characteristics than male patients. For instance, the mean tumor size in females (8.6 cm) was significantly smaller than that of male patients (11.6 cm) (*P*=0.02). In addition, the nodular type of HCC appeared to be more frequently found among female patients, whereas the massive and diffuse types were more common among males (*P*=0.01). Furthermore, the tumors in the female group tended to be of a less advanced stage according to Okuda's criteria (*P*=0.04) and less frequently associated with portal or hepatic vein invasion (*P*=0.03). Nonetheless, no significant differences between groups were observed as to the degree of tumor differentiation, the prevalence of extrahepatic metastasis or ruptured HCC.

Table 2 Clinicopathologic data of female and male patients with HCC at initial diagnosis

Characteristics	Female (n=39)	Male (n=260)	P
Mean tumor size (cm)	8.1±3.9	11.6±4.5	0.02
Tumor size			
≤5 cm:>5cm	9:30	30:230	0.04
Gross appearance of HCC			
Nodular:Multinodular:	12:10:14:3	30:52:115:63	0.01
Massive:Diffuse			
Tumor cell differentiation			
Well:Moderately:Poorly	3:5:4	11:66:32	NS
Okuda's staging (I:II:III)	13:23:3	43:180:37	0.04
Portal or hepatic vein invasion (+:-)	6:33	84:176	0.03
Extrahepatic metastasis (+:-)	5:34	37:223	NS
Ruptured HCC (+:-)	1:38	29:231	NS
Therapy for HCC (+:-)	22:17	105:155	NS
Modality of therapy			
Surgical resection (+:-)	9:30	27:233	0.02
Chemoembolization (+:-)	13:26	43:217	0.01
Systemic chemotherapy (+:-)	0:39	31:229	0.02

Quantitative variables were expressed as mean±SD; (+:-) indicates positive:negative.

Likewise, there was no statistically significant difference between groups in terms of the number of patients treated with specific therapeutic modalities. However, female patients were more likely than male patients to undergo surgical resection, which included segmental and lobar resection, or treated with transcatherter arterial chemoembolization (TACE) (*P*=0.02 and 0.01, respectively). In contrast, a significantly higher proportion of male patients were treated with systemic chemotherapy than females (*P*=0.02).

The median survival time of all patients in this study, regardless of their gender, was 5 mo. The Kaplan-Meier survival curves demonstrated that the overall median survival for female and male patients were 14 and 4 mo, respectively (*P*=0.004, using log-rank test) (Figure 1). For patients who were treated with any specific therapeutic modality, the median survival for the female and male group were 17 and 7 mo, respectively (*P*=0.025). In the untreated cases, the median survival of the female group was longer than that of the male group (9 and 3 mo, respectively), however, this difference did not achieve statistical significance (*P*=0.24).
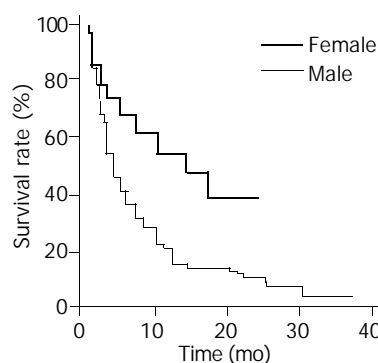

Figure 1 Overall survival of male and female patients with HCC.

Univariate analysis of the main variables was performed to determine significant risk factors associated with the overall survival. In addition to male sex, serum AFP levels >400 IU/mL, Okuda's stage II and III HCC, massive or diffuse types of tumors, tumor mass size over 5 cm in diameter, venous invasion and

extrahepatic metastasis, and an unfavorable prognosis were observed in patients who did not receive any specific therapy for HCC. Stepwise Cox regression multivariate analysis revealed that high serum AFP levels, venous invasion, extrahepatic metastasis and absence of specific therapy were significantly and independently predictive for unfavorable prognosis (Table 3). Nonetheless, gender was not selected in the final analysis as an independent predictor of survival.

Table 3 Independent predictors influencing survival in HCC

Variables	Regression coefficient (95% CI)	*P* value[1]
AFP (>400 IU/mL)	1.67 (1.03-2.71)	0.037
Portal or hepatic vein invasion	1.73 (1.04-2.89)	0.035
Extrahepatic metastasis	2.37 (1.30-4.37)	0.005
No therapy	2.87 (1.63-5.04)	0.0002

95% CI: 95% confidence interval; [1]*P* value based on multiivariate Cox regression analysis

DISCUSSION

Various types of cancer occur more frequently in male than in female patients. Such is also the case with HCC. In fact, marked male predominance in HCC incidence is observed in both high- and low-risk areas, regardless of ethnic and geographic diversity[15]. Despite this, the exact reasons for sex difference in the incidence of HCC are unclear. It has been reported that DNA synthetic activities are higher in male than in female cirrhotics and this might be one of the possible explanations for the gender discrepancy in HCC[16]. However, in patients who had already developed HCC, a significant difference in tumor cellular proliferation between male and female patients was not detected[11]. It has also been suggested that the effect of sex hormones may contribute, at least in part, to the greater incidence of HCC observed in male patients. Although the mechanism remains to be elucidated, studies from animal models has implicated that the hormonal effect may be related to testosterone's ability in enhancing transforming growth factor (TGF) alpha related hepatocarcinogenesis and hepatocyte proliferation[17].

Beside this, other possible factors contributing to the male predominance in HCC include the association with HBV infection, the higher proportion of male cirrhotics and differences in life-style habits, such as heavy alcohol consumption and smoking[6,10]. However, in this study, no significant difference was found between groups in the prevalence of associated cirrhosis. Likewise, although HBsAg carriers were slightly more common in males, this discrepancy did not reach statistical significance. Notably, this was also the case with the prevalence of chronic HCV infection in our study. In contrast, the prevalence of heavy alcohol consumption was significantly different, being higher in male than in female patients. Indeed, alcoholic cirrhosis has long been recognized as a risk factor for developing HCC, although its role in direct hepatocarcinogenesis is uncertain[18]. Nonetheless, it is reasonable to speculate that chronic alcohol abuse might accelerate cancer development in some cases with HBV- or HCV-associated cirrhosis and this may be partially responsible for the male preponderance of HCC in our series.

In addition, to confirm the marked male predominance, our study has demonstrated that male patients with HCC had a less favorable prognosis than females after initial diagnosis. Specifically, better survival in females was observed in those who had undergone surgical resection or treated with TACE. For untreated cases, the influence of gender on prognosis seemed to be limited since significant difference in survival between groups was not achieved, although there was a trend for females to survive longer. These results were consistent

with previous reports in which a better prognosis was observed in females following hepatic resection[9-13]. For instance, according to the study in Japan by Nagasue *et al*., significantly better survival rates were found in females after 4 years of hepatic surgery[9]. A previous report on Chinese patients by Cong *et al*. also demonstrated that the survival rates after surgery were approximately 50% and 25% in females and males, respectively[10]. Likewise, a study in Hong Kong by Ng *et al*., indicated that females had a lower incidence of tumor recurrence following the surgical operations, with a median disease free survival of 19.5 mocompared with 4.5 mo for males[11]. Recently, Lee *et al*. reported that female cirrhotics with HCC had 5-year disease survival rates after hepatic resection, which was higher than males (approximately 65% and 30%, respectively)[12]. Conversely, such favorable prognosis in females was not consistently observed among patients with inoperable tumors[6-8].

Thus, it could be speculated that the prognosis of HCC is not directly influenced by the sex of the patients. This is confirmed in our study that gender was not selected as an independent predictor of survival from the multivariate analysis. In fact, a better prognosis in females was probably attributed to a less advanced stage of HCC at initial diagnosis and, as a result, a higher proportion of cases was likely to undergo surgical resection or treated with TACE. In this study, for example, approximately 25% and 35% of female patients were treated with hepatic resection or TACE, respectively, while only approximately 10% and 15% of males were treated with such modalities. It has been generally recognized that hepatic resection is one of the most effective therapeutic modalities offering a hope of cure for patients with HCC[19,20]. Moreover, a non-surgical approach such as TACE appears to be beneficial in prolonging survival for some patients with unresectable tumors[21-22].

In addition to therapeutic factors, some pathobiologic features indicative of tumor invasiveness, such as venous involvement, appear to be significant factors influencing the survival of HCC[23]. It has also been demonstrated that the presence of venous invasion is associated with a higher intrahepatic recurrence rate after the resection of the tumor[24]. Although HCC is characterized by its propensity for vascular invasion, it is interesting that female patients with HCC had a much lower prevalence of venous involvement than males. It seems, therefore, that this is probably one of the main factors contributing to different survival rates between the two sexes in our study. Similarly, yet to be addressed, are the effects of other tumor pathologic features, such as tumor encapsulation during the disease-free period after surgical resection of HCC[25]. Previous data have demonstrated that females have a significantly higher prevalence of tumor encapsulation than males (80% and 45%, respectively). Furthermore, the tumors in females were frequently less invasive in terms of lower prevalence of tumor microsatellites and positive histological margin[11].

In conclusion, our data indicated that female patients with HCC had certain clinicopathologic features different from those in male patients. Moreover, females with HCC appeared to have better survival rates than males. This better prognosis in females was related to more favorable tumor characteristics such as a lower prevalence of hepatic or portal venous invasion and less advanced stages at initial diagnosis. As a result, female patients were more likely than male patients to undergo hepatic resection or to be treated with TACE.

REFERENCES

1   **Chen CJ,** Yu MW, Liaw YF. Epidemiological characteristics and risks factors of hepatocellular carcinoma. *J Gastroenterol Hepatol* 1997; **12**: S290-308

2   **Tang ZY.** Hepatocellular carcinoma-cause, treatment and metastasis. *World J Gastroenterol* 2001; **7**: 445-454

3   **McGlynn KA,** Tsao L, Hsing AW, Devesa SS, Fraumeni JF Jr. International trends and patterns of primary liver cancer. *Int J Cancer* 2001; **94**: 225-236

4   **Srivatanakul P.** Epidemiology of liver cancer in Thailand. *Asian Pac J Cancer Prev* 2001; **2**: 117-121

5   **Tangkijvanich P,** Hirsch P, Theamboonlers A, Nuchprayoon I, Poovorawan Y. Association of hepatitis viruses to hepatocellular carcinoma in Thailand. *J Gastroenterol* 1999; **34**: 227-233

6   **Lai CL,** Gregory PB, Wu PC, Lok AS, Wong KP, Ng MM. Hepatocellular carcinoma in Chinese males and females. Possible causes for the male predominance. *Cancer* 1987; **60**: 1107-1110

7   **Calvet X,** Bruix J, Gines P, Bru C, Sole M, Vilana R, Rodes J. Prognostic factors of hepatocellular carcinoma in the west: a multivariate analysis in 206 patients. *Hepatology* 1990; **12**: 753-760

8   **Falkson G,** Cnaan A, Schutt AJ, Ryan LM, Falkson HC. Prognostic factors for survival in hepatocellular carcinoma. *Cancer Res* 1988; **48**: 7314-7318

9   **Nagasue N,** Galizia G, Yukaya H, Kohno H, Chang YC, Hayashi T, Nakamura T. Better survival in women than in men after radical resection of hepatocellular carcinoma. *Hepatogastroenterology* 1989; **36**: 379-383

10 **Cong WM,** Wu MC, Zhang XH, Chen H, Yuan JY. Primary hepatocellular carcinoma in women of Mainland China. A clinicopathologic analysis of 104 patients. *Cancer* 1993; **71**: 2941-2945

11 **Ng IO**, Ng MM, Lai EC, Fan ST. Better survival in female patients with hepatocellular carcinoma. Possible causes from a pathologic approach. *Cancer* 1995; **75**: 18-22

12 **Lee CC**, Chau GY, Lui WY, Tsay SH, King KL, Loong CC, Hshia CY, Wu CW. Better post-resectional survival in female cirrhotic patients with hepatocellular carcinoma. *Hepatogastroenterology* 2000; **47**: 466-469

13 **Dohmen K,** Shigematsu H, Irie K, Ishibashi H. Longer survival in female than in male with hepatocellular carcinoma. *J Gastroenterol Hepatol* 2003; **18**: 267-272

14 **Trevisani F,** Caraceni P, Bernardi M, D' Intino PE, Arienti V, Amorati P, Stefanin GF, Grazi G, Mazziotti A, Fornale L. Gross pathological types of hepatocellular carcinoma in Italian patients. Relationship with demographic, environmental and clinical factors. *Cancer* 1993; **72**: 1557-1563

15 **El-Serag HB.** Hepatocellular carcinoma: an epidemiologic view. *J Clin Gastroenterol* 2002; **35**(5 Suppl 2): S72-78

16 **Tarao K,** Ohkawa S, Shimizu A, Harada M, Nakamura Y, Ito T, Tamai S, Hoshino H, Okamoto N, Iimori K. The male preponderance in incidence of hepatocellular carcinoma in cirrhotic patients may depend on the higher DNA synthetic activity of cirrhotic tissue in men. *Cancer* 1993; **72**: 369-374

17 **Matsumoto T,** Takagi H, Mori M. Androgen dependency of hepatocarcinogenesis in TGF alpha transgenic mice. *Liver* 2000; **20**: 228-233

18 **Adami HO,** Hsing AW, McLaughlin JK, Trichopoulos D, Hacker D, Ekbom A, Perrson I. Alcoholism and liver cirrhosis in the etiology of primary liver cancer. *Int J Cancer* 1992; **51**: 898-902

19 **Befeler AS,** Di Bisceglie AM. Hepatocellular carcinoma: diagnosis and treatment. *Gastroenterolgy* 2002; **122**: 1609-1619

20 **Qian J,** Feng GS, Vogl T. Combined interventional therapies of hepatocellular carcinoma. *World J Gastroenterol* 2003; **9**: 1885-1891

21 **Pawarode A**, Tangkijvanich P, Voravud N. Outcome of primary hepatocellular carcinoma treatment: an 8-year experience with 368 patients in Thailand. *J Gastroenterol Hepatol* 2000; **15**: 860-864

22 **Lo CM**, Ngan H, Tso WK, Liu CL, Lam CM, Poon RT, Fan ST, Wong J. Randomized controlled trial of transarterial lipiodal chemoembolization for unresectable hepatocellular carcinoma. *Hepatology* 2002; **35**: 1164-1171

23 **Ringe B,** Pichlmayr R, Wittekind C, Tusch G. Surgical treatment of hepatocellular carcinoma: Experience with liver resection and transplantation in 198 patients. *World J Surg* 1991; **15**: 270-285

24 **Nagasue N,** Uchida M, Makino Y, Takemoto Y, Yamanoi A, Hayashi T, Chang YC, Kohno H, Nakamura T, Yukaya H. Incidence and factors associated with intrahepatic recurrence following resection of hepatocellular carcinoma. *Gastroenterology* 1993; **105**: 488-494

25 **Ng IO,** Lai EC, Ng MM, Fan ST. Tumor encapsulation in hepatocellular carcinoma. A pathologic study of 189 cases. *Cancer* 1992; **70**: 690-693

Edited by Ma JY **Proofread by** Xu FM

• LIVER CANCER •

Effect of phosphorus-32 glass microspheres on human hepatocellular carcinoma in nude mice

Dong-Sheng Zhang, Lu Liu, Li-Qiang Jin, Mei-Ling Wan, Qun-Hui Li

Dong-Sheng Zhang, Li-Qiang Jin, Mei-Ling Wan, Qun-Hui Li,
School of Basic Medical Sciences, Southeast University, Nanjing
210009, Jiangsu Province, China
Lu Liu, Experimental Center of Modern Medical Sciences, Southeast
University, Nanjing 210009, Jiangsu Province, China
Supported by the Science and Technology Commission of Jiangsu
Province, No.BJ93007 and Natural Science Foundation of Jiangsu
Province, No. BK2001003
Correspondence to: Professor Dong-Sheng Zhang, School of Basic
Medical Sciences, Southeast University, 87 Ding Jia Qiao Road,
Nanjing 210009, Jiangsu Province, China. b7712900@jlonline.com
Telephone: +86-25-83272502 **Fax:** +86-25-57712900
Received: 2003-11-21 **Accepted:** 2003-12-29

Abstract

AIM: To study the effects of phosphorus-32 glass microspheres
(^{32}P-GMS) on human hepatocellular carcinoma in nude mice.

METHODS: Human liver cancer cell line was implanted into
the dorsal subcutaneous tissue of 40 BALB/c nude mice.
Then the 40 tumor-bearing BALB/ c nude mice were allocated
into treatment group (n=32) and control group (n=8). In
the former group different doses of ^{32}P-GMS were injected
into the tumor mass, while in the latter nonradioactive [31]P-
GMS was injected into the tumor mass. The experimental
animals were sacrificed on the 14th day. The ultrastructural
changes of tumor in both treatment group and control group
were studied with transmission electron microscopy (TEM)
and stereology.

RESULTS: In treatment group, a lot of tumor cells were
killed and the death rate of tumor cells was much higher
(35-70%). Ultrastructurally, severe nuclear damage was
observed in the death cells. The characteristics of appoptosis
such as margination of heterochromatin was also found in
some tumor cells. Besides, well differentiated tumor cells,
degenerative tumor cells and some lymphocytes were seen.
The skin and muscle adjacent to the tumor were normal. In
control group, the tumor consisted of poorly differentiated
tumor cells, in which there were only a few of dead cells
(5%). Stereologicl analysis of ultrastructral morphology
showed that Vv of nuclei (53.31±3.46) and Vv of nucleoli
(20.40±1.84) in the control group were larger than those
(30.21±3.52 and 10.96±2.52) in the treatment group
respectively (P<0.01), and Vv of RER (3.21±0.54) and Vv of
mitochondria (4.53±0.89) in the control group were smaller
than those (8.67±1.25 and 7.12±0.95) in the treatment group
respectively (P<0.01, 0.05). Sv of the membrane of microvilli
and canaliculi (27.12 um^2/100 um^3±11.84 um^2/100 um^3) in the
control group was smaller than that (78.81 um^2/100 um^3±
19.69 um^2/100 um^3) in the treatment group (P<0.01). But Vv
of lipid particles (3.71±1.97) and Vv of vacuoles (5.72±1.58)
were much larger than those (0.30±0.16 and 0.35±0.15) in
the treatment group respectively (P<0.05, P<0.01).

CONCLUSION: The experimental results indicate that local
administration of ^{32}P-GMS can produce obvious effect on

liver cancer cells and the anticancer effect of ^{32}P-GMS is
directly proportional to the dose administrated. Ultrastructural
stereology can also show the effect of ^{32}P-GMS on the
normalization of tumor cells, which is beneficial to the
prognosis and treatment of patients. Moreover, local
administrtion of ^{32}P-GMS is also safe.

INTRODUCTION

In recent years, nuclide labeled nontoxic and undegradable
micro-carriers such as phosphorus-32 glass microsphere ([32]P-
GMS)[1,2] and yttrium-90 glass microsphere[3-5] have been
successfully developed and gained much attention as a new
radioactive medcine for treating malignant liver neoplasms.
Experimental researches using micro-carriers such as microsphere,
microcapsule, nano-microsphere (nano-sphere), liposome
and nano-liposome in treating malignant tumors have been
carried out for more than a decade and gained much interesting
development. Microspheres conjugated with anticancer drugs
including traditional Chinese medicine could release drugs
slowly into the cancer tissues, thus keeping their anti-cancer
effect for a long time[6-9]. However, there are only a few reports
about the researches of cytocidal effect of local internal
irradiation of ^{32}P-GMS on tumor cells. The ultrastructural
stereology study of human liver cancer cell treated by ^{32}P-GMS
has not been reported[10,11]. So the authors used a human liver
tumor-bearing nude mouse model to explore the anticancer
effect of ^{32}P-GMS and the ultrastructural stereology changes
in the tumor with TEM.

MATERIALS AND METHODS

Materials
^{32}P-GMS By activating of standardized glass microspheres
through nuclear-chemical reaction, nonradioactive [31]P ([31]P-
GMS, cold sphere) was transformed into radioactive ^{32}P glass
microsphere (provided by Nuclear Power Research Institute
of China). It had the following properties. The diameter of glass
sphere was 46-76 μm, ^{32}P physical half-life was 14.28 d, average
β ray energy per disintegration was 0.695 MeV, and soft tissue
penetration distance was max. 8.0 mm, averaging 3.2 mm.
^{32}P-GMS suspension was prepared by mixing ^{32}P-GMS with
super-liquidized iodized oil or 500 g/L glucose solution to
the concentrations of 370 MBq.mL/L and 37 MBq.mL/L
on an oscillator.
Animal experiment Human liver cancer cell line subset (H-
CS) with higher oncogenicity and liability of metastasis was
implanted into the dorsal subcutaneous tissue of 40 BALB/c
nu/nu nude mice (male, mean body mass 19.2 g, aged 4 wk,
derived from Shanghai Experimental Animal Center, Chinese
Academy of Sciences) at the dosage of 0.1-0.2 mL (1×10^7 tumor
cells for each animal).

Forty tumor-bearing nude mice with the tumor mass diameter of 0.7-1.0 cm, different doses (7 320 Gy, 3 660 Gy, 1 830 Gy, 366 Gy and 183 Gy) of ^{32}P-GMS were injected to the mass center of 32 nude mice (subgroup A: $n=6$, B: $n=6$, C: $n=8$, D: $n=6$, E: $n=6$) in the treatment group and non-radioactive ^{31}P-GMS to the mass center of 8 nude mice as the control group. The experimental animals were sacrificed on the 14th day.

Preparation of electron microscopcial sections Biopsy specimens from all the tumors and their adjacent tissues were immediately placed in 40 g/L glutaraldehyde and allowed to stand for 2 h at room temperature. Then the tissue was washed 3 times and postfixed for 1 h in 10 g/L osmium tetroxide. After rinsed in distilled water and dehydrated in acetone, the tissue specimens were embedded in Epon 812, polymerized for 48 h, ultrathin sectioned and stained. The electron microscopical sections were viewed in a H600 transmission electron microscope. At the same time, all specimens from tumors and their adjacent tissues were subjected to gross inspection, light microscopy to observe the morphological changes, and compared with the ultrastructural changes, and then the death rate of tumor cells was calculated. Death rate=the number of death cells/the number of total cells.

Method of stereological study Test grid method was used[12]. The areas of teat web was 120 mm×90 mm, and the length of each small grid was 5 mm. There were 432 tested dots in test web. The TEM pictures were magnified to 30 000-fold, and 30 pictures were taken in each group. When the picture was tested, the test web was put on the picture to test the constructure observed. Stereological parameters (volume density Vv; surface density Sv) were used to test the cell organallae such as nucleus, nucleolus, RER and mitochondron, lysosome, lipid, vesicles and membrane of microvilli and canaliculi. The point counting method was used. The standard deviation and standard error of stereological parameters in each group were calculated. The statistical method used was t test.

The formula of volume density Vv is

$$V_v = \frac{\sum_{i=1}^{n} P_{x_i}}{\sum_{i=1}^{n} P_{r_i}}$$

(n: the number of pictures, i: the ordinal number of pictures, Pxi: the number of test points within the scope of some constructures in i picture, Pri: the number of test points within the section scope of the frames of reference in the same picture as above).

The formula of surface density Sv is

$$S_v = \frac{2\sum_{i=1}^{n} I_{x_i}}{z\sum_{i=1}^{n} P_{r_i}}$$

(n: the number of pictures, i: the ordinal number of pictures, Ixi: the number of the points of transversal intersection of some membranes and test line in i picture, Pri: the number of test points within the section scope of the frames of reference in the same picture as above, $2/z$ is coefficient).

RESULTS

Ultrastructure observation

In the treatment group, the tumor cells of subgroup A revealed necrotic injury and a lot of tumor cells were killed (Figure 1A). In the severely injured cells the nuclei lysed, cell membrane disrupted and numerous debries were found. The injured tumor cells showed condensation of nuclear chromatin, peripheral aggregation of heterochromatin in pieces, damaged organellae in cytoplasm, disappearance of mitochondrial cristae and ribosomes, appearance of a few of vacuoles and lipid particles. The death rate of tumor cells in the subgroup A was much higher (70%). In subgroup B, many tumor cells presented histological structures similar to those in subgroup A (the death rate: 65%), but with many lysosomes. Some were differentiated

tumor cells with the characteristics of round nuclei with small nucleoli, evenly distributed chromatin, mainly euchromatin, lots of mitochondria and rough endoplasmic reticula in the cytoplasm, formation of plenty of microvilli at the interface of tumor cells (Figure 1B). The capillaries between the moderately differentiated tumor cells had thickened or loosened basal membranes with local defects. Abundant fibroblasts and collagen fibers could be found in the matrix. There was a tendency to form bile canaliculi somewhere between tumor cells (Figure 1C). Under light microscope, the tumor tissues both in subgroups A and B showed scattered focal necrosis. The tumor cells in subgroup C (the death rate: 50%) showed different morphologic appearances, some damaged mildly and others severely, but some were moderately differentiated with plenty of cytoplasmic free polyribosomes. Plasma cells were scattered among the tumor cells, and some lymphocytes protruded the pseudopodia when they were contacted with the tumor cells. There were residual tumor cells showing active proliferation. In subgroups D and E (the death rate: 35%), the histological structure was manifested in various complicated forms, and active multiplication of tumor cells was readily seen. Under light microscope, the histological characteristics in subgroups C, D and E were the arrangement of tumor cells transformed from dense to loose with scattered spot necrosis. No abnormality was found in the muscle and dermal cells of adjacent skin nearby the tumor.

In the control group, most tumor cells were poorly differentiated and rapidly multiplicated (Figure 1D), with characteristics of irregular large nuclei with deep indentations and plenty of chromatins, several peripherally aggregated large and prominent nucleoli. In cytoplasm, a lot of free polyribosomes, vacuoles and lipid particles were presented, while mitochondria, glycogen and rough endoplasmic reticulum were scant. Only a few of dead cells (5%) were found in this group. In the nearby interstitial tissue infiltrated tumor cells, degenerative lymphocytes, damaged fibroblasts, loose collagen fibers were found.
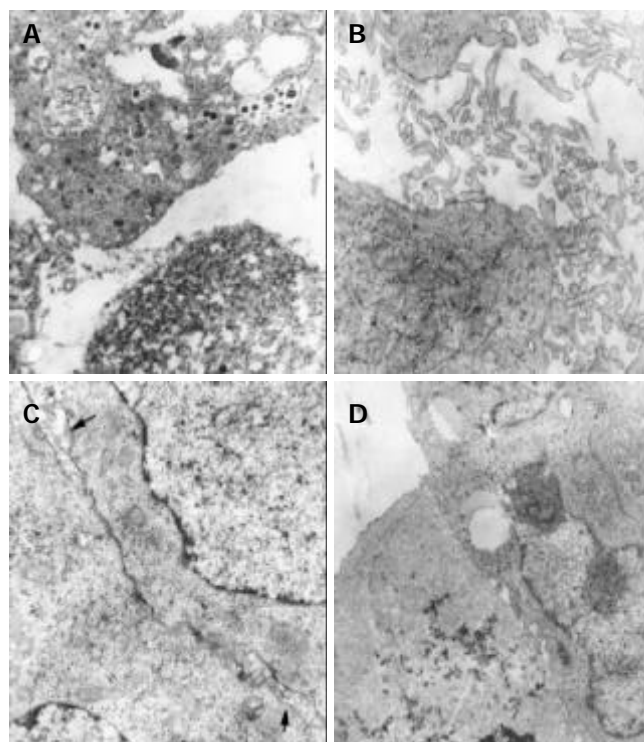

Figure 1 Ultrastructural characterictics of effect of ^{32}P-GMS on human hepatocellular carcinoma. A: Necrosed tumor cells (×12 000). B: Microvilli on the surface of tumor cells and mitochondria in cytoplasm (×18 000). C: Formation of bile duct-like structure in tumor cells (arrow, ×18 000). D: Heteromorphic tumor cells with cleavage of nuclei and scanty microvilli on surface (×12 000).

Stereological study

The results of stereological analysis of ultrastructural morphology are summarized in Tables 1, 2 and 3.

Table 1 Comparision of liver cancer cell Vv in control group and treatment group

Constructure	Liver cancer cell Vv(mean±SD)×100%	
	Control group	Treatment group
Nuclei	53.31±3.46[b]	30.21±3.52[b]
Cytoplasm	46.79±3.46	69.79±3.52
Mitochondria	4.53±0.89[a]	7.12±0.95[a]
Lysosomes	2.07±0.22	1.94±1.12
RER	3.21±0.54[d]	8.67±1.25[d]
Lipid particles	3.71±1.97[c]	0.30±0.16[c]
Vacuoles	5.72±1.58[f]	0.35±0.15[f]

Nuclei Vv in control group was larger than that in treatment group, [a]$P<0.05$. Vv of RER in control group was smaller than that in treatment group, [b]$P<0.01$. Vv of mitochondria in control group was smaller than that in treatment group, [d]$P<0.01$. Vv of lipid particles was larger in control group than that in treatment group, [c]$P<0.05$. Vv of vacuoles was larger in control group than that in treatment group, [f]$P<0.01$.

Table 2 Comparision of nucleoli Vv of liver cancer cells in control group and treatment group

Constructure	Nucleoli Vv liver cancer cell Vv(mean±SD)×100%	
	Control group	Treatment group
Nucleoli	20.40±1.84[b]	10.96±2.52[b]
Nuclei	79.60±1.84	89.04±2.52

Nucleoli Vv in control group was larger than that in treatment group, [b]$P<0.01$.

Table 3 Comparision of Sv in membranes of microvilli and canaliculi of liver cancer cells in control group and treatment group

Constructure	Sv of liver cancer cell (mean±SD)×100%	
	Control group	Treatment group
Membrane of microvilli and canaliculi	27.12 um²/100 um³ ±11.84 um²/100 um³[b]	78.81 um²/100 um³ ±19.69 um²/100 um³[b]

Sv of the membranes of microvilli and canaliculi of liver cancer cells in control group was smaller than that in treatment group, [b]$P<0.01$.

DISCUSSION

Anticancer effect and mechanism of ^{32}P-GMS

On the 14th day of local injection of ^{32}P-GMS to the tumor, the tumor cell death rate was 35-70% in different treatment groups, and was 5% in control group. The results showed that local internal irradiation of ^{32}P-GMS had cytocidal effects on tumor cells and the anticancer effect of ^{32}P-GMS was directly proportional to the dose administrated.

Anticancer mechanism of ^{32}P-GMS mainly includes two parts. The first is that β-ray energy of ^{32}P-GMS could directly destroy or injury DNA of tumor cells to induce cell death because of the breakage, disaggregation and synthetic obstruction of DNA. The second is that β-ray irradiation conducted ionization and irradiation of the water molecules in intracellular environment to produce several kinds of free radicals and superoxides which indirectly killed the tumor cells by injuring the biological macromolecules[13,14]. Besides, researches also showed that β-ray could induce cell-death related gene expressions to accelerate the apoptosis of tumor cells[15]. Because ^{32}P-GMS internal irradiation is one kind of continued low linear energy transfer(LET) irradiation, its indirect effect on tumor cells might be much more important[16].

Ultrastructure charactericts and significance of effect of ^{32}P-GMS on tumor

In specimens of different treatment groups, the tumor cells might exhibit as survived, degenerative or necrosed (in early or typical changes). It seems that this reflected the whole course of tumor cell progression from degeneration to death after irradiation. The ultrastructural changes demonstrated that under the effect of high-dose irradiation, the tumor tissues received a lethal radiation energy in a short period, resulting in nonexistence of tumor cells which had a high ability to synthesize endogenous proteins. Under the appropriate dose of irradiation, besides the necrosis of most tumor cells, the tendency to derive to nearly normal histological pictures appeared, such as microvilli on the cell surface, formation of bile canaliculi-like structure. These demonstrated that ^{32}P-GMS had the ability to kill actively proliferative tumor cells and to promote their normalization. On the other hand, proliferation of connective tissue after irradiation could lead to disorganization, which could destroy the survived tumor cells. This was consistent with what was reported[13]. At the lower dose of irradiation, plasma cells and some lymphocytes were scattered among tumor cells, but this was rarely seen in the high-dose subgroup. Whether the immune function during treatment can be enhanced to some extent is still unknown. The irradiation injured some interstitial tissues such as thickened or loosened basal membrane of capillaries with local defects and damaged collagen fibers. But acute irradiative inflammation was not found and the tissue adjacent the tumor was normal, indicating that local administration of ^{32}P-GMS is safe.

Stereological ultrastructure analysis of effect of ^{32}P-GMS on tumor

Stereological analysis is a kind of image analysis technology widely used in pathomorphological researches. Researches discovered that image analysis was of importance to explore the criteria for pathological diagnosis, grading and morphogenesis of human hepatocellular carcinoma[17-19]. Compared with qualitative analysis, stereological analysis was much more objective.

Differentiated malignant tumor cells have some characteristics under electron microscope. The general characteristics of poorly differentiated and rapidly multiplicated tumor cells included irregular large nuclei, peripherally aggregated large and prominent nucleoli, lots of free polyribosomes in cytoplasm, scanty mitochondria and rough endoplasmic reticulum[20,21]. The characteristics of differentiated tumor cells are different, including round nuclei with small nucleoli, mitochondria and rough endoplasmic reticula in the cytoplasm, formation of microvilli at the interface of tumor cells. There was a tendency to form bile canaliculi somewhere between liver tumor cells. Stereological results showed that Vv of nuclei (53.31±3.46) and Vv of nucleoli (20.40±1.84) in the control group were larger than those (30.21±3.52 and 10.96±2.52) in the treatment group respectively ($P<0.01$) and Vv of RER (3.21±0.54) and Vv of mitochondria (4.53±0.89) in the control group were smaller than those (8.67±1.25 and 7.12±0.95) in the treatment group respectively ($P<0.01, 0.05$). Sv of the membrane of microvilli and canaliculi (27.12 um²/100 um³±11.84 um²/100 um³) in the control group was smaller than that (78.81um²/100 um³ ±19.69 um²/100 um³) in the treatment group ($P<0.01$). The results indicated that local administration of ^{32}P-GMS could produce obvious anticancer effects, besides, it played a role in

making poorly differentiated tumor cells become well differentiated ones, which was obviously beneficial to the prognosis and treatment of patient. Stereological study also showed that Vv of lipid particles (3.71±1.97) and Vv of vacuoles (5.72±1.58) in control group were much larger than those (0.30±0.16, and 0.35±0.15) in treatment group ($P<0.05$, $P<0.01$). There is a possibility that the cells with lipid particles and vacuoles were degenerative cells which were much easier to be killed by β-ray energy of ^{32}P-GMS, so the Vv of lipid particles and vacuoles in treatment group was smaller than that in control group.

In conclusion, local administration of ^{32}P-GMS has obvious anticancer effects on liver cancer cells, which is directly proportional to the dose administrated. Ultrastructural stereology can also show the role of ^{32}P-GMS in promoting the normalization of tumor cells. Moreover, local administration of ^{32}P-GMS is safe.

REFERENCES

1   **Liu L**, Sun WH, Wu FP, Han DQ, Teng GJ, Fan J. An experimental study of treatment of liver cancer by locally administration with phosphate-32 glass microspheres & estimation of *tissue-absorbed dose. Nanjing Tiedao Yixueyuan Xuebao* 1997; **16**: 223-226

2   **Liu L**, Fan J, Zhang J, Du MH, Wu FP, Teng GJ. Experimental treatment of carcinoma in a mouse model by local injection of phosphorus-32 glass microspheres. *J Vasc Interv Rad* 1998; **9**: 166

3   **Herba MJ**, Illescas FF, Thirlwell MP, Boos GJ, Rosenthall L, Atri M, Bret PM. Hepatic malignacies: improved treatment with intraarterial Y-90. *Radiology* 1988; **169**: 311-314

4   **Wollner I**, Knutsen C, Smith P, Prieskorn D, Chrisp C, Andrews J, Juni J, Warber S, Klevering J, Crudup J, Ensminger W. Effects of hepatic arterial yttrium 90 glass microspheres in dogs. *Cancer* 1988; **61**: 1336-1344

5   **Andrews JC**, Walker SC, Ackermann RJ, Cotton LA, Ensminger WD, Shapiro B. Hepatic radioembolization with yttrium-90 containing glass microspheres: preliminary results and clinical follow-up. *J Nucl Med* 1994; **35**: 1637-1644

6   **Zhang DS**, Jia XP, Fan XS, Jin LQ, Wan ML, Li QH, Zheng J, Gu N. Preparation and characterization of magnetic nano-microspheres containing arsenic trioxide. *Dianzi Xianwei Xuebao* 2002; **21**: 507-508

7   **Zhang DS**, Fan XS, Jia XP, Zheng J, Gu N, Ding AW, Jin LQ, Wan ML, Li QH. Effects of Nano-magnetoliposomes containing arsenic trioxide on heLa cells. *Zhonghua Zhongxiyi Zazhi* 2003; **4**: 1289-1292

8   **Fan XS**. The use of magnetic liposomes in cancer therapy. *Guowai Yixue Zhongliuxue Fence* 2003; **30**: 147-149

9   **Lu XL**. Advances of nanotechnology in breast cancer treatment. *Guowai Yixue Zhongliuxue Fence* 2003; **30**: 201-204

10 **Zhang DS**, Liu L, Wan ML, Li QH, Hong DR. Phosphorus-32 glass microspheres to treat human hepatocellular carcinoma in nude mice. *Zhonghua Shiyan Waike Zazhi* 1999; **16**: 327-328

11 **Liu L**,Teng GJ, Zhang DS, Song JZ, He SC, Guo JH, Fang W. Toxicology of intrahepatic arterial administration of interventional phosphorous-32 glass microspheres to domestic piges. *Chin Med J* 1999; **112**: 632-636

12 **Han ZB** , Cai WQ. Application of electron microscopy in clinical medicine. *Chong Qing: ,Chong Qing Publishing House* 1988: 74-82

13 **Editorial board of pratical oncology**. Practical Oncology. Vol. 1. *Beijing: People' s Health Publishing House* 1977: 406-413

14 **Liu L**, Jiang Z, Teng GJ, Song JZ, Zhang DS, Guo QM, Fang W, He SC, Guo JH. Clinical and experimental study on regional administration of phosphorus-32 glass microspheres in treating hepatic carcinoma. *World J Gastroenterol* 1999; **5**: 492-505

15 **Zheng DX.** Advance in apoptosis research. *Zhonghua Binglixue Zazhi* 1996; **25**: 50-53

16 **Wang YY**, Wang DZ, Zheng GY, Mao ZY. Apoptosis induced by interstitial irradiation with ^{32}P glass microspheres combination with hyperthermia in mous solid tumor S180. *Huaxi Kouqiang Yixue Zazhi* 2001; **19**: 118-119

17 **Shen LJ**, Zhang ZJ, Ou YM, Zhang HX, Huang R, He Y, Wang MJ, Xu GS. Computed morphometric analysis and expression of alpha fetoprotein in hepatocellular carcinoma and its related lesion. *World J Gastroenterol* 2000; **6**: 415-416

18 **Zhang ZJ**, Shen LJ, Ou YM, Huang R, Zhang HX, He Y, Xu GS. Image analysis on the pathological morphogenesis and forecasting diagnosis of human hepatocarcinoma. *Zhongguo Tishixue Tuxiang Fenxi* 2000; **5**: 230-234

19 **Zhang ZJ**, Shen LJ, Huang R, Zhang HX, Ou YM, He Y, Xu GS, Wang MJ. Morphometric application to grading of human hepatocellular carcinoma. *Zhonghua Xiaohua Zazhi* 1995; **15**: 327-329

20 **Bo AH**, Shun SX, Li JL. Medical electron microscopy. *Beijing: People' s Health Publishing House* 2000: 69-94

21 **Wu ZB**. Basis of Ultrastructural Pathology. *Beijing: People' s Health Publishing House* 1990: 20-99

Edited by Wang XL and Xu FM

• LIVER CANCER •

Structure analysis and expressions of a novel tetratransmembrane protein, lysosoma-associated protein transmembrane 4 b associated with hepatocellular carcinoma

Xin-Rong Liu, Rou-Li Zhou, Qing-Yun Zhang, Ye Zhang, Yue-Ying Jin, Ming Lin, Jing-An Rui, Da-Xiong Ye

Xin-Rong Liu, Rou-Li Zhou, Ye Zhang, Yue-Ying Jin, Ming Lin, Department of Cell Biology and Genetics, School of Basic Medical Sciences, Peking University, Beijing 100083, China
Qing-Yun Zhang, Department of Clinical Laboratory, School of Oncology, Peking University, Beijing 100037, China
Jing-An Rui, Da-Xiong Ye, Department of General Surgery/Pathology, Peking Union Medical College Hospital, Beijing 100032, China
Supported by the 248 Major R&D Program of Beijing, No. H020220020310 and Special Fund for Promotion of Education, Ministry of Education, China
Correspondence to: Dr. Rou-Li Zhou, Department of Cell Biology and Genetics, School of Basic Medical Sciences, Peking University, Beijing 100083, China. rlzhou@bjmu.edu.cn
Telephone: +86-10-82801034   **Fax:** +86-10-62358270
Received: 2003-07-12   **Accepted:** 2003-07-30

Abstract

AIM: To analyze the structure and expressions of the protein encoded by an HCC-associated novel gene, lysosome-associated protein transmembrane 4 β (*LAPTM4B*).

METHODS: Primary structure and fundamental characteristics of LAPTM4B protein were analysed with bioinformatics. Expressions of LAPTM4B in HCC tissues and various cell lines were detected using polyclonal antibodies and Western blot.

RESULTS: *LAPTM4B* encoded two isoforms of proteins with molecular masses 35-ku and 24-ku, respectively. The expression level of LAPTM4B-35 protein in HCC tissues was dramatically upregulated and related to the differentiation status of HCC tissues, and it was also high in some cancer cell lines. Computer analysis showed LAPTM4B was an integral membrane protein with four transmembrane domains. LAPTM4B showed relatively high homology to LAPTM4A and LAPTM5 in various species.

CONCLUSION: *LAPTM4B* gene encoded two isoforms of tetratransmembrane proteins, LAPTM4B-35 and LAPTM4B-24. The expression of LAPTM4B-35 protein is upregulated and associated with poor differentiation in human HCC tissues, and also at high levels in some cancer cell lines. LAPTM4B is an original and conserved protein.

INTRODUCTION

We have previously reported the cloning and identification of a novel gene, which was designated by the International Nomenclature Committee as lysosomal associated protein transmembrane 4 β (*LAPTM4B*)[1-4]. *LAPTM4B* was overexpressed in 87.3% human hepatocellular carcinomas (HCC) at mRNA level performed by Northern blot[2]. BLAST program analysis showed that the *LAPTM4B* gene was mapped to chromosome 8 q22.1, spanning approximately at least 50 kb. It is composed of seven exons separated by six introns. The cloned full-length cDNA sequence (GenBank accession number: AY057051) of *LAPTM4B* is 2.2 kb and contains two ATGs at the 5' end with an interval of 273 bp and two polyadenylation signals: aataaa and aattaaa[2].

In this study, primary structures of proteins encoded by *LAPTM4B* gene were analyzed using bioinformatics. Specific polyclonal antibodies directing against two epitopes of the 10-peptides localized at the N-terminus (28-37aa) and in between the 3rd and 4th transmembrane domains (232-241aa) of LAPTM4B, respectively, were prepared. The expressions of LAPTM4B proteins in HCC, paired noncancerous liver (PNL), normal liver (NL) tissues and various cancer cell lines were detected by Western blot. The functions of LAPTM4B protein was discussed.

MATERIALS AND METHODS

Specimens
Fresh HCC and paired noncancerous liver specimens were obtained during operations on patients with HCC, normal liver tissues were obtained during operations on patients with hepatohemangioma.

Cell lines and culture
Human hepatoma cell lines BEL-7402, QGY-7701, SMMC-7721, HLE and human hepatic cell line L-02, human cervical cancer cell line HeLa, human prostate carcinoma cell lines PC3M and PC3, human pulmonary giant cell carcinoma cell lines BE1 and LH7, and human melanoma cell lines WM451 and WM983A were maintained in RPMI 1640 (GIBco BRL) medium supplemented with 100 mL/L fetal bovine serum.

Protein extraction[5-7]
The tissues stored at -80 ℃ or living cells were homogenized and extracted with lysis buffer (pH7.6) containing 10 mmol/L Tris, 150 mmol/L NaCl, 1 mmol/L EDTA, 5 g/L NP40, 1 mmol/L PMSF, 1 μg/mL aprotinin, 1 μg/mL pepstatin A. After centrifugation at 12 000 g for 10 min at 4 ℃, the supernatants were collected and the proteins were quantitated by Bradford microassay.

Peptide synthesis and antibody preparation[8-10]
Two KLH-conjugated 10 peptides (KLH- Ala-Lys-Gly-Thr-Asp-Pro-Ala-Glu-Ala-Arg and KLH-Pro-Tyr-Arg-Asp-Asp-Val-Met-Ser-Val-Asn) were synthesized by Invitrogen Company. Rabbits were immunized subcutaneously with 1 mg of KLH-peptide conjugates emulsified in Freund's complete adjuvant (GIBco BRL). The immunization was repeated with the antigens in Freund's incomplete adjuvant (GIBco BRL) 4 wk after the first

injection and 2 wk after the second injection. The anti-sera were designated as LAPTM4B-N28-37-pAb and LAPTM4B-EC2-pAb, respectively. The titers of these two sera were both above 1×10^5 detected by ELISA with peptide-coated plates. The pre-immune sera did not show any reactivity to the peptides.

Western blotting

Proteins in cell lysates were fractionated by 100 g/L SDS-PAGE and then electrotransferred onto a nitrocellulose filter (Bio-Rad). The filters were blocked at 4 ℃ overnight with blocking buffer (pH7.6) containing 50 g/L fat free dry milk. Then the filters were incubated with indicated antibody for 2 h at room temperature. After washed with TBST (pH6.0), the filters were incubated at room temperature for 1 h with horseradish peroxidase conjugated goat anti-rabbit IgG at 1:2 000 dilution in TBS-5 g/L fat free dry milk. Immunoreactive bands were visualized using ECL detection reagents (Santa Cruz).

Bioinformatics analysis tool

The Bioinformatics analysis tool included BLAST and FASTA for basic local alignment of sequences, PCGENE software for predicting primary structure and fundamental characteristics of the protein, Kyte&Doolittle hydrophobicity index for calculating hydrophobicity value, ClustalW software for multiple sequence alignment and DNAMAN software for displaying phylogenic tree.

RESULTS

Bioinformatics analysis of primary structure of LAPTM4B protein

The primary structure of LAPTM4B is shown in Figure 1. The *LAPTM4B* cDNA may encode two putative proteins with 35 ku (317 aa) and 24 ku (226 aa). Computer analysis (PCGENE) showed that LAPTM4B was an integral membrane protein with four highly conserved hydrophobic transmembrane domains, forming two extracellular loops (EC1 and EC2), a cytoplasmic loop and intracellular amino- and carboxyl tails. The transmembrane regions were located at 117-133, 163-179, 200-216, and 243-259 aa, respectively. The full amino acid sequence contained one N-glycosylation site, eight phosphorylation sites, and four N-myristoylation sites. A tyrosine phosphorylation site was predicted at 285 aa at C-terminal region, which depending on phosphorylation might form a binding site for specific SH2 domain in some signaling proteins. It was also predicted that LAPTM4B containing proline-rich motif (PXXP) at N-terminal region would be a SH3 domain binding protein. Moreover, LAPTM4B contained typical lysosomal targeting signals (3 YXX φ motifs)[11] at C-terminal region. Human LAPTM4B
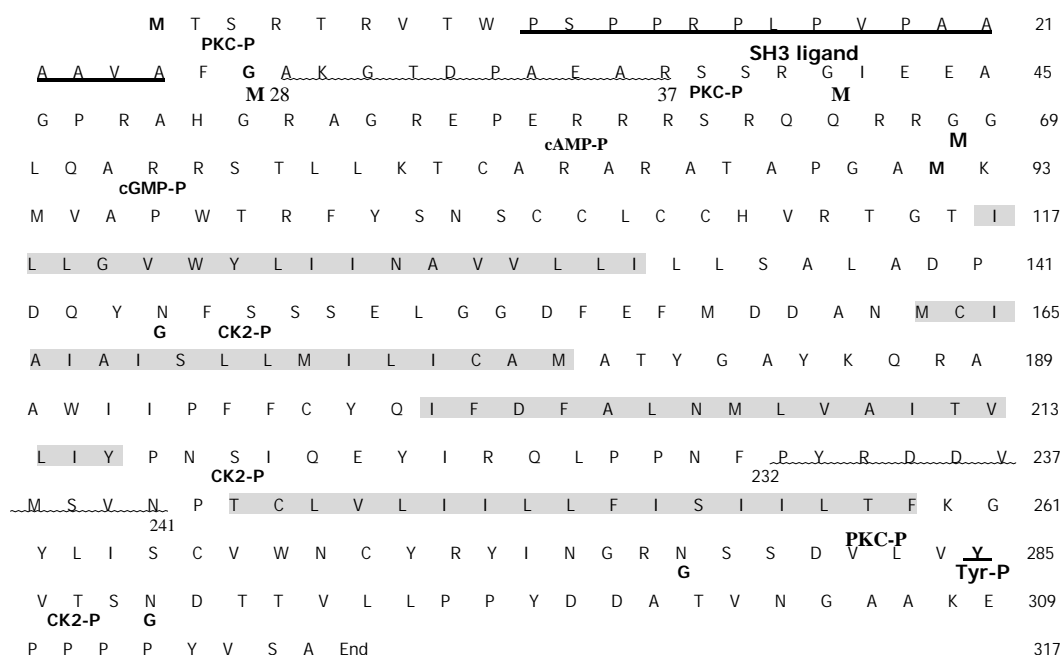

Figure 1 Putative amino-acid sequence of LAPTM4B. The four transmembrane domains are shadowed with gray color. Two translation initiation sites are thick black. Putative SH3 ligand is indicated by thick underlining. The sequence containing 10 amino acid residues (28aa-37aa or 232aa-241aa) and used as immunogen is wavy underlined. PKC-P, cAMP-P, cGMP-P, CK2-P, Tyr-P: various phosphorylation sites; G: N-glycosylation site; M: myristylation site.
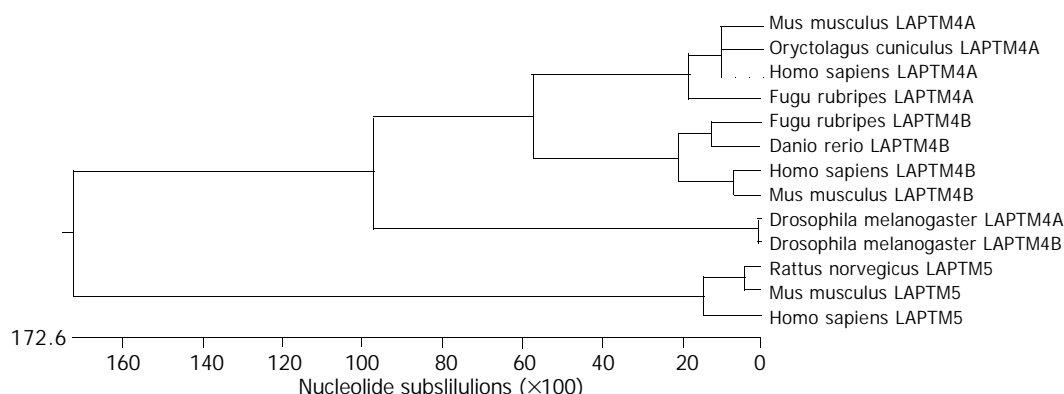

Figure 2 Phylogenic tree of LAPTM4B.

shared 92% homology with mouse LAPTM4B (GenBank accession number: AAH1912)[12] at amino acid level, suggesting that LAPTM4B was highly conserved within vertebrate species. The region from 140 aa to 317 aa of LAPTM4B was highly conserved compared with mouse LAPTM4B. But the N-terminal region from 1 aa to 91 aa (between the first ATG and the second ATG) of LAPTM4B-35 was highly specific and no homological sequence was found using BLAST in nr database. LAPTM4B also showed 46% homology to a lysosomal tetra-transmembrane protein, LAPTM4A, at amino acid level. The orthodog of LAPTM4A in murine was a nucleoside transporter in intracellular membrane-bound compartments, and mediated a multidrug resistance phenotype in drug-sensitive strains of *S. cerevisiae*[12-14].

The phylogenic tree (Figure 2) was constructed according to multiple sequence alignment results. It showed that LAPTM4B, LAPTM4A and LAPTM5 proteins were distributed in clusters. Human LAPTM4B showed the most close homology to Mus musculus and also had certain homology to Dannio rerio and Fugu rubripes, as well as Drosophila melanogaster, but was far-away from Yeast. In addition, LAPTM4B showed relatively high homology to LAPTM4A and LAPTM5 in various species to a certain extent, and LAPTM4B was closer to LAPTM4A than LAPTM5. These results indicated that LAPTM4B was an original and conserved protein.

Expression of LAPTM4B protein in HCC tissues

As shown in Figure 3, 2 proteins with molecular masses 35-ku and 24-ku both reacted with LAPTM4B-EC2-pAb were identified by Western blot in HCC, PNL and NL tissues, and designated as LAPTM4B-35 and LAPTM4B-24, respectively. Nevertheless, only one band at the 35 ku position appeared when LAPTM4B-N28-37-pAb was used for Western blot in HCC tissues, indicating that LAPTM4B-35 was translated from the whole ORF and initiated from the first ATG, whereas LAPTM4B-24 was translated from the second ATG. Furthermore, LAPTM4B proteins were significantly overexpressed in HCC tissues than in PNL and NL tissues. Notably, the expression levels of LAPTM4B-35 were significantly related to the differentiation status of HCC tissues, they were higher in poorly differentiated HCCs than in moderately and well differentiated HCCs (Figure 4)[4]. In addition, the ratio of LAPTM4B-35 to LAPTM4B-24 was remarkably higher in HCC than in PNL and NL (Table 1). However, the ratio of LAPTM4B-35 to LAPTM4B-24 in PNL was kept at the same level as in NL, even though LAPTM4B-35 and LAPTM4B-24 were both slightly increased. Thus the development of HCC might be associated with the raised ratio of LAPTM4B-35 to LAPTM4B-24.
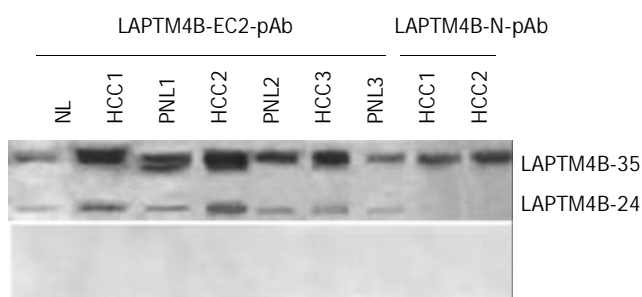

Figure 3 Expressions of LAPTM4B proteins in HCC tissues identified by Western blot with various antibodies. Top: Western Blot profiles performed with anti serum. LAPTM4B-EC2-pAb: polyclonal antibody directing against the epitope localized at the EC2 domain between the 3rd and 4th transmembrane regions of LAPTM4B. LAPTM4B-N28-37-pAb: polyclonal antibody directing against the epitope localized at the N-terminal region of LAPTM4B. Bottom: Western blot profiles performed with pre-immune serum.
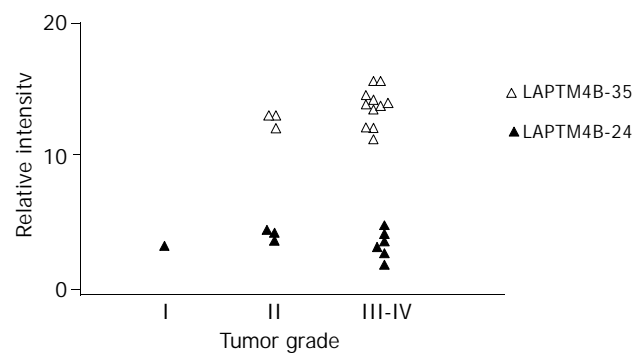

Figure 4 Correlation between LAPTM4B-35 protein expression and pathological grade of HCC.

Table 1 Relative intensity of LAPTM4B-35 and LAPTM4B-24 (mean±SD)

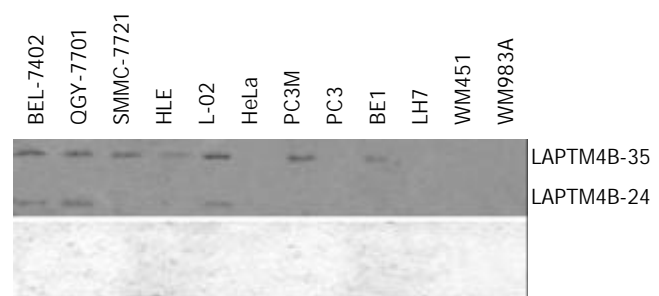|	HCC	PNL	NL
LAPTM4B-35	13.32±1.98[b]	4.58±1.31	2.78±0.11
LAPTM4B-24	3.59±1.78[b]	1.76±1.24	1.00±0.02
LAPTM4B-35/LAPTM4B-24 (ratio)	3.71	2.60	2.78

[b]$P<0.01$ *vs* PNL and NL.

Figure 5 Expression of LAPTM4B proteins in various cell lines shown via Western blot with LAPTM4B-EC2-pAb. Top: Western blot profiles performed with LAPTM4B-EC2-pAb. Bottom: Western blot profiles performed with pre-immune serum.

Table 2 Relative intensity of LAPTM4B-35 and LAPTM4B-24 in various cell lines

Cell line	LAPTM4B-35	LAPTM4B-24	LAPTM4B-35/-24 (ratio)
BEL-7402	3.98	2.09	1.91
QGY-7701	3.21	2.20	1.45
SMMC-7721	2.98	-	-
HLE	2.24	-	-
L-02	3.32	2.56	1.29
Hela	-	-	-
PC3M	2.96	-	-
PC3	-	-	-
BE1	1.47	-	-
LH7	-	-	-
WM451	-	-	-
WM983A	-	-	-

Expression of LAPTM4B proteins in various cell lines

LAPTM4B proteins in 12 cell lines were detected by Western blot with LAPTM4B-EC2-pAb (Figure 5). With exception of HLE cells, LAPTM4B proteins were remarkably expressed in

all of HCC-derived cell lines including BEL-7402, QGY-7701 and SMMC-7721, and human hepatic cell line L-02 cells. The ratio of LAPTM4B-35 to LAPTM4B-24 was higher in HCC cell lines than in immortal hepatic cell line L-02 (Table 2), suggesting that disturbance of LAPTM4B-35 to LAPTM4B-24 equilibrium in expressions might cause the malignant transformation in hepatocarcinogenesis. Moreover, the expressions of LAPTM4B-35 were also higher in highly metastatic cell lines[15-17], including prostate carcinoma PC-3M and pulmonary giant cell carcinoma BE1 cell lines than in the syngenic low metastatic cell lines, including PC-3 and LH7 cell lines. Therefore, the overexpression of LAPTM4B-35 was likely related to cancer cell invasion and metastasis. However, LAPTM4B was not detected in human cervical carcinoma cell line HeLa and human melanoma cell lines WM451 and WM983A[15], indicating that overexpression of LAPTM4B-35 was somehow specific for some carcinomas.

DISCUSSION

HCC is one of the most common cancers world-wide, and is the major cause of malignant deaths in Asia and Africa[18-20]. The pathogenesis of HCC is particularly complex. The current model for HCC carcinogenesis postulated a multistage progression involving an accumulation of genetic alterations[21,22], including activation of oncogenes N-ras, H-ras, K-ras, c-erbA, c-met, and c-myc etc.[23,24], repression or mutation of tumor suppressor genes[25], besides the transcriptional activation of c-jun and nuclear factor NF-κB by HBV and HCV[26,27]. But the roles of these genes in cell proliferation, differentiation, and premalignant status in liver malignancy are far from elucidated.

We previously reported[2] that *LAPTM4B* was a novel gene associated with HCC, and significantly overexpressed in HCC as shown via Northern blot and *in situ* hybridization. *LAPTM4B* is also widely expressed in human tissues with a relatively high level in the testis, heart and skeletal muscles, and moderately in the ovary, kidney and pancreas, and poorly in the liver, spleen, and thymus, and lowest in the lung and peripheral leukocytes. It was remarkably overexpressed in 87.3% (48/55 cases) HCC tissues when compared with PNL and NL tissues. Furthermore, the *LAPTM4B* mRNA expression levels were significantly related to the differentiation status of HCC tissues. They were highest in poorly differentiated HCCs, higher in moderately differentiated HCCs, and relatively low in well differentiated HCCs.

Here we report the expressions of LAPTM4B proteins in HCC, PNL, NL and a number of cell lines via Western blot analysis using two antibodies, LAPTM4B-N28-37-pAb or LAPTM4B-EC2-pAb, which were prepared by immunization with two KLH-conjugated 10-peptides whose sequences are localized at either the second extracellular loop (EC2) between the third and fourth transmembrane regions or the N-terminal region in the cytoplasma. These two 10-peptides used as immunogens were highly specific, i.e. having very low homology compared to known proteins of Homo sapiens. By using PCGENE software, the 10-peptides should have characteristics of high hydrophilicity and no residues of putative glycosylation and phosphorylation. KLH was conjugated with the N-termini of 10-peptides in order to increase immunogenicity. Two isoforms of LAPTM4B, LAPTM4B-35 and LAPTM4B-24, whose mass was coincident with the predicted products translated from the first and second ATG in ORF, were identified. Expressions of LAPTM4B-35 proteins were highly upregulated in HCC with poor differentiation. This result was coincident with expression of *LAPTM4B* mRNA in HCC tissues. LAPTM4B expressions were also high in human HCC cell lines and some other cancer cell lines. Transient transfection of murine BHK cells was performed with two plasmids, *pcDNA3/LAPTM4B-AE*

containing a full-length cDNA of *LAPTM4B* ORF and *pcDNA3/LAPTM4B-BE* containing the same ORF sequence but with 273 nucleotides deleted at 5' end, respectively. The transfectants in AE-series expressed mainly LAPTM4B-35 and slightly LAPTM4B-24, and proliferated very rapidly and formed colonies powerfully. However, the transfectants in BE-series expressed only LAPTM4B-24, and lost potentials of long term survival and growth. Therefore, it is suggested that LAPTM4B-24 may play an antagonistic role in cell survival and proliferation, and the equilibrium of LAPTM4B-35 and LAPTM4B-24 in expression is involved in controlling cell survival/proliferation and differentiation. The disequilibrium in expressions of LAPTM4B-35 and LAPTM4B-24 may be involved in malignant transformation of hepatocytes and carcinogenesis.

REFERENCES

1   **Liu J**, Zhou R , Zhang N, Rui J, Jin C. Biological function of a novel gene overexpressed in human hepatocellular carcinoma. *Chin Med J* 2000; **113**: 881-885

2   **Shao GZ**, Zhou RL, Zhang QY, Zhang Y, Liu JJ, Rui JA, Wei X, Ye DX. Molecular cloning and characterization of LAPTM4B, a novel gene upregulated in hepatocellular carcinoma. *Oncogene* 2003; **22**: 5060-5069

3   **He J**, Shao G, Zhou R. Effects of the novel gene, LAPTM4B, highly expression in hepatocellular carcinoma on cell proliferation and tumorigenesis of NIH3T3 cells. *Beijing Daxue Xuebao* 2003; **35**: 348-352

4   **Liu X,** Zhou R, Zhang Q, Zhang Y, Shao G, Jin Y, Zhang S, Lin M, Rui J, Ye D. Identification and characterization of LAPTM4B encoded by a human hepatocellular carcinoma-associated novel gene. *Beijing Daxue Xuebao* 2003; **35**: 340-347

5   **Schuck S**, Honsho M, Ekroos K, Shevchenko A, Simons K. Resistance of cell membranes to different detergents. *Proc Natl Acad Sci U S A* 2003; **100**: 5795-5800

6   **Jones MN**. Surfactants in membrane solubilisation. *Int J Pharm* 1999; **177**: 137-159

7   **Shetty J**, Diekman AB, Jayes FC, Sherman NE, Naaby-Hansen S, Flickinger CJ, Herr JC. Differential extraction and enrichment of human sperm surface proteins in a proteome: identification of immunocontraceptive candidates. *Electrophoresis* 2001; **22**: 3053-3066

8   **Shen L**, Guo ZY, Chen Y, Liu LY, Feng YM. Expression, purification, characterization of amphioxus insulin-like peptide and preparation of polyclonal antibody to it. *Shengwu Huaxue Yu Shengwu Wuli Xuebao* 2001; **33**: 629-633

9   **Hadidi S**, Yu K, Chen Z, Gorczynski RM. Preparation and functional properties of polyclonal and monoclonal antibodies to murine MD-1. *Immunol Lett* 2001; **77**: 97-103

10   **Missbichler A**, Hawa G, Schmal N, Woloszczuk W. Sandwich ELISA for proANP 1-98 facilitates investigation of left ventricular dysfunction. *Eur J Med Res* 2001; **6**: 105-111

11   **Hogue DL**, Nash C, Ling V, Hobman TC. Lysosome-associated protein transmembrane 4 alpha (LAPTM4 alpha) requires two tandemly arranged tyrosine-based signals for sorting to lysosomes. *Biochem J* 2002; **365**(Pt 3): 721-730

12   **Hogue DL**, Ellison MJ, Young JD, Cass CE. Identification of a novel membrane transporter associated with intracellular membranes by phenotypic complementation in the yeast Saccharomyces cerevisiae. *J Biol Chem* 1996; **271**: 9801-9808

13   **Cabrita MA**, Hobman TC, Hogue DL, King KM, Cass CE. Mouse transporter protein, a membrane protein that regulates cellular multidrug resistance, is localized to lysosomes. *Cancer Res* 1999; **59**: 4890-4897

14   **Hogue DL**, Kerby L, Ling V. A mammalian lysosomal membrane protein confers multidrug resistance upon expression in Saccharomyces cerevisiae. *J Biol Chem* 1999; **274**: 12877-12882

15   **Li S**, Fang W, Zhong H. Expression of tumor metastasis suppressor gene KAI1/CD82 in human cancer cell lines with different metastasis potential. *Zhonghua Yixue Zazhi* 1999; **79**: 708-710

16   **Kim IY**, Kim BC, Seong do H, Lee DK, Seo JM, Hong YJ, Kim HT, Morton RA, Kim SJ. Raloxifene, a mixed estrogen agonist/antagonist, induces apoptosis in androgen-independent human prostate cancer cell lines. *Cancer Res* 2002; **62**: 5365-5369

17   **Liu Y**, Zheng J, Fang W, You J, Wang J, Cui X, Wu B. Identification of metastasis associated gene G3BP by differential display in human cancer cell sublines with different metastatic potentials G3BP as highly expressed in non-metastatic. *Chin Med J* 2001; **114**: 35-38

18   **Liu YH**, Zhou RL, Rui JA. Detection of hepatoma cells in peripheral blood of HCC patients by nested RT-PCR. *World J Gastroenterol* 1998; **4**: 106-108

19   **Bosch FX**, Ribes J, Borras J. Epidemiology of primary liver cancer. *Semin Liver Dis* 1999; **19**: 271-285

20   **Rui JA**, Wang SB, Chen SG, Zhou R. Right trisectionectomy for primary liver cancer. *World J Gastroenterol* 2003; **9**: 706-709

21   **Kondoh N**, Wakatsuki T, Ryo A, Hada A, Aihara T, Horiuchi S, Goseki N, Matsubara O, Takenaka K, Shichita M, Tanaka K, Shuda M, Yamamoto M. Identification and characterization of genes associated with human hepatocellular carcinogenesis.

Cancer Res 1999; **59**: 4990-4996

22   **Qin LX**, Tang ZY. The prognostic molecular markers in hepatocellular carcinoma. *World J Gastroenterol* 2002; **8**: 385-392

23   **Luo D**, Liu QF, Gove C, Naomov N, Su JJ, Williams R. Analysis of N-ras gene mutation and p53 gene expression in human hepatocellular carcinomas. *World J Gastroenterol* 1998; **4**: 97-99

24   **Ueki T**, Fujimoto J, Suzuki T, Yamamoto H, Okamoto E. Expression of hepatocyte growth factor and its receptor c-met proto-oncogene in hepatocellular carcinoma. *Hepatology* 1997; **25**: 862-866

25   **Zhu AX**. Hepatocellular carcinoma: are we making progress? *Cancer Invest* 2003; **21**: 418-428

26   **Henkler F**, Waseem N, Golding MH, Alison MR, Koshy R. Mutant p53 but not hepatitis B virus X protein is present in hepatitis B virus-related human hepatocellular carcinoma. *Cancer Res* 1995; **55**: 6084-6091

27   **Sansonno D**, Cornacchiulo V, Racanelli V, Dammacco F. *In situ* simultaneous detection of hepatitis C virus RNA and hepatitis C virus-related antigens in hepatocellular carcinoma. *Cancer* 1997; **80**: 22-33

Edited by Zhu LH and Wang XL **Proofread by** Xu FM

• LIVER CANCER •

Quantitative detection of *common deletion* of mitochondrial DNA in hepatocellular carcinoma and hepatocellular nodular hyperplasia

Jian-Yong Shao, Hong-Yi Gao, Yu-Hong Li, Yu Zhang, You-Yong Lu, Yi-Xin Zeng

Jian-Yong Shao, Hong-Yi Gao, Yu-Hong Li, Yu Zhang, Yi-Xin Zeng, Cancer Center, Sun Yat-Sen University, Guangzhou 510060, Guangdong Province, China
You-Yong Lu, Beijing Institute for Cancer Research, Beijing Laboratory of Molecular Oncology, School of Oncology, Peking University, Beijing 100034, China
Correspondence to: Jian-Yong Shao, M.D., Ph.D., Department of Pathology, Cancer Center, Sun Yat-Sen University, 651 Dong Feng Road East, Guangzhou 510060, Guangdong Province, China. jyshao@gzsums.edu.cn
Telephone: +86-20-87343391   **Fax:** +86-20-87343391

Abstract

AIM: To study the deletion of mitochondiral DNA in hepatocellular carcinoma and hepatocellular nodular hyperplasia and its significance in the development of cancer.

METHODS: Deleted mtDNA (CD-mtDNA) and wild type mtDNA (WT-mtDNA) were quantitatively analyzed by using real-time PCR in 27 hepatocellular carcinomas (HCC) and corresponding noncancerous liver tissues and 27 hepatocellular nodular hyperplasiae (HNH).

RESULTS: A novel CD (4 981 bp) was detected in 85% (23/27) and 83%(22/27) of HCC and HNH tumor tissues, respectively, which were significantly higher than that in paired noncancerous liver tissues (57%, 15/27) ($P<0.05$). The CD/WT-mtDNA ratio in HCC tumors was 0.00092 (median, interquartile range, 0.0001202-0.00105), which was significantly higher than that in paired noncancerous liver tissues (median, 0.000, quartile range, 0-0) ($P=0.002$, Mann-Whitney Test), and was 25 of times of that in HNH tissues (median, 0.0000374, quartile range, 0-0.0004225) ($P=0.002$, Mann-Whitney test).

CONCLUSION: CD-mtDNA mutation plays an important role in the development and progression of HCC.

INTRODUCTION

Heptacellular carcinoma (HCC) is one of the common malignancies worldwide, and has been ranked the 2nd cancer killer in China. Hepatitis B and C viruses (HBV and HCV) and dietary aflatoxin intake remain the major causative factors of HCC[1]. Previous studies also revealed that frequent genetic aberrations were involved in heptocarcinogenesis[2,3]. However, the molecular mechanisms of hepatocarcinogenesis remain unclear. Recently, morphological features of the tumor, both gross and histological, have been found to be significantly associated with tumor recurrence and patient survival.

Nuclear gene alterations are correlated to invasion, metastasis, recurrence of HCC,which are regarded as biomarkers for the malignant phenotype of HCC, and related to the prognosis and therapeutic outcomes. These biomarkers include p53 gene mutation[4], VEGF overexpression[5,6], apoptosis related genes, cell adhesion and extracellular matrix related genes such as E-cadherin, β-catenins, CD44s, MMPs and their inhibitor TIMPs[7-13].

Human mitochaondrial DNA (mtDNA) is located in cytoplasm, is becoming the study hotspot for its alteration in correlation with its tumorigenesis. Mitochondria are involved in apoptosis[14], and probably also tumorigenesis[15], which has led researchers to examination the potential roles of mtDNA alterations in the development and maintenance of cancers.

The most abundant change in mtDNA is called common deletion (4 977 bp, CD). CD-containing mitochondrial DNA (CD-mtDNA) was first observed in patients with mitochondrial myopathies, and was also found to accumulate in patients with heteroplasmic mtDNA mutations and in normal individuals during aging, particularly in postmitotic tissues such as muscle and brain[16]. The CD-mtDNA mutation has been detected in several types of human tumors including thyroid Hürthle cell tumor[17], gastric cancer[18], and hepatocellular carcinoma[19]. However, knowledge about the common deletion of mtDNA in HCC in China is poor. This is the first report of a high incidence (70%) of a novel CD-mtDNA (4 981 bp) in tumor tissues of HCC and hepatocellular nodular hyperplasia (HNH) from southern China, and the first analysis correlating CD-mtDNA level to clinicopathological parameters and age.

MATERIALS AND METHODS

Clinical data and histopathologic analysis of tumor samples

Patients with histologically proved HCC and HNH at the Cancer Center, Sun Yat-Sen University (Guangzhou, China) were recruited with informed consent from January 1999 to January 2003. Samples consisted of 27 surgically resected HCC and 27 HNH specimens. In HCC specimens, the tumor tissue and paired adjacent noncancerous liver tissue were obtained independently for mtDNA analysis. In serum, hepatitis B viral surface antigen and HCV antibody titer were detected by enzymed-linked immunosorbent assay and radio-immunoassay. Grading of differentiation was performed according to the method of Edmondson and Steiner. Tumors were classified into well differentiated group (grades 1 and 2) and poorly differentiated group (grades 3 and 4). The tumor size was classified into small (tumor mass <3 cm in greatest diameter) and large (tumor mass size >3 cm in greatest diameter). There were 24 males and 3 females aged from 40 to 79 years, with an average age of 58 years.

DNA extraction

Total (nuclear and mitochondria) DNA was extracted from

Table 1 TaqMan primers and probes for detection of WT-mtDNA and CD-mtDNA

Target	Amplicon	Oligonucleotide sequence (5'-3')
Wild Type mtDNA	101 bp	WT1 forward primer (7 878-7 897): 5´-AATCAATTGGCGACCAATGG-3´
		WT2 reverse primer (7 979-7 958): 5´-CGCCTGGTTCTAGGAATAATGG-3´
		WT probe (7 899-7 917): 5' FAM-ACTGAACCTACGAGTACAC-MGB-3'
Common Deletion mtDNA	132 bp	CD1 forward primer (8 448-8 472): 5'-TATTAAACACAAACTACCACCTACC-3'
		CD2 reverse primer (13 560-13 539): 5'-GGCTCAGGCGTTTGTGTATGAT-3'
		CD probe: (13 456-13 471): 5' FAM- ACC ATTGGC AGC CTA G -MGB 3'

paraffin-embedded tissues of HNH, HCC and adjacent noncancerous liver tissues using the QIAamp DNeasy Tissue Kit (Qiagen, Hilden, Germany). Prior to DNA extraction, a microdissection technique was used in certain cases when tumor tissues and non-tumor tissues were mixed in one sample to enrich tumor cells[20]. Five 10- μm thick sections were cut and placed into a 1.5 mL Eppendorff tube. The sections were deparaffinized twice with xylene and alcohol.

Conventional PCR detection of CD-mtDNA

In this investigation, we developed a real-time PCR protocol that reliably quantified mtDNA through amplification of different regions of the mitochondrial genomes: one just outside the CD region in cytochrome c oxidase II (MTCO2) coding region (IS), and one overlapping the CD itself (Figure 1). PCR primers for detection of CD-mtDNA were designed according to MITOMAP Human mtDNA Cambridge Sequence data (www.mitomap.org). Real-time PCR primers and fluorogenic probes for regions of WT-mtDNA (forward primer, L7878-7897; reverse primer, H7979-7958; probe, L7899-7917) and CD-mtDNA (forward primer, L8448-8472; reverse primer, H13560-13539; probe, L13456-13471) were designed with the Primer Express software (Table 1).

Conventional PCR was performed in 20 μL volume consisting of 2 μL 10×PCR buffer, 25 μmol/L of each dNTP, 2.5 U Taq polymerase, 15 pmol/L of each primer and 50 ng of DNA template. The reaction was performed in a PE2700 thermocycler (Applied Biosystem Inc., USA). PCR reaction included at 95 ℃ for 10 min, 40 cycles at 94 ℃ for 30 s, at 60 ℃ for 30 s and at 72 ℃ for 30 s. The PCR products were separated on 20 g/L agarose gels at 80 V for 60 min, visualized by ethidium bromide staining and UV light, and photographed. The results of amplification of CD-mtDNA by conventional PCR in HCC and HNH tissues are shown in Figure 2A.
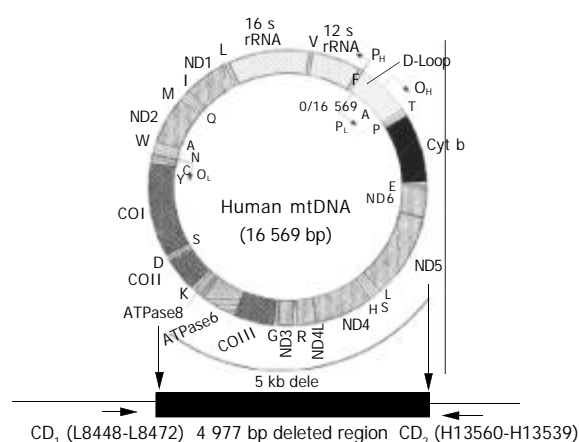

Figure 1 Human mitochondrial DNA showing the 4 997-bp deletion. The genes disrupted by the 4 997 bp deletion between nucleotide positions 8 469 and 13 447 encode four polypeptides for complex I (ND3, ND4, ND4L and ND5), one for complex IV (CO III) and two for complex V (ATP8 and ATP6), and five tRNA genes for the amino acids G, R, H, S and L. CD represent the PCR primers position that flank the common deletion region.
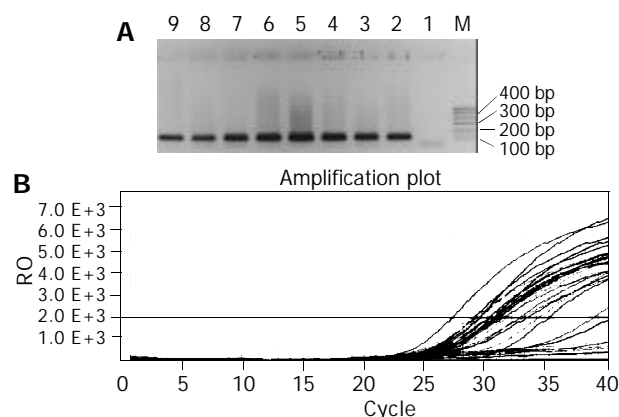

Figure 2 Detection results of CD-mtDNA in HCC. A: Conventional PCR results: Lane M, marker, Lane 1, negative control, Lane 2, positive control, Lane 3-4, nasopharygitis samples, and Lane 5-8, NPC samples; B: Real-time PCR result shows the amplification plot of fluorescence intensity against the PCR cycle. Each plot corresponds to a HCC sample. The *X* axis denotes the cycle number of a quantitative PCR reaction. The *Y* axis denotes the Rn, which is the fluorescence intensity over the background. The correlation coefficient is 0.994.

TaqMan-PCR

The principles of real-time PCR and methods for absolutely quantification of target DNA were described[18]. The quantitative TaqMan-PCR method could provide real-time measurement of target input.

Triplicate amplification reactions were performed in a 96-well microplate. Total WT-mtDNA and CD-mtDNA reactions (25 μL) each containing 100 ng DNA, 1×TaqMan Universal PCR Master Mix, 300 mmol/L of each dNTP and 300 mmol/Lof each IS or CD primer were performed. The reactions were completed by adding 100 nmol/L of the specific WT or CD probe. PCR and fluorescence analysis were performed using the ABI GeneAmp 7900HT sequence detection system (Applied Biosystems Inc., USA). Amplification conditions included at 50 ℃ for 2 min (for optimal AmpErase UNG activity), at 95 ℃ for 10 min (for deactivation of AmpErase UNG and activation of AmpliTaq Gold), then 40 cycles at 95 ℃ 15 s and at 60 ℃ for 1 min (for probe/primer hybridization and DNA synthesis).

Analysis of the reactions was carried out in an ABI PRISM 7900HT sequence detector equipped with the sequence detection software version 2.0 (PE Applied Biosystems, Foster City, USA). Absolute DNA quantification was performed using the standard curve method. Reactions were carried out with different concentrations (10^{10}, 10^9, 10^8, 10^7, 10^6, 10^5, 10^4 copies/mL) of two standard plasmids in parallel with test reactions. The standard plasmids, one carrying sequences flanking the common deletion and one carrying a unique mtDNA sequence independent of the CD, allowed the generation of two standard curves showing the number of copies of total WT-mtDNA or CD-mtDNA versus the measured CT. The CT values of samples were then converted to the number of DNA copies by comparing the sample CT to that of a known concentration of plasmid DNA.

The amount of mutation corresponded to the concentration ratio of CD-mtDNA to WT-mtDNA within each sample. If DNA was not detected within 40 cycles (CT=40), it was considered absent from a particular sample. The amplification plot CD-mtDNA detected by TaqMan PCR in HCC tissues is presented in Figure 2B.

The CD-mtDNA PCR products were sequenced using the ABI PRISM BigDye termination cycle sequencing ready reaction kit on an ABI PRISM377 sequencer (Applied Biosystem Inc., USA). Blast sequencing analysis confirmed that PCR products of the CD-mtDNA were homologous to the Cambridge version of the mtDNA sequence.

Statistical analysis

The levels of CD/MT-mtDNA ratio in different groups were compared using the Mann-Whitney rank-sum test. The chi-square test and Fisher's exact test were used to assess the difference in different groups. A P value less than 0.05 was considered statistically significant.

RESULTS

The 132 bp PCR fragment amplified from CD-mtDNA was cloned and sequenced to confirm the deletion junction created by the CD, which was characterized by the presence of one of the two 13 bp repeats that normally flanked wild-type mtDNA. Sequence comparison (Human mtDNA Cambridge Sequence data, www. mitomap.org) revealed that the common deletion region in our HCC samples was a 4 981 bp fragment extending from position 8 470 bp to 13 450 bp (Figure 3). This was a novel mtDNA deletion belonging to the 4 977 bp deletion subtype that was first reported in liver diseases.

Incidence of CD-mtDNA by conventional PCR detection

CD-mtDNA was detected by conventional PCR in 70% (19/27), 63% (17/27) and 44% (12/27) in HCC tumors, HNH tissues and HCC adjacent liver tissues, respectively. The detected rate of CD-mtDNA in HCC and HNH tumors by conventional PCR was significantly higher than that in adjacent liver tissues ($P<0.05$, chi-square test). There was no significant difference in CD-mtDNA detected rate between HCC and HNH ($P>0.05$, chi-square test).

By quantitative TaqMan-PCR, the detection rate of CD-mtDNA in HCC tumors, HNH tissues and adjacent liver tissues was 70% (19/27), 63% (17/27) and 44% (12/27), respectively. When these results were combined with those of conventional PCR, CD-mtDNA was detected in 85% (23/27) of HCC, 83% (22/27) of HNH, and 57% (15/27) of HCC paired adjacent liver tissues. The detected CD-mtDNA rate in HCC and HNH tumors was significantly higher than that in paired noncancerous liver tissues ($P<0.05$, chi-square test). (Figure 4).
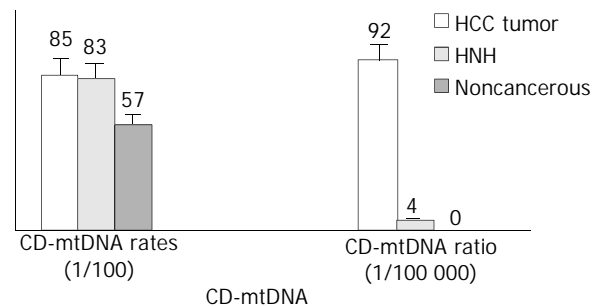

Figure 4 Correlations of CD-mtDNA with HCC and HNH. The CD-mtDNA rate in HCC and HNH lesions was significantly higher than that in paired noncancerous tissues; the CD/WT-mtDNA ratio in HCC was significant higher than that in paired noncancerous liver tissues ($P=0.02$), and was about 25 times that in HNH lesions ($P=0.02$).

CD/WT-mtDNA ratio in HCC and HNH lesions

We evaluated the relative level of CD-mtDNA by calculating the ratio of CD-mtDNA to WT-mtDNA in each sample. In this study, the CD/WT-mtDNA ratio was 0.00092 (median, interquartile range, 0.0001202-0.00105) in HCC tumor, 0.000 (median, quartile range, 0-0) in paired noncancerous liver tissues, and 0.0000374 (median, quartile range, 0-0.0004225) in HNH tissues. The CD/WT-mtDNA ratio in HCC tumor was significantly higher than that in paired noncancerous liver tissues ($P=0.002$, Mann-Whitney test), and was 25 times of that in HNH tissues ($P=0.002$, Mann-Whitney test, Figure 4). No correlation of the detected rate and the ratio of CD-mtDNA with ageing, staging, tumor size, HBV infection and differentiation of patients with HCC were found.

DISCUSSION

It has been found that human mitochondrial DNA (mtDNA) has a double-stranded circular molecule of 16 569 bp that encodes 37 genes: 2 rRNAs, 22 tRNAs and 13 polypeptides[21]. The mtDNA was present in high copy levels (10^3-10^4 copies per cell) in virtually all cells, and the vast majority of an individual's copies were identical at birth[22]. It has been generally accepted that high mutation rates of mtDNA are caused by a lack of protective histones, inefficient DNA repair systems, and continuous exposure to mutagenic effects of oxygen radicals generated by oxidative phosphorylation[23,24]. The deletion was thought to be the product of an intragenomic recombination event between two 13 bp direct repeats (positions 8 470-8 482 and 13 447-13 459) after a single-strand break caused by ultraviolet A (UVA) or ROS[25].

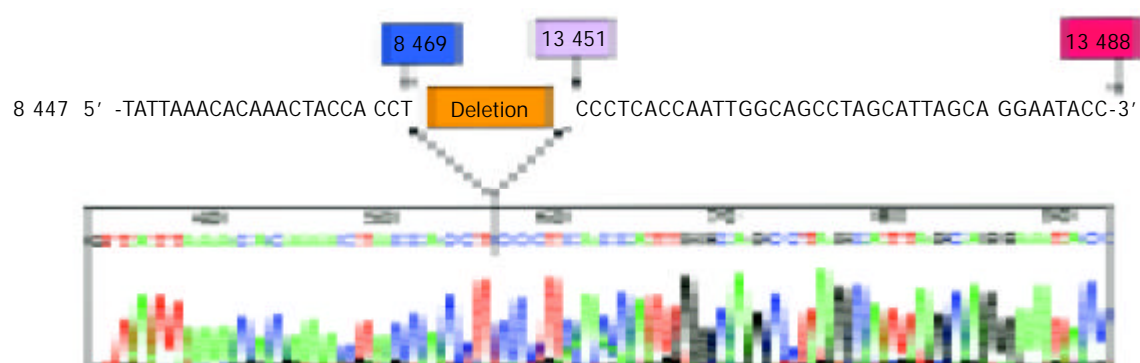Recently, somatic mutations in mitochondrial DNA (mtDNA)

Figure 3 Sequencing result of the amplified CD-mtDNA from HCC. Comparison with the MITOMAP Human mtDNA Cambridge Sequence data (www.mitomap.org), the deletion region (red bar region) is a 4981 bp deletion from position 8 470 to 13 450 of the mtDNA.

have been detected in various cancers including HCC. Mutations in the D-loop were frequent events and could be used as a molecular tool to determine clonality of HCC[26]. There are controversial reports of CD-mtDNA mutation in HCC. CD-mtDNA was reported to be detected in HCC tumors and noncancerous liver tissues, whereas lower level even no CD-mtDNA was detected in HCC tumors[27,28]. In this investigation, we detected a novel CD-mtDNA mutation (4 981 bp) in 85% HCC, which was higher than that in gastric cancer (50%)[18], but less than that in thyroid Hürthle cell tumors (100%)[17]. Moreover, we found that both the detected CD-mtDNA rate and CD/WT-mtDNA ratio in HCC were higher than those in paired noncancerous liver tissues of individuals with HCC. This result was different from previous studies. The different risk factors and different genetic background in HCC tumorigenesis between Chinese and Japanese might explain the disparity of the results. Further studies are required to determine if CD-mtDNA mutation is correlated with malignant transformation.

However, the biological impact of mtDNA deletion on HCC tumors is not entirely clear. Defects in mitochondrial function have long been suspected to contribute to the development and progression of cancer. These mutations could contribute to neoplastic transformation by changing cellular energy capacities, increasing mitochondrial oxidative stress, and/or modulating apoptosis[25]. Diaz *et al.*[29] reported that mtDNA with large deletions, but not with pathogenic point mutations, repopulated organelles significantly faster than wild-type genomes in the same cell. Under proliferating conditions, cells harboring relatively high levels of deleted mtDNAs showed a slight reduction in the mutated fraction. This was consistent with the observation that patients with mitochondrial diseases had relatively low percentages of mutated mtDNA in proliferating peripheral blood cells and fibroblasts[30]. This situation paralleled the accumulation of large-scale mtDNA deletions in postmitotic tissues, where selection based on cellular growth or survival did not take place, and abnormal organelle proliferation would lead to an increase in mtDNA replication rates[31,32]. Amuthanl[33] showed that damage to mtDNA and the mitochondrial membrane might change nuclear gene expression, leading to overexpression of genes including cathepsin L, transforming growth factor (TGFβ), and mouse melanoma antigen (MMA), which are well known markers for tumor progression. Singh[34] showed that mtDNA played an important role in cellular sensitivity to cancer therapeutic agents. Since each cell contains many mitochondria with multiple copies of mtDNAs, it is possible that wild-type and mutant mtDNA can co-exist in a state called heteroplasmy. Thus, the biological impact of a given mutation may vary, depending on the proportion of mutant mtDNAs carried by individuals.

It has been shown that mtDNA deletions accumulate with age in many tissues. However, in tumors, the CD has been associated with external factors such as radiation and cigarette smoking[35-37]. In this investigation, we found that although there was no significant difference in detected CD-mtDNA rate between HCC and paired adjacent liver tissues as well as HNH, the CD-mtDNA ratio in HCC was significantly higher than that in HNH (25-fold) and paired noncancerous liver tissues. These results suggest that CD-mtDNA mutation may be accumulated during the hepatocyte transformation. No correlation of CD-mtDNA with ageing, staging and HBV infection of the individuals with HCC and HNH was found. In this investigation, the high detected rate and high ratio of CD-mtDNA in HCC and HNH suggested that this rapid and quantitative assay of CD-mtDNA and WT-mtDNA copy number was potentially useful in a variety of molecular and evolutionary fields of HCC.

In conclusion, this is the first quantitative study of frequent occurrence of CD-mtDNA mutations in patients with HCC. This study provides further evidence that CD-mtDNA mutation might play an important role in the development and progression of HCC. Studies evaluating the CD-mtDNA mutations as a biomarker may be potentially useful for early diagnosis of HCC.

REFERENCES

1   **Tang ZY.** Hepatocellular carcinoma-cause, treatment and metastasis. *World J Gastroenterol* 2001; **7**: 445-454

2   **Shao J,** Li Y, Li H, Wu Q, Hou J, Liew C. Deletion of chromosomes 9p and 17 associated with abnormal expression of p53, p16/MTS1 and p15/MTS2 gene protein in hepatocellular carcinomas. *Chin Med J* 2000; **113**: 817-822

3   **Fujimoto Y,** Hampton LL, Wirth PJ, Wang NJ, Xie JP, Thorgeirsson SS. Alterations of tumor suppressor genes and alleilic losses in human hepatocellular carcinomas in China. *Cancer Res* 1994; **54**: 281-285

4   **Shiota G,** Kishimoto Y, Suyama A, Okubo M, Katayama S, Harada K, Ishida M, Hori K, Suou T, Kawasaki H. Prognostic significance of serum anti-p53 antibody in patients with hepatocellular carcinoma. *J Hepatol* 1997; **27**: 661-668

5   **Poon RT,** Ng IO, Lau C, Zhu LX, Yu WC, Lo CM, Fan ST, Wong J. Serum vascular endothelial growth factor predicts venous invasion in hepatocellular carcinoma: a prospective study. *Ann Surg* 2001; **233**: 227-235

6   **Niu Q,** Tang ZY, Ma ZC, Qin LX, Zhang LH. Serum vascular endothelial growth factor is a potential biomarker of metastatic recurrence after curative resection of hepatocellular carcinoma. *World J Gastroenterol* 2000; **6**: 565-568

7   **Wei Y,** Van Nhieu JT, Prigent S, Srivatanakul P, Tiollais P, Buendia MA. Altered expression of E-cadherin in hepatocellular carcinoma: correlations with genetic alterations, beta-catenin expression, and clinical features. *Hepatology* 2002; **36**: 692-701

8   **Endo K,** Ueda T, Ueyama J, Ohta T, Terada T. Immunoreactive E-cadherin , alpha-catenin, beta-catenin, and gamma-catenin proteins in hepatocellular carcinoma: relationships with tumor grade, clinicopathologic parameters, and patients' survival. *Hum Pathol* 2000; **31**: 558-565

9   **Cui J,** Zhou XD, Liu YK, Tang ZY, Zile MH. Abnormal β-catenin gene expression with invasiveness of primary hepatocellular carcinoma in China. *World J Gastroenterol* 2001; **7**: 542-546

10 **Endo K,** Terada T. Protein expression of CD44 (standard and variant isoforms) in hepatocellular carcinoma: relationships with tumor grade, clinicopathologic parameters, p53 expression, and patient survival. *J Hepatol* 2000; **32**: 78-84

11 **Jiang YF,** Yang ZH, Hu JQ. Recurrence or metastasis of HCC: predictors, early detection and experimental antiangiogenic therapy. *World J Gastroenterol* 2000; **6**: 61-65

12 **Bu W,** Huang X, Tang Z. The role of MMP-2 in the invasion and metastasis of hepatocellular carcinoma (HCC) Article in Chinese. *Zhonghua Yixue Zazhi* 1997; **77**: 661-664

13 **Fox SB,** Taylor M, Grondahl-Hansen J, Kakolyris S, Gatter KC, Harris AL. Plasminogen activator inhibitor-1 as a measure of vascular remodelling in breast cancer. *J Pathol* 2001; **195**: 236-243

14 **Green DR,** Reed JC. Mitochondria and apoptosis. *Science* 1998; **281**: 1309-1312

15 **Cavalli LR,** Liang BC. Mutagenesis, tumorigenicity, and apoptosis: are the mitochondria involved? *Mutat Res* 1998; **398**: 19-26

16 **Corral-Debrinski M,** Horton T, Lott MT, Shoffner JM, Beal MF, Wallace DC. Mitochondrial DNA deletions in human brain: regional variability and increase with advanced age. *Nat Genet* 1992; **2**: 324-329

17 **Maximo V,** Soares P, Lima J, Cameselle-Teijeiro J, Sobrinho-Simoes M. Mitochondrial DNA somatic mutations (point mutations and large deletions) and mitochondrial DNA variants in human thyroid pathology: a study with emphasis on Hurthle cell tumors. *Am J Pathol* 2002; **160**: 1857-1865

18 **Maximo V,** Soares P, Seruca R, Rocha AS, Castro P, Sobrinho-Simoes M. Microsatellite instability, mitochondrial DNA large deletions, and mitochondrial DNA mutations in gastric carcinoma. *Genes Chromosomes Cancer* 2001; **32**: 136-143

19 **Fukushima S,** Honda K, Awane M, Yamamoto E, Takeda R, Kaneko I, Tanaka A, Morimoto T, Tanaka K, Yamaoka Y. The frequency of 4977 base pair deletion of mitochondrial DNA in

various types of liver disease and in normal liver. *Hepatology* 1995; **21**: 1547-1551

20 **Moskaluk CA**, Kern SE. Microdissection and polymerase chain reaction amplification of genomic DNA from histologic tissue sections. *Am J Pathol* 1997; **150**: 1547-1552

21 **Anderson S,** Bankier AT, Barrell BG, de Bruijn MH, Coulson AR, Drouin J, Eperon IC, Nierlich DP, Roe BA, Sanger F, Schreier PH, Smith AJ, Staden R, Young IG. Sequence and organization of the human mitochondrial genome. *Nature* 1981; **290**: 457-465

22 **Lightowlers RN**, Chinnery PF, Thunball DM, Howell N. Mammalian mitochondrial genetics: heredity, heteroplasmy and disease. *Trends Genet* 1997; **13**: 450-455

23 **Wallace DC.** Diseases of the mitochondrial DNA. *Annu Rev Biochem* 1992; **61**: 1175-1212

24 **Wallace DC.** Mitochondrial genetics: a paradigm for aging and degenerative diseases? *Science* 1992; **256**: 628-632

25 **Shoffner JM,** Lott MT, Voljavec AS, Soueidan SA, Costigan DA, Wallace DC. Spontaneous Kearns-Sayre/chronic external ophthalmoplegia plus syndrome associated with a mitochondrial DNA deletion: a slip-replication model and metabolic therapy. *Proc Natl Acad Sci U S A* 1989; **86**: 7952-7956

26 **Nomoto S,** Yamashita K, Koshikawa K, Nakao A, Sidransky D. Mitochondrial D-loop mutations as clonal markers in multicentric hepatocellular carcinoma and plasma. *Clin Cancer Res* 2002; **8**: 481-487

27 **Nishikawa M,** Nishiguchi S, Shiomi S, Tamori A, Koh N, Takeda T, Kubo S, Hirohashi K, Kinoshita H, Sato E, Inoue M. Somatic mutation of mitochondrial DNA in cancerous and noncancerous liver tissue in individuals with hepatocellular carcinoma. *Cancer Res* 2001; **61**: 1843-1845

28 **Yamamoto H,** Tanaka M, Katayama M, Obayashi T, Nimura Y, Ozawa T. Significant existence of deleted mitochondrial DNA in cirrhotic liver surrounding hepatic tumor. *Biochem Biophys Res Commun* 1992; **182**: 913-920

29 **Diaz F**, Bayona-Bafaluy MP, Rana M, Mora M, Hao H, Moraes CT. Human mitochondrial DNA with large deletions repopulates organelles faster than full-length genomes under relaxed copy number control. *Nucleic Acids Res* 2002; **30**: 4626-4633

30 **Moraes CT,** DiMauro S, Zeviani M, Lombes A, Shanske S, Miranda AF, Nakase H, Bonilla E, Werneck LC, Servidei S. Mitochondrial DNA deletions in progressive external ophthalmoplegia and Kearns-Sayre syndrome. *N Engl J Med* 1989; **320**: 1293–1299

31 **Johnston W,** Karpati G, Carpenter S, Arnold D, Shoubridge EA. Late-onset mitochondrial myopathy. *Ann Neurol* 1995; **37**: 16–23

32 **Moslemi AR,** Melberg A, Holme E, Oldfors A. Clonal expansion of mitochondrial DNA with multiple deletions in autosomal dominant progressive external ophthalmoplegia. *Ann Neurol* 1996; **40**: 707–713

33 **Amuthan G**, Biswas G, Zhang SY, Klein-Szanto A, Vijayasarathy C, Avadhani NG. Mitochondria-to-nucleus stress signaling induces phenotypic changes, tumor progression and cell invasion. *EMBO J* 2001; **20**: 1910-1920

34 **Singh KK,** Russell J, Sigala B, Zhang Y, Williams J, Keshav KF. Mitochondrial DNA determines the cellular response to cancer therapeutic agents. *Oncogene* 1999; **18**: 6641-6646

35 **Kotake K,** Nonami T, Kurokawa T, Nakao A, Murakami T, Shimomura Y. Human livers with cirrhosis and hepatocellular carcinoma have less mitochondrial DNA deletion than normal human livers. *Life Sci* 1999; **64**: 1785-1791

36 **Rogounovitch TI,** Saenko VA, Shimizu-Yoshida Y, Abrosimov AY, Lushnikov EF, Roumiantsev PO, Ohtsuru A, Namba H, Tsyb AF, Yamashita S. Large deletions in mitochondrial DNA in radiation-associated human thyroid tumors. *Cancer Res* 2002; **62**: 7031-7041

37 **Ballinger SW,** Bouder TG, Davis GS, Judice SA, Nicklas JA, Albertini RJ. Mitochondrial genome damage associated with cigarette smoking. *Cancer Res* 1996; **56**: 5692-5697

Edited by Ren SY and Wang XL **Proofread by** Xu FM

• LIVER CANCER •

Expression of *cytochrome P4502E1* gene in hepatocellular carcinoma

Xiao-Bo Man, Liang Tang, Xiu-Hua Qiu, Li-Qun Yang, Hui-Fang Cao, Meng-Chao Wu, Hong-Yang Wang

Xiao-Bo Man, Liang Tang, Xiu-Hua Qiu, Hui-Fang Cao, Hong-Yang Wang, International Co-operation Laboratory on Signal Transduction, Eastern Hepatobiliary Surgery Hospital, 225 Changhai Road, Shanghai 200438, China
Li-Qun Yang, Department of Anesthesiology, Eastern Hepatobiliary Surgery Hospital, 225 Changhai Road, Shanghai 200438, China
Meng-Chao Wu, Department of Clinical Surgery, Eastern Hepatobiliary Surgery Hospital, 225 Changhai Road, Shanghai 200438, China
Correspondence to: Dr. Hong-Yang Wang, International Co-operation Laboratory on Signal Transduction, Eastern Hepatobiliary Surgery Hospital, 225 Changhai Road, Shanghai 200438, China. hywangk@online.sh.cn
Telephone: +86-21-25070856   **Fax:** +86-21-65566851
Received: 2003-06-10   **Accepted:** 2003-08-16

Abstract

AIM: To investigate *cytpchrome P4502E1* (*CYP2E1)* gene expression in occurrence and progression of hepatocellular carcinoma (HCC).

METHODS: The human liver arrayed library was spotted onto the nylon membranes to make cDNA array. Hybridization of cDNA array was performed with labeled probes synthesized from RNA isolated from HCC and adjacent liver tissues. Sprague-Dawley rats were administrated diethylnitrosamine (DENA) to induce HCC. *CYP2E1* expression was detected by the method of RT-PCR and Northern blot analysis.

RESULTS: *CYP2E1* was found by cDNA array hybridization to express differently between HCC and liver tissues. *CYP2E1* only expressed in liver, but did not express in HCC tissues and expressed lowly in cirrhotic tissues. In the progression of cirrhosis and HCC, the expression level of *CYP2E1* was gradually decreased and hardly detected until the late stage of HCC.

CONCLUSION: Using arrayed library to make cDNA arrays is an effective method to find differential expression genes. *CYP2E1* is a unique gene expressing in liver but did not express in HCC. *CYP2E1* expression descended along with the initiation and progression of HCC, which is noteworthy further investigations in its significance in the development of HCC.

INTRODUCTION

Hepatocellular carcinoma (HCC) is one of the most common cancers in China and the world[1,2]. Although the wide use of diagnostic technology and the improvement in curative treatment may evolve to a better scenario, it still represents more than 5% of all cancers[3]. To investigate HCC associated genes is very helpful to elucidating the molecular mechanism of proliferation, differentiation and transformation of hepatocytes in the occurrence and development of HCC[4,5]. cDNA microarray analysis is a powerful technique in the investigation of cancer associated gene identification and function[6]. The gene expression can be simultaneously monitored in a large scale with cDNA microarray[7]. The potential analysis of the expression of thousands of genes in one experiment provided new insights into the molecular study of the occurrence and development of HCC[8-10].

In the present study, a method of making cDNA array from the arrayed library was developed to identify the differentially expressed genes. *CYP2E1*, the gene encoding cytochrome P450 2E1 (CYP2E1), a member of cytochrome P450s present in prokaryotes and through the eukaryotes[11], was identified to express in normal liver or cirrhotic tissues adjacent to tumors but not express in HCC tissues. CYP2E1 is one of the important members of cytochrome P450 superfamily, with functions ranging from catalysis of the conversion of ethanol to acetaldehyde and from acetate to metabolization of many exotic drugs and procarcinogens[12]. A rat HCC model was then induced to study *CYP2E1* expression in the procession of HCC. The results showed that *CYP2E1* expression descended along with the initiation, promotion and progression of HCC. It is suggested that *CYP2E1* is correlated to HCC and noteworthy further investigations for its significance in the development of HCC.

MATERIALS AND METHODS

Arrayed library preparation
The human liver cDNA library (Invitrogen, USA) was cultured on the agar plate and were picked into 96-well microplates with 200 μL culture medium. After an overnight culture, 1 μL of the bacterial medium in each well was diluted into 20 μL from which 1 μL was transferred to the corresponding 96-well PCR microplates and the remaining was added to 50 μL glycerol and stored at -80 ℃.

PCR amplification of plasmids
PCR reaction was carried out with oligonucleotide T7 (5' gga aga agg gaa ctg att cag 3') and oligonucleotide BGHR (5' cac atc cag atc ata tgc cag 3') as forward primer and reverse primer. The procedure of PCR was made with denaturing at 94 ℃ for 4 min followed by 35 cycles of reaction including denaturing at 94 ℃ for 50 s, annealing at 58 ℃ for 50 s and elongation at 72 ℃ for 90 s, and a final bonus extension elongation at 72 ℃ for 7 min. The amplified products were randomly selected for electrophoresis to validate PCR efficiency.

DNA arrays preparation
The PCR products in the microplates were spotted with TAS (BioRobotics, UK) onto the 8 cm×12 cm nylon membrane to form 2×2×96 array in each membrane. The 0.7 mm diameter 96-pin spotting setting was used. Each product from a well was spotted onto the same position 3 times. The membranes were denatured immediately in the denature buffer (1.5 mol/L

NaCl, 0.5 mol/L NaOH) for 5 min and then equalized in the equalizing buffer (0.9 mol/L NaCl, 0.5 mol/L Tris, pH7.5) for 5 min followed by baking at 80 ℃.

DENA-induced HCC in rats

DENA (Sigma, USA) was diluted into 1×10^{-4} concentration in drinkable water. Male Sprague-Dawley rats were obtained from the Experimental Animal Center of Chinese Academy of Sciences, Shanghai. The rats in HCC group were administrated DENA via drinking DENA-diluted water while the rats in control group drank clean water. Three HCC-induced rats and one control rat were sacrificed by decollation under pentobarbital anesthesia every week. The liver tissue was immediately stored in liquid nitrogen for RNA isolation and fixed for histological analysis.

Total RNA and mRNA isolation

Total RNA was isolated from 0.1 g frozen tissues in 1 mL Trizol™ reagent (Invitrogen, USA) according to the manufacturer' s instructions. Isolation of mRNA was carried out with the Oligotex™mRNA Mini kit (Qiagen, Germany) from 250 µg total RNA.

Labeling of cDNA from mRNA of HCC tissues

Probes for the array hybridization were labeled with Atlas™ SpotLight™labeling kit (Clontech, USA) according to the user' s manual. A 2 µg mRNA respectively from paired HCC tumor and adjacent normal or cirrhotic tissues was added with 2.5 µL CDS Primer Mix and incubated at 70 ℃ for 10 min. Reaction buffer (5×) 5 µL, Labeling Mix (10×) 2.5 µL, DTT (100 mmol/L) 1.25 µL were added and incubated at 48 ℃ for 5 min. PowerScript reverse transcriptase (1.25 µL) per reaction and 10 mL of Master Mix were added and incubated at 48 ℃ for an additional 45 min. The reaction was stopped by adding 0.5 mL of 0.5 mol/L EDTA (pH8.0) and then purified routinely.

Hybridization of DNA array

DNA array hybridization and detection were preceded with SpotLight™chemiluminescent hybridization & detection kit (Clontech, USA). The array membranes were wetted and pre-hybridized while a biotinylated array probe was denatured. Cot-1 and the biotinylated probe were added to pre-hybridization solution to incubate overnight. The membranes were washed and blocked, and added with enough stabilized Streptavidin-HRP conjugate. After equilibrated, the membranes were covered with the luminol/peroxide working solution and incubated at room temperature for 5 min and exposed the membrane to film for an appropriate time to obtain desired signals.

RT-PCR of CYP2E1 in rats

First strand cDNA was reversibly transcribed from total RNA with SuperScript™II reverse transcriptase (Invitrogen, USA). The procedure of RT-PCR of CYP2E1 was carried out in normal rat tissues with the oligonucleotide (5' act tct acc tgc tga gca c 3') and oligonucleotide (5' ttc agg tct cat gaa cgg g 3') as forward and reverse primer respectively and with denaturing at 94 ℃ for 4 min followed by 33 cycles of reaction including denaturing at 94 ℃ for 50 s, annealing at 55 ℃ for 50 s and extension at 72 ℃ for 1 min, and a final bonus extension for 7 min. An 874-bp sequence product was amplified.

Cloning of rat CYP2E1

The PCR product was purified using the QIAquick PCR purification kit (Qiagen, Germany) and cloned into the T-vector (Promega, USA) directly and transfected into DH5-alpha bacteria. The plasmid was purified to be sequenced and confirmed according to the GenBank sequence.

Northern blot analysis

The plasmid was digested and electrophoresed. The template fragment was purified from agarose gel using the gel extracting kit (Qiagen, Germany). The probe was labeled from 25 ng template DNA by the random primer method using DNA polymerase I large (Klenow) fragment (Promega, USA) with $\alpha\text{-}^{32}$p-dCTP followed by purification using the QIAquick purification kit (Qiagen, Germany). Total RNA (40 µg) justified by 28 s and 18 s intensity of each sample, was loaded. Electrophoresis was carried out under denaturing conditions and RNA was transferred onto nitrocellulose membrane and cross-linked by baking at 80 ℃ for 2 h. The filters were then prehybridized, hybridized, and washed under high stringency conditions. All blots were screened by Fuji BAS2000 and analyzed by LABwork software and then exposed at -80 ℃ to Kodak X-ray film for 2 wk.

RESULTS

Identification of CYP2E1 as an HCC-silent gene with cDNA array gene expression profile analysis

The arrayed library clones were spotted onto each nylon membrane to 2×2×96 array from 4 microplates. There were 96 subarrays in one membrane. The arrayed membranes were denatured, fixed and preserved under dry condition. The mRNA from HCC tissues and corresponding adjacent liver tissues was labeled to hybridize to the above arrayed membranes. A spot then identified low signals in HCC tissues but high signals in corresponding adjacent liver tissues (Figure 1). It was suggested that the gene was a liver-expressing gene that was downregulated in HCC tissues. According to the position of the spot in membrane, the clones in microplates of arrayed library was recruited and sequenced as CYP2E1.
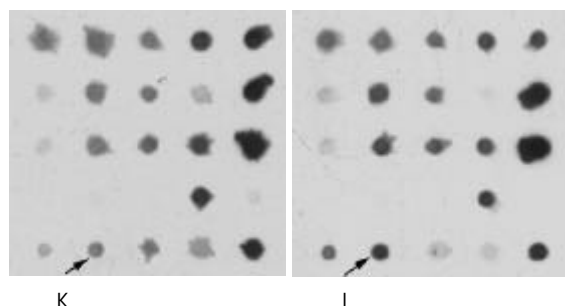

Figure 1 Differential expression profile of cDNA array hybridization result. Part of the membrane is displayed. The clones the arrows point represent CYP2E1. K: HCC tissue, L: adjacent liver tissue.

HCC model of DENA-induced rats

The liver tissue from DENA-induced rats that were killed after 3 wk appeared almost normal as the control rats. The pathological examination indicated the liver lesion in these rats. The livers of rats after the 4th wk were smaller than those of control rats and the color of the liver surface was much dingy. Cirrhotic nodi could be seen on the liver surface of rats killed in the 7th wk and cirrhosis could be detected as early as in the 5th wk by pathological examination. There were few liver cancer nodi in 1 rat detected in the 9th wk. So the 9th wk might be the boundary between cirrhosis and HCC in the present study. In the 10th wk, HCC could be detected in all rats and HCC nodi could be seen by naked eyes after the 10th wk. After the 16th wk, HCC nodi were spread almost all over the rat liver.

CYP2E1 expression in normal tissues

Twelve types of human normal tissues except liver were used

for Northern blot analysis of *CYP2E1* expression. *CYP2E1* did not express at all in the 12 normal human tissues. To represent the expression level of *CYP2E1* in these organs, the RNA sample of heart, brain, lung, intestine and liver were selected with 2 cases of HCC tissues and 1 case of kidney cancer tissue to be transferred onto one membrane for Northern blot analysis. The hybridization result showed that *CYP2E1* indeed only expressed in non-tumor liver tissues (Figure 2). The expression pattern of *CYP2E1* in rats was the same as in human. By RT-PCR analysis, it was indicated that *CYP2E1* was only amplified from normal liver tissues and did not express in other tissues (Figure 3).
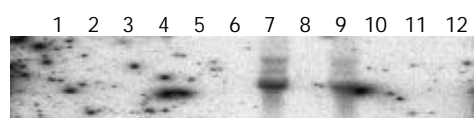

Figure 2 *CYP2E1* expression in normal human organs and HCC tissues detected by Northern blot analysis. 1: heart, 2: brain, 3: muscle, 4: intestine, 5: stomach, 6: lung, 7: liver tissues adjacent to HCC, 8: HCC, 9: liver tissues adjacent to HCC, 10: HCC, 11: renal tissues adjacent to carcinoma, 12: renal carcinoma.
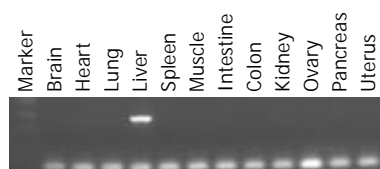

Figure 3 *CYP2E1* expression in normal organs of rat detected by RT-PCR analysis.
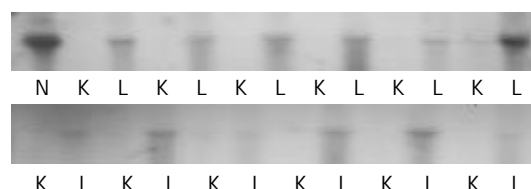

Figure 4 *CYP2E1* expression in human HCC tissues detected by Northern blot analysis. N: normal liver, K: HCC, L: liver tissue adjacent to HCC.
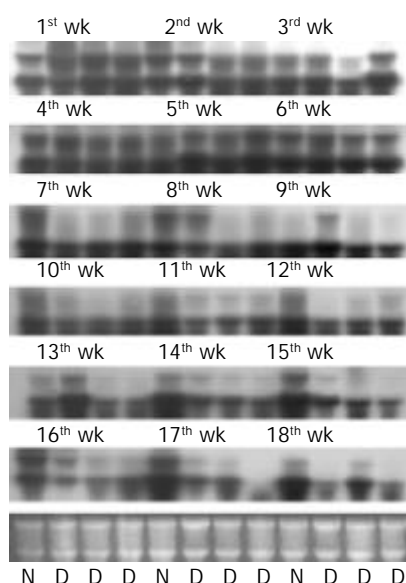

Figure 5 *CYP2E1* expression in occurrence and development of rat HCC detected by Northern blot analysis. There were 12

lanes in one membrane including specimen of 3 wk. Ribosomal RNA of 28 s and 18 s as control was in the bottom. N: normal control group, D: DENA-induced group.

CYP2E1 expression in HCC

Northern blot analysis showed that *CYP2E1* expressed in normal liver tissues and adjacent tissues with cirrhosis. There was no hybridization signal in HCC tissues from all 14 cases. *CYP2E1* was significantly downregulated in HCC (Figure 4). The rat HCC model simulated the progression of HCC. The change of expression was analyzed also by Northern blot (Figure 5). In the early liver lesion stage of the DENA-induced rats after 1-3 wk, *CYP2E1* expression was slightly upregulated compared with normal livers. But after 4 wk, the gene was down-regulated and when cirrhosis occurred after 5 wk, the expression level was almost the same in the liver between the 2 groups. It was obvious that the cirrhotic tissues of the rats expressed at lower level than the normal livers after 7 wk. When the DENA-induced rats progressed to the stage of tumor from the 10th wk, *CYP2E1* expressed at much lower level than normal livers and liver of cirrhotic stages. Until the very later stage of HCC, the expression level was very low and the hybridization signal was hardly detected.

DISCUSSION

An ideal support allowed effective immobilization of probe onto its surface, and robust hybridization of target with the probe[13]. Nylon membrane, as a standard support used for making microarrays[14,15] could hold more DNA. The hybridization and detection of membranes arrays cost much less. Here we used the nylon membranes as the matrix of cDNA arrays. The DNA on the membranes was denatured before cross-linking to the matrix by baking the array at 80 ℃. In many cases, the cDNA targets were chosen directly from cDNAs library of interest for DNA microarray manufacturing[16]. The collection should include an aggregation of gene clones as many as possible. On the other hand, for certain purpose of an investigation, most genes on a large content array might not be necessary. The method to make cDNA microarray in this study arose from the concept of arrayed library. The cDNA plasmid library was transferred to the microplates to be the arrayed library, which was copied to the nylon membranes to make the DNA arrays after PCR amplification. Because most genes on the arrays did not differently express between samples, the tumor and normal tissues, for example, the sequencing expense of these genes could be saved. It was after the array hybridization, the genes that were detected to express differently would be selected from the arrayed library and were sequenced for further studies. In this study, most genes showed no differential expression between HCC and adjacent liver tissues. Only the differently expressed genes were sequenced for further investigations. *CYP2E1* was identified as a liver profound but HCC silent gene.

P450 enzymes were found in almost all eukaryotes and prokaryotes[17]. CYP2E1 enzyme had a molecular weight of 57 KD and the encoding gene was located on chromosome 10 spanning 11 413 base pairs[18,19]. *CYP2E1* was found to play an important role in its polymorphism during tumor occurrence. The significance of this polymorphism currently unclear[20,21]. To date, the results in possible associations between *CYP2E1* genetic polymorphisms and alcoholic liver disease susceptibility have been varied and often contradictory[22]. Because hepatic CYP2E1 has been shown to activate various carcinogens, there has been interest in whether certain *CYP2E1* polymorphisms might predispose to liver cancer[23,24]. It was demonstrated that possession of the less common *Rsa* I/*Pst* I allele was associated with increased susceptibility to HCC[25].

Although CYP2E1 was said to be located in most tissues with the largest concentration in the liver, it was constitutively expressed in the liver and only induced to express in other tissues by treatment with acetone, ethanol, isoniazid and other compounds, many of which are substrates for the enzyme[26-28]. This study showed that *CYP2E1* expressed only in the liver but did not express in the other normal organs in human and rats. So it could be concluded that *CYP2E1* is the liver-specific functional gene. Furthermore, *CYP2E1* was found to loose expression in HCC. Northern blot analysis was performed to validate the result of chip experiment. *CYP2E1* expressed at a high level in normal or cirrhotic tissues but was silent in HCC tissues from 14 cases of HCC. So *CYP2E1* did not express in HCC. To further understand the expression of *CYP2E1* in the initiation, promotion and progression of HCC, the DENA-induced rat HCC model was made to study the role of *CYP2E1* in the process of HCC. The development of rat HCC underwent the progression of liver lesion and cirrhosis until the tumor occurrence. The results showed that at the early stage of the rat model the expression level of *CYP2E1* in the liver lesion tissues was slightly higher than that in normal rat liver in the first to third week. Because CYP2E1 was involved in the metabolism of nitrosamines, DENA might induce *CYP2E1* expression. But along with the aggravation of liver lesion and development of cirrhosis, the expression level of *CYP2E1* was gradually descended. After the progressing stage of HCC, *CYP2E1* did not express as in human HCC. There were very low signals because at the late stages of HCC the tumor were grown sporadically and the samples were intermixed with cirrhotic tissues where *CYP2E1* still expressed. The expression pattern of *CYP2E1* in the HCC was worth of further studies. It is suggested that these differential expression might help further understand the molecular genetic and gene regulation mechanism of HCC progression. Because *CYP2E1* does not express in HCC cells, there might be a guided biological treatment for HCC with its potential substrate.

REFERENCES

1   **Qin LX**, Tang ZY. The prognostic significance of clinical and pathological features in hepatocellular carcinoma. *World J Gastroenterol* 2002; **8**: 193-199
2   **Ince N,** Wands JR. The increasing incidence of hepatocellular carcinoma. *N Engl J Med* 1999; **340**: 798-799
3   **Llovet JM**, Beaugrand M. Hepatocellular carcinoma: present status and future prospects. *J Hepatol* 2003; **38**(Suppl 1): S136-S149
4   **Thorgeirsson SS**, Grisham JW. Molecular pathogenesis of human hepatocellular carcinoma. *Nat Genet* 2002; **31**: 339-346
5   **Tannapfel A**, Wittekind C. Genes involved in hepatocellular carcinoma: deregulation in cell cycling and apoptosis. *Virchows Arch* 2002; **440**: 345-352
6   **Berns A**. Gene expression in diagnosis. *Nature* 2000; **403**: 491-492
7   **Young RA**. Biomedical discovery with DNA arrays. *Cell* 2000; **102**: 9-15
8   **Chen X**, Cheung ST, So S, Fan ST, Barry C, Higgins J, Lai KM, Ji J, Dudoit S, Ng IO, Van De Rijn M, Botstein D, Brown PO. Gene expression patterns in human liver cancers. *Mol Biol Cell* 2002; **13**: 1929-1939
9   **Delpuech O**, Trabut JB, Carnot F, Feuillard J, Brechot C, Kremsdorf DR. Identification, using cDNA macroarray analysis, of distinct gene expression profiles associated with pathological and virological features of hepatocellular carcinoma. *Oncogene* 2002; **21**: 2926-2937
10   **Lee JS**, Thorgeirsson SS. Functional and genomic implications of global gene expression profiles in cell lines from human hepatocellular cancer. *Hepatology* 2002; **35**: 1134-1143
11   **Peterson JA**, Graham SE. A close family resemblance: the importance of structure in understanding cytochromes P450. *Structure* 1998; **6**: 1079-1085
12   **Tanaka E**, Terada M, Misawa S. Cytochrome P450 2E1: its clinical and toxicological role. *J Clin Pharm Ther* 2000; **25**: 165-175
13   **Southern E**, Mir K, Shchepinov M. Molecular interactions on microarrays. *Nat Genet* 1999; **21**(Suppl): 5-9
14   **Schlaak JF**, Hilkens CM, Costa-Pereira AP, Strobl B, Aberger F, Frischauf AM, Kerr IM. Cell-type and donor-specific transcriptional responses to interferon-alpha. Use of customized gene arrays. *J Biol Chem* 2002; **277**: 49428-49437
15   **Mochii M**, Yoshida S, Morita K, Kohara Y, Ueno N. Identification of transforming growth factor-beta- regulated genes in caenorhabditis elegans by differential hybridization of arrayed cDNAs. *Proc Natl Acad Sci U S A* 1999; **96**: 15020-15025
16   **Cheung VG**, Morley M, Aguilar F, Massimi A, Kucherlapati R, Childs G. Making and reading microarrays. *Nat Genet* 1999; **21** (1 Suppl): 15-19
17   **Nelson DR,** Koymans L, Kamataki T, Stegeman JJ, Feyereisen R, Waxman DJ, Waterman MR, Gotoh O, Coon MJ, Estabrook RW, Gunsalus IC, Nebert DW. P450 superfamily: update on new sequences, gene mapping, accession numbers and nomenclature. *Pharmacogenetics* 1996; **6**: 1-42
18   **Umeno M**, McBride OW, Yang CS, Gelboin HV, Gonzalez FJ. Human ethanol-inducible P450IIE1: complete gene sequence, promoter characterization, chromosome mapping, and cDNA-directed expression. *Biochemistry* 1988; **27**: 9006-9013
19   **Umeno M**, Song BJ, Kozak C, Gelboin HV, Gonzalez FJ. The rat P450IIE1 gene: complete intron and exon sequence, chromosome mapping, and correlation of developmental expression with specific 5' cytosine demethylation. *J Biol Chem* 1988; **263**: 4956–4962
20   **Tsutsumi M**, Takada A, Wang JS. Genetic polymorphisms of cytochrome P4502E1 related to the development of alcoholic liver disease. *Gastroenterology* 1994; **107**: 1430-1435
21   **Ueshima Y**, Tsutsumi M, Takase S, Matsuda Y, Kawahara H. Acetaminophen metabolism in patients with different cytochrome P-4502E1 genotypes. *Alcohol Clin Exp Res* 1996; **20**(1 Suppl): 25A–28A
22   **Wong NA**, Rae F, Simpson KJ, Murray GD, Harrison DJ. Genetic polymorphisms of cytochrome p4502E1 and susceptibility to alcoholic liver disease and hepatocellular carcinoma in a white population: a study and literature review, including meta-analysis. *Mol Pathol* 2000; **53**: 88-93
23   **Chen CJ**, Yu MW, Liaw YF. Epidemiological characteristics and risk factors of hepatocellular carcinoma. *J Gastroenterol Hepatol* 1997; **12**: S294-308
24   **Yu MW**, Gladek-Yarborough A, Chiamprasert S, Santella RM, Liaw YF, Chen CJ. Cytochrome p4502E1 and glutathione S-transferase M1 polymorphisms and susceptibility to hepatocellular carcinoma. *Gastroenterology* 1995; **109**: 1266-1273
25   **Ladero JM**, Agundez JA, Rodriguez-Lescure A, Diaz-Rubio M, Benitez J. RsaI polymorphism at the cytochrome P4502E1 locus and risk of hepatocellular carcinoma. *Gut* 1996; **39**: 330-333
26   **Rumack BH**. Acetaminophen hepatotoxicity: the first 35 years. *J Toxicol Clin Toxicol* 2002; **40**: 3-20
27   **Johansson I**, Eliasson E, Norsten C, Ingelman-Sundberg M. Hydroxylation of acetone by ethanol-and acetone-inducible cytochrome P-450 in liver microsomes and reconstituted membranes. *FEBS Lett* 1986; **196**: 59-64
28   **Nakajima T**, Elovaara E, Park SS, Gelboin HV, Hietanen E, Vainio H. Immunochemical characterization of cytochrome P-450 isozymes responsible for benzene oxidation in the rat liver. *Carcinogenesis* 1989; **10**: 1713-1717

• COLORECTAL CANCER •

Constitutive activation of Stat3 signaling pathway in human colorectal carcinoma

Xiang-Tao Ma, Shan Wang, Ying-Jiang Ye, Ru-Yu Du, Zhi-Rong Cui, Ma Somsouk

Xiang-Tao Ma, Shan Wang, Ying-Jiang Ye, Ru-Yu Du, Department of Surgery, Peking University People's Hospital, Beijing 100044, China
Zhi-Rong Cui, Division of Surgical Oncology, Peking University People's Hospital, Beijing 100044, China
Ma Somsouk, Gastrointestinal Unit, Department of Medicine, Massachusetts General Hospital, Harvard Medical School, 32 Fruit Street, Boston, MA 02114, USA
Supported by the National Natural Science Foundation of China, No. 30271269
Correspondence to: Dr. Shan Wang, Department of Surgery, Peking University People's Hospital, Beijing 100044,
China. shwang60@sina.com
Telephone: +86-10-68792772   **Fax:** +86-10-68318386
Received: 2003-10-24   **Accepted:** 2003-12-08

Abstract

AIM: Signal transducers and activators of transcription (STATs) are a family of transcription factors activated in response to cytokines and growth factors. Constitutive activation of Stat3 has been observed in a growing number of tumor-derived cell lines, as well as tumor specimens from human cancers. The purpose of this study was to investigate the expression of p-Stat3, activated form of Stat3, and its downstream mediators including cyclin D1 and Bcl-x_L in colorectal carcinoma (CRC), and to explore the possible mechanism of Stat3 signaling pathway in the tumorigenesis of colorectal carcinoma.

METHODS: Tissue samples from 45 patients of primary colorectal carcinoma were selected for studying Stat3 signaling pathway protein expression. Western blot analysis was used to measure the expression of p-Stat3, cyclin D1, and Bcl-x_L proteins in colorectal carcinomas. Furthermore, the expression patterns of these proteins were analyzed for their distribution at the cellular level by immunohistochemical staining of the tissues.

RESULTS: Protein levels of p-Stat3, cyclin D1, and Bcl-x_L were increased in colorectal carcinomas compared with adjacent normal mucosae ($P < 0.05$). Elevated levels of p-Stat3 were correlated with the nodal metastasis and the stage ($P < 0.05$). Overexpression of cyclin D1 was associated with the nodal metastasis ($P < 0.05$). There was also a significant correlation between the expressions of p-Stat3 and cyclin D1 ($r = 0.382$, $P < 0.05$).

CONCLUSION: Constitutive activation of Stat3 may play an important role in the tumorigenesis of colorectal carcinoma, and the detailed mechanism of Stat3 signaling pathway in CRC deserves further investigation.

INTRODUCTION

Colorectal carcinoma (CRC) is a very common malignancy in developed countries and the incidence of CRC has been increasing rapidly in the latter part of the twentieth century in urban China[1,2]. Although there have been advances in surgical and cytotoxic treatments of colorectal carcinoma, the overall survival percentage has not changed in recent years. While significant progresses have been achieved in identifying oncogenes and tumor suppressor genes involved in the tumorigenesis of colorectal carcinoma, the molecular mechanisms in colorectal carcinoma are still poorly understood. Recently, with the delineation of important signal transduction cascades, it has become clear that the signal transducers and activators of transcription (STATs) signaling pathway may play an important role in the malignant transformation of a number of human malignancies[3].

STATs are transcription factors activated in response to cytokines and growth factors. At present, seven STATs have been identified in mammals: Stat1, Stat2, Stat3, Stat4, Stat5a, Stat5 b, and Stat6. Stat5 a and Stat5 b are encoded by distinct genes whereas Stat1 and Stat3 exhibit two isoforms, each resulting from alternative splicing[4]. These proteins have a conserved structural organization and range in size from 750 to 900 amino acids. Activated STATs rapidly translocate into nuclei, bind to recognition sequences in the promoter region of target genes, and regulate their transcription. Recent studies have demonstrated the essential roles of STATs proteins in modulating the process of cell proliferation, differentiation, and apoptosis[5-7].

Constitutively activated STAT proteins have been observed in a wide variety of human tumor cell lines and primary tumors including leukemia, multiple myeloma, breast cancer, prostate cancer, and other cancers[8-13]. Further investigation demonstrated that activation of Stat3 was associated with the transformation by v-Src and other viral oncoproteins[13-15]. Stat3 has been classified as an oncogene because constitutively activated Stat3 was found to mediate oncogenic transformation in cultured cells and tumor formation in nude mice[16,17]. Stat3 activation may not only provide a growth advantage, but also confer resistance to conventional therapies that rely on the mechanism of apoptosis to eliminate tumor cells[18]. The events downstream from constitutive activation of Stat3 that promote tumorigenesis are unclear but could include deregulation of cell cycle progression and/or providing protection against apoptosis. Recent studies showed that constitutive activation of Stat3 correlated with cyclin D1 expression and might provide a prognostic marker in head and neck cancer[19], and activated Stat3 contributed to the process of apoptosis in ovarian cancer cells by regulating the expression of Bcl-x_L[20]. These findings suggest that constitutive activation of Stat3 participates in the development of different human malignancies. However, the expression and activation of Stat3 protein in human colorectal carcinomas have not been studied. It is important to know whether or not constitutive activation of Stat3 signaling pathway plays a central role in human colorectal carcinomas.

In the present study, we examined the expression of p-Stat3, the activated form of Stat3, cyclin D1, and Bcl-x_L in 45 primary

tumor samples obtained from patients with CRC. Our results demonstrate that constitutive activation of Stat3 signaling pathway may play an important role in the tumorigenesis of colorectal carcinoma. Furthermore, activation of Stat3 is correlated with the overexpression of cyclin D1 in colorectal carcinoma.

MATERIALS AND METHODS

Materials

PVDF membranes for Western blot analysis were purchased from Millipore (Bedford, MA), and x-ray film was from Eastman Kodak (Rochester, NY). All antibodies were from Santa Cruz Biotechnology (Santa Cruz, CA). Prestained molecular mass markers were from GIBCO/BRL (Grand Island, NY). The enhanced chemiluminescence (ECL) system for Western blot analysis was from Amersham (Arlington Heights, IL). Concentrated protein assay dye reagents were from Bio-Rad Laboratories (Hercules, CA). All other reagents were of molecular biology grade and were purchased from either Sigma (St. Louis, MO) or Amresco (Solon, OH).

Patients and tissue samples

Primary colorectal adenocarcinomas and adjacent normal mucosae distant from the tumor (5-10 cm away) were obtained from 45 patients undergoing colorectal cancer resection at the Department of Surgery, Peking University People's Hospital from February, 1999 to February, 2000. No patient had received chemotherapy or radiation therapy before surgery. The samples were collected after informed consent was obtained from the patients at the time of surgery. Malignant tissues and adjacent normal mucosae were immediately snap-frozen in liquid nitrogen within 15-20 min after surgical removal to ensure preservation of Stat3 activities. Detailed clinicopathological parameters including gender, age, site of primary tumor, stage, and degree of differentiation are shown in Table 1. Staging of the tumors was conducted according to the American Joint Committee on Cancer (AJCC)/International Union Against Cancer (UICC) TNM Classification after brief histological studies.

Table 1 Clinicopathological parameters of 45 patients with colorectal carcinoma

Clinicopathological parameters		Numbers (%)
Gender	Male	24 (53.3)
	Female	21 (46.7)
Age (yr)	Range	35-81
	Mean	61.7
	Median	66.0
Primary site	Colon	25 (55.6)
	Rectum	20 (44.4)
	I	1 (0.22)
	II	24 (53.3)
	III	14 (31.1)
	IV	6 (13.3)
Depth of invasion and	T1-T2 N0	7 (15.6)
Lymph node involvement	T3-T4 N0	18 (40.0)
	T1-T2 N1-2N2	12 (26.7)
	T3-T4 N1-N2	8 (17.8)
Distant Metastasis	M0	39 (86.7)
	M1	6 (13.3)
Histological grade	G1	12 (26.7)
	G2	22 (48.9)
	G3	11 (24.4)
Tumor size	>5 cm	22 (48.9)
	$\leqslant$5 cm	23 (51.1)

T1: tumor invades the submucosa; T2: tumor invades the mus-cularis propria; T3: tumor invades through the muscularis propria into the subserosa or perirectal tissues; T4: tumor directly invades other organs or structures and/or perforates visceral peritoneum; N0: no regional lymph node metastasis; N1: metastasis in one to three regional lymph nodes; N2: metastasis in four or more regional lymph nodes; M0: no distant metastasis; M1: distant metastasis; G1: well differentiated tumor; G2: moderately differentiated tumor; G3: poorly differentiated tumor.

Western blot analysis

Tissues were lysed with lysis buffer (150 mmol/L NaCl, 10 g/L sodium deoxycholate, 10 g/L Triniton X-100, 1 g/LSDS, 10 mmol/L Tris, pH 7.2, 1 mmol/L $Na_3 VO_4$, 1 mmol/L phenylmethylsulfonyl fluoride, 1 mmol/L NaF, 0.1 mmol/L aprotinin, and 1 mmol/L leupeptin). After centrifugation at 13 000 g for 30 min at 4 ℃, the protein concentrations in the cell lysates were determined by the Bradford assay. For Western blot analysis, whole cell extracts were mixed with 2×sodium dodcyl sulfate (SDS) sample buffer (125 mmol/L Tris· HCl, pH 6.8, 40 g/L SDS, 200 mL/L glycerol, 100 mL/L 2-mercaptoethanol) at 1:1 ratio and were heated for 5 min at 100 ℃. Proteins (50 μg/lane) were separated by electrophoresis on 7.5-10% gradient SDS-polyacrylamide gel and transferred onto a PVDF membrane. Prestained molecular weight markers were included in each gel. Membranes were blocked for 30 min in Tris-buffered saline (TBS: 10 mmol/L Tris· HCl, pH 7.5 and 150 mmol/L NaCl) with 5 g/L Tween-20 (TBST) and 50 g/L BSA. After blocking, membranes were incubated at 4 ℃ overnight with Stat3 (C-20) phospho-independent, phospho-specific (Tyr-705) p-Stat3 (B-7); cyclin D1 (M-20), and Bcl-x_L (H-62) antibody in TBST and 10 g/L BSA respectively. Additionally, anti-glyceraldehydes-3-phosphate dehydrogenase (GAPDH) antibody was used to determine the amount of endogenous GAPDH protein to serve as an internal control. After the membranes were washed three times with TBST (5 min each), they were incubated with horseradish peroxidase-conjugated secondary antibody in TBST and 10 g/L BSA for 30 min. Subsequently, membranes were washed three times with TBST and developed by using the enhanced chemiluminescence (ECL) detection system. The optical density (OD) was measured by densitometry using a Storm PhosphoImager (Molecular Dynamics, Sunnyvale, CA) and the result was shown as relative expression for tumor (T) versus normal mucosae (N).

Immunohistochemical staining

Tissue samples were fixed in 40 g/L buffered formaldehyde, and embedded in paraffin. Five-micrometer sections of normal mucosa and colorectal carcinoma were cut and mounted onto poly-L-lysine-coated glass slides, air-dried, and heated for 2 h at 60 ℃ in an oven. The sections were dewaxed in xylene, rehydrated in descending alcohols, and endogenous peroxidase activity was blocked using 3 mL/L H_2O_2-methanol solution. These sections were then subjected to an antigen retrieval procedure; slides were heated in citrate buffer 10 mmol/L (pH 6.0) for 10 min. The sections were then cooled and washed in phosphate-buffered saline (pH 7.4) and nonspecific binding sites were blocked by incubating with 50 mL/L goat serum for 30 min in a humidified chamber at room temperature. The slides were incubated at 4 ℃ overnight with appropriate primary antibody [Stat3 (C-20), dilution 1:75; p-Stat3 (B-7), dilution 1:150; cyclin D1 (M-20), dilution 1:100; Bcl-x_L (H-62), dilution 1:100]. Immunologic reaction was developed using 3-3-diaminobenzidine in TBS containing 0.2 mL/L hydrogen peroxide. The slides were counterstained with hematoxylin. Negative controls were performed by substituting the primary antibody with Tris-buffered saline.

Statistical analysis

Statistical analysis was performed with SPSS software version 10.0 (SPSS Inc., Chicago, IL). Data were presented as mean±SD.

The relationship between levels of p-Stat3, cyclin D1 or Bcl-x$_L$ and various clinicopathological parameters was determined by Student's *t* test or one-way ANOVA. The association between p-Stat3, cyclin D1 and Bcl-x$_L$ expression was analyzed by Pearson's correlation coefficient. *P*<0.05 was considered statistically significant.

RESULTS

Activated Stat3 was constitutively expressed in colorectal carcinoma

One objective was to determine whether Stat3 was constitutively activated in human colorectal carcinoma and whether activation of Stat3 correlated with various clinicopathological parameters in patients with CRC. To determine whether Stat3 was activated in CRC, we performed Western blot analysis using antibody to p-Stat3, activated form of Stat3. Representative cases are shown in Figure 1. Of the 45 CRC samples examined, 57.8% (26 of 45) of the samples showed strong p-Stat3 expression. Quantitative evaluation of the relative expression (tumor versus normal mucosae) of these experiments demonstrated an average 2.6-fold increase in the level of p-Stat3 protein in cancers compared with adjacent normal mucosae (*P*=0.002, Table 2). Both cytoplasmic and nuclear localizations of the Stat3 (p-Stat3) were detected in CRC primary tumors (Figure 2). When we examined possible correlations with various clinicopathological parameters, we found that increased levels of p-Stat3 were significantly correlated with the existence of nodal metastasis (*P*=0.018). We also found that the levels of p-Stat3 were increased in stages III and IV, whereas its levels were decreased in stages I and II (*P*=0.026). No statistically significant correlation was observed between p-Stat3 expression and gender, age, primary site, size, and grade of tumors (Table 3).

Expression of downstream mediators of Stat3 in colorectal carcinoma

We next investigated the expression of cyclin D1 and Bcl-x$_L$, which could be potential downstream mediators of Stat3 in

CRC. We found that cyclin D1 and Bcl-x$_L$ were overexpressed in CRC tissues (*P*<0.05, Table 2). When we examined possible correlations with various clinicopathological parameters, we found that increased expression of cyclin D1 correlated with the nodal metastasis (*P*=0.041), whereas increased expression of Bcl-x$_L$ did not significantly correlate with any of these parameters (Figure 1, Table 3). The expression pattern of cyclin D1 and Bcl-x$_L$ was also checked with immunohistochemistry. Representative examples of immunohistochemical staining are shown in Figure 2. Furthermore, we studied the possible correlations between expression of p-Stat3 and downstream mediators. When these data were analyzed by Pearson's correlation coefficient, we found a significant association between expressions of p-Stat3 and cyclin D1 (*r*=0.382, *P*<0.05). No statistically significant correlation was observed between p-Stat3 and Bcl-x$_L$ expressions (*r*=0.162, *P*>0.05).

Figure 1 Expressions of Stat3, p-Stat3, cyclin D1, and Bcl-x$_L$ in colorectal carcinoma. Lysates were made as described under Materials and Methods. GAPDH represents the internal protein control. Elevated levels of Stat3, p-Stat3 (Tyr-705), cyclin D1, and Bcl-x$_L$ in tumor (T) tissues were compared to adjacent normal mucosae (N).

Figure 2 Expressions of Stat3, p-Stat3, cyclin D1, and Bcl-x$_L$ in colorectal carcinoma. A: Cytoplasmic staining of Stat3 in CRC (original magnification ×200); B: Nuclear staining of p-Stat3 in CRC (original magnification ×200); C: Nuclear staining of cyclin D1 in CRC (original magnification ×200); D: Cytoplasmic staining of Bcl-x$_L$ (original magnification ×200).

Table 2 Expressions of p-Stat3, cyclin D1, and Bcl-x$_L$ in colorectal carcinoma (mean±SD)

Items	n	Percentage (%)	A Value Tumor	A Value Normal	t	P
p-Stat3	45	57.8 (26/45)	114 263±53 598	55 971±28 762	3.573	0.002
cyclin D1	45	64.4 (29/45)	58 321±24 872	22 563±11 160	5.191	0.0001
Bcl-x$_L$	45	68.9 (31/45)	71 032±43 425	37 281±14 622	4.627	0.0001

Table 3 Correlations between p-Stat3, cyclin D1, Bcl-x$_L$ and clinicopathological parameters in colorectal carcinoma (mean±SD)

Item	n	p-Stat3	P	cyclin D1	P	Bcl-x$_L$	P
Gender							
Male	24	2.7±0.6	0.846	4.1±1.6	0.913	3.7±1.2	0.746
Female	21	2.5±0.5		4.3±1.8		3.3±1.1	
Age (yr)							
≥65	22	2.8±0.7	0.736	4.8±2.1	0.825	3.4±1.5	0.870
<65	23	2.4±0.4		3.6±1.3		3.6±0.8	
Stage							
III+IV	20	3.6±0.6	0.026	5.2±1.9	0.065	4.2±1.3	0.235
I+II	25	1.8±0.5		3.4±1.5		3.1±1.0	
Histological Grade							
G1	12	2.3±0.5	0.778	4.7±1.8	0.732	3.9±1.3	0.894
G2	22	2.4±0.6	0.645	4.2±1.4	0.627	3.3±1.0	0.771
G3	11	3.4±0.6	0.530	3.6±2.2	0.565	3.6±1.2	0.832
Node Metastasis							
Positive	27	3.8±0.8	0.018	5.5±1.9	0.041	4.4±1.4	0.162
Negative	18	1.6±0.4		3.3±1.5		2.9±1.0	
Distant Metastasis							
M1	6	3.6±0.8	0.638	5.4±2.2	0.612	5.2±1.6	0.324
M0	39	2.5±0.5		4.0±1.6		3.3±1.1	
Tumor Size							
≥5 cm	22	3.0±0.7	0.582	4.5±1.8	0.776	3.8±1.3	0.735
<5 cm	23	2.2±0.4		3.9±1.6		3.2±1.0	

G1: well differentiated tumor, G2: moderately differentiated tumor, G3: poorly differentiated tumor, M0: no distant metastasis, M1: distant metastasis.

DISCUSSION

Though significant progresses have been achieved in delineating the molecular mechanisms of colorectal carcinoma tumorigenesis, specific signal transduction pathways involved in CRC have not been fully characterized[21]. Increasing reports suggested that Stat3 signaling pathway played a critical role in malignant transformation and tumor progression[3]. Constitutive activation of Stat3 has been detected in a wide variety of human primary tumors and tumor cell lines including blood malignancies, breast cancer, and other cancers[8-13]. In the current study, we provided evidences that constitutive activation of Stat3 signaling might play an important role in human colorectal carcinoma.

Western blot analysis with p-Stat3 antibody showed that the activated form of Stat3 was elevated in the majority (57.8%) of CRC samples. Both cytoplasmic and nuclear localizations of Stat3 (p-Stat3) were also detected in CRC primary tumors. Nagpal et al.[22] reported in their work on head and neck carcinomas that 58.9% (53/90) of HNSCC tumors showed very high Stat3 protein accumulation, and none of the normal epithelium samples showed Stat3 absence. Campbell et al.[23] found that in 51 human primary tissues from normal prostate, benign prostatic hyperplasia, and prostate cancer, p-Stat3 was observed more prominently in the nuclei of cells residing in malignant glands compared to those in nonmalignant samples. As previously discussed, there were a growing number of evidences associating constitutive or aberrant activation of Stat3 with human cancers. The presence of p-Stat3 and its up-regulation in colorectal carcinoma could have important implications in colorectal cancer biology.

Because the above results provided evidence that Stat3 was constitutively activated in colorectal carcinomas, it was of interest to determine whether activation of stat3 correlated with various clinicopathological parameters in patients with CRC. When we examined possible correlations with various parameters, we found that increased levels of p-Stat3 significantly correlated with the existence of nodal metastasis and its stage but not with other parameters. Masuda et al.[19] indicated in their work on HNSCC, that elevated levels of the activated form of Stat3 had a significant association with the clinical stage of HNSCC. Ni et al.[24,25] demonstrated that Stat3 DNA binding activity was correlated with malignant potential in both human prostate cancer cell lines and a large series of rat Dunning prostate cancer cell lines. The most aggressive cell lines were found to have the highest Stat3 DNA binding activities. Blockade of activated Stat3 by dominant-negative Stat3 constructs significantly suppressed their growth *in vitro* and tumorigenicity *in vivo*. This specific activation of Stat3 in the tumorigenesis of colorectal carcinoma could qualify it as a potential diagnostic marker.

Tumor progression could be facilitated by activation of genes that regulate proliferation and/or apoptosis. However, the downstream events from constitutively activated Stat3 are not fully understood. Cyclin D1, an important cell cycle regulator, was overexpressed and associated with the poor prognosis in colorectal carcinoma[26]. We investigated the expression of cyclin D1 in CRC tissues. When we examined possible correlations with various parameters, we found that increased levels of cyclin D1 correlated with the nodal metastasis, and there was a significant correlation between overexpressions of p-Stat3 and cyclin D1. However, the precise mechanism underlying the overexpression of cyclin D1 in CRC is unclear. In the majority of the cases of CRC, cyclin D1 gene was not amplified, suggesting that the increased expression of cyclin D1 was due to defects at the level of gene transcription[27]. The similar discrepancy between cyclin D1 overexpression and gene amplification was also reported in breast and HNSCC cancers[28,29]. Constitutive activation of Stat3 constructs has been shown to activate the cyclin D1 promoter in rodent fibroblast cell lines[16], and overexpression of cyclin D1 was associated with increased activation of Stat3 in ovarian carcinoma and HNSCC[20,30]. Therefore, frequent overexpression of cyclin D1 in CRC might be attributable, at least in part, to increased levels of p-Stat3.

Another important downstream mediator is Bcl-x$_L$. Bcl-x$_L$ is a member of Bcl-2 family that could play a critical role in apoptosis[31]. Previous studies showed that Bcl-x$_L$ was overexpressed in colorectal carcinomas, and Bcl-x$_L$ might be a useful prognostic marker in CRC[32,33]. We also found that Bcl-x$_L$ was overexpressed in CRC tissues, but the increased protein level did not significantly correlate with the clinicopathological parameters in CRC. No statistically significant correlation was observed between p-Stat3 and Bcl-x$_L$ expressions. Bromberg et al.[16] observed that Stat3 could tra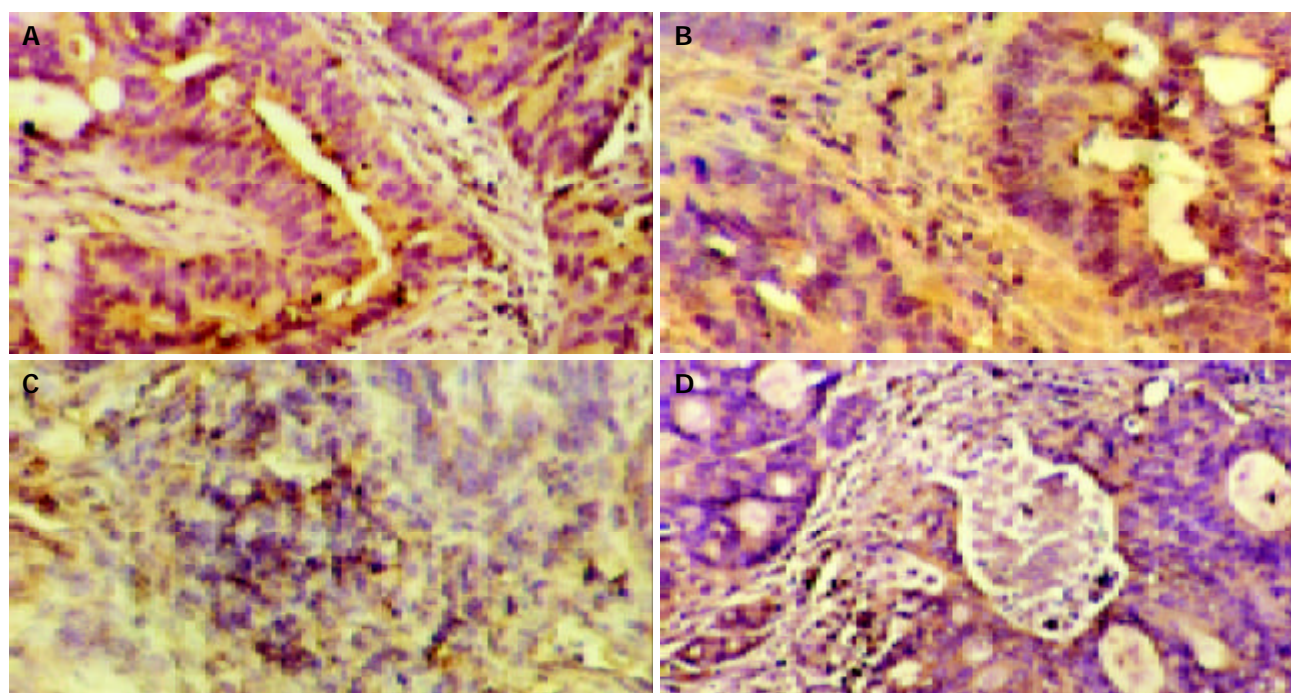nscriptionally up-regulate the expression of Bcl-x$_L$ in Stat3 transformed cell lines. Evidence suggested that blocking of the activated Stat3 in multiple myeloma cells and ovarian cancer cells could down-regulate the expression of Bcl-x$_L$ and enhance the apoptosis, and the cells regained the sensitivity to chemotherapy[9,20]. The precise mechanism by which activation of Stat3 enhances the transcription of Bcl-x$_L$ in CRC remains to be determined.

Our results demonstrated that in comparison with normal

mucosae, p-Stat3 protein was overexpressed in human colorectal carcinomas. Expression of p-Stat3 was associated with the presence of nodal metastasis and its stage. Our clinical data also provides evidence that there is a strong association of p-Stat3 and cyclin D1 overexpression in CRC. These results suggest that constitutive activation of Stat3 signaling pathway may play an important role in the tumorigenesis of colorectal carcinoma, and the detailed mechanism of Stat3 signaling pathway in CRC deserves further investigation.

ACKNOLEDGEMENTS

REFERENCES

1   **Jemal A**, Thomas A, Murray T, Thun M. Cancer statistics, 2002. *CA Cancer J Clin* 2002; **52**: 23-47

2   **Jin F**, Devesa SS, Chow WH, Zheng W, Ji BT, Fraumeni JF Jr, Gao YT. Cancer incidence trends in urban shanghai, 1972-1994: an update. *Int J Cancer* 1999; **83**: 435-440

3   **Bromberg J**. Stat proteins and oncogenesis. *J Clin Invest* 2002; **109**: 1139-1142

4   **Darnell JE Jr**. STATs and gene regulation. *Science* 1997; **277**: 1630-1635

5   **Levy DE**, Darnell JE Jr. Stats: transcriptional control and biological impact. *Nat Rev Mol Cell Biol* 2002; **3**: 651-662

6   **Smithgall TE**, Briggs SD, Schreiner S, Lerner EC, Cheng H, Wilson MB. Control of myeloid differentiation and survival by Stats. *Oncogene* 2000; **19**: 2612-2618

7   **Mora LB**, Buettner R, Seigne J, Diaz J, Ahmad N, Garcia R, Bowman T, Falcone R, Fairclough R, Cantor A, Muro-Cacho C, Livingston S, Karras J, Pow-Sang J, Jove R. Constitutive activation of Stat3 in human prostate tumors and cell lines: direct inhibition of Stat3 signaling induces apoptosis of prostate cancer cells. *Cancer Res* 2002; **62**: 6659-6666

8   **Spiekermann K**, Biethahn S, Wilde S, Hiddemann W, Alves F. Constitutive activation of STAT transcription factors in acute myelogenous leukemia. *Eur J Haematol* 2001; **67**: 63-71

9   **Catlett-Falcone R**, Landowski TH, Oshiro MM, Turkson J, Levitzki A, Savino R, Ciliberto G, Moscinski L, Fernandez-Luna JL, Nunez G, Dalton WS, Jove R. Constitutive activation of Stat3 signaling confers resistance to apoptosis in human U266 myeloma cells. *Immunity* 1999; **10**: 105-115

10 **Garcia R**, Bowman TL, Niu G, Yu H, Minton S, Muro-Cacho CA, Cox CE, Falcone R, Fairclough R, Parsons S, Laudano A, Gazit A, Levitzki A, Kraker A, Jove R. Constitutive activation of Stat3 by the Src and JAK tyrosine kinases participates in growth regulation of human breast carcinoma cells. *Oncogene* 2001; **20**: 2499-2513

11 **Dhir R**, Ni Z, Lou W, DeMiguel F, Grandis JR, Gao AC. Stat3 activation in prostatic carcinomas. *Prostate* 2002; **51**: 241-246

12 **Grandis JR**, Drenning SD, Zeng Q, Watkins SC, Melhem MF, Endo S, Johnson DE, Huang L, He Y, Kim JD. Constitutive activation of Stat3 signaling abrogates apoptosis in squamous cell carcinogenesis *in vivo*. *Proc Natl Acad Sci U S A* 2000; **97**: 4227-4232

13 **Feng DY**, Zheng H, Tan Y, Cheng RX. Effect of phosphorylation of MAPK and Stat3 and expression of c-fos and c-jun proteins on hepatocarcinogenesis and their clinical significance. *World J Gastroenterol* 2001; **7**: 33-36

14 **Bromberg JF**, Horvath CM, Besser D, Lathem WW, Darnell JE Jr. Stat3 activation is required for cellular transformation by v-src. *Mol Cell Biol* 1998; **18**: 2553-2558

15 **Bowman T**, Broome MA, Sinibaldi D, Wharton W, Pledger WJ, Sedivy JM, Irby R, Yeatman T, Courtneidge SA, Jove R. Stat3-mediated Myc expression is required for Src transformation and PDGF-induced mitogenesis. *Proc Natl Acad Sci U S A* 2001; **98**: 7319-7324

16 **Bromberg JF**, Wrzeszczynska MH, Devgan G, Zhao Y, Pestell RG, Albanese C, Darnell JE Jr. Stat3 as an oncogene. *Cell* 1999; **98**: 295-303

17 **Bowman T**, Garcia R, Turkson J, Jove R. STATs in oncogenesis. *Oncogene* 2000; **19**: 2474-2488

18 **Real PJ**, Sierra A, De Juan A, Segovia JC, Lopez-Vega JM, Fernandez-Luna JL. Resistance to chemotherapy via Stat3-dependent overexpression of Bcl-2 in metastatic breast cancer cells. *Oncogene* 2002; **21**: 7611-7618

19 **Masuda M**, Suzui M, Yasumatu R, Nakashima T, Kuratomi Y, Azuma K, Tomita K, Komiyama S, Weinstein IB. Constitutive activation of signal transducers and activators of transcription 3 correlates with cyclin D1 overexpression and may provide a novel prognostic marker in head and neck squamous cell carcinoma. *Cancer Res* 2002; **62**: 3351-3355

20 **Huang M**, Page C, Reynolds RK, Lin J. Constitutive activation of stat 3 oncogene product in human ovarian carcinoma cells. *Gynecol Oncol* 2000; **79**: 67-73

21 **Oving IM**, Clevers HC. Molecular causes of colon cancer. *Eur J Clin Invest* 2002; **32**: 448-457

22 **Nagpal JK**, Mishra R, Das BR. Activation of Stat-3 as one of the early events in tobacco chewing-mediated oral carcinogenesis. *Cancer* 2002; **94**: 2393-2400

23 **Campbell CL**, Jiang Z, Savarese DM, Savarese TM. Increased expression of the interleukin-11 receptor and evidence of STAT3 activation in prostate carcinoma. *Am J Pathol* 2001; **158**: 25-32

24 **Ni Z**, Lou W, Lee SO, Dhir R, DeMiguel F, Grandis JR, Gao AC. Selective activation of members of the signal transducers and activators of transcription family in prostate carcinoma. *J Urol* 2002; **167**: 1859-1862

25 **Ni Z**, Lou W, Leman ES, Gao AC. Inhibition of constitutively activated Stat3 signaling pathway suppresses growth of prostate cancer cells. *Cancer Res* 2000; **60**: 1225-1228

26 **Maeda K**, Chung Y, Kang S, Ogawa M, Onoda N, Nishiguchi Y, Ikehara T, Nakata B, Okuno M, Sowa M. Cyclin D1 overexpression and prognosis in colorectal adenocarcinoma. *Oncology* 1998; **55**: 145-151

27 **Tetsu O**, McCormick F. Beta-catenin regulates expression of cyclin D1 in colon carcinoma cells. *Nature* 1999; **398**: 422-426

28 **Lin SY**, Xia W, Wang JC, Kwong KY, Spohn B, Wen Y, Pestell RG, Hung MC. Beta-catenin, a novel prognostic marker for breast cancer: its roles in cyclin D1 expression and cancer progression. *Proc Natl Acad Sci U S A* 2000; **97**: 4262-4266

29 **Quon H**, Liu FF, Cummings BJ. Potential molecular prognostic markers in head and neck squamous cell carcinomas. *Head Neck* 2001; **23**: 147-159

30 **Kijima T**, Niwa H, Steinman RA, Drenning SD, Gooding WE, Wentzel AL, Xi S, Grandis JR. STAT3 activation abrogates growth factor dependence and contributes to head and neck squamous cell carcinoma tumor growth *in vivo*. *Cell Growth Differ* 2002; **13**: 355-362

31 **Tsujimoto Y**, Shimizu S. Bcl-2 family: life-or-death switch. *FEBS Lett* 2000; **466**: 6-10

32 **Krajewska M**, Moss SF, Krajewski S, Song K, Holt PR, Reed JC. Elevated expression of Bcl-X and reduced Bak in primary colorectal adenocarcinomas. *Cancer Res* 1996; **56**: 2422-2427

33 **Biroccio A**, Benassi B, D' Agnano I, D' Angelo C, Buglioni S, Mottolese M, Ricciotti A, Citro G, Cosimelli M, Ramsay RG, Calabretta B, Zupi G. c-Myb and Bcl-x overexpression predicts poor prognosis in colorectal cancer: clinical and experimental findings. *Am J Pathol* 2001; **58**: 1289-1299

• COLORECTAL CANCER •

Postprocessing techniques of CT colonography in detection of colorectal carcinoma

Ming-Yue Luo, Hong Shan, Li-Qing Yao, Kang-Rong Zhou, Wen-Wei Liang

Ming-Yue Luo, Hong Shan, Wen-Wei Liang, Department of Radiology, the Third Affiliated Hospital, Sun Yat-Sen University, Guangzhou 510630, Guangdong Province, China
Li-Qing Yao, Endoscopy Center, Zhongshan Hospital, Fudan University Medical School, Shanghai 200032, China
Kang-Rong Zhou, Department of Radiology, Zhongshan Hospital, Fudan University Medical School, Shanghai 200032, China
Correspondence to: Dr. Ming-Yue Luo, Department of Radiology, the Third Affiliated Hospital, Sun Yat-Sen University, Guangzhou 510630, Guangdong Province, China. myluo@yahoo.com.cn
Telephone: +86-20-85516867   **Fax:** +86-20-87536401
Received: 2003-06-04   **Accepted:** 2003-09-18

Abstract

AIM: To evaluate the value of postprocessing techniques of CT colonography, including multiplanar reformation (MPR), virtual colonoscopy (VC), shaded surface display (SSD) and Raysum, in detection of colorectal carcinomas.

METHODS: Sixty-four patients with colorectal carcinoma underwent volume scanning with spiral CT. MPR, VC, SSD and Raysum images were obtained by using four kinds of postprocessing techniques in workstation. The results were comparatively analyzed according to circumferential extent, lesion length and pathology pattern of colorectal carcinomas. All diagnoses were proved pathologically and surgically.

RESULTS: The accuracy of circumferential extent of colorectal carcinoma determined by MPR, VC, SSD and Raysum was 100.0%, 82.8%, 79.7% and 79.7%, respectively. There was a significant statistical difference between MPR and VC. The consistent rate of lesion length was 89.1%, 76.6%, 95.3% and 100.0%, respectively. There was a statistical difference between VC and SSD. The accuracy of discriminating pathology pattern was 81.3%, 92.2%, 71.9% and 71.9%, respectively. There was a statistical difference between VC and SSD. MPR could determine accurately the circumference of colorectal carcinoma, Raysum could determine the length of lesion more precisely than SSD, VC was helpful in discriminating pathology patterns.

CONCLUSION: MPR, VC, SSD and Raysum have advantage and disadvantage in detection of colorectal carcinoma, use of these methods in combination can disclose the lesion more accurately.

INTRODUCTION

Multiplanar reformation (MPR), virtual colonoscopy (VC), shaded surface display (SSD) and Raysum images could be obtained after source data of CT colonography are processed in workstation. Numerous literatures on CT colonography are based on examination of colon polypi[1-17]. No research report on the diagnosis of colorectal carcinoma with postprocessing techniques of MPR, VC, SSD and Raysum is available. The aim of this study was to investigate the clinical value of four postprocessing techniques in detection of colorectal carcinomas by comparing the results of 64 colorectal carcinomas.

MATERIALS AND METHODS

Clinical data
Sixty-four patients (39 men, 25 women, aged 20-78 years, mean age 55.6 years) with colorectal carcinomas were studied. All cases were diagnosed surgically and pathologically.

Examination protocol
The whole procedure of CT colonography included patient preparation, volume scanning and image postprocessing[18-20].

Patient preparation
A liquid diet for 48 h was used and 500 mL of 200 g/L mannite mixed with 1 000 mL of 50 g/L glycol saline solution was administered orally in the evening prior to examination.

Anisodamine hydrochloride injection (654-2) (10 mg) was administered intramuscularly 10 min before CT scanning to alleviate colon spasm, minimize peristalsis and allow optimal colonic distention. The patient lay on right lateral decubitus position on CT table after dwelling a rectal enema tube. Then, the patient lay on supine, and room air was gently insufflated into the colorectum to distend the colon as long as the patient was tolerable.

Volume scanning
A HighSpeed advantage helical CT scanner (General Electric Medical System) was used to acquire a standard scout view image of the abdomen and pelvis to assess the degree of colorectal distension, room air was further insufflated if required. Images were acquired by using 3.0 mm collimation with a pitch of 2.0, 100-120 mA, 120 kV, and a 512×512 matrix. The range of scanning encompassed the entire colon from the rectum to cecum.

Image postprocessing
Image reconstruction data were transferred to a workstation (Sun Sparc 20 workstation, GE Advantage Windows 2.0 image analysis software) via picture archive and communication system, after retro-reconstructing the initial image data of scanning with 1.5 mm thickness, 0.5 mm interval. MPR, VC, SSD and Raysum images were obtained with postprocessing techniques in workstation.

MPR image: axial, coronal, sagittal and oblique images were acquired with the center on colorectal carcinoma segment by using CT software to display wall, lumen and adjacent structure of the lesion.

VC image: intraluminal image was obtained by applying Navigator software with about - 700 HU threshold from the rectum to cecum. Lesions were observed with Fly-through program along the longitudinal lumen[21].

SSD image: image reconstruction of colorectal area was performed with SSD software, then the interested colorectal segment were obtained by trimming off unnecessary part with Scalpel program, magnification and rotation were done to demonstrate colorectal carcinoma.

Raysum image: transparent image of interested colorectum was acquired by using Raysum software on the basis of SSD image to display the situation of endolumen and wall.

Statistical analysis

The following 3 aspects were comparatively analyzed according to surgery and pathology results. According to the invasive extent of colorectal carcinoma along the wall, tumors were divided into <1/2, 1/2-3/4 and >3/4 circumference. According to the longitudinal length of the lesion, it was classified into categories of 2.0-3.0 cm, 3.1-5.0 cm and 5.1-11.0 cm, respectively. The pathology pattern was classified into massive, ulcerous, infiltrative, ulcerous and infiltrative types.

Results of 4 kinds of postprocessing techniques were compared with surgical observation and pathology results. Accuracy of diagnosis with 4 kinds of postprocessing techniques was compared by using *U* test.

RESULTS

Examination results of circumferential extents, lesion lengths and pathology patterns in 64 colorectal carcinomas with 4 kinds of postprocessing techniques (Table 1)

Diagnostic accordance of 64 colorectal carcinomas with 4 kinds of postprocessing techniques (Table 2)

DISCUSSION

MPR, VC, SSD and Raysum images obtained by postprocessing technique displayed colorectal carcinoma in different manners with different clinical values.

Circumferential extent

The accuracy of circumferential extent of colorectal carcinoma determined with MPR, VC, SSD and Raysum was 100.0%, 82.8%,

79.7% and 79.7%, respectively (Tables 1, 2). Significant statistical difference between MPR and VC, MPR and SSD, MPR and Raysum were obtained, respectively.

Table 2 Diagnosis accordance of 64 colorectal carcinomas with postprocessing techniques

Postprocessing technique	Circumferential extent		Lesion length		Pathological pattern	
	Case (*n*)	%	Case (*n*)	%	Case (*n*)	%
MPR	64	100.0	57	89.1	52	81.2
VC	53	82.8	49	76.6	59	92.2
SSD	51	79.7	61	95.3	46	71.9
Raysum	51	79.7	64	100.0	46	71.9
χ^2 value	14.748[b]		22.430[b]		10.909[a]	

[a]$P<0.05$ *vs* pathological pattern, [b]$P<0.01$ *vs* circumferential extent and lesion length.

MPR had two dimensional axial, coronal, sagittal and oblique reconstruction images in series, on the center of colorectal carcinoma segments. MPR might reflect different density tissues by using different attenuation scales with high density resolution and it has no obvious artifact. It could clearly display intraluminal lesion and range invaded by carcinoma along its wall and adjacent structure, and accurately determine the circumferential extent of colorectal carcinoma[22].

VC, SSD and Raysum images could be obtained by using appropriate CT threshold values with transparence of the part beyond them, could make use of only certain information without favorable disclosure of lesions in detail. Sometimes, they had difficulty in showing directly the condition of colorectal wall when thickening was not obvious. Therefore, the determination of circumferential extent of colorectal carcinoma was not so accurate as MPR (Figure 1A-C).

Length of tumors

The correction rate of lesion lengths determined with MPR, VC, SSD and Raysum was 89.1%, 76.6%, 95.3% and 1 00.0%, respectively (Tables 1, 2).

Table 1 Circumferential extents, lesion lengths and pathology patterns in 64 colorectal carcinomas determined with postprocessing techniques

Item	Diagnostic accordance (*n*)					Accurate diagnosis (%)			
	S&p c	MPR	VC	SSD	Raysum	MPR	VC	SSD	Raysum
Circumf extent	64	64	53	51	51	100.0	82.8	79.7	79.7
<1/2 circum	7	7	6	6	6	100.0	85.7	85.7	85.7
1/2-3/4 circum	14	14	12	11	11	100.0	85.7	78.6	78.6
>3/4 circum	43	43	35	34	34	100.0	81.4	79.1	79.1
Lesion length (cm)	64	57	49	61	64	89.1	76.6	95.3	100.0
2.0-3.0	6	6	6	6	6	100.0	100.0	100.0	100.0
3.1-5.0	33	31	26	32	33	93.9	78.8	97.0	100.0
5.1-11.0	25	20	17	23	25	80.0	68.0	92.0	100.0
Pathology pattern	64	52	59	46	46	81.2	92.2	71.9	71.9
Massive type	38	32	38	27	27	84.2	100.0	71.1	71.1
Ulcerous type	5	4	4	3	4	80.0	80.0	60.0	80.0
Infiltrative type	13	11	12	11	12	84.6	92.3	84.6	92.3
Ulc and inf type	8	5	5	5	3	62.5	62.5	62.5	37.5

S & p c=Surgery and pathology case, Circumf=Circumferential, circum=circumference, Ulc and inf=Ulcerous and infiltrative. For circumferential extent, comparison between MPR and VC, $U=3.472$, $P<0.001$; comparison between VC and SSD, $U=0.449$, $P>0.05$; comparison between SSD and Raysum, $U=0.000$, $P>0.05$. For Lesion length, comparison between MPR and VC, $U=1.875$, $P>0.05$; comparison between VC and SSD, $U=3.034$, $P<0.05$; comparison between SSD and Raysum $U=1.759$, $P>0.05$. For pathologic pattern, comparison between MPR and VC, $U=1.817$, $P>0.05$; comparison between VC and SSD, $U=2.991$, $P<0.05$; comparison between SSD and Raysum, $U=0.000$, $P>0.05$.

Figure 1 Massive rectal carcinoma in a 74 years old man. VC, SSD displayed an irregular mass, but unable to determine circumferential extent (A, B). MPR showed the mass with 1/4 circumference around rectal wall (C).
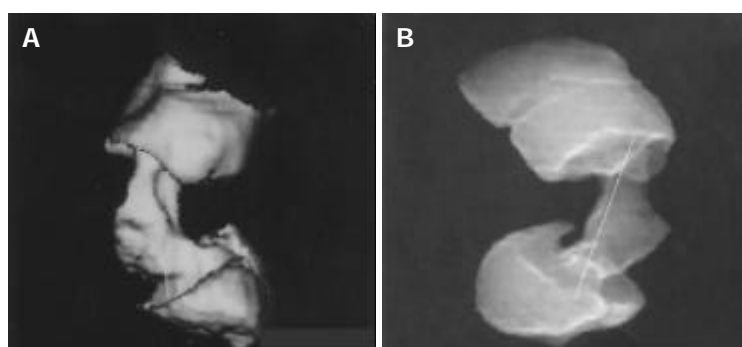

Figure 2 Infiltrative rectal carcinoma in a 46 years old man. SSD disclosed the two ends of carcinoma and measured its length (A). Raysum manifested the two ends of carcinoma more clearly and measured its length more accurately than SSD (B).
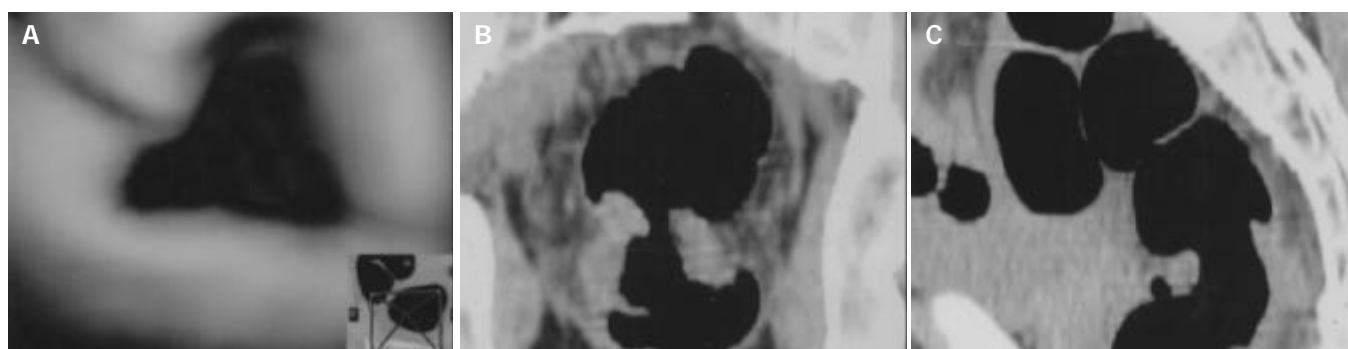

Figure 3 Infiltrative rectal carcinoma in a 48 years old man. VC demonstrated the carcinoma around rectal wall (A). Combination of coronal and sagittal images of MPR revealed an infiltrative carcinoma, but was not so obvious as VC (B, C).

SSD image displayed the surface of colorectal lumen from outside to inside, being similar to the image of filling phase in double contrast barium enema. It could be locally magnified and rotated polygonally to demonstrate colorectal carcinoma as clear as possible and show lesion lengths and morphology of two ends. But it utilized only certain information and did not reveal the lesion in detail due to the appropriate CT threshold value and transparence of the part beyond it. Moreover, because of partial covering of lesions by the colorectum, sometimes its manifestation was not quite precise[23]. Its correction rate of lesion lengths was 95.3 % in our series.

Raysum was obtained on the basis of SSD image similar to the image of mucosa phase in double contrast barium enema. It could display the situation of endolumen and wall by transparence and avoid the disadvantages of partial overlapping of lesions by colorectum with SSD, hence clearly revealing lesion lengths and morphology at two ends and accurately manifesting the lesion lengths[24] (Figure 2A, B).

MPR was a two dimensional image formed by reconstruction. But the colorectum was tortuous in structure, moreover, it was complicated by the presence of colorectal carcinoma. Therefore, measurement of the lesion length with MPR was not accurate[25]. In our study its accuracy was 89.1%.

VC could obtain virtual cubic images from colorectal endolumen. Its image was similar to that of fiberoptic colonoscopy. It could directly show the surface morphology of colorectal carcinoma, and its distal and proximal situations. But its manifestation of lesion lengths had a comparatively great error[3,4,14,18,26-28]. The correct rate was only 76.6% in our series.

Pathological patterns

The accuracy of pathology patterns determined by MPR, VC, SSD and Raysum was 81.3%, 92.2%, 71.9% and 71.9%, respectively (Tables 1, 2). Significant statistical differences between VC and SSD were noticed.

VC image could disclose the surface morphology of colorectal carcinoma and its distal and proximal situations directly with observations from endolumen, favoring the discrimination of pathology patterns. However, there was certain difficulty in revealing the detail of carcinoma. It had errors in discriminating

pathology patterns[29-30]. The correction rate was 92.2% in our study.

MPR was a two-dimensional image formed by reconstruction, and was combined with axial, coronal, sagittal and oblique images. But it had no direct three dimensional manifestation with a relative great error in discriminating pathology patterns (Figure 3A-C).

SSD, Raysum images could display the surface of colorectal lumen from outside to inside, similar to the images of filling and mucosa phase in double contrast barium enema. But they could use certain information and could not show carcinoma details, and were fairly inaccurate in discriminating pathology patterns. Its correction rate was only 71.9% in our series.

In conclusion, MPR, VC, SSD and Raysum have both advantage and disadvantage in detection of colorectal carcinoma. MPR can accurately determine the circumferential extent, Raysum can fairly determine the length of lesions, and is more trustworthy than SSD, VC is helpful in discriminating pathology patterns. Their combination can disclose colorectal carcinomas more accurately.

ACKNOWLEDGEMENTS

REFERENCES

1   **Podolsky DK.** Going the distance--the case for true colorectal-cancer screening. *N Engl J Med* 2000; **343:** 207-208
2   **Fletcher RH.** The end of barium enemas? *N Engl J Med* 2000; **342:** 1823-1824
3   **Bond JH.** Virtual colonoscopy–promising, but not ready for widespread use. *N Engl J Med* 1999; **341:** 1540-1542
4   **Fenlon HM,** Nunes DP, Schroy PC 3rd, Barish MA, Clarke PD, Ferrucci JT. A comparison of virtual and conventional colonoscopy for the detection of colorectal polyps. *N Engl J Med* 1999; **341:** 1496-1503
5   **Zalis ME,** Perumpillichira J, Del Frate C, Hahn PF. CT colonography: digital subtraction bowel cleansing with mucosal reconstruction initial observation. *Radiology* 2003; **226:** 911-917
6   **Yee J,** Kumar NN, Hung RK, Akerkar GA, Kumar PR, Wall SD. Comparison of supine and prone scanning separately and in combination at CT colonography. *Radiology* 2003; **226:** 653-661
7   **Summers RM,** Jerebko AK, Franaszek M, Malley JD, Johnson CD. Colonic polyps: complementary role of computer-aided detection in CT colonography. *Radiology* 2002; **225:** 391-399
8   **McFarland EG,** Pilgram TK, Brink JA, McDermott RA, Santillan CV, Brady PW, Heiken JP, Balfe DM, Weinstock LB, Thyssen EP, Littenberg B. CT colonography: multiobserver diagnostic performance. *Radiology* 2002; **225:** 380-390
9   **Lefere PA,** Gryspeerdt SS, Dewyspelaere J, Baekelandt M, Van Holsbeeck BG. Dietary fecal tagging as a cleansing method before CT colonography: initial results polyp detection and patient acceptance. *Radiology* 2002; **224:** 393-403
10   **Yoshida H,** Masutani Y, MacEneaney P, Rubin DT, Dachman AH. Computerized detection of colonic polyps at CT colonography on the basis of volumetric features: pilot study. *Radiology* 2002; **222:** 327-336
11   **Yee J,** Akerkar GA, Hung RK, Steinauer-Gebauer AM, Wall SD, McQuaid KR. Colorectal neoplasia: performance characteristics of CT colonography for detection in 300 patients. *Radiology* 2001; **219:** 685-692
12   **Summers RM,** Johnson CD, Pusanik LM, Malley JD, Youssef AM, Reed JE. Automated polyp detection at CT colonography: feasibility assessment in a human population. *Radiology* 2001; **219:** 51-59
13   **Ferrucci JT.** Colon cancer screening with virtual colonoscopy: promise,

polyps, politics. *Am J Roentgenol* 2001; **177:** 975-988
14   **Luo MY,** Zhou KR, Yao LQ. Experimental study of simulated polyp in pig colon: detection with CT virtual colonoscopy. *Zhongguo Yixue Yingxiang Jishu* 2000; **16:** 719-721
15   **Luo MY,** Zhou KR, Yao LQ. Comparative study on the detecting colorectal polyps with virtual colonoscopy or other postprocessing techniques. *Linchuang Fangshexue Zazhi* 2000; **19:** 699-702
16   **Summers RM,** Beaulieu CF, Pusanik LM, Malley JD, Jeffrey RB Jr, Glazer DI, Napel S. Automated polyp detector for CT colonography: feasibility study. *Radiology* 2000; **216:** 284-290
17   **Macari M,** Milano A, Lavelle M, Berman P, Megibow AJ. Comparison of time-efficient CT colonography with two- and three-dimensional colonic evaluation for detecting colorectal polyps. *Am J Roentgenol* 2000; **174:** 1543-1549
18   **Luo M,** Shan H, Zhou K. CT virtual colonoscopy in patients with incomplete conventional colonoscopy. *Chin Med J* 2002; **115:** 1023-1026
19   **Zalis ME,** Hahn PF. Digital subtraction bowel cleansing in CT colonography. *Am J Roentgenol* 2001; **176:** 646-648
20   **Fletcher JG,** Johnson CD, Welch TJ, MacCarty RL, Ahlquist DA, Reed JE, Harmsen WS, Wilson LA. Optimization of CT colonography technique: prospective trail in 180 patients. *Radiology* 2000; **216:** 704-711
21   **Neri E,** Giusti P, Battolla L, Vagli P, Boraschi P, Lencioni P, Caramella D, Bartolozzi C. Colorectal cancer: role of CT colonography in preoperative evaluation after incomplete colonoscopy. *Radiology* 2002; **223:** 615-619
22   **McFarland EG,** Brink JA, Pilgram TK, Heiken JP, Balfe DM, Hirselj DA, Weinstock L, Littenberg B. Spiral CT colonography: reader agreement and diagnostic performance with two- and three-dimensional image-display techniques. *Radiology* 2001; **218:** 375-383
23   **Hopper KD,** Iyriboz AT, Wise SW, Neuman JD, Mauger DT, Kasales CJ. Mucosal detail at CT virtual reality: surface versus volume rendering. *Radiology* 2000; **214:** 517-522
24   **Glick S.** double-contrast barium enema for colorectal cancer screening: a review of the issues and a comparison with other screening alternatives. *Am J Roentgenol* 2000; **174:** 1529-1537
25   **Macari M,** Megibow AJ. Pitfalls of using three-dimensional CT colonography with two-dimensional imaging correlation. *Am J Roentgenol* 2001; **176:** 137-143
26   **Makin GB,** Breen DJ, Monson JR. The impact of new technology on surgery for colorectal cancer. *World J Gastroenterol* 2001; **7:** 612-621
27   **Spinzi G,** Belloni G, Martegani A, Sangiovanni A, Del Favero C, Minoli G. Computed tomographic colonography and conventional colonoscopy for colon diseases: a prospective, blinded study. *Am J Gastroenterol* 2001; **96:** 394-400
28   **Mendelson RM,** Foster NM, Edwards JT, Wood CJ, Rosenberg MS, Forbes GM. Virtual colonoscopy compared with conventional colonoscopy: a developing technology. *Med J Aust* 2000; **173**: 472-475
29   **Pescatore P,** Glucker T, Delarive J, Meuli R, Pantoflickova D, Duvoisin B, Schnyder P, Blum AL, Dorta G. Diagnostic accuracy and interobserver agreement of CT colonography (virtual colonoscopy). *Gut* 2000; **47:** 126-130
30   **Johnson CD,** Ahlquist DA. Computed tomography colonography (virtual colonoscopy): a new method for colorectal screening. *Gut* 1999; **44:** 301-305

• VIRAL HEPATITIS •

Dendritic cells from chronic hepatitis B patients can induce HBV antigen-specific T cell responses

Ruo-Bing Li, Hong-Song Chen, Yao Xie, Ran Fei, Xu Cong, Dong Jiang, Song-Xia Wang, Lai Wei, Yu Wang

Rou-Bing Li, Hong-Song Chen, Ran Fei, Xu Cong, Dong Jiang, Song-Xia Wang, Lai Wei, Yu Wang, Hepatology Institute, People's Hospital, Peking University, Beijing 100044, China
Yao Xie, Ditan Hospital, Beijing 100011, China
Co-correspondents: Yu Wang
Correspondence to: Dr. Hong-Song Chen, Hepatology Institute, People's Hospital, Peking University, Beijing 100044, China. chen2999@sohu.com
Telephone: +86-10-68314422 Ext 5726   **Fax:** +86-10-68321900

Abstract

AIM: To determine whether dendritic cells (DCs) from chronic hepatitis B patients could induce HBV antigen-specific T cell responses or not.

METHODS: DCs were generated from peripheral blood mononuclear cells of patients with chronic hepatitis B (CHB) infection and healthy donors. We compared the phenotypes of these DCs and their ability to secrete cytokines and to participate in mixed lymphocyte reactions. In addition, autologous lymphocytes were cultured with DCs loaded with HBV core region peptide HBcAg8-27, an epitope recognized by cytotoxic T lymphocytes (CTL), and bearing human leucocyte antigen (HLA)-A2 for 10 d. Cytokine secretion and lytic activity against peptide-pulsed target cells were assessed.

RESULTS: DCs with typical morphology were generated successfully by culturing peripheral blood mononuclear cells (PBMCs) from CHB patients with AIM-V containing GM-CSF and IL-4. Compared with DCs from normal donors, the level of CD80 expressed in DCs from CHB patients was lower, and DCs from patients had lower capacity of stimulate T cell proliferation. When PBMCs isolated from patients with chronic or acute hepatitis B infection and from normal donors were cocultured with HBcAg18-27 peptide, the antigen-specific memory response of PBMCs from acute hepatitis B patients was stronger than that of PBMCs from chronic hepatitis B patients or normal donors. PBMCs cocultured with DCs treated with HBcAg18-27 CTL epitope peptide induced an antigen-specific T cell reaction, in which the level of secreted cytokines and lytic activity were higher than those produced by memory T cells.

CONCLUSION: DCs from patients with CHB can induce HBV antigen-specific T cell reactions, including secretion of cytokines essential for HBV clearance and for killing cells infected with HBV.

INTRODUCTION

In patients infected by hepatitis B virus (HBV), the virus may easily escape from immune surveillance, thus inducing tolerance and becoming a persistent infection. Persistently infected patients produce a weak or undetectable HBV-specific CTL response[1]. Therefore, when treating chronically infected patients with HBV, the population of T cells recognizing HBV should be increased, thus producing an effective immune response.

Dendritic cells (DCs) are the most potent antigen presenting cells throughout the body. These cells express high levels of MHC class I and II antigens, as well as costimulatory molecules, and play essential roles in triggering primary immune responses[2,3]. The use of DCs, as a type of natural adjuvant, has been applied to the immunotherapy of melanomas and prostate gland carcinomas[4]. In addition, administration of DCs activated by cytokines to transgenic mice has been shown to break CTL immune tolerance and induce specific CTL reactions against HBV[5]. The aim of this study was to compare the anti-HBV activity of DCs derived from patients infected with HBV with those from healthy donors. DCs derived from different individuals were cultured, reacted with a peptide specific to the HBV antigen, HBcAg18-27, and cocultured with autogeneic PBMCs to determine if this procedure could induce antigen-specific CTL, which could then be utilized to kill target cells loaded with HBV antigens or to secrete specific cytokines.

MATERIALS AND METHODS

Patients

Of the HBV patients, four were studied during an episode of acute hepatitis B, and 12 (8 males, 4 females; average age, 38.3 years) were chronically infected with HBV. In addition, 20 patients were HLA-A2 positive, and 4 patients were HLA-A2 negative. We also included eight uninfected healthy volunteers (4 males, 4 females; average age, 35.2 years) as normal controls, of them six were HLA-A2 positive and two were HLA-A2 negative.

The diagnosis of acute and chronic hepatitis B was based on standard diagnostic criteria, as formulated by the 5th China Infection Disease and Parasitology Conference in 2000. HBV-infected patients had no complications of other organs. Normal controls had no clinical history of HBV infection and were serologically negative for HBV markers. All patients and normal controls were serologically negative for antibodies to HIV and HCV.

Cytokines and regents

Recombinant human GM-CSF was purchased from Leucomax Corp (Germany), and recombinant human IL-4 and TNF-α were purchased from Peprotech Corp (England). Ficoll-Hypaque fluid was from Dingguo Corporation, Beijing. Mouse anti-human HLA-A*02 monoclonal antibody (BB7.2 cell line) was a gift from Professor. Wei-Feng Chen, and T_2 cell line was a gift from Professor. Yan-Fang Sui. FITC-conjugated mouse monoclonal antibodies to human CD86, CD14, and CD3, and PE-labeled mouse monoclonal antibodies to human CD80, HLA-DR, CD54, CD11c, and CD19, were obtained from B-D Corp (USA). Mouse monoclonal antibodies to human CD83 and CD1a, FITC- and

PE-labeled goat anti-mouse Ig (H+L) antibodies, PE-labeled mouse anti-human IFN-γ, TNF-α, and IL-2 were all purchased from Pharmingen Corp (USA). CytoTox 96 non-radioactive cytotoxicity assay kits were from Promega Corp (USA). AIMV and RPMI 1 640 were from GIBCO Corp (USA), and IL-12 ELISA kit was from Endogen Corp (USA).

Synthetic peptide
HLA-A2 restricted HBcAg18-27 CTL epitope peptide, FLPSDFFPSV, was synthesized by Saibaisheng Biological Corporation(Beijing) and purified to >90% homogeneity by HPLC. The lyophilized peptide was dissolved in DMSO at a concentration of 2 mg/mL, and stored at -20 ℃.

Isolation of PBMCs
Following informed consent obtained from each subject, 100 mL anticoagulated venous blood was obtained from each, and peripheral blood mononuclear cells (PBMCs) were isolated by Ficoll-Hypaque density gradient centrifugation (density, 1.077). Cells at the interface were transferred to RPMI 1 640 incomplete medium containing 100 U/mL penicillin and 100 U/mL streptomycin, and washed twice.

Generation of DCs from PBMCs
DCs were cultured as described previously[6,7] with slight modifications. PBMCs were suspended in DC culture medium (AIMV), plated at a density of 2×10^7 cells/well in 6-well polystyrene culture plates, and cultured overnight at 37 ℃ in 950 ml/L air/50 ml/L CO_2. Nonadherent cells were removed by gently swirling the plate, and the adherent cells were cultured in AIMV containing 1 000 U/mL recombinant human GM-CSF and 500 U/mL recombinant human IL-4 at 37℃ in 950 ml/L air/50 ml/L CO_2 and refed daily with half volumes of fresh medium. Cells and culture supernatants were harvested on d 3,5,7,9,11, 13, and 15. Where indicated, TNF-α (20 ng/mL) was added on d 7, and the cells and supernatant were harvested on d 9.

Flow cytometric analysis
The phenotype of harvested DCs was analyzed by flow cytometry (Becton Dickinson, FACScalibur). Cells (5×10^5) were suspended in PBS, centrifuged at 313 r/min for 5 min at 4℃, incubated for 30 min at 4℃ with fluorescent monoclonal antibody, and fixed in 4 g/L paraformaldehyde.

IL-12 detection
IL-12 concentration in cell supernatants was assayed by ELISA, using standard curves according to the manufacturer's instructions.

Allogeneic mixed lymphocyte reaction
To test T cell stimulatory function of DCs, DCs were irradiated with 60Co (3 000 rad), suspended in AIMV and placed in 96-well flat bottom culture plates at densities of 0.5, 1.0, and 2.5×10^4 cells/well. Responder T cells were added to each well, at a density of 5×10^5 cells/well, and cultured for 120 h. The ratio of DC:T was 1:20, 1:50, and 1:100, and each assay was performed in triplicate. T cells plated without DCs were utilized as negative controls. During the last 16 h of incubation, 1Ci/well of [3H] thymidine was added. On d 5, the cells were harvested, and the amounts of [3H] thymidine incorporated into responder cells were counted with a beta counter.

Isolation of CD8+ T cells
Purified populations of T cells were isolated from PBMCs using magnetic beads. Briefly, PBMCs were incubated with anti-CD8 MACS (Miltenyi Biotech, Germany) according to the manufacturer's protocol. Cells retained by MACS beads were regarded as CD8 positive cells, with purity greater than 90%.

Stimulation of PBMCs with synthetic peptide
PBMCs from patients and normal donors were plated in 24-well plates at densities of 2×10^6 cells/well, in 2 mL RPMI1 640 containing IL-2 (50 mg/L). Synthetic peptides were added to the cell cultures at a final concentration of 20 mg/L. As a negative control, DMSO alone was added to the wells. After 1 h, 0.7 μL Golgistop was added per mL culture medium, cells were collected 4 h later, and intracellular cytokine stain (ICCS) was applied.

Intracellular cytokine stain assay
Harvested cells were washed twice with PBS, 10 μL FITC-labelled mouse anti-human CD8 Ab was added to each tube, and the tubes were incubated in the dark on ice for 30 min. To each tube 250 μL FACS permeabilization solution was added, and the tubes were incubated for 20 min on ice in the dark. Cells were washed twice with 1 mL/tube FACS perm-wash and incubated with PE-conjugated mouse monoclonal antibody to human IFN-γ, IL-2, or TNF-α for 30 min on ice in the dark. The cells were washed with FACS perm-wash solution, PBS + 1 g/L BSA was added, and the cells were loaded onto a FACS calibur flow cytometer within 24 h, with data analysis performed using Cell Quest software (Becton Dickinson). A total of 400 000 events were measured in each analysis. PE-conjugated mouse Ab was used as isotype controls. A lymphocyte gate was set to exclude monocytes, debris and dead cells.

CTL generation
CD8+ responders for peptide-specific CTL were generated from nonadherent PBMCs. CD8+ T cells were stimulated with DCs loaded with peptide at a stimulator-to-responder (S:R) ratio of 1:30. These cells were cultured in RPMI containing 100 g/L fetal calf serum (FCS) and IL-2 (50 mg/L). Responders were restimulated every 5 d with DCs pulsed with peptide. As controls, CD8+ T cells were stimulated with unpulsed DC. Six h before harvesting, 0.7 μL Golgistop was added to per mL culture medium. On d 10, CD8+T cells were harvested, ICCS was applied, and CTL cytotoxicity assays were performed.

CTL cytotoxicity assay
HLA-A2 restricted antigen recognition by CTL was assessed by a standard cytotox 96 non-radioactive cytotoxicity assay. Recognition of HBcAg18-27 peptide by CTL was assessed using T2 cells preincubated for 4 h with 20 μg/mL peptide. Target cells were resuspended at a density of 1×10^5 cells/mL, thus making the ratios of effectors to target cells 30:1, 10:1, and 3:1, with a triplicate set of wells prepared for each ratio and for the controls. The percent of lyses was calculated as:

$$\text{Percent of lysis (\%)} = \frac{100 \times A \text{ (experimental-effector spontaneous-target spontaneous)}}{A \text{ (target maximum-target spontaneous)}}$$

Statistical analysis
Result were expressed as mean±SD and analyzed using the Student's *t* test. *P*<0.05 was regarded as statistically significant.

RESULTS

Detection of DC surface markers
PBMCs were isolated from patients and healthy donors and cultured overnight. After removal of the nonadherent cells, the remaining adherent monocytes were cultured in AIMV containing GM-CSF and IL-4. Cell cultures were observed after 24 h, becoming larger after 48 h and exhibiting DC morphology with veiled processes and dendrites (Figure 1). The yields of DCs from hepatitis B patients and normal donors did not differ significantly.
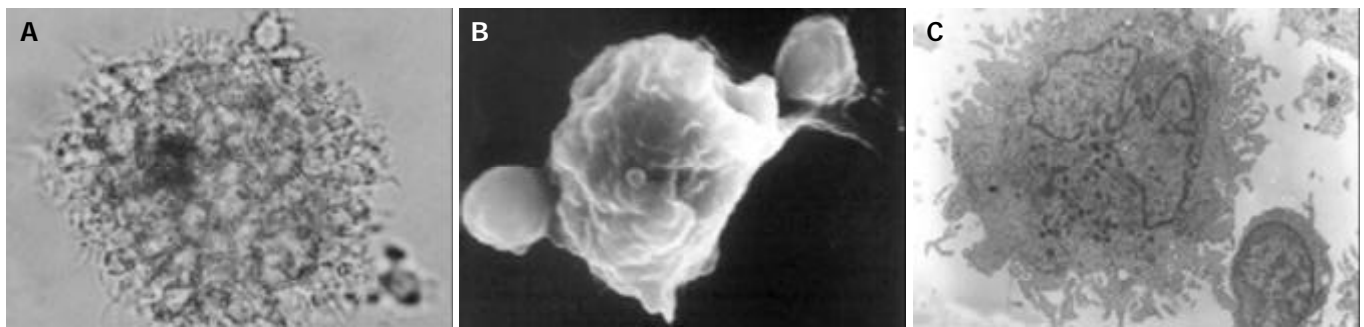
Figure 1 Morphology of dendritic cells after 7 and 9 d. A: Cluster of DCs after 9 d (light microscope, ×100); B: A DC on day 7 (scanning electron microscope, ×5 000); C: A DC on day 7 (transmitting electron microscope, ×5 000).

DCs were identified by their typical morphology and by CD86/HLA-DR double positive expression. These cells were harvested and counted, and surface markers were measured over time. The number of DCs peaked on d 9, decreasing gradually thereafter. The expression of DC- related cell markers was first detected on d 3. After cultured for 7 d with GM-CSF and IL-4, these DCs expressed costimulatory and MHC molecules, showing that cells derived from both patients and controls were morphologically compatible with DCs. Among the MHC and costimulatory molecules examined, we found that CD80 expression in patients with hepatitis B was weaker than that in normal donors (Table 1).

Table 1 Phenotype of DCs from HB patients and normal donors (n=10,%, mean±SD)

DC Antigen	Positive DCs of HB patients	Positive DCs of normal donors	P
CD86	89.89±1.14	91.17±3.41	0.633
CD80	36.86±2.30	59.87±6.31	0.021
CD1a	23.25±7.04	32.92±4.58	0.405
HLA-DR	97.29±1.09	97.11±1.14	0.852
CD83	23.25±7.34	33.18±11.12	0.265

Responses to TNF-a in DCs from HBV patients and healthy donors
Following addition of 20 μg/mL TNF-α to the culture medium on the 5th d of culture, the cells and culture supernatants were harvested 48 h later. When cell phenotypes were assayed by flow cytometry, we found that the expression of CD83 was weaker in cells cultured in the absence of TNF-α than in its presence. However, culture in the presence of TNF-α did not alter the expression of CD86, CD80 or HLA-DR. While production of IL-12 by cultured DCs from hepatitis B patients and healthy donors did not differ, the secretion of IL-12 was significantly increased in cells cultured with TNF-α (Figure 2).
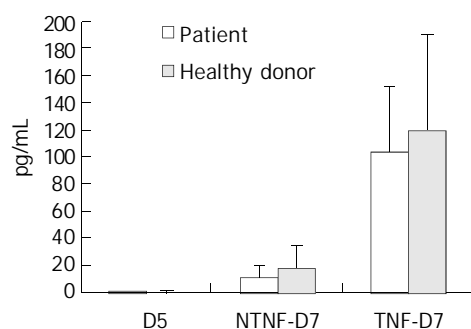

Figure 2 Effect of TNF-α on DC secretion of IL-12.

DCs from HB patients and healthy donors were cultured for 5 d, at which time TNF-α was added to some of the cultures

(TNF-D7) but not to others (NTNF-D7), and incubation was continued for an additional 2 d. IL-12 secretion was measured on d 5 and 7. Each bar represents mean±SD of DCs from 6 different individuals.

Immune stimulatory activity of DCs
When we tested T cell-stimulatory activity of DCs in allogeneic MLR, we found that patients with chronic hepatitis B tended to have decreased T cell-stimulatory activity compared with normal donors, but the difference did not attain statistical significance (Figure 3).
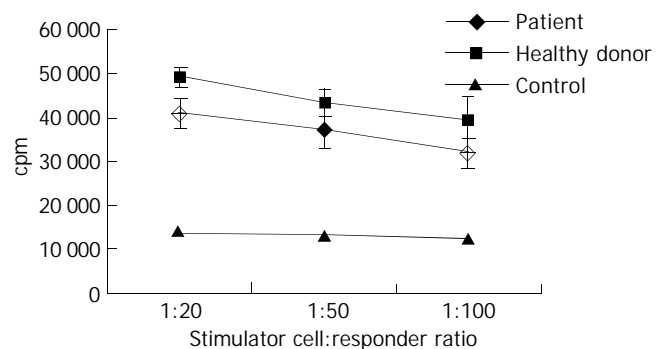

Figure 3 MLR of DCs against allogeneic T cells.

Each MLR was set up in triplicate in flat-bottom 96-well plates. The responder T cells were obtained from a healthy donor, while irradiated DCs were used as stimulators at different ratios to T cells. Each point represents the mean±SD. of measurements from 6 different individuals.

T cell memory response to HBcAg18-27 CTL epitope
PBMCs isolated from patients with chronic hepatitis B (CHB) and acute hepatitis B (AHB) and from normal donors were incubated with HBcAg 18-27 peptide for 6 h, and ICCS was used to determine the frequency of HBcAg 18-27 peptide reactive T cells secreting cytokines. We found that stimulated PBMCs from the AHB group produced significantly stronger T cell memory reactions than PBMCs from either of the other groups (P<0.05) (Table 2).

DCs from CHB patients induced specific immune responses of CD8+ T cells
DCs primed with HBcAg18-27 peptide were cultured with lymphocytes for 10 d to determine whether peptide-reactive T cells were able to secrete various cytokines, including IFN-γ, IL-2 and TNF-α. Using the ICCS assay, we found that DCs from CHB patients induced peptide-reactive T cells to secrete cytokines (Figure 4), to a significantly greater degree than that secreted by peptide-stimulated PBMCs (P<0.05). We also

observed significant differences between DCs and PBMCs of CHB patients (Table 3).

Table 2 Memory immune responses of PBMCs from patients with chronic hepatitis B (CHB), acute hepatitis B (AHB) and normal donors (mean±SD)

Group	n	Percent CD8+T cells secreting cytokines		
		IFN-γ/CD8	IL-2/CD8	TNF-α/CD8
CHB	7	0.18±0.14	0.13±0.05	0.37±0.18
AHB	4	4.26±2.49	4.80±2.23	4.57±2.29
Donor	6	0.28±0.13	0.59±0.27	0.68±0.33
P value[a]		0.019	0.024	0.010
P value[c]		0.013	0.031	0.010

[a]$P<0.05$ AHB *vs* CHB. [c]$P<0.05$ AHB *vs* Donor.

Table 3 CD8+T cell immune responses induced by peptide-pulsed DCs (mean±SD)

Group	n	Percent of CD8+ T cells secreting cytokines (%)		
		IFN-γ/CD8	IL-2/CD8	TNF-α/CD8
CHB[1]	7	0.28±0.15	0.46±0.13	0.68±0.15
CHB[2]	4	0.59±0.39	0.74±0.16	1.52±0.38
P value[a]		0.043	0.049	0.028

1: T cells induced by unpulsed DCs; 2: T cells induced by peptide-pulsed DCs; a: comparison of CHB[1] and CHB[2].
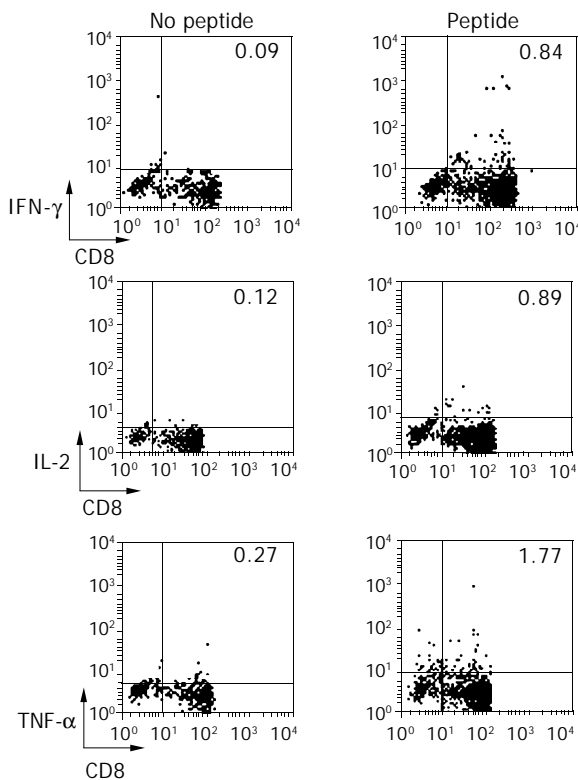

Figure 4 Cytokine secretion of peptide-reactive T cells induced by DCs from one CHB patient. T cells from one CHB patient was incubated with autologous DCs pulsed with the HBV-specific peptide HBcAg 18-27 (Peptide) or without peptide (No peptide), and T cell response was detected by flow cytometry by measuring cytokine secretion by the activated T cells. The dot-plots show levels of intracellular staining for IFN-γ, IL-2 and TNF-α (y-axis) and surface CD8 molecule (x-axis). The number in the upper-right quadrant indicates the percentage of CD8-positive T cells that secret cytokines.

CTL cytotoxicity induced by DCs loaded with peptide

Target cells were divided into 2 groups, with one group incubated with peptide and the other group without. CTL cytotoxicity of the DCs from CHB patients against T cells incubated with peptide was (57.28±20.00)%, (47.54±20.70)%, and (21.38±12.86)% at effector to target cell ratios of 30:1, 10:1, and 3:1, respectively, while CTL cytotoxicity of these same DCs against T cells incubated without peptide was (30.38±10.00)%, (26.99±12.72)%, and (13.74±3.22)%, respectively (Figure 5).
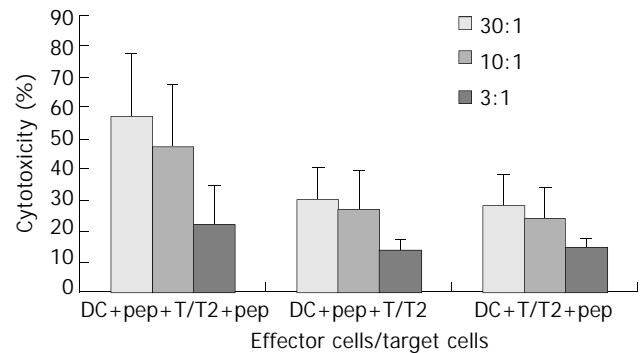

Figure 5 T cell cytotoxicity induced by DCs in CHB patients. DC+pep+T, T cells induced by DCs loaded with specific peptide; DC+T, T cells induced by DCs without peptide; T2+pep, peptide-loaded target cells; T2, target cells.

DISCUSSION

DCs are the most potent antigen presenting cells crucial for activating CD8+ killer T cells and CD4+ helper T cells. DCs release bioactive cytokine IL-12, which can stimulate NK cells, induce Th1 type cytokine production and foster the development of cytotoxic T lymphocytes. DCs may thus be a powerful natural adjuvant for the treatment of tumors and viral infections. It is now known that the function of DCs is not fixed, depending on alterations in the cellular environment. Alterations in DC function may result from the effects of anti-inflammatory cytokines, including IL-10 and TGF-β, and on the characteristics of pathogens.

It was observed that, the functional activity of DCs was decreased, as measured by the stimulation of allogeneic T cell proliferation. In patients with chronic hepatitis B, however, it was unclear if DCs could act as natural adjuvants. In HBV transgenic (Tg) mice, DC function was normal, and there were CTLs specific for HBsAg, which were functionally quiescent. When cytokine-activated DCs were administered to these Tg mice, tolerance was broken, and antiviral reactions were induced[2]. In contrast, the expression of MHC II (I a) and CD86 and the ability of DCs to induce cell proliferation were lower in Tg than in normal mice[8].

In this study, we isolated PBMCs from the peripheral blood of patients with chronic hepatitis B infection and from healthy donors and compared the functional activity of their DCs. We found that, while CD80 expression was lower on DCs from patients than on those from healthy donors, other surface markers including HLA and costimulatory molecules were expressed to an equal extent. Functionally, DCs from CHB patients were able to stimulate the proliferation of allogeneic T cells, but to a lower extent than observed with DCs from non-CHB donors.

T cell activation requires costimulatory molecules (*e.g.*, CD28-B7), which provide a second signal. The B7 family is comprised primarily of B7-1 (CD80) and B7-2 (CD86). Although their function is not fully known, several studies have shown that CD80 signals preferentially promote development of Th1 cells, whereas CD86 signals promote Th2 development. While

CD80 gene knockout mice have a normal immunoglobulin superfamily repertoire, a complete deficiency of CD86 would destroy humoral immunity. B7 receptors have two ligands. CD28 provides a costimulatory signal essential to T cell activation, whereas CTLA-4 blocks T cell proliferation. CTLA-4 bound with greater affinity to CD80 than to CD86, suggesting that the binding of CD80 tends to inhibit T cell proliferation[9-11]. Our finding, that CD80 expression by DCs from patients with chronic hepatitis B was weaker than that from healthy donors, might be related to the inhibition of T cell activation seen in these patients and to the decreased function of DCs from these patients observed in our MLR assay. In addition, our results confirmed Akbar's study[7], in that the decreased functional activity of patient DCs results in the inability of these cells to present antigens to T cells, thus leading to reduced induction of a specific cytotoxic reaction. This, in turn, resulted in a lower rate of killing of infected cells and a reduction in the suppression of viral replication, finally leading to a state of persistent infection.

When pathogens invade a host, a potent immune response is produced to eliminate the pathogens. At the end stage of this immune response, the majority of effector T and B cells gradually undergo apoptosis, while a smaller number differentiate into long-lived memory T or B cells. Memory T cells produce vigorous secondary responses to antigen and rapidly eliminate pathogens. For example, the infected cells were cytolysed by CTLs. On the other hand, the primary difference between memory and naïve T cells is that, when they are activated, the former had higher reactivity to antigens and secreted more cytokines[12-14]. Thus, when an individual is infected with HBV, certain soluble products of the immune response, especially IFN-γ, IL-2, and TNF-α, can suppress HBV gene expression, as well as replication in vivo.

Hepatocellular HBV gene expression has been shown to be profoundly suppressed by non-cytolytic regulatory signals delivered by HBsAg-specific CTL through their secretion of IFN-γ and induction of TNF-α following antigen recognition. These effects were mediated by a posttranscriptional mechanism that selectively accelerates the degradation of cytoplasmic HBV mRNA[15]. We therefore assayed the cytokines secreted by CD8+T cells to illuminate the immune response of individuals to viral infection. We found that PBMCs from patients with CHB and AHB and from normal donors could be stimulated by HBcAg18-27 peptide. However, stimulated PBMCs from patients with AHB produced stronger memory reactions than those from patients with CHB or healthy donors, suggesting that AHB PBMCs have potent memory immune reactions to this specific antigen, whereas CHB PBMCs are at least partially tolerant to this antigen. The mechanism of tolerance includes factors from the host and from the virus. New-born babies contaminated by HBV transmitted from their mothers were in a state of immune tolerance to HBV and about 90% carry HBV as a persistent infection.

T cells play an important role in the immune system. Not only do they have effector functions, but also they are the major regulators of immune function. T cell activation requires two signals, one from the T cell receptor that recognizes the complex of MHC and antigen on the surfaces of antigen presenting cells (APCs), and the other from costimulatory molecules such as CD28-B7. To determine whether the immune tolerance of DCs from CHB patients could be broken, we primed DCs with HBcAg18-27 and incubated them with lymphocytes, and we assayed CTL generation. Our finding, that an antigen-specific T cell reaction was induced when these peptide-primed DCs were co-cultured with CD8+ T cells, and that the cytotoxic activity of CTLs against target cells cultured with peptide was higher than that against target cells cultured without peptide, suggested that DCs from patients with CHB could break immune tolerance and induce an HBV antigen-specific T cell reactions.

DCs have great potential in anti-viral therapy as antigen presenting cells. Our findings showed that, although the function of patient DCs was lower than that of control DCs, the former still expressed signals necessary for T cell activation, released of IL-12 and stimulation of allogeneic T cell proliferation. Moreover DCs from these patients could break immune tolerance to induce HBV antigen-specific T cell responses. IL-12 is a critical cytokine secreted by DCs, which can induce the production of specific T cells, suggesting that TNF-α is an important factor in immunotherapy. Thus, our findings suggest that DCs originating from cytokine activated PBMCs of CHB patients can be utilized in immunotherapy, which will be a potential treatment for hepatitis B.

REFERENCES

1   **Chisari FV**. Cytotoxic T cells and viral hepatitis. *J Clin Invest* 1997; **99**: 1472-1477

2   **Hart DN**. Dendritic cells: unique leukocyte population which control the primary immune response. *Blood* 1997; **90**: 3245-3287

3   **Steinman RM**. The dendritic cell system and its role in immunogenicity. *Annu Rev Immunol* 1991; **9**: 271-296

4   **Rescigno M**, Granucci F, Ricciardi-Castagnoli P. Dendritic cells at the end of the millennium. *Immunol Cell Biol* 1999; **77**: 404-410

5   **Shimizu Y**, Guidotti LG, Fowler P, Chisari FV. Dendritic cell immunization breaks cytotoxic T lymphocyte tolerance in hepatitis B virus transgenic mice. *J Immunol* 1998; **161**: 4520-4529

6   **Romani N**, Reider D, Heuer M, Ebner S, Kampgen E, Eibl B, Niederwieser D, Schuler G. Generation of mature dendritic cells from human blood. An improved method with special regard to clinical applicability. *J Immunol Methods* 1996; **196**: 137-151

7   **Romani N**, Gruner S, Brang D, Kampgen E, Lenz A, Trockenbacher B, Konwalinka G, Fritsch PO, Steinman RM, Schuler G. Proliferating dendritic cell progenitors in human blood. *J Exp Med* 1994; **180**: 83-93

8   **Akbar SM**, Inaba K, Onji M. Upregulation of MHC class II antigen on dendritic cells from hepatitis B virus transgeneic mice by interferon-γ: abrogation of immune response defect to a T-cell-dependent antigen. *Immunology* 1996; **87**: 519-527

9   **Freeman GJ**, Boussiotis VA, Anumanthan A, Bernstein GM, Ke XY, Rennert PD, Gray GS, Gribben JG, Nadler LM. B7-1and B7-2 do not deliver identical costimulatory signals, since B7-2 but not B7-1 preferentially costimulates the initial production of IL-4. *Immunity* 1995; **2**: 523-532

10 **Kuchroo VK**, Das MP, Brown JA, Ranger AM, Zamvil SS, Sobel RA, Weiner HL, Nabavi N, Glimcher LH. B7-1and B7-2 costimulatory molecules activate differentially the Th1/Th2 developmental pathways: application to autoimmune disease therapy. *Cell* 1995; **80**: 707-718

11 **Coyle AJ**, Gutierrez-Ramos JC. The expanding B7 superfamily: increasing complexity in costimulatory signals regulating T cell function. *Nat Immunol* 2001; **2**: 203-209

12 **Ahmed R**, Gray D. Immunological memory and protective immunity: understanding their relation. *Science* 1996; **272**: 54-60

13 **Sprent J**, Surh CD. Generation and maintenance of memory T cells. *Curr Opin Immunol* 2001; **13**: 248-254

14 **Champangne P**, Dumont AR, Sekaly RP. Learning to remember: generation and maintenance of T-cell memory. *DNA Cell Biol* 2001; **20**: 745-760

15 **Chisari FV**. Viruses, immunity, and cancer: lessons from hepatitis B. *Am J Pathol* 2000; **156**: 1117-1132

• VIRAL HEPATITIS •

Selection of a peptide mimicking neutralization epitope of hepatitis E virus with phage peptide display technology

Ying Gu, Jun Zhang, Ying-Bing Wang, Shao-Wei Li, Hai-Jie Yang, Wen-Xin Luo, Ning-Shao Xia

Ying Gu, Jun Zhang, Ying-Bing Wang, Shao-Wei Li, Hai-Jie Yang, Wen-Xin Luo, Ning-Shao Xia, The Key Laboratory of Ministry of Education for Cell Biology and Tumor Cell Engineering, Xiamen University, Xiamen 361005, Fujian Province, China
Supported by Grant from Science and Technology Projects of Fujian Province, China; No.2002 F013; Excellent Scholar Incubation Plan of the Ministry of Education, China
Correspondence to: Ning-Shao Xia, The Key Laboratory of Ministry of Education for Cell Biology and Tumor Cell Engineering, Xiamen University, Xiamen 361005, Fujian Province, China. nsxia@jingxian.xmu.edu.cn
Telephone: +86-592-2184110   **Fax:** +86-592-2184110
Received: 2003-10-27   **Accepted:** 2003-12-08

Abstract

AIM: To select the peptide mimicking the neutralization epitope of hepatitis E virus which bound to non-type-specific and conformational monoclonal antibodies (mAbs) 8C11 and 8H3 fromed 7-peptide phage display library, and expressed the peptide recombinant with HBcAg in *E.coli*, and to observe whether the recombinant HBcAg could still form virus like particle (VLP) and to test the activation of the recombinant polyprotein and chemo-synthesized peptide that was selected by mAb 8H3.

METHODS: 8C11 and 8H3 were used to screen for binding peptides through a 7-peptide phage display library. After 4 rounds of panning, monoclonal phages were selected and sequenced. The obtained dominant peptide coding sequences was then synthesized and inserted into amino acid 78 to 83 of hepatitis B core antigen (HBcAg), and then expressed in *E.coli*. Activity of the recombinant proteins was detected by Western blotting, VLPs of the recombinant polyproteins were tested by transmission electron microscopy and binding activity of the chemo-synthesized peptide was confirmed by BIAcore biosensor.

RESULTS: Twenty-one positive monoclonal phages (10 for 8C11, and 11 for 8H3) were selected and the inserted fragments were sequenced. The DNA sequence coding for the obtained dominant peptides 8C11 (N′-His-Pro-Thr-Leu-Leu-Arg-Ile-C′, named 8C11A) and 8H3 (N′-Ser-Ile-Leu-Pro- Tyr-Pro-Tyr-C′, named 8H3A) were then synthesized and cloned to the HBcAg vector, then expressed in *E.coli*. The recombinant proteins aggregated into homodimer or polymer on SDS-PAGE, and could bind to mAb 8C11 and 8H3 in Western blotting. At the same time, the recombinant polyprotein could form virus like particles (VLPs), which could be visualized on electron micrograph. The dominant peptide 8H3A selected by mAb 8H3 was further chemo-synthesized, and its binding to mAb 8H3 could be detected by BIAcore biosensor.

CONCLUSION: These results implicate that conformational neutralizing epitope can be partially modeled by a short peptide, which provides a feasible route for subunit vaccine development.

INTRODUCTION

Hepatitis E is an acute hepatitis caused by hepatitis E virus (HEV) in developing countries, where it occurs sporadically and in an epidemic form. The causative agent, HEV, is transmitted primarily by the fecal-oral route, and it accounts for about 15-20% sporadic cases of acute hepatitis in China[1,2]. HEV is an icosahedron non-enveloped virus, and its genome is a single-stranded positive-sense, 3′-polyadenylated RNA about 7.5 kb in length. It contains 3 open reading frames (ORFs). ORF1 codes for a polyprotein of 1 693 amino acids and contains domains homologous to a viral methyltransferase, a papainlike cysteine protease, an RNA helicase, and an RNA-dependent RNA polymerase, and the most hypervariable region of HEV genome. ORF2 codes for the viral capsid protein of 660 amino acids, while ORF3 codes for a 123-amino-acid-long polypeptide with unknown function.

It has been proved that the major viral capsid protein encoded by ORF2 contains the protective epitope[3]. We recombined a fragment of HEV ORF2 and expressed the polypeptide named NE2 in *E.coli* recently[4], and proved it to be a protective antigen[5], which naturally forms homodimer by virtue of its interface domain[6]. Three anti-NE2 neutralization mAbs, 8C11, 8H3 and 13D8 were selected, which could recognize 2 separated neutralization conformational surface epitopes of HEV, 8C11 and 13D8 against one and 8H3 against the other. The 3 mAbs can neutralize HEV *in vitro* and *in vivo* test of Rhesus monkey[7-9].

8C11 and 8H3 were used to screen binding peptides from a heptapeptide phage display library, which could mimic the 2 neutralizing epitopes of HEV binding to 8C11 and 8H3 respectively. The obtained dominant peptides' DNA sequences were then synthesized and cloned into amino acid 78 to 83 of hepatitis B core antigen (HBcAg), then expressed in *E.coli*. While it has been proven that HBcAg could be expressed in eukaryocytes or prokarocytes, and assembled into VLP automatically. The inserted sequence between amino acids 73 and 94 could be expressed on the HBcAg VLP surface[10]. Because HBcAg is an immunodominant immunogen[11], which results in the immunodominance of the insertion, we expressed the linear epitopes, which could conformationally mimic epitope on the surface of HBcAg, resulting in a VLP antigen, and prove its activity. This assay would not only mimic the neutralizing epitope of HEV but also provide insights into a novel route for subunit vaccine development.

MATERIALS AND METHODS

Monoclonal antibodies

8C11 and 8H3 mAbs, which could conformationally bind to neutralizing epitopes of HEV were prepared in our

laboratory[7,9]. Affinity purified antibody phosphatase labeled goat anti-mouse IgG (H+L) was from Kirkegaard & Perry Laboratory (2 Cessua Court, Gaithersburg Maryland 20879, USA).

Affinity selection and amplification of peptide library
Heptapeptide phage display library and host strain *E.coli* ER2738 were purchased from New England BioLabs Company. Anti-HEV mAbs binding phages were isolated from the phage display library by successive cycles of selection and amplification. The biopanning procedure was essentially used as described in the phage display library user manual. Briefly, mAbs 8C11 and 8H3 (100 μg/mL) were coated on 96-well microtiter plates. After blocked with 20 g/L BSA, 100 μL diluted phage (10 uL of the original library) was piped onto the coated plate and shaked gently for 1 h at room temperature, the plates were washed for 10 times with PBST (10 g/L Tween 20). The bound phages were eluted with 100 μL 10 mmol/L Gly-Cl (pH 2.2), 1 mg/mL BSA, rocked gently for 10 min. The eluate was piped into a microcentrifuge tube and neutralized with 10 μL 1 mol/L Tris-HCl (pH 9.1). The eluate was added to 20 mL ER2738 culture and incubated at 37 ℃ with vigorous shaking for 4.5 h. The culture was transferred to a centrifuge tube and spun for 10 min at 10 000 g at 4 ℃. The supernatant was collected and 1/6 volume of PEG/NaCl (200 g/L PEG8000, 2.5 mol/L NaCl) was added. The phage was allowed to precipitate at 4 ℃ overnight. PEG precipitation was spun for 15 min at 10 000 g at 4 ℃. The pellet was re-suspended in 1 mL PBS, and re-precipitated with PEG/NaCl. Finally the pellet was suspended in 200 μL PBS, and stored at 4 ℃. The amplified eluate was titered as general methods. The concentration of target mAbs was lowered to 50 μg/mL, at the same time the concentration of Tween-20 was risen to 50 g/L in the washing step, then was panned 3 more times by repeating the above steps. After 4 rounds panning, individual monoclones were sequenced. The single-stranded DNA of M13 phages was purified by using the M13 mini kit purchased from Shanghai Huashun Biotech Ltd, and then sequenced by Shanghai Boya Ltd.

Construction of recombinant expression vector for peptide
The recombinant expression vector named pC149-mut was composed in our laboratory. The peptide of amino acids 1 to 149 of HBcAg expressed in *E.coli* formed viral like particles (VLPs). The amino acid residues 78 to 83 were exposed at the VLP's surface. According to this we cloned the HBcAg's genome of amino acid residues 1 to 149 into the expression vector pTO-T7[12] of *E.coli*, and designed a linker to replace the immunodominant epitope located at 79 to 80aa of HBc and composed the mutant vector pC149-mut. After exogenous gene was inserted into the amino acid residues 78 to 83, recombinant C antigen was still able to form VLP and expose the exogenous epitope.

We designed the primer (Table 1) according to the dominant sequence of selected monoclonal phages, and the linker sequence of pC149-mut vector. Therefore, we could insert heptapeptide exogenome into the vector and co-express it with HBcAg using 8C11AFP or 8H3AFP as a former primer and

149 mutRP as a lower primer, and using the pC149-mut vector as a template. PCR was carried out after pre-denaturation at 94 ℃ for 5 min, 25 cycles of denaturation at 94 ℃ for 50 s, annealing at 56 ℃ for 50 s, and extension at 72 ℃ for 25 s, then extension at 72 ℃ for 10 min. The PCR fragment was cloned into pMD 18-T vector and formed positive clones containing the genome of peptide 8C11A (CATCCTACTC TTTTGCGTATT), which could bind to mAb 8C11 or the genome of peptide 8H3A (TCTATTCTGCCGTATCCTTAT), which could bind to mAb 8H3. Then they were digested with *Bam*H I and *Eco*R I, and the product fragment was linked into the pC149-mut vector to compose the expression vector named pC149-mut-8C11A or pC149-mut-8H3A (Figure 1).

Expression and purification of recombinant polyprotein
Host stain ER2566 was cultured and transformed with the recombinant vector pC149-mut-8C11A or pC149-mut-8H3A in LB culture medium at 37 ℃ in a shaker, till the A_{600} reached 0.8-1.0, then the culture was incubated with 0.2 mmol/L IPTG for 6 h at 37 ℃. The cells were spun to be collected and were disintegrated by an ultrasonic disintegrator (Uilbra-Cell VGX500 of SONICS & MATERIALS Co.). The insoluble protein was spun and collected, then suspended and deposited 2 times into 10 g/L Triton X-200. The pellet was finally suspended into buffer A (4 mol/L Urea, 20 mmol/L Tris-HCl pH 8.5, 5 mmol/L EDTA, 100 mmol/L NaCl), dialysed in PBS overnight. The lysate was spun and collected.

Western blotting
Boiled supernatant of ultrasonic lysate and boiled deposition of ultrasonic lysate and control samples (the expression of pC149-mut could not react with mAbs, and the recombinant polyprotein NE2 was used to select mAbs including 8C11 and 8H3[7,9]) were dissolved in 120 g/L SDS-PAGE, transferred to a nitrocellulose membrane. Each contained one lane of the protein molecular mass mark between 18.3 and 215 ku. The membrane containing proteins with 5 g/L non-fat dry milk as blocking solution was incubated for 90 min and reacted with the test mAb 8H3 or 8C11 diluted in 5 g/L non-fat dry milk. The immunocomplexes were detected by using Ap-labeled goat-anti-mouse IgG, BCIP and NBT as substrates.

Transmission electron microscopy of chimeric VLPs
After renatured by the methods described above, the particles were adsorbed to carbon-coated grids, stained with 2 g/L uranyl acetate, and examined by JEM-100CXII electron microscope at about ×100 000 magnification.

Active analysis of recombinant proteins by BIAcore biosensor
Heptapeptide named 8H3A (N'-Ser-Ile-Leu-Pro-Tyr-Pro-Tyr-C') was synthesized and purified by Xi'an Meilian Ltd (Xi'an, China). Then the biosensor chip was coupled with anti-mouse Fc, which was carried out according to the user manual. Briefly, the sensor chip CM5 with CM Dextran on its reaction-surface was activated with EDC and NHS, and then the flow cells were treated with a standard amine-coupling reagent (injecting 10 mm/L NaOAc, pH4.8, instead of protein) or with amine-coupling reagents and anti-mouse Fc polyclonal antibody. The

Table 1 Primers for expression vector of mimic peptide

Primer ID	Primer sequence
8C11AFP	GGATCC<u>CATCCTACTCTTTTGCGTATT</u>GGTGGTGGAGGTTCAGG
8H3AFP	GGATCC<u>TCTATTCTGCCGTATCCTTAT</u>GGTGGTGGAGGTTCAGG
149 mutRP	GAATTCTTAAACAACAGTAGTTT

The underlined sequences are the insert genes coding the selected peptides.

coupling density of the antibody was 900 RU. Experiments were run at 25 ℃. After mAb 8H3 was bound to anti-mouse Fc antibody, peptide 8H3A was injected. The data of association and dissociation indicating the reaction between mAb 8H3 and peptide 8H3A were collected. Biacore X biosensor, CM5 sensor chip and reagent of EDC & NHS were from Amersham Biosciences Company (Uppsala, Sweden).

RESULTS

Sequence characteristics of peptide binding to neutralizing mAb 8C11 or 8H3

After 4 rounds of biopanning, 21 monoclonal phages were selected for sequencing (in which 10 phage could bind to mAb 8C11, and the other 11 could bind to mAb 8H3). According to the DNA sequence, the peptide sequence of the phage displayed was made out (Figure 2). Heptapeptide with amino acid sequence HPTLLRI was dominant (50%) in the 10 monoclones bound to mAb 8C11. While in the 11 monoclones bound to mAb 8H3, the preponderant amino acid sequence was SILPYPY (27.3%). Furthermore, in the heptapeptide binding to mAb 8H3, the amino acid sequence of S*LP, S*P, S*L or LP was also more frequent, indicating that S, L and P would be more important to form the domain binding to mAb 8H3. Likewise, amino acids P, T and L were found to be more important in the interaction between peptide and mAb 8C11.
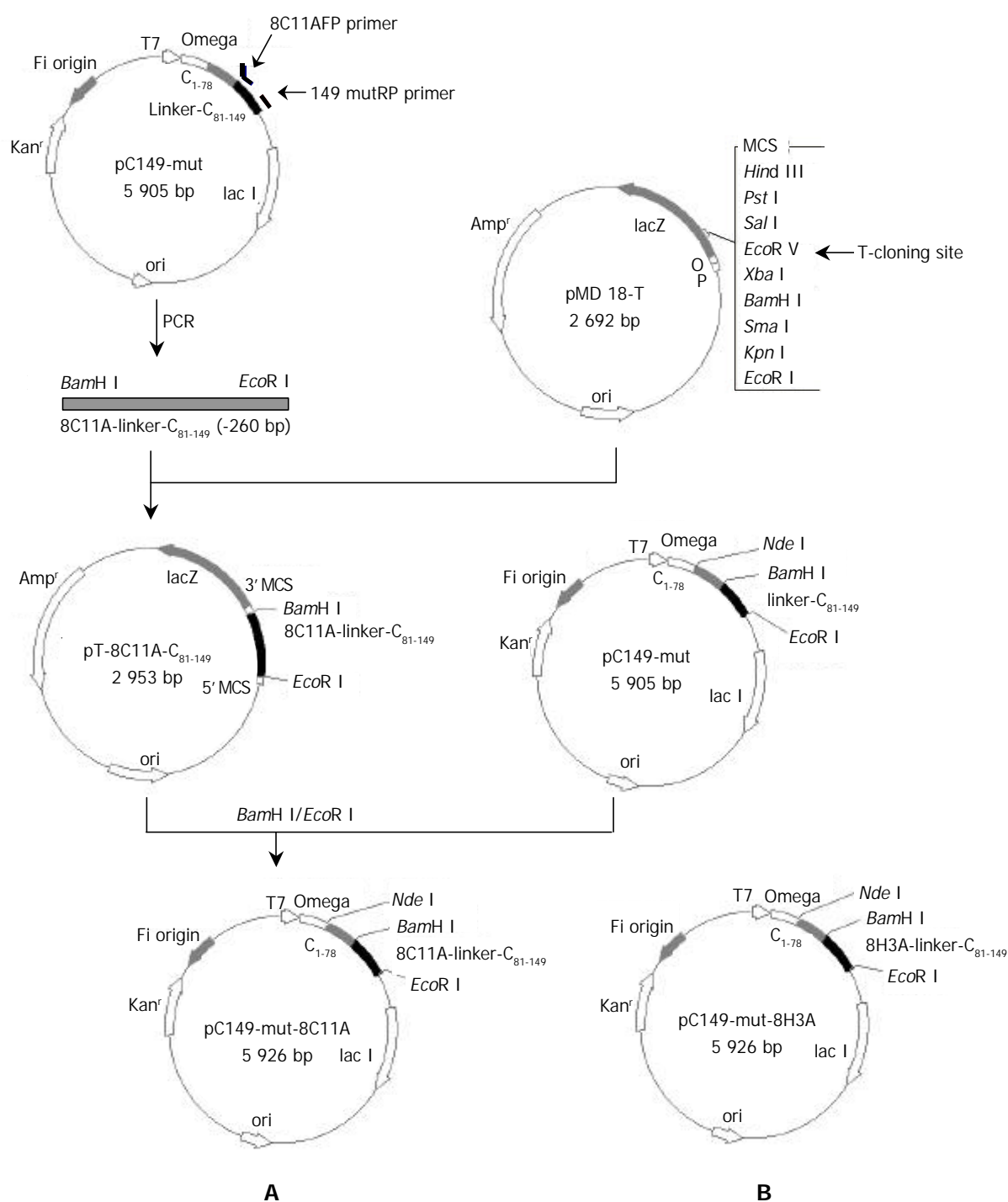

Figure 1 Expression vector construction of pC149-mut-8C11A and pC149-mut-8H3A. A: Construction of pC149-mut-8C11A, B: Map of pC149-mut-8H3A, which was constructed as pC149-mut-8C11A except using the primer 8H3AFP instead of 8C11AFP.
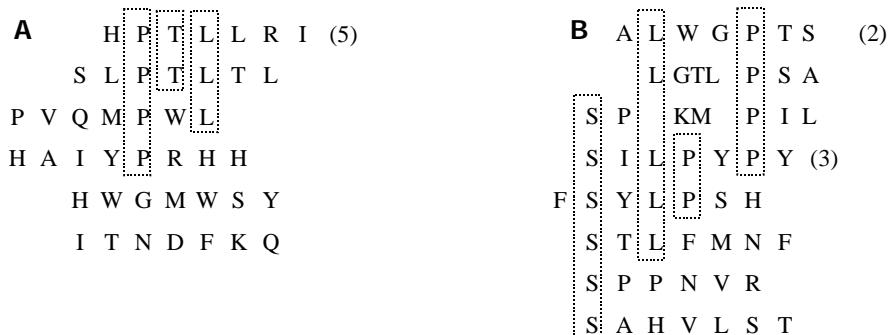
A

```
    H P T L L R I  (5)
    S L P T L T L
  P V Q M P W L
  H A I Y P R H H
      H W G M W S Y
      I T N D F K Q
```

B

```
  A L W G P T S   (2)
    L GTL  P S A
  S P  KM  P I L
  S I L P Y P Y  (3)
F S Y L P S H
  S T L F M N F
  S P P N V R
  S A H V L S T
```

Figure 2 Sequences of peptides selected by monoclonal antibodies. A: Selected by mAb 8C11, B: Selected by mAb 8H3.

Expression and western blotting of peptide mimic neutralization epitope

Dominant peptides 8C11A (N' -His-Pro-Thr-Leu-Leu-Arg-Ile-C') and 8H3A (N' -Ser-Ile-Leu-Pro-Tyr-Pro-Tyr-C') were cloned into the vector pC149-mut named C8C11A and C8H3A respectively, and expressed. The result of expression was shown in Figure 3. Recombinant polyprotein C8C11A was found in the insoluble cell pellet, and formed dimer (about M_r40 000 in mass) on the SDS-PAGE mainly while the monomer (about M_r20 000) was hard to be seen. As to the Western blotting result, it was the dimer that could interact with mAb 8C11 in the same level as the monomer of NE2 protein (about M_r29 000). C8H3A fusions were also found in the insoluble cell pellet. Beside the dimer, a monomer was in the majority, but only the -M_r40 000 dimer was able to bind to mAb 8H3 when tested by Western blotting.

Figure 3 Expression and Western blotting of pC149-mut-8C11A and pC149-mut-8H3A. A, C: SDS-PAGE, B, D: Western blotting of mAbs 8C11 and 8H3 respectively, A, B: pC149-mut-8C11A, C, D: pC149-mut-8H3A. 1, Protein molecular weight marker; 2, Supernatant of ultrasonic lysate; 3, Deposition of ultrasonic lysate; 4, C149-mut control; 5, Purified NE2 antigen

Electron micrograph of VLP

The renatured recombinant polyprotein particles were adsorbed to carbon-coated grids, stained with 20 g/L uranyl acetate, and examined with TEM. The recombinant HBcAg with 8C11A or 8H3A on its surface and HBcAg could form VLPs and VLPs' diameter was about 20 nm (Figure 4).

Figure 4 Virus like particles assemblied by recombinant protein C8C11A, C8H3A or C149 mut (Negative staining electron microscopy, ×100 000).

Figure 5 Binding curve of chemo-synthesized seven peptide 8H3A against monoclonal antibody 8H3 in BIAcore biosensor.

Interaction between chemo-synthesized heptapeptide 8H3A and mAb 8H3

The mAb 8H3 was bound to the anti-mouse Fc polyclonal antibody coupled on the cells of CM5 chip. After mAb 8H3 was bound to the anti-mouse Fc antibody, peptide 8H3A (1 mg/mL) was injected and the data of association and dissociation were collected. Chemo-synthesized heptapeptide 8H3A could bind to mAb 8H3, but not stably (Figure 5).

DISCUSSION

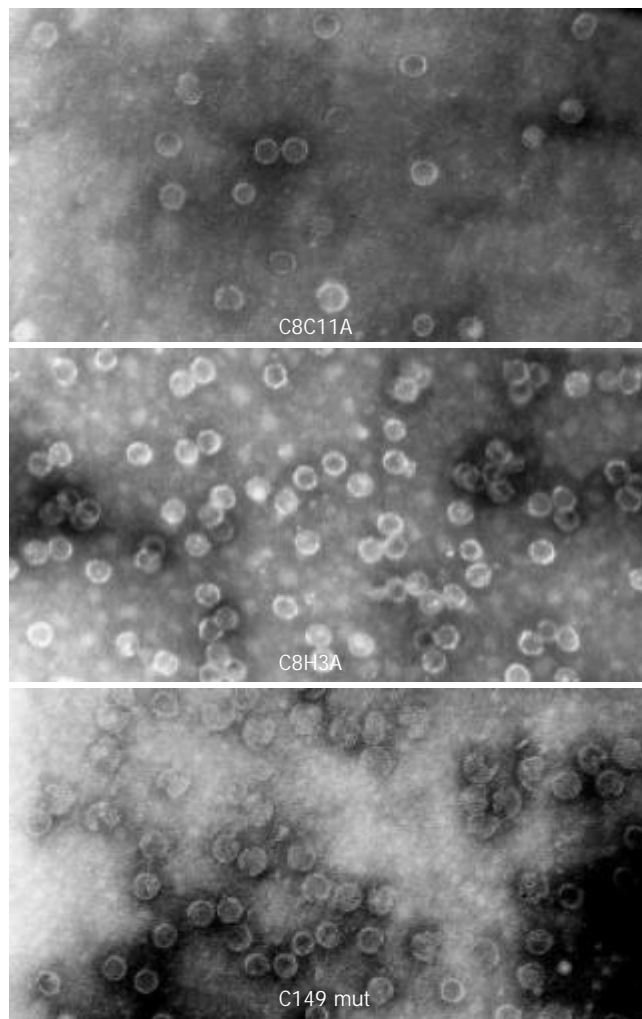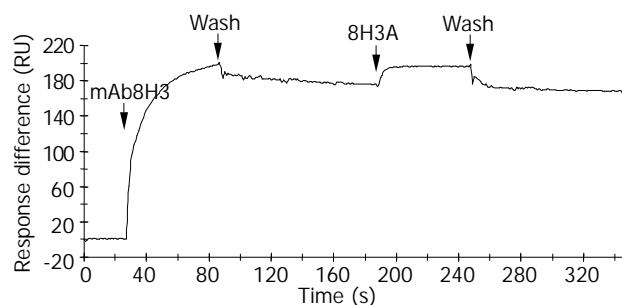Phage display technique has been widely used in constructing antibody library or biopanning of random peptides according to their biological activities, and in many other fields or so[13,14]. As a new technique, it makes use of the characteristics of the coat protein of the phage, that is, a peptide is expressed as a fusion with the phage coat protein pIII, resulting in the display of fused protein on the surface of virion. Phage display technique allows rapid identification and amplification of the peptide ligands for target molecules by the affinity of their specifical-binding. Recently, random peptide libraries displayed on phage have been widely used in many fields, such as identification and analysis of a peptide mimic the epitope of HIV[15] and HIV-1-infected cells[16], identification of enzyme inhibitors[17] and immunodepressants[18], and many antigens etc.[19-22]. Phage display technique is specially useful to mimic a variety of half-antigens and non-peptide target molecules' function, which is a very useful way to produce mimic peptide medication. Many reports have been available on the peptides mimicing epitope, which can neutralize *Neisseria meningitidis*[23,24] and many other bacteria to produce bacterial vaccines.

There are still no cell models of HEV, or effective methods to produce HEV artificially. Different sections of HEV capsid protein were expressed, and the structures of the recombinant polyproteins were analysed, which can help us to speculate the crude structure of HEV capsid. We cloned a section of HEV ORF2 (named NE2) and expressed this recombinant protein in *E.coli*. It was found that NE2 formed polymer spontaneously, from dimer to hexamer concretely. This was very similar to the assemble process of HEV capsid protein[4,25,26]. NE2 was used to immunize Rhesus monkey, and induce protective antibodies. The above findings indicate that polyprotein NE2 mimics the crude structure of HEV ORF2[4]. Monoclonal antibodies were selected by immunizing BALB/c mice with NE2[7,9], 3 of which named 8C11, 8H3 and 13D8 were identified to be mAbs which could recognize 2 different epitopes of HEV. These 3 mAbs were proved to be neutralizing mAb by *in vivo* neutralization test in rhesus. The 2 epitopes recognized by mAbs (1 bound to 8C11 and 13D8, and the other to 8H3) were tested to be conformational epitopes. We panned the random phage display heptapeptide library, which displayed the linear eptiope constructed by heptapeptide, and the peptides could mimic the neutralizing eptiope that could bind to the 2 mAbs (8C11 and 8H3). Furthermore, heptapeptides were recombined on HBcAg for expression in *E.coli*, and their activities were tested by Western blotting. The recombinant polyprotein expressed by plasmid pC149-mut-8C11A appeared to be the dimer of M_r 40 000 on SDS-PAGE, which could bind to mAb 8C11 similar to the monomer of NE2. While the production of plasmid pC149-mut-8H3A could form monomer (M_r 20 000) and dimer (M_r 40 000) on SDS-PAGE, and only the dimer could react with mAb on Western blotting. Maybe it is because that 7 amino acid peptide is too short, and to display it on the surface of recombinant HBcAg is in need of assistance of special conformation, HBcAg is a large protein while the monomer recombinant HBcAg can not display the exogenesis epitope of heptapeptide, so the activity of the monomer is not obvious.

The chemo-synthesized heptapeptide 8H3A could bind to mAb 8H3, but the binding was not stable. Comparing the dominant peptides' sequence with the primary structure of NE2, no same sequence was found, conforming that the epitopes recognized by mAbs 8C11 and 8H3 are not constructed by continuous amino acid of NE2, but the function of their spatial structure is similar to the mimic peptides.

The immunogenicity of HBcAg is the highest in all kinds of antigens of HBV. The design of vector pC149-mut was to insert foreign genes into amino acids 78 to 83[10], the immunogenicity of that position was better. The inserted amino acid could replace the epitope that reacts with B cells easily, thus reducing their interference with the exogenous epitope in immune response. This feature made HBcAg to be a very useful vector for multi-epitope chimeric vaccine[10,27], so did the pC149-mut vector, which was designed accordingly. In this study, heptapeptide was cloned into pC149-mut between the amino acids 78 to 83 of HBcAg, and the recombinant polyprotein could form VLP, which displayed the foreign heptapeptide on their surface and kept its immunogenicity. The known neutralizing epitopes of viruses are almost conformational epitopes, so the genetically engineered vaccine needs the recombinant protein to be in correct conformation, and be able to preserve the immunity. These 2 qualifications could result in a mass of genetically engineered screen. But if using the peptides which mimic the conformational neutralizing epitopes, using the plasmid pC149-mut as a vector to mimic peptide vaccine expression will get VLP antigens, which remain the activation of neutralizing epitopes, and ensure the immunity of the vaccine, at the same time result in protective immunity. On the one hand, this tactics makes it available to unite more than one kind of virus's neutralizing epitopes on the VLP antigen. That is to say, it is a way to develop polyvalent vaccines, which shows new direction in the development of new vaccine[28-31]. The preventer of polyvalent vaccine is that the neutralizing epitopes are almost conformational, if in term of the routine method the conformational epitope cannot be exactly formed. On the other hand, if the chemo-synthesized peptide is used, the immunity will be influenced because of the low molecular mass of peptide. In a word, using the recombinant vector to express the protein, which can form VLP, and using the linear functional mimic epitope, which is displayed on the surface of VLP antigen instead of the conformational neutralizing epitope, is a new feasible idea to settle the difficulties in polyvalent vaccines.

REFERENCES

1   **Zhuang H,** Cao XY, Liu CB, Wang GM. Epidemiology of hepatitis E in China. *Gastroenterol Jpn* 1991; **26** (Suppl 3): 135-138
2   **Huang RT,** Li XY, Xia XB, Yuan XT, Liu MX, Li DR. Antibody detection and sequence analysis of sporadic HEV in Xiamen region. *World J Gastroenterol* 1999; **5**: 270-272
3   **Purcell RH**, Emerson SU. Hepatitis E virus In Knipe DM, Howley PM, Griffin DE, eds. Fields virology, 4thed. vol2. Philadelphia: *Lippincott Raven Pub* 2001: 3051-3061
4   **Li SW,** Zhang J, He ZQ, Ge SX, Gu Y, Ling J, Liu RS, Xia NS. The study of aggregate of the ORF2 peptide of hepatitis E virus expressed in Escherichia coli. *Shengwu Gongcheng Xuebao* 2002; **18**: 463-467
5   **Ge SX,** Zhang J, Huang GY, Pang SQ, Zhou KJ, Xia NS. The Immuno-protect study of a hepatitis E virus ORF2 peptide expressed in E.coli. *Weishengwu Xuebao* 2003; **43**: 35-42
6   **Li SW**, He ZQ, Wang YB, Chen YX, Liu RS, Lin J, Gu Y, Zhang J, Xia NS. Interface domain of hepatitis E virus capsid protein homodimer. *Shengwu Gongcheng Xuebao* 2004; **20**: 90-98
7   **Gu Y,** Zhang J, Li SW, Ge SX, He ZQ, Zhu ZH, Xian YL, Li YM, Xia NS. Characerazation of the anti-HEV ORF2 monoclonal antibodies by biosensor. *Xibao Yu Fenzi Mianyixue Zazhi* 2002; **18**: 617-620

8   **Ge SX,** Zhang J, Peng G, Huang GY, He ZQ, Gu Y, Zhu ZH, Ng MH, Xia NS. Development and evaluation of ELISAs for anti-hepatitis E virus IgM and IgG detection based on polmerized recombinant antigen. *Bingdu Xuebao* 2003; **19**: 78-86

9   **Gu Y,** Ge SX, Huang GY, Li SW, Zhu ZH, He ZQ, Chen YX, Wang YB, Zhang J, Xia NS. Identification of neutralizing mono-clonal antibodies to the hepatitis E virus. *Bingdu Xuebao* 2003; **19**: 217-223

10   **Bottcher B,** Wynne SA, Crowther RA. Determination of the fold of the core protein of hepatitis B virus by electron cryomicroscopy. *Nature* 1997; **386**: 88-91

11   **Ding CL,** Yao K, Zhang TT, Zhou F, Xu L, Xu JY. Generation of cytotoxic T cell against HBcAg using retrovirally transduced dendritic cells. *World J Gastroenterol* 2003; **9**: 1512-1515

12   **Luo WX,** Zhang J, Yang HJ, Li SW, Xie XY, Pang SQ, Li SQ, Xia NS. Construction and application of an Escherichia coli high effective expression vector with an enhancer. *Shengwu Gongcheng Xuebao* 2000; **16**: 578-581

13   **Yu ZC,** Ding J, Nie YZ, Fan DM, Zhang XY. Preparation of single chain variable fragment of MG7 mAb by phage display technology. *World J Gastroenterol* 2001; **7**: 510-514

14   **Wu BP,** Xiao B, Wan TM, Zhang YL, Zhang ZS, Zhou DY, Lai ZS, Gao CF. Construction and selection of the natural immune Fab antibody phage display library from patients with colorectal cancer. *World J Gastroenterol* 2001; **7**: 811-815

15   **Ferrer M,** Sullivan BJ, Godbout KL, Burke E, Stump HS, Godoy J, Golden A, Profy AT, van Schravendijk MR. Structural and functional characterization of an epitope in the conserved C-terminal region of HIV-1 gp120. *J Pept Res* 1999; **54**: 32-42

16   **MacDonald NJ,** Shivers WY, Narum DL, Plum SM, Wingard JN, Fuhrmann SR, Liang H, Holland-Linn J, Chen DH, Sim BK. Endostatin binds tropomyosin. A potential modulator of the anti-tumor activity of endostatin. *J Biol Chem* 2001; **276**: 25190-25196

17   **Kiczak L,** Kasztura M, Koscielska-kasprzak K, Dadlez M, Otlewski J. Selection of potent chymotrypsin and elastase inhibitors from M13 phage library of basic pancreatic trypsin inhibitor (BPTI). *Biochim Biophys Acta* 2001; **1550**: 153-163

18   **Aramburu J,** Yaffe MB, Lopez-Rodriguez C, Cantley LC, Hogan PG, Rao A. Affinity-driven peptide selection of an NFAT inhibitor more selective than cyclosporin A. *Science* 1999; **285**: 2129-2133

19   **Shchelkunov SN,** Nesterov AE, Ryazankin IA, Ignat' ev GM, Sandakhchiev LS. Development of a candidate polyvalent live vaccine against human immunodeficiency, hepatitis B, and orthopox viruses. *Dokl Biochem Biophys* 2003; **390**: 180-183

20   **Ragupathi G,** Livingston P. The case for polyvalent cancer vaccines that induce antibodies. *Expert Rev Vaccines* 2002; **1**: 193-206

21   **Cardo-Vila M**, Arap W, Pasqualini R. Alpha v beta 5 integrin-dependent programmed cell death triggered by a peptide mimic of annexin V. *Mol Cell* 2003; **11**: 1151-1162

22   **Xu L**, Jin BQ, Fan DM. Selection and identification of mimic epitopes for gastric cancer-associated antigen MG7 Ag. *Mol Cancer Ther* 2003; **2**: 301-306

23   **Grothaus MC,** Srivastava N, Smithson SL, Kieber-Emmons T, Williams DB, Carlone GM, Westerink MA. Selection of an immunogenic peptide mimic of the capsular polysaccharide of Neisseria meningitidis serogroup A using a peptide display library. *Vaccine* 2000; **18**: 1253-1263

24   **Prinz DM**, Smithson SL, Westerink MA. Two different methods result in the selection of peptides that induce a protective antibody response to Neisseria meningitidis serogroup C. *J Immunol Methods* 2004; **285**: 1-14

25   **Zhang JZ,** Ng MH, Xia NS, Lau SH, Che XY, Chau TN, Lai ST, Im SW. Comformational antigenic determinants generated by interactions between a bacterially expressed recombinant peptide of the hepatits E virus structural protein. *J Med Virol* 2001; **64**: 125-132

26   **Im SW,** Zhang JZ, Zhuang H, Che XY, Zhu WF, Xu GM, Li K, Xia NS, Ng MH. A bacterially expressed peptide prevents experimental infection of primates by the hepatitis E virus. *Vaccine* 2001; **19**: 3726-3732

27   **Pumpens P**, Razanskas R, Pushko P, Renhof R, Gusars I, Skrastina D, Ose V, Borisova G, Sominskaya I, Petrovskis I, Jansons J, Sasnauskas K. Evaluation of HBs, HBc, and frCP virus-like particles for expression of human papillomavirus 16 E7 oncoprotein epitopes. *Intervirology* 2002; **45**: 24-32

28   **Sompuram SR**, Kodela V, Ramanathan H, Wescott C, Radcliffe G, Bogen SA. Synthetic peptides identified from phage-displayed combinatorial libraries as immunodiagnostic assay surrogate quality-control targets. *Clin Chem* 2002; **48**: 410-420

29   **Poloni F**, Puddu P, Moretti F, Flego M, Romagnoli G, Tombesi M, Capone I, Chersi A, Felici F, Cianfriglia M. Identification of a LFA-1 region involved in the HIV-1-induced syncytia formation through phage-display technology. *Eur J Immunol* 2001; **31**: 57-63

30   **Li BW**, Rush A, Zhang SR, Curtis KC, Weil GJ. Antibody responses to Brugia malayi antigens induced by DNA vaccination. *Filaria J* 2004; **3**: 1

31   **Combredet C**, Labrousse V, Mollet L, Lorin C, Delebecque F, Hurtrel B, McClure H, Feinberg MB, Brahic M, Tangy F. A molecularly cloned Schwarz strain of measles virus vaccine induces strong immune responses in macaques and transgenic mice. *J Virol* 2003; **77**: 11546-11554

Edited by Xu FM and Wang XL

• VIRAL HEPATITIS •

Community-based survey of HCV and HIV coinfection in injection drug abusers in Sichuan Province of China

Yu-Hua Ruan, Kun-Xue Hong, Shi-Zhu Liu, Yi-Xin He, Feng Zhou, Guan-Ming Qin, Kang-Lin Chen, Hui Xing, Jian-Ping Chen, Yi-Ming Shao

Yu-Hua Ruan, Kun-Xue Hong, Shi-Zhu Liu, Yi-Xin He, Feng Zhou, Hui Xing, Jian-Ping Chen, Yi-Ming Shao, Center for AIDS/STD Control and Prevention, Chinese Center for Disease Control and Prevention, Beijing 100050, China
Guan-Qming Qin, Sichuan Provincial Center for Disease Control and Prevention, Chengdu 610031, Sichuan Province, China
Kang-Lin Chen, Xichang Center for STD and Leprosy Control, Xichang County 615000, Sichuan Province, China
Supported by the National Key Technologies Research and Development Program of China during Tenth Five-Year Plan Period, No. 2001BA705B02 and National Natural Science Foundation of China, No. 30170823
Correspondence to: Dr. Yi-Ming Shao, Division of Virology and Immunology, National Center for AIDS/STD Control and Prevention, Chinese Center for Disease Control and Prevention, 27 Nanwei Road, Xuanwu District, Beijing 100050, China. yshao@public3.bta.net.cn
Telephone: +86-10-63166184   **Fax:** +86-10-63154638
Received: 2003-10-10   **Accepted:** 2003-12-08

Abstract

AIM: To investigate the prevalence and risk factors of HCV/HIV coinfection in injection drug abusers (IDAs) in Lianshan Yi Autonomous Prefecture of Sichuan province, China.

METHODS: From November 8, 2002 to November 29, 2002, a community-based survey was conducted to investigate the demographic characteristics, patterns of shared injectors devices and sexual behaviors in IDAs. Blood samples were also collected to test HCV and HIV infection. A total of 379 subjects were recruited in the study through community outreach and peer recruiting methods.

RESULTS: Of the 379 IDAs, the HCV prevalence and HIV prevalence were 71.0% and 11.3%, respectively, and HCV/HIV coinfection was 11.3%. HCV infection was found in 100% and 67.3% of HIV-positive and HIV-negative IDAs, respectively. HIV prevalence was 16.0% in HCV positive IDAs while none of the HCV negative IDAs was positive for HIV. Ethnicity, shared needles or syringes and cotton in the past 3 mo and syphilis infection were associated with HCV/HIV coinfection shown by univariate analysis using chi-square test. Multivariate logistic regression analysis showed that shared needles or syringes in the past 3 mo (Odds ratio=3.121, 95% CI: 1.278-7.617, $P<0.05$) and syphilis infection (Odds ratio=2.914, 95% CI: 1.327-6.398, $P<0.01$) were significantly associated with HCV infection. No statistically significant association was found in univariate analysis between sexual behaviors and HCV/HIV coinfection.

CONCLUSION: Shared needles and syringes in the past 3 mo and syphilis infection were significantly associated with HCV infection. Further sero-epidemiological prospective cohort studies should be conducted to clarify the impact of syphilis and high risk sexual behaviors on HCV transmission through unprotected sexual intercourse.

Ruan YH, Hong KX, Liu SZ, He YX, Zhou F, Qin GM, Chen KL,

Xing H, Chen JP, Shao YM. Community-based survey of HCV and HIV coinfection in injection drug abusers in Sichuan Province of China. *World J Gastroenterol* 2004; 10(11): 1589-1593
http://www.wjgnet.com/1007-9327/10/1589.asp

INTRODUCTION

Since the first case in China of an injection drug abuser (IDA) with AIDS was reported in Yunnan Province along the border with Burma (Myanmar) in 1985[1], China has experienced a rapid increase in the number of HIV/AIDS cases. The majority of HIV infections in China were currently found in rural residents in the western provinces. Furthermore, 71% of documented HIV cases were IDAs. The IDA population is at high risk for HIV infection and also has a high prevalence of HCV. The major mode of HCV and HIV transmission among IDAs is through shared drug injection devices[2-9]. Because unprotected sexual intercourse is widespread among injection drug abusers, unsafe sexual intercourse is also a notable mode of HIV transmission in IDAs and general population. On the other hand, the association between HCV transmission and high-risk sexual behaviors needs to be clarified[10-15]. Some studies have reported that HCV transmission through unsafe sexual intercourse can be enhanced in HIV positive patients due to HCV viremia and more active HCV infection with persistent viremia[16,17]. Clinical progression is more rapid in patients with HCV/HIV coinfection than in patients with HIV only. The prognostic value of HCV infection for both clinical and immunological progression is significant at early stages of HIV infection[18-24]. Furthermore, HIV coinfection in patients with HCV is associated with more rapid progression to liver failure and liver cancer. The HCV and HIV epidemics are a significant public health problem in China because of high HCV prevalence among HIV-positive IDAs. Studies have investigated HCV/HIV coinfection among IDAs recruited from detoxification centers or re-education centers in China. However, few community- or population-based studies have been performed on HCV/HIV coinfection among IDAs in China, especially in regard to the relationship between risk factors, such as shared injection devices and sexual behaviors, and HCV/HIV coinfection or HCV infection.

A community-based survey of HCV/HIV coinfection among IDAs was conducted in Xichang County, Sichuan Province, China, in November 2002. The aim of the cross-sectional study was to identify the specific risk factors for HCV/HIV coinfection among IDAs in Sichuan Province, China.

MATERIALS AND METHODS

Materials
Study participants were recruited through a community-based outreach method that involved the distribution of information materials regarding the study to the community. The outreach campaign was especially targeted to the known IDA groups. During the informed consent process, potential participants in our study were invited to be peer recruiters with the offer of financial incentives for recruiting other IDAs in the community.

After providing written informed consent, potential study participants underwent a screening interview designed to identify IDAs eligible for the study. All participants were at least 18 years of age, and injected drugs at least one time in the past 3 mo. Those who met the inclusion criteria then completed an HCV and HIV risk assessment interview, received HIV pre-test and risk reduction, underwent phlebotomy for HCV and HIV antibody testing, and received HIV post-testing counseling.

Sichuan Province is located in southwest China and the main drug transportation route from Yunnan and Guangxi to Xinjiang. Xichang County is located in Lianshan Yi Autonomous Prefecture of southwest Sichuan. The total population of Xichang County is 617 000. From November 8, 2002 to November 29, 2002, 379 IDAs based in the community of Xichang County were enrolled by the Xichang Center for STD and Leprosy Control to estimate the prevalence of HCV/HIV coinfection and to investigate the risk factors associated with HCV and HIV infection. The study protocol and informed consent were approved by the Institutional Review Board (IRB) of the Center for AIDS/STD Control and Prevention, Chinese Center for Disease Control and Prevention. Informed consent was obtained from all study participants before being interviewed.

Methods

Each study participant was assigned a unique and confidential identification number that was subsequently used to label questionnaire responses and serum specimens. An interviewer-administered questionnaire was used to collect data on risk factors for HCV and HIV infection. Questions were concerned with demographic characteristics, drug use and drug injection behaviors, condom use and sexual behaviors. Demographic variables included age, gender, ethnicity, education, employment, marital status, and home ownership. Questions pertaining to drug use investigated the frequency of drug use and drug injection in the past 3 mo and the frequency of shared injection devices in the past 3 mo, including shared needles or syringes, cookers, cotton, rinse water, and use of front- or back-loading. Assessment of sexual behaviors included questions regarding sex behaviors with a steady partner or other partner(s) in the past 6 mo, condom use in the past month, exchange of money for sex partner in the past 6 mo, and the addition of any new sex partners in the past 6 mo. The interview, counseling and blood collection were performed at the site clinic of the Xichang Center for STD and Leprosy Control.

Each serum or plasma sample was collected from IDAs by venipuncture and tested for antibodies to HIV by enzyme-linked immunosorbent assay (ELISA; Beijing Wantai Biological Medicine Company, China). Positive results were confirmed by an HIV-1/HIV-2 Western immunoblot assay (HIV BLOT 2.2 WB; Genelabs, Singapore). Samples were considered as HIV-positive when both ELISA and Western immunoblot results were positive. Samples were tested for antibodies to HCV by ELISA (Beijing Jinhao Biological Production Company, China). The presence of antibodies to syphilis was tested by ELISA (Beijing Jinhao Biological Production Company, China), positivity was confirmed by passive particle agglutination test for detection of antibodies to *Treponema pallidum* (TPPA; Fujirebio, Inc., Japan).

EpiData software (EpiData 2.1 for Windows; The EpiData Association, Odense, Denmark) was used for data double entry and validation. Statistical analysis of chi-square test or Fisher's exact test was performed to screen behaviors and demographic characteristics associated with high risk for HCV and HIV infection. A multivariate logistic regression model was constructed to select independent risk factors of HCV infection and to control confoundings among various risk factors which provided both P-values and 95% confidence intervals for the Odds ratio (OR) point estimates. Data analyses were carried out using the statistical analysis system (SAS 8.2 for Windows; SAS Institute Inc., North Carolina, USA).

RESULTS

Prevalence of HCV and HIV coinfection in IDAs

A total of 379 IDAs were investigated in this study. As shown in Table 1, HCV prevalence and HIV prevalence were 71.0% and 11.3%, respectively. HCV/HIV coinfection was 11.3%. HCV infection was found in 100% and 67.3% of HIV-positive and HIV-negative IDAs, respectively. HIV prevalence was 16.0% among HCV-positive IDAs and none of the HCV-negative IDAs was found to be HIV-positive.

Table 1 Prevalence of HCV/HIV coinfection in IDAs in Xichang County, Sichuan Province, China

HCV	HIV		Total
	Positive	Negative	
Positive	43	226	269
Negative	0	110	110
Total	43	336	379

Risk factors for HCV and HIV infection in IDAs

Table 2 presents the results of univariate analysis of demographics, risk variables of injection drug abusers in the past 3 mo, sexual behaviors in the past 6 mo, and syphilis infection. HCV/HIV coinfection showed a statistically significant association with ethnicity ($P<0.01$), frequency of shared needles or syringes ($P<0.05$) and cotton in the past 3 mo ($P<0.05$) and syphilis infection ($P<0.01$). The frequency of drug injection, shared rinse water and cooker in the past 3 mo all showed a strong but not statistically significant correlation with HCV/HIV coinfection, with P values near 0.05.

Stepwise multivariate logistic regression analyses were performed using risk factors of ethnicity; Frequency of drug injection, shared needles or syringes, rinse water, cooker and cotton in the past 3 mo and syphilis infection were included in the initial model to investigate the association with HCV infection. As shown in Table 3, shared needles or syringes in the past 3 mo ($P<0.05$) and syphilis infection ($P<0.01$) were independently associated with HCV infection.

DISCUSSION

Among male IDAs in preparatory cohorts for HIV vaccine trials in Thailand, the prevalence of HCV and HCV/HIV coinfection was 96.4% and 50.7%[25]. In a study on IDAs from drug detoxification centers in Yunnan Province of China in 2000, the prevalence of HCV was 99.3% in HIV-positive IDAs[26]. Lai *et al.*[27] reported 15.4% HIV infection and 63.5% HCV infection in IDAs in Guangxi Zhuang Autonomous Region of China; HCV incidence was about 10 times more than HIV incidence. These studies showed that the prevalence of HCV and HIV was high in IDAs, and that HCV transmission was more rapid than HIV transmission.

In previous studies of HIV-positive populations in Xichang County in Sichuan Province, the prevalence of HCV was found to be approximately 60% in HIV-positive individuals[28,29]. In this study, we found a relatively high prevalence (11.3%) of HCV/HIV coinfection in IDAs in Xichang County. Shared needles or syringes in the past 3 mo ($P<0.05$) was significantly associated with HCV infection after demographic characteristics and other risk factors were controlled. However, multivariate analysis showed that shared devices were indirectly related to drug injection, such as cotton, rinse water, cookers, and front- or back-loading, while not significantly associated with HCV/HIV coinfection or with HCV infection. Univariate analysis showed

Table 2 Risk factors associated with HCV/HIV coinfection in IDAs in Xichang County, Sichuan Province, China

	Factor	Total n	HCV/HIV coinfection		HCV infection		χ^2	P
			n	Prevalence (%)	n	Prevalence (%)		
General								
Gender	Male	313	38	12.1	180	57.5		
	Female	66	5	7.6	46	69.7	3.45	0.178
Age(yr)	<29	208	25	12.0	123	59.1		
	≥29	171	18	10.5	103	60.2	0.21	0.901
Ethnicity	Han	243	20	8.2	142	58.4		
	Other	136	23	16.9	84	61.8	10.29	0.006
Years of education	≤6	158	22	13.9	94	59.5		
	>6	221	21	9.5	130	58.8	2.93	0.231
Marriage	Yes	113	16	14.2	66	58.4		
	No	266	27	10.2	160	60.2	1.30	0.521
Employed	Yes	167	20	12.0	91	54.5		
	No	212	23	10.8	135	63.7	3.52	0.172
Own home	Yes	132	20	15.2	76	57.6		
	No	247	23	9.3	150	60.7	2.94	0.23
Drug abuse and drug injection behaviors (past 3 mo)								
Frequency of	<1 time/d	79	6	7.6	42	53.2		
Drug injection	≥1 time/d	300	37	12.3	184	61.3	5.53	0.063
Frequency of shared	<2 times/wk	332	35	10.5	193	58.1		
Needles or syringes	≥2 times/wk	47	8	17.0	33	70.2	7.42	0.025
Frequency of	<2 times/wk	336	36	10.7	196	58.3		
Shared rinse water	≥2 times/wk	43	7	16.3	30	69.8	5.67	0.059
Frequency of	<2 times/wk	335	36	10.7	195	58.2		
Shared cooker	≥2 times/wk	44	7	15.9	31	70.5	5.95	0.051
Frequency of shared cotton	No	352	36	10.2	213	60.5		
	Yes	27	7	25.9	13	48.1	6.19	0.045
Front- or back-loading	No	364	40	11.0	220	60.4		
	Yes	15	3	20.0	6	40.0		0.180[1]
Sexual behaviors (past 6 mo)								
Steady sex partner	No	209	25	12.0	124	59.3		
	Yes	170	18	10.6	102	60.0	0.18	0.914
Sex behavior with non-steady sex partner	No	241	25	10.4	144	59.8		
	Yes	138	18	13.0	82	59.4	0.72	0.698
Steady sex partner of IDU	No	308	35	11.4	182	59.1		
	Yes	71	8	11.3	44	62.0	0.24	0.889
Gave money for sex behavior	No	303	32	10.6	186	61.4		
	Yes	76	11	14.5	40	52.6	2.09	0.351
Received money for sex	No	334	39	11.7	195	58.4		
Behavior	Yes	45	4	8.9	31	68.9	1.82	0.403
Addition of new sex partner(s)	No	264	25	9.5	160	60.6		
	Yes	115	18	15.7	66	57.4	3.08	0.214
Presence of syphilis infection	No	321	30	9.3	189	58.9		
	Yes	58	13	22.4	37	63.8	13.07	0.001

Note: [1]χ^2 Fisher's exact test.

Table 3 Multivariate logistic regression analyses of risk factors associated with HCV prevalence in IDAs in Xichang County, Sichuan Province, China

Factor	β	SEM	P-value	Odds ratio	95% CI
Shared needle or syringe in the past 3 mo	1.1380	0.4553	0.0124	3.121	1.278-7.617
Syphilis infection	1.0695	0.4013	0.0077	2.914	1.327-6.398

that shared cotton in the past 3 mo was associated with HCV/HIV coinfection. Some studies reported that factors of indirectly shared injection devices, including cotton, rinse water, and cookers, posed significant risks for HIV infection in IDAs[30-32].

The modes of HCV transmission have been a matter of important controversy in literature[10-15]. Although a high prevalence of HCV was found in STD patients, female workers and homosexual partners might be suggestive of sexual transmission, drug injection might also play a significant role in HCV transmission[14]. Furthermore, drug injection was the main risk factor associated with HCV infection in homosexual and bisexual men, while the other risk factors after adjusting injection drug abuse included the number of sexual partners in the past year, anal sex and oral sex behaviors[33]. Moreover, Alter *et al.*[15] reported that unsafe heterosexual behavior, anal sex and oral sex behavior were associated with HCV infection, suggesting that both sex behavior and injection drug abuse may play significant roles in HCV transmission. Univariate and multivariate analysis showed that syphilis infection was associated with HCV/HIV coinfection and HCV infection.

However, univariate analysis showed that high risk sexual behaviors were not associated with HCV/HIV coinfection. Lai et al.[27] reported that history of sexually transmitted diseases was independently associated with HIV infection in Guangxi Zhuang Autonomous Region. A study showed that the total number of past sexual partners was associated with HCV infection, but there was no relationship between HCV infection and the total number of sexual partners or sexual behaviors in the past several months[34]. Two studies of STD individuals confirmed the important role that IDA played a role in HCV infection and sexual transmission played a minor role in HCV epidemiologies, such as homosexuality/bisexuality, syphilis seropositivity, and a history of syphilis[35,36]. In our study, persistent use of condom (vaginal sex only) and non-use of condom in IDAs with steady sex partners, and non steady sex partners accounted for 7.6% (9/119) and 88.2% (105/119), 14.6% (13/89) and 68.5% (61/89) in the past month, respectively. This was the first evidence in our study that syphilis infection might contribute to HCV infection in IDAs in Sichuan Province, and syphilis infection is a significant indicator of past high risk sexual behaviors, which increase risk for HCV sexual transmission.

Further sero-epidemiological prospective cohort studies should be conducted to clarify the impact of syphilis and high risk sexual behaviors on HCV transmission through unprotected sexual intercourse.

ACKNOWLEDGEMENTS

REFERENCES

1   **Ma Y**, Li ZZ, Zhang KX, Yang WQ, Ren XH, Yang YF, Ning DM, Cun SZ, Wang BH, Liu SQ, Zhang JP, Zhao SD. Identification of HIV infection among drug users in China. *Zhonghua Liuxing Bingxue Zazhi* 1990; **11**: 184-185
2   **Yin N**, Mei S, Li L, Wei FL, Zhang LQ, Cao YZ. Study on the epidemiology and distribution of human immunodeficiency virus-1 and hepatitis C virus infection among intravenous drug users and illegal blood donors in China. *Zhonghua Liuxing Bingxue Zazhi* 2003; **24**: 962-965
3   **Zhong RX**, Luo HT, Zhang RX, Li GR, Lu L. Investigation on infection of hepatitis G virus in 105 cases of drug abusers. *World J Gastroenterol* 2000; **6**(Suppl 3): 63-63
4   **Hahn JA**, Page-Shafer K, Lum PJ, Ochoa K, Moss AR. Hepatitis C virus infection and needle exchange use among young injection drug users in San Francisco. *Hepatology* 2001; **34**: 180-187
5   **Maier I**, Wu GY. Hepatitis C and HIV co-infection: a review. *World J Gastroenterol* 2002; **8**: 577-579
6   **Murray JM**, Law MG, Gao Z, Kaldor JM. The impact of behavioural changes on the prevalence of human immunodeficiency virus and hepatitis C among injecting drug users. *Int J Epidemiol* 2003; **32**: 708-714
7   **Wu NP**, Li D, Zhu B, Zou W. Preliminary research on the co-infection of human immunodeficiency virus and hepatitis virus in intravenous drug users. *Chin Med J* 2003; **116**: 1318-1320
8   **Quaglio GL**, Lugoboni F, Pajusco B, Sarti M, Talamini G, Mezzelani P, Des Jarlais DC. Hepatitis C virus infection: prevalence, predictor variables and prevention opportunities among drug users in Italy. *J Viral Hepat* 2003; **10**: 394-400
9   **Taketa K**, Ikeda S, Suganuma N, Phornphutkul K, Peerakome S, Sitvacharanum K, Jittiwutikarn J. Differential seroprevalences of hepatitis C virus, hepatitis B virus and human immunodeficiency virus among intravenous drug users, commercial sex workers and patients with sexually transmitted diseases in Chiang Mai, Thailand. *Hepatol Res* 2003; **27**: 6-12

10   **Valdivia JA**, Rivera S, Ramirez D, De Los Rios R, Bussalleu A, Huerta-Mercado J, Pinto J, Piscoya A. Hepatitis C virus infection in female sexual workers from northern lima. *Rev Gastroenterol Peru* 2003; **23**: 265-268
11   **Hammer GP**, Kellogg TA, McFarland WC, Wong E, Louie B, Williams I, Dilley J, Page-Shafer K, Klausner JD. Low incidence and prevalence of hepatitis C virus infection among sexually active non-intravenous drug-using adults, San Francisco, 1997-2000. *Sex Transm Dis* 2003; **30**: 919-924
12   **Fletcher S.** Sexual transmission of hepatitis C and early intervention. *J Assoc Nurses Aids Care* 2003; **14**(Suppl 5): S87-S94
13   **Russi JC**, Serra M, Vinoles J, Perez MT, Ruchansky D, Alonso G, Sanchez JL, Russell KL, Montano SM, Negrete M, Weissenbacher M. Sexual transmission of hepatitis B virus, hepatitis C virus, and human immunodeficiency virus type 1 infections among male transvestite comercial sex workers in Montevideo, Uruguay. *Am J Trop Med Hyg* 2003; **68**: 716-720
14   **Brettler DB**, Mannucci PM, Gringeri A, Rasko JE, Forsberg AD, Rumi MG, Garsia RJ, Rickard KA, Colombo M. The low risk of hepatitis C virus transmission among sexual partners of hepatitis C-infected hemolic males: an international multicenter study. *Blood* 1992; **80**: 540-543
15   **Alter MJ**, Coleman PJ, Alexander WJ, Kramer E, Miller JK, Mandel E, Hadler SC, Margolis HS. Importance of heterosexual activity in the trasmission of hepatitis B and non-A, non-B hepatitis. *JAMA* 1989; **262**: 1201-1205
16   **Mendes-Correa MC,** Barone AA, Guastini C. Hepatitis C virus seroprevalence and risk factors among patients with HIV infection. *Rev Inst Med Trop Sao Paulo* 2001; **43**: 15-19
17   **Lissen E**, Alter HJ, Abad MA, Torres Y, Perez-Romero M, Leal M, Pineda JA, Torronteras R, Sanchez-Quijano A. Hepatitis C virus infection among sexually promiscuous groups and the heterosexual partners of hepatitis C virus infected index cases. *Eur J Clin Microbiol Infect Dis* 1993; **12**: 827-831
18   **Romero M**, Perez-Olmeda M, Garcia-Samaniego J, Soriano V. Management of chronic hepatitis C in patients co-infected with HIV: Focus on safety considerations. *Drug Saf* 2004; **27**: 7-24
19   **Livry C**, Binquet C, Sgro C, Froidure M, Duong M, Buisson M, Grappin M, Quantin C, Portier H, Chavanet P, Piroth L. Acute liver enzyme elevations in HIV-1-infected patients. *HIV Clin Trials* 2003; **4**: 400-410
20   **Quintana M**, del Amo J, Barrasa A, Perez-Hoyos S, Ferreros I, Hernandez F, Villar A, Jimenez V, Bolumar F. Progression of HIV infection and mortality by hepatitis C infection in patients with haemophilia over 20 years. *Haemophilia* 2003; **9**: 605-612
21   **Hisada M**, Chatterjee N, Zhang M, Battjes RJ, Goedert JJ. Increased hepatitis C virus load among injection drug users infected with human immunodeficiency virus and human T lymphotropic virus type II. *J Infect Dis* 2003; **188**: 891-897
22   **Klein MB**, Lalonde RG, Suissa S. The impact of hepatitis C virus coinfection on HIV progression before and after highly active antiretroviral therapy. *J Acquir Immune Defic Syndr* 2003; **33**: 365-372
23   **Greub G**, Ledergerber B, Battegay M, Grob P, Perrin L, Furrer H, Burgisser P, Erb P, Boggian K, Piffaretti JC, Hirschel B, Janin P, Francioli P, Flepp M, Telent A. Clinical progression, survival, and immune recovery during antiretroviral therapy in patients with HIV-1 and hepatitis C virus coinfection: the Swiss HIV Cohort Study. *Lancet* 2000; **356**: 1800-1805
24   **Piroth L**, Duong M, Quantin C, Abrahamowicz M, Michardiere R, Aho LS, Grappin M, Buisson M, Waldner A, Portier H, Chavanet P. Does hepatitis C virus co-infection accelerate clinical and immunological evolution of HIV-infected patients? *AIDS* 1998; **12**: 381-388
25   **Paris R**, Sirisopana N, Benenson M, Amphaiphis R, Tuntichaivanich C, Myint KSA, Brown AE. The association between hepatitis C virus and HIV-1 in preparatory cohorts for HIV vaccine trials in Thailand. *AIDS* 2003; **17**: 1363-1367
26   **Zhang CY**, Yang RG, Xia XS, Qin SY, Dai JP, Zhang ZB, Peng ZZ, Wei T, Liu H, Pu DC, Luo JH, Takebe YT, Ben KL. High

prevalence of HIV-1 and hepatitis C virus coinfection among injection drug users in the southeastern region of Yunnan, China. *JAIDS* 2002; **29**: 191-196

27 **Lai SH**, Liu W, Chen J, Yang JY, Li ZJ, Li RJ, Liang FX, Liang SL, Zhu QY, Yu XF. Changes in HIV-1 incidence in Heroin Users in Guangxi province, China. *JAIDS* 2001; **26**: 365-370

28 **Yang TL**, Xu YC, Hu XH. The prevalence of HIV, HBC and HCV among drug users in Xichang county of Sichuan province. *Yufang Yixue Qingbao Zazhi* 2001; **17**: 170-171

29 **Wei DY**, Ma MJ, Gong WH, Han YH. The survey of HIV, HBV and HCV infection. *Yufang Yixue Qingbao Zazhi* 2000; **16**: 187

30 **Denis B**, Dedobbeleer M, Collet T, Petit J, Jamoulle M, Hayani A, Brenard R. High prevalence of hepatitis C virus infection in belgian intravenous drug users and potential role of the "cotton-filter" in transmission: the GEMT study. *Acta Gastroenterol Belg* 2000; **63**: 147-153

31 **Hagan H**, Thiede H, Weiss NS, Hopkins SG, Duchin JS, Alexander ER. Sharing of drug preparation equipment as a risk factor for hepatitis C. *Am J Public Health* 2001; **91**: 42-46

32 **Thorpe L**, Ouellet L, Hershow R, Bailey S, Williams II, Monerrosso E. The multiperson use of non-syringe injection equipment and risk of hepatitis C infection in a cohort of young adult injection drug users, Chicago 1997-1999. *Ann Epidemiol* 2000; **10**: 472-473

33 **Osmoda DH**, Charlebois E, Sheppard HW, Page K, Winkelstein W, Moss AR, Reingold A. Comparison of risk factors for hepatitis C and hepatitis B virus infection in homosexual men. *J Infec Dis* 1993; **167**: 66-71

34 **Zhou PY**, Xu JH, Liao KH, Xu M, Wang JS. A survey of HCV prevalence and sexual behavior among STD patients in STD clinic. *Zhonghua Pifuke Zazhi* 1999; **32**: 403-404

35 **Fiscus SA**, Kelly WF, Battigelli DA, Weber DJ, Schoenbach VJ, Landis SE, Wilber JC, Van der Horst CM. Hepatitis C virus seroprevalence in clients of sexually transmitted disease clinics in North Carolina. *Sex Transm Dis* 1994; **21**: 155-160

36 **Bodsworth NJ**, Cunningham P, Kaldor J, Donovan B. Hepatitis C virus infection in a large cohort of homosexually active men: independent associations with HIV-1 infection and injecting drug use but not sexual behaviour. *Genitourin Med* 1996; **72**: 118-122

Edited by Wang XL and Xu FM

• BASIC RESEARCH •

Modulation of human enteric epithelial barrier and ion transport function by Peyer's patch lymphocytes

Jie Chen, Lai-Ling Tsang, Lok-Sze Ho, Dewi K. Rowlands, Jie-Ying Gao, Chuen-Pei Ng, Yiu-Wa Chung, Hsiao-Chang Chan

Jie Chen, Lai-Ling Tsang, Lok-Sze Ho, Dewi K. Rowlands, Chuen-Pei Ng, Yiu-Wa Chung, Hsiao-Chang Chan, Epithelial Cells Biology Research Center, Department of Physiology, Faculty of Medicine, Chinese University of Hong Kong, Hong Kong, China
Jie-Ying Gao, Department of Immunology, Institute of Microbiology and Epidemiology, Academy of Military Medical Sciences, Beijing 100071, China
Jie Chen, Department of Biology, Faculty of Medicine, Shanxi Medical University, Taiyuan 030001, Shanxi Province, China
Supported by Strategic Program of Chinese University of Hong Kong, and Distinguished Yong Investigator Fund of the National Natural Science Foundation of China, 30029002
Correspondence to: Dr. Hsiao-Chang Chan, Department of Physiology, Chinese University of Hong Kong, Shatin, NT, Hong Kong, China. hsiaocchan@cuhk.edu.hk
Telephone: +852-2609-6839 **Fax:** +852-2603-5022
Received: 2003-12-28 **Accepted:** 2004-02-11

Abstract

AIM: To investigate the role of Peyer's patch lymphocytes in the regulation of enteric epithelial barrier and ion transport function in homeostasis and host defense.

METHODS: Mouse Peyer's patch lymphocytes were co-cultured with human intestinal epithelial cell line Caco-2 either in the mixed or separated (isolated but permeable compartments) culture configuration. Barrier and transport functions of the Caco-2 epithelial monolayers were measured with short-circuit current (I_{sc}) technique. Release of cytokines was measured by enzyme-linked immunosorbent assay (ELISA) and cytokine mRNA expression was analyzed by semi-quantitative RT-PCR. Barrier and iontransport functions of both culture conditions following exposure to *Shigella* lipopolysaccharide (LPS) were also examined.

RESULTS: The transepithelial resistance (TER) of the epithelial monolayers co-cultured with Peyer's patch lymphocytes was maintained whereas that of the Caco-2 monolayers alone significantly decreased after eight days in culture. The forskolin-induced anion secretion, in either absence or presence of LPS, was significantly suppressed in the both co-cultures as compared with the Caco-2 cells alone. Furthermore, only the mixed co-culture condition induced the expression and release of mIL-6 from Peyer's patch lymphocytes, which could be further enhanced by LPS. However, both co-culture conditions suppressed expression and release of epithelial hIL-8 under the unstimulated conditions, while the treatment with LPS stimulated their hIL-8 expression and release.

CONCLUSION: Peyer's patch lymphocytes may modulate intestinal epithelial barrier and ion transport function in homeostasis and host defense via cell-cell contact and cytokine signaling.

Chen J, Tsang LL, Ho LS, Rowlands DK, Gao JY, Ng CP, Chung YW, Chan HC. Modulation of human enteric epithelial barrier

and ion transport function by Peyer's patch lymphocytes. *World J Gastroenterol* 2004; 10(11): 1594-1599

http://www.wjgnet.com/1007-9327/10/1594.asp

INTRODUCTION

The mucosal surface of the gastrointestinal tract is lined by a single layer of epithelial cells jointed together at their apical poles by tight junctions, forming a barrier that separates the luminal contents from the effector immune cells underneath. It has become increasingly clear that the intense immunological activities occurring at the enteric mucosal surface involve interactions between epithelial and immune cells[1,2]. Accumulating evidence suggests that epithelial cells can produce cytokines and chemokines that attract and activate immune cells with potentially important effects on the immediate and long-term host defense functions. Effective immune surveillance of the mucosal surface requires transport of intact macromolecules and micro-organisms across the epithelial barrier to the cells of mucosal immune system. Groups of organized mucosal lymphoid follicles, named Peyer's patches, lined along the gastrointestinal tract in a specialized overlying epithelium, are the sites for transporting, processing and presenting foreign antigens. In Peyer's patches, each follicle is separated from the overlying epithelium by a subepithelial "dome" region that is rich in lymphocytes and dendritic cells. It is apparent that the immune cells in the dome region interact intimately with the overlying epithelium, giving rise to mucosal immune response without the needs of systemic involvement[3]. Although a mucosal lympho-epithelial internet has been proposed to mediate the interactions between epithelial and immune cells, details of the interactions are far from understood. The close contact between Peyer's patch lymphocytes and intestinal epithelial cells suggests that these lymphocytes may play a role in the modulation of epithelial barrier/transport functions in homeostasis as well as host defense. However, no evidence has been provided so far concerning the role of Peyer's patch lymphocytes in intestinal epithelial physiology.

In addition to their major defensive role as a passive barrier, the intestinal epithelial cells also play an active role in physiology and pathophysiology of the gut. While the absorptive properties of the epithelium are known to be of vital importance for the nutrition of the body, as well as the maintenance electrolytes and fluid balance, the secretory activities of the epithelium are also important for protective purpose. Luminally directed transport of Cl^- and HCO_3^- is the driving force for fluid secretion that flushes away noxious substances from the intestinal mucosal surface. Secretory diarrhea is often the consequence for increased water and electrolyte secretion upon invasion by microorganisms. *Escherichia*, *Salmonella* and *Shigella* are the most important bacterial causes of diarrhea worldwide[4]. The pathogenesis of bacteria-induced diarrhea with regard to the involvement of Peyer's patch lymphocytes remains largely unknown although the barrier function and ion secretory responses of the intestinal epithelium have been shown to be affected by both proinflammatory and anti-inflammatory cytokines[5-7].

The co-culture of characterized epithelial cells with defined immune cell populations and subsequent analysis of epithelial physiology have contributed significantly to our appreciation of the immune regulation of epithelial function[8,9]. Kerneis *et al.*[10] have successfully induced functional M cells by co-culturing Caco-2 cells, a human intestinal surface epithelial cell line, with murine Peyer's patch lymphocytes. This phenomenon indicates the profound influence of Peyer's patch lymphocytes on intestinal epithelial phenotypes[11]. Thus, to investigate the role of Peyer's patch lymphocytes in intestinal epithelial barrier/transport function during infection, we adopted this co-culture system to build an infection model with *Shigella* LPS, one of the major virulence factors of Gram-negative bacteria that is responsible for eliciting a wide array of immune responses[11,12]. The present study includes different co-culture configurations: One consisting of upper and lower compartments with a permeable filter separating the epithelial layer and lymphocytes, and the other mixing both epithelial cells and lymphocytes in the same compartment. Using these co-culture configurations, epithelial-immune interactions through cell-cell contact as well as cytokine signaling could be examined independently.

MATERIALS AND METHODS

Isolation of peyer's patch lymphocytes

BALB/c mice (SPF, female, 6-8 wk old) were obtained from the Animal House of Chinese University of Hong Kong. The lymphoid follicles of the Peyer's patch were carefully excised from the intestinal serosal side and placed in 10 mL phosphate buffered saline (PBS, pH 7.4, GIBCO 10010-31) supplemented with 20 mL/L FBS and 2% penicillin-streptomycin. The collected patches were triturated by pipetting up and down a few times and smashing through a metallic grid (mesh: 100). Individual lymphocytes were released in the liquid below the metallic grid. The lymphocytes were washed with PBS, the distribution of Peyer's patch T and B cell populations was consistent with previous data when they were checked by flow cytometry[10], then diluted to the expected concentration.

Enteric epithelial cell culture

Human colonic cell line Caco-2, which is a villus cell-like colonic cell line[13], was purchased from American Type Culture Collection (Rockville, MD). The cells were grown in Dulbecco Modified Eagle's minimal essential medium (DMEM, high glucose, GIBC-BRL) with 100 mL/L fetal bovine serum (FBS, GIBCO 16000-044), 2 mmol/L L-glutamine (GIBCO-BRL), 100 μmol/L non-essential amino acid (GIBCO-BRL), 200 units/mL penicillin and 200 μg/mL streptomycin (GIBCO-BRL) at 37 ℃ in a 50 mL/L CO_2 atmosphere. Caco-2 cells were seeded at a density of 3×10^5 cells on a floating permeable support, which was made of a membrane filter (Millipore, 0.45 μm pore size) with a silicone rubber ring attached on top of it for confining the cells (0.45 cm² growth area).

Co-culture configurations

Three types of culture configurations were established in this study: (1) Caco-2 culture alone: Caco-2 cells (3×10^5 cells) were grown as a homogenous polarized monolayer according to the epithelial cell culture method mentioned above and served as the control. (2) Separated co-culture: Epithelial cells (3×10^5 cells) were plated on a permeable support (growth area of 0.45 cm² as described), which floated above 2 mL culture medium containing Peyer's patch lymphocytes (5×10^6 cells) in a Petri dish (3.5-cm diameter). (3) Mixed co-culture: Caco-2 cells (3×10^5 cells) were directly mixed with Peyer's patch lymphocytes (1×10^6 cells), and then were seeded on the same permeable support described above and grown at 37 ℃ in a 50 mL/L CO_2 atmosphere.

Shigella F2a-12 LPS pretreatment

When the Caco-2 cells grown as polarized monolayers on the membrane filter reached confluence on the 4th d, *Shigella F2a-12* LPS (5 μg/mL, obtained from the Immunology Department of Institute of Microbiology & Epidemiology, Academy of Military Medical Sciences) was added to the apical side of the epithelial monolayers and treated for 8, 24 and 48 h at 37 ℃ in a 50 mL/L CO_2 atmosphere.

Short-circuit current measurements (Isc)

The *Isc* measurement has been described previously[14]. In short, the confluent monolayers were clamped vertically between the two halves of an Ussing chamber. Monolayers were short circuited (transepithelial potential difference clamped at zero) using a voltage-clamp amplifier (DVC-1000; World Precision Instruments Inc., New Haven, CT, USA). The resulting *Isc* was displayed on-line on a pen recorder (Kipp and Zonen, Delft, The Netherlands). Transepithelial electrical resistance (TER) was determined based on Ohm's law by clamping the tissue intermittently at a value of 0.2 mV. For most measurements, the monolayers were bathed in normal Krebs-Henseleit solutions (NaCl, 117 mmol/L ; KCl, 4.7 mmol/L; $MgCl_2$, 1.2 mmol/L; $NaHCO_3$, 24.8 mmol/L; KH_2PO_4, 1.2 mmol/L; $CaCl_2$, 2.56 mmol/L; Glucose, 11.1 mmol/L) with 950 mL/L O_2 and 50 mL/L CO_2.

Semi-quantitative RT-PCR

Caco-2 monolayers grown on the filters (Millipore, 0.22 μm pore size, cell growth area of 7.065 cm²) were harvested for RT-PCR after 8-h and 24-h *Shigella F2a-12* LPS pre-treatment. The specific primers for hIL-8[15] were 5' tct ctt ggc agc ctt cct 3' (sense) and 5' gaa gtt tca ctg gca tct tca c 3' (antisense), corresponding to the nucleotides 98-427 with the expected cDNA size of 390 bp (Tm 58 ℃, 30 cycle); mIL-6[16] were 5' ctg caa gag act tcc atc cag 3' (sense) and 5' tcc agt ttg gta gca tcc atc 3' (antisense), corresponding to the nucleotides 45-340 with the expected cDNA size of 296 bp (Tm 55 ℃, 35 cycle). Their expression was compared to the house-keeping gene GAPDH (forward: 5' tcc cat cac cat ctt cca g 3' and reverse: 5' tcc acc act gac acg ttg 3'). RT-PCR was performed using the PTC-200 Peltier Thermal Cycler (MJ Research Company) and software for analysis data is GraphPad Prism 3.02.

Enzyme-linked immunosorbent assay (ELISA)

After confluent Caco-2 monolayers on the Millipore filter was challenged by *Shigella F2a-12* LPS pretreatment for 8 and 24 h, the culture medium was collected and kept at -20 ℃ until evaluation hIL-8 and mIL-6 bioassay using ELISA kits (BIOSOURCE Company) according to manufacturer's instructions.

Statistical analysis

All data were expressed as mean±SE. The number of experiments represents independent measurements on separate monolayers. Comparisons between groups of data were made by one-way ANOVA. A "*P*" value of less than 0.05 was considered statistically significant.

RESULTS

Co-culture with Peyer's patch lymphocytes results in better maintenance of epithelial barrier function but LPS decreases it

Polarized monolayers of Caco-2 were tested for transepithelial resistance (TER) at various times (the 4th, 6th and 8th d after co-culture) (Figure 1). A significant decrease in TER was observed in Caco-2 alone after eight days in culture, whereas high TER could still be maintained for either mixed or separated co-cultures for the same period of time (Figure 1). However, after treatment with *Shigella* LPS (5 μg/mL) for 48 h, TER measured on the

6th d of co-culture, decreased significantly in both co-culture groups but not in Caco-2 alone (Figure 2).
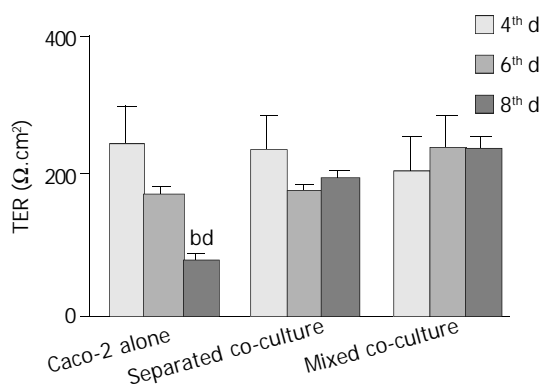

Figure 1 Comparison of time-dependent changes in transepithelial resistance (TER) of different culture groups. Data in all panels are mean±SE for 4 experiments, significant differences relative to its own 4-d of culture in Caco-2 alone ([b]$P<0.01$), and to its own 6th day culture of Caco-2 alone ([d]$P<0.001$) are indicated.
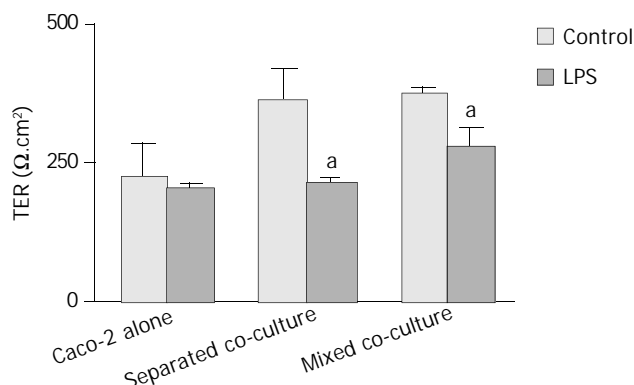

Figure 2 Effect of *Shigella* F2a-12 LPS on transepithelial resistance (TER) of different culture groups. Cultured monolayers were exposed to LPS 48-h prior to TER measurement on the 6 d of culture. Comparison of TER in the absence or presence of *Shigella* F2a-12 LPS among the three culture groups. The values indicate mean±SE; $n=5$; [a]$P<0.05$ (compared to its own control).
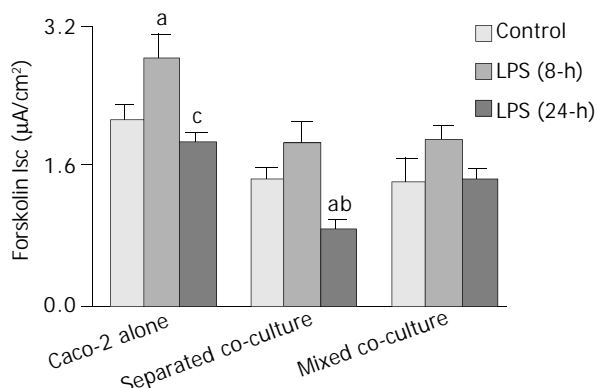

Figure 3 Effect of *Shigella* F2a-12 LPS on the Forskolin-induced *Isc*. Comparison of the Forskolin (4 μg/mL, basoateral addition)-induced *Isc* in the absence or presence of LPS for 8-h and 24-h under different culture conditions. The values indicate mean±SE; $n=12$; [a]$P<0.05$ (compared to its own control); [c]$P<0.05$ and [b]$P<0.001$ (compared to its own LPS treatment for 8-h).

Co-culture with Peyer's patch lymphocytes alters anion secretory responses

The *Isc* responses of the co-cultures and Caco-2 alone to the challenge of an adenylate cyclase activator, forskolin, were characterized. As shown in Figure 3, significantly lower *Isc* response was observed in both co-cultures than that of the Caco-2 alone control in the absence of LPS. Increased responses in all groups were observed after 8-h LPS treatment. Significantly more upregulated *Isc* response was observed in Caco-2 alone group (Figure 3). After 24 h of LPS treatment, the *Isc* responses of the separated co-culture and Caco-2 alone groups decreased significantly as compared with that of 8-h LPS treatment but not the mixed co-culture (Figure 3). No significant differences in the basal *Isc* among the groups were observed, nor did it change significantly upon treatment with LPS (data not shown).
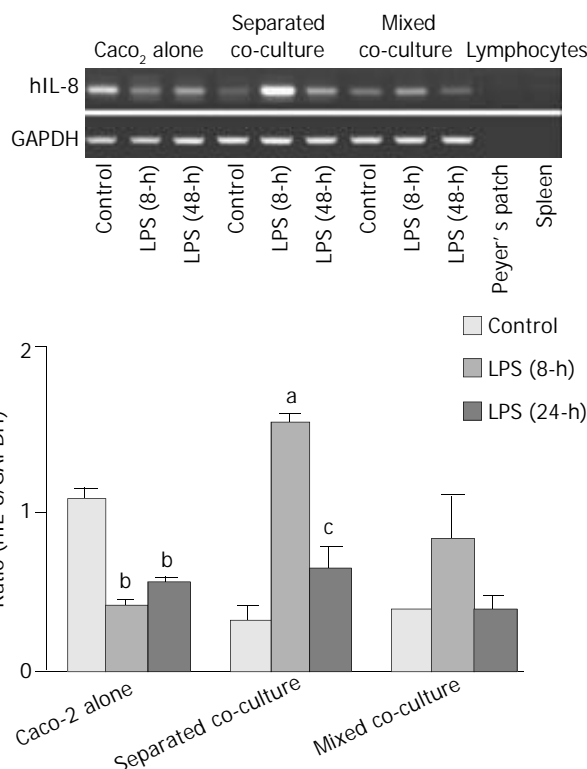

Figure 4 Induction of hIL-8 expression in Caco-2 cells by *Shigella* F2a-12 LPS in different culture groups. Comparison of hIL-8 expression in Caco-2 cells in the absence or presence of LPS for 8-h and 24-h between three culture groups by semi-quantitative RT-PCR with Peyer's patch lymphocytes as negative control. The values indicate mean±SE; [a]$P<0.05$, [b]$P<0.01$ (compared to its own control); [c]$P<0.05$ (compared to separated co-culture LPS pre-treatment for 8-h).

Separated co-culture results in enhanced expression and release of hIL-8 from Caco-2 cells

To examine the mRNA expression of hIL-8, primers specific for hIL-8 were used in RT-PCR experiments, and the RNA from mouse Peyer's patch lymphocytes was used as negative control to detect any potential. The results are shown in Figure 4. The highest level of hIL-8 expression was observed in the Caco-2 alone as compared to the other two co-cultures when they were cultured in the absence of LPS. However, after treatment with LPS for 8 h, lower hIL-8 expression was observed in the Caco-2 culture alone while increased hIL-8 expression was evident in both co-cultures. The increase in the hIL-8 expression was particularly more enhanced in the separated co-culture. After 24 h, the expression of hIL-8 in the co-cultures returned closer to their basal levels but the expression in the Caco-2 alone remained low as compared with its own control. The expression of hIL-8 was not detected in mouse Peyer's patch lymphocytes confirming that the above expression profile of hIL-8 was associated with human intestinal epithelial cells.

ELISA using a human kit was conducted to confirm the release of hIL-8 from different cultures with mouse Peyer's patch lymphocytes as a control for cross-reactivity. The results showed that the levels of hIL-8 released from the Caco-2 alone culture under the unstimulated condition and 8-h LPS treatment were significantly greater than that from both co-cultures (Figure 5). However, following the 24-h LPS treatment, levels of hIL-8 in both co-culture groups increased considerably while a decrease was observed in Caco-2 alone (Figure 5). A detectable amount of hIL-8 was also observed from mouse Peyer's patch lymphocytes (1×10^6 cells), indicating the presence of condition cross-reactivity of human IL-8 antibody to mouse IL-8 (Figure 5).
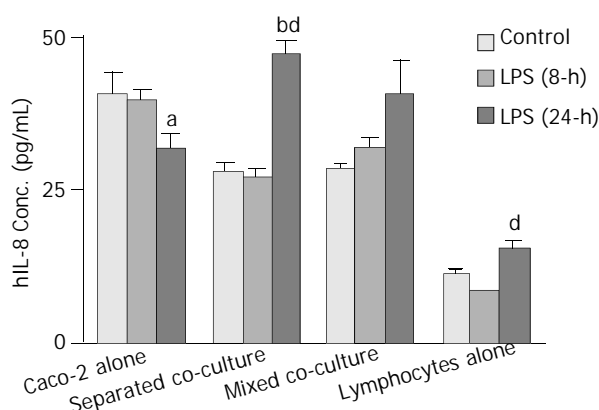

Figure 5 Comparison of *Shigella* F2a-12 LPS-induced hIL-8 release from different culture groups by ELISA. **C**ulture groups and Peyer's patch lymphocytes alone (control, 1×10^6 cells) were treated with LPS for 8-h and 24-h. The presented values indicate mean±SE; *n*=8; [b]*P*<0.001 (compared to its own control); [a]*P*<0.05 and [d]*P*<0.001 (compared to its own LPS treatment for 8-h).
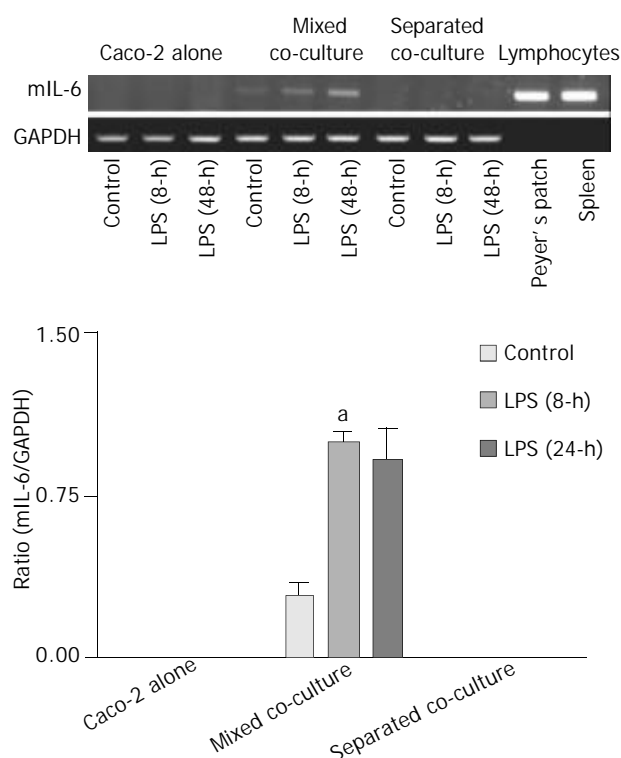

Figure 6 Induction of mIL-6 expression by *Shigella* F2a-12 LPS in different culture groups. Comparison of mIL-6 expression in the absence or presence of LPS for 8-h and 24-h among the culture groups by semi-quantitative RT-PCR with mouse Peyer's patch lymphocytes as positive control. The values indicate mean±SE [a]*P*<0.01 (compared to the mixed control).

The mixed co-culture condition triggers expression and release of mIL-6 from Peyer's patch lymphocytes

Using primers specific for mIL-6, the expected RT-PCR product of mIL-6 was detected in the mixed co-culture and mouse lymphocytes but not in the Caco-2 culture alone or separated co-culture, where only the epithelial cells in the upper compartment were subjected to RT-PCR, thus excluding detection of IL-6 from the Peyer's patch lymphocytes in the medium. The expression of mIL-6 in the mixed co-culture further increased after 8 and 24 h of treatment with LPS (Figure 6).

The release of mIL-6 from different cultures, as well as mouse Peyer's patch lymphocytes (1×10^6 cells), was measured using a mouse ELISA kit. The results showed that no groups except the mixed co-culture had detectable mIL-6 release either in the absence or presence of LPS treatment (Figure 7). The level of mIL-6 measured in the mixed co-culture group significantly increased after 24-h LPS treatment (Figure 7).
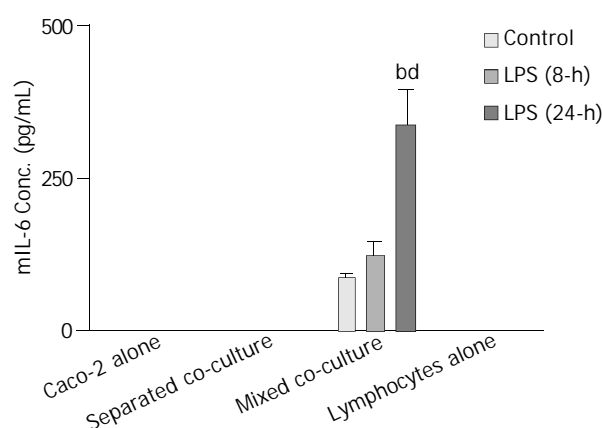

Figure 7 Comparison of *Shigella* F2a-12 LPS-induced mIL-6 release from different culture groups by ELISA. Culture groups and Peyer's patch lymphocytes (1×10^6 cells) were treated with LPS for 8-h and 24-h. The values indicate mean±SE; *n*=5; [b]*P*<0.01 (compared to mixed co-culture control) and [d]*P*<0.01 (compared to the mixed LPS treatment for 8-h).

DISCUSSION

The present study has demonstrated for the first time the role of Peyer's patch lymphocytes in intestinal epithelial physiology in homeostasis as well as host defense. Both epithelial barrier function and anion secretory activities, under normal or infected conditions, were affected by the presence of Peyer's patch lymphocytes to various extent depending on the co-culture configurations. TER has been used as an index of epithelial barrier integrity, which is sometimes compromised in certain infections, possibly as a direct result of modulation by immune cells[17]. Previous studies in co-cultures of epithelial cells and immune cells, including lamina propria mononuclear cells (LPMC)[18] and intraepithelial lymphocytes[19], invariably resulted in disruption of epithelial barrier function as indicated by a decrease in TER. However, the present study did not observe significant reduction in the TER in the Caco-2 co-cultures with Peyer's patch lymphocytes, either in the separated or mixed configuration, as compared with the Caco-2 culture alone. On the contrary, the TER in both co-cultures could be maintained up to eight days whereas that in Caco-2 control decreased drastically. These results suggest that unlike other types of immune cells previously studied, Peyer's patch immune cells, which consist mostly of lymphocyte (99%)[10], play a distinct homeostatic regulatory role in maintaining the barrier function of the epithelial monolayers. However, TER of both co-cultures decreased substantially after treatment with *Shigella* LPS for

48 h, indicating that *Shigella* LPS may have direct effect on epithelial barrier function without the modulation of Peyer's patch lymphocytes. This notion is also supported by the observed mRNA expression of tight junction-associated protein ZO-1 in both co-cultures with Peyer's patch lymphocytes (data not shown). It has been shown that LPS accounts for a large part of the transepithelial signaling caused by apical *Shigella* bacteria that induces adherence and transmigration of basal polymorphonuclear leukocytes (PMNs), which disrupt the monolayer permeability and facilitate bacterial invasion[20].

Similar to the barrier function, the epithelial secretory activities, in both homeostasis and infection, were also affected by the presence of Peyer's patch lymphocytes, depending on the configuration of the co-cultures. In normal conditions (or in the absence of LPS), reduced forskolin-induced *Isc* was observed when Peyer's patch lymphocytes were co-cultured with Caco-2 and the *Isc* response in the Caco-2 alone group was significantly increased after LPS challenge up to eight hours. These results suggest that the forskolin-induced *Isc* response could be suppressed by Peyer's patch lymphocytes. However, down-regulation of forskolin-induced anion secretion could be seen in all groups 24 h after LPS challenge, suggesting that cytokine signaling also plays a role at later stages of infection, perhaps affecting the expression of ion channels. Interestingly, the *Isc* response of anion secretion in the mixed co-culture showed no significant change in the absence or presence of LPS, suggesting that cell-cell contact is important for modulation of epithelial anion secretion by Peyer's patch lymphocytes. In contrast to many previous results obtained from *in vitro* epithelial model cells showing anion secretion stimulated by bacteria[21] or immune and inflammatory modulators produced by inflammatory cells[22], the present results show no change in the forskolin-induced anion secretion in the mixed co-cultures in the absence or presence of LPS. Reduced secretory responsiveness has also been observed in the epithelial cell models that are co-cultured with a number of different immune cells[7]. This is also consistent with the observation that colonic mucosa from patients with chronic inflammatory bowl disease respond poorly to secretagogues[23]. Thus, it appears that the epithelial secretory response in homeostasis and infection is modulated by immune cells including Peyer's patch lymphocytes. The present results showed that Peyer's patch lymphocytes suppressed epithelial secretory activity, especially upon LPS challenge, suggesting that the secretory diarrhea caused by bacterial infection may not be solely due to enhanced water and electrolyte secretion. Recent studies have suggested that the inhibition of Na+-K+-ATPase by interferon γ that leads to the reduction of Na+ absorption may be a major cause of inflammation-associated diarrhea[24]. The inhibition of Na+-K+-ATPase induced by interferon γ may also account for the presently observed Peyer's patch lymphocyte-suppressed anion secretion since secondary active anion secretion depends on the Na+ gradient generated by the Na+-K+-ATPase. Further studies examining the expression of various ion channels and transporters including Na+-K+-ATPase and CFTR in response to LPS challenge are currently undertaken in our laboratory.

The present results suggest that the modulation of epithelial physiology by Peyer's patch lymphocytes involves both cell-cell contact and cytokine signaling. The mouse-human hybrid co-cultures in different configurations, mixed and separated, not only allow the distinction of contact-dependent and independent signaling mechanisms but also the identification of the source of cytokines, although homology between human and mouse cytokine may result in cross-reactivity as seen in the ELISA results showing detectable hIL-8 measured from mouse Peyer's patch lymphocytes using a human kit. Further experiment with RT-PCR using species-specific primers could also be conducted to confirm the source of cytokines. In fact, the ELISA results were closely correlated with the RT-PCR results with a time lag in the response to LPS. This observation is consistent with the fact that the transcriptional changes occur prior to the translational changes[25].

The more prominent effects on forskolin-induced anion secretion observed in the mixed co-culture as compared to that in the separated co-culture indicate the importance of cell-cell contact in addition to cytokine communication. In fact, cell-cell contact appears to be absolutely required for the enhancement of the expression and release of mIL-6 from Peyer's patch lymphocytes under both normal condition and LPS challenge. This observation is of physiological significance considering the close contact between Peyer's patch lymphocytes and intestinal epithelial cells in the Peyer's patches. IL-6 is known to be produced by a number of cell types including antigen-presenting cells and B cells and it is involved in the acute phase response, B cell maturation and macrophage differentiation[26]. IL-6 has also been reported to activate transcription of a variety of molecules including cytokines and receptors[27]. Therefore, cell-cell contact-induced IL-6 release from Peyer's patch lymphocytes may affect the expression of epithelial ion channels and transporters and lead to modulation of epithelial function. On the other hand, more enhanced expression and release of hIL-8 from Caco-2 cells was observed in the separated co-culture than the mixed co-culture. This is consistent with the properties of IL-8 as a chemokine for attracting immune cells to the site of inflammation since the separation of Peyer's patch lymphocytes from Caco-2 cells in the separated co-culture presents a need for IL-8 to signal the recruitment of lymphocytes. However, there is no need for production of IL-8 if the lymphocytes are present next to the epithelial cells as in the mixed co-culture. Epithelial hIL-8 production has been implicated in the disruption of the epithelial barrier function by *Shigella*[28] as well as other entroinvasive bacteria[29]. Bacterial invasion turns the infected epithelial cells to become strongly proinflammatory with subsequent IL-8 production that attracts polymorphonuclear leukocytes (PMNs), ultimately leading to the disruption of the epithelium. This study only investigated the mIL-6 and hIL-8 expression and release from lymphocytes and epithelial cell to illustrate possible interactions through soluble factors between epithelial and immune cells. Other cytokines may also play a role in the regulation of epithelial physiology by Peyer's patch lymphocytes. The observed expression and release of mIL-6 and hIL-8, constitutively and in response to the LPS challenge, suggest that they may be involved in mediating the modulatory effects of Peyer's patch lymphocytes on epithelial barrier and ion transport function in homeostasis and host defense. Further studies are required to identify their specific roles as well as the involvement of other immune mediators in the modulation of epithelial physiology.

In summary, being the sensory arm of the intestinal mucosa, Peyer's patches are not only involved in transporting, processing and presentation of antigens/pathogens that are essential to eliciting mucosal immune response, but also play an important role in modulating epithelial physiology. This function is distinct from other types of lymphocytes previously studied. Our results indicated that lymphocytes in Peyer's patches receive information from mucosal surface epithelial cells, via both cell-cell contact and cytokine signaling, and in return modulate epithelial barrier and ion transport function in both homeostasis and host defense. Since immune modulation determines the epithelial responsiveness to infection, the co-cultures of epithelial cells with Peyer's patch lymphocytes may provide useful models in studying the initiation process involved in the pathogenesis of inflammation-associated diarrhea.

REFERENCES

1   **Berin MC**, McKay DM, Perdue MH. Immune-epithelial inter-

actions in host defense. *Am J Trop Med Hyg* 1999; **60**: 16-25

2   **Hamzaoui N**, Pringault E. Interaction of microorganisms, epithelium, and lymphoid cells of the mucosa-associated lymphoid tissue. *Ann N Y Acad Sci* 1998; **859**: 65-74

3   **Neutra MR**, Mantis NJ, Kraehenbuhl JP. Collaboration of epithelial cells with organized mucosal lymphoid tissues. *Nat Immunol* 2001; **2**: 1004-1009

4   **Farthing MJ**. Novel targets for the pharmacotherapy of diarrhoea: a view for the millennium. *J Gastroenterol Hepatol* 2000; **15**(Suppl): G38-G45

5   **Beltinger J**, McKaig BC, Makh S, Stack WA, Hawkey CJ, Mahida YR. Human colonic subepithelial myofibroblasts modulate transepithelial resistance and secretory response. *Am J Physiol* 1999; **277**: C271-C279

6   **Lu J**, Philpott DJ, Saunders PR, Perdue MH, Yang PC, McKay DM. Epithelial ion transport and barrier abnormalities evoked by superantigen-activated immune cells are inhibited by interleukin-10 but not interleukin-4. *J Pharmacol Exp Ther* 1998; **287**: 128-136

7   **McKay DM**, Singh PK. Superantigen activation of immune cells evokes epithelial (T84) transport and barrier abnormalities via IFN-gamma and TNF alpha: inhibition of increased permeability, but not diminished secretory responses by TGF-beta2. *J Immunol* 1997; **159**: 2382-2390

8   **McKay DM**, Croitoru K, Perdue MH. T cell-monocyte interactions regulate epithelial physiology in a coculture model of inflammation. *Am J Physiol* 1996; **270**: C418-C428

9   **Kanzato H**, Manabe M, Shimizu M. An *in vitro* approach to the evaluation of the cross talk between intestinal epithelium and macrophages. *Biosci Biotechnol Biochem* 2001; **65**: 449-451

10   **Kerneis S**, Bogdanova A, Kraehenbuhl JP, Pringault E. Conversion by Peyer's patch lymphocytes of human enterocytes into M cells that transport bacteria. *Science* 1997; **277**: 949-952

11   **Kerneis S**, Caliot E, Stubbe H, Bogdanova A, Kraehenbuhl J, Pringault E. Molecular studies of the intestinal mucosal barrier physiopathology using cocultures of epithelial and immune cells: a technical update. *Microbes Infect* 2000; **2**: 1119-1124

12   **Heumann D**, Roger T. Initial responses to endotoxins and Gram-negative bacteria. *Clin Chim Acta* 2002; **323**: 59-72

13   **Takahashi A**, Iida T, Naim R, Naykaya Y, Honda T. Chloride secretion induced by thermostable direct haemolysin of vibrio parahaemolyticus depends on colonic cell maturation. *J Med Microbiol* 2001; **50**: 870-878

14   **Cuthbert AW**, George AM, MacVinish L. Kinin effects on electrogenic ion transport in primary cultures of pig renal papillary collecting tubule cells. *Am J Physiol* 1985; **249**: F439-F447

15   **Rodriguez BL**, Rojas A, Campos J, Ledon T, Valle E, Toledo W, Fando R. Differential interleukin-8 response of intestinal epithelial cell line to reactogenic and nonreactogenic candidate vaccine strains of vibrio cholerae. *Infect Immun* 2001; **69**: 613-616

16   **Faruqi TR**, Gomez D, Bustelo XR, Bar-Sagi D, Reich NC. Rac1 mediates STAT3 activation by autocrine IL-6. *Proc Natl Acad Sci U S A* 2001; **98**: 9014-9019

17   **Rescigno M**, Rotta G, Valzasina B, Ricciardi-Castagnoli P. Dendritic cells shuttle microbes across gut epithelial monolayers. *Immunobiology* 2001; **204**: 572-581

18   **Willemsen LE**, Schreurs CC, Kroes H, Spillenaar Bilgen EJ, Van Deventer SJ, Van Tol EA. A coculture model mimicking the intestinal mucosa reveals a regulatory role for myofibroblasts in immune-mediated barrier disruption. *Dig Dis Sci* 2002; **47**: 2316-2324

19   **Taylor CT**, Murphy A, Kelleher D, Baird AW. Changes in barrier function of a model intestinal epithelium by intraepithelial lymphocytes require new protein synthesis by epithelial cells. *Gut* 1997; **40**: 634-640

20   **Sansonetti PJ**. Molecular and cellular mechanisms of invasion of the intestinal barrier by enteric pathogens. The paradigm of Shigella. *Folia Microbiol* 1998; **43**: 239-246

21   **Resta-Lenert S**, Barrett KE. Enteroinvasive bacteria alter barrier and transport properties of human intestinal epithelium: role of iNOS and COX-2. *Gastroenterology* 2002; **122**: 1070-1087

22   **O'Loughlin EV**, Pang GP, Noltorp R, Koina C, Batey R, Clancy R. Interleukin 2 modulates ion secretion and cell proliferation in cultured human small intestinal enterocytes. *Gut* 2001; **49**: 636-643

23   **Sandle GI**, Higgs N, Crowe P, Marsh MN, Venkatesan S, Peters TJ. Cellular basis for defective electrolyte transport in inflamed human colon. *Gastroenterology* 1990; **99**: 97-105

24   **Sugi K**, Musch MW, Field M, Chang EB. Inhibition of Na^+,K^+-ATPase by interferon gamma down-regulates intestinal epithelial transport and barrier function. *Gastroenterology* 2001; **120**: 1393-1403

25   **Pedron T**, Thibault C, Sansonetti PJ. The invasive phenotype of Shigella flexneri directs a distinct gene expression pattern in the human intestinal epithelial cell line Caco-2. *J Biol Chem* 2003; **278**: 33878-33886

26   **Diehl S**, Rincon M. The two faces of IL-6 on Th1/Th2 differentiation. *Mol Immunol* 2002; **39**: 531-536

27   **Sitaraman SV**, Merlin D, Wang L, Wong M, Gewirtz AT, Si-Tahar M, Madara JL. Neutrophil-epithelial crosstalk at the intestinal lumenal surface mediated by reciprocal secretion of adenosine and IL-6. *J Clin Invest* 2001; **107**: 861-869

28   **Sansonetti PJ**. Microbes and microbial toxins: paradigms for microbial-mucosal interactions III. Shigellosis: from symptoms to molecular pathogenesis. *Am J Physiol Gastrointest Liver Physiol* 2001; **280**: G319-G323

29   **Fleckenstein JM**, Kopecko DJ. Breaching the mucosal barrier by stealth: an emerging pathogenic mechanism for enteroadherent bacterial pathogens. *J Clin Invest* 2001; **107**: 27-30

Edited by Ma JY and Xu FM

• BASIC RESEARCH •

Association of differentially expressed genes with activation of mouse hepatic stellate cells by high-density cDNA mircoarray

Xiao-Jing Liu, Li Yang, Feng-Ming Luo, Hong-Bin Wu, Qu-Qiang

Xiao-Jing Liu, Hong-Bin Wu, Qu Qiang, Laboratory of Department of Internal Medicine, West China Hospital, Sichuan University, Chengdu 610041, Sichuan Province, China
Li Yang, Department of Gastroenterology of West China Hospital, Sichuan University, Chengdu 610041, Sichuan Province, China
Feng-Ming Luo, Department of Internal Medicine of West China Hospital, Sichuan University, Chengdu 610041, Sichuan Province, China
Supported by the National Natural Science Foundation of China, No.39800054 and No.39700068
Correspondence to: Xiao-Jing Liu, Department of Internal Medicine, West China Hospital, Sichuan University, 37 Wainan Guoxuexiang, Chengdu 610041, Sichuan Province, China. xiaojingliu67@yahoo.com
Telephone: +86-28-85422388
Received: 2003-10-08   **Accepted:** 2003-12-08

Abstract

AIM: To characterize the gene expression profiles associated with activation of mouse hepatic stellate cell (HSC) and provide novel insights into the pathogenesis of hepatic fibrosis.

METHODS: Mice HSCs were isolated from BALB/c mice by *in situ* perfusion of collagenase and pronase and single-step density Nycodenz gradient. Total RNA and mRNA of quiescent HSC and culture-activated HSC were extracted, quantified and reversely transcripted into cDNA. cDNAs from activated HSC were labeled with Cy5 and cDNAs from the quiescent HSC were labeled with Cy3, which were mixed with equal quantity, then hybridized with cDNA chips containing 4 000 genes. Chips were washed, scanned and analyzed. Increased expression of 4 genes and decreased expression of one gene in activated HSC were confirmed by reverse transcription- polymerase chain reaction (RT-PCR).

RESULTS: A total of 835 differentially expressed genes were identified by cDNA chip between activated and quiescent HSC, and 465 genes were highly expressed in activated HSC. The differentially expressed genes included those involved in protein synthesis, cell-cycle regulation, apoptosis, and DNA damage response.

CONCLUSION: Many genes implicated in intrahepatic inflammation, fibrosis and proliferation were up-regulated in activated HSC. cDNA microarray is an effective technique in screening for differentially expressed genes between two different situations of the HSC. Further analysis of the obtained genes will help understand the molecular mechanism of activation of HSC and hepatic fibrosis.

INTRODUCTION

Liver fibrosis is a common consequence of chronic liver injury and is characterized by the progressive accumulation of extracellular matrix (ECM) proteins, particularly type I and III collagens. Hepatic stellate cells (HSC) are the major source of ECM in hepatic fibrosis and HSC is one of the sinusoid-constituent cells that plays multiple roles in the liver pathophysiology. After hepatic injury, HSC undergoes an activation process, characterized by loss of vitamin A, trans-differentiation to a smooth muscle α-actin (α-SMA)-positive myofibroblast like cell type, increased proliferation and increased production of ECM proteins[1,2]. Activation and transformation of HSC from the vitamin A-storing phenotype (also called "quiescent" phenotype) to the "myofibroblastic" one has been identified as a critical step in hepatic fibrogenesis and is regulated by several factors including cytokines and oxidative stress[3-5]. However, the molecular mechanism for HSC activation is not well understood. The activation of HSC involves many genes from multiple pathogenic pathways.

cDNA microarray analysis is a powerful descriptive method of examining the expression profile of hundreds to thousands of genes in unison. It has become an increasingly popular tool to investigate the function of genes, especially those genes involved in tumor generation and growth[6]. Recently, cDNA array has been used to identify differentially expressed genes in HCV-associated cirrhosis and achieve new insights into HCV liver injury[7].

Further advances in our knowledge about HSC activation requires more genes to be identified. Microarray technology provides us with a genomic approach to explore the genetic markers and molecular mechanisms leading to hepatic fibrosis. To this end, we have used cDNA microarray analysis to detect genes whose mRNA expression changes in the cultured activated HSC. RT-PCR analysis confirmed up-regulation of 4 previously unreported transcripts and down-regulation of one gene transcript in the activated HSC. The identification of these genes provides new insight into the understanding of HSC activation and hepatic fibrogenesis. Culturing HSC on plastic surface converts them from a quiescent phenotype to an activated phenotype similar to *in vivo* activation and this cultured-induced activation has been extensively studied as a model of the activation secondary to liver fibrogenesis[8,9]. Therefore, we used the *in vitro* model in which the activation of HSC was induced by growth on plastic dishes to study the differentially expressed genes associated with the activation of HSC.

MATERIALS AND METHODS

Materials
Male BALB/c mice were obtained from Experimental Animal Center of West China Medical School, Sichuan University (Chengdu, Sichuan). All animals were treated humanely according to the national guideline for the care of animals.

Pronase, DNase I and Collagenase B were from Roche Molecular Biochemicals (Mannhein, Germany). Nycodenz was from Sigma (St. Louis, USA). Dulbecco' s modified medium (DMEM), trypsin-EDTA and new-born calf serum were from Invitrogen Corp (Grand Island, USA). Monoclonal antibodies against desmin, α-smooth muscle actin (α-SMA) were obtained from Dako (Glostrup, Denmark). Gene chips (MGEC-40s) were

purchased from BioStar Genechip Inc. (Shanghai, P.R.China), and each chip contains 4 000 mouse cDNAs, including 1 500 cDNAs of known sequence and function, and 2 500 novel cDNAs whose function has not been known in the public database.

Methods

HSC isolation and culture HSC was isolated from male Balb/c mice by *in situ* pronase, collagenase perfusion and single-step Nycodenz gradient according to our previous report. The purity of primary HSC after 3 d in culture was approximately 95% as estimated by vitamin A auto-fluorescence and immunocytochemistry with antibody against desmin. Therefore, HSC cultured in uncoated plastic dishes spontaneously acquired an activated phenotype, characterized by expression of α-SMA and by loss of vitamin A droplets. After reaching confluence (about 10-14 d after plating), activated HSC was detached by trypsin, and split in a 1:2 ratio. Experiments were performed on primary cells cultured for 3 d and activated HSC of the third passages using 3 independent cell lines, and the purity of activated HSC exceeded 98%.

Preparation of RNA and cDNA microarray Total RNA was isolated from primary mouse HSC and sub-confluent culture-activated mouse HSC (passage 3), using Trizol reagent (Invitrogen Life Technologies Inc, USA) according to the manufacturer's protocol. Poly (A) mRNA was isolated from total RNA using Oligotex mRNA Midi Kit (Qiagen, USA) according to the manufacturer's protocol.

All microarray procedures were performed by BioStar Genechip Inc. (Shanghai, P.R.China). Equal quantities of mRNA from each cell phenotype were used to prepare probes, hybridized to gene chips (MGEC-40 s, Biostar Genechip Inc.), and analyzed for the quantity of mRNA encoded by 4 000 mouse genes. The preparation of Cy5 and Cy3 probes from mRNA samples and the hybridization were conducted by the BioStar Genechip Inc.

RT-PCR assays To validate the expression pattern identified on the expression arrays, 4 genes (MIF, Annexin VI, N-Cadherin, DAD1) from the up-regulated genes and one gene (BHMT) from the down-regulated genes in activated HSC were picked and semi-quantitative RT-PCR was performed to confirm their changed expression with cDNA templates from activated and quiescent HSC. The total RNA was isolated from HSC using Trizol reagent, precipitated in ethanol and resuspended in sterile RNAase-free water and stored at -70 ℃, as described previously. One-step reverse transcription-polymerase chain reaction (RT-PCR) was performed according to the method of the supplier (TaKaRa Biotechnology Co., Ltd, Dalian). Primers were designed using the Primer 3 program from Whitehead Institute for Biomedical Research (Cambridge, MA, USA)[10], synthesized and purified by PAGE in Genebase BRL Custom Primers (Genebase Biotechnology Co., Shanghai). Primer sequences are shown in Table 1. The PCR products was analyzed by 20 g/L agarose gel electrophoresis with TAE buffer at 80 V for 40 min, visualized with ethidium bromide and photographed under UV light by Gel Documentation system (Gel Doc 2000™, Bio-Rad, USA). The semi-quantitative analysis was performed using the volume analysis in the Quantity One Software (Bio-Rad, USA). Each detected gene/GAPDH quotient is the indication of the detected gene. Experiments were performed for at least five times with similar results.

Statistical analysis

RT-PCR results were expressed as mean±SD. Differences between means were analyzed with Student t test for paired samples. A value of $P<0.05$ was considered statistically significant.

RESULTS

Expression pattern of genes in activated HSC

Differences in gene expression patterns between mouse activated HSC and quiescent HSC were assessed using microarray analysis. This array allows a quantitative measurement of 4 000 known genes and expressed sequence tags. Genes that differed in intensity by at least 2-fold were considered to be differentially regulated. Figure 1 shows that the cDNA array images along with color charts indicating up-regulated genes with red, down-regulated ones with green and non-changed with yellow. Of the 4 000 genes analyzed by mircoarray, a total of 835 genes (20.8%) revealed differential expression in the activated HSC when compared with the quiescent HSC (Tables 2-4). Of the 835 genes with altered expression in the activated HSC, 462 genes (including 204 known function genes) revealed elevated expression whereas 373 genes (including 132 known function genes) revealed reduced expression. Array analysis identified many differentially expressed genes that are important in inflammation, fibrosis, proliferation, signaling, apoptosis and oxidative stress.

Validation of array data with RT-PCR

To further investigate the reliability of our array data, we picked 5 differential expressed genes and measured the expression of the genes in the activated and quiescent HSC. Figures 2 and 3 and Table 5 show that the different expression pattern of each of the five genes as determined by RT-PCR were similar to those observed with cDNA array, confirming the reliability of our array data.

Table 1 Primer sequences for RT-PCR

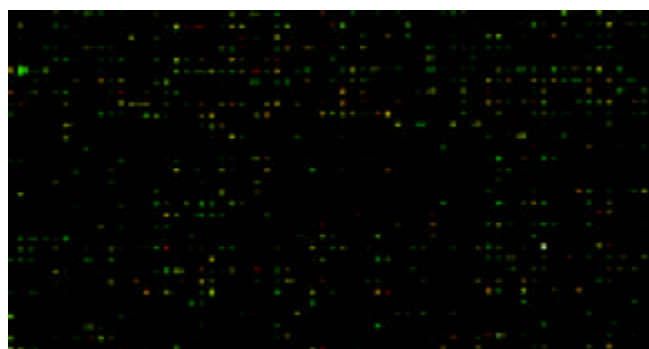| Gene name	Primer sequence	Expected product size
Betaine homocysteine methyltransferase (BHMT)	Left 5' –GCC TAT AGC GGC TAC CAT GT-3' Right 5' -CTC TGC AAT GGC CCT GAT GT-3'	399 bp
Defender against cell death protein 1 (DAD1)	Left 5' -TTC GGC TAC TGT CTC CTC GT -3' Right 5' -ACG AGG TGC AGG ATA GTG CT-3'	197 bp
Annexin VI	Left 5' -TAC CCC GGA GTA TTT TGC TG-3' Right 5' -GTC CCC TCC ACA TAG CTT CA-3'	220 bp
Neural cadherin (N-Cadherin)	Left 5' -ATA CAG TGT CAC TGG GCC AG- 3' Right 5' -CGT AAG TGG GAT TGC CTT CC- 3'	499 bp
Macrophage migration inhibitory factor (MIF)	Left 5' -TTT TAG TGG CAC GAG CGA CC-3' Right 5' -AAG CGA AGG TGG AAC CGT TC- 3'	199 bp
GAPDH	Left 5' -ACC ACA GTC CAT GCC ATC AC-3' Right 5' -TCC ACC ACC CTG TTG CTG TA-3'	452 bp

Figure 1 cDNA microarray scanning result of gene expression profile between quiescent HSC and activated HSC.
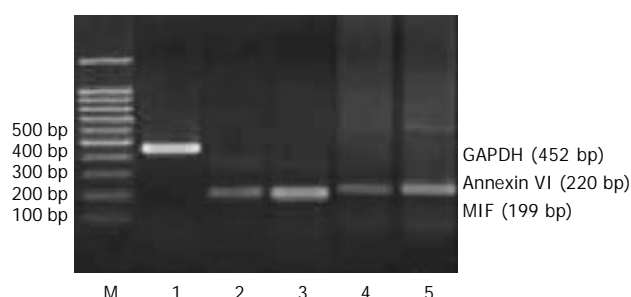

Figure 2 Electrophoresis analysis of RT-PCR products. Lane M: 100 bp DNA ladder; Lane 1: GAPDH; Lane 2, 3: MIF amplified from quiescent HSC and activated HSC mRNA respectively; Lane 3 shows increased expression of MIF in activated HSC compared with lane 2 in quiescent HSC. Lane 4, 5: Annexin VI amplified from quiescent HSC and activated HSC mRNA respectively; Lane 5 shows increased expression of Annexin VI in activated HSC compared with lane 4 in quiescent HSC.

Figure 3 Electrophoresis analysis of RT-PCR products. Lane M: 100 bp DNA ladder; Lane 1: GAPDH; Lane 2, 3: N-Cadherin amplified from quiescent HSC and activated HSC mRNA respectively; Lane 3 shows increased expression of N-Cadherin in activated HSC compared with lane 2 in quiescent HSC. Lane 4, 5: DAD1 amplified from quiescent HSC and activated HSC mRNA respectively; Lane 5 shows increased expression of Annexin VI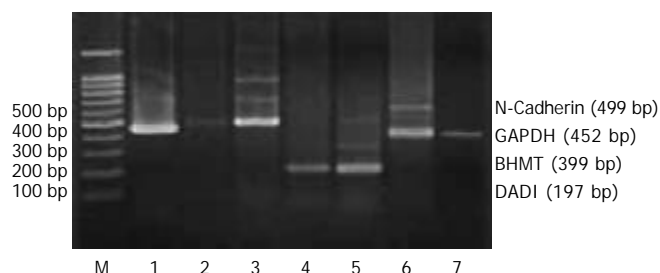 in activated HSC compared with lane 4 in quiescent HSC. Lane 6, 7: BHMT amplified from quiescent HSC and activated HSC mRNA respectively; Lane 7 shows decreased expression of BHMT in activated HSC compared with lane 6 in quiescent HSC.

DISCUSSION

Genome-wide expression profiling by microarray of cDNA or oligonucleotide probes on a glass or nylon substrate is an exceptionally powerful tool for the study of gene regulation. This methodology has been used to investigate the phenomena particularly appropriate for the analysis of expressed liver genes[7]. cDNA microarrays were used to profile changes in gene expression in activated HSC. Scatter plot analysis showed that approximately 20.8% of all mouse genes examined on the 4 000 gene microarrays exhibited altered expression, with 11.5% showing up-regulation and 9.3% showing down-regulation. These genes will be future studied.

Table 2 Part of the previously reported up-regulated genes in activation of HSC

GenBank accession number	Gene name	Ratio (Cy5/Cy3)	Potential gene function
M73741	Alpha-B2-crystallin, complete cds	155.619	Small heat shock protein gene, an early marker for HSC activation
X52046	Procollagen, type III, alpha 1	119.092	Extracellular matrix (ECM), over- expressed in hepatic fibrosis
M18194	Fibronectin mRNA	29.958	ECM, over expressed in hepatic fibrosis
J02870	Laminin receptor mRNA	6.62	ECM receptor (integrin), cell adhesion
L08115	CD9 antigen	6.094	Cell membrane glycoprotein, involved in cell activation and adhesion
U16163	Prolyl 4-hydroxylase alpha (II)-subunit mRNA, complete cds	4.555	An enzyme which is essential for the collagen synthesis in HSC
X62622	TIMP-2 mRNA for tissue inhibitor of metalloproteinase, type 2	3.732	Inhibition for ECM degradation
X04017	mRNA for cysteine-rich glycoprotein SPARC	3.435	Regulation of cell shape, adhesion, migration and proliferation
AF070470	SPARC-related protein (SRG) mRNA, complete cds	3.181	Regulation of cell shape, adhesion, migration and proliferation
M21495	Cytoskeletal gamma-actin mRNA,	3.092	Relate skeleton structure of cell
AF188297	TGF-beta receptor binding protein (Trip1) mRNA, complete cds	2.976	TGF-beta mediated signaling pathway
AJ245923	alpha-tubulin 8 (Tuba 8 gene) mRNA	2.901	Relate skeleton structure of cell
AF053454	Tetraspan TM4SF (Tspan-6) mRNA, complete cds	2.896	Cell development, differentiation, motility
AF013262	Lumican gene, complete cds	2.862	Small, leucine-rich proteoglycan which involves in the regulation of collagen figril assembly
L02526	Protein kinase (MEK) mRNA	2.714	Signaling molecule in MAPK family
Y00769	mRNA for integrin beta subunit	2.521	Signaling molecular in cell adhesion, proliferation and migration

Table 3 A portion of up-regulated genes in activated HSC

GenBank accession number	Gene name	Ratio (Cy5/Cy3)	Potential gene function
AF061017	UDP-glucose dehydrogenase, mRNA complete cds	15.56	Glycosaminoglycan , hyaluronan and heparan sulfate biosynthesis
X65553	mRNA for poly (A) binding protein	7.405	A regulator of translation initiation
AF029844	Elongation factor 1-beta homology mRNA, complete cds	6.305	Translation factor and has multi-functions
NM_010798	Macrophage migration inhibitory factor (Mif), mRNA	5.847	Proinflammatory peptide and a mediator of growth factor dependent ERK MAP kinase activation and cell cycle progression
M31131	Neural cadherin (N-cadherin) mRNA	5.559	Cell adhesion molecule
AB029930	mRNA for caveolin-1 beta isoform	4.945	Inhibit the eNOS activity
D12618	mRNA for nucleosome assembly protein-1, complete cds	4.528	Histone H2A-H2B shutting protein that promotes histone deposition, and is important for maintaining chromatin structure
M22432	Protein synthesis elongation factor Tu (eEF-Yu, eEf-1-1alpha) mRNA, complete cds	4.344	Translation factor involved in the protein biosynthesis
D31717	mRNA for ribophorin	4.319	Glycoprotein synthesis
NM_012052	Ribosomal protein S3 (Rps3), mRNA	4.297	Protein biosynthesis
X72711	mRNA for replication factor C (140 Kda), long subunit	4.245	DNA synthesis and repair, and a regulator of NF-kappa B
X13460	Annexin VI, p68 (Mouse mRNA for p68 protein of the lipocortin family)	4.218	Calcium binding protein
NM_011290	Ribosomal protein L6 (Rp16), mRNA	4.089	Protein biosynthesis
U12273	Apurinic/apyrimidinic endonuclease (APEX) gene, complete cds	3.488	A DNA repair enzyme and an activator of several transcription factors
D42048	mRNA for squalene epoxidase	3.298	Rate-limiting enzyme of cholesterol biosynthesis
AJ250491	mRNA for receptor activity modifying protein 3 (Ramp3) gene	3.255	Complex with the calcitonin receptor-like receptor, establishing a functional receptor for adrenomedullin
L04280	Ribosomal protein (RPL12) mRNA	3.172	Protein biosynthesis
K02927	Ribonucleotide reductase subunit M1 mRNA, complete cds	3.156	Rate-limiting enzyme in DNA synthesis and repair
AF087568	Palmitoyl-protein thioesterase precursor mRNA, complete cds	3.059	Cell survival signaling
AF020039	NADP-dependent isocitrate dehydrogenase (Idh) mRNA, complete cds	3.038	A key enzyme of the tricarboxylic acid cycle
X57960	Ribosomal protein L7	2.962	Protein biosynthesis
U09816	GM2 activator protein (Gm2a) mRNA	2.888	Enzymatic hydrolysis of GM2
AB018575	Cdc 7 mRNA, complete cds	2.816	Essential for G1/S transition
AF041054	E1B19K/Bcl-2 binding protein homology (Nip3) mRNA, nuclear gene encoding mitochondria protein, complete cds	2.813	Nips is a pro-apoptotic mitochondria protein
L04128	Ribosomal protein L18 (rpL18) mRNA	2.751	Protein biosynthesis
Z31554	(129/SV) Cctd mRNA for CCT (chaperonin containing TCP-1) delta subunit	2.743	Stabilize the cytoskeletal protein actin and tubulin
D63784	mRNA for MIDA1, complete cds	2.703	Regulate cell growth
AF026481	eIF-1A (eIF-1A) mRNA, complete cds	2.682	Translation initiation factor
U35249	CDK-activating kinase assembly factor p36/MAT1, complete cds	2.645	An assembly factor and a targeting subunit of cyclin-dependent kinase-activating kinase that is involved in cell cycle control, transcription and DNA repair
M76131	Elongation factor (ef-2) mRNA, 3' end	2.614	Protein biosynthesis
X64713	mRNA for cyclin B1	2.576	Cell cycle regulatory protein
D26091	mRNA for mCDC47, complete cds	2.570	A member of the minichromosome maintenance (Mcm) family involve in the DNA replication licensing system
U78085	Ribosomal protein S5 mRNA	2.507	Protein synthesis
AF141322	Caveolin-2 mRNA, complete cds	2.458	Inhibit the eNOS activity
M33934	IMP dehydrogenase mRNA, complete cds	2.429	An enzyme involved in de novo synthesis of guanine nucleotides
U83628	Defender against cell death protein 1 (DAD1) mRNA, complete cds	2.372	Apoptotic suppressor gene

Table 4 Part of down-regulated genes in the activated HSC

GenBank accession number	Gene name	Ratio (Cy5/Cy3)	Potential gene function
D49949	mRNA for IGIF precursor poly-peptide in (Interleukin 18), complete cds	0.065	In the development of Th1 cells and tissue injury inflammatory reaction
U63146	Retinal binding protein (RBP) mRNA	0.125	Retinoid storage and metabolism
AF035644	Potentially prenylated protein tyrosine phosphatase mPRL-2 mRNA, complete cds	0.226	Cellular regulation
X58287	mR-PTPu gene for protein tyrosine phosphatase, receptor-type M	0.280	Cellular regulation
AF033381	Betaine homocysteine methyl transferase (BHMT) mRNA, complete cds	0.299	A key liver enzyme that is important for homocysteine homeostasis
M75720	Alpha-1 serine protease inhibitor 3 mRNA, complete cds	0.308	Anti-inflammatory effect
U20497	P19 protein mRNA, complete cds	0.324	CDK4&CDK6 inhibitor, cell cycle inhibitor
D85596	AMP deaminase H-type, complete cds	0.339	Involved in the biosynthesis, inter-conversion and degradation of purine compounds
Y10138	Gene encoding prostaglandin D synthase	0.361	A PGD producing enzyme and a retinoid transporter
NM_013498	CAMP response element modulator (CREM) mRNA	0.366	Down-regulator of CAMP-induced transcription
U67187	G protein signaling regulator RGS2 (rgs2) mRNA, complete cds	0.369	Negatively regulate G-coupled receptor function
AF023919	PK-120 precursor (itih-4) mRNA, complete cds	0.421	Inter-alpha-trypsin-inhibitor H4, is a potential regulator for ECM proteins
AF077950	Protein inhibitor of activated STAT protein PIAS 1 mRNA, complete cds	0.433	Inhibition of STAT-1-mediated gene activation
M75718	Alpha-1 protease inhibitor 4 mRNA, complete cds	0.437	Anti-inflammatory activity
D38046	mRNA for type II DNA topoisomerase beta isoform, complete cds	0.445	An essential enzyme that alters DNA topology which is important for cell survive and apoptosis
AF073996	myotubularin (Mtm1) mRNA complete cds	0.464	Subfamily of protein tyrosine phosphatases

Table 5 Semi-quantitative analysis of RT-PCR results

Groups	Mean±SD (quotient of the detected gene/GAPDH)	N	p value
MIF from quiescent HSC	0.269±0.016	5	
MIF from activated HSC	0.759±0.046	5	<0.05
N-Cadherin from quiescent HSC	0.177±0.063	5	
N-Cadherin from activated HSC	0.776±0.087	5	<0.05
Annexin VI from quiescent HSC	0.137±0.04	5	
Annexin VI from activated HSC	0.478±0.025	5	<0.05
DAD1 from quiescent HSC	0.174±0.016	5	
DAD1 from activated HSC	0.593±0.047	5	<0.05
BHMT from quiescent HSC	0.602±0.083	5	
BHMT from activated HSC	0.134±0.059	5	<0.05

In the up-regulated genes associated with the activation of HSC, some genes have already been reported (Table 2). Alpha B-crystallin was first reported by Lang et al[11] recently as an early marker for HSC activation. In our experiment, the ratio of Cy5 to Cy3 for its mRNA was the highest in all the genes in the gene-chip, suggesting that mRNA expression of alpha B-crystallin in activated HSC up-regulated mostly comparing with the quiescent HSC. The mRNA expression for procollagen type III[12], fibronectin[13], laminin receptor, prolyl 4-hydroxylase[14], TIMP-2, TGF-beta and its receptor binding protein[15], MEK[16] and integrin beta[17] was increased in activated HSC. Tetraspanins (TM4SF) super family which includes CD9, CD53, CD81 and CD151 were highly expressed in the activated human HSC and have been implicated in HSC migration, a key event in liver tissue wound healing and fibrogenesis[18]. Secreted protein, acidic and rich in cysteine (SPARC), which functions in tissue remodeling, was expressed by activated HSC in chronic hepatitis, suggesting the involvement of SPARC in hepatic fibrogenesis after chronic injuries[19]. Lumican is a small leucine-rich proteoglycan, which contributes to cell migration, proliferation, tissue hydration and collagen fibrillogenesis, and its expression is increased in HSC in diseased liver during the process of fibogenesis[20]. Although we employed different methods, animal models or different sources of HSC, our experimental data was consistent with the results observed by others, demonstrating that the technique of cDNA microarray has a higher reliability. In addition, the expression of those that were not previously linked to the activation of HSC was also

found to be changed. These include genes involved in the control of HSC morphology, growth, differentiation, migration and apoptosis.

Analysis of the genes showed elevated expression in the activated HSC clustered into distinct functional groups. Genes showing elevated expression included many genes involved in the formation and remodeling of the extracellular matrix (ECM) and in the regulation of cellular response (including cell adhesion, proliferation and migration) to the ECM, such as procollagen type III, fibronectin, TIMP-2, TGF beta, UDP-glucose dehydrogenase (AF061017), N-cadherin (M131131) and lumican (AF013262).

The enzyme UDP-glucose dehydrogenase (Udpgdh)(EC 1.1.1.22) converts UDP-glucose to UDP-glucutonate, a critical component of the glycosaminoglycans, hyluronan, chondroitin sulfate and heparan sulfate[21]. It is known that heparan sulfate proteoglycans are essential cofactors in cell-matrix adhesion processes, in cell-cell recognition system, and in receptor-growth factor interactions. Cultured human HSC can synthesize all four cyndecans and the increased expression of glycosaminoglycans and hyaluronic acid may be important in the deposition of matrix components and activation of growth factors accompanying fibrogenesis. Our results suggested that the increased expression of heparan sulfate proteoglycans in activated HSC might be partially caused by the elevated expression of the enzyme UDP-glucose dehydrogenase.

Neural cadherin (N-cadherin) is an adhesion molecule of the cadherin family, whose expression was up regulated in response of smooth muscle cells to arterial injury[22]. AnnexinVI is a 68-Kda protein of the annexin family, a group of structural similar, calcium-dependent, phospholipid-binding proteins[23]. Our cDNA microarray data along with the RT-PCR results showed increased expression of N-cadherin and annexin VI in activated HSC, suggesting their regulations might be important for the hepatic fibrogenesis.

In all cells, protein synthesis is coordinated by the ribosome, and the large ribonucleoprotein is composed of at least 50 distinct molecules and several large RNA molecules. Genes showing elevated expression included many genes that encode ribosomal proteins and proteins involved in the translation and protein synthesis, such as mRNA for poly A-binding protein (X65553), elongation factor 1-beta homology mRNA (AF029844), elongation factor Tu (M22432), ribosomal protein S3 (NM_012052), S5 (U78085), L6 (NM_011290), L12 (L04280), L18 (L04128) and eukaryotic initiation factor 1A (eIF1A) (AF026481). HSC proliferated during the process of activation, so it is not surprising that many genes involved in the protein synthesis up-regulated in the activated HSC.

Our work has identified some previously unreported genes involved in DNA synthesis and repair showing elevated expression in the activated HSC, such as replication factor C gene (X72711), apurinic/apyrimidinic endonuclease (APEX) gene (U12273), ribonucleotide reductase subunit M1 (M1-RR) mRNA (K02917), and IMP dehydrogenase mRNA (M33934), an enzyme involved in de novo synthesis of guanine nucleotides.

Replication factor C (RFC) is a clamp loader, catalyzes assembly of circular proliferating cell nuclear antigen clamps around primed DNA, enabling processive synthesis by DNA polymerase during DNA replication and repair. The Rel A (p65) subunit of NF-kappa B is an important regulator of inflammation, proliferation and apoptosis, but the large subunit of RFC can function as a regulator of Rel A. In addition to its previously described function in DNA replication and repair, RFC plays an important role as a regulator of transcription factor NF-kappa B activity[24].

APEX nuclease is a mammalian DNA repair enzyme having apurinic/apyrimidinic endonuclease, 3' -5' -exonuclease, DNA 3' repair diesterase and DNA 3' -phosphatase activities. It is also a redox factor (Ref-1), stimulating DNA binding activity of

AP-1 binding proteins such as Fos and Jun[25]. Ribonucleotide reductase (RR) is a cytoplasmatic enzyme catalyzing the reduction of all four ribonucleotides to their corresponding deoxyribonucleotides, so it is a rate-limiting enzyme in the DNA synthesis and repair. Its activity strongly correlates to the rate of DNA synthesis, and the expression of M1-RR antigen was found to correlate positively with the expression of Ki-67 and PCNA, the cell cycle markers of proliferating cells[26]. We conclude that mechanisms for DNA synthesis and repair are activated during the process of HSC activation.

Elevated expression was also observed for a number of genes involved in the control of cell growth, survival, differentiation and apoptosis. Palmitoyl-protein thioesterase (PPT) is a newly described lysomal enzyme that hydrolyzes long chain fatty acids from lipid-modified cysteine residues in proteins, and its precursor mRNA (AF087568) was up-regulated in activated HSC. It was reported that inhibition of PPT increased the susceptibility of neurons to apoptotic cell death[27]. Id, a helix-loop-helix protein not only regulates cell differentiation negatively, but also promote growth and apoptosis, and an Id-associate protein, MIDA1 (Mouse Id associate1), regulated cell growth positively. MIDA1 is a novel sequence-specific DNA binding protein with some different properties from the usual transcription factors and may act as a mediator of Id-mediated growth-promoting function through its DNA binding activity[28], and its gene expression was increased in the activated HSC.

The cyclin-dependent kinase (CDK)-activating kinase (CAK) is involved in cell cycle control, transcription, and DNA repair, and MAT1 gene (U35249), an assembly factor and a targeting subunit of CAK, was also up regulated in the activated HSC. It was reported that abrogation of MAT1 expression by retrovirus-mediated gene transfer of antisense MAT1 RNA in cultured rat aortic smooth muscle cells (SMC) retarded SMC proliferation and inhibits cell activation from a nonproliferation state, and this effect was due to G1 phase arrest and apoptotic cell death[29].

Up-regulation of the DAD1 (U83628), a putative anti-apoptosis gene identified in several distantly related organisms[28], was observed as well as the Nip3 (AF041054), a proapoptotic member of the Bcl-2 family of cell death factors[29] in the activated HSC. CDC7, an evolutionarily conserved serine-threonine kinase, plays a pivotal role in linking cell cycle regulation to genome duplication, being essential for the firing of DNA replication origins[30]. Our microarray experiments also identified elevated expression for CDC7 gene (AB018575) and cyclin B_1 (X64713) in the activated HSC. The strategy for terminating the proliferation of activated HSC by apoptosis might be an exciting therapy for patients with chronic liver injury and fibrosis[10,31], therefore, our experimental data about the differentially expressed genes involved in apoptosis will give some new ideas on induce apoptosis in HSC.

Macrophage migration inhibitory factor (MIF)(NM_010798), a pro-inflammatory peptide and a mediator of growth factor-dependent ERK MAP kinase activation and cell cycle progression[32], was up-regulated by the process of HSC activation. MIF has been shown to contribute significantly to the development of immuno-pathology in several models of inflammatory, such as glomerulonephritis[33]. Our RT-PCR results confirmed the increased expression of MIF mRNA in the activated HSC. This is the first study to demonstrate that activated HSC can produce MIF *in vitro*, and its up-regulation in activated HSC might suggest a role for MIF in the hepatic fibrogenesis *in vivo*. It is necessary to carry further more research to understand how MIF regulates proliferation in activated HSC.

Down-regulation was observed for genes encoding interleukin 18 (D49949) and retinal binding protein (RBP) (U63146) in the activated HSC. IL-18 has an anti-fibrotic effect and it was reported that intrasplenic transplantation of IL-18

gene modified hepatocytes could be a candidate for therapeutic intervention in hepatic fibrosis through induction of a dominant Th1 response[34]. HSCs are the body's major cellular storage sites for retinoid, but the immortalized rat HSC cell line HSC-T6 failed to express RBP[35]. Our cDNA microarray results were consistent with the previous reports.

In the activated HSC, reduced expression was observed for genes involved in general cellular regulation including a family of protein-tyrosine phosphatase (PTPases) and some negative regulators of cell growth signaling, such as P19 protein (U20497), CAMP response element modulator (Crem)(NM_013498), G protein signaling regulator RGS2 (U67187), and protein inhibitor of activated STAT protein - PIAS1 (AF077950). The PTPases included the potentially prenylated protein tyrosine phosphatase mPRL-2 (AF035644)[36], myotubularin (Mtm1)(AF071996)[37] and mR-PTPu gene for protein tyrosine phosphatase, receptor type M. Protein tyrosine kinase and phosphatase play diverse roles in involving energy metabolism, cell proliferation and stimulation of MHC class I molecule pathway. Down-regulation was also observed for the alpha-1 serine protease inhibitor 3 (M75720), alpha-1 protease inhibitor 4 (M75718) and PK-120 precursor (itih-4)(AF023919), a serine protease inhibitor.

P19 is a tumor suppressing protein and belongs to a family of cyclin D-dependent kinase inhibitors of CDK4 and CDK6, which play a key role in human cell cycle control[38]. Addition of p19 protein can lead to inhibition of the CDK's activity and may cause the cells to arrest at G1 phase. Transcriptional factors binding to camp-response elements (CREs) in the promoters of various genes belong to the basic domain-leucine zipper super family and are composed of three genes in mammals, CREB, CREM, and ATF-1. Activation is classically brought about by signaling-dependent phosphorylation of a key acceptor site (Ser133 in CREB) by a number of possible kinases, including PKA, CamKIV and RSK-2. Repression may involve dynamic dephosphorylation of the activators and decreased association with CREB-binding protein (CBP). Another pathway of transcriptional repression on CRE sites implicates the inducible repressor ICER (inducible camp early repressor), a product of the CREM gene. Being an inducible repressor, ICER is involved in auto-regulatory feedback loops of transcription that govern the down-regulation of early response genes, such as the proto-oncogene c-fos[39]. It is known that CREB is one of the transcription factors whose expression is increased in the activated HSC during the liver injury[40], but the important role of CREM in the pathophysiology of liver fibrogenesis has not been studied. Similarly, Jak-Stat signaling is one of the signaling pathways in the HSC proliferation and activation[41], but the role of a negative regulator in this cytokine signaling, protein inhibitor of activated STAT-1 (PIAS-1), has not been understood. Thus, our microarray data might provide novel potential approaches to the treatment of hepatic fibrogenesis in patients with chronic liver diseases.

Reduced mRNA expression was also found for betaine-homocysteine methyl transferase (BHMT). BHMT is a key liver enzyme for homocysteine (Hcy) homeostasis. It catalyzes the synthesis of methionine from betaine and homocysteine, utilizing a zinc ion to activate Hcy. Elevated plasma levels of Hcy have been shown to interfere with normal cell function in a variety of tissues and organs, such as the vascular wall and the liver. It is known that Hcy is able to induce the expression and synthesis of the TIMP-1 in variety of cell types ranging from vascular smooth muscle cells to hepatocytes, HepG2 cells and HSCs. In HSCs, Hcy also stimulates alpha$_1$ (I) procollagen mRNA expression, promotes activating protein-1 (AP-1) binding activity[42]. Hcy is a key metabolite in methionine metabolism, which takes place mainly in the liver. Hyperhomocysteinemia may develop as a consequence of defects in Hcy-metabolizing genes (such as BHMT); nutritional conditions leading to vitamin B (6), B (12), or folate deficiencies; or chronic alcohol consumption. We postulated that hyperhomocysteinemia in the hepatic fibrosis was partly due to the reduced expression of BHMT gene in the activated HSC.

We used cDNA array analysis to detect genes whose mRNA expression changes in the activated mouse HSC after culture on the plastic dishes. RT-PCR analysis confirmed the up-regulation of four previously unreported transcripts and down-regulation of one gene in activated HSC. The identity of these genes provides new insights into the understanding of activation of HSC during the liver injury and hepatic fibrogenesis.

REFERENCES

1   **Reeves HL**, Friedman SL. Activation of hepatic stellate cells–a key issue in liver fibrosis. *Front Biosci* 2002; **7**: d808-826

2   **Dai WJ**, Jiang HC. Advances in gene therapy of liver cirrhosis: a review. *World J Gastroenterol* 2001; **7**: 1-8

3   **Mann DA**, Smart DE. Transcriptional regulation of hepatic stellate cell activation. *Gut* 2002; **50**: 891-896

4   **Pinzani M**, Marra F. Cytokine receptors and signaling in hepatic stellate cells. *Semin Liver Dis* 2001; **21**: 397-416

5   **Liu XJ**, Yang L, Mao YQ, Wang Q, Huang MH, Wang YP, Wu HB. Effects of the tyrosine protein kinase inhibitor genistein on the proliferation, activation of cultured rat hepatic stellate cells. *World J Gastroenterol* 2002; **8**: 739-745

6   **Tan ZJ**, Hu XG, Cao GS, Tang Y. Analysis of gene expression profile of pancreatic carcinoma using cDNA microarray. *World J Gastroenterol* 2003; **9**: 818-823

7   **Shackel NA**, McGuinness PH, Abbott CA, Gorrell MD, McCaughan GW. Insights into the pathobiology of hepatitis C virus-associated cirrhosis: analysis of intrahepatic differential gene expression. *Am J Pathol* 2002; **160**: 641-654

8   **Liu C**, Gaca MD, Swenson ES, Vellucci VF, Reiss M, Wells RG. Smads 2 and 3 are differentially activated by transforming growth factor-beta (TGF-beta) in quiescent and activated hepatic stellate cells. Constitutive nuclear localization of Smads in activated cells is TGF-beta-independent. *J Biol Chem* 2003; **278**: 11721-11728

9   **Galli A**, Crabb DW, Ceni E, Salzano R, Mello T, Svegliati-Baroni G, Ridolfi F, Trozzi L, Surrenti C, Casini A. Antidiabetic thiazolidinediones inhibit collagen synthesis and hepatic stellate cell activation *in vivo* and *in vitro*. *Gastroenterology* 2002; **122**: 1924-1940

10   **Rozen S**, Skaletsky H. Primer 3 on the WWW for general users and for biologist programmers. *Methods Mol Biol* 2000; **132**: 365-386

11   **Lang A**, Schrum LW, Schoonhoven R, Tuvia S, Solis-Herruzo JA, Tsukamoto H, Brenner DA, Rippe RA. Expression of small heat shock protein alpha B-crystallin is induced after hepatic stellate cell activation. *Am J Physiol Gastrointest Liver Physiol* 2000; **279**: G1333-1342

12   **Wei HS**, Li DG, Lu HM, Zhan YT, Wang ZR, Huang X, Zhang J, Cheng JL, Xu QF. Effects of AT1 receptor antagonist, losartan, on rat hepatic fibrosis induced by CCl$_4$. *World J Gastroenterol* 2000; **6**: 540-545

13   **Svegliati-Baroni G**, Ridolfi F, Di Sario A, Saccomanno S, Bendia E, Benedetti A, Greenwel P. Intracellular signaling pathways involved in acetaldehyde-induced collagen and fibronectin gene expression in human hepatic stellate cells. *Hepatology* 2001; **33**: 1130-1140

14   **Aoyagi M**, Sakaida I, Suzuki C, Segawa M, Fukumoto Y, Okita K. Prolyl 4-hydroxylase inhibitor is more effective for the inhibition of proliferation than for inhibition of collagen synthesis of rat hepatic stellate cells. *Hepatol Res* 2002; **23**: 1-6

15   **Tahashi Y**, Matsuzaki K, Date M, Yoshida K, Furukawa F, Sugano Y, Matsushita M, Himeno Y, Inagaki Y, Inoue K. Differential regulation of TGF-beta signal in hepatic stellate cells between acute and chronic rat liver injury. *Hepatology* 2002; **35**: 49-61

16   **Kim KY**, Rhim T, Choi I, Kim SS. N-acetylcysteine induces cell cycle arrest in hepatic stellate cells through its reducing activity. *J Biol Chem* 2001; **276**: 40591-40598

17 **Yang C**, Zeisberg M, Mosterman B, Sudhakar A, Yerramalla U, Holthaus K, Xu L, Eng F, Afdhal N, Kalluri R. Liver fibrosis: insights into migration of hepatic stellate cells in response to extracellular matrix and growth factors. *Gastroenterology* 2003; **124**: 147-159

18 **Mazzocca A**, Carloni V, Sciammetta S, Cordella C, Pantaleo P, Caldini A, Gentilini P, Pinzani M. Expression of transmembrane 4 superfamily (TM4SF) proteins and their role in hepatic stellate cell motility and wound healing migration. *J Hepatol* 2002; **37**: 322-330

19 **Nakatani K**, Seki S, Kawada N, Kitada T, Yamada T, Sakaguchi H, Kadoya H, Ikeda K, Kaneda K. Expression of SPARC by activated hepatic stellate cells and its correlation with the stages of fibrogenesis in human chronic hepatitis. *Virchows Arch* 2002; **441**: 466-474

20 **Gressner AM**, Krull N, Bachem MG. Regulation of proteoglycan expression in fibrotic liver and cultured fat-storing cells. *Pathol Res Pract* 1994; **190**: 864-882

21 **Ge X**, Penney LC, van de Rijn I, Tanner ME. Active site residues and mechanism of UDP-glucose dehydrogenase. *Eur J Biochem* 2004; **271**: 14-22

22 **Jones M**, Sabatini PJ, Lee FS, Bendeck MP, Langille BL. N-cadherin upregulation and function in response of smooth muscle cells to arterial injury. *Arterioscler Thromb Vasc Biol* 2002; **22**: 1972-1977

23 **de Diego I**, Schwartz F, Siegfried H, Dauterstedt P, Heeren J, Beisiegel U, Entich C, Grewal T. Cholesterol modulates the membrane binding and intracellular distribution of annexin 6. *J Biol Chem* 2002; **277**: 32187-32194

24 **Anderson LA**, Perkins ND. Regulation of RelA (p65) function by the large subunit of replication factor C. *Mol Cell Biol* 2003; **23**: 721-732

25 **Ranalli TA**, Tom S, Bambara RA. AP endonuclease 1 coordinates flap endonuclease 1 and DNA ligase I activity in long patch base excision repair. *J Biol Chem* 2002; **277**: 41715-41724

26 **Chen S**, Zhou B, He F, Yen Y. Inhibition of human cancer cell growth by inducible expression of human ribonucleotide reductase antisense cDNA. *Antisense Nucleic Acid Drug Dev* 2000; **10**: 111-116

27 **Dawson G**, Dawson SA, Marinzi C, Dawson PE. Anti-tumor promoting effects of palmitoyl: protein thioesterase inhibitors against a human neurotumor cell line. *Cancer Lett* 2002; **187**: 163-168

28 **Inoue T**, Shoji W, Obinata M. MIDA1 is a sequence specific DNA binding protein with novel DNA binding properties. *Genes Cells* 2000; **5**: 699-709

29 **Wu L**, Chen P, Shum CH, Chen C, Barsky LW, Weinberg KI, Jong A, Triche TJ. MAT1-modulated CAK activity regulates

30 **Kim JM**, Nakao K, Nakamura K, Saito I, Katsuki M, Arai K, Masai H. Inactivation of Cdc7 kinase in mouse ES cells results in S-phase arrest and p53-dependent cell death. *EMBO J* 2002; **21**: 2168-2179

31 **Abriss B**, Hollweg G, Gressner AM, Weiskirchen R. Adenviral-mediated transfer of p53 or retinoblastoma protein blocks cell proliferation and induces apoptosis in culture-activated hepatic stellate cells. *J Hepatol* 2003; **38**: 169-178

32 **Liao H**, Bucala R, Mitchell RA. Adhesion-dependent signaling by macrophage migration inhibitory factor (MIF). *J Biol Chem* 2003; **278**: 76-81

33 **Fingerle-Rowson G**, Koch P, Bikoff R, Lin X, Metz CN, Dhabhar FS, Meinhardt A, Bucala R. Regulation of macrophage migration inhibitory factor expression by glucocorticoids *in vivo*. *Am J Pathol* 2003; **162**: 47-56

34 **Zhang LH**, Pan JP, Yao HP, Sun WJ, Xia DJ, Wang QQ, He L, Wang J, Cao X. Intrasplenic transplantation of IL-18 gene-modified hepatocytes: an effective approach to reverse hepatic fibrosis in schistosomiasis through induction of dominant Th1 response. *Gene Ther* 2001; **8**: 1333-1342

35 **Vogel S**, Piantedosi R, Frank J, Lalazar A, Rockey DC, Friendman SL, Blaner WS. An immortalized rat liver stellate cell line (HSC-T6): a new cell model for the study of retinoid metabolism *in vitro*. *J Lipid Res* 2000; **41**: 882-893

36 **Si X**, Zeng Q, Ng CH, Hong W, Pallen CJ. Interaction of farnesylated PRL-2, a protein-tyrosine phosphatase, with the beta-subunit of geranylgeranyltransferase II. *J Biol Chem* 2001; **276**: 32875-32882

37 **Maehama T**, Taylor GS, Dixon JE. PTEN and myotubularin: novel phosphoinositide phosphatases. *Annu Rev Biochem* 2001; **70**: 247-279

38 **Zeeb M**, Rosner H, Zeslawski W, Canet D, Holak TA, Balbach J. Protein folding and stability of human CDK inhibitor p19 (INK4d). *J Mol Biol* 2002; **315**: 447-457

39 **Servillo G**, Della Fazia MA, Sassone-Corsi P. Coupling cAMP signaling to transcription in the liver: pivotal role of CREB and CREM. *Exp Cell Res* 2002; **275**: 143-154

40 **Eng FJ**, Friedman SL. Transcriptional regulation in hepatic stellate cells. *Semin Liver Dis* 2001; **21**: 385-395

41 **Saxena NK**, Ikeda K, Rockey DC, Friedman SL, Anania FA. Leptin in hepatic fibrosis: evidence for increased collagen production in stellate cells and lean littermates of ob/ob mice. *Hepatology* 2002; **35**: 762-771

42 **Garcia-Tevijano ER**, Berasain C, Rodriguez JA, Corrales FJ, Arias R, Martin-Duce A, Caballeria J, Mato JM, Avila MA. Hyperhomocysteinemia in liver cirrhosis: mechanism and role in vascular and hepatic fibrosis. *Hypertension* 2001; **38**: 1217-1221

Edited by Ma JY **Proofread by** Xu FM

• BASIC RESEARCH •

Leflunomide attenuates hepatocyte injury by inhibiting Kupffer cells

Hong-Wei Yao, Jun Li, Ji-Qiang Chen, Shu-Yun Xu

Hong-Wei Yao, Ji-Qiang Chen, Zhejiang Respiratory Drugs Research Laboratory of State Drugs Administration of China, School of Medicine, Zhejiang University, Hangzhou 310031, Zhejiang Province, China
Jun Li, Shu-Yun Xu, Institute of Clinical Pharmacology, Anhui Medical University, Hefei, 230032, Anhui Province, China
Supported by Natural Science Foundation of Anhui Province, No. 98446733
Correspondence to: Professor Jun Li, Institute of Clinical Pharmacology, Anhui Medical University, Hefei, 230032, Anhui Province, China. amuicplj@mail.hf.ah.cn
Telephone: +86-551-5161040   **Fax:** +86-551-5161040
Received: 2003-11-13   **Accepted:** 2003-12-29

Abstract

AIM: To investigate the importance of direct contact between Kupffer cells (KCs) and hepatocytes (HCs) during hepatic inflammatory responses, and the effect of leflunomide's active metabolite, A_{771726}, on cytokines in KCs, HCs and KC cocultures (DC cocultures).

METHODS: KCs and HCs in liver were isolated by digestion with pronase and collagenase. Lipopolysaccharide (LPS)-induced inflammatory response in monocultures of rat HCs and KCs was compared with that in DC cocultures. Tumor necrosis factor-α (TNF-α) and interleukin-1 (IL-1) concentrations in different culture supernatants were measured with ELISA. TNF-α mRNA in KCs of inflammatory liver injury was analyzed with reverse transcriptase polymerase chain reaction (RT-PCR).

RESULTS: DC cocultures strongly exhibited the production of TNF-α and IL-1 compared with other cultures, and these cytokines were mainly produced by KCs, especially by activated KCs. Time course studies revealed an increased production of TNF-α preceding the IL-1 production, suggesting that increased TNF-α levels could be involved in the increase of IL-1 production. Leflunomide's active metabolite, A_{771726}, had significantly inhibitory effect on TNF-α and IL-1 at protein and transcription levels, and the reduced production of IL-1 by A_{771726} was associated with the inhibitory action of A_{771726} on TNF-α.

CONCLUSION: Leflunomide can inhibit hepatocyte damage by inhibiting proinflammatory cytokine release from KCs.

INTRODUCTION

Tissue inflammation plays a critical role in liver pathology via induction of cellular injury. In fact, infiltration of mononuclear phagocytes into the liver correlates with the severity of liver injury. Moreover, proinflammatory cytokines such as tumor necrosis factor-α (TNF-α) and interleukin-1 (IL-1) have been linked to the promotion of liver injury[1-3], and the anti-inflammatory cytokine interleukin-10 (IL-10) was believed to inhibit liver injury[4,5]. Kupffer cells (KCs) are among the first cells that respond to endotoxins, including lipopolysaccharides (LPS), and are considered to be the primary macrophages involved in the clearance of gut-derived bacteria or bacterial toxins. High portal level of LPS could lead to a pronounced secretion of proinflammatory mediators by KCs and ultimately to endotoxin-induced liver injury[6,7]. KCs are located in hepatic sinusoids and lie in between or on top of endothelial cells. However, they do have direct cell contacts with parenchymatous hepatocytes (HCs) through their cytoplasmic extentions. Cellular communication between KCs and HCs has been thought to occur mainly by production of cytokines and excretion of inflammatory mediators such as eicosanoids, nitric oxide (NO), and/or reactive oxygen species (ROS)[8,9]. Proinflammatory cytokines, TNF-α and IL-1in particular, have been shown to be early and important mediators of HC injury[8,10].

Leflunomide, an isoxazole derivative and a unique immunomodulatory agent, is capable of treating rheumatoid arthritis, allograft and xenograft rejection, systemic lupus erythematosus, Crohn's disease, and prostate cancer[11-16]. Leflunomide is a prodrug that could be rapidly converted in the cell to an active metabolite, A_{771726}[17-19]. Our investigations demonstrated that leflunomide had therapeutic actions on acute and chronic liver diseases[20-22]. In order to study the mechanisms of leflunomide on liver injury, the interaction between KCs and HCs *in vitro*, and the effect of leflunomide's active metabolite, A_{771726}, on TNF-α and IL-1 were investigated.

MATERIALS AND METHODS

Animals and reagents
Male Sprague-Dawley rats weighing 200-250 g were purchased from Animal Center of Anhui Medical University. Rats were allowed to take food and tap water *ad libitum. Bacillus Calmétte-Guérin* (BCG) was purchased from Institute of Shanghai Biological company. Collagenase, Nycodenz, LPS from *Escherichia coli* O111:B4, 3-(4,5-dimethylthiazol-2-yl)-2, 5-diphenyltetrazolium bromide (MTT), and ELISA kits of TNF-α and IL-1 were obtained from Sigma Chemical (St. Louis, Mo). Powdered 1640 medium was obtained from GIBCO Co., USA. Leflunomide and its active metabolite, A_{771726}, were kindly donated by Cinkate Co., USA.

Preparation of inflammatory liver injury
Each rat was injected with 15 mg BCG in 0.2 mL saline via tail vein, and 14 d later with 10 μg LPS in 0.2 mL saline[23]. At 16 h post-injection of LPS, rats were anesthetized and KCs were isolated.

Preparation of HCs
The procedure for isolation of rat HCs was based on Seglen's method[24], with some modifications. The obtained cell suspension was diluted in modified Hanks' buffered salt solution

(pH 7.65, 4 ℃, 9.2 mmol/L HEPES, 9.91 g/L Hanks' buffered salt solution without Ca^{2+} and Mg^{2+}) and centrifuged at 200 *g* for 5 min. The supernatant was discarded, and cells were resuspended with PBS (pH 7.4) to a final volume of 100 mL and centrifuged for 2 min at 50 *g*. The supernatant, containing mainly nonparenchymal cells, was collected for isolation of KCs (see Preparation of KCs). Pellets containing mainly HCs were resuspended in RPMI 1640 medium and washed 4 times for 2 min at 50 *g*. After the final wash step, cells were counted and diluted with RPMI 1640 medium supplemented with 50 mL/L FBS, glutamine (2 mmol/L), and gentamicin (50 µg/mL) to a final concentration of 1×10^6 cells/mL. Viability of cultures was ≥95% as assessed by trypan blue dye exclusion. Light microscopic observations revealed a purity of 90-95% HCs for HC cultures.

Preparation of KCs
The procedure for KCs isolation was based on the method of Smedsrod *et al*[25], with slight modifications. Supernatants (see Preparation of HC cultures) containing mainly nonparenchymal cells were transferred to four 50 mL Falcon tubes followed by centrifugation at 50 *g* in a swing-out rotor at 4 ℃ for 2 min. This procedure was repeated twice to discard the remaining HCs. After the final step, supernatants were centrifuged at 200 *g* in a swing-out rotor at 4 ℃ for 10 min, and discarded. The resulting pellets were resuspended in PBS to a final volume of 40 mL. The nonparenchymal cell suspension was prepared by centrifugation on a double-layered (17.2%/11.5%) Nycodenz solution. After centrifugation at 1400 *g* for 20 min (4 ℃), KCs and endothelial cells were present at the boundary between the upper and lower layers. The cell suspension containing both KCs and endothelial cells, was collected and centrifuged at 200 *g* for 10 min, and the resulting pellets were diluted with RPMI 1640 medium (without serum) and washed again. Hereafter, the pellets consisting of 50% KCs and 50% endothelial cells were diluted in RPMI 1640 medium (without serum) to a final concentration of 2×10^6 cells/mL. To separate KCs from endothelial cells, cells were plated on tissue culture plates at 37 ℃ and 50 mL/L CO_2 for 30 min followed by a single wash step discarding the nonadherent endothelial cells. Viability of KCs was ≥95% as determined by trypan blue dye exclusion assay. Immunohistochemistry and fluoroscopy revealed a purity of ≥85% KCs for KC cultures.

Cell cultures
HCs were cultured at a density of 0.5×10^6 cells/well in 24-well culture dishes using RPMI 1640 medium, supplemented with 50 mL FBS, glutamine (2 mmol/L), and gentamicin (50 µg/mL). KCs were cultured in RPMI 1640 medium containing 100 mL/L FBS, 2 mmol/L glutamine, and 50 µg/mL gentamicin at a density of 0.5×10^6 cells/well in 24-well culture dishes. DC cocultures consisted of 0.5×10^6 attached KCs in 24-well tissue culture plates with the addition of 0.5×10^6 HCs in direct contact. RPMI 1640 medium supplemented with 50 mL/L FBS, glutamine (2 mmol/L), and gentamicin (50 µg/mL) was used. After an attachment period of 4 h, the medium was replaced by a fresh medium in all culture types.

Experimental design
After a recovery period of 24 h at 37 ℃ and 50 mL/L CO_2, the medium was replaced by a medium containing 0, 1, 5, or 10 µg/mL LPS. Because HCs are known to produce various important serum compounds such as LPS-binding protein, medium of KC cultures still contained 50 mL/L FBS. After 2, 4, 8, and 24 h of incubation, tissue culture supernatants were collected for analysis of cytokines. To study the effect of A_{771726} on excretion of TNF-α and IL-1 in DC coculture supernatants, A_{771726} was dissolved with RPMI 1640 medium and added to DC cocultures

from 0 h to 4 h (0-4 h), to 24 h (0-24 h) and from 4 h to 24 h (4-24 h) after incubation with LPS, respectively.

Measurement of TNF-α and IL-1
TNF-α and IL-1 concentrations in cell culture supernatants were measured using commercial ELISA kits with recombinant rat TNF-α and IL-1 as standard. Measurements were performed in duplicate.

Semiquantitative RT-PCR assay for TNF-α mRNA in KCs of inflammatory liver tissue
After incubation with or without A_{771726} (0.001-10 µmol/L), KCs of inflammatory liver tissue were harvested and kept at -70 ℃ until RNA extraction. Total cellular RNA was extracted using RNA easy kits (Invitrogen, USA). To test the efficacy of reverse transcriptase, RT-PCR was performed for GDPH mRNA. Briefly, the first strain of cDNA was synthesized by reverse transcriptase and pooled. The resulting cDNA samples were adjusted to PCR buffer conditions and run for PCR simultaneously. The primers for TNF-α were 5' -CGAGTGACAAGCCCGTAGCC and 5' -GGATGAACACGCCAGTCGCC. The primers for GDPH were 5' -CCACCCATGGCAAATTCCATGGCA and 5' - TCTAGACGGCAGGTCAGGTCCACC[26]. The amplification of TNF-α and GDPH genes was expected to generate 753 bp and 600 bp fragments, respectively. Amplification was performed for 35 cycles, each consisting of denaturation at 94 ℃ for 1 min, annealing at 51 ℃ for 1 min, and extension at 72 ℃ for 2 min. Ten µL of reaction mixture was loaded to 10 g/L agarose gel containing 0.5 µg/mL ethidium bromide for electrophoresis, the gel was then placed under ultraviolet ray for semi-quantitation detection.

Statistics
Unless stated otherwise, data were expressed as mean±SD and evaluated using two-way ANOVA followed by Student' s *t* test for comparison between 2 groups. $P<0.05$ was considered statistically significant.

RESULTS
Proinflammatory cytokine production after stimulation with LPS
The production of TNF-α and IL-1 was measured after incubation of HC and KC cultures, and DC cocultures in medium with or without LPS. A time course study showed that maximal cytokine levels in KC cultures and DC cocultures were observed after 4 h incubation for TNF-α and 24 h incubation for IL-1 respectively (Figure 1). Moreover, TNF-α and IL-1 levels in culture supernatants were positive correlated with the concentration of LPS (Figure 2). TNF-α and IL-1 levels at 2, 4, 8, 24 h in DC cocultures were significantly higher than those in KC or HC cultures (Figure 1). However, two cytokines levels in HC cultures showed no statistically significant changes throughout the experiments (Figures 1-2).

Effect of A_{771726} on TNF-α and IL-1 production in DC cocultures after stimulation with LPS
Based on the results as above, we selected DC cocultures stimulated with 10 µg/mL LPS as targets, and A_{771726} was added to DC cocultures with different time course. After 4 h incubation (0-4 h), TNF-α and IL-1 production in DC cocultures stimulated with LPS (10 µg/mL) was significantly inhibited in A_{771726} (0.1, 10 µmol/L) and dexamethasone (2×10^{-5} µmol/L) group (Figure 3 A). Likewise, TNF-α and IL-1 production in DC cocultures was also significantly inhibited after 24 h incubation (0-24 h) in A_{771726} (10 µmol/L) group (Figure 3B). Because the concentration of TNF-α reached its maximal level after 4 h incubation, we designed a protocol that A_{771726} was added to DC cocultures from 4 h to 24 h after incubation (4-24 h). The results showed

that the concentration of TNF-α and IL-1 in DC cocultures supernatants was not inhibited in A_{771726} (10 μmol/L, 4-24 h) group (Figure 3B). Furthermore, TNF-α and IL-1 levels in A_{771726} (10 μmol/L, 0-24 h) group were significantly lower than those in A_{771726} (10 μmol/L, 4-24 h) group.
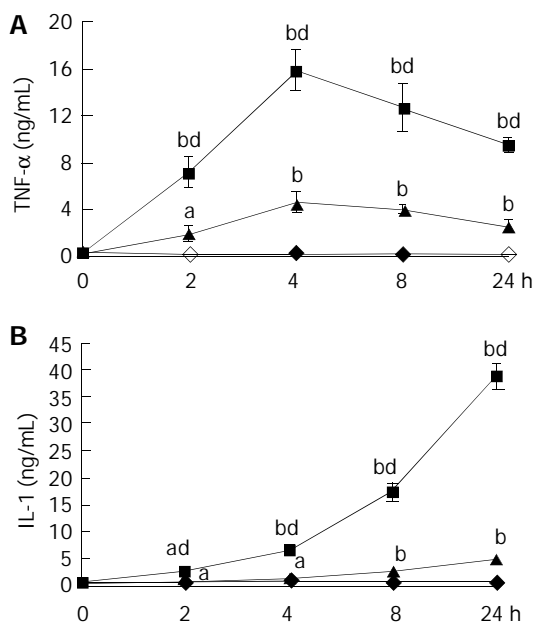

Figure 1 Changes of TNF-α and IL-1 levels in different type culture supernatants with LPS (10 μg/mL) (*n*=3, mean±SD). DC, solid line; KC, dot line; HC, dashed line. [a]*P* <0.05, [b]*P* <0.01 for IL-1 levels in DC, KC, and HC *vs.* control. [d]*P* <0.01, *vs* KC and HC. A: Changes of TNF-α levels in different type culture supernatants with LPS. B: Changes of IL-1 levels in different type culture supernatants with LPS.
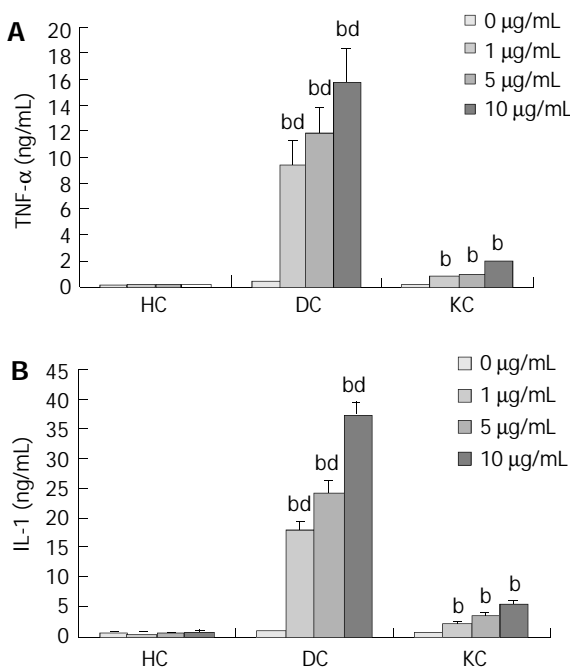

Figure 2 Changes of TNF-α and IL-1 levels in culture supernatants of HC, DC, KC after 4 h and 24 h incubation with various concentrations of LPS (*n*=3, mean±SD). [b]*P* <0.01 for TNF-α and IL-1 levels in DC, KC *vs* control; [d]*P* <0.01 for DC coculture *vs* other cultures after 0, 1, 5, and 10 μg/mL LPS. A: Changes of TNF-α levels in culture supernatants of HC, DC, KC after 4 h incubation with various concentrations of LPS. B: Changes of IL-1 levels in culture supernatants of HC, DC, KC after 24 h incubation with various concentrations of LPS.

Effect of A_{771726} on TNF-α mRNA in KCs of inflammatory liver tissue

A_{771726} had significantly inhibitory actions on the production of TNF-α in supernatants of DC cocultures. To gain insights into the potentially inhibitory action of A_{771726} on TNF-α via transcriptional level, TNF-α mRNA was analyzed by RT-PCR in KCs during liver inflammation induced by injection with BCG and LPS. Gel electrophoresis and semiquantitation analysis showed that A_{771726} significantly reduced the expression of TNF-α mRNA in KCs of inflammatory liver tissue induced by BCG and LPS (Figure 4, Table 1).
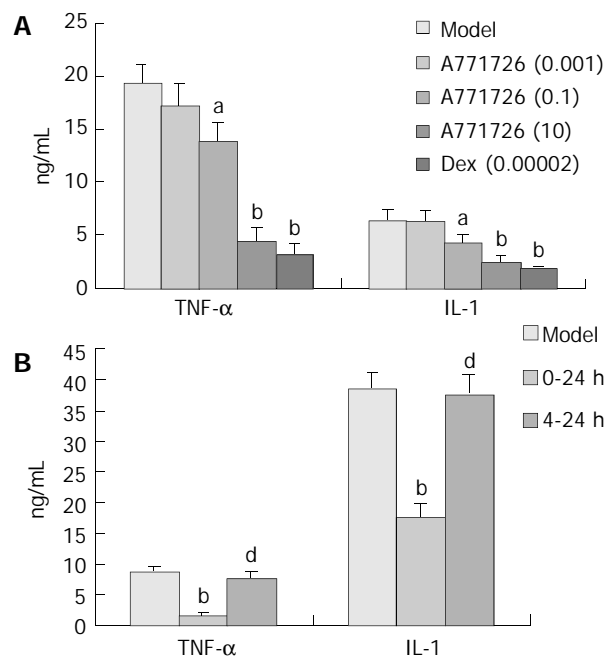

Figure 3 Effect of A_{771726} on TNF-α and IL-1 levels in culture supernatants of DC stimulated by LPS (10 μg) with different administration time (*n*=3, mean±SD). [a]*P*<0.05, [b]*P*<0.01, *vs* model; [d]*P*<0.01, *vs* 0-24 h group.
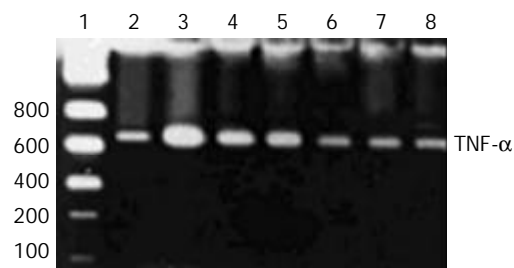

Figure 4 Effect of A_{771726} on TNF-α mRNA of KCs in immunological liver injury rats. 1: DNA marker; 3: model; 2: Dexamethasone; 4-8: A_{771726} at concentration of 1×10^{-3}, 1×10^{-2}, 1×10^{-1}, 1×10^{0}, 1×10^{1} μmol/L.

Table 1 Effect of A_{771726} on TNF-α mRNA in KCs of inflammatory liver injury rats (*n*=3, mean±SD)

Group	Dose (μmol/L)	TNF-α
Model	–	2.669±0.252
A_{771726}	1×10^{-3}	2.507±0.051
	1×10^{-2}	2.213±0.044[a]
	1×10^{-1}	1.955±0.080[b]
	1×10^{0}	1.432±0.067[b]
	1×10^{1}	0.987±0.048[b]
Dexamethasone	2×10^{-5}	1.021±0.110[b]

[a]*P*<0.05, [b]*P*<0.01, *vs* Model.

DISCUSSION

In the intact liver, HCs are in direct contact with KCs. The present experiments were designed to assess whether direct contact between HCs and KCs was of influence on the LPS-induced inflammatory response. When compared the production of TNF-α and IL-1 in the different culture types, direct cell-to-cell contact between KCs and HCs seemed to be essential, because an 4- or 7-fold increase of TNF-α and IL-1, could be observed in DC cocultures. Although the cytokine levels in KC cultures were markedly lower than those observed in DC cocultures, incubation of KC cultures with LPS still resulted in an abundant cytokine response. LPS-induced cytokine expression in DC cocultures or KC cultures has been extensively studied, but in this study we showed that direct contact between KCs and HCs significantly increased TNF-α and IL-1 production by rat KCs. However, the levels of two cytokines in HC cultures showed no statistically significant changes throughout the experiments. The results indicated proinflammatory mediators such as TNF-α and IL-1 in culture supernatants were mainly produced by KCs, especially activated KCs. Time course studies performed with these cultures revealed an increased production of TNF-α preceding the IL-1 production, suggesting that increased TNF-α levels could be involved in IL-1 production. The results were consistent with Shito's report[1] that TNF-α could be a cause of liver injury and might help regulate the expression of IL-1.

Leflunomide was mainly used to inhibit the activity of dihydroorotate dehydrogenase (DHODH) involved in *de novo* pyrimidine biosynthesis. But at a high concentration, it mainly inhibited protein tyrosine kinases initiating signaling, and therefore reduced the cell response to mitogens and cytokines. Recent evidences suggested the anti-inflammatory and immunoregulatory effects of leflunomide were related with its ability to suppress TNF-α and IL-1 selectively over their inhibitors in T lymphocyte/monocyte activation, and the activation of nuclear factor kappa B, a potent mediator of inflammation when stimulated by inflammatory stimuli. We found that TNF-α and IL-1 levels in supernatants of DC cocultures were apparently inhibited by A_{771726} (0.1, 10 μmol/L, 0-4 h) and A_{771726} (10 μmol/L, 0-24 h). However, TNF-α and IL-1 levels in supernatants of DC cocultures were not affected in A_{771726} (10 μmol/L, 4-24 h) group, and the levels of the two cytokines in A_{771726} (10 μmol/L, 0-24 h) group were significantly lower than those in A_{771726} (10 μmol/L, 4-24 h) group. The results indicated that the inhibitory action of A_{771726} on TNF-α and IL-1 levels was generated mainly from 0-4 h incubation, and reduced production of IL-1 by A_{771726} was associated with the inhibitory action of A_{771726} on TNF-α. Furthermore, RT-PCR analysis showed that A_{771726} significantly reduced the expression of TNF-α mRNA in KCs of inflammatory liver tissue induced by BCG+LPS. The results showed A_{771726} had significantly inhibitory effects on production of TNF-α in KCs at transcriptional level.

Although further work is required to demonstrate whether A_{771726} has other targets in inflammatory liver injury, A_{771726} can inhibit hepatocyte damage by inhibiting proinflammatory cytokine release from KCs.

REFERENCES

1   **Shito M,** Balis UJ, Tompkins RG, Yarmush ML, Toner M. A fulminant hepatic failure model in the rat: involvement of interleukin-1beta and tumor necrosis factor-alpha. *Dig Dis Sci* 2001; **46:** 1700-1708

2   **Bradham CA,** Plumpe J, Manns MP, Brenner DA, Trautwein C. Mechanisms of hepatic toxicity. I. TNF-induced liver injury. *Am J Physiol* 1998; **275:** G387-392

3   **Nishioji K,** Okanoue T, Mori T, Sakamoto S, Itoh Y. Experimental liver injury induced by *Propionibacterium acnes* and li-popolysaccharide in macrophage colony stimulating factor-deficient osteopetrotic (op/op) mice. *Dig Dis Sci* 1999; **44:** 1975-1984

4   **Sermon F,** Le Moine O, Gustot T, Quertinmont E, Louis H, Nagy N, Degraef C, Deviere J. Chronic alcohol exposure sensitizes mice to galactosamine-induced liver injury through enhanced keratinocyte chemoattractant and defective IL-10 production. *J Hepatol* 2003; **39:** 68-76

5   **Louis H,** Le Moine O, Goldman M, Deviere J. Modulation of liver injury by interleukin-10. *Acta Gastroenterol Belg* 2003; **66:** 7-14

6   **Enomoto N,** Ikejima K, Yamashina S, Hirose M, Shimizu H, Kitamura T, Takei Y, Sato And N, Thurman RG. Kupffer cell sensitization by alcohol involves increased permeability to gut-derived endotoxin. *Alcohol Clin Exp Res* 2001; **25**(6 Suppl): 51S-54S

7   **Lukkari TA,** Jarvelainen HA, Oinonen T, Kettunen E, Lindros KO. Short-term ethanol exposure increases the expression of Kupffer cell CD14 receptor and lipopolysaccharide binding protein in rat liver. *Alcohol Alcohol* 1999; **34:** 311-319

8   **Wang JH,** Redmond HP, Wu QD, Bouchier-Hayes D. Nitric oxide mediates hepatocyte injury. *Am J Physiol* 1998; **275:** G1117-1126

9   **Kmiec Z.** Cooperation of liver cells in health and disease. *Adv Anat Embryol Cell Biol* 2001; **161:** 1-151

10   **Hoek JB,** Pastorino JG. Ethanol, oxidative stress, and cytokine-induced liver cell injury. *Alcohol* 2002; **27:** 63-68

11   **Sanders S,** Harisdangkul V. Leflunomide for the treatment of rheumatoid arthritis and autoimmunity. *Am J Med Sci* 2002; **323:** 190-193

12   **Osiri M,** Shea B, Robinson V, Suarez-Almazor M, Strand V, Tugwell P, Wells G. Leflunomide for the treatment of rheumatoid arthritis: a systematic review and metaanalysis. *J Rheumatol* 2003; **30:** 1182-1190

13   **Williams JW,** Mital D, Chong A, Kottayil A, Millis M, Longstreth J, Huang W, Brady L, Jensik S. Experiences with leflunomide in solid organ transplantation. *Transplantation* 2002; **73:** 358-366

14   **Kessel A,** Toubi E. Leflunomide in systemic lupus erythematosus. *Harefuah* 2002; **141:** 355-357

15   **Prajapati DN,** Knox JF, Emmons J, Saeian K, Csuka ME, Binion DG. Leflunomide treatment of Crohn's disease patients intolerant to standard immunomodulator therapy. *J Clin Gastroenterol* 2003; **37:** 125-128

16   **Ko YJ**, Small EJ, Kabbinavar F, Chachoua A, Taneja S, Reese D, DePaoli A, Hannah A, Balk SP, Bubley GJ. A multi-institutional phase ii study of SU101, a platelet-derived growth factor receptor inhibitor, for patients with hormone-refractory prostate cancer. *Clin Cancer Res* 2001; **7:** 800-805

17   **Lucient J,** Dias VC, LeGatt DF, Yatscoff RW. Blood distribution and single-dose pharmacokinetics of leflunomide. *Ther Drug Monit* 1995; **17:** 454-459

18   **Li J,** Yao HW, Jin Y, Zhang YF, Li CY, Xu SY. Pharmacokinetics of leflunomide in Chinese healthy volunteers. *Acta Pharmacol Sin* 2002; **23:** 551-555

19   **Rozman B**. Clinical pharmacokinetics of leflunomide. *Clin Pharmacokinet* 2002; **41:** 421-430

20   **Yao HW,** Li J, Jin Y, Zhang YF, Li CY, Xu SY. Effect of leflunomide on immunological injury in mice. *World J Gastroenterol* 2003; **9:** 320-323

21   **Yao HW,** Jin Y, Li J, Zhang YF, Li CY, Xu SY. Effect of leflunomide on immunological injury. *Yaoxue Xuebao* 2001; **36:** 727-730

22   **Yao HW,** Jin Y, Li J, Zhang YF, Li CY, Xu SY. Effect of leflunomide on the acute chemical injury. *Anhui Yiyao* 2001; **5:** 7-9

23   **Zhang GL,** Lin ZB, Zhang B. Effects of selective induceble nitric oxide synthase inhibitor on immunological hepatic injury in rat. *Zhonghua Yixue Zazhi* 1998; **78:** 540-543

24   **Seglen PO.** Preparation of isolated rat liver cells. *Methods Cell Biol* 1976; **13:** 29-83

25   **Smedsrod B,** Pertoft H, Eggertsen G, Sundstrom C. Functional and morphological characterization of cultures of Kupffer cells and liver endothelial cells prepared by means of density separation in Percoll, and selective substrate adherence. *Cell Tissue Res* 1985; **241:** 639-649

26   **Yin F,** Yang YJ, Yu PL, Mao DA, Tao YG. Tumor necrosis factor –α in brain tissues of rats with pertussis bacilli induced brain edema. *Chin J Contemp Pediatr* 2000; **2:** 82-85

Edited by Wang XL and Xu CT **Proofread by** Xu FM

• BASIC RESEARCH •

A rapid and efficient method to express target genes in mammalian cells by baculovirus

Tong Cheng, Chen-Yu Xu, Ying-Bin Wang, Min Chen, Ting Wu, Jun Zhang, Ning-Shao Xia

Tong Cheng, Chen-Yu Xu, Ying-Bin Wang, Min Chen, Ting Wu, Jun Zhang, Ning-Shao Xia, Key Laboratory of Cell Biology and Tumor Cell Engineering of Ministry of Education, Xiamen University, Xiamen 361005, Fujian Province, China
Supported by the grant from 863 Program, No.2001AA628120
Correspondence to: Professor Ning-Shao Xia, Key Laboratory of Cell Biology and Tumor Cell Engineering of Ministry of Education, Xiamen University, Xiamen 361005, Fujian Province, China. nsxia@jingxian.xmu.edu.cn
Telephone: +86-592-2184110   **Fax:** +86-592-2184110
Received: 2003-10-27   **Accepted:** 2003-12-08

Abstract

AIM: To investigate the modification of baculovirus vector and the feasibility of delivering exogenous genes into mammalian cells with the culture supernatant of Spodoptera frugiperta (Sf9) cells infected by recombinant baculoviruses.

METHODS: Two recombinant baculoviruses (BacV-CMV-EGFPA, BacV-CMV-EGFPB) containing CMV-EGFP expression cassette were constructed. HepG2 cells were directly incubated with the culture supernatant of Sf9 cells infected by recombinant baculoviruses, and reporter gene transfer and expression efficiencies were analyzed by flow cytometry (FCM). The optimal transduction conditions were investigated by FCM assay in HepG2 cells. Gene-transfer and expression efficiencies in HepG2 or CV1 cells by baculovirus vectors were compared with lipofectAMINE, recombinant retrovirus and vaccinia virus expression systems. Twenty different mammalian cell lines were used to investigate the feasibility of delivering exogenous genes into different mammalian cells with the culture supernatant of infected Sf9 cells.

RESULTS: CMV promoter could directly express reporter genes in Sf9 cells with a relatively low efficiency. Target cells incubated with the 1:1 diluted culture supernatant (moi=50) for 12 h at 37 ℃ could achieve the highest transduction and expression efficiencies with least impairment to cell viability. Under similar conditions the baculovirus vector could achieve the highest gene-transfer and expression efficiency than lipofectAMINE, recombinant retrovirus and vaccinia virus expression systems. Most mammalian cell lines could be transduced with recombinant baculovirus. In primate adherent culture cells the recombinant baculovirus could arrive the highest infection and expression efficiencies, but it was not very satisfactory in the cell lines from mice and suspended culture cells.

CONCLUSION: Mammalian cells incubated with the culture supernatant of infected Sf9 cells could serve as a very convenient way for rapid and efficient expression of foreign genes in mammalian cells, but it might be more suitable for primate adherent culture cells.

INTRODUCTION

The baculovirus (*Autographa californica* multiple nuclear polyhedrosis virus, AcMNPV) insect cell expression system has been extensively developed and widely used for the production of numerous recombinant proteins in insect cells[1-5]. As the previous reports described, baculovirus had a strict host range, which was only limited to lepidopteran insects. However, researchers have reported that baculoviruses can be taken up by some mammalian cells[6,7], but are incapable of replicating in these mammalian cells[8,9]. A modified AcMNPV containing promoters that are active in mammalian cells, such as Rous sarcoma virus (RSV) promoter and cytomegalovirus immediate early (CMV-IE) promoter, can express exogenous genes in mammalian cells[10-14]. So a new way could be chosen by researchers for experiments of delivering target genes into mammalian cells, besides the conventional lipid transfection and mammalian viral vector expression systems, such as retrovirus expression system, adenovirus expression system. Previous reports have described that recombinant baculoviruses used in gene-transfer experiments were often concentrated by ultracentrifugation. Although this way can markedly increase the virus titer, but it needs to culture a large number of cells to obtain sufficient viruses, and the manipulation is complex and burdensome. So it is inconvenient in some daily common experiments.

Bac-to-Bac system is the most often used baculovirus-based expression system for the production of recombinant proteins in insect cells. In our research, based on the Bac-to-Bac system recombinant baculoviruses were constructed, which contain the enhanced green fluorescent protein (eGFP) gene driven by CMV promoter, to investigate the modification of baculovirus vector and the feasibility of delivering exogenous genes into mammalian cells with the culture supernatant of Sf9 cells infected by recombinant baculoviruses. Compared with lipid transfection, retrovirus and vaccinia virus expression system, efficiencies of gene transfer and expression in mammalian cells by the culture supernatant of infected Sf9 cells were superior to the traditional ways. Since direct application of the culture supernatant could simplify the procedures of delivering foreign genes into mammalian cells by baculovirus vectors, it could serve as a valuable tool for some daily common experiments.

MATERIALS AND METHODS

Cell lines

Spodoptera frugiperda (Sf9) cell line was purchased from Invitrogen (California, USA). CV1, 293, 143B, HepG2, PLC/PRF/5, BNL 1ME A.7R.1, WI-38, DMS-114, JC, L-929, P815, PT67 cell lines were obtained from the American Type Culture Collection. Hela, CHO, NIH3T3, Raji, CNE, MCF-7, BGC-223 cell lines were stored in our laboratory. LCL-cm and pT67-EGFP cell lines were constructed in our laboratory.

Bacteria and plasmids

E.coli DH5α was stored in our laboratory. *E.coli* DH10Bac was purchased from Invitrogen (California, USA). pcDNA3.1

(+) was purchased from Invitrogen (California, USA). pEGFP was purchased from Clontech (California, USA). pMD18-EF1A, pCDNA3.1-EGFP was constructed in our laboratory.

Construction of shuttle vectors

Plasmid pEGFP was digested with *Bam*HI and *Eco*RI, a 760 bp fragment containing EGFP gene was retrieved and inserted into the pFastBacl backbone that was digested with *Bam*HI and *Eco*RI to form pFB-EGFP. EGFP gene was moved from pEGFP to pcDNA3.1(+) as an *Eco*RI-*Bam*HI fragment to construct pN31-EGFP. An 1.6 kb BglII-*Eco*RI fragment from pN31-EGFP, containing CMV-IE promoter/enhancer and EGFP gene, was inserted into the pFastBacl backbone which was digested with *Bam*HI and *Eco*RI to obtain pFB-CMV-EGFPA. A *Bgl*II-*Bam*HI fragment containing the polyadenylation signal was inserted into the *Bam*HI site of pFastBacl to construct pFB-EF1A. An 1.6 kb *Sal*I-*Eco*RI fragment from pN31-EGFP was inserted into pFB-EF1A which was digested with *Xho*I and *Eco*RI to construct pFB-CMV-EGFPB (Figure 1).

Construction of recombinant baculoviruses[15]

Shuttle vectors pFB-EGFP, pFB-CMV-EGFPA, pFB-CMV-EGFPB were transformed into *E.coli* DH10Bac cells, which were incubated on LB agar plates containing 100 μg/mL Bluo-gal, 40 μg/mL IPTG, 7 μg/mL gentamicin, 50 μg/mL kanamycin, 10 μg/mL tetracycline for 24-48 h at 37 ℃ White colonies were inoculated into LB medium containing the same antibiotics and bacmid DNA was isolated according to the standard manual (Invitrogen).

pUC/M13 amplification primers were directed at sequences on either side of the mini*att*Tn7 site within the *lac*Zα-complementation region of bacmid. If transposition occurred, the PCR product produced by these primers (at 94 ℃ for 50 s, at 55 ℃ for 50 s, at 72 ℃ for 5 min, 30 cycles, at 72 ℃ for 10 min) was 2 300 bp plus the size of the insert. The PCR product of bacmid alone was about 300 bp, bacmid transposed with pFB-EGFP was 3 060 bp, bacmid transposed with pFB-CMV-EGFPA was 3 978 bp, and bacmid transposed with pFB-CMV-EGFPB was 4 633 bp.

Sf9 cells were cultured in Grace's supplemented insect medium containing 100 mL/L fetal bovine serum (HyClone). Recombinant baculoviruses were generated by Bac-to-Bac system according to the standard manual (Invitrogen). Viruses were amplified to a high titer by propagation in Sf9 cells. Virus titers were measured by plaque assay on Sf9 cells.

Transduction of mammalian cells by recombinant baculoviruses

Mammalian cells were seeded in 24-well culture dishes about 50 000 cells per well and incubated in a 37 ℃ CO$_2$ incubator for 12 h. Culture medium was removed, replaced with the collected culture supernatant (500 μL), and incubated for 1-24 h at 37 ℃ After removal of viruses, fresh medium was added

and cultures were incubated at 37 ℃. Cells that grew in suspension were pelleted by centrifugation before addition of virus inoculums. Forty-eight h post transduction, cultures were examined for eGFP expression using fluorescence microscopy and FCM.

Fluorescence microscopy

The cells transduced with recombinant baculoviruses were observed by Nikon ECLIPSE TE200 inverted microscope, and fluorescence photos were collected by the digital camera Nikon coolpix990.

Flow cytometry

After 48 h, transduction cultures were harvested with trypsin and washed with Dulbecco's PBS. Dispersive cells were pelleted by centrifugation (1 500 r/min, 5 min) and resuspended in Dulbecco's PBS with 50 mL/L fetal bovine serum and filtered by a nylon filter. Data collection was performed on a flow cytometer (FCM, Beckman Coulter EPICS XL), the exciting spectrum was 488 nm, and the detection spectrum was 525 nm. About 20 000 signals were collected per specimen. The negative control was the cells without treatment with the viruses, the eGFP positive domain (B domain) was set and the percentage of cell numbers in B domain of the negative control sample did not exceed 2%. The transfer efficiency of reporter genes was obtained by subtracting the percentage of cell numbers in B domain of the negative control from the percentage of cell numbers in B domain of the target sample. The reporter gene expression efficiency was reflected by mean fluorescence intensity of positive cells in the B domain.

Mammalian cells transfected by LipofectAMINE

Cells were seeded in 24-well culture dishes about 50 000 cells per well and incubated in a 37 ℃ CO$_2$ incubator for 12 h. One μg of target DNA was diluted into 50 μL free-serum culture medium (solution A), 2 μL LipofectAMINE reagent was diluted into 50 μL free-serum culture medium (solution B), the two solutions were mixed gently and incubated for 45 min at room temperature. The cells were washed twice with 1 mL free-serum culture medium. Five hundred μL free-serum culture medium and transfection mixture was added, cells were incubated for 6 h in a 37 ℃ incubator. The transfection mixture was removed and 500 μL supplemented culture media containing 100 mL/L fetal bovine serum was added. After 48 h transfection cultures were examined for GFP expression by FCM.

Mammalian cells infected by retrovirus

pT67-EGFP cell line constructed in our laboratory could produce recombinant retroviruses containing the EGFP expression cassette. Mammalian cells were seeded in 24-well culture dishes about 50 000 cells per well and incubated in a 37 ℃ CO$_2$ incubator for 12 h. The culture medium was removed
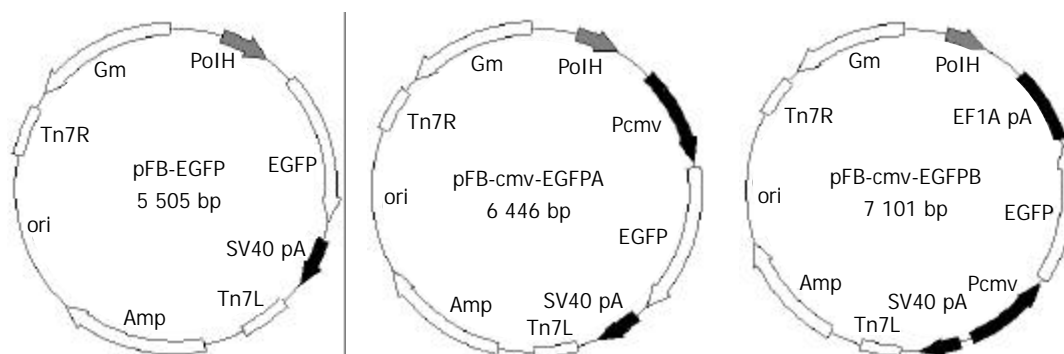

Figure 1 Plasmids pFB-EGFP, pFB-CMV-EGFPA and pFB-CMV-EGFPB.

and replaced with the collected culture supernatant of pT67-EGFP (500 μL), and incubated at 37 ℃ for 12 h. After removal of the viruses, fresh medium was added and cultures were incubated at 37 ℃. After 48 h, infection cultures were examined for GFP expression by FCM.

Mammalian cells infected by vaccinia virus

The recombinant vaccinia viruses containing the EGFP expression cassette were constructed in our laboratory. Mammalian cells were seeded in 24-well culture dishes about 50 000 cells per well and incubated in a 37 ℃ CO_2 incubator for 12 h. The culture medium was removed and replaced with the collected vaccinia viruses diluted by PBS (500 μL), and incubated at 37 ℃ for 1 h. After removal of the viruses, fresh medium was added and cultures were incubated at 37 ℃. After 24 h, infection cultures were examined for GFP expression by FCM.

RESULTS

EGFP expression in Sf9 cells driven by different promoters

The recombinant baculoviruses (BacV-EGFP, BacV-CMV-EGFPA, BacV-CMV-EGFPB) were constructed with the reporter gene coding for eGFP under the control of either the PH promoter of baculovirus or the immediate early promoter of CMV. Sf9 cells were infected by the recombinant baculoviruses at a moi of 10. After 72 h, cells were observed by inverted fluorescence microscope (Figure 2). High level of eGFP expression was observed in Sf9 cells infected by BacV-EGFP, whereas low levels of eGFP expression were found in Sf9 cells infected by BacV-CMV-EGFPA or BacV-CMV-EGFPB, showing that CMV promoter was utilized weakly in insect cells, resulting in low expression of eGFP in these cultures.

EGFP expression in HepG2 cells transduced with different recombinant baculoviruses

The culture supernatants of Sf9 cells infected by recombinant baculoviruses (BacV-EGFP, BacV-CMV-EGFPA, and BacV-CMV-EGFPB) for 4 d were collected and virus titers were determined by plaque assay. All the collected culture supernatants were diluted with fresh Grace' s culture medium to make the virus titers 1.0×10^7 pfu/mL. HepG2 cells were incubated with the collected supernatants (moi=100) for 8 h at 37 ℃. Twenty-four h post transduction, gene transfer and expression efficiencies were analyzed by inverted microscopy and FCM (Figure 3). High levels of eGFP expression could be detected in HepG2 cells transduced with BacV-CMV-EGFPA or BacV-CMV-EGFPB, and the gene transfer and expression efficiencies were similar. In contrast, no eGFP expression was found in HepG2 cells transduced with BacV-EGFP, showing that the PH promoter of baculoviruses was inactive in HepG2 cells. During the experiment, the morphological characteristics and growth of HepG2 cells were normal.

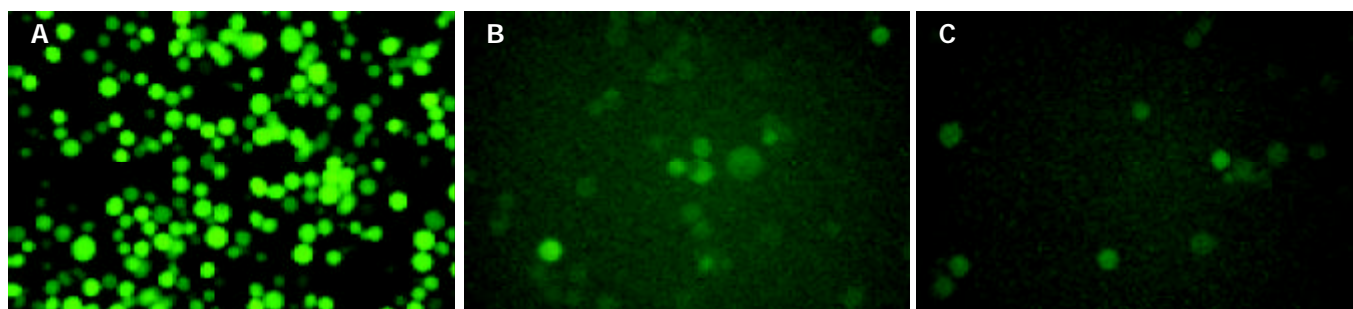**Figure 2** Fluorescence photos of Sf9 cells infected with recombinant baculoviruses. A: BacV–EGFP; B: BacV-CMV-EGFPA; C: BacV-CMV-EGFPB.
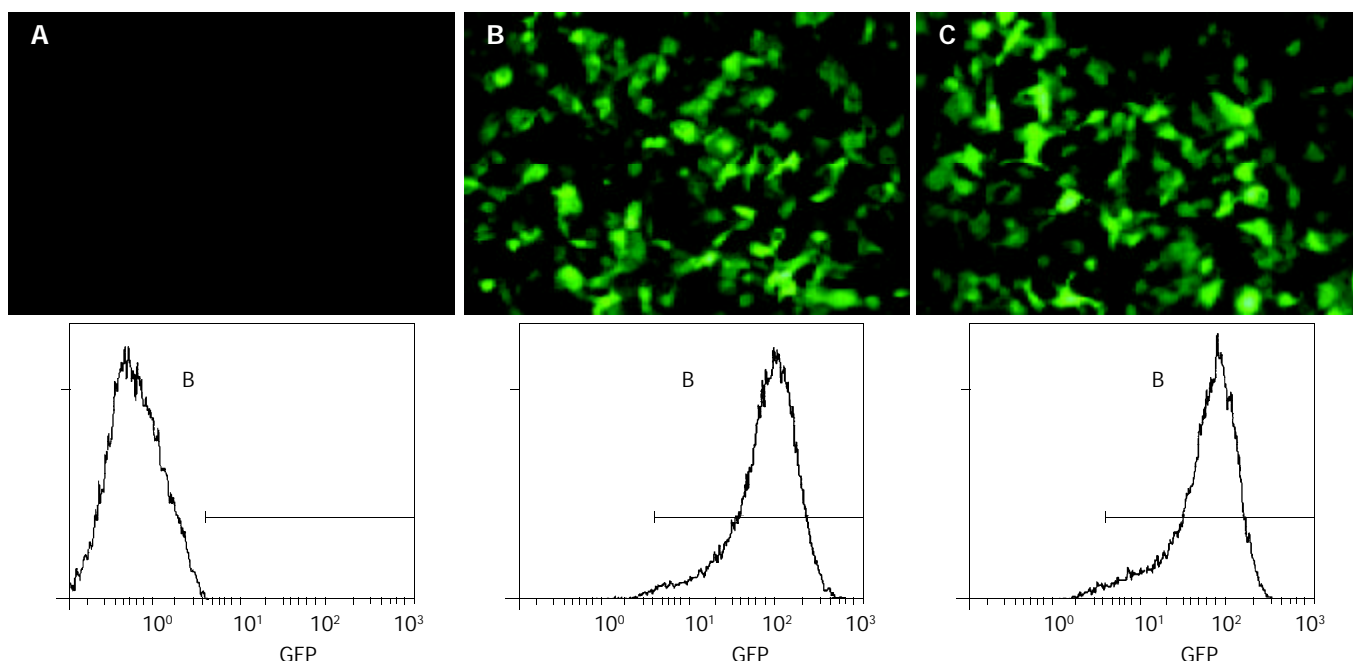

Figure 3 Fluorescence photos (up) and FCM analysis (down) of HepG2 cells transduced with recombinant baculoviruses. A: BacV–EGFP; B: BacV-CMV-EGFPA; C: BacV-CMV-EGFPB.

Effects of different dilution ratio and incubation time on efficiencies of gene transfer and expression

To optimize the way of delivering exogenous genes into mammalian cells with the culture supernatant of Sf9 cells infected by recombinant baculoviruses, HepG2 cells were incubated with the collected culture supernatant serially diluted by DMEM culture medium containing 100 mL/L fetal bovine serum and the transduction time ranged from 1 h to 24 h. After 24 h, the reporter gene transfer and expression efficiencies were analyzed by FCM (Figure 4). With increase of incubation time and moi, the efficiencies of gene transfer and expression in target cells increased.

Continuous expression of eGFP in HepG2 cells by baculovirus vector

HepG2 cells seeded in 24-well culture dishes were incubated with the culture supernatant of Sf9 cells infected by BacV-CMV-EGFPA (moi=50). Culture medium was changed every two days. The cells were harvested at various times and quantitatively assayed for eGFP expression by FCM. As shown in Figure 5, the expression of EGFP could be detected during a long time post transduction and peaked 24-48 h after transduction, which implied that the target gene could be continuously expressed in mammalian cells by recombinant baculovirus vectors.

Comparison of different gene delivery methods

pcDNA3.1(+)-EGFP was transfected into HepG2 and CV1 cells by LipofectAMINE. After 48 h, the reporter gene transfer and expression efficiencies were analyzed by FCM. pT67-EGFP cell line was constructed in our laboratory, which could produce the recombinant retroviruses containing the EGFP expression cassette. HepG2 and CV1 cells were incubated with the collected culture supernatant of pT67-EGFP for 12 h at 37 ℃. After 48 h, the reporter gene transfer and expression efficiencies were analyzed by FCM. HepG2 and CV1 cells were incubated with the culture supernatant of Sf9 cells infected by BacV-CMV-EGFPA for 12 h at 37 ℃ (moi=50). After 48 h, the reporter gene transfer and expression efficiencies were analyzed by FCM. The recombinant vaccinia viruses containing the EGFP expression cassette were constructed in our laboratory. HepG2 and CV1 cells were incubated with the collected vaccinia viruses diluted by PBS at 37 ℃ for 1 h. After 24 h, infection cultures were examined for GFP expression by FCM.

As shown in Table 1, under the similar conditions recombinant baculoviruses and vaccinia viruses could achieve higher gene-transfer and expression efficiencies than lipofectAMINE and recombinant retrovirus system. But obvious cytopathic effects could be observed at 24-32 h on HepG2 or CV1 cells infected by vaccinia viruses, while in mammalian cells transduced with recombinant baculoviruses, no cytopathic effect could be observed during the experiment.

Table 1 Comparison of gene-transfer and expression efficiency in HepG2 and CV1 cells among different gene-transfer systems

	Gene-transfer rate (%)		Mean fluorescence intensity	
	HepG2	CV1	HepG2	CV1
LipofectAMINE	29.6	34.2	138.1	103.4
Retro-EGFP	13.5	18.2	95.8	76.6
Vaccinia-EGFP	93.5[a]	94.2[a]	172.5[a]	148.4[1]
BacV-CMV-EGFPA	92.5	95.6	294.5	232.1

[1]Cytopathic effects could be observed within 24 h post infection and most cells were lysised within 48 h.

Baculovirus-mediated gene delivery to various mammalian cell lines

To investigate the feasibility of delivering the reporter gene into various mammalian cells with the culture supernatant of

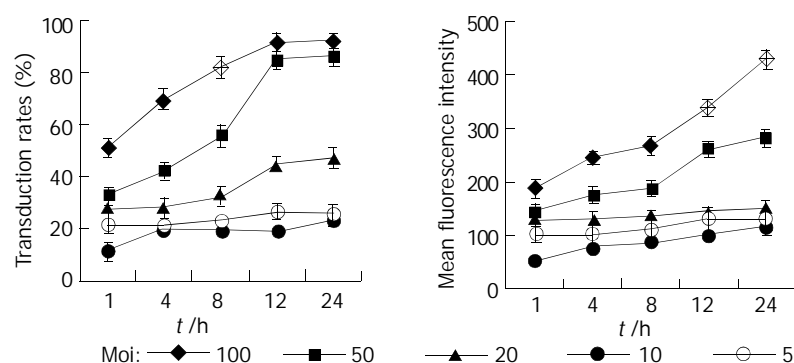**Figure 4** Effect of different moi and incubation time on gene transfer and expression efficiencies in HepG2 cells transduced with BacV-CMV-EGFPA.
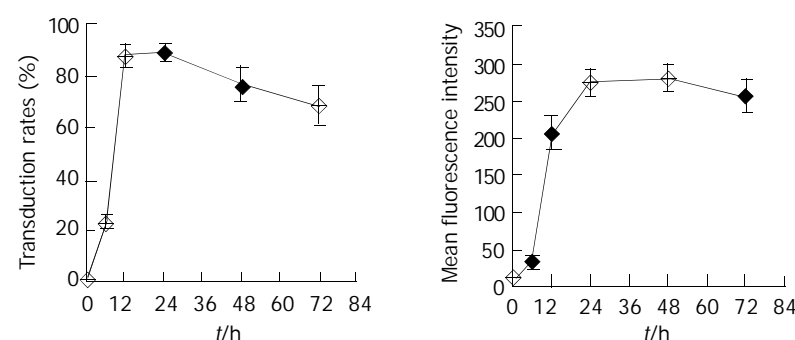

Figure 5 Reporter gene transfer and expression efficiencies at different times in HepG2 cells transduced with BacV-CMV-EGFPA.

infected Sf9 cells, twenty different mammalian cell lines were used, including twelve human cell lines (WI-38, Hela, HepG2, 293, PLC/PRF/5, 143B, MCF-7, BGC-223, DMS 114, CNE, Raji, LCL-cm), seven mice cell lines (BNL 1ME A.7R.1, CHO-K1, L-929, JC, PT67, NIH3T3, P815), and one monkey cell line (CV1). These cells were incubated with the infected Sf9 cell culture supernatant diluted with complete culture medium for the corresponding mammalian cells at ratio 1:1(vol:vol) for 12 h (BacV-CMV-EGFPA, moi=50). After 48 h, the reporter gene transfer and expression efficiencies were analyzed by FCM (Table 2). Results showed that most mammalian cell lines could be transduced with recombinant baculoviruses by this way.

Activity of CMV promoter in different mammalian cell lines

In our research the susceptibility of mammalian cells lines to recombinant baculoviruses was determined by the expression of reporter gene in different cells. So the results might be affected by different expression efficiencies of reporter gene in different cell lines. The reporter gene used in these experiments was the EGFP gene, which was one of the most widely used reporter genes and had many advantages such as no cytoxicity to host cells, easy detectable, more sensitive[16,17]. The CMV promoter was usually used in experiments, which had the ability to give strong expression of target genes in a variety of mammalian cell types[18].

We investigated the activity of CMV promoter in different mammalian cell lines used in our experiments by FCM. Plasmid pcDNA3.1-EGFP containing an expression cassette of EGFP reporter gene under control of CMV promoter, was transfected by LipofectAMINE into some mammalian cells especially those difficult for baculoviruses to enter. After 48 h, reporter gene transfer and expression efficiencies were analyzed by FCM (Table 3). Results showed that CMV promoter could effectively direct the expression of reporter gene in these mammalian cells. Although the expression efficiencies differed in various cell lines, all the expressions could be detected by FCM. So the gene transfer efficiencies to mammalian cells by

Table 2 Comparison of gene-transfer and expression efficiencies in different mammalian cell lines transduced with BacV-CMV-EGFPA

Organism	Tissue	Growth properties	Transduction efficiency(%)	Mean fluorescence intensity
Human				
WI-38	Lung fibroblast	Adherent		
Hela	Adenocarcinoma	Adherent		
HepG2	Hepatocellular carcinoma	Adherent		
293	Kidney	Adherent		
PLC/PRF/5	Hepatoma	Adherent		
143B	Osteosarcoma	Adherent		
MCF-7	Gastric carcinoma	Adherent		
BGC-223	Breast carcinoma	Adherent		
DMS 114	Small cell lung cancer	Adherent		
CNE	Nasopharyngeal carconoma	Suspension		
Raji	Burkitt's lymphoma	Suspension		
LCL-cm	B lymphocyte	Suspension		
Mouse				
BNL 1ME A.7R.1	Liver	Adherent		
CHO-K1	Ovary	Adherent		
L-929	Subcutaneous connective tissue	Adherent		
JC	Adenocarcinoma	Adherent		
PT67	Embryo fibroblast	Adherent		
NIH3T3	Embryo fibroblast	Adherent		
P815	Mastocytoma	Suspension		
Monkey				
CV1	Normal kidney	Adherent		

Table 3 Comparison of gene-transfer and expression efficiencies in different mammalian cell lines transfected with pcDNA3.1-EGFP

Organism	Tissue	Growth properties	Transfection efficiency(%)	Mean fluorescence intensity
Human				
WI-38	Lung fibroblast	Adherent	24.53	58.3
HepG2	Hepatocellular carcinoma	Adherent	18.60	79.4
Hela	Adenocarcinoma	Adherent	19.82	42.7
293	Kidney	Adherent	61.45	86.6
Raji	Burkitt's lymphoma	Suspension	5.56	14.6
LCL-cm	B lymphocyte	Suspension	7.62	17.4
Mouse				
BNL 1ME A.7R.1	Liver	Adherent	13.09	19.1
CHO-K1	Ovary	Adherent	47.36	48.6
JC	Adenocarcinoma	Adherent	12.54	22.8
PT67	Embryo fibroblast	Adherent	22.63	31.6
NIH3T3	Embryo fibroblast	Adherent	25.31	35.3
P815	Mastocytoma	Suspension	12.78	16.8

recombinant baculoviruses containing CMV-EGFP expression cassette could basically show the ability of baculoviruses to enter different mammalian cell lines.

Efficiencies of gene transfer into suspended or adherent culture cells by recombinant baculoviruses

The cells used in our experiments were derived from primate or mice. We compared the transfer efficiencies of reporter gene in adherent or suspended culture cells of these two cell types (Table 4). The result showed that in primate cell lines the efficiencies of gene transfer into adherent culture cells were markedly higher than those of gene transfer into the suspended culture cells ($t=20.6484$, $P<0.05$). In mice cell lines, only one suspended culture cell line was used in our experiment, its gene transfer efficiency by baculovirus vector was also markedly lower than the adherent culture cell line from the same organism. Furthermore we also noticed that, the efficiencies of gene transfer into the primate adherent culture cells were markedly higher than those of gene transfer into the adherent culture cells from mice ($t=7.9674$, $P<0.05$), and the efficiencies of reporter gene transfer to the suspended culture cells from primate and mice were both low, the difference between them was not distinct. In primate adherent culture cells recombinant baculoviruses could arrive the highest infection and expression efficiencies, but they were not very satisfactory in the cell lines from mice and suspended culture cells.

Table 4 Comparison of transduction efficiencies in adherent and suspended culture cells of different species transduced with BacV-CMV-EGFPA

		Adherent culture	Suspended culture
Primate	Total	10	3
	Mean transduction efficiency(%)	77.25±11.37	1.12±0.53
Mice	Total	6	1
	Mean transduction efficiency(%)	21.84±15.85	0.61

DISCUSSION

It has been proved that recombinant baculoviruses could serve as a powerful tool for delivering foreign genes into mammalian cells[19]. Previous reports have described that recombinant baculoviruses used in gene-transfer experiments were often concentrated by ultracentrifugation. This could yield a large number of recombinant viruses with high purity, but it needed to culture a large number of cells to obtain sufficient viruses, and the manipulation was complex and burdensome. We investigated the feasibility of delivering exogenous genes into mammalian cells directly with the culture supernatant of Sf9 cells infected by recombinant baculoviruses. The results showed that when the incubation time was identical, with the increase of dilution ratio and the decrease of moi, the reporter gene transfer and expression efficiencies were decreased; when the dilution ratio and moi were identical, with the prolongation of incubation time, the gene transfer and expression efficiencies were increased too, suggesting that virus titers and incubation time were the most important factors that affected the efficiencies of the gene transfer and expression, and the virus titer was the crucial factor. In direct morphological observation in the transduced cells, we found that the growth of target cells was affected when undiluted culture supernatant was used or the incubation time was long. The morphological characteristics of some cells were abnormal, and the number of dead cells increased. So according to the observed results of the morphology and growth of transduced cells, we thought that incubating

target mammalian cells with the culture supernatant of infected Sf9 cells ($\geqslant 1.0\times10^7$pfu/mL) 1:1(vol:vol) diluted by the mammalian cell complete culture medium for 12 h in a 37 ℃ CO_2 incubator (moi=50) could achieve the highest efficiency of gene transfer and expression, together with the least impairment to cell viability.

In our research twenty mammalian cell lines were used to investigate the feasibility of delivering reporter genes into various mammalian cells with the culture supernatant of infected Sf9 cells. The results showed that the reporter gene could be effectively transferred into the majority of mammalian cell lines by recombinant baculovirus vectors. The gene transfer efficiencies in adherent culture cells from human or monkey by baculovirus vectors were markedly higher than those from mice, indicating that the susceptibility of mammalian adherent culture cell lines to baculoviruses might be different between different species. Furthermore, baculoviruses could be hardly taken up by suspended culture cells. A total of four suspended culture cell lines were used in our experiment, three from human, and one from mice. Their efficiencies of gene transfer by baculovirus vectors were not more than 2%, markedly lower than those of the adherent culture cell lines from the same species respectively. Similar results were also observed by Condreay *et al*[20].

Numerous methods have been developed for introducing target genes into mammalian cells including chemical-based procedures, electroporation, and mammalian viral vector-based systems. Lipid transfection, retrovirus expression system and vaccinia virus expression system were most often used in experiments among these methods. The advantages of lipid transfection were short time-used, wide host range, but in common cases the transfection efficiencies were low, and was not suitable for some experiments that needed high transfection efficiencies[21]. Retroviruses could infect many mammalian cell lines, and were able to integrate with host cell genomes stably. But retroviruses could only be taken up by the cells in mitosis phase, and the infection efficiencies in the non dividing cells were very low[22,23]. The successful application of the retrovirus expression system needs high virus titers. If the culture supernatants of retrovirus package cell line were directly used in the gene transfer experiment, the virus titers were usually difficult to meet our need. So increasing the virus titer of recombinant retroviruses has become an important research content in the application of retrovirus expression system, and this was also an important factor that restricted the wide application of the retrovirus expression system[24,25]. A package cell line that can stably generate high titer recombinant viruses would also take a long time for cloning. The vaccinia virus expression systems have been widely used for *in vitro* production and functional characterization of proteins and live vaccines in vaccine research[26,27]. The life cycle of poxviruses occurs exclusively within the cytoplasm of infected cells and can lead to the lysis of infected cells within 12-24 h[28]. So the vaccinia virus expression system is unsuitable for continuous expression of foreign genes in target cells. Similar problems also occur in application of other mammalian viral vector-based systems. The cost and time-used in application of these expression systems were too expensive and burdensome for some daily common experiments.

As described in our report, the culture supernatant of Sf9 cells infected by recombinant baculoviruses could be directly used for delivery of foreign genes into mammalian cells. Their virus titer was sufficient for efficient gene transfer experiments. So under common circumstances without special requirements, there is no need for concentration and purification of the virus, which can markedly decrease our workloads, and improve our work. In comparison to lipid transfection system, retrovirus expression system and vaccinia virus expression system, we

could find that under similar conditions recombinant baculoviruses could achieve the highest gene-transfer and expression efficiencies in mammalian cells. Baculoviruses are inherently unable to replicate in mammalian cells, have few or no microscopically observable cytopathic effects on target cells. These modified recombinant baculoviruses containing mammalian cell-active expression cassettes could be used more widely in a variety of gene transfer. We also noticed that the gene transfer and expression efficiencies in mice cells and suspended culture cells by recombinant baculoviruses containing CMV promoter were not satisfactory, suggesting that although recombinant baculoviruses could serve as a very convenient tool for gene transfer in mammalian cells, but they also have limitations and might not be suitable for all cell lines.

REFERENCES

1   **Miller LK.** Baculoviruses for foreign gene expression in insect cells. *Biotechnology* 1988; **10**: 457-465
2   **Luckow VL**, Summers MD. Signals important for high-level expression of foreign genes in Autographa californica nuclear polyhedrosis virus expression vectors. *Virology* 1988; **167**: 56-71
3   **Ren H**, Zhu FL, Zhu SY, Song YB, Qi ZT. Immunogenicity of HGV NS5 protein expressed from Sf9 insect cells. *World J Gastroenterol* 2001; **7**: 98-101
4   **Li B**, Wu HY, Qian XP, Li Y, Chen WF. Expression, purification and serological analysis of hepatocellular carcinoma associated antigen HCA587 in insect cells. *World J Gastroenterol* 2003; **9**: 678-682
5   **Hou LH**, Du GX, Guan RB, Tong YG, Wang HT. *In vitro* assay for HCV serine proteinase expressed in insect cells. *World J Gastroenterol* 2003; **9**: 1629-1632
6   **Groner A**, Granados RR, Burand JP. Interaction of Autographa californica nuclear polyhedrosis virus with two nonpermissive cell lines. *Intervirology* 1984; **21**: 203–209
7   **Carbonell LF**, Miller LK. Baculovirus interaction with nontarget organisms: a virus-borne reporter gene is not expressed in two mammalian cell lines. *Appl Environ Microbiol* 1987; **53**: 1412-1417
8   **Tjia ST**, zu Altenschildesche GM, Doerfler W. Autographa californica nuclear polyhedrosis virus (AcNPV) DNA does not persist in mass cultures of mammalian cells. *Virology* 1983; **125**: 107–117
9   **Carbonell LF**, Klowden MJ, Miller LK. Baculovirus-mediated expression of bacterial genes in dipteran and mammalian cells. *J Virol* 1985; **56**: 153–160
10 **Hofmann C**, Sandig V, Jennings G, Rudolph M, Schlag P, Strauss M. Efficient gene transfer into human hepatocytes by baculovirus vectors. *Proc Natl Acad Sci U S A* 1995; **92**: 10099-10103
11 **Boyce FM**, Bucher NLR. Baculovirus-mediated gene transfer into mammalian cells. *Proc Natl Acad Sci U S A* 1996; **93**: 2348-2352
12 **Shoji I**, Aizaki H, Tani H, Ishii K, Chiba T, Saito I, Miyamura T, Matsuura Y. Efficient gene transfer into various mammalian cells, including non-hepatic cells, by baculovirus vectors. *J Gen Virol* 1997; **78**(Pt 10): 2657-2664
13 **Delaney WE**, Isom HC. Hepatitis B virus replication in human HepG2 cells mediated by hepatitis B virus recombinant baculovirus. *Hepatology* 1998; **28**: 1134–1146
14 **Duisit G**, Saleun S, Douthe S, Barsoum J, Chadeuf G, Moullier P. Baculovirus vector requires electrostatic interactions including heparan sulfate for efficient gene transfer in mammalian cells. *J Gene Med* 1999; **1**: 93-102
15 Bac-to-Bac baculovirus expression systems instruction manual. Invitrogen life technologies 2002
16 **Chalfie M**, Tu Y, Euskirchen G, Ward WW, Prasher DC. Green fluorescent protein as a marker for gene expression. *Science* 1994; **263**: 802-805
17 **Kain SR**, Adams M, Kondepudi A, Yang TT, Ward WW, Kitts P. Green fluorescent protein as a reporter of gene expression and protein localization. *Biotechniques* 1995; **19**: 650-655
18 **Davis MG**, Huang ES. Transfer and expression of plasmids containing human cytomegalovirus immediate-early gene 1 promoter-enhancer sequences in eukaryotic and prokaryotic cells. *Biotechnol Appl Biochem* 1988; **10**: 6-12
19 **Kost TA**, Condreay JP. Recombinant baculoviruses as mammalian cell gene-delivery vectors. *Trends Biotechnol* 2002; **20**: 173-180
20 **Condreay JP**, Witherspoon SM, Clay WC, Kost TA. Transient and stable gene expression in mammalian cells transduced with a recombinant baculovirus vector. *Proc Natl Acad Sci U S A* 1999; **96**: 127-132
21 **Bebok Z**, Abai AM, Dong JY, King SA, Kirk KL, Berta G, Hughes BW, Kraft AS, Burgess SW, Shaw W, Felgner PL, Sorscher EJ. Efficiency of plasmid delivery and expression after lipid-mediated gene transfer to human cells *in vitro*. *J Pharmacol Exp Ther* 1996; **279**: 1462-1469
22 **Chuck AS**, Clarke MF, Palsson BO. Retroviral infection is limited by Brownian motion. *Hum Gene Ther* 1996; **7**: 1527-1534
23 **Miller DG**, Adam MA, Miller AD. Gene transfer by retrovirus vectors occurs only in cells that are actively replicating at the time of infection. *Mol Cell Biol* 1990; **10**: 4239-4242
24 **Chuck AS**, Palsson BO. Consistent and high rates of gene transfer can be obtained using flow-through transduction over a wide range of retroviral titers. *Hum Gene Ther* 1996; **7**: 743-750
25 **Bowles NE**, Eisensmith RC, Mohuiddin R, Pyron M, Woo SL. A simple and efficient method for the concentration and purification of recombinant retrovirus for increased hepatocyte transduction *in vivo*. *Hum Gene Ther* 1996; **7**: 1735-1742
26 **Mackett M**, Smith GL, Moss B. Vaccinia virus: a selectable eukaryotic cloning and expression vector. *Biotechnology* 1992; **24**: 495-499
27 **Whitman ED**, Tsung K, Paxson J, Norton JA. *In vitro* and *in vivo* kinetics of recombinant vaccinia virus cancer-gene therapy. *Surgery* 1994; **116**: 183-188
28 **Moss B**. Genetically engineered poxviruses for recombinant gene expression, vaccination and safety. *Proc Natl Acad Sci U S A* 1996; **93**: 11341–11348

Edited by Wang XL and Xu CT   **Proofread by** Xu FM

• BASIC RESEARCH •

Risk factors of development of gut-derived bacterial translocation in thermally injured rats

Zhong-Tang Wang, Yong-Ming Yao, Guang-Xia Xiao, Zhi-Yong Sheng

Zhong-Tang Wang, Yong-Ming Yao, Zhi-Yong Sheng, Department of Microbiology and Immunology, Burns Institute, 304th Hospital of PLA, Beijing 100037, China
Guang-Xia Xiao, Institute of Burn Research, Southwestern Hospital, Third Military Medical University, Chongqing 400038, China

Correspondence to: Yong-Ming Yao, M.D., Department of Microbiology and Immunology, Burns Institute, 304th Hospital of PLA, 51 Fu-Cheng Road, Beijing 100037, China. c_ff@sina.com
Telephone: +86-10- 66867394   **Fax:** +86-10-68429998

Abstract

AIM: Studies have demonstrated that gut-derived bacterial translocation (BT) might play a role in the occurrence of sepsis and multiple organ dysfunction syndrome (MODS). Yet, no convincing overall analysis of risk factors for BT has been reported. The purpose of this study was to evaluate the related factors for the development of BT in burned rats.

METHODS: Wistar rats were subjected to 30% third-degree burns. Then samples were taken on postburn d 1, 3, and 5. Incidence of BT and counts of mucosal bifidobacteria, fungi and *E. coli*, mucus sIgA, degree of injury to ileal mucosa, and plasma interleukin-6 were observed. Univariate analysis and multivariate logistic regression analysis were performed.

RESULTS: The overall BT rate was 53.9% (69 in 128). The result of univariate analysis showed that the levels of plasma endotoxin and interleukin-6, the counts of mucosal fungi and *E. coli*, and the scores of ileum lesion were markedly increased in animals with BT compared with those without (P=0.000-0.005), while the levels of mucus sIgA and the counts of mucosal bifidobacteria were significantly reduced in animals with translocation compared with those without (P=0.000). There was a significant positive correlation between mucus sIgA and the counts of mucosal bifidobacteria (r=0.74, P=0.001). Moreover, there were strong negative correlations between scores of ileum-lesion and counts of bifidobacteria (r=-0.67, P=0.001). Multivariate logistic regression revealed that ileum lesion score (odds ratio [OR] 45.52, 95% confidence interval [CI] 5.25-394.80), and counts of mucosal bifidobacteria (OR 0.039, 95% CI 0.0032-0.48) were independent predictors of BT secondary to severe burns.

CONCLUSION: Ileal lesion score and counts of mucosal bifidobacteria can be chosen as independent prognosis factors of the development of BT. Specific interventions targeting these high-risk factors might be implemented to attenuate BT, including strategies for repair of damaged intestinal mucosae and restoration of the balance of gastrointestinal flora.

INTRODUCTION

Sepsis and multiple organ dysfunction syndrome (MODS) remain the leading causes of death 72 h after a severe burn and other traumas. Early MODS after a severe injury is usually due to an excessive and overwhelming malignant systemic inflammatory response and massive hemorrhagic shock as a result of the initial insults. On account of the finding that as many as 30% patients died of early sepsis and MODS with no identifiable septic foci[1], some investigators postulated that systemic infections might be originated from the gut.

At present, many animal and a few clinical studies have demonstrated that gut-derived bacterial translocation does play a role in the occurrence of early sepsis and MODS[2-5]. Because most of the pathogens come from the gut, the gastrointestinal tract is even termed as an "undrained abscess" under certain circumstances such as trauma, endotoxemia, hemorrhage, and thermal injury. A generally accepted theory is that translocation of luminal bacteria and toxins is mechanically linked to the following factors, namely disruption of the normal balance in indigenous microflora with subsequent overgrowth of potentially pathogenic bacteria, impaired intestinal immunologic barrier of the host, and disruption of the mucosal physical barrier of the gut[1]. However, to our knowledge, what role these three factors play in the incidence of bacterial translocation under some conditions has not been fully elucidated.

In the past decade, literature on the mechanisms and methods of treatment and prevention of bacterial translocation has been substantial. However, to date no convincing overall analysis of risk factors for bacterial translocation has been reported.

The purpose of our study was to clarify the individual role of intestinal mucosa, mucosal flora, and gut sIgA in producing bacterial translocation in scalded rats, in an attempt to propose a formula for predicting the probability of incidence of bacterial translocation by using univariate analysis and multivariate logistic regression.

MATERIALS AND METHODS

Animals

Wistar rats, weighing 180 to 220 g, male and female in equal number, were purchased from the Experiment Animal Center of Third Military Medical University in Chongqing, China. Animals were housed in separate steel cages in a temperature-controlled room with a 12-h light-dark cycle, and acclimatized for at least seven days prior to use. Animals had free access to an irradiated commercial rodent diet and autoclaved water *ad lib*. All experimental manipulations were undertaken in accordance with the NIH Guide for the Care and Use of Laboratory Animals, with the approval of the Scientific Investigation Board of the Institute of Burn Research, Southwestern Hospital, Third Military Medical University, Chongqing, China.

Burn injury

After an overnight fast, rats were weighed, numbered, and anesthetized with sodium pentobarbital (40 mg/kg body mass, i.p.), with the dorsal hair shaved, and then subjected to 30% total body surface area skin full-thickness thermal injury, which was produced by exposure to 94 ℃ water bath for 18 s using a wood template with an aluminium wand for fixing rat abdomen. Rats were quickly dried and resuscitated with Ringer's lactate (40 mL/kg, i.p.) immediately after injury. Animals were then allowed to fully recover from anesthesia before being returned to their cages, and had free access to radiated commercial rodent chow and autoclaved water *ad lib*. Sulphadiazine silver suspension (20 g in 100 mL water) was applied to the wounds once a day to prevent infection. Samples were taken on post-burn d 1, 3, and 5. Fifty animals were included at each time point except for sham burned group with ten.

Microbiologic analysis

Techniques for culturing and bacterial translocation studies were performed with a modification of the methodology described by Tadros *et al*[6]. After the animals were anesthetized (50 mg/kg body mass, i.p.), their abdomens were shaved, sterilized with tincture of iodine and 750 mL/L alcohol, and opened through a midline incision with sterile scissors. Under aseptic conditions, blood was obtained from portal vein and vena cava under direct visualization, and a swab culture was taken from the exposed belly cavity. Then mesenteric lymph nodes (MLN), spleen, liver, and kidney were obtained and weighed. Each organ was homogenized in brain heart infusion broth. Two hundred µL homogenates from tissues, as well as 200 µL blood, were inoculated on both Gram-negative bacteria-specific MacConkey's agar and blood agar. A duplicate culture was made for each specimen. All specimens were incubated at 37 ℃ for 24 h. Positive specimens were sub-cultured, and the bacteria were identified by standard bacteriologic techniques. Cultures were considered positive when more then 100 colonies per gram of tissue were found. No culture for obligate anaerobics was made, because they had a low tendency to translocate to extra-intestinal sites.

Following removal of the aforementioned organs, the terminal ileal loop was excised, opened longitudinally, then its content was wiped off lightly with sterile cotton swabs, rinsed three times with 10 mL sterile 0.01 mol/L phosphate-buffered saline (PBS). The residual liquid was dried with sterile filter paper. The specimen was then put into a CO_2 filled bottle immediately. The samples were weighed, homogenized with a sterile blender, and diluted by 10 -fold with brain heart infusion broth. One hundred µL desired diluted specimen was poured separately onto the *E. coli*-specific MacConkey's agar, bifidobacteria-specific BLB agar, and fungi-specific medium (modified by including Imipenium 30 µg/mL). The cultures were all duplicated. Plates were incubated for 24 h for aerobic bacterial culture, and 72 h for anaerobic and fungus cultures, at 37 ℃, respectively. Then colonies of bacteria or fungi were counted, and the suspiciousness was identified using standard microbiologic technique. All plates and brain-heart infusion were purchased from Shanghai Med&Chem Institute, Shanghai, China.

Quantitative culture results were expressed as the number of $\log_{10}$ colony-forming units (CFU) per gram tissue. The terminal ileal loop was used because bacterial translocation correlated with colonization of the ileum rather than that of the colon[6]. The limit detection of the assay was 10 bacteria.

Plasma endotoxin measurement

Portal blood was collected and put into pyrogen-free polypropylene tubes containing 2 µL of sterile heparin. Platelet-rich plasma was obtained by centrifugation at 4 ℃, 260 r/min for 10 min, and then aliquots of which were prepared and transferred to sterile pyrogen-free tubes under laminar air flow, and stored at -35 ℃ until use. Plasma endotoxin concentration was measured by the chromogenic limulus amebocyte lysate (LAL) method. The procedure followed was based on the protocol provided with the kit (Shanghai Med&Chem Institute, Shanghai, China). Briefly, in order to avoid activation and inhibitory effects of plasma on LAL test, 0.1 mL serum specimen was diluted (1:10) in apyrogenic sterile water 0.2 mL and Tris-HCl buffer 0.2 mL, boiled for 10 min, and then supernatant obtained by centrifugation at 4 ℃, 5 000 r/min for 10 min was used for detection. The supernatants were coincubated for 25 min at 37 ℃ with LAL, and 3 min after chromogenic substrate was added, reaction was stopped with an aqueous solution of 0.5 g/L naphthyl ethylenediamine. Absorbance was read in a spectrophotometer at 545 nm. The absorbance of a control was subtracted from these absorbances in order to adjust the samples' intrinsic color development. The endotoxin concentration was corrected for dilution and calculated from a standard curve derived from assay of standard (Escherichia coli 0111:B4, 1EU [endotoxin units]=100 pg) supplied by the company. This method was sensitive to 0.03 EU/mL of endotoxin. Depyrogen of detection material was approved by ^{60}Co exposure.

Measurement of intestinal mucus sIgA

Duodenum, jejunum and ileum were excised, cut into 3 segments, opened longitudinally. Intestinal contents were wiped off with bamboo sticks. Intestinal mucus was collected by scraping with glass slides, and dissolved in 1 mL 0.01 mol/L PBS [including 1 mmol/L dithiothreitol (DTT), 100 µg/mL phenylmethyl sulfonylfluoride (PMSF), 10 µg/mL Leupeptin, 10 µg/mL soybean trypsin inhibitor, and 2 µg/mL aprotinin]. The solution was centrifuged at 30 000 *g* at 4 ℃ for 10 min. The supernatant was aspirated and frozen until use.

The supernatants were diluted to 1:400 with 0.01 mol/L PBS for measurement of sIgA concentrations by radioimmunoassay (RIA), based on the protocol supplied with the kit (Biotinge-Tech. Co., Beijing, China). In short, samples were added into glass tubes, incubated with polystyrene-balls which were coated with mouse anti-rat sIgA mAb (Sigma chemical co., St Louis, MO), at 37 ℃ for 2 h, washed 4 times with deionized water, then ^{125}I conjugated goat anti-rat IgA antibody was added. They were kept at room temperature over night. After washed four times, the balls were transferred into another tube for detection. Additionally, a rat myeloma IgA (Zymed, San Francisco, CA) diluted into 15.6 ng/mL, 31.3 ng/mL, 62.5 ng/mL, 125 ng/mL, 250 ng/mL, 500 ng/mL, 1 000 ng/mL, and 2 000 ng/mL, was serially measured for a standard curve. Radionuclide counts were determined in term of disintegrations per minute (dpm) using a gama counter and calibrated by subtracting the background count. Interassay and intraassay coefficients of variation were < 10%. The assay had a sensitivity of 20 pg/mL. Total protein in supernatants was estimated using the Lowry method, simultaneously. Therefore, the concentrations of sIgA from gut mucus were expressed as µg per mg of protein (sIgA µg/mg protein).

Microscopic evaluation

Ileum specimens were dehydrated in progressive concentrations of ethanol, cleared in xylene, and embedded in paraffin. Deparaffinized 4-µm thick sections were stained with hematoxylin-eosin. Glass slides were coded to allow two experienced histopathologists to examine the tissue sections blindly. The degree of intestinal tissue injuries was evaluated using a grading scale from 0 to 8[7]. Grade 0 was defined as

normal mucosa. Pathognomonic for grades 1 to 3 was an increasing subepithelial space of the villi. In grade 4, the villi were denuded, and grade 5 was characterized by loss of the villi. In grade 6, the intestinal crypt layer was also injured, and in grade 7, the entire intestinal mucosa was necrotic. Grade 8 represented transmural infarction.

ELISA for IL-6

Caval blood was collected, centrifuged at 260 r/min for 10 min. Samples were serially diluted with 0.01 mol/L PBS, and IL-6 was determined by sandwich ELISA. The following procedure was based on the protocol supplied with the kit (Bioting-Tech. Co., Beijing, China). Briefly, 96-well plates (Corning Costar, Cambridge, MA) were coated with 100 μL anti-IL-6 mAb diluted in 0.1 mL bicarbonate buffer (pH 8.2) and incubated at 4 ℃ for 48 h. The wells were blocked with PBS containing 10 g/L BSA at room temperature for 1 h. Serial 2-fold dilutions of plasma were added to duplicate wells over night at 4 ℃. Then the wells were incubated with biotinylated anti-IL-6 Ab, at 37 ℃ for 1 h, and then with peroxidase-labeled anti-biotin Ab for 1 h, and developed with ABTS reagent (Sigma). Similarly, a standard curve ranging from 0 to 2 000 pg/mL was plotted using recombinant human IL-6. Absorbance was then read at 410 nm, and the amount of IL-6 in each sample was computed from the standard curve. Interassay and intraassay coefficients of variation were <10%. The assay had a sensitivity of 100 pg/mL.

Statistical analysis

The software package Stata for Windows (Version 6.0) was used for analysis. Results were expressed as mean±SD, except for data of the grading of mucosal injury, which were expressed as median and range. Continuous variables were compared by Student's *t* test or Wilcoxon- Mann-Whitney rank sum test, whereas the Chi-square test (χ^2 test) was used for comparing proportions. Correlation analysis, univariate and stepwise multivariate logistic regression analysis, with bacterial translocation as the dependent variable, were used to identify factors associated with bacterial translocation to develop a model to predict the probability of incidence. A *P* value of 0.05 or less was considered to statistically significance.

RESULTS

Incidence of bacterial translocation

The overall mortality was 14.7%(22 in 150) during the experiment. The incidence of bacterial translocation was 53.9%(69 in 128) after burn. There were 17 positively cultured strains from abdominal cavity swabs, which were coincident with those strains cultured in organs. The rate of bacterial translocation was 84%, 59%, and 28% on post-burn d 1, 3, and 5, respectively (84% *vs* 59%, *P*=0.02; 84% *vs* 28%, *P*=0.000; 59% *vs* 28%, *P*=0.04), while it was 10% in shame-burn animals.

Univariate analysis

Univariate analysis showed that the levels of plasma endotoxin and interleukin-6, the counts of mucosal fungi and *E. coli*, and the scores of ileum lesion were markedly increased in animals with bacterial translocation compared with those without (*P*=0.000-0.005), while mucus sIgA and the counts of mucosal bifidobacteria were significantly reduced in animals with bacterial translocation compared with those without (*P*=0.000). Moreover, the ratio of bifidobacteria to *E. coli* was decreased significantly from 2 000:1 in animals without bacterial translocation to 10:1 in animals with translocation (Table 1).

Table 1 Univariate analysis of suspected factors for development of bacterial translocation

	BT[1] (*n*=69)	Non-BT[2] (*n*=59)	*t*- or *z*-value	*P*-value
Endotoxin (EU/mL)	0.158±0.0447	0.110±0.0348	6.443	0.000
Microbe flora[3]				
Fungi	3.80±0.8	3.2±0.7	2.859	0.005
E. coli	4.90±1.0	4.0±1.0	5.076	0.000
Bifidobacteria	6.10±0.6	7.3±0.5	6.967	0.000
SigA (μg/mg protein)	55.78±9.81	87.51±10.69	16.857	0.000
Ileo-lesion score	4(2-6)	2(0-4)	9.178	0.000
IL-6 (pg/mL)	871±588	499±308	4.125	0.0001

[1]Animals with bacterial translocation;[2] Animals without bacterial translocation; [3]Mucosal micro-flora ($\log_{10}$ CFU/g tissue).

Table 2 Correlation analysis of data associated with bacterial translocation

	X1	X2	X3	X4	X5	X6	X7
X1	1.0000						
X2	0.7166	1.0000					
X3	0.4586	0.3847	1.0000				
X4	-0.5135	-0.4029	-0.5516	1.0000			
X5	-0.5434	-0.4416	-0.4795	0.7363	1.0000		
X6	0.4834	0.3369	0.3663	-0.6676	-0.7312	1.0000	
X7	0.4807	0.3679	0.2550	-0.3772	-0.3772	0.3549	1.0000

X1: endotoxin levels (EU/mL), X2: counts of fungi ($\log_{10}$ CFU/g tissue), X3: counts of *E. coli* ($\log_{10}$ CFU/g tissue), X4: counts of bifidobacteria ($\log_{10}$ CFU/g tissue), X5: mucous sIgA levels (μg/mg protein), X6: ileal lesion score, X7: IL-6 levels (pg/mL).

Table 3 Independent predictors of bacterial translocation evaluated by multivariate analysis

	Coefficient	Odds ratio (95% CI[1])	*z*-value	*P*-value
X6[2]	3.8182±1.1022	45.52(5.25-394.80)	3.464	0.001
X4[3]	-3.2424±1.2757	0.039(0.003-0.48)	-2.542	0.011
Constant	9.9220±8.7435		1.135	0.256

[1]Confidence interval; [2]Ileal lesion score; [3]Counts of bifidobacteria ($\log_{10}$ CFU/g tissue).

Correlations among experimental findings

As shown at Table 2, there was a significant positive correlation between levels of endotoxin and counts of mucosal fungi and *E. coli*, scores of ileum lesion, and levels of interleukin-6 (r=0.72, 0.46, 0.48, 0.48, respectively. P<0.001), and between mucus sIgA and counts of mucosal bifidobacteria (r=0.74, P<0.001). Moreover, there were strong negative correlations between scores of ileum lesion and counts of bifidobacteria and concentrations of sIgA (r=-0.67, -0.73, respectively. P<0.001), as well as significant negative correlations between counts of mucosal bifidobacteria and levels of endotoxin, and counts of fungi and *E. coli* (r=-0.51, -0.40, -0.55, respectively, P<0.01). Figures 1 and 2 respectively showed the correlation between levels of mucus sIgA and counts of mucosal bifidobacteria, and between counts of mucosal bifidobaacteria and scores of ileum lesion.
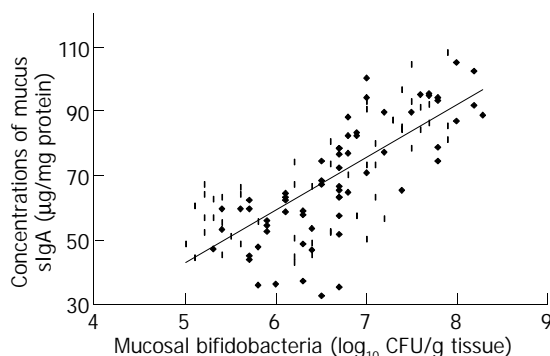

Figure 1 Correlation between counts of mucosal bifidobacteria and intestinal mucous sIgA (r=0.74, P=0.000).
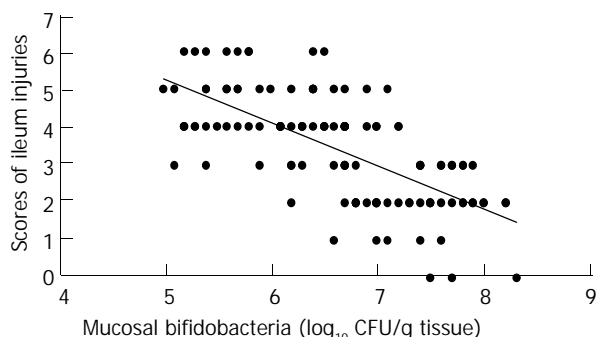

Figure 2 Correlation between counts of mucosal bifidobacteria and scores of ileum injury (r=-0.67, P=0.000).

Multivariate analysis

In multivariate analysis, as shown in Table 3, only two variables in seven parameters remained independent prognosis factors of the development of bacterial translocation associated with postburn injuries. Ileal lesion score was considered as the auxo-action factor, and the counts of mucosal bifidobacteria as the prevention factor. This model was described by the following formula: P (bacterial translocation)=e^{logit}/($1+e^{logit}$) {logit=9.9220-3.2424 [$\log_{10}$(count of bifidobacteria/g tissue)] +3.8182 (ileal-lesion score)}, with likelihood ratio χ^2=141.28, and the accuracy of the formula for burn rats was (50+67)/ 128=91% when ileal-lesion score was no less then 4, and the counts of bifidobacteria was no more then 10^6 CFU/g tissue.

DISCUSSION

Intestinal mucosa is a key barrier to prevent the invasion and spread of microorganisms that normally reside within the gut lumen. Under certain conditions, however, bacteria and their products such as endotoxin, can cross this barrier and get access to visceral organs via lymph or blood stream, a process that has been referred to as bacterial translocation. Factors that could promote bacterial translocation included overgrowth of Gram-negative enteric bacilli, impaired host immune defenses, and injury to the intestinal mucosa resulting in increased intestinal permeability[1]. These mechanisms could act in concert to promote synergistically the systemic spread of indigenous translocating bacteria to cause lethal sepsis. Many pathological conditions could evoke bacterial translocation, such as ionization radiation, endotoxemia, dystrophia, peritonitis, renal failure, intestinal obstruction, lesion of mucosa, hemorrhagic shock, long-term fasting, deficiency in secretory IgA, total parenteral nutrition, severe trauma, massive operation, and extensive burn. Recently, some measures were taken to prevent and treat bacterial translocation secondary to trauma with bactericidal/permeability increasing protein, glucagons-like peptide, growth hormone, insulin-like growth factor I, inhibitor of angiotensin II, C1 inhibitor, bombesin, inhibitors of NO synthase, glutamine, lactulose, interleukin-1alpha, probiotics and selective digestive tract decontamination[6,8-17], and their effects on the incidence of bacterial translocation were found to be resulted from ameliorating indigenous flora, strengthening the mucosal barrier, and promoting host systemic or intestinal immunity. However, what role does each of the above mentioned factors play in inciting bacterial translocation is yet to be clarified.

At the early stage of severe burns, there was a considerable change in gut mucosal flora, while only mild alternations occurred in intestinal luminal flora. It is noteworthy that bacterial translocation correlated with the state of colonization in ileum rather than in colon[16]. With these facts in mind, in the present study, we paid more attention to the changes in mucosal microorganisms of the terminal ileal loop. Bifidobacterium, which was the most common species in feces of human[18,19], *E. coli*, which was known to be the most commonly translocated microorganism[4,20,21], as well as fungi, which commonly constituted the pathogens of nosocomial infection in an intensive care unit (ICU), were chosen as representatives of intestinal microflora. Concomitantly, the main pathological changes were located in mucosa of the terminal ileum[22], the scores of lesion in ileum, reflecting the status of mucosa barrier[7], and the levels of mucus sIgA, showing the function of intestinal immunity[23], were determined. The levels of plasma endotoxin and IL-6 were used to evaluate the systemic inflammatory reactions[24,25]. Furthermore, univariate analysis was used to identify the relationship between different variables with occurrence of bacterial translocation, correlation analysis was used for the compliance with the examined variables, and then logistic regression analysis was used to determine the independent predicting factors associated with bacterial translocation.

Bacterial translocation might result from a breach of the intestinal mucosa, as a result of ischemia, atrophy, mechanical injury, *etc*. Repair of injured mucosa depended on the improvement of local microcirculation[26]. During burn shock, with re-distribution of blood circulation, the gastrointestinal suffered a prolonged ischemia, even when systemic hemodynamic parameters were normalized. This condition is known as compensatory covert shock. Our data showed that this hypoxic condition produced injuries to the mucosa of terminal ileum, followed by a significantly increased incidence of bacterial translocation at the early postburn stage. Moreover, the scores of ileal lesion had a significantly positive correlation with serum endotoxin levels. It has been documented that translocated endotoxin could trigger systemic inflammatory response through LBP/CD14 sensibility-increasing system[27], and resulted in an over-release of inflammatory factors such as TNF-α, IL-6, which might further damage intestinal

mucosae[25,27].

There was a marked negative correlation between scores of ileal lesion and mucosal bifidobacteria counts or mucus sIgA. The injury to intestinal mucosa predisposed bacteria to escape from the intestinal wall, while mucosal bifidobacteria and mucus sIgA might be protective against it[15,23,28].

Katouli and colleagues demonstrated that the composition and diversity of gut flora were associated with bacterial translocation, and the proportion and quantity of *E. coli* might influence the incidence of bacterial translocation secondary to hemorrhagic shock[20]. Our results showed that the counts of bifidobacteria decreased by 16-fold, and the counts of *E. coli* and fungi increased respectively by 8- and 4-fold in animals in which bacterial translocation was found. Moreover, the ratio of bifidobacteria to *E. coli* was decreased from 2 000:1 in animals without translocation to 16:1 in animals with translocation. This result might imply that the number of bifidobacteria, especially the ratio of bifidobacteria to *E. coli*, might be of more significance as a marker of bacterial translocation than the quantity and proportion of *E. coli*. Multivariate analysis showed that only the count of mucosal bifidobacteria was the independent predictor for the incidence of bacterial translocation, indicating that bifidobacteria, the predominant anaerobes in the gut, might play a key role in maintaining the biological barrier. The work of others showed that bifidobacteria as a mucosal flora could prevent other intestinal bacteria from adhering to intestinal epithelia through a competitive mechanism, and by producing lactic acid and acetate to create a harmful environment of lowered pH for the growth of *E. coli*, Salmonella, and methicillin-resistant Staphylococcus aureus[28-35]. Our data supported these assertions that administration of bifidobacteria could restore the disrupted gut micro-ecology, which was favorable to the host. As a result, endotoxin release was lessened, and the incidence of bacterial translocation was lowered.

Local immunological defense of the gut was mainly provided by the gut-associated lymphoid tissue (GALT), principally in the form of secretory IgA. sIgA, the predominant immunoglobulin present in mucosal secretions, was the first line of defense on the intestinal mucosal surface[23]. The importance of the mucosal immune system has been extensively recognized, for it relates to the potential pathogenic role of gut flora. Failure of the barrier function of the gut challenged by stress of severe trauma could lead to the translocation of viable enteric bacteria and endotoxin[1]. Our results showed that mucous sIgA was reduced by 56% in animals with bacterial translocation as compared to animals without translocation. However, the concentration of intestinal mucous sIgA was excluded as an independent predictor when examined by multivariate statistical analysis. This might be partially due to the significant positive correlation between the level of sIgA and the count of bifidobacteria. Moreover, the synthesis and excretion of sIgA depended mainly on healthy and stable commensal bacteria[23,30,34]. Overgrowth of Gram-negative bacteria after hemorrhagic shock might also suppress intestinal immunological function and sIgA secretion, augmenting bacterial translocation[36,37]. On the contrary, selective decontamination of the digestive tract (SDD) or supplement of exogenous bifidobacteria could attenuate the incidence of bacterial translocation accompanied by improved intestinal and systemic immunity[15,17,23].

In summary, the development of bacterial translocation was closely associated with overgrowth of pathogens such as fungi and *E. coli*, lowering of intestinal immunologic barrier function, breaching of gut mucosal barrier, and systemic inflammatory reaction subsequent to severe burns. The independent factors related to bacterial translocation were ileal injury score and the counts of gut bifidobacteria. Among them, the score of ileal injury was considered as the augmentative factor, and the counts of mucosal bifidobacteria as the protective factor. Thus specific interventions targeting the high-risk factors, including repair of damaged intestinal mucosa by improving gut microcirculation and improvement of gastrointestinal micro-ecology by increasing the quantity and proportion of bifidobacteria, might be beneficial to the attenuation of bacterial translocation. Moreover, determination of the quantity of bifidobacteria and the ratio of bifidobacteria to *E. coli* in feces might be used to predict the occurrence of bacterial translocation.

REFERENCES

1   **Swank GM**, Deitch EA. Role of the gut in multiple organ failure: bacterial translocation and permeability changes. *World J Surg* 1996; **20**: 411-417

2   **Sheng ZY**, Dong YL, Wang XH. Bacterial translocation and multiple system organ failure in bowl ischemia and reperfusion. *J Trauma* 1992; **32**: 148-153

3   **Yeh DC**, Wu CC, Ho WM, Cheng SB, Lu IY, Liu TJ, Peng FK. Bacterial translocation after cirrhotic liver resection: a clinical investigation of 181 patients. *J Surg Res* 2003; **111**: 209-214

4   **MacFie J**, O' Boyle C, Mitchell CJ, Buckly PM, Johnstone D, Sudworth P. Gut origin of sepsis: a prospective study investigating associations between bacterial translocation, gastric microflora, and septic morbidity. *Gut* 1999; **45**: 223-228

5   **Steinberg SM**. Bacterial translocation: what it is and what it is not. *Am J Surg* 2003; **186**: 301-305

6   **Tadros T**, Traber DL, Heggers JP, Herndon DN. Angiotensin II inhibitor DuP753 attenuates burn- and endotoxin-induced gut ischemia, lipid peroxidation, mucosal permeability, and bacterial translocation. *Ann Surg* 2000; **231**: 566-576

7   **Park PO**, Haglund U. Regeneration of small bowel mucosa after intestinal ischemia. *Crit Care Med* 1992; **20**: 135-139

8   **Ding LA**, Li JS. Effects of glutamine on intestinal permeability and bacterial translocation in TPN-rats with endotoxemia. *World J Gastroenterol* 2003; **9**: 1327-1332

9   **Koutelidakis I**, Papaziogas B, Giamarellos-Bourboulis EJ, Makris J, Pavlidis T, Giamarellou H, Papaziogas T. Systemic endotoxaemia following obstructive jaundice: the role of lactulose. *J Surg Res* 2003; **113**: 243-247

10   **Ulusoy H**, Usul H, Aydin S, Kaklikkaya N, Cobanoglu U, Reis A, Akyol A, Ozen I. Effects of immunonutrition on intestinal mucosal apoptosis, mucosal atrophy, and bacterial translocation in head injured rats. *J Clin Neurosci* 2003; **10**: 596-601

11   **Fujino Y**, Suzuki Y, Kakinoki K, Tanioka Y, Ku Y, Kuroda Y. Protection against experimental small intestinal ischaemia-reperfusion injury with oxygenated perfluorochemical. *Br J Surg* 2003; **90**: 1015-1020

12   **Li JY**, Lu Y, Hu S, Sun D, Yao YM. Preventive effect of glutamine on intestinal barrier dysfunction induced by severe trauma. *World J Gastroenterol* 2002; **8**: 168-171

13   **Cevikel MH**, Ozgun H, Boylu S, Demirkiran AE, Sakarya S, Culhaci N. Nitric oxide regulates bacterial translocation in experimental acute edematous pancreatitis. *Pancreatology* 2003; **3**: 329-335

14   **Tadros T**, Traber DL, Heggers JP, Herndon DN. Effects of interleukin-1alpha administration on intestinal ischemia and reperfusion injury, mucosal permeability, and bacterial translocation in burn and sepsis. *Ann Surg* 2003; **237**: 101-109

15   **Wang ZT**, Yao YM, Xiao GX, Cao WH, Sheng ZY. Bifidobacterial supplement enhances the expression and excretion of intestinal sIgA in severely burned rats. *Zhonghua Waike Zazhi* 2003; **41**: 385-388

16   **Wang ZT**, Yao YM, Xiao GX, Sheng ZY. Improvement of bifidobacterial supplement on the barrier function of intestinal mucosa and microbe flora induced by thermal injury in rats. *Zhongguo Weizhongbing Jijiu Yixue* 2003; **15**: 154-158

17 **Yao YM**, Lu LR, Yu Y, Liang HP, Chen JS, Shi ZG, Zhou BT, Sheng ZY. Influence of selective decontamination of the digestive tract on cell-mediated immune function and bacteria/endotoxin translocation in thermally injured rats. *J Trauma* 1997; **42**: 1073-1079

18 **Locascio M**, Holgado AP, Perdigon G, Oliver G. Enteric bifidobacteria: isolation from human infants and challenge studies in mice. *Can J Microbiol* 2001; **47**: 1048-1052

19 **Satokari RM**, Vaughan EE, Akkermans AD, Saarela M, de Vos WM. Bifidobacterial diversity in human feces detected by genus-specific PCR and denaturing gradient gel electrophoresis. *Appl Environ Microbiol* 2001; **67**: 504-513

20 **Nettelbladt CG**, Katouli M, Bark T, Svenberg T, Mollby R, Ljungqvist O. Orally inoculated Escherichia coli strains colonize the gut and increase bacterial translocation after stress in rats. *Shock* 2003; **20**: 251-256

21 **Eaves-Pyles T**, Alexander JW. Comparison of translocation of different types of microorganisms from the intestinal tract of burned mice. *Shock* 2001; **16**: 148-152

22 **Mosenthal AC**, Xu D, Deitch EA. Elemental and intravenous total parenteral nutrition diet-induced gut barrier failure is intestinal site specific and can be prevented by feeding nonfermentable fiber. *Crit Care Med* 2002; **30**: 396-402

23 **Macpherson AJ**, Gatto D, Sainsbury E, Harriman GR, Hengartner H, Zinkernagel RM. A primitive T cell-independent mechanism of intestinal mucosal IgA responses to commensal bacteria. *Science* 2000; **288**: 2222-2226

24 **Gong JP**, Wu CX, Liu CA, Li SW, Shi YJ, Yang K, Li Y, Li XH. Intestinal damage mediated by Kupffer cells in rats with endotoxemia. *World J Gastroenterol* 2002; **8**: 923-927

25 **Yao YM**, Bahrami S, Redl H, Fuerst S, Schlag G. IL-6 release after intestinal ischemia/reperfusion in rats is under partial control of TNF. *J Surg Res* 1997; **70**: 21-26

26 **Akin ML**, Gulluoglu BM, Erenoglu K, Terzi K, Erdemoglu A, Celenk T. Hyperbaric oxygen prevents bacterial translocation in thermally injured rats. *J Invest Surg* 2002; **15**: 303-310

27 **Fang WH**, Yao YM, Shi ZG, Yu Y, Wu Y, Lu LR, Sheng ZY. Effect of recombinant bactericidal/permeability-increasing protein on endotoxin translocation and lipopolysaccharide-binding protein/CD14 expression in rats after thermal injury. *Crit Care Med* 2001; **29**: 1452-1459

28 **Caplan MS,** Miller-Catchpole R, Kaup S, Russell T, Lickerman M, Amer M, Xiao Y, Thomson R Jr. Bifidobacterial supplementation reduces the incidence of necrotizing enterocolitis in a neonatal rat model. *Gastroenterology* l999; **117**: 577-583

29 **Urao M**, Fujimoto T, Lane GJ, Seo G, Miyano T. Does probiotics administration decrease serum endotoxin levels in infants? *J Pediatr Surg* 1999; **34**: 273-276

30 **Hooper LV**, Gordon JI. Commensal host-bacterial relationships in the gut. *Science* 2001; **292**: 1115-1118

31 **He F**, Ouwehand AC, Hashimoto H, Isolauri E, Benno Y, Salminen S. Adhesion of *Bifidobacterium spp.* to human intestinal mucus. *Microbiol Immunol* 2001; **45**: 259-262

32 **Eizaguirre I**, Urkia NG, Asensio AB, Zubillaga I, Zubillaga P, Vidales C, Garcia-Arenzana JM, Aldazabal P. Probiotic supplementation reduces the risk of bacterial translocation in experimental short bowel syndrome. *J Pediatr Surg* 2002; **37**: 699-702

33 **Wang ZT**, Xiao GX, Xiao J, Wang HJ, Peng YZ, Luo QZ. Effects of bifidobacteria preparation on restoring the disorder of intestinal flora induced by Meropenium in severely burned patients. *Zhonghua Shaoshang Zazhi* 2002; **18**: 111-112

34 **Guarner F**, Malagelada JR. Gut flora in health and disease. *Lancet* 2003; **361**: 512-519

35 **Gilmore MS**, Ferretti JJ. Microbiology. The thin line between gut commensal and pathogen. *Science* 2003; **299**: 1999-2002

36 **Gordon DM**, Diebel LN, Liberati DM, Myers TA. The effects of bacterial overgrowth and hemorrhagic shock on mucosal immunity. *Am Surg* 1998; **64**: 718-721

37 **Choudhry MA**, Fazal N, Goto M, Gamelli RL, Sayeed MM. Gut-associated lymphoid T cell suppression enhances bacterial translocation in alcohol and burn injury. *Am J Physiol Gastrointest Liver Physiol* 2002; **282**: G937-947

Edited by Wang XL and Xu FM

• BASIC RESEARCH •

Gene expression profiles of hepatocytes treated with La(NO₃)₃ of rare earth in rats

Hui Zhao, Wei-Dong Hao, Hou-En Xu, Lan-Qin Shang, You-Yong Lu

Hui Zhao, Wei-Dong Hao, Hou-En Xu, Lan-Qin Shang, Department of Toxicology, Peking University Health Science Center, Beijing 100083, China
You-Yong Lu, School of Oncology, Beijing Institute for Cancer Research, Peking University, Beijing 100034, China
Supported by grant of Key Project of National Natural Science Foundation of China, No. 29890280-3
Correspondence to: Wei-Dong Hao, Department of Toxicology, Peking University Health Science Center, No 38 Xue Yuan Road, Beijing 100083, China. whao@bjmu.edu.cn
Telephone: +86-10-82802352   **Fax:** +86-10-62015583
Received: 2002-08-01   **Accepted:** 2002-08-31

Abstract

AIM: To compare the gene expression between La(NO₃)₃-exposed and control rats *in vivo*.

METHODS: Rats were fed La(NO₃)₃ once daily at a dose of 20 mg/kg for one month by gavage. Gene expression of hepatocytes was detected using mRNA differential display (DD) technique and cDNA microarray and compared between treated and control groups.

RESULTS: Six differentially expressed sequence tags were cloned by DD, of which five were up regulated and one was down regulated in treated rats. Two sequences were determined. One band was novel. The other shared 100% sequence homology with AU080263 Sugano mouse brain mncb Mus musculus cDNA clone MNCb-5435 5′ . With DNA microarray, 136 differentially expressed genes were identified including 131 over-expressed genes and 5 under-expressed genes. Most of these differentially expressed genes were cell signal and transmission genes, genes associated with metabolism, protein translation and synthesis.

CONCLUSION: La(NO₃)₃ could change the expression levels of some kinds of genes. Further analysis of the differentially expressed genes would be helpful for understanding the wide biological effect spectrum of rare earth elements.

Zhao H, Hao WD, Xu HE, Shang LQ, Lu YY. Gene expression profiles of hepatocytes treated with La(NO₃)₃ of rare earth in rats. *World J Gastroenterol* 2004; 10(11): 1625-1629
http://www.wjgnet.com/1007-9327/10/1625.asp

INTRODUCTION

Rare earth (RE) includes 17 elements. According to the physical and chemical nature, 16 elements except for scandium (Sc) are categorized into two groups. One is called light RE, which is represented by cerium, including lanthanum (La), cerium (Ce), praseodymium (Pr), neodymium (Nd), promethium (Pm), samarium (Sm) and europium (Eu). The other is called heavy RE, which is represented by yttrium, including gadolinium (Gd), terbium (Tb), dysprosium (Dy), holmium (Ho), erbium (Er), thulium (Tm), ytterbium (Yb), lutetium (Lu) and yttrium (Y).

Recently, RE has become one of the common xenobiotics in our surroundings as it is widely used in industry, stockbreeding and medicine, especially as trace fertilizers in agriculture, and they can be concentrated by food chain. Therefore, understanding the effects of RE on health has become more and more important.

Studies on RE toxicology have lasted for a long time. However, deeper exploration of its mechanism is highly needed. It is well known the biological effect spectrum of RE is wide and the dose-response relationship is complicated. For example, RE elements could induce chromosome damage of blood lymphocytes[1] and liver damage[2-4], depress learning and memory[5], increase or suppress cell-mediated immunity of the spleen[6], inhibit gap junctional intercellular communication[7], *etc*. However, safety evaluation of RE is not easy, and the research of biomarkers by molecular biology is in its infancy. It is necessary to find more sensitive biomarkers by new techniques and methods, and to acquire a deeper understanding of the mechanism.

In this paper, the molecular mechanism of RE toxicity was explored by DD and cDNA microarray. La(NO₃)₃, which is the major component in RE trace fertilizers, was selected as the study material.

MATERIALS AND METHODS

La(NO₃)₃ treatment of rats

In the study of DD, 86-week-old Wistar rats were chosen. One half of them were male, and the others were female. To guarantee the treated rats and control had similar heredity backgrounds, the rule of same-breeding and same-sex control was applied. A La (NO₃)₃-treated rat and its control were called a pair of test animals. There were two pairs of male rats and female rats, respectively. Treated rats were fed La(NO₃)₃ once daily at a dose of 20 mg/kg for one month by gavage. Control rats were fed distilled water. One pair of female rats was chosen in the study of cDNA microarray. Parts of isolated rat livers were used to observe morphology of hepatocytes by light microscopy and electron microscopy. Others were snap frozen in liquid nitrogen and then stored at -80 ℃ until RNA extraction.

Preparation of total RNA

Total RNA was prepared with single-step method by acid guanidinium isothiocyanate-phenol-chloroform according to Chomczynski and Sacchi[8]. In brief, 0.5 g liver was homogenized with 2.5 mL solution D, then 0.25 mL 0.2 mol/L NaAc/0.1 mmol/L ATA, 2.75 mL phenol, 0.55 mL chloroform/isoamyl alcohol (24:1) were added and shaken in order. It was cooled on ice for 15 min and centrifuged at 10 000 g at 4 ℃ for 20 min. The supernatant was removed put into new tubes and 2.75 mL isopropanol was added to precipitate at -20 ℃. It was then centrifuged at 10 000 g at 4 ℃ for 20 min. The supernatant was discarded and the pellet was dissolved in RNA denature buffer, then 15 μL 3 mol/LNaAc and 330 μL 1 000 mL/L ethanol were added to precipitate at -20 ℃ for 1 h. Contaminated chromosomal DNA was digested with DNAse I (Promega).

Differential Display (DD)

For reverse transcription, RNA (in 1.0 μL DEPC treated water) was mixed with 2.0 μL AP1 (Beckman) and incubated at 70 ℃

for 5 min, then cooled on ice immediately. The solution was mixed with 8.8 μL DEPC treated water, 4.0 μL 5×reverse transcript buffer, 2.0 μL dNTP (250 μmol/L), 2.0 μL DTT (100 mmol/L) and 0.2 μL MMLV reverse transcriptase (200 U/μL, GIBCO). Reverse transcription was performed at 42 ℃ for 5 min, then at 50 ℃ for 50 min, and finally at 70 ℃ for 15 min.

For amplification of cDNA, AP1 was chosen as anchor 3' primer and ARP1-ARP4 were selected as arbitrary 5' primers. A 2 μL cDNA was mixed with 8.2 μL DEPC treated water, 2.0 μL 10×PCR buffer (Promega), 2.0 μL MgCl$_2$ (25 mmol/L, Promega), 1.6 μL dNTP (2.5 mmol/L), 2.0 μL ARP (2 μmol/L), 2.0 μL AP (2 μmol/L) and 0.2 μL TaqE (2.0 U/μL, Promega). The PCR amplification program was at 95 ℃ for 2 min, then 4 cycles at 92 ℃ for 15 s, at 50 ℃ for 30 s, and at 72 ℃ for 2 min, followed by 30 cycles at 92 ℃ for 15 s, at 60 ℃ for 30 s, at 72 ℃ for 2 min, and finally at 72 ℃ for 7 min.

A 7 μL PCR mixture was redissolved in 4 μL loading dye, heated at 95 ℃ for 2 min, then run on 80 g/L polyacrylamide-urea gels at 9 mA. DNA fragments on gels were displayed by silver stain method. Bands representing cDNA, which appeared to be differentially expressed, were excised and reamplified under the same conditions as above except the primers. In this procedure, T7 promoter and M13 reverse (-48) were used.

DNA sequence analysis
DNA sequence analysis was carried out with dye-terminator method in ABI DNA sequencer. DNA sequences were identified by comparison to those in GenBank BLASTn on Internet.

cDNA microarray
cDNA probes were prepared through reverse transcription and then purified. The probes from normal rats were labeled with Cy3-dUTP, and the probes from La(NO$_3$)$_3$-treated rats were labeled with Cy5-dUTP. The chips were scanned using ScanArray3000 laser scanner (General Scanning, Inc) at two wavelengths to detect emissions from both Cy3 and Cy5. The acquired images were analysed using ImaGene3.0 software (BioDiscovery, Inc.). The intensity of each spot at the two wavelengths represented the quantity of Cy3-dUTP and Cy5-dUTP, respectively. Each ratio of Cy3 and Cy5 was computed. Overall intensities were normalized by a coefficient according to the ratios of the located 40 housekeeping genes. To minimize artifacts arising from low expression values, only the genes with raw intensity values larger than 800 counts for one or both of Cy3 and Cy5 were chosen for differential analysis.

RESULTS

Effects of La(NO$_3$)$_3$ on morphology of rat hepatocytes
La(NO$_3$)$_3$ had no significant effects on histopathology by light microscopy. Swollen or cavitated mitochondria were observed in hepatocytes by electron microscopy (Figure 1).

Differential expression of La(NO$_3$)$_3$-induced genes of rat hepatocytes
Six differentially expressed bands in two pairs of rats, were obtained (Figure 2). Among them, five were up regulated and one was down regulated in treated rats. Two bands were sequenced. The results were as follows. LaFT1-4-1: The expression level of EST in treated rats was higher than that in control. Its length was about 160 bp (Figure 3A). EST was compared with known ESTs in GeneBank BLASTn. The homology was low (≤15%). LaFT1-4-1 was novel. Its sequence was as follow: 5'-AGCGGATAACA ATTTCACACAGGAGTAGCAGACCCTGCCCCCAGGAAA TAACACACACTAAACTCTCAAAAAAAAAAAGCCCTATA GTGAGTCGTATTACACCCTATAGTGAGTCGTATTAGC GGATAACAATTTCACACAGGACGCCCTATAGTGAGTA-3'.

LaMT1-4-1: The expression level of EST in treated rats was higher than that in control. Its length was about 144 bp (Figure 3B). The EST was compared with known ESTs in GenBank BLASTn and it shared 100% sequence homology with AU080263 Sugano mouse brain mncb Mus musculus cDNA clone MNCb-5435 5'. Its sequence was as follow: 5'-ACTCAAAGGCGGTAATACGG TTATCCACAGAATCAGGGGATAACGCAGGAAAGAA CATGTGAGCAAAAGGCCAGCAAAAGGCCAGGAAC CGTAAAAAGGCCGCGTTGCTGGCGTTTTTCCATAGG CTCCGCCCCCCTGACGAGC-3'.
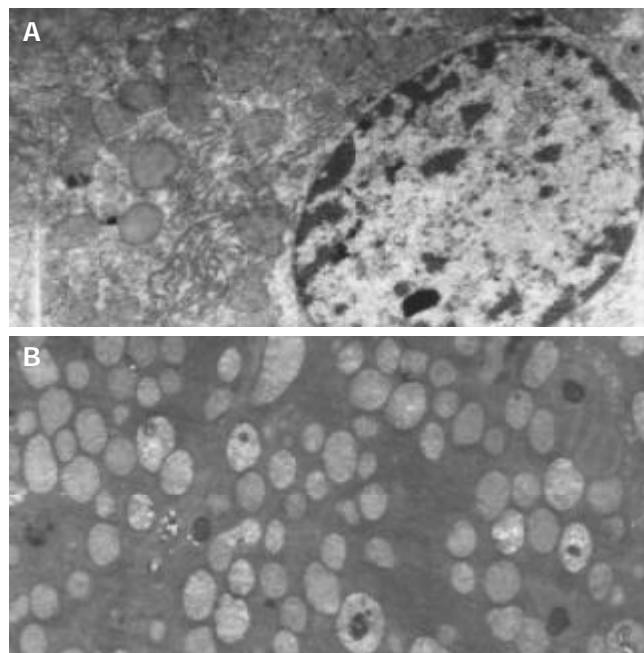

Figure 1 Electron microscopic images of hepatocytes. A: Normal mitochondria in control hepatocytes (TEM×6 700), B: Swollen or cavitated mitochondria in treated hepatocytes (TEM×5 800).
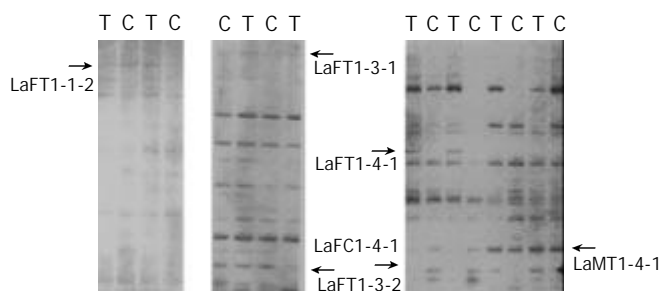

Figure 2 Polyacrylamide-urea gel of DNA fragments. Six differentially expressed bands in two pairs of rats were obtained. "T" above the bands and in name represents treated group, while "C" represents control group, "M" represents male, and "F" represents female. Among the bands, the expression levels of LaFT1-1-2, LaFT1-3-1, LaFT1-3-2, LaFT1-4-1 and LaMT1-4-1 were increased in treated rats. However, the level of LaFC1-4-1 was decreased.

Profile of gene expression in La(NO$_3$)$_3$-treated rat liver
HGEC-40D expression profile microarray, which consisted of 4 096 human cDNAs containing 60 control genes and 4 036 target genes, was provided by United Gene Holdings, Ltd. For every gene, there were two parallels in microarray. Target genes were divided into 15 types: oncogenes and tumor suppressor genes, ionic passage and transportation protein genes, cell cycle protein genes, stress reaction protein genes, cell skeleton

and movement protein genes, genes related to cell apoptosis, DNA synthesis, repair and recombination genes, DNA binding, transcription and transcription factor genes, cell receptor genes, immunity related genes, cell signal and transmission genes, metabolism related genes, protein translation and synthesis genes, growth related genes, and others.
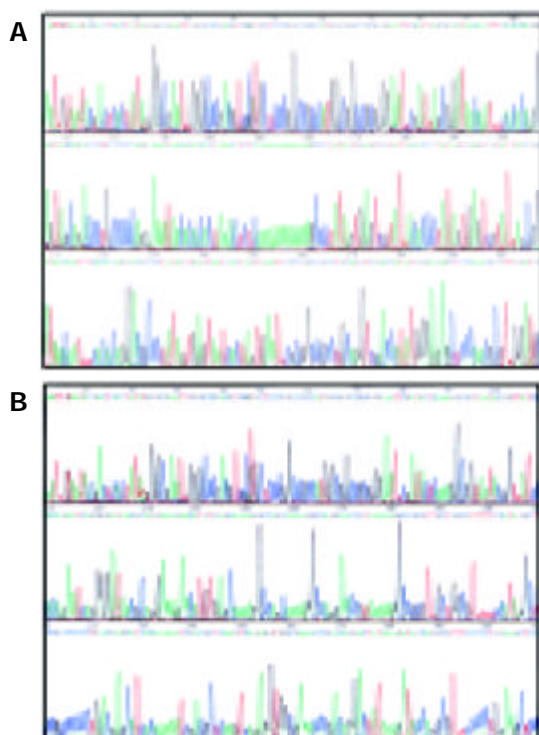
In order to monitor the preparation and hybridization of DNA microarray, positive and negative controls were arranged. Forty housekeeping genes were used as positive controls. 821 gene (8 spots) and 1×spot solution (8 spots) were used as negative control spots. Positive control spots showed high intensity of signals and negative control spots showed low intensity, which proved the reliability of the data.

Cy3 fluorescent signal (labeled control) and Cy5 fluorescent signal (labeled treated group) were represented with red and green respectively. For overlying two signals of one spot, the spot showed green if the intensity of Cy3 signal was stronger (indicating down-regulation tendency), the spot showed red if the intensity of Cy5 signal was stronger (indicating up-regulation tendency), the spot showed yellow if the intensities of Cy3 and Cy5 signals were similar. In this study, the result of microarray is shown in Figure 4.
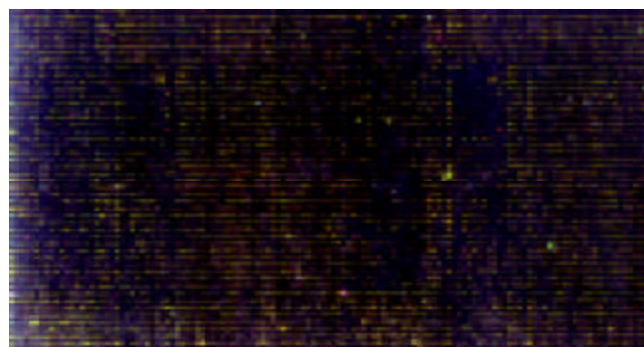

A
B

Figure 3 Sequences of cDNA. A: Sequence of LaFT1-4-1. Its length was about 160 bp. The primers used were AP1 and ARP4. B: Sequence of LaMT1-4-1. Its length was about 144 bp. The primers used were AP1 and ARP4.

Figure 4 Two overlying fluorescent signals.

We screened out 136 differentially expressed genes according to the following rules. The ratio of Cy3 and Cy5 signal was larger than 2 or smaller than 0.5, the raw intensity value of one or both of Cy3 and Cy5 was larger than 800, the trend of up-regulation or down-regulation in parallels was the same. Of the

Table 1 Profile of gene expression in La(NO$_3$)$_3$-treated rat liver

Trend	GenBank-ID	Definition	Average ratio
up	ab023148	Homo sapiens mRNA for KIAA0931 protein, partial cds.	23.4
	hsu38545	Human ARF-activated phosphatidylcholine-specific phospholipase D1a (hPLD1) mRNA, complete cds.	10.1
	hstrke	H.sapiens TRK E mRNA.	8.7
	humrp17a	Human ribosomal protein L7a (surf 3) large subunit mRNA, complete cds.	7.8
	humcda24a	Homo sapiens CD24 signal transducer mRNA, complete cds.	6.9
	hsu76111	Human translation repressor NAT1 mRNA, complete cds.	6.4
	af125042	Homo sapiens bisphosphate 3' -nucleotidase mRNA, complete cds.	6.1
	hsu43701	Human ribosomal protein L23a mRNA, complete cds.	6.0
	hsu85946	Homo sapiens brain secretory protein hSec10p (HSEC10) mRNA, complete cds.	5.7
	ae000136	Escherichia coli K-12 MG1655 section 26 of 400 of the complete genome.	5.6
	af077951	Homo sapiens protein inhibitor of activated STAT protein PIAS1 mRNA, complete cds.	5.3
	af044671	Homo sapiens MM46 mRNA, complete cds.	5.1
	hsu35048	Human TSC-22 protein mRNA, complete cds.	5.1
	af068302	Homo sapiens choline/ethanolamine phosphotransferase (CEPT1) mRNA, complete cds.	5.1
	hsy17392	Homo sapiens mRNA for prefoldin subunit 1.	5.0
	af131820	Homo sapiens clone 25077 mRNA sequence, complete cds.	4.8
	af094481	Homo sapiens trinucleotide repeat DNA binding protein p20-CGGBP (CGGBP) gene, complete cds.	4.8
	ab020636	Homo sapiens mRNA for KIAA0829 protein, partial cds.	4.4
	ab020697	Homo sapiens mRNA for KIAA0890 protein, complete cds.	4.4
down	ab011098	Homo sapiens mRNA for KIAA0526 protein, complete cds.	0.466
	hsifi56r	Human mRNA for 56-ku protein induced by interferon.	0.437
	hssgk	Homo sapiens sgk gene.	0.405
	hsu87967	Human ATP diphosphohydrolase mRNA, complete cds.	0.364
	humkuant	Human Ku autoimmune antigen gene, complete cds.	0.352

136 genes with altered expression, 131 genes had an elevated expression and 5 genes had a reduced expression. Most of the differentially expressed genes were cell signal and transmission genes, genes related to metabolism, protein translation and synthesis genes. Five down-regulated and 19 up-regulated genes with their differential expression levels more than 4-fold and having similar trends, are described in Table 1.

DISCUSSION

Studies on toxicities of RE elements by different intake pathways showed that the liver was the target organ of RE element toxicity[9-15], and 20 mg/kg was believed to be the effective dose in oral administration[15]. So, rats treated with La(NO$_3$)$_3$ at a dose of 20 mg/kg by gavage were chosen in our study.

mRNA differential display could provide a unique and powerful experimental system to study differential gene expression. In this study, six differentially expressed tags were obtained. Of the 2 bands sequenced, one (LaFT1-4-1) was novel.

The technique of DNA microarray could allow expression monitoring of thousands of genes in parallel[16]. This technique promotes the identification of differentially expressed genes and investigation of the function of genes. In this study, human cDNA microarray was used. The genomes of human and rodent were very similar[17,18], the homology of human genes and rat genes was over 70%. So it is of significance to analyse rat samples by a HGEC-40D expression profile microarray. One hundred and thirty-six differentially expressed genes were found by DNA microarray, which included mainly cell signal and transmission genes, genes related to metabolism, protein translation and synthesis genes. These genes accounted for 15%, 14% and 13%, respectively. Analysis on capital genes was described as follows.

Some genes encoding mitochondrial proteins were up regulated. The levels of homo sapiens NADH-ubiquinone oxidoreductase B22 subunit mRNA, ND2 gene, NDUFA5 gene and NDUFS8 gene were elevated 2.543, 3.540, 3.645 and 3.767 fold respectively, which were possibly associated with the damage of mitochondria.

Twelve differentially expressed KIAA genes were found in the study. Eleven were up regulated and one was down regulated. The expression level of KIAA0931 was elevated 23.4-fold. A family of KIAA includes new genes published by Kazusa DNA Research Institute in Japan. The functions of KIAA genes were supposed to be related to cell signal transmission, cell structure and cell movement based on the sequence studies[19-21].

Phosphatidylcholine-specific phospholipase D1a (hPLD), is an important member of cell signal transducers. Active hPLD could produce biological effects by the following mechanisms. Phosphatidic acid (PA), diacyl-glycerol (DG) and lysophosphatidic acid (LPA), which are the direct and indirect products of hPLD, are important second messengers. Hydrolysis of phosphatidyl choline (PC) by hPLD could change local components of the membranes, consequently the characteristics of the membranes[22]. It has been revealed that the process of hydrolysis of PC is related to many physiological activities including metabolism, cell cleavage, secretion, immunity, inflammatory reaction[23]. In this study the expression level of hPLD gene was elevated by 10.1-fold, suggesting that activated hPLD which affects cell signal transmission is an important pathway of La(NO$_3$)$_3$ toxicity.

Signal transducer and activator of transcription (STAT) proteins play an important role in cell proliferation and differentiation induced by cytokines. STAT1 protein is believed to be the transcription factor of IFN reactivity. In addition, the mice with Stat1 gene picked out were found to be lacking of congenital immunity to viruses and bacteria[24]. Protein inhibitor of activated STAT1 (PIAS1) could depress the activity of STAT1

by blocking STAT1 binding to specific DNA[25]. PIAS1 gene was up regulated 5.3-fold in the study. It was suggested that La(NO$_3$)$_3$ might affect congenital immunity and the reactivity to IFN.

There were 7 differentially expressed genes related to immunity, of which 6 genes were up regulated and 1 was down regulated. In the up-regulated genes, H12.3 protein gene could regulate lymphocyte proliferation[26]. CD9 antigen gene[27], β-globulin gene, immuno-globulin light chain gene, CD24 signal transducer gene were related to humoral immunity. Calnexin protein gene played a role in cellular immunity and humoral immunity[28]. The results suggested that La(NO$_3$)$_3$ had effects on both cellular immunity and humoral immunity. This was in good agreement with the results obtained by other researchers[29-31].

In conclusion, the expression profiles of certain genes of La(NO$_3$)$_3$ treated rats differed markedly from those of control rats. This is consistent with the wide biological effect spectrum of RE elements. Multiple genes may join together to play a same role. Further analysis of the differentially expressed genes would be helpful for understanding the wide biological effect spectrum of RE elements. It would be interesting to explore further if the differentially expressed genes could be used as more sensitive biomarkers.

REFERENCES

1   **Xu HE**, Gao GH, Jia FL, Wangh XY, Xie Q, Liu HS, Wang NF. Effect of mixed rare earth Changle on the micronuclei formation of blood lymphocytes in rats. *Zhonghua Yufang Yixue Zazhi* 2000; **34**(Suppl): 5-7

2   **Nakamura Y**, Tsumura Y, Tonogai Y, Shibata T, Ito Y. Differences in behavior among the chlorides of seven rare earth elements administered intravenously to rats. *Fundam Appl Toxicol* 1997; **37**: 106-116

3   **Tuchweber B**, Trost R, Salas M, Sieck W. Effect of praseodymium nitrate on hepatocytes and Kupffer cells in the rat. *Can J Physiol Pharmacol* 1976; **54**: 898-906

4   **Salas M**, Tuchweber B, Kovacs K, Garg BD. Effect of cerium on the rat liver: an ultrastructural and biochemical study. *Beitr Pathol* 1976; **157**: 23-44

5   **Li XQ**, Jiang JJ, Yang L, Liu M, Yang LY. Effect of low level mixed rare earth Changle on learning and memory, locomotor activity and NMDA-and M-receptors activity and morphology of divisions of hippocampal cortex in rats. *Zhonghua Yufang Yixue Zazhi* 2000; **34**(Suppl): 20-23

6   **Liu JM**, Chen D, Wang XM, Nie YX, Li Y, Li J. Long-term effect of Changle and La(NO$_3$)$_3$ on level of IL-2 and γ-IFN of splenic lymphocytes in rats. *Zhonghua Yufang Yixue Zazhi* 2000; **34** (Suppl):49-51

7   **Guo XB**, Gao ZH, Luo LZ, Yao BY. Effects of rare earth compounds on metabolic cooperation between Chinese hamster V79 cells. *Zhonghua Yufang Yixue Zazhi* 2000; **34**(Suppl): 17-19

8   **Chomczynski P**, Sacchi N. Single-step method of RNA isolation by acid guanidinium thiocyanate-phenol-chloroform extraction. *Anal Biochem* 1987; **162**: 156-159

9   **Godin DV**, Frohlich J. Erythrocyte alterations in praseodymium-induced lecithin: cholesterol acyltransferase(LCAT) deficiency in the rat: comparison with familial LCAT deficiency in man. *Res Commun Chem Pathol Pharmacol* 1981; **31**: 555-566

10 **Langer GA**, Frank JS. Lanthanum in heart cell culture. Effect on calcium exchange correlated with its localization. *J Cell Biol* 1972; **54**: 441-455

11 **Arvela P**, Kraul H, Stenback F, Pelkonen O. The cerium-induced liver injury and oxidative drug metabolism in DBA/2 and C57BL/6 mice. *Toxicology* 1991; **69**: 1-9

12 **Spencer A**, Wilson S, Harpur E. Gadolinium chloride toxicity in the mouse. *Hum Exp Toxicol* 1998; **17**: 633-637

13 **Hirano S**, Kodama N, Shibata K, Suzuki KT. Metabolism and toxicity of intravenously injected yttrium chloride in rats. *Toxicol Appl Pharmacol* 1993; **121**: 224-232

14 **Shinohara A**, Chiba M, Inaba Y. Distribution of terbium and increase of calcium concentration in the organs of mice i.v.-

administered with terbium chloride. *Biomed Environ Sci* 1997; **10**: 73-84

15 **Chen AJ**, Chen D, Liu Y, Liu P, Wang XM, Nie YX, Wang X, Sun SY. The long term effect of low dose of Changle on the structure and function of liver in rats. *Zhonghua Yufang Yixue Zazhi* 2000; **34**(Suppl): 46-48

16 **Schena M**, Shalon D, Davis RW, Brown PO. Quantitative monitoring of gene expression patterns with a complementary DNA microarray. *Science* 1995; **270**: 467-470

17 **Pennisi E**. Genomics. Sequence tells mouse, human genome secrets. *Science* 2002; **298**: 1863-1865

18 **Pennisi E**. Genomics. Charting a genome's hills and valleys. *Science* 2002; **296**: 1601-1603

19 **Nagase T**, Ishikawa K, Miyajima N, Tanaka A, Kotani H, Nomura N, Ohara O. Prediction of the coding sequences of unidentified human genes. IX. The complete sequences of 100 new cDNA clones from brain which can code for large proteins *in vitro*. *DNA Res* 1998; **5**: 31-39

20 **Nagase T**, Ishikawa K, Suyama M, Kikuno R, Hirosawa M, Miyajima N, Tanaka A, Kotani H, Nomura N, Ohara O. Prediction of the coding sequences of unidentified human genes. XII. The complete sequences of 100 new cDNA clones from brain which code for large proteins *in vitro*. *DNA Res* 1998; **5**: 355-364

21 **Nagase T**, Ishikawa K, Suyama M, Kikuno R, Hirosawa M, Miyajima N, Tanaka A, Kotani H, Nomura N, Ohara O. Prediction of the coding sequences of unidentified human genes. XIII. The complete sequences of 100 new cDNA clones from brain which code for large proteins *in vitro*. *DNA Res* 1999; **6**: 63-70

22 **Exton JH**. Phospholipase D: Enzymology, mechanisms of regulation, and function. *Physiol Rev* 1997; **77**: 303-320

23 **Morris AJ**, Engebrecht J, Frohman MA. Structure and regulation of phospholipase D. *Trends Pharmacol Sci* 1996; **17**: 182-185

24 **Coffman RL**, Lebman DA, Rothman P. Mechanism and regulation of immunoglobulin isotype switching. *Adv Immunol* 1993; **54**: 229-270

25 **Liu B**, Liao J, Rao X, Kushner SA, Chung CD, Chang DD, Shuai K. Inhibition of Stat1-mediated gene activation by PIAS1. *Proc Natl Acad Sci U S A* 1998; **95**: 10626-10631

26 **Guillemot F**, Billault A, Auffray C. Physical linkage of a guanine nucleotide-binding protein-related gene to the chicken major histocompatibility complex. *Proc Natl Acad Sci U S A* 1989; **86**: 4594-4598

27 **Boucheix C**, Benoit P, Frachet P, Billard M, Worthington RE, Gagnon J, Uzan G. Molecular cloning of the CD9 antigen. A new family of cell surface proteins. *J Biol Chem* 1991; **266**: 117-122

28 **Hochstenbach F**, David V, Watkins S, Brenner MB. Endoplasmic reticulum resident protein of 90 kilodaltons associates with the T- and B-cell antigen receptors and major histocompatibility complex antigens during their assembly. *Proc Natl Acad Sci U S A* 1992; **89**: 4734-4738

29 **Wang YZ**, Li ZX, Li F, Li M, Shi Y. Effects of RE elements on workers' immune function. *Zhiye Yixue* 1995; **22**: 7-8

30 **Zhang ZS**, Xue B, Chen XA. Effects of RE nitrate on the function of T- lymphocytes, B- lymphocytes and macrophage. *Weisheng Dulixue Zazhi* 1993; **7**: 157-158

31 **Wei XT**, Ma N, Lei ZM, Xue B, Xu HE. Effects of La(NO$_3$)$_3$ on the immune function and cell apoptosis of splenic lymphocytes and thymocytes. *Zhonghua Yufang Yixue Zazhi* 2000; **34** (Suppl): 42-45

Edited by Zhu LH and Wang XL **Proofread by** Xu FM

• BASIC RESEARCH •

Competitive inhibition of adherence of enterotoxigenic *Escherichia coli*, enteropathogenic *Escherichia coli* and *Clostridium difficile* to intestinal epithelial cell line Lovo by purified adhesin of *Bifidobacterium adolescentis* 1027

Shi-Shun Zhong, Zhen-Shu Zhang, Ji-De Wang, Zhuo-Sheng Lai, Qun-Ying Wang, Ling-Jia Pan, Yue-Xin Ren

Shi-Shun Zhong, Zhen-Shu Zhang, Ji-De Wang, Zhuo-Sheng Lai, Qun-Ying Wang, Ling-Jia Pan, Yue-Xin Ren, Chinese PLA Institute of Digestive Diseases, Nanfang Hospital, First military Medical University, Guangzhou 510515, Guangdong Province, China
Supported by Natural Science Foundation of Guangdong Province, No.010621
Correspondence to: Dr. Shi-Shun Zhong, Chinese PLA Institute of Digestive Disease, Nanfang Hospital, First military Medical University, Guangzhou 510515, Guangdong Province, China. zdoctor@sohu.com
Telephone: +86-20-61641530
Received: 2004-01-10   **Accepted:** 2004-02-18

Abstract

AIM: To observe competitive inhibition of adherence of enterotoxigenic *Escherichia coli* (ETEC), enteropathogenic *Escherichia coli* (EPEC) and *Clostridium difficile* (*C. difficile*) to intestinal epithelial cell line Lovo by purified adhesin of *Bifidobacterium adolescentis* 1027 (B. ado 1027).

METHODS: The binding of bacteria to intestinal epithelial cell line Lovo was counted by adhesion assay. The inhibition of adherence of ETEC, EPEC and *C. difficile* to intestinal epithelial cell line Lovo by purified adhesin of B. ado 1027 was evaluated quantitatively by flow cytometry.

RESULTS: The purified adhesin at the concentration of 10 μg/mL, 20 μg/mL and 30 μg/mL except at 1 μg/mL and 5 μg/mL could inhibit significantly the adhesion of ETEC, EPEC and *C. difficile* to intestinal epithelial cell line Lovo. Moreover, we observed that a reduction in bacterial adhesion was occurred with increase in the concentration of adhesin, and MFI (Mean fluorescent intensity) was decreased with increase in the concentration of adhesin.

CONCLUSION: The purified adhesin of B. ado 1027 can inhibit the adhesion of ETEC, EPEC and C. difficile to intestinal epithelial cell line Lovo in a dose-dependent manner.

INTRODUCTION

It is well known that enterotoxigenic *Escherichia coli* (ETEC) and enteropathogenic *Escherichia coli* (EPEC) are major cause of diarrhoea in neonates and travelers. The gastrointestinal tract appears to be a reservoir for *E. coli* which are able to translocate across the intestinal mucosa. *Clostridium difficile* (*C. difficile*),

a gram-positive spore-forming anaerobic bacillus, is the most common cause of infectious diarrhoea in hospitalized patients[1]. Adherence of bacteria to intestinal epithelium is known to be a prerequisite for colonization and infection of the gastrointestinal tract by many gastrointestinal pathogens[2-4]. The intestinal epithelium is the primary site of contact for pathogens with host cells and plays an important role in the cross-talk between epithelial cells, luminal micro-organisms and immune cells. Therefore, inhibition of bacterial adhesion to the intestinal surface may prevent enteropathogens from translocating across the intestinal mucosa.

Bifidobacterium is known to be a predominant constituent of the human intestinal microflora[5]. The presence of bifidobacteria in the human intestine has been reported to contribute to human health and well being[6,7]. Adherence of bifidobacteria to intestinal mucus is regarded as one of the prerequisites for successful colonization[8], antagonistic activity against enteropathogens[9,10], modulation of the immune system[11]. In addition, mucosal adhesion has been proposed as one of the main selection criteria for probiotic strains[12-14]. Recently, studies have focused on its anti-infectious effects, particularly the inhibition activity against enteropathogens for protecting human[15-17]. As the production and preservation of live bifidobacterium are difficult, so its application is restricted. Bernet *et al.*[18] observed that the occurrence of bifidobacteria adhering to the human intestinal cells by a mechanism of adhesion which involved a proteinaceous component. Fujiwara *et al.*[19,20] clarified that bifidobacterium longum SBT2928 produced a proteinaceous factor which prevented the binding of ETEC to the binding receptor gangliotetraosylceramide (GA1). Zheng *et al.*[21] extracted and purified a protein with a molecular weight of 16 ku from spent culture supernatant of *Bifidobacterium adolescentis* 1027 (B. ado 1027). In the present study, competitive inhibition of adherence of ETEC, EPEC and *Clostridium difficile* to intestinal epithelial cells by purified adhesin of B. ado 1027 was observed by adhesion assay and flow cytometry assay.

MATERIALS AND METHODS

Bacterial strains

B. ado 1027 was isolated from healthy infants feces and identifiedby API-20A and TAB system (British). *B. ado* 1027 was cultured in sulfglycolic acid salt broth at 37 ℃ for 48 h under anaerobic conditions. ETEC and EPEC were obtained from Department of Epidemiology, First Military Medical University. ETEC and EPEC were cultured in agitation, nutrient broth at 37 ℃ for 48 h. A toxin-producing *C. difficile* strain (VPI10463) was obtained from Lanzhou Institute of Biological Products (China). *C. difficile* strain was grown in brain-heart infusion broth at 37 ℃ for 48 h under anaerobic conditions. All bacteria were harvested from the broth culture by centrifugation at 2 500 r/min for 10 min, followed by resuspension of the pellet in phosphate buffered saline (PBS, pH 7.4) to a concentration of 1×10^8 colony forming units (cfu)/mL.

Cell line

Human intestinal epithelial cell line Lovo was obtained from American type culture collection (ATCC) and was maintained in RPMI-1 640 (Gibco) supplemented with 2 mmol/L *L*-glutamine and 100 mL/L FCS at 37 ℃ in a humidified atmosphere containing 50 mL/L CO_2. For the adhesion assay, monolayer of Lovo cell was prepared on glass coverslips which were placed in six-well tissue culture plates (Corning Glass Works, Corning, N.Y.).

Extraction and purification of adhesin

The adhesin of bifidobacterium was extracted and purified as reported earlier by Zheng *et al*[21]. In short, the adhesin of bifidobacterium was isolated and purified by Superdex 75 gel filtration and Q-Sepharose FF ion exchange chromatography, and the adhesin was analyzed by SDS-PAGE. It was a protein with a molecular weight of 16 Ku , stored at -20 ℃.

In vitro adhesion assay

The adherence of bacteria strains to Lovo cells was examined as described previously[22-24]. Briefly, the Lovo monolayer prepared on glass coverslips which were placed in six-well tissue culture plates, was washed twice with PBS. The adhesin (1 µg/mL, 5 µg/mL, 10 µg/mL, 20 µg/mL, and 30 µg/mL) of bifidobacterium was added to each well of the tissue culture plate, and the plate was incubated at 37 ℃ in a humidified atmosphere containing 50 mL/L CO_2. After 30 min of incubation, the monolayer was washed one time with PBS. The suspensions of bacteria (1mL) were added to each well, respectively. After 3 h of incubation at 37 ℃ atmosphere, the monolayer was washed twice with sterile PBS, fixed with methanol, stained with Gram stain, and examined microscopically. For each monolayer on a glass coverslip, the number of adherent bacteria was evaluated in 30 random microscopic areas. Adherence was evaluated by two different technicians to eliminate bias. Bifidobacterium+bacteria and alone bacteria group were used as controls of adhesion.

Mean fluorescent intensity (MFI) of human intestinal epithelial cell with adherent bacteria were detected by flow cytometer

The fluorochrome FITC (Fluorescein isothiocyanate) was used in this study. All bacteria were washed 2 times in bicarbonate buffer (0.1 mol/L, pH 9.2), and labelled with fluorochrome FITC (1.5 mg/mL) by incubating 1×10^8 bacteria/mL at 4 ℃ for 1 h. Excess fluorochrome was removed by washing 5 times with PBS at 1 500 *g*. All bacteria were resuspended in PBS which contained B. ado 1027 (1×10^8/mL), adhesin of different concentrations and non-adhesin. Fluorescently labelled bacteria (1×10^8) were incubated with 1×10^5 epithelial cells for 2 h at 37 ℃. After incubation, cells were washed three times with PBS to remove non-adherent bacteria. MFI (wave-length of excitation: 488 nm, wave-length of emission: 575 nm) of human intestinal epithelial cells with adherent bacteria was measured in a FACS-420 flow cytometer (Coulter, U.S). A total of 10 000 cells was acquired and the data were analysed with the Cell Quest software program from Coulter.

Statistical analysis

Values were expressed as mean±SD. Statistical comparisons between the means were made with students *t* test by SPSS 10.0 version. A *P* value of <0.05 was assumed for statistical significance.
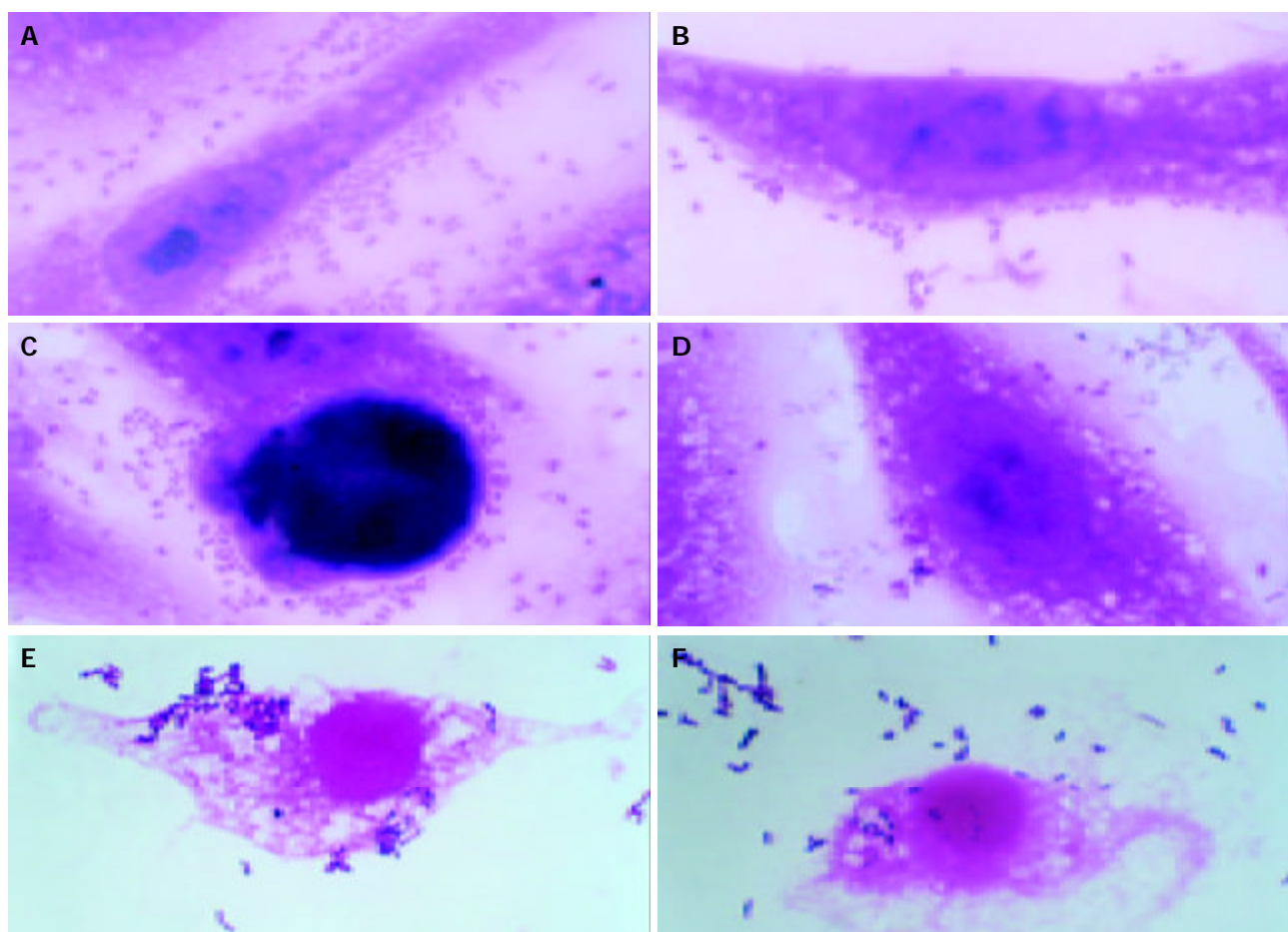

Figure 1 Gram staining of ETEC, EPEC and *Clostridium difficile* (×1000). Competitive inhibition of adherence of ETEC, EPEC and *Clostridium difficile* to intestinal epithelial cells by purified adhesin of B. ado 1027 was observed by adhesion assay. A: adherence of ETEC to intestinal epithelial cells without adhesin; B: adherence of ETEC to intestinal epithelial cells with adhesin; C: adherence of EPEC to intestinal epithelial cells without adhesin; D: adherence of ETEC to intestinal epithelial cells with adhesin; E: adherence of *C. difficile* to intestinal epithelial cells without adhesin; and F: adherence of *C. difficile* to intestinal epithelial cells with adhesin.

RESULTS

Effect of purified adhesin of B. ado 1027 on adherence of ETEC, EPEC and C. difficile to intestinal epithelial cells

The adhesion assay was performed after Lovo cell and different concentrations adhesin were incubated at 37 ℃ for 30 min. As shown in Table 1, the purified adhesin at the concentration of 10 µg/mL, 20 µg/mL and 30 µg/mL except at 1 µg/mL and 5 µg/mL could significantly inhibit the adhesion of ETEC, EPEC and clostridium difficile to intestinal epithelial cell line Lovo. Adhesion of ETEC, EPEC or *Clostridium difficile* to intestinal epithelial cell was significantly decreased when the concentration of purified adhesin was 10 µg/mL, 20 µg/mL or 30 µg/mL ($P<0.05$, $P<0.01$). Moreover, we observed that the ability of inhibition was enhanced with increase in the concentration of adhesin. These results indicated that purified adhesin of *B. ado* 1027 was involved in the adhesion of bacteria. The adhesion of ETEC and EPEC to intestinal epithelial cell was linear (Figures 1A, B, C and D). The adhesion of *C. difficile* to intestinal epithelial cell was like cluster (Figures 1E and F). The number of adherence of ETEC, EPEC and clostridium difficile to intestinal epithelial cells with adhesin was less than that of without adhesin. Inhibition of adherence of ETEC, EPEC and *Clostridium difficile* to intestinal epithelial cell by purified adhesin of B. ado 1027 was not significantly different between adhesin (30 µg/mL) and bacteria+ *B. ado* 1027 group (1×10^8/mL).

Table 1 Effect of purified adhesin of B. ado 1027 on adhesion of ETEC, EPEC and *C. difficile* to intestinal epithelial cell line Lovo

Group	Bacteria/cell		
	ETEC	EPEC	*C.difficile*
Adhesin (0 µg/mL)	108.83±16.34	110.27±13.12	110.00±16.91
Adhesin (1 µg/mL)	106.00±14.46	107.77±13.28	108.07±14.54
Adhesin (5 µg/mL)	102.97±7.65	104.20±10.82	104.23±9.62
Adhesin (10 µg/mL)	81.37±7.18[b]	81.73±9.01[b]	78.83±6.23[b]
Adhesin (20 µg/mL)	41.23±7.13[b]	42.37±7.54[b]	38.77±7.82[b]
Adhesin (30 µg/mL)	11.97±4.42[b]	11.33±4.35[b]	11.40±4.20[b]
B. ado 1027	10.87±3.22	10.07±3.32	11.73±3.66

[b]$P<0.01$ *vs* adhesin (0 µg/mL).

Table 2 Mean fluorescent intensity (MFI) of human intestinal epithelial cell with adherent ETEC, EPEC and *C. difficile*

Group	MFI		
	ETEC	EPEC	*C.difficile*
Adhesin (0 µg/mL)	5.76±0.43	5.26±0.29	5.14±0.21
Adhesin (1 µg/mL)	5.55±0.44	5.06±0.32	5.06±0.14
Adhesin (5 µg/mL)	5.10±0.24	4.83±0.28	4.84±0.15
Adhesin (10 µg/mL)	3.91±0.20[b]	3.67±0.35[b]	3.25±0.32[b]
Adhesin (20 µg/mL)	2.23±0.43[b]	2.21±0.32[b]	2.19±0.26[b]
Adhesin (30 µg/mL)	1.41±0.23[b]	1.25±0.18[b]	0.89±0.14[b]
B. ado 1027	1.25±0.23	0.98±0.13	0.79±0.19

[b]$P<0.01$ *vs* adhesin (0 µg/mL) group

Flow cytometric analysis of bacteria adherence to intestinal epithelial cell

ETEC, EPEC and a toxin-producing C. difficile strain (VPI10463) were assessed for their ability to adhere to human intestinal epithelial cell line Lovo (Table.2). There was no significant difference in MFI of ETEC, EPEC or *C. difficile* when the concentrations of adhesin were 1 µg/mL and 5 µg/mL. However, MFI was significantly decreased when the concentrations of adhesin were 10 µg/mL, 20 µg/mL and 30 µg/mL ($P<0.05$, $P<0.01$).

MFI was decreased with increase in the concentration of adhesin. There was no significant difference in MFI between adhesin (30 µg/mL) and bacteria+ *B. ado* 1027 group (1×10^8/mL).

DISCUSSION

Adherence of pathogenic to the intestinal mucus is regarded a prerequisite for prolonged transient colonization and infection of the gastrointestinal tract, and plays an important role in invasion and in yileding and secretion of virulence factor[25]. Bifidobacteria, the predominant bacteria in the human intestinal microflora, are considered to be microorganisms with a great influence on human health[26]. There have been many studies demonstrating that strains of bifidobacteria have anti-infectious properties against enteropathogenic bacteria[18,27-29]. However, there existed a few flaws when live bifidobacteria agents was used in gut barrier dysfunction: live bifidobacteria was difficult to produce and preserve, and also difficult to breed sufficiently due to lack of local gas and growth substrate. Bernet *et al.*[18] and Zheng *et al.*[30] reported the occurrence of bifidobacteria adhering to the human intestinal cells by a mechanism of adhesion which involves a proteinaceous component. Fujiwara *et al.*[31] reported that SBT2928 produced a proteinaceous factor, binding inhibitory factor (BIF), which prevented the binding of the ETEC to GA1 *in vitro*, and the binding of ETEC to the human intestinal epithelial cell line HCT-8 was reduced by BIF treatment in a dose-dependent manner. These results showed there was adhesin component in bifidobacteria.

Adherence assay which can Gram stain and microscopically examine bacteria to human intestinal epithelial has been accepted widely for quantitative and direct visual. However, light microscopic methods, while useful, are tedious and time-consuming and may be prone to observer error. Flow cytometry allows analysis of cell populations by virtue of their physical characteristics and has been used previously to assess the adherence of *Helicobacter pylori*[32]. With this approach, it is possible to distinguish differences in cell populations based on changes in fluorescent intensities for test and control populations. When compared with conventional microscopy, it is also possible to examine much larger numbers of cells in a shorter time period[33]. The present study used Gram stain and flow cytometry to demonstrate competitive inhibition of adherence of ETEC, EPEC and *C. difficile* to intestinal epithelial cell line Lovo by purified adhesin of B. ado 1027. Our study showed that the purified adhesin at the concentration of 10 µg/mL, 20 µg/mL and 30 µg/mL except at 1 µg/mL and 5 µg/mL could significantly inhibit the adhesion of ETEC, EPEC and *C. difficile* to intestinal epithelial cell line Lovo. Moreover, we observed that the ETEC, EPEC and *C. difficile* adhesion were reduced by adhesin treatment in a dose-dependent manner. Inhibition of the binding of ETEC, EPEC and *C. difficile* to intestinal epithelial cell was not significantly different between adhesin (30 µg/mL) and bacteria+ B. ado 1027 group. The results of flow cytometry analysis of bacteria adherence to intestinal epithelial cell also confirmed it. MFI was decreased with increase in the concentration of adhesin. These results indicated that purified adhesin of B. ado 1027 was involved in the adhesion of bacteria. Two basic factors, receptor and adhesin, are required for classical adhesion. One of the mechanisms by which probiotic bacteria can protect epithelial is receptor competition[34]. Our results suggest that adhesin functions by blocking the binding site of ETEC, EPEC and *C. difficile* to intestinal epithelial cell. Adhesin produced by bifidobacterial may play an important role in protecting the host. Future studies need to carry out a survey of the resistance of adhesin against the activities of digestive enzymes in the gastrointestinal tract of human. In addition, it is important to determine whether all strains or all species of bifidobacteria produce adhesin or a similar protein(s)

which prevents the binding of pathogens to receptor in intestinal epithelial surfaces.

We also observed that the adhesive behaviors of bacteria to intestinal epithelial cell line Lovo were different. The adhesion of ETEC and EPEC to intestinal epithelial cell was linear, whereas the adhesion of *C. difficile* to intestinal epithelial cell was like cluster. This suggests that different bacteria may have different distribution of receptor on cell surface.

In conclusion, the purified adhesin of *B. ado* 1027 can effectively inhibit adherence of ETEC, EPEC and C. difficile to intestinal epithelial cell *in vitro*. However, whether adhesin could prevent diseases related with ETEC, EPEC and *C. difficile*, still needs to be proved *in vivo* by human clinical studies.

REFERENCES

1   **Kelly CP**, LaMont JT. Clostridium difficile infection. *Annu Rev Med* 1998; **49**: 375-390

2   **Kagnoff MF**, Eckmann L. Epithelial cells as sensors for microbial infection. *J Clin Invest* 1997; **100**: 6-10

3   **Raupach B**, Mecsas J, Heczko U, Falkow S, Finlay BB. Bacterial epithelial cell cross talk. *Curr Top Microbiol Immunol* 1999; **236**: 137-161

4   **Eckmann L**, Kagnoff MF, Fierer J. Intestinal epithelial cells as watchdogs for the natural immune system. *Trends Microbiol* 1995; **3**: 118-120

5   **Finegold SM,** Sutter VL, Sugihara PT, Elder HA, Lehman SM, Phillips RL. Fecal microbial flora in Seventh Day Adventist populations and control subjects. *Am J Clin Nutr* 1977; **30**: 1781-1792

6   **Bezkorovainy A**. Probiotics: determinants of survival and growth in the gut. *Am J Clin Nutr* 2001; **73**(2 Suppl): 399S-405S

7   **Isolauri E**. Probiotics in human disease. *Am J Clin Nutr* 2001; **73**: 1142S-1146S

8   **Alander M**, Satokari R, Korpela R, Saxelin M, vilpponen-Salmela T, Mattila-Sandholm T, von Wright A. Persistence of colonization of human colonic mucus by a probiotic strain, Lactobacillus rhamnosus GG after oral consumption. *Appl Environ Microbiol* 1999; **65**: 351-354

9   **Coconnier MH**, Bernet MF, Chauviere G, Servin AL. Adhering heat-killed human Lactobacillus acidophilus strain LB, inhibits the process of pathogenically of diarrhoeagenic bacteria in culture human intestinal cells. *J Diarrhoeal Dis Res* 1993; **11**: 235-242

10   **Coconnier MH**, Bernet MF, Kernis S, Chauviere G, Fourniat J, Servin AL. Inhibition of adhesion of enteroinvasive pathogens to human intestinal Caco-2 cells by Lactobacillus acidophilus strain LB decrease bacterial invasion. *FEMS Microbiol Lett* 1993; **110**: 299-305

11   **Schiffrin EJ**, Brassart D, Servin AL, Rochat F, Donnet-Hughes A. Immune modulation of blood leukocytes in human by lactic acid bacteria: criteria for strain selection. *Am J Clin Nutr* 1997; **66**: 515S-520S

12   **Del Re B**, Sgorbati B, Miglioli M, Palenzona D. Adhesion, autoaggregation and hydrophobicity of 13 strains of Bifidobacterium longum. *Lett Appl Microbiol* 2000; **31**: 438-442

13   **Kirjavainen PV**, Ouwehand AC, Isolauri E, Salminen SJ. The ability of probiotic bacteria to bind to human intestinal mucus. *FEMS Microbiol Lett* 1998; **167**: 185-189

14   **He F**, Ouwehand AC, Isolauri E, Hashimoto H, Benno Y, Salminen S. Comparison of mucosal adhesion of Bifidobacteria isolated from healthy and allergic infants. *FEMS Immunol Med Microbiol* 2001; **30**: 43-47

15   **Matsumoto M,** Tani H, Ono H, Ohishi H, Benno Y. Adhesive property of bifidobacterium lactis LKM512 and predominant bacteria of intestinal microflora to human intestinal mucin.

Curr Microbiol 2002; **44**: 212-215

16   **Lee YJ,** Yu WK, Heo TR. Identification and screening for antimicrobial activity against Clostridium difficile of Bifidobacterium and Lactobacillus species isolated from healthy infant faeces. *Int J Antimicrob Agents* 2003; **21**: 340-346

17   **Setoyama H,** Imaoka A, Ishikawa H, Umesaki Y. Prevention of gut inflammation by Bifidobacterium in dextran sulfate-treated gnotobiotic mice associated with Bacteroides strains isolated from ulcerative colitis patients. *Microbes Infect* 2003; **5**: 115-122

18   **Bernet MF**, Brassart D, Neeser JR, Servin AL. Adhesion of human bifidobacterial strains to cultured human intestinal epithelial cells and inhibition of enteropathogen-cell interactions. *Appl Environ Microbiol* 1993; **59**: 4121-4128

19   **Fujiwara S**, Hashiba H, Hirota T, Forstner JF. Proteinaceous factor(s) in culture supernatant fluids of bifidobacteria which prevents the binding of enterotoxigenic Escherichia coli to gangliotetraosylceramide. *Appl Environ Microbiol* 1997; **63**: 506-512

20   **Fujiwara S**, Hashiba H, Hirota T, Forstner JF. Purification and characterization of a novel protein produced by Bifidobacterium longum SBT2928 that inhibits the binding of enterotoxigenic Escherichia coli Pb176 (CFA/II) to gangliotetraosylceramide. *J Appl Microbiol* 1999; **86**: 615-621

21   **Zheng YJ**, Pan LJ, Wang LS, Zhou DY, Guo LA, Yan Z. Purified of bifidobacterium adhesin. *Chin J Microbiol Immunol* 1999; **19**: 196

22   **Zheng YJ**, Pan LJ, Ye GA, Zhou DY. Competitive inhibition of adherence of EPEC and ETEC to intestinal epithelial by human Bifidobacterial strains. *Chin J Microbiol* 1999; **11**: 329-331

23   **Tuomola EM**, Ouwehand AC, Salminen SJ. The effect of probiotic bacteria on the adhesion of pathogens to human intestinal mucus. *FEMS Immunol Med Microbiol* 1999; **26**: 137-142

24   **Coconnier MH**, Klaenhammer TR, Kerneis S, Bernet MF, Servin AL. Protein-mediated adhesion of Lactobacillus acidophilus BG2FO4 on human enterocyte and mucus-secreting cell lines in culture. *Appl Environ Microbiol* 1992; **58**: 2034-2039

25   **Cotter PA**, Miller JF. Triggering bacterial virulence. *Science* 1996; **273**: 1183-1184

26   **Rycroft CE**, Fooks LJ, Gibson GR. Methods for assessing the potential of prebiotics and probiotics. *Curr Opin Clin Nutr Metab Care* 1999; **2**: 481-484

27   **Shu Q**, Gill HS. A dietary probiotic (Bifidobacterium lactis HNO19) reduces the severity of Escherichia coli O157: H7 infection in mice. *Med Microbiol Immunol* 2001; **189**: 147-152

28   **Madsen KL**. The use of probiotics in gastrointestinal disease. *Can J Gastroenterol* 2001; **15**: 817-822

29   **Bai AP,** Ouyang Q, Zhang W, Wang CH, Li SF. Probiotics inhibit TNF-α -induced interleukin-8 secretion of HT29 cells. *World J Gastroenterol* 2004; **10**: 455-457

30   **Zheng YJ**, Pan LJ, Ye GA, Zhou DY. Study on the adherence of human Bifidobacteria to cultured human intestinal epithelial cells. *Chin J Microbiol Immunol* 1997; **17**: 85-87

31   **Fujiwara S**, Hashiba H, Hirota T, Forstner JF. Inhibition of the binding of enterotoxigenic Escherichia coli Pb176 to human intestinal epithelial cell line HCT-8 by an extracellular protein fraction containing BIF of Bifidobacterium longum SBT2928: suggestive evidence of blocking of the binding receptor gangliotetraosylceramide on the cell surface. *Int J Food Microbiol* 2001; **67**: 97-106

32   **Clyne M**, Drumm B. Adherence of *Helicobacter pylori* to the gastric mucosa. *Can J Gastroenterol* 1997; **11**: 243-248

33   **Drudy D**, O' Donoghue DP, Baird A, Fenelon L, O' Farrelly C. Flow cytometric analysis of Clostridium difficile adherence to human intestinal epithelial cells. *J Med Microbiol* 2001; **50**: 526-534

34   **Madsen K**, Cornish A, Soper P, Mckaigney C, Jijon H, Yachimec C, Doyle J, Jewell L, De Simone C. Probiotic bacteria enhance murine and human intestinal epithelial barrier function. *Gastroenterology* 2001; **121**: 580-591

• BASIC RESEARCH •

Blockage of transforming growth factor b receptors prevents progression of pig serum-induced rat liver fibrosis

Wei Jiang, Chang-Qing Yang, Wen-Bin Liu, Yi-Qing Wang, Bo-Ming He, Ji-Yao Wang

Wei Jiang, Chang-Qing Yang, Wen-Bin Liu, Yi-Qing Wang, Bo-Ming He, Ji-Yao Wang, Department of Gastroenterology, Zhongshan Hospital, Fudan University, Shanghai 200032, China
Correspondence to: Professor Ji-Yao Wang, Department of Gastroenterology, Zhongshan Hospital, Fudan University, Shanghai 200032, China. jiyao_wang@ hotmail.com
Telephone: +86-21-64041990 Ext 2420   **Fax:** +86-21-34160980
Received: 2003-08-26   **Accepted:** 2003-10-29

Abstract

AIM: To test the hypothesis that introduction of antisense TβR I and TβR II eukaryotic expressing plasmids into a rat model of immunologically induced liver fibrosis might block the action of TGF-β_1 and halt the progression of liver fibrosis.

METHODS: RT-Nest-PCR and gene recombination techniques were used to construct rat antisense TβR I and TβR II recombinant plasmids which could be expressed in eukaryotic cells. The recombinant plasmids and empty vector (pcDNA3) were encapsulated by glycosyl-poly-L-lysine and then transducted into rats of pig serum-induced liver fibrosis model. Expression of exogenously transfected gene was assessed by Northern blot, and hepatic expressions of TβR I and TβR II were evaluated by RT-PCR and Western blot.We also performed ELISA for serum TGF-β_1, hydroxyproline of hepatic tissues, immunohistochemistry for collagen types I and III, and VG staining for pathological study of the liver tissues.

RESULTS: The exogenous antisense TβR I and TβR II plasmids could be well expressed *in vivo*, and block mRNA and protein expression of TβR I and TβR II in the fibrotic liver at the level of mRNA respectively. These exogenous plasmid expressions reduced the level of TGF-β_1 (antisense TβR I group 23.998±3.045 ng/mL, antisense TβR II group 23.156±3.131 ng/mL, disease control group 32.960±3.789 ng/mL; F=38.19, 36.73, P<0.01). Compared with disease control group, the contents of hepatic hydroxyproline (antisense TβR I group 0.169±0.015 mg/g liver, antisense TβR II group 0.167±0.009 mg/g liver, disease control group 0.296±0.026 mg/g liver; F=14.39, 15.48, P<0.01) and the deposition of collagen types I and III decreased in the two antisense treatment groups (antisense TβR I group, collagen type I 669.90±50.67, collagen type III 657.29±49.48; antisense TβR II group, collagen type I 650.26±51.51, collagen type III 661.58±55.28; disease control group, collagen type I 1209.44±116.60, collagen type III 1175.14±121.44; F=15.48 to 74.89, P<0.01). Their expression also improved the pathologic classification of liver fibrosis models (compared with disease control group, χ^2=17.14, 17.24, P<0.01). No difference was found in the level of TGF-β_1, the contents of hepatic hydroxyproline and collagen types I and III and pathologic grade between pcDNA3 control group and disease control group or between the two antisense treatment groups (F =0.11 to 1.06, χ^2=0.13 to 0.16, P>0.05).

CONCLUSION: Antisense TβR I and TβR II recombinant plasmids have certain reverse effects on liver fibrosis and can be used as possible candidates for gene therapy.

INTRODUCTION

Liver fibrosis is a common sequel to diverse liver injuries. In the formation of liver fibrosis and cirrhosis, synthesis of collagen increases and its degradation decreases. It has been thought that liver fibrosis can be reversed and liver cirrhosis is irreversible[1-5]. Profound studies have been conducted on the treatment of liver fibrosis. However, this disease is still lack of efficient therapy[6-11]. Searching for a new therapy seems very important.

In the formation of liver fibrosis and cirrhosis, many cytokines produce marked effects through autocrine and paracrine[1,2,5]. Molecular mechanisms involved in fibrogenesis reveal that transforming growth factorβ (TGF-β), especially TGF-β_1, plays a pivotal role[12-16]. Signaling by TGF-β occurs through a family of transmembranes and ser/thr kinase receptors. Both components of the receptor complex, known as receptor I (TβR I) and receptor II (TβR II) are essential for signal transduction[17,18]. So in theory, blockage of TGF-β signal transduction by inhibiting the expression of TβR I and/or TβR II may have therapeutic effects on liver fibrosis.

At present, gene therapy for liver fibrosis targeting TGF-β mainly includes inhibiting the expression of TGF-β_1 (for instance, antisense TGF-β_1 RNA) and using deficient TβR II[19-21]. But therapeutic researches which target TβR I or use antisense TβR II as a therapeutic tool have not been reported. In the present experiments, we constructed antisense TβR I and TβR II eukaryotic expressing plasmids and performed *in vivo* transfection. We aimed to test the hypothesis that introduction of these two exogenous plasmids into a rat model of immunologically induced liver fibrosis might block the action of TGF-β_1 and halt the progression of liver fibrosis.

MATERIALS AND METHODS

Construction of recombinant plasmid

Nested primers were designed and synthesized according to rat TβR I and TβR II cDNA sequences (GenBank)[22,23]. The length of amplified PCR products was anticipated to be 470 bp, 606 bp (Table 1). Total RNA was extracted from normal rat liver with Trizol reagent (GIBCO, USA) according to the manufacturer's directions. RT-Nest-PCR was used to construct TβR I and TβR II cDNA fragments. Samples were heated at 94 ℃ for 7 min and subjected to 32 PCR cycles of denaturation at 94 ℃ for 1 min, annealing at 55 ℃ for 1 min, extension at 72 ℃ for 1 min, followed by a final extension at 72 ℃ for 5 min. After separation, reclaim and purification, the PCR products of TβR I and TβR II were

connected with T vector (Promega, USA) and then transferred into JM-109 strain. PT/ TβR I and PT/ TβR II were successfully constructed after IPTG/X-gal screening. The target fragments were cut and inserted reversely into eukaryotic expressing plasmid pcDNA3 (Invitrogen, CA), and then transferred into JM-109 strain again. By using enzyme-cutting identification (TβR I: *Eco*RI and *Xho*I; TβR II: *Eco*RI and *Bam*HI) and DNA autosequencing (PE377 Auto sequencer, USA), the successful constructions of antisense TβR I and TβR II eukaryotic expressing plasmids were proved (Figure 1).

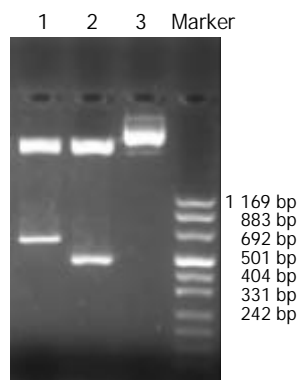**Figure 1** Enzyme-cutting identification of the recombinant plasmids, Lane 1: pANTI-RII, Lane 2: pANTI-RI, Lane 3: pcDNA3.

Table 1 Primer pairs for PCR reactions

RI 1: 5' ACAGGCGCAAACAGTGGCAG 3' (18-33)

RI 2: 5' AGTCTCGTAGCACAATGGTCC 3' (643-661)

RI 3: 5' TTCAC<u>CTCGAG</u>AGTGGCAGCGGGACC 3' (25-39)
     Xho I

RI 4: 5' CTACC<u>GAATTC</u>TGGACCATCAGCATAAG 3' (456-470)
     *Eco*R I

RII 1: 5' TTCATAGGCTCGGTTCGCGG 3' (199-213)

RII 2: 5' GCAGTTGTCGCTGAAATCCA 3' (882-901)

RII 3: 5' AACAT<u>GAATTC</u>GGTCTATGACGAGCG 3' (227-241)
     *Eco*R I

RII 4: 5' ACAAT<u>GGATCC</u>GAAGATGGCAATGACAG 3' (795-811)
     *Bam*H I

Experimental protocols

Forty-six male Sprague-Dawley rats (weighing 100 to 120 g) provided by Experimental Animal Center, Zhongshan Hospital, Fudan University, were randomly divided into the following 5 groups: 10 in experimental liver fibrosis model induced by pig-serum as disease control group (M), 10 in antisense TβR I plasmid transfection as treatment group (A), 10 in antisense TβR II plasmid transfection as treatment group (B), 10 in pcDNA3 transfection as pcDNA3 control group (C) and 6 in normal control group (N). Animals in the normal control group received 0.5 mL of NS twice weekly by intraperitoneal injection for 8 wk. Rats in the other 4 groups received 0.5 mL of pig-serum twice weekly by intraperitoneal injection for 8 wk[24]. Among groups A, B and C, the recombinant antisense TβR I and TβR II plasmids and empty vector (pcDNA3) of 100 µg each time were encapsulated by glycosyl-poly-L-lysine (G-PLL) and then transducted into rats of liver fibrosis model via caudal vein every 2 wk respectively. The molecular ratio of galactose and poly-L-lysine was 15:28 and the average molecular weight of G-PLL was 8.5 ku. All experimental rats were sacrificed at the end of the 8th wk. The middle lobes of the livers were removed and specimens were fixed in Carnoy's fixative (glacial acetic acid, chloroform, and ethanol at a volume ratio of 1:3:6) and

then embedded in paraffin for histological analysis. The remaining tissue was quickly partitioned and immediately stored in liquid nitrogen and then frozen below -70 ℃. After that the rats were humanely killed.

RNA isolation and Northern blot analysis for exogenous gene and hepatic T*b*R I and T*b*R II expression

For Northern blot analysis, 30 µg of total tissue RNAs was separated by electrophoresis on a 1% denaturing agarose gel, transferred to a Hybond-N membrane (Amersham, UK) and fixed by baking for 2 h at 80 ℃. The probe for pcDNA3 according to its special T7 promoter sequence (the oligonucleotide fragment: 5'-CAGAGGGATATCACTCAGCATAAT-3'), which was to detect exogenous gene expression, was labeled with [α-^{32}P]dATP using DNA tailing kit (Roche, Germany). TβR I and TβR II cDNA probes were labeled with [α-^{32}P]dCTP using a high prime DNA labeling kit (Roche, Germany) to detect rat TβR I and TβR II expression. Blots were pre- hybridized for at least 3 h at 42 ℃, and then hybridized for 20 h at 42 ℃. Auto radiographs were exposed for indicated times to Kodak films at -70 ℃ for 7 d. As an internal standard (loading control) the blots were re-hybridized with [α-^{32}P] β-actin.

RT-PCR analysis for T*b*R I and T*b*R II mRNA expression

Total RNA of 1 µg from each sample was reversely transcribed and amplified using an RT-PCR kit (ShengNeng-BoCai Biotechnology Co. Shanghai, China). The RT-PCR reaction contained 12.5 pmol each primer (TβR I: sense sequence 5' -TCACTAGATCGCCCTTTCAT-3' ; antisense sequence 5' -GATAATCCGACACCAACCAC-3' , a product of 355 bp; TβR II: sense sequence 5' -CCACGACCCCAAGTTCACCT-3' , antisense sequence 5' -TGGGCAGCAGTTCCGTATTG-3' , a product of 428 bp) for detecting the TβR I and TβR II mRNA expression in rat liver tissues. Additionally primer pairs (sense sequence 5' - TGGGACGATATGGAGAAGAT -3' ; antisense sequence 5' - ATTGCCGATAGTGATGACCT -3') were used for amplifying the expression of β-actin (a product of 521 bp) as internal control. Samples were placed in a thermocycler with the incubation program at 37 ℃ for 60 min, at 90 ℃ for 5 min, then 30 cycles at 94 ℃ for 45 s, at 54 ℃ for 45 s, and at 72 ℃ for 1 min, and a final extension at 72 ℃ for 5 min. Products of RT-PCR were electrophoresed on a 20 g/L agarose gel to show the amplified bands. The areas under curve of the bands were calculated by Photo-Treater (Tanon GIS-1000, China). The ratio of the objective band and β-actin (control) represented the relative value of expression of the objective band.

Western blot for hepatic T*b*R I and T*b*R II expression

Lysates from 50 mg rat liver tissues were prepared with RIPA buffer [1×PBS, 10 g/L NP40, 5 g/L sodium deoxycholate, 1 g/L SDS, 10 mmol/L PMSF (in isopropanol), 36 µg/mL aprotinin and 1mmol/L sodium orthovanadate]. Tissue lysates were centrifuged at 3000 r/min for 10 min at 4 ℃, and protein concentrations were determined by BCA protein assay (Pierce, IL). Protein samples (100 µg) were heated for 5 min at 100 ℃ and separated on 120 g/L SDS-PAGE and then transferred to PVDF membranes (Schleicher&Schuell, Germany) in Tris-glycine buffer (pH 8.5) plus 200 mL/L methanol. The membranes were blocked overnight in 50 mL/L non-fat dried milk in Tris-buffer containing 1 g/L Tween-20 and then washed with Tris-buffer. The blots were incubated overnight at 4 ℃ with rabbit TβR I, TβR II and β-actin polyclonal IgG (Santa Cruz, USA) diluted 1:200 in Tris-buffer. The blots were washed and then incubated with AP-conjugated secondary antibodies (Santa Cruz, USA) at 1:500 dilution for 2 h at room temperature. The protein bands were visualized with BCIP/NBT (DAKO, USA) system.

ELISA assay of serum TGF-b₁

Assay of serum TGF-β_1 content was performed with double antibody ABC-ELISA method according to the previous reports of Ueno et al.[21] and Roth et al.[25].

Hepatic hydroxyproline (OH-Pro) content

Hydroxyproline content was determined by the previous method with some modification[26]. A total of 500 mg of liver tissues was hydrolyzed in 6 mol/L HCl solution at 120 ℃ for 24 h. The hydroxyproline content of the liver was expressed as micrograms per gram of wet weight.

Immunohistochemistry of hepatic collagen types I and II

After dewaxed with xylene and rehydrated through a graded alcohol series, sections were digested with 4 g/L trypsin. The sections were incubated with rabbit polyclonal antibodies against types I or II collagen (diluted 1:100) at 37 ℃ for 60 min and then overnight at 4 ℃. Then the sections were incubated with Envision™ secondary antibodies of biotinylated sheep anti-rabbit IgG (DAKO, USA) at 37 ℃ for 30 min and then with the substrate solution (3,3-diaminobenzidine tetrahydrochloride in H_2O_2 in Tris buffer pH 7.4) for 10 min, followed by counterstaining with hematoxylin. The sections were washed 3 times with 0.01 mol/L PBS (pH7.4) after each step. For control staining, PBS was used instead of the primary antibody. The slides were then analyzed with an image analyzing system (LeiCA-Q500IW System, Germany) to obtain the integral light density and the average area of positive staining. The multiplication of both parameters represented the relative contents of hepatic collagen types I and II.

Histology

Sections from paraffin-embedded blocks were dewaxed and stained with Van Gieson method. Fibrosis was scored according to the classification which graded liver fibrosis into seven degrees (0-VI).

Statistical analysis

All values were expressed as mean±SD. Differences between groups were analyzed by one-way ANOVA (SPSS10.0 software) and the pathological grading of fibrosis of each group was analyzed by trend analysis and chi-square test (EPI5.0 software). $P<0.05$ was considered statistically significant.

RESULTS

General situation of animals

No animal died during the experimental period. No significant difference was found in the levels of ALT (51±9 U/L vs 53±8 U/L) and Cr (91±13 μmol/L vs 92±14 μmol/L) between pcDNA3 control group and disease control group ($P>0.05$). No significant difference was found in the height or weight of rats among antisense TβR I, antisense TβR II and pcDNA3 control groups ($P>0.05$).

Expression of exogenous gene and TbR I, TbR II gene in liver tissues by Northern blot

The exogenous gene expression could be detected in transfection groups (antisense TβR I, antisense TβR II and pcDNA3 control groups) by Northern blot, but not in disease control group (Figure 1). The expression of TβR I mRNA was much higher in pcDNA3 control group and disease control group than in antisense TβR I group. The expression of TβR II was also much higher in pcDNA3 control group and disease control group than in antisense TβR II group at mRNA level (Figure 2).

Hepatic TbR I and TbR II mRNA expression by RT-PCR

The expression of antisense TβR I RNA induced a decreased mRNA level of TβR I in antisense TβR I group (1.039±0.110)

compared with pcDNA3 control group (1.453±0.112) and disease control group (1.472±0.099) ($P<0.01$). The expression of antisense TβR II RNA also induced a decreased mRNA level of TβR II in antisense TβR II group (0.805±0.105) compared with pcDNA3 control group (1.743±0.151) and disease control group (1.798±0.139) ($P<0.01$). No difference was found in the level of TβR I and TβR II mRNA between pcDNA3 control and disease control groups ($P>0.05$).
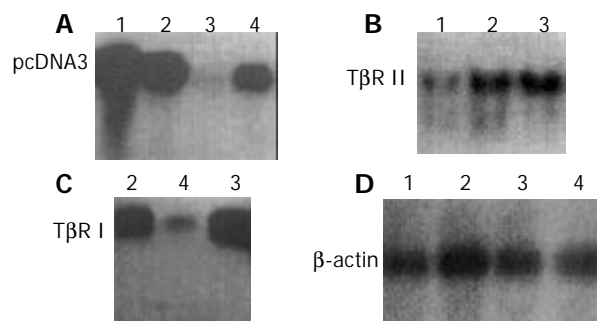

Figure 2 Expression of exogenous transfected gene assessed by Northern blot, A: Hybridization using ³²P labeled oligo-nucleotide probe which targets T7 promoter; B: Hybridization by using ³²P labeled TβR II cDNA probe; C: Hybridization by using ³²P labeled TβR I cDNA probe; D: β-actin probe used as control. Lane 1: Antisense TβR II group; Lane 2: pcDNA3 control group; Lane 3: Disease control group; Lane 4: Antisense TβR I group.
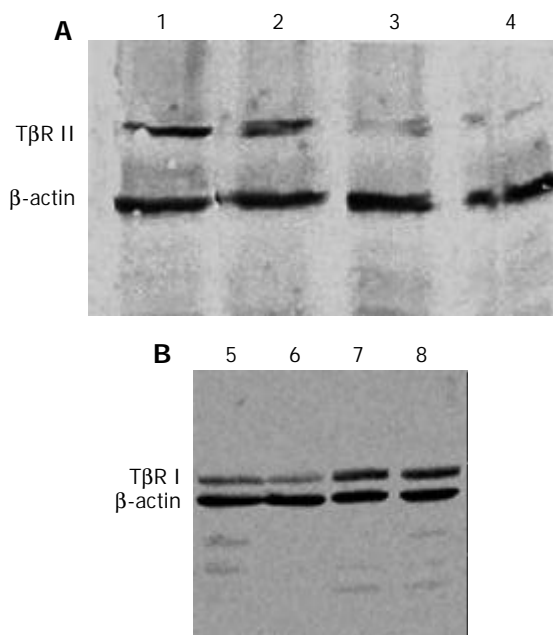

Figure 3 Hepatic protein expression of TβR I, TβR II assessed by Western blot, A: Hepatic protein expression of TβR II; B: Hepatic protein expression of TβR I; Lanes 1,8: Disease control group; Lanes 2,7: pcDNA3 control group; Lane 3: Antisense TβR II group; Lanes 4,6: Normal control group; Lane 5: Antisense TβR I group.

Hepatic TbR I and TbR II protein expression by Western blot

The expression of TβR I protein was decreased in antisense TβR I group and the expression of TβR II protein was also decreased in antisense TβR II group when compared with pcDNA3 control group and disease control group, but they were still slightly higher than those in normal control group. The expressions of TβR I and TβR II protein in pcDNA3 control group were similar to those in disease control group (Figure 3).

Table 2 Effects of transfected plasmid on the content of hepatic hydroxyproline and deposition of collagen types I and III (mean±SD)

Group	Number	Hydroxyproline (mg/g liver)	Collagen I	Collagen III
Disease control group	10	0.296±0.026[d]	1 209.44±116.60[d]	1 175.14±121.44[d]
Antisense TβR II group	10	0.167±0.009[bd]	650.26±51.51[bd]	661.58±55.28[bd]
Antisense TβR I group	10	0.169±0.015[d]	669.90±50.67[d]	657.29±49.48[d]
pcDNA3 control group	10	0.284±0.025[d]	1 205.70±110.11[d]	1 149.89±91.61[d]
Normal control group	6	0.128±0.004	449.33±35.95	421.15±20.15

[b]*P*<0.01 *vs* disease control group and pcDNA3 control group, [d]*P*<0.01 *vs* normal control group.

Table 3 Pathological grade of liver fibrosis at the 8th week

Group	Grade							Total
	0	I	II	III	IV	V	VI	
Disease control group[d]	0	0	0	1	4	4	1	10
Antisense TβR II group[db]	1	7	2	0	0	0	0	10
Antisense TβR I group[db]	1	6	3	0	0	0	0	10
pcDNA3 control group[d]	0	0	0	1	5	3	1	10
Normal control group	6	0	0	0	0	0	0	6

[b]*P*<0.01 *vs* disease control group and pcDNA3 control group, [d]*P*<0.01 *vs* normal control group.

ELISA assay of serum TGF-*b*₁

The level of serum TGF-β_1 was reduced in antisense TβR I group (23.998±3.045 ng/mL) and antisense TβR II group (23.156±3.131 ng/mL) compared with pcDNA3 control group (32.275±1.884 ng/mL) and disease control group (32.960±3.789 ng/mL), but was still higher than that in normal control group (14.338±2.421 ng/mL) (*P*<0.01). No significant difference was found between antisense TβR I and antisense TβR II groups (*P*>0.05).

Effects of antisense T*b*R I and T*b*R II plasmid transfection on hepatic hydroxyproline and collagen types I and II content

The hepatic hydroxyproline content and the accumulation of hepatic collagen types I and III in antisense TβR I and antisense TβR II groups were significantly decreased compared with disease control and pcDNA3 control groups (*P*<0.01). No statistical difference was found between pcDNA3 control and disease control groups or between antisense TβR I and antisense TβR II groups (*P*>0.05). Hepatic hydroxyproline content and accumulation of collagen in these four groups were significantly higher than those in normal control group (*P*<0.01) (Table 2).

Effects of transfected plasmid on patho-histology

The fibrosis grade of antisense TβR I and antisense TβR II groups alleviated significantly compared with disease control and pcDNA3 control groups (*P*<0.01). All these four groups had significantly higher fibrosis grades when compared to normal control group (*P*<0.01). No significant difference was found between disease control and pcDNA3 control groups or between antisense TβR I and antisense TβR II groups (*P*>0.05) (Table 3).

DISCUSSION

Pig serum-induced rat hepatic fibrosis is a model that shows an intense immune response to the administration of heterologous serum. Histologically, the changes were characterized by mononuclear cell infiltration and fibrotic response in the periportal area, followed by the septum formation connecting portal tract with central veins without hepatocyte injury[24].

In the formation of liver fibrosis and cirrhosis, a number of cytokines could produce marked effects through autocrine and paracrine[25,26]. Molecular mechanisms involved in fibrogenesis revealed that transforming growth factorβ (TGF-β), especially TGF-β_1, played a pivotal role in the regulation of the production, degradation and accumulation of extracellular matrix (ECM)[1,21,27]. Secreted as a latent precursor, TGF-β is activated at sites of injury. Active TGF-β binds to specific, high-affinity receptors present on most cells, initiating a signaling cascade that results in biological effects. Signaling by TGF-β occurs through a family of transmembranes and ser/thr kinase receptors. Both components of the receptor complex, known as receptor I (TβR I) and receptor II (TβR II) are essential for signal transduction. Signaling is initiated by binding of TGF-β to the TβR II. Once bound, the TGF-β/ TβR II complex then recruits TβR I into a heteromeric complex. Within the heteromeric complex, the kinase domain of type II receptor could transphosphorylate and activate type I receptor kinase, which then functioned to propagate the signal to downstream targets[21-23]. At present, gene therapy for liver fibrosis targeting TGF-β receptor mainly used adenoviral vectors expressing a dominant-negative type II TGF-β receptor or an adenovirus expressing an entire ectodomain of human TGF-β type II receptor fused to Fc portion of human IgG to block the TGF-β signal transduction[19,21].

Antisense technique has been used to inhibit the target genes and proteins expressed in experimental rat hepatic fibrosis[7]. We used RT-Nest-PCR and gene recombination techniques to construct rat antisense TβR I and TβR II recombinant plasmids successfully which could be expressed in eucaryotic cells. We transducted the exogenous plasmid into the fibrotic liver based on our previous research on gene target therapy. The exogenous antisense TβR I and TβR II recombinant plasmids were well expressed *in vivo*, and could block the mRNA and protein expression of TβR I and TβR II in the fibrotic liver induced by pig serum.

In our study, serum TGF-β_1 analysis showed the expression of TGF-β_1 was decreased after the expression of TβR I and TβR II was blocked. Our results were similar to the previous report that used deficient TβR II in treating experimental liver fibrosis. It was indicated that the production of active TGF-β_1 was inhibited after the expression of TGF-β receptors was blocked and the signal transduction of TGF-β was also inhibited.

Collagen types I and III constitute the main components of increased ECM in liver fibrosis. It has been proposed that degradation of collagen types I and III is very important in the

reversion of liver fibrosis[5,28,29]. In our study, the recombinant plasmid could be delivered to liver by G-PLL and expressed in the tissue of liver. In addition, there was a significant decrease of collagen deposition after the recombinant antisense TβR I and TβR II plasmids was transduced into fibrotic liver through mensuring the hepatic hydroxyproline content and immunohistochemistry of collagen types I and III. This suggested that the recombinant plasmids could increase the degrading capacity of collagen types I and III, decrease the deposition of ECM, and probably reverse hepatic fibrosis. In the data analysis, there was a significant difference in fibrosis grades between the disease control group and the recombinant plasmid transfected group. It showed that the antisense TβR I and TβR II plasmids had significant ameliorative effects on liver fibrosis.

No difference was found in the level of TGF-β_1, the contents of hepatic hydroxyproline and collagen types I and III and the pathologic grade between empty plasmid control and disease control groups or between the two antisense treatment groups. It indicated that the signal transduction of TGF-β could be inhibited by blocking the expression of either TβR I or TβR II and the effects of antisense TβR I and antisense TβR II plasmids on experimental liver fibrosis were similar. Both TβR I and TβR II were essential for signal transduction.

In summary, our results demonstrate that TGF-β_1 plays an important role in liver fibrosis development especially in degradation of collagens. Antisense TβR I and antisense TβR II recombinant plasmids have certain reverse effects on liver fibrosis and could be used as possible candidates for gene therapy. As a new therapeutic means, gene therapy has a long way to go, especially in transductive efficiency, gene targeting, stability and adverse effects.

REFERENCES

1 **Alcolado R**, Arthur MJ, Iredale JP. Pathogenesis of liver fibrosis. *Clin Sci* 1997; **92**: 103-112

2 **Olaso E**, Friedman SL. Molecular regulation of hepatic fibrogenesis. *J Hepatol* 1998; **29**: 836-847

3 **Huang ZG**, Zhai WR, Zhang YE, Zhang XR. Study of heteroserum-induced rat liver fibrosis model and its mechanism. *World J Gastroenterol* 1998; **4**: 206-209

4 **Benyon RC**, Iredale JP. Is liver fibrosis reversible? *Gut* 2000; **46**: 443-446

5 **Neubauer K**, Saile B, Ramadori G. Liver fibrosis and altered matrix synthesis. *Can J Gastroenterol* 2001; **15**: 187-193

6 **Lieber CS**. Prevention and treatment of liver fibrosis based on pathogenesis. *Alcohol Clin Exp Res* 1999; **23**: 944-949

7 **Rockey DC**. Gene therapy for hepatic fibrosis-bringing treatment into the new millennium. *Hepatology* 1999; **30**: 816-818

8 **Cheng ML**, Wu YY, Huang KF, Luo TY, Ding YS, Lu YY, Liu RC, Wu J. Clinical study on the treatment of liver fibrosis due to hepatitis B by IFN-alpha1 and traditional medicine preparation. *World J Gastroenterol* 1999; **5**: 267-269

9 **Wang LT**, Zhang B, Chen JJ. Effect of anti-fibrosis compound on collagen expression of hepatic cells in experimental liver fibrosis of rats. *World J Gastroenterol* 2000; **6**: 877-880

10 **Du B**, You S. Present situation in preventing and treating liver fibrosis with TCM drugs. *J Tradit Chin Med* 2001; **21**: 147-152

11 **Murphy F**, Arthur M, Iredale J. Developing strategies for liver fibrosis treatment. *Expert Opin Investig Drugs* 2002; **11**: 1575-1585

12 **Bachem MG**, Meyer D, Melchior R, Sell KM, Gressner AM. Activation of rat liver perisinusoidal lipocytes by transforming growth factors derived from myofibroblastlike cells. A potential mechanism of self perpetuation in liver fibrogenesis. *J Clin Invest* 1992; **89**: 19-27

13 **Okuno M**, Moriwaki H, Imai S, Muto Y, Kawada N, Suzuki Y, Kojima S. Retinoids exacerbate rat liver fibrosis by inducing the activation of latent TGF-beta in liver stellate cells. *Hepatology* 1997; **26**: 913-921

14 **Pinzani M**, Marra F, Carloni V. Signal transduction in hepatic stellate cells. *Liver* 1998; **18**: 2-13

15 **Friedman SL**. Molecular regulation of hepatic fibrosis, an integrated cellular response to tissue injury. *J Biol Chem* 2000; **275**: 2247-2250

16 **Bissell DM**, Roulot D, George J. Transforming growth factor β and the liver. *Hepatology* 2001; **34**: 859-867

17 **Wrana JL**, Attisano L, Wieser R, Ventura F, Massague J. Mechanism of activation of the TGF-beta receptor. *Nature* 1994; **370**: 341-347

18 **Willis SA**, Zimmerman CM, Li LI, Mathews LS. Formation and activation by phosphorylation of activin receptor complexes. *Mol Endocrinol* 1996; **10**: 367-379

19 **Qi Z**, Atsuchi N, Ooshima A, Takeshita A, Ueno H. Blockade of type beta transforming growth factor signaling prevents liver fibrosis and dysfunction in the rat. *Proc Natl Acad Sci U S A* 1999; **96**: 2345-2349

20 **Lin JS**, Song YH, Kong XJ, Li B, Liu NZ, Wu XL, Jin YX. Preparation and identification of anti-transforming growth factor beta1 U1 smallnuclear RNA chimeric ribozyme *in vitro*. *World J Gastroenterol* 2003; **9**: 572-577

21 **Ueno H**, Sakamoto T, Nakamura T, Qi Z, Astuchi N, Takeshita A, Shimizu K, Ohashi H. A soluble transforming growth factor beta receptor expressed in muscle prevents liver fibrogenesis and dysfunction in rats. *Hum Gene Ther* 2000; **11**: 33-42

22 **Choi ME**, Kim EG, Huang Q, Ballermann BJ. Rat mesangial cell hypertrophy in response to transforming growth factor-beta 1. *Kidney Int* 1993; **44**: 948-958

23 **Bassing CH**, Yingling JM, Howe DJ, Wang T, He WW, Gustafson ML, Shah P, Donahoe PK, Wang XF. A transforming growth factor beta type I receptor that signals to activate gene expression. *Science* 1994; **263**: 87-89

24 **Tsukamoto H**, Matsuoka M, French SW. Experimental models of hepatic fibrosis: a review. *Semin Liver Dis* 1990; **10**: 56-65

25 **Roth S**, Schurek J, Gressner AM. Expression and release of the latent transforming growth factor β binding protein by hepatocytes from rat liver. *Hepatology* 1997; **25**: 1398-1405

26 **Sakaida I**, Hironaka K, Uchida K, Suzuki C, Kayano K, Okita K. Fibrosis accelerates the development of enzyme-altered lesions in the rat liver. *Hepatology* 1998; **28**: 1247-1252

27 **Takiya S**, Tagaya T, Takahashi K, Kawashima H, Kamiya M, Fukuzawa Y, Kobayashi S, Fukatsu A, Katoh K, Kakumu S. Role of transforming growth factor β_1 on hepatic regeneration and apoptosis in liver diseases. *J Clin Pathol* 1995; **48**: 1093-1097

28 **Branch AD**. A hitchhiker' s guide to antisense and nonantisense biochemical pathways. *Hepatology* 1996; **24**: 1517-1529

29 **Brenner DA,** Waterboer T, Choi SK, Lindquist JN, Stefanovic B, Burchardt E, Yamauchi M, Gillan A, Rippe RA. New aspects of hepatic fibrosis. *Hepatology* 2000; **32**(1 Suppl): 32-38

• CLINICAL RESEARCH •

Imaging diagnosis of 12 patients with hepatic tuberculosis

Ri-Sheng Yu, Shi-Zheng Zhang, Jian-Jun Wu, Rong-Fen Li

Ri-Sheng Yu, Jian-Jun Wu, Rong-Fen Li, Department of Radiology, Second Affiliated Hospital, Zhejiang University School of Medicine, Hangzhou 310009, Zhejiang Province, China
Shi-Zheng Zhang, Department of Radiology, Sir Run Run Shaw Hospital, Zhejiang University School of Medicine, Hangzhou 310009, Zhejiang Province, China
Correspondence to: Dr. Ri-Sheng Yu, Department of Radiology, the Second Affiliated Hospital, Zhejiang University School of Medicine, Hangzhou 310009, Zhejiang Province, China. yurisheng2003@yahoo.com.cn
Telephone: +86-571-87783860   **Fax:** +86-571-87783804
Received: 2003-08-30   **Accepted:** 2003-10-22

Abstract

AIM: To assess CT, MR manifestations and their diagnostic value in hepatic tuberculosis.

METHODS: CT findings in 12 cases and MR findings in 4 cases of hepatic tuberculosis proved by surgery or biopsy were retrospectively analyzed.

RESULTS: (1) CT findings: One case of serohepatic type of hepatic tuberculosis had multiple-nodular lesions in the subcapsule of liver. Parenchymal type was found in 10 cases, including multiple, miliary, micronodular and low-density lesions with miliary calcifications in 2 cases; singular, low-density mass with multiple flecked calcifications in 3 cases; multiple cystic lesions in 1 case; multiple micronodular and low-density lesions fusing into multiloculated cystic mass or "cluser" sign in 3 cases; and singular, macronodular and low-density lesion with multiple miliary calcifications in 1 case. One case of tuberculous cholangitis showed marked dilated intrahepatic ducts with multiple flecked calcifications in the porta hepatis. (2) MR findings in 4 cases were hypointense on both T1-weighted imagings and T2-weighted imagings in one case, hypointense on T1-weighted imagings and hyperintense on T2-weighted imagings in 3 cases. Enhanced MR in 3 cases was slightly shown peripheral enhancement or with multilocular enhancement.

CONCLUSION: Various types of hepatic tuberculosis have different imaging findings, and typical CT and MR findings can suggest the diagnosis.

INTRODUCTION

During the second half of the twentieth century, as a result of improved nutrition, reduced crowding, public health measures, and effective chemotherapy, a dramatic decrease in the incidence of tuberculosis was seen in the world[1]. But in recent years, increased incidence of tuberculosis has been attributed to several causes, including AIDS epidemic, iv drug abuse and increase in the number of immunocompromised patients[2,3]. Hepatic tuberculosis is the most common manifestation of upper abdominal parenchymatous organ tuberculosis and its incidence has also been increasing.

Imaging features of hepatic tuberculosis have been described by several researchers at computed tomography (CT) and magnetic resonance imaging (MRI), the imaging appearance of these lesions is considered as nonspecific and, a histopathological or bacteriological confirmation is often required[4-7].

The CT and MRI features of 12 patients with pathologically proven hepatic tuberculosis examined between 1984 and 1999 were analyzed retrospectively to improve the imaging diagnostic accuracy and differentiation of hepatic tuberculosis.

MATERIALS AND METHODS

Subjects

Of the 12 hepatic tuberculosis patients, 7 were male and 5 female, aged from 18 to 69 years (mean, 38.2 years). The diagnosis was proved by surgery (8 cases), liver biopsy (3 cases) and abdominoscopy (1 case). The duration of symptoms ranged from 1 to 18 mo. The most frequent clinical symptoms and signs were right upper abdominal pain ($n=10$), upper abdominal tenderness ($n=8$), low-grade fever ($n=8$), night sweat ($n=6$), weight-loss and fatigue ($n=5$), abdominal mass ($n=1$), hepatomegly ($n=4$) and jaundice ($n=2$). Among the 12 cases, 4 were accompanied by extra-hepatic tuberculosis. Laboratory test showed anemia ($n=10$), raised erythrocyte sedimentation rate ($n=9$) and abnormal liver function ($n=7$). Tuberculin test was positive in 4 out of 5 patients tested. Eight patients were examined with ultrasound, but only 2 were correctly diagnosed. All the 12 patients had chest x-ray, and evidences of pulmonary tuberculosis were found in 2.

CT scanning

CT was performed with Siemens Somatom DR3 and HiQ units for the patients in routine fasting state. Some patients were given 500 mL of diluted iodinated contrast medium (10 g/L meglumine diatrizoate) orally 30 min before scanning. Scan scope ranged from the dome of diaphragm to the last plane of liver. All patients were examined with plain scanning at first and then using 600 g/L meglumine diatrizoate 60-80 mL for enhanced scanning with section thickness of 8-10 mm and internal of 10 mm.

MR scanning

MR was performed with a superconducting unit (Impact; Siemens, Germany) operating at a field strength of 1.0 T by using a body coil. The matrix size for data acquisition was 256×128, and a 6-10-mm section thickness with a section gap of 0-4-mm. Conventional fast spin-echo (TSE) included T1-weighted images (700/12 ms, TR/TE) and T2-weighted images (2 600-5 000/128-165 ms, TR/TE). If necessary, FLASH T1-weighted images with transverse angle of 70-75° were added. Post-contrasted MRI was obtained on FLASH T1-weighted images and TSE T1-weighted images after 0.2 mmol/kg GD-DTPA. Some patients were examined by using T1-weighted imaging fat suppression.

RESULTS

CT findings of hepatic tuberculosis based on its pathologic classification

Serohepatic type One case of serohepatic type of hepatic tuberculosis had multiple-nodular hypodense lesions with slightly peripheral enhancement in the subcapsule of liver and thickened subcapsule of quadratus lobe on CT (Figure 1).

Figure 1 Serohepatic type: multiple-nodular hypodense lesions in the subcapsule of liver and thickened subcapsule of quadrotus lobe on CT.

Parenchymal type Ten cases of parenchymal type of hepatic tuberculosis were divided into 3 subtypes: (1) Miliary tuberculosis (*n*=2): CT showed multiple, miliary, micronodular and low-density lesions with size ranging from 0.6 cm to 1.8 cm and no marked enhancement (Figure 2). Multiple miliary calcifications were found in 1 case. (2) Nodular tuberculosis (*n*=7): Nodule was more than 2.0 cm in diameter. Singular, slightly low-density (ranging from 34-42 Hu) lesions in liver were seen in 3 cases with multiple flecked calcifications in 2 cases (Figure 3), and with slightly peripheral enhancement in 2 cases, no marked enhancement in 1 case. Multi-nodular lesions were in 4 cases. One case of scattered multi-nodular lesions was two isolated cystic masses, with 23 Hu and 29 Hu respectively, and had no marked enhancement (Figure 4). Gathered multiple masses were found in the other 3 cases. CT revealed multiple micronodular and low-density lesions fusing into multiloculated cystic mass or "cluser" sign with multiloculated enhancement. (3) Mixed tuberculosis (*n*=1): CT demonstrated singular, macronodular and low-density lesion with slightly enhanced rim and multiple miliary calcifications (Figure 5).

Figure 2 Miliary tuberculosis: scattered distribution of multiple, miliary, micronodular and low-density lesions in liver.

Figure 3 Nodular tuberculosis: singular low-density mass with multiple flecked calcifications in the right lobe of liver and tuberculous lymphadenopathy encroaching on head of pancreas.

Figure 4 Nodular tuberculosis: cystic mass with 23 Hu in the right lobe of liver.

Figure 5 Mixed tuberculosis: singular, round-like and low-density lesion and multiple miliary calcifications in the right lobe of liver.

Tuberculous cholangitis One case of tuberculous cholangitis showed slightly diffuse hepatomegly, marked- dilated intrahepatic ducts, multiple calcificated lymph nodes in the porta hepatis and other regional distribution of lymph nodes in abdomen, and a large amount of hyperdense ascites. It was proved by surgery and pathology that tuberculosis of common hepatic duct involved left and right intrahepatic ducts and secondary marked dilated distant ducts. Lymph node tuberculosis and tuberculous peritonitis were also diagnosed pathologically.

MR findings

MR was performed in 4 patients. One case of serohepatic type of hepatic tuberculosis diagnosed on CT was reexamined with MR after therapy, showing multiple-nodular lesions with hypointense on T1-weighted images and hyperintense on T2-weighted images in the subcapsule of liver. The lesions had slightly peripheral enhancement after contrast administration. The other 3 cases were classified as parenchymal type of hepatic tuberculosis on CT, including miliary tuberculosis, mixed tuberculosis and nodular tuberculosis. Miliary tuberculosis showed multiple, miliary, micronodular lesions with hypointense on T1-weighted images and hyperintense on T2-weighted images. Mixed tuberculosis showed singular, macronodular lesion presented as a hypointense mass on both T1-weighted images and T2-weighted images (Figure 6) with peripheral enhancement. In this case, the lesion presented round-like on axial plane but irregular strip with multilocular enhancement on coronary and sagittal planes (Figure 7). Nodular tuberculosis revealed multiple micronodular lesions fusing into multiloculated cystic mass, which was hypointense on T1-weighted images and marked hyperintense on T2-weighted images, with multiloculated enhancement (Figure 8).

Abdominal extra-hepatic tuberculosis

Among the 12 cases, 4 had lymph node tuberculosis, showing enlarged lymph nodes, with ringed peripheral enhancement or calcifications in 2 cases respectively (Figure 3). Pancreatic tuberculosis, adrenal tuberculosis and tuberculous peritonitis were found in 1 case.

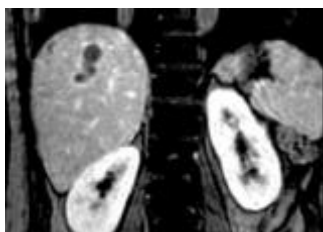**Figure 6** MR T2-weighted images showing singular, round-like hypointense lesion.

Figure 7 MRI showing irregular strip lesion with multilocular enhancement on coronary plane.
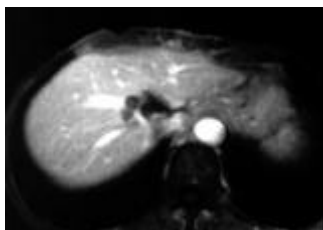

Figure 8 Enhanced MRI showing multiple micronodular lesions fusing into multiloculated cystic mass near the second porta hepatis.

DISCUSSION

Hepatic tuberculosis is considered to be a rare clinical entity. Unless there was a high index of suspicion, the diagnosis was often overlooked[1,4]. Hepatic tuberculosis can be manifested by relatively nonspecific clinical presentation. The most frequent clinical symptoms and signs were right upper abdominal pain, upper abdominal tenderness, low-grade fever, night sweat, weight-loss and fatigue, abdominal mass, hepatomegly and jaundice[4,8,9]. Anemia, raised ESR, abnormal hepatic function and positive tuberculin test could be found in laboratory examinations.

Classification

Classification of hepatic tuberculosis has remained in dispute by now[8-10]. The authors of this article considered it comprehensive and reasonable to classify hepatic tuberculosis into serohepatic type, parenchyma type and tuberculous cholangitis. In a sense, we do not agree that tuberculous cholangitis belonged to parenchymal type of hepatic tuberculosis[8]. The parenchymal type is the most common one among the 3 types, which can be further divided into 3 subtypes, *i.e.* miliary tuberculosis, nodular tuberculosis and mixed tuberculosis.

CT findings of various types of hepatic tuberculosis

Parenchyma type Miliary tuberculosis: This subtype is the most common form of hepatic tuberculosis and was found in 80-100% of autopsied patients with disseminated pulmonary tuberculosis[11]. It is depicted as multiple or diffuse miliary micronodular lesions ($\leqslant$2.0 cm in diameter on CT), often as a

part of tuberculosis in the whole body. So clinically it was not difficult to diagnose correctly[9,12]. Radiographic examination could detect hepatomegly and micronodular lesions, but it was extremely difficult to find noncalcificated lesions with less than 0.5 cm in diameter with CT[12-17]. In this series, CT revealed multiple, miliary, micronodular, hypodense lesions (>0.5 cm in diameter) scattered in liver in 2 cases with miliary calcifications in one case.

Nodular tuberculosis: The lesion, with a diameter >2 cm, is less common and has been found to be fused by miliary lesions or micronodular lesions[4]. Because nodular lesion is apt to be found by CT and MRI, most reported hepatic tuberculosis belongs to nodular tuberculosis[10,12-15,17-28]. Pathological features of this subtype are more complex than those of other subtypes. If tuberculous granuloma had no evident caseating necrosis or had a large amount of fibrous tissue existed, CT revealed a hypodense mass with slightly peripheral enhancement and no features on imaging findings could be found, it was difficult to diagnose it correctly[13]. In tuberculous granuloma, when calcium deposited calcificans punctata or even "powdery" calcificans, it might appear in the hypodense lesion that could be detected on CT and is therefore helpful to the diagnosis[6,13,24-26]. Two cases in this study were found to have calcificans punctata in the lesion center. When marked caseation or liquefaction necrosis emerged in the center of tuberculous granuloma, it means tuberculous abscess was formed and CT manifestation would be a cystic lesion with slightly or no enhanced rim[12,17,18]. In this study there were two isolated cystic masses with no marked enhancement. Compared with liver cyst, the CT findings of the isolated cystic masses were higher than those of liver cyst and the wall of isolated cystic was more blurring. When multiple micronodular lesions fused into macronodular mass, CT present as a "clunter" sign or a mutilotulated cystic mass with mutilobulated enhancement[13,19], which could be considered as a special CT feature but small pyogenic hepatic abscesses needed to be ruled out firstly[29]. Such manifestation was characterized by a less marked enhancement and a shorter duration, being different from bacterial hepatic abscess. Three cases in this study were found.

Mixed tuberculosis (or miliary macronodular tuberculosis): One case showed multiple miliary calcifications with singular hypodense lesion. We considered that one of the typical CT features of hepatic tuberculosis might be multiple, various-dense lesions, indicating that there are lesions developed in different pathologic stage coexisting in hepatic tuberculosis, including tuberculous granuloma, liquefaction necrosis, fibrosis or calcification.

Tuberculous cholangitis Tuberculous cholangitis is rare and occurs mainly in children. Obstructive jaundice is the most common in clinic. Pathology revealed regional or diffuse duct dilation with duct wall thickening and stiffening[8]. Imaging findings showed irregular dilated intrahepatic ducts or diffuse miliary calcifications along the course of the bile ducts. The latter was considered as a typical feature of tuberculous cholangitis[13,30]. In our case, CT demonstrated mild diffuse hepatomelgy, marked dilated intrahepatic ducts and multiple flecked calcifications in the porta hepatis, complicated with tuberculous peritonitis.

Serohepatic type Serohepatic type of hepatic tuberculosis is the most uncommon one in the 3 types and was depicted as miliary tuberculous lesions in the subcapsule of liver or "frosted liver", formed by thickened subcapsule[8]. To our knowledge, the imaging findings of this type have not been reported. In our case, CT revealed multi-nodular hypodense lesions in the subcapsule of liver and thickened subcapsule of quadratus lobe. On MRI, multi-nodular lesions appeared as hypointense areas on T1-weighted imagings and as hyperintense areas on T2-weighted imagings, with slightly peripheral enhancement

after contrast administration. The features of CT and MRI were consistent with pathological features.

MR findings

MRI of hepatic tuberculosis showed a hypointense nodule with a hypointense rim on T1-weighted imagings, and hypointense, isointense or hyperintense with a less intense rim on T2-weighted imagings, and peripheral enhancement or internal septal enhancement on post-contrasted MRI[20,21,24,31]. MR findings were related to different pathological stages of tuberculosis[20,24,31]. At the early and medium stages of granuloma with or without caseation or liquefaction necrosis, the lesion showed a low signal intensity on T1-weighted imagings and a high signal intensity on T2-weighted imagings. Similar lesions with hypointense on T1-weighted imaging and hypo- and iso-intense on T2-weighted imagings were corresponding to fibrous stage of tuberculosis and may have slightly or no peripheral enhancement. Tuberculous granuloma at early or medium stage and fibro-proliferous lesions all depicted as a low-density area on CT but as various signal intensities on T2-weighted imaging, which is the main advantage of MRI in the diagnosis of hepatic tuberculosis. In addition, 3D-MR imaging is helpful to distinguish the pattern of lesions and diagnose the disease. But MRI is limited to detect calcification. MR findings in 4 cases of this study were hypointense on T1-weighted imaging, hypointense in one case and hyperintense on T2-weighted imaging in 3 cases. Calcificated lesions on CT showed no signal intensity on MRI. In 2 cases in our study, lesions with hyperintense on T2-weighted imaging were pathologically proved by surgery to be a caseation necrosis in tuberculous granuloma and hypointense, and were proved to be a complete fibrosis. In short, CT and MRI have some characteristic manifestations valuable for the qualitative diagnosis of hepatic tuberculosis.

REFERENCES

1   **Hassan I**, Brilakis ES, Thompson RL, Que FG. Surgical management of abdominal tuberculosis. *J Gastrointest Surg* 2002; **6**: 862-867
2   **Yilmaz T**, Sever A, Gur S, Killi RM, Elmas N. CT findings of abdominal tuberculosis in 12 patients. *Comput Med Imaging Graph* 2002; **26**: 321-325
3   **Yang ZG**, Min PQ, Sone S, He ZY, Liao ZY, Zhou XP, Yang GQ, Silverman PM. Tuberculosis versus lymphomas in the abdominal lymph nodes: evaluation with contrast-enhanced CT. *Am J Roentgenol* 1999; **172**: 619-623
4   **Fang SG**, Yang JZ. Diagnosis of hepatic tuberculosis. *Shijie Huaren Xiaohua Zazhi* 1999; **7**: 412-413
5   **Suri R**, Gupta S, Gupta SK, Singh K, Suri S. Ultrasound guided fine needle aspiration cytology in abdominal tuberculosis. *Br J Radiol* 1998; **71**: 723-727
6   **Tan TC**, Cheung AY, Wan WY, Chen TC. Tuberculoma of the liver presenting as a hyperechoic mass on ultrasound. *Br J Radiol* 1997; **70**: 1293-1295
7   **Xing X,** Xia S. Diagnosis and treatment of hepatic tuberculoma. *Chin J Tuberc Respir Dis* 1997; **20**: 169-171
8   **Wu JP**, Qiu FZ. Huang Jiasi Surgery. 5th ed. *Beijing: People's hygiene publisher* 1992: 1324-1325
9   **Li YH**, Chi J. Clinical and pathological features of hepatospleic tuberculosis. *J Chin Med Univ* 1996; **25**: 193-194
10 **Levine C**. Primary macronodular hepatic tuberculosis: US and CT appearances. *Gastrointest Radiol* 1990; **15**: 307-309
11 **Thoeni RF**, Margulis AR. Gastrointestinal tuberculosis. *Semin Roentgenol* 1979; **14**: 283-294
12 **Xie R**, Zhou X, Chen J. CT diagnosis of tuberculosis of civer and spleen. *Chin J Tuberc Respir Dis* 1999; **22**: 237-238
13 **Hou MH**, Xue YS, Gen SQ, Liu QW, Huang H, Wang J, Gou LX, Jian ZJ, Ju CQ. CT manifestation of hepatic tuberculosis. *Chin J Radiol* 1996; **30**: 151-154
14 **Suri S**, Gupta S, Suri R. Computed tomography in abdominal tuberculosis. *Br J Radiol* 1999; **72**: 92-98
15 **Leder RA**, Low VH. Tuberculosis of the abdomen. *Radiol Clin North Am* 1995; **33**: 691-705
16 **Jadvar H**, Mindelzun RE, Olcott EW, Levitt DB. Still the great mimicker: abdominal tuberculosis. *Am J Roentgenol* 1997; **168**: 1455-1460
17 **Oto A**, Akhan O, Ozmen M. Focal inflammatory diseases of the liver. *Eur J Radiol* 1999; **32**: 61-75
18 **Reed DH**, Nash AF, Valabhji P. Radiological diagnosis and management of a solitary tuberculous hepatic abscess. *Br J Radiol* 1990; **63**: 902-904
19 **Malde HM**, Chadha D. The "cluster" sign in macronodular hepatic tuberculosis: CT features. *J Comput Assist Tomogr* 1993; **17**: 159-161
20 **Kawamori Y**, Matsui O, Kitagawa K, Kadoya M, Takashima T, Yamahana T. Macronodular tuberculoma of the liver: CT and MR findings. *Am J Roentgenol* 1992; **158**: 311-313
21 **Fan ZM**, Zeng QY, Huo JW, Bai L, Liu ZS, Luo LF, Yang JC, Zhou XH. Macronodular multi-organs tuberculoma: CT and MR appearances. *J Gastroenterol* 1998; **33**: 285-288
22 **Varela M**, Fernandez J, Navasa M, Bruix J. Pseudotumoral hepatic tuberculosis. *J Hepatol* 2003; **39**: 654
23 **Lupatkin H**, Brau N, Flomenberg P, Simberkoff MS. Tuberculous abscesses in patients with AIDS. *Clin Infect Dis* 1992; **14**: 1040-1044
24 **Maeda N**, Tanaka S, Andachi H, Osaki M, Horie Y, Suou T, Kawasaki H. Solitary hepatic tuberculoma with chronic hepatitis C diagnosed by polymerase chain reaction using paraffin-embedded resected specimen. *Hepatol Res* 1999; **15**: 80-89
25 **Kok KY**, Yapp SK. Isolated hepatic tuberculosis: report of five cases and review of the literature. *J Hepatobiliary Pancreat Surg* 1999; **6**: 195-198
26 **Stoupis C**, Taylor HM, Paley MR, Buetow PC, Marre S, Baer HU, Vock P, Ros PR. The Rocky liver: radiologic-pathologic correlation of calcified hepatic masses. *Radiographics* 1998; **18**: 675-685
27 **Hickey N**, McNulty JG, Osborne H, Finucane J. Acute hepatobiliary tuberculosis: a report of two cases and review of the literature. *Eur Radiol* 1999; **9**: 886-889
28 **Andronikou S**, Welman CJ, Kader E. The CT features of abdominal tuberculosis in children. *Pediatr Radiol* 2002; **32**: 75-81
29 **Jeffrey RB Jr**, Tolentino CS, Chang FC, Federle MP. CT of small pyogenic hepatic abscesses: the cluster sign. *Am J Roentgenol* 1988; **151**: 487-489
30 **Abascal J**, Martin F, Abreu L, Pereira F, Herrera J, Ratia T, Menendez J. Atypical hepatic tuberculosis presenting as obstrctive jaundice. *Am J Gastroenterol* 1988; **83**: 1183-1186
31 **Yan FH**, Zeng MS, Cheng WZ, Liu R, Zhou KR, Fang J, Ji Y. MRI findings of hepatic tuberculosis. *Linchuang Fangshexue Zazhi* 2002; **21**: 439-442

• CLINICAL RESEARCH •

Tumor type M_2 pyruvate kinase expression in gastric cancer, colorectal cancer and controls

Bo Zhang, Jian-Ying Chen, Dao-Da Chen, Guo-Bin Wang, Ping Shen

Bo Zhang, Jian-Ying Chen, Dao-Da Chen, Guo-Bin Wang, Department of General Surgery, Affiliated Xiehe Hospital of Huazhong University of Science and Technology, Wuhan 430022, Hubei Province, China
Ping Shen, Department of Biology, Wuhan University, Wuhan 430074, Hubei Province, China
Co-correspondents: Ping Shen
Correspondence to: Bo Zhang, Department of General Surgery, Affiliated Xiehe Hospital of Huazhong University of Science and Technology, Wuhan 430022, Hubei Province, China. wavestor@whu.edu.cn
Telephone: +86-27-87648533
Received: 2003-09-18   **Accepted:** 2003-10-07

Abstract

AIM: Tumor formation is generally linked to an expansion of glycolytic phosphometabolite pools and aerobic glycolytic flux rates. To achieve this, tumor cells generally overexpress a special glycolytic isoenzyme, termed pyruvate kinase type M_2. The present study was designed to evaluate the use of a new tumor marker, tumor M_2-PK, in discriminating gastrointestinal cancer patients from healthy controls, and to compare with the reference tumor markers CEA and CA72-4.

METHODS: The concentration of tumor M_2-PK in body fluids could be quantitatively determined by a commercially available enzyme-linked immunosorbent assay (ELISA)-kit (ScheBo® Tech, Giessen, Germany). By using this kit, the tumor M_2-PK concentration was measured in EDTA-plasma of 108 patients. For the healthy blood donors a cut-off value of 15 U/mL was evaluated, which corresponded to 90% specificity. Overall 108 patients were included in this study, 54 patients had a histological confirmed gastric cancer, 54 patients colorectal cancer, and 20 healthy volunteers served as controls.

RESULTS: The cut-off value to discriminate patients from controls was established at 15 U/mL for tumor M_2-PK. The mean tumor M_2-PK concentration of gastric cancer was 26.937 U/mL. According to the TNM stage system, the mean tumor M_2-PK concentration of stage I was 16.324 U/mL, of stage II 15.290 U/mL, of stage III 30.289 U/mL, of stage IV 127.31 U/mL, of non-metastasis 12.854 U/mL and of metastasis 35.711 U/mL. The mean Tumor M_2-PK concentration of colorectal cancer was 30.588 U/mL. According to the Dukes stage system, the mean tumor M_2-PK concentration of Dukes A was 16.638 U/mL, of Dukes B 22.070 U/mL, and of Dukes C 48.024 U/mL, of non-metastasis 19.501 U/mL, of metastasis 49.437 U/mL. The mean tumor M_2-PK concentration allowed a significant discrimination of colorectal cancers (30.588 U/mL) from controls (10.965 U/mL) ($P<0.01$), and gastric cancer (26.937 U/mL) from controls (10.965 U/mL) ($P<0.05$). The overall sensitivity of tumor M_2-PK for colorectal cancer was 68.52%, while that of CEA was 43.12%. In gastric cancer, tumor M_2-PK showed a high sensitivity of 50.47%, while CA72-4 showed a sensitivity of 35.37%.

CONCLUSION: Tumor M_2-PK has a higher sensitivity than markers CEA and CA72-4, and is a valuable tumor marker for the detection of gastrointestinal cancer.

INTRODUCTION

Pyruvate kinase plays a key role in the glycolytic pathway. One of its functions is to control nucleotide triphosphate generation[1-3]. Different isoforms of this enzyme exist (pyruvate kinases L, R, M_1, M_2, Tumor M_2), which are tissue-specifically expressed in various organisms. All isoforms are known to be homotetramers in their active state. In tumor cells, however, tetrameric pyruvate kinase M_2 isoenzyme is disrupted and predominant in a dimeric form. It has been suggested that at least a part of the mechanisms is to disrupt the tetrameric form of pyruvate kinase M_2 phosphorylated by receptor tyrosine kinases. The concentration of dimeric pyruvate kinase M_2 isoenzyme is dramatically increased in a metabolic state characteristic for tumor cells. It is thus called tumor M_2-PK[4,5]. Tumor M_2-PK is also present in body fluids, most likely released from tumor cells by tumor necrosis and cell turnover. It can be detected by a sandwich-ELISA based on two monoclonal antibodies. Furthermore, it has been demonstrated that tumor M_2-PK determination should be carried out in EDTA-plasma for its stability[6-9].

Circulating tumor markers are an established index of monitoring systemic therapies in a number of solid tumors. In the diagnosis of gastrointestinal cancer, CA19-9, CA72-4 and CEA are the major tumor markers. Since the diagnosis of gastrointestinal cancer was dependent on endoscopies and cytology more than these tumor markers, the present study was designed to evaluate the use of a new tumor marker tumor M_2-PK in discriminating gastrointestinal cancer patients from healthy donors in order to increase the sensitivity of the diagnosis for gastrointestinal cancer[10-13].

It was previously shown for renal and pancreatic carcinoma that tumor M_2-PK determination in circulation could provide a good discrimination of benign disease from malignant one and might correlate with stage of disease[14-18]. Only limited data are available on tumor M_2-PK in gastrointestinal cancer. Thus, we investigated this new marker in patients with gastrointestinal cancer focusing on whether tumor M_2-PK plasma levels increased in gastrointestinal cancer patients in comparison to healthy controls, whether tumor M_2-PK was correlated with the classical tumor marker CEA, whether tumor M_2-PK gave any predictive information on response to therapy.

MATERIALS AND METHODS

Patients

A total of 108 consecutive patients with histological confirmed primary gastrointestinal cancer were included in the study. The

mean age was 47.9 years (ranging from 32 to 66 years). There were 76 men and 32 women. Among them, 54 were gastric cancer patients (25 non metastasized, 29 metastasized), 54 were colorectal cancer patients (20 non-metastasized, 34 metastasized). According to TNM stage system, 5 gastric cancer patients were classified as stage I, 24 as stage II, 23 as stage III, 2 as stage IV. According to Dukes stage system, 14 colorectal cancer patients were classified as Dukes A, 19 as Dukes B, 21 as Dukes C. Twenty healthy donors served as a control group.

Methods

The test kit (ScheBo· Tu M_2-PK, ScheBo®Tech GmbH, Giessen, Germany) required 10 μL EDTA-plasma per sample and was performed according to the manufacturer's instructions. Samples were collected as EDTA-blood, followed by centrifugation (2 000 r/min, 10 min) and removal of the supernatant plasma. Tumor M_2-PK concentration in EDTA-plasma was determined immunologically using a sandwich enzyme-linked immunosorbent assay (ELISA) based on two monoclonal antibodies (clones I and II) specific for tumor M_2-PK. The antibodies did not cross-react with other isoforms of pyruvate kinase.

The ELISA plate was coated with a monoclonal antibody that only recognized tumor M_2-PK. Tumor M_2-PK from EDTA plasma samples and standards bound to the antibody and thus were immobilized on the plate. EDTA plasma samples were diluted (1:100) with sample/washing buffer, 50 μL of diluted sample and ready-to-use standard were transferred into wells, incubated for 60 min at room temperature. Then the wells were emptied of the sample and each well was washed 3 times with sample/washing buffer (250 μL/well). The plate was inverted and tapped on a clean paper towel to remove any remaining liquid. Fifty μL/well of the 1:100 biotin-conjugated second monoclonal antibody was added and incubated for 30 min at room temperature. After washing, 50 μL/well of ready-to-use POD-streptavidin was added and incubated for 30 min in dark at room temperature. After washing, 100 μL of ready-to-use substrate solution was added to each well, and incubated for 30 min in dark at room temperature. The substrate reaction was stopped by adding 100 μL of stop solution per well. The contents were mixed well by agitating the plate. The optical density was read at 405 nm wavelengths with a micro titer plate reader between 5 and 30 min after addition of the stop solution. The contents were mixed well before measuring. The 492 nm was used as a reference wavelength.

For determination of CEA and CA72-4, serum samples (25 μL, undiluted) were measured using the fully automatic, competitive chemiluminescent immunoassay with a diagnosis kit.

Statistical analysis

Data were statistically analyzed with origin 6.1 for windows. All P values were resulted from a two-sided test. P value less than 0.05 was considered statistically significant.

RESULTS

The mean tumor M_2-PK concentration of gastric cancer was 26.937 U/mL. According to the TNM stage system, the mean tumor M_2-PK concentration of stage I was 16.324 U/mL, of stage II 15.290 U/mL, of stage III 30.289 U/mL, of stage IV 127.31 U/mL, of non-metastasis 12.854 U/mL and of metastasis 35.711 U/mL (Table 1).

The mean tumor M_2-PK concentration of colorectal cancer was 30.588 U/mL. According to the Dukes stage system, the mean tumor M_2-PK concentration of Dukes A was 16.638 U/mL, of Dukes B 22.070 U/mL, of Dukes C 48.024 U/mL, of non-metastasis 19.501 U/mL, and of metastasis 49.437 U/mL (Table 2).

The mean tumor M_2-PK concentration allowed a significant discrimination of colorectal cancers (30.588 U/mL) from controls (10.965 U/mL) (t=3.173, P=0.0022, $P<0.01$), gastric cancer (26.937 U/mL) from controls (10.965 U/mL) (t=2.314, P=0.024, $P<0.05$) (Table 3 and Figure 1).
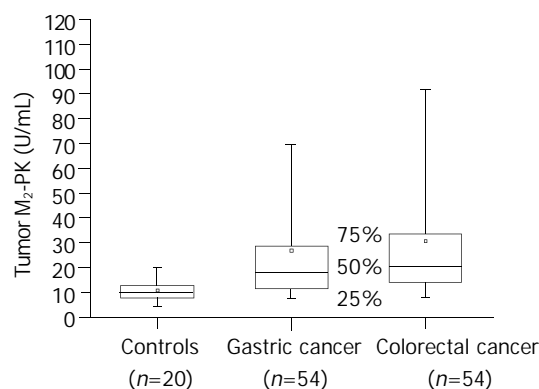

Figure 1 Concentrations of tumor M_2-PK in patients with gastrointestinal tumors and controls.

Table 1 Concentration of tumor M_2-PK and common clinical status in 54 patients with gastric cancer

No.	Tumor M_2-PK (U/mL)	TNM stage	Metastasis	No.	Tumor M_2-PK (U/mL)	TNM stage	Metastasis
1	9.26	II	N	28	24.52	IIIB	M
2	36.5	IIIA	N	29	16.6	II	M
3	23.08	II	N	30	9.26	II	N
4	23.08	IIIB	M	31	37.85	IA	N
5	165.3	IIIA	M	32	17.06	II	N
6	18.06	II	N	33	34.81	IIIA	M
7	8.81	II	N	34	14.81	II	N
8	17.34	II	N	35	23.49	II	M
9	6.87	IB	M	36	28.25	IIIA	M
10	17.91	IIIB	N	37	12.87	II	N
11	24.07	IIIB	M	38	10.62	II	M
12	12.67	II	N	39	118.02	IV	M
13	28.4	IIIB	M	40	28.75	IIIA	N
14	56.76	IIIA	N	41	14.31	II	M
15	6.42	IIIA	M	42	32.4	II	M
16	28.7	IIIB	M	43	7.61	II	N
17	7.47	IA	N	44	12.23	IA	N
18	13.9	IIIA	M	45	18.1	II	M
19	14.5	II	M	46	25.17	IIIA	M
20	69.24	IIIB	M	47	10.63	II	N
21	12.33	IIIA	M	48	8.84	II	N
22	28.66	IIIB	M	49	19.35	IIIA	N
23	136.6	IV	M	50	41.11	II	M
24	11.36	II	N	51	11.38	IIIA	N
25	7.62	II	N	52	21.75	IIIA	M
26	17.2	IB	N	53	30.03	IIIB	M
27	11.36	IIIA	M	54	11.3	II	N

N=non metastasis, M=metastasis.

The sensitivity of tumor M_2-PK for a cutoff point of 15 U/mL was compared to the established tumor markers CEA (cutoff point of 3.0 μg/μL) and CA72-4 (cut-off point of 4 KU/L). The overall sensitivity of tumor M_2-PK to colorectal cancer was 68.52%, while that of CEA was 43.12%. In gastric cancer, tumor M_2-PK showed a higher sensitivity of 50.47%, while CA72-4

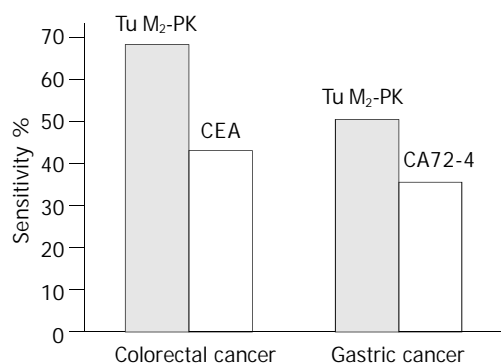showed a sensitivity of 35.37% (Figure 2).

Figure 2 Comparison of sensitivities of tumor M$_2$-PK, CEA, CA72-4 in different gastrointestinal tumors.

Table 2 Concentration of tumor M$_2$-PK and common clinical status in 54 patients with colorectal cancer

No.	Tumor M$_2$-PK (U/mL)	Dukes stage	Metastasis	No.	Tumor M$_2$-PK (U/mL)	Dukes stage	Metastasis
1	16.14	A	N	28	11.35	A	N
2	14.35	A	N	29	37.86	A	M
3	21.96	A	N	30	41.3	A	M
4	9.86	B	N	31	21.5	B	N
5	28.71	B	N	32	13.6	B	N
6	16.29	A	N	33	6.42	A	N
7	29.75	C1	M	34	10.76	C1	N
8	20.93	A	N	35	15.78	A	N
9	18.83	C1	M	36	12.4	C1	N
10	14.8	C1	M	37	56.4	C1	M
11	20.93	A	N	38	76.32	A	M
12	15.09	C1	M	39	14.85	C1	N
13	113.8	C1	M	40	8.76	C1	N
14	18.55	B	N	41	22.35	B	M
15	67.02	C1	M	42	28.13	C1	M
16	20.05	B	N	43	33.46	B	M
17	20.05	A	N	44	25.78	A	N
18	17.95	C1	M	45	7.93	C1	N
19	91.7	C1	M	46	13.44	C1	N
20	20.2	B	N	47	48.66	B	M
21	29.75	C1	M	48	106.3	C1	M
22	86.16	C1	M	49	14.78	C1	N
23	53.11	C1	M	50	10.66	C1	N
24	108.75	B	N	51	23.35	B	N
25	42.19	A	N	52	30.16	A	N
26	7.72	A	N	53	6.11	A	N
27	19.26	B	N	54	9.45	B	N

N=non metastasis, M=metastasis.

Table 3 Detection of tumor M$_2$-PK in patients with gastrointestinal cancer and healthy donors

	n	Min (U/mL)	Max (U/mL)	Mean (U/mL)	Median (U/mL)	SD
Controls	20	4.62	20.73	10.965	9.43	4.774
Gastric cancer	54	6.42	165.3	26.937	17.34	30.604
Colorectal cancer	54	6.11	113.8	30.588	20.05	27.385

DISCUSSION

The metabolic state of tumor cells is different from that of normally proliferating cells. Tumor cells exhibit an increased glycolysis to lactate initiated by multiple steps, including a switch of isoenzyme pattern and activity. Pyruvate kinase is a key enzyme of glycolysis. Different isoforms of this enzyme exist (pyruvate kinases L, R, M$_1$, M$_2$, tumor M$_2$) and are tissue-specifically expressed in various organisms. The L-type is found in the liver and proximal tubules of normal kidneys, erythrocytes express the R-type, the M$_1$-type predominates in skeletal muscle, heart and brain, and the M$_2$-type is expressed in the lung, distal tubules of normal kidney, fetal and undifferentiated or proliferating tissues. All isoforms are known to be homotetramers in their active state.

In tumor cells, pyruvate kinase isoenzyme M$_2$ is strongly overexpressed and shifted into the dimeric state. The tetrameric form has a high affinity to phosphoenolpyruvate (PEP), whereas the dimeric form has a considerably lower PEP affinity, which consequently leads to an increase of phosphometabolite pool. The concentration of the dimeric pyruvate kinase M$_2$ isoenzyme is dramatically increased in a metabolic state characteristic of tumor cells. It is thus called tumor type M$_2$ pyruvate kinase (tumor M$_2$-PK) by means of specific monoclonal antibodies against tumor M$_2$-PK, which does not cross-react with the pyruvate kinase M$_2$ tetramer and other pyruvate kinase isoforms. A sensitive immunoassay (ELISA) was employed to measure tumor M$_2$-PK in body fluids.

It was previously shown that tumor M$_2$-PK determination in the circulation provided a good discrimination of benign disease from a malignant one and might correlate with stage of disease[19-22]. Only limited data are available on tumor M$_2$-PK in gastrointestinal cancer. In the present study, tumor M$_2$-PK in the diagnosis of gastrointestinal cancer was evaluated.

Since proliferating cells had an altered metabolism with an over-expression of the dimeric form of the tumor-specific pyruvate kinase isoenzyme tumor M$_2$-PK, the present study was initiated to evaluate tumor M$_2$-PK in diagnosis of gastrointestinal cancer, in comparison with the established tumor markers CEA and CA72-4. Significant discrimination of tumor patients from healthy controls was observed[23-28]. In the diagnosis of colorectal cancer, the sensitivity of tumor M$_2$-PK was higher than that of CEA. But the sensitivity of tumor M$_2$-PK in the diagnosis of gastric cancer was lower than that in the diagnosis of colorectal cancer, whereas it was higher than that of CA72-4.

From the presented data, it is concluded that tumor M$_2$-PK can be used as a valuable diagnostic marker for gastrointestinal cancer. Further studies should focus on disease monitoring, therapy evaluation and the combination of tumor M$_2$-PK with other tumor markers[29-32].

REFERENCES

1   **Mazurek S**, Grimm H, Boschek CB, Vaupel P, Eigenbrodt E. Pyruvate kinase type M2: a crossroad in the tumor metabolome. *Br J Nutr* 2002; **87**(Suppl 1): S23-29
2   **Mazurek S**, Eigenbrodt E. The tumor metabolome. *Anticancer Res* 2003; **23**: 1149-1154
3   **Mazurek S**, Zwerschke W, Jansen-Durr P, Eigenbrodt E. Effects of the human papilloma virus HPV-16 E7 oncoprotein on glycolysis and glutaminolysis: role of pyruvate kinase type M2 and the glycolytic-enzyme complex. *Biochem J* 2001; **356**(Pt 1): 247-256
4   **Mazurek S**, Grimm H, Oehmke M, Weisse G, Teigelkamp S, Eigenbrodt E. Tumor M2-PK and glutaminolytic enzymes in the metabolic shift of tumor cells. *Anticancer Res* 2000; **20**: 5151-5154
5   **Oremek GM**, Gerstmeier F, Sauer-Eppel H, Sapoutzis N, Wechsel HW. Pre-analytical problems in the measurement of tumor type pyruvate kinase (tumor M2-PK). *Anticancer Res*

2003; **23**(2A): 1127-1130

6   **Hugo F**, Fischer G, Eigenbrodt E. Quantitative detection of tumor M2-PK in serum and plasma. *Anticancer Res* 1999; **19**(4A): 2753-2757

7   **Zwerschke W**, Mazurek S, Massimi P, Banks L, Eigenbrodt E, Jansen-Durr P. Modulation of type M2 pyruvate kinase activity by the human papillomavirus type 16 E7 oncoprotein. *Proc Natl Acad Sci U S A* 1999; **96**: 1291-1296

8   **Schneider J**, Morr H, Velcovsky HG, Weisse G, Eigenbrodt E. Quantitative detection of tumor M2-pyruvate kinase in plasma of patients with lung cancer in comparison to other lung diseases. *Cancer Detect Prev* 2000; **24**: 531-535

9   **Roigas J**, Schulze G, Raytarowski S, Jung K, Schnorr D, Loening SA. Tumor M2 pyruvate kinase in plasma of patients with urological tumors. *Tumour Biol* 2001; **22**: 282-285

10   **Hardt PD**, Ngoumou BK, Rupp J, Schnell-Kretschmer H, Kloer HU. Tumor M2-pyruvate kinase: a promising tumor marker in the diagnosis of gastro-intestinal cancer. *Anticancer Res* 2000; **20**: 4965-4968

11   **Schulze G**. The tumor marker tumor M2-PK: an application in the diagnosis of gastrointestinal cancer. *Anticancer Res* 2000; **20**: 4961-4964

12   **Hardt PD**, Toepler M, Ngoumou B, Rupp J, Kloer HU. Fecal pyruvate kinase concentrations (ELISA based on a combination of clone 1 and clone 3 antibodies) for gastric cancer screening. *Anticancer Res* 2003; **23**(2A): 855-857

13   **Hardt PD**, Toepler M, Ngoumou B, Rupp J, Kloer HU. Measurement of fecal pyruvate kinase type M2 (tumor M2-PK) concentrations in patients with gastric cancer, colorectal cancer, colorectal adenomas and controls. *Anticancer Res* 2003; **23**(2A): 851-853

14   **Oremek GM**, Teigelkamp S, Kramer W, Eigenbrodt E, Usadel KH. The pyruvate kinase isoenzyme tumor M2 (Tu M2-PK) as a tumor marker for renal carcinoma. *Anticancer Res* 1999; **19**: 2599-2601

15   **Wechsel HW**, Petri E, Bichler KH, Feil G. Marker for renal cell carcinoma (RCC): the dimeric form of pyruvate kinase type M2 (Tu M2-PK). *Anticancer Res* 1999; **19**(4A): 2583-2590

16   **Oremek GM**, Sapoutzis N, Kramer W, Bickeboller R, Jonas D. Value of tumor M2 (Tu M2-PK) in patients with renal carcinoma. *Anticancer Res* 2000; **20**: 5095-5098

17   **Roigas J**, Deger S, Schroeder J, Wille A, Turk I, Brux B, Jung K, Schnorr D, Loening SA. Tumor type M2 pyruvate kinase expression in metastatic renal cell carcinoma. *Urol Res* 2003; **26**

18   **Roigas J**, Schulze G, Raytarowski S, Jung K, Schnorr D, Loening SA. Tumor M2 pyruvate kinase in renal cell carcinoma. Studies of plasma in patients. *Urologe A* 2000; **39**: 554-556

19   **Schneider J**, Velcovsky HG, Morr H, Katz N, Neu K, Eigenbrodt E. Comparison of the tumor markers tumor M2-PK, CEA, CYFRA 21-1, NSE and SCC in the diagnosis of lung cancer. *Anticancer Res* 2000; **20**: 5053-5058

20   **Schneider J**, Neu K, Grimm H, Velcovsky HG, Weisse G, Eigenbrodt E. Tumor M2-pyruvate kinase in lung cancer patients: immunohistochemical detection and disease monitoring. *Anticancer Res* 2002; **22**(1A): 311-318

21   **Schneider J**, Peltri G, Bitterlich N, Neu K, Velcovsky HG, Morr H, Katz N, Eigenbrodt E. Fuzzy logic-based tumor marker profiles including a new marker tumor M2-PK improved sensitivity to the detection of progression in lung cancer patients. *Anticancer Res* 2003; **23**(2A): 899-906

22   **Schneider J**, Peltri G, Bitterlich N, Philipp M, Velcovsky HG, Morr H, Katz N, Eigenbrodt E. Fuzzy logic-based tumor marker profiles improved sensitivity of the detection of progression in small-cell lung cancer patients. *Clin Exp Med* 2003; **2**: 185-191

23   **Pottek T**, Muller M, Blum T, Hartmann M. Tu-M2-PK in the blood of testicular and cubital veins in men with testicular cancer. *Anticancer Res* 2000; **20**: 5029-5033

24   **Luftner D**, Mesterharm J, Akrivakis C, Geppert R, Petrides PE, Wernecke KD, Possinger K. Tumor type M2 pyruvate kinase expression in advanced breast cancer. *Anticancer Res* 2000; **20**: 5077-5082

25   **Hoopmann M**, Warm M, Mallmann P, Thomas A, Gohring UJ, Schondorf T. Tumor M2 pyruvate kinase-determination in breast cancer patients receiving trastuzumab therapy. *Cancer Lett* 2002; **187**: 223-228

26   **Schneider J**, Neu K, Velcovsky HG, Morr H, Eigenbrodt E. Tumor M2-pyruvate kinase in the follow-up of inoperable lung cancer patients: a pilot study. *Cancer Lett* 2003; **193**: 91-98

27   **Oremek GM**, Rox S, Mitrou P, Sapoutzis N, Sauer-Eppel H. Tumor M2-PK levels in haematological malignancies. *Anticancer Res* 2003; **23**(2A): 1135-1138

28   **Oremek GM**, Muller R, Sapoutzis N, Wigand R. Pyruvate kinase type tumor M2 plasma levels in patients afflicted with rheumatic diseases. *Anticancer Res* 2003; **23**: 1131-1134

29   **Aisaki K**, Kanno H, Oyaizu N, Hara Y, Miwa S, Ikawa Y. Apoptotic changes precede mitochondrial dysfunction in red cell-type pyruvate kinase mutant mouse erythroleukemia cell lines. *Jpn J Cancer Res* 1999; **90**: 171-179

30   **Steinberg P**, Klingelhoffer A, Schafer A, Wust G, Weisse G, Oesch F, Eigenbrodt E. Expression of pyruvate kinase M2 in preneoplastic hepatic foci of N-nitrosomorpholine-treated rats. *Virchows Arch* 1999; **434**: 213-220

31   **Oremek GM**, Rutner F, Sapoutzis N, Sauer-Eppel H. Tumor marker pyruvate kinase type tumor M2 in patients suffering from diabetic nephropathy. *Anticancer Res* 2003; **23**(2A): 1155-1158

32   **Pezzilli R**, Migliori M, Morselli-Labate AM, Campana D, Ventrucci M, Tomassetti P, Corinaldesi R. Diagnostic value of tumor M2-pyruvate kinase in neuroendocrine tumors. A comparative study with chromogranin A. *Anticancer Res* 2003; **23**: 2969-2972

Edited by Wang XL and Zhu LH **Proofread by** Xu FM

• CLINICAL RESEARCH •

Epidemiology of gastroesophageal reflux disease: A general population-based study in Xi'an of Northwest China

Jin-Hai Wang, Jin-Yan Luo, Lei Dong, Jun Gong, Ming Tong

Jin-Hai Wang, Jin-Yan Luo, Lei Dong, Jun Gong, Department of Gastroenterology, Second Hospital of Xi'an Jiaotong University, Xi'an 710004, Shaanxi Province, China
Ming Tong, Department of Preventive Medicine, Medical College of Xi'an Jiaotong University, Xi'an 710061, Shaanxi Province, China
Correspondence to: Dr. Jin-Hai Wang, Department of Gastroenterology, Second Hospital of Xi'an Jiaotong University, Xi'an 710004, Shaanxi Province, China. jinhaiwang@hotmail.com
Telephone: +86-29-7679290   **Fax:** +86-29-7231758
Received: 2003-11-21   **Accepted:** 2003-12-16

Abstract

AIM: Gastroesophageal reflux disease (GERD) is a common disorder in the Western population, but detailed population-based data in China are limited. The aim of this study was to understand the epidemiology of symptomatic gastroesophageal reflux (SGER) in adults of Xi'an, a northwestern city of China, and to explore the potential risk factors of GERD.

METHODS: Symptoms suggestive of GERD, functional dyspepsia (FD), irritable bowel syndrome (IBS), upper respiratory diseases and some potential risk factors were investigated in a face-to-face manner in a region-stratified random samples of 2 789 residents aged 18-70 years in Xi'an by using a standardized questionnaire.

RESULTS: With a response rate of 91.8%, the prevalence of SGER was 16.98% (95% CI, 14.2-18.92) in Xi'an adults, and no gender-related difference was observed ($P>0.05$). SGER was more common among subjects aged 30-70 years than in those aged 18-29 years ($P<0.05$). The prevalence of SGER in rural, urban and suburban subjects was 21.07%, 17.44% and 12.12%, respectively, and there was a significant difference between rural, urban and suburban regions ($P<0.05$). Compared with subjects without SGER, the prevalence of symptoms suggestive of FD and IBS, pneumonia, asthma, bronchitis, laryngitis, pharyngitis, chronic cough, wheeze, globus sensation, oral ulcer and snore was significantly increased in subjects with SGER ($P<0.01$). Heavy smoking (OR=4.94; CI, 3.70-6.61), heavy alcohol use (OR=2.85; CI, 1.67-4.49), peptic ulcer (OR=5.76; CI, 3.99-8.32), cerebral palsy (OR=3.97; CI, 1.97-8.00), abdominal operation (OR=2.69; CI, 1.75-4.13), obesity (OR=2.16; CI, 1.47-3.16), excessive food intake (OR=1.43; CI, 1.17-1.75), sweet food (OR=1.23; CI, 0.89-1.54), and consumption of coffee (OR=1.23; CI, 0.76-2.00) were independently associated with SGER. The episodes of GERD were commonly precipitated by dietary factors (66.05%), followed by body posture (26.54%), ill temper (23.72%), fatigue (22.32%) and stress (10.93%).

CONCLUSION: GERD is common in Xi'an's adult population with a mild or moderate degree. The etiology and pathogenesis of GERD are probably associated with FD, IBS, and some respiratory, laryngopharyngeal and odontostological diseases or symptoms. Some lifestyles, diseases and dietary factors are the risk factors of GERD.

INTRODUCTION

Gastroesophageal reflux disease (GERD) is a common disorder, and approximately 17-38% of adults in the Western population experienced heartburn and/or acid regurgitation, the main symptoms of GERD, at least once per week; with 4-9% having daily symptoms[1-3]. Some patients with GERD would develop Barrett's esophagus, intestinal metaplasia of esophageal mucosa that predisposes to adenocarcinoma of the esophagus[4-8], which has increased rapidly since 1970s[9,10]. Patients with esophageal carcinoma have been proved to have a low 5-year survival rate[11,12] In addition to the risk of cancer, GERD is well recognized to be associated with some upper respiratory diseases, having an adverse impact on the quality of life, and the cost of long-term medical therapy is substantial. Therefore, it is of much importance to understand the prevalence of GERD and to identify the potential risk factors to prevent GERD and GERD-related diseases. As detailed population-based data on GERD in China are currently limited, we aimed in this study to estimate the prevalence of SGER in Xi'an adults, to determine the relationship between GERD and FD, IBS, and upper respiratory diseases, and to explore the risk factors of GERD.

MATERIALS AND METHODS

Subjects

Xi'an is a northwestren city of China, consisting of 7 administrative districts and 3 counties. Of the administrative districts 4 are in the urban region and 3 in the suburban region, and the counties are all in the rural region. Each district includes numerous neighboring communities including multiple residential areas, and each of the county covers several townships governing a number of villages. Based on the 1997 census data obtained from the local government and the proportion of population within the regions, we randomly selected one or more residential areas or villages in the urban, suburban and rural regions, respectively. Finally, a total of 2 789 subjects entered this survey, including 911 subjects from the urban region, 853 from the suburban region, and 1 025 from the rural region. The proportion of subjects in different regions was similar to that of Xi'an population ($P>0.05$), and the selected samples were matched for age and gender with Xi'an population ($P>0.05$).

Questionnaire

The questionnaire was designed on the basis of previous works from two university hospitals[13], but modified to suit the local conditions. The modified version contained 8 fractions covering a total of 130 relative questions (items), of which 15 were specifically concerned with the frequency and severity of symptoms suggestive of GERD in the past years. Other questions included those concerning general condition of the subject (self-reported

height and weight), the symptoms suggestive of functional dyspepsia (FD) and irritable bowel syndrome (IBS) in the past year, symptoms or history of respiratory, laryngopharyngeal, and odontostological diseases in the past year; history of illness and operation, personal habits (smoking, alcohol), and dietary habits.

Definitions

The following definitions for symptom categories and diseases were used. Only symptoms occurring in the past year before the interview were considered. (1) Heartburn: a burning pain or burning sensation behind the sternum in the chest. (2) Acid regurgitation: a bitter or sour-tasting fluid reflux into the throat or mouth. (3) Food regurgitation: eaten food reflux into the mouth. Heartburn, acid regurgitation, and food regurgitation were considered to be the main symptoms of GERD. Each of the typical symptoms was estimated according to its severity and frequency, which measured on a 4-score scale. The severity was assessed as follows: 0, none; 1, mild (could be ignored); 2, moderate (could not be ignored but did not affect lifestyle); 3, severe (affected lifestyle). The score of symptom frequency was estimated as follows: 0, none or less than one occasion per month on average; 1, several occasions (1 to3) a month; 2, several occasions (1 to 6) a week; 3, one or more than one occasions daily. Based on the scores of the severity and frequency of the main GERD symptoms, a total score (range, 0 to 18) of each subject was calculated. (4) SGER: subjects with a total score (St) no less than 3. (5) Chest pain: any pain or discomfort felt inside the chest more than once per month on average but not including any pain caused by diagnosed heart disease. (6) Dysphagial: a feeling that food stuck in the throat or chest more than one per month. (7) Symptoms suggestive of FD and IBS and symptoms of respiratory, laryngopharyngeal, and odontostological diseases: any of these symptoms presented more than once a week on average in the past year. (8) History of diseases or operations: any disease or operation diagnosed or performed in a hospital before the interview. (9) Alcohol use: taking 300 g of alcohol per month. (10) Heavy alcohol use: taking 210 g or more of alcohol per week. (11) Smoking status: defined as current smoking, current non-smoking, and heavy smoking (more than one pack a day). (12) Obesity: a body mass index $\geq$30 kg/m^2. (13) Coffee and special beverages: drinking more than one cup per day on average. (14) Dietary habits: taking special food more than one servings per day on average.

Training of interviewers

The team of interviewers was constituted mainly by medical students studying preventive medicine in our university, who were trained by the same two professors, one was a physician of gastroenterology and understood well the relative definitions, and the other was a specialist in preventive medicine and had rich experience in survey.

Assessment of feasibility

Before the actual study, a pilot study was conducted among 100 unselected outpatients attending our gastroenterological clinic, to test the appropriateness of the questionnaire and to familiarize the interviewers with the survey procedure and the definitions. The problems that the interviewers encountered during the pilot study were discussed and their solutions were provided accordingly.

Survey design and response rate

According to the list of selected subjects and guiding by the members of residents or village's committee, all subjects were interviewed face to face at their home by the interviewers. The completed questionnaires were checked and kept by same physician. The absent subjects were registered and two reminder interviews were conducted at weekly intervals. Finally, the survey was closed after 16 wk. Among the 2 789 selected subjects, 74 had moved away, 58 could not be interviewed due to their absence during the survey period, 6 died, and 91 explicitly refused to participate in the study. A total of 2 560 subjects were successfully interviewed within a period of 4 mo, resulting in a response rate of 91.8%. There was no difference between the responders and non-responders with respect to their age and gender (P>0.05), and the constitution of the non-responder in different regions was reasonably similar (P>0.05). Twenty-eight individuals were subsequently excluded from the analysis because of inadequately questionnaires. Data from 2 532 questionnaires were entered in a computer.

Statistical analysis

The questionnaires were coded for analysis, and the data were entered in a computer and analyzed by using DBASE¢ósoftware. The prevalence was derived with 95% confidence intervals (95%CI). Comparison of the data was performed using EP15.0 χ^2 test. The odds ratios (OR) and 95% CI for each significant variable in the final model were calculated from the coefficients estimated in the logistic regression model. All P values were two-tailed, with the level of statistical significance specified at 0.05.

RESULTS

Main symptoms of GERD

The prevalence of heartburn for at least once monthly, weekly and daily episodes was 10.98% (278/2 532), 4.07% (103/2 532) and 1.66% (42/2 532), respectively. That for acid regurgitation monthly was 21.01% (532/2 532), weekly 7.78% (197/2 532), and daily 3.53% (89/2 532). For food regurgitation, the prevalence was 8.57% (217/2 532), 3.28% (83/2 532), and 1.42% (36/2 532) for at least one occasion monthly, weekly, and daily, respectively.

Symptomatic gastroesophageal reflux

The distribution of the total score of main GERD symptoms in the responders is shown in Table 1. The prevalence of SGER was 16.98% (95%CI, 14.20-18.92), of which, 13.11%, 2.92%, and 0.95% were considered as mild, moderate, and severe, respectively. Responders with SGER were more likely to be a mild or moderate degree.

Table 1 The distribution of total score of main GERD symptoms of responders (n=2 532)

Total score (St)	Responders (n)	Rate (%)
$\leq$2	2 102	83.02
$\geq$3 (SGER)	430	16.98
3-7 (mild)	332	13.11
8-12 (moderate)	74	2.92
13-18 (severe)	24	0.95

Relationship between SGER and gender, age, and region

There was no statistically significant difference between men and women in the prevalence of GERD (61.71% vs 17.25%, P>0.05), and the ratio of male/female was 1:1.03. The prevalence of SGED was relatively constant across each of 10-year age interval (Table 2, χ^2 for trend; P= 0.075), but by cutting χ^2 apart, we found that the prevalence of GERD was significantly higher in the responders aged 30-70 years than in those aged 18-29 years (χ^2=4.40, P<0.05), and the group aged 50-59 years had the highest prevalence of SGEG (21.39%). The responders in the urban and rural regions were more likely than the responders in suburban regions to have SGER (21.07% and 17.44% vs 12.12%, P<0.05). However, SGER was similarly prevalent in the urban and rural regions (P>0.05).

Table 2 The prevalence of SGED in each age group

Age group (yr)	Responders (n)	Responders with SGED (n)	Prevalence of SGED(%)
<20	64	9	14.06
20-29	517	73	14.12
30-39	621	106	17.07
40-49	584	100	17.12
50-59	360	77	21.39
60-69	354	60	16.95
70	32	5	15.63
18-70	2 532	430	16.98

Association between SGER and respiratory, laryngopharyngeal, and odontostoloical diseases

Table 3 summarized the prevalence of some respiratory, laryngopharyngeal, and odontostological diseases or symptoms in responders with and without SGER. The responders with SGER reported a higher prevalence of pneumonia, asthma, bronchitis, pharyngitis, laryngitis, chronic cough, wheeze, globus sensation, oral ulcer, and snore than the responders without SGER.

Table 3 The prevalence of respiratory, laryngopharyngeal, and odontostological diseases or symptoms in responders with and without SGER

Disease or symptom	Responders with SGER(n=430) n	Rate (%)	Responderswithout SGER(n=2 102) n	Rate (%)	P value
Pneumonia	12	2.79	15	0.73	<0.01
Asthma	28	6.51	46	2.19	<0.01
Bronchitis	66	15.35	187	8.90	<0.01
Pharyngitis	35	8.14	82	3.90	<0.01
Laryngitis	102	23.73	248	11.80	<0.01
Chronic cough	92	21.40	232	11.04	<0.01
Wheeze	33	7.67	80	3.80	<0.01
Globus sensation	102	23.72	104	4.95	<0.01
Oral ulcer	77	17.91	162	7.71	<0.01
Snore	121	28.14	362	12.27	<0.01

Relationship between SGER and other common gastrointestinal symptoms

The prevalence rate of pain behind the sternum, dysphagia, retching, nausea, vomiting, epigastric discomfort, epigastric fullness, epigastric pain, diarrhoea, and constipation in responders with SGER was significantly higher than that in the responders without SGER (*P*<0.01, Table 4).

Table 4 Other common gastrointestinal symptoms in responders with and without GERD

Symptom	Responders with SGER (n=430) n	Rate (%)	Responders without SGER (n=2 102) n	Rate (%)	P value
Pain behind breastbone	100	23.25	84	4.14	<0.01
Dysphagia	24	5.58	20	0.95	<0.01
Retching	164	38.14	228	10.85	<0.01
Nausea	137	31.86	148	7.04	<0.01
Vomiting	78	18.14	71	3.38	<0.01
Epigastric discomfort	161	37.44	216	10.28	<0.01
Epigastric fullness	201	46.74	303	14.41	<0.01
Epigastric pain	122	28.37	147	6.99	<0.01
Diarrhoea	59	13.72	102	5.07	<0.01
Constipation	93	21.63	199	9.47	<0.01

The potential risk factors

The data obtained from Table 5 showed that heavy smoking (OR=4.94; CI, 3.70-6.61), heavy alcohol use (OR=2.85; CI, 1.67-4.49), peptic ulcer (OR=5.76; CI, 3.99-8.32), abdominal operation (OR=2.69; CI, 1.75-4.13) were strongly associated with SGER; obesity (OR=2.16; CI, 1.47-3.16) was moderately associated. The association between SGER and current smoking (OR=1.27; CI, 1.17-1.38), excessive food intake (OR=1.43; CI, 1.17-1.75), sweet food (OR=1.23; CI, 0.98-1.54), and coffee (OR=1.23; CI, 0.76-2.00) still existed , but it was mild. The prevalence of SGER was not influenced by tea (OR=1.13; CI, 0.91-1.44), pepper food (OR=1.07; CI, 0.86-1.32), and fat intake (OR=1.00; CI, 0.81-1.23).

Precipitating factors for SGER

Of 430 responders with SGER, 79.07% (340/432) reported the episodes of SGER with specially precipitating factors. Some dietary factors (sweet foods, peppery foods, fat or oil foods, and sour beverage) were the most common precipitating factors (66.05%), followed by body posture (26.54%), ill temper (23.72%), fatigue (22.32%), and stress (10.93%).

Table 5 The Association Between SGER and Selected Risk Factors

Selected risk factors	Factor exposure			Non-factor exposure			P value	OR[1] (95%CI)
	Responders n	Responders with SGER n	Rate (%)	Responders n	Responders with SGER n	Rate (%)		
Current smoking	992	189	19.05	1 540	241	15.65	<0.05	1.27(1.17-1.38)
Heavy smoking	219	99	45.21	2 313	320	13.84	<0.01	4.94(3.70-6.61)
Heavy alcohol use	74	26	35.14	2 458	404	16.44	<0.01	2.85(1.67-4.49)
Peptic ulcer	59	31	52.54	2 473	399	16.13	<0.01	5.76(3.99-8.32)
Abdominal operation	99	34	34.34	2 433	396	16.28	<0.01	2.69(1.75-4.13)
Erebral palsy	18	8	44.44	2 514	422	16.78	<0.01	3.97(1.97-8.00)
Obesity	139	41	29.50	2 392	389	16.26	<0.01	2.16(1.47-3.16)
Over intake	614	129	21.01	1 918	301	15.69	<0.01	1.43(1.17-1.75)
Sweet food	695	133	19.14	1 837	297	16.17	>0.05	1.23(0.98-1.54)
Coffee	85	17	20.00	2 447	413	16.88	>0.05	1.23 0.76-2.00)
Tea	798	145	18.17	1 734	285	16.44	>0.05	1.13(0.91-1.44)
Pepper food	1 533	266	17.35	999	164	16.42	>0.05	1.07(0.86-1.32)
Fat intake	1 065	181	17.00	1 467	249	16.97	>0.05	1.00(0.81-1.23)

[1]OR ¨R2.6: a strong association; OR=1.7-2.5: a moderate association; OR=1.2-1.6: a mild association; OR=0.9-1.1: no association.

DISCUSSION

Population-based research well suits the purpose of investigating the epidemiology of gastroesophageal reflux disease, which is a common disorder in the community. The diagnosis could be made on the basis of its specific symptoms of heartburn and acid regurgitation without further diagnostic test[14]. Thus, the methodology utilizing a self-reported questionnaire has become popular in population-based study of GERD[1-3]. However, this kind of research can be limited by the varied ability of the interviewees to comprehend the definitions used and also by the relatively low response rates. Our research was conducted face to face in subjects' home with the guidance by the members of local community, therefore a high response rate (91.8%) was insured, significant responder bias was avoided, and the definitions were understood accurately assisted by the explanation provided by the trained interviewers, making possible a semi-quantitative diagnosis of SGER which was made by quantifying not only the frequency, but also the severity of main GERD symptoms so as to exclude those subjects with trivial symptoms. The prevalence of heartburn for at least weekly episodes in our study was 4.07%, similar to the prevalence rates reported in other two studies in Asia[15,16], but was lower than those of Western population, such as the rate of 17.8% in Americans[2], 14.7% in Australians[17], 15% in Finlanders[18] and 11.76% in Belgians[19].

In the past few years, there has been an increase in the frequency of GERD in Asia, but the related information remains scarce[20]. The prevalence of GERD in Western adult population varied between 17% and 38%, depending on the definitions and methodology used[1,2,3]. A community-based study showed that the ethnic-adjusted prevalence of GERD was 1.6% in Singapore, in which GERD was defined as the presence of heartburn and/or acid regurgitation at least once a month[15]. The prevalence of SGER was 16.98% in the present study. Although these studies are not comparable because of differences in methodologies and definitions used, the different prevalence of GERD may suggests that the prevalence of GERD actually varies between these populations. These differences were probably caused by genetic factors, environmental factors, dietary habits, and health habits. In our study, the variation of the prevalence of SGER in different regions was more likely to be explained by these factors. We found that the prevalence rate of SGER did not differ between men and women, which agreed with many studies[1,2,15]. Our data also suggested that elder subjects were more likely to have SGER. The reasons are mainly that old people had a poor esophageal acid clearance and decreased defense mechanisms against reflux of acid gastric contents on the esophageal mucosa[21,22].

The association between GERD and atypical reflux symptoms[2], FD[1,15,17,], and IBS[23-26] was assessed in some studies, but no related studies were conducted in China. The high prevalence of atypical reflux symptoms (pain behind the sternum and dysphagia) and symptoms suggestive of FD (retching, nausea, vomiting, epigastric discomfort, epigastric fullness, *etc.*), and IBS (epigastric pain, diarrhoea, and constipation.) in the responders with SGER in this population-based study confirmed the association among these symptoms. Subjects with aggravated dysphagia and pain behind the sternum caused by heart or coronary diseases were excluded in the analysis, so to some extent, the high prevalence of non-obstructive dysphagia and non-cardiac chest pain in subjects with SGER suggested that these two symptoms might be a late sequela of GERD. The considerable overlap among symptoms suggestive of GERD, FD and IBS may imply the same etiology and pathogenesis in these diseases. This conclusion, however, needs to be tested by further clinical and experimental studies.

Clinical studies have shown a cause-effect relationship between GERD and some respiratory, laryngopharyngeal, and odontostological diseases or symptoms[27-32]. This association was further confirmed by our population-based research. Therefore, when a general medical therapy failed to improve the patients' conditions, a 24-h pH monitoring was necessary to detect pathological reflux, and a medical antireflux treatment would be more effective to relieve these conditions with pathological reflux[28].

Laboratory studies demonstrated a correlation between both weight and body mass index with gastroesophageal reflux[33,34]. This correlation was still held in our population-based study. Cigarette smoking could reduce lower esophageal sphincter pressure and predispose strain-induced reflux[35,36]. Our research confirmed the association between smoking and SGER, and the association was weaker when cigarette consumption was decreased. We also observed a more than twofold increase in the prevalence of SGER in heavy alcohol users (42.9%) as compared with non-drinkers (15.7%). Although weight loss, smoking and drinking cessation have been recommended for patients with GERD, some patients reported improvement in their symptoms by doing so[37], a multicentre-randomized clinical trial is still needed to certify the efficacy of these therapies for GERD.

We also found that GERD was strongly associated with peptic ulcer, post abdominal operation conditions (chlolecystectomy and gastrectomy), and erebral palsy (intellectually disabled and sequela of apoplexy) which were not reported by the other population-based studies. High gastric acid output and abnormal gastric empty are responsible for the increased prevalence of GERD in patients with peptic ulcer. Abdominal operations change the normal anatomic structure of upper gastrointestinal tract and commonly cause alkaline reflux. The main reasons for the high prevalence of SGER in individuals with erebral palsy were the abnormal motility of esophagus or gastric tract of these patients and a number of common medications used (calcium channel blockers and tricyclic antidepressants) which promote GER by relaxing the lower esophageal sphincter[38, 39]

Consumption of special foods such as fat, chocolate, mints, coffee, onion, citrus fruit and tomato products and eating habits have been shown to be associated with temporary GER or relaxed LES in laboratory settings[40-42]. However, our population-based study demonstrated that excessive food intake, sweat foods, and coffee were only weekly associated with SGER and no positive association was observed between SGER and fat intake, tea, and peppery foods. Our results were partly similar to the observation by Paul and his colleagues, whose nationwide population-based case-control study showed that GER symptoms and the risk of adenocarcinoma of esophagus or gastric cardia were not associated with dietary factors[43]. The main explanation is that the quantity of these special foods was difficult to be accurately assessed in population-based study other than in a laboratory experiment. Another conceivable explanation is that the consumption of these foods might not be enough in quantity and/or frequency to cause GERD symptoms. The finding that episodes of SGER were commonly precipitated by dietary factors in our study also supports the above explanations.

In summary, GERD is common in Xi'an adult population, and a significant health problem in the community. The etiology and pathogenesis of GERD are probably associated with FD, IBS, and some respiratory, laryngopharyngeal and odontostological diseases or symptoms. Some life habits, diseases and dietary factors are the risk factors for GERD, and avoidance of these risk factors should be recommended as a primary prevention therapy of GERD.

REFERENCES

1   **Kennedy T**, Jones R. The prevalence of gastro-oesophageal reflux symptoms in a UK population and the consultation behaviour of patients with these symptoms. *Aliment Pharmacol The*r 2000; **14**: 1589-1594

2   **Locke GR** 3rd, Talley NJ, Fett SL, Zinsmeister AR, Melton LJ 3rd. Prevalence and clinical spectrum of gastroesophageal reflux: a population-based study in Olmsted County. *Gastroenterology* 1997; **112**: 1448-1456

3   **Talley NJ**, Zinsmeister AR, Schleck CD, Melton LJ 3rd. Dyspepsia and dyspepsia subgroups: a population-based study. *Gastroenterology* 1992; **102**: 1259-1268

4   **Bytzer P**, Christensen PB, Damkier P, Vinding K, Seersholm N. Adenocarcinoma of the esophagus and Barrett's esophagus: a population-based study. *Am J Gastroenterol* 1999; **94**: 86-91

5   **Falk GW**. Barrett's esophagus. *Gastroenterology* 2002; **122**: 1569-1591

6   **Buttar NS**, Wang KK, Leontovich O, Westcott JY, Pacifico RJ, Anderson MA, Krishnadath KK, Lutzke LS, Burgart LJ. Chemoprevention of esophageal adenocarcinoma by COX-2 inhibitors in an animal model of Barrett's esophagus. *Gastroenterology* 2002: **122**: 1101-1112

7   **Shirvani VN**, Ouatu-Lascar R, Kaur BS, Omary MB, Triadafilopoulos G. Cyclooxygenase 2 expression in Barrett's esophagus and adenocarcinoma: Ex vivo induction by bile salts and acid exposure. *Gastroenterology* 2000; **118**: 487-496

8   **Sampliner RE**. Practice guidelines on the diagnosis, surveillance, and therapy of Barrett's esophagus. *Am J Gastroenterol* 1998; **93**: 1028-1033

9   **Devesa SS**, Blot WJ, Fraumeni JF Jr. Changing patterns in the incidence of esophageal and gastric carcinoma in the united states. *Cancer* 1998; **83**: 2049-2053

10 **Cameron AJ**, Lomboy CT. Barrett's esophagus: age,prevalence and extent of columnar epithelium. *Gastroenterology* 1992; **103**: 1241-1245

11 **Sampliner RE**. Effect of up to 3 years of high-dose lansoprazole on Barrett's esophagus. *Am J Gastroenterol* 1994; **89**: 1844-1848

12 **Sharma P**, Sampliner RE, Camargo E. Normalization of esophageal pH with high- dose proton pump inhibitors therapy dose not result in regression of Barrett's esophagus. *Am J Gastroenterol* 1997; **92**: 582-585

13 **Pan GZ**, Xu GM, Ke MY, Han SM, Guo HP, Li ZS, Fang XC, Zou DW, Lu SC, Liu J. Epidemiological study on symptomatic gastroesophageal reflux disease in China: Beijing and Shanghai. *Chin J Dig Dis* 2000; **1**: 2-8

14 **Hollenz M**, Stolten M, Labenz J. Prevalence of gastro-oesophageal reflux disease in general practice. *Dtsch Med Wochenschr* 2002; **127**: 1007-1012

15 **Ho KY**, Kang JY, Seow A. Prevalence of gastrointestinal symptoms in a multiracial Asian population, with particular reference to reflux-type symptoms. *Am J Gastroenterol* 1998; **93**: 1816-1822

16 **Ho KY**. Gastroesophageal reflux disease is uncommon in Asia: evidence and possible explanations. *World J Gastroenterol* 1999; **5**: 4-6

17 **Talley NJ**, Boyce P, Jones M. Identification of distinct upper and lower gastrointestinal symptom groupings in an urban population. *Gut* 1998; **42**: 690-695

18 **Isolauri J**, Laippala P. Prevalence of symptoms suggestive of gastro-oesophageal reflux disease in an adult population. *Ann Med* 1995; **27**: 67-70

19 **Louis E**, DeLooze D, Deprez P, Hiele M, Urbain D, Pelckmans P, Deviere J, Deltenre M. Heartburn in Belgium: prevalence, impact on daily life, and utilization of medical resources. *Eur J Gastroenterol Hepatol* 2002; **14**: 279-284

20 **Lim LG**, Ho KY. Gastroesophageal reflux disease at the turn of millennium. *World J Gastroenterol* 2003; **9**: 2135-2136

21 **Huang X**, Zhu HM, Deng CZ, Porro GB, Sangaletti O, Pace F, Gastroesophageal reflux: the features in elderly patients. *World J Gastroenterol* 1999; **5**: 421-423

22 **Ter RB**, Johnston BT, Castell DO. Influence of age and gender on gastroesophageal reflux in symptomatic patients. *Dis Esophagus* 1998; **11**: 106-108

23 **Pimentel M**, Rossi F, Chow EJ, Ofman J, Fullerton S, Hassared P, Lin HC. Increased prevalence of irritable bowel syndrome in patients with gastroesophageal reflux. *J Clin Gastroenterol* 2002; **34**: 221-224

24 **Holtmann G**, Goebell H, Talley NJ. Functional dyspepsia and irritable bowel syndrome: is there a common pathophysiological basis? *Am J Gastroenterol* 1997; **92**: 954-959

25 **Stanghellini V**, Tosetti C, Paternico A, De Giorgio R, Barbara G, Salvioli B, Corinaldesi R. Predominant symptoms identify different subgroups in functional dyspepsia. *Am J Gastroenterol* 1999; **94:** 2080- 2085

26 **Kennedy TM**, Jones RH, Hungin APS, O'flanagan H, Kelly P. Irritable bowel syndrome, gastro-oesophageal reflux, and bronchial hyper-responsiveness in the general population. *Gut* 1998; **43**: 770-774

27 **Tomonaga T**, Awad ZT, Filipi CJ, Hinder RA, Selima M, Tercero F, Marsh RE, Shiino Y, Welch R. Symptom predictability of reflux-induced respiratory disease. *Dig Dis Sci* 2002; **47**: 9-14

28 **Tauber S**, Gross M, Issing WJ. Association of laryngopharyngeal symptoms with gastroesophageal reflux disease. *Laryngoscope* 2002; **112**: 879-886

29 **Jiang SP**, Liang RY, Zeng ZY, Liu QL, Liang YK, Li JG. Effects of antireflux treatment on bronchial hyper-responsiveness and lung function in asthmatic patients with gastroesophageal reflux disease. *World J Gastroenterol* 2003; **9**: 1123-1125

30 **Giacchi RJ**, Sullivan D, Rothstein SG. Compliance with anti-reflux therapy in patiebts with otolaryngologic manifestation of gastroesophageal reflux disease. *Laryngoscope* 2000; **110**: 19-22

31 **Branski RC**, Bhattacharyya N, Shapiro J. The reliability of the assessment of endoscopic laryngeal findings associaied with laryngoph aryngeal reflux disease. *Laryngoscope* 2002; **112**: 1019-1024

32 **Garcia-Compean D**, Gonzalez MV, Galindo G, Mar DA, Trevino JL, Martinez R, Bosques F, Maldonado H. Prevalence of gastroesophageal reflux disease in patients with extraesophageal symptoms referred from otolaryngology, allergy, and cardiology practices: a prospective study. *Dig Dis* 2000; **18**: 178-182

33 **Fisher BL**, Pennathur A, Mutnick JLM, Little AG. Obesity correlates with gastroesophageal reflux. *Dig Dis Sci* 1999; **44**: 2290-2294

34 **Locke GR** 3rd, Talley NJ, Fett SL, Zinsmeister AR, Melton LJ 3rd. The factors associated with symptoms of gastroesophageal reflux. *Am J Med* 1999; **106**: 642-649

35 **Pandolfino JE**, Kahrilas PJ. Smoking and gastro-oesophageal reflux disease. *Eur J Gastroenterol Hepatol* 2000; **12**: 837-842

36 **Kadakia SC**, De La Baume HR, Shaffer RT. Effects of transdermal nicotine on lower esophageal sphincter and esophageal motility. *Dig Dis Sci* 1996; **41**: 2130-2134

37 **Häuser W**, Grandt D. Tobacco associated gastrointestinal disorders: smoking cessation therapy –a task for gastrenterololgists. *Z Gastroenterol* 2002; **40**: 815-821

38 **Bohmer CJ**, Klinkenberg-knol EC, Niezen-de Boer RC, Meuwissen SG. The prevalence of gastro-oesophageal reflux disease based on non-specific symptoms in institutionalized, intellectually disable individuals. *Eur J Gastroenterol Hepatol* 1997; **9**: 187-190

39 **Böhmer CJM**, Klinkenberg-Knol EC, Niezen-de Boer MC, Meuwissen SGM. Gastroesophageal reflux disease in intellectually disabled individuals: how often, how serious, how manageable? *Am J Gastroenterol* 2000; **95**: 1868-1872

40 **Cranley JP**, Achkar E, Fleshler B. Abnormal lower esophageal sphincter pressure responses in patients with orange juice-induced heartburn. *Am J Gastroenterol* 1986; **81**: 104-106

41 **Allen ML**, Mellow MH, Robinson MG, Orr WC. The effect of raw onions on acid reflux and reflux symptoms. *Am J Gastroenterol* 1990; **85**: 377-380

42 **Cohen S**, Booth GH Jr. Gastric acid secretion and low-esophageal-sphincter pressure in response to coffee and caffeine. *N Engl J Med* 1975; **293**: 897-899

43 **Terry P**, Lagergren J, Wolk A, Nyren O. Reflux-inducing dietary factors and risk of adenocarcinoma of the esophagus and gastric cardia. *Nutrition Cancer* 2000; **38**: 186-191

Edited by Chen WW and Wang XL **Proofread by** Xu FM

• CLINICAL RESEARCH •

Serum hepatic enzyme manifestations in patients with severe acute respiratory syndrome: Retrospective analysis

Hui-Juan Cui, Xiao-Lin Tong, Ping Li, Ying-Xu Hao, Xiao-Guang Chen, Ai-Guo Li, Zhi-Yuan Zhang, Jun Duan, Min Zhen, Bin Zhang, Chuan-Jin Hua, Yue-Wen Gong

Hui-Juan Cui, Xiao-Lin Tong, Ping Li, Ying-Xu Hao, Xiao-Guang Chen, Ai-Guo Li, Zhi-Yuan Zhang , Jun Duan, Min Zhen, Bin Zhang, Chuan-Jin Hua, Chinese-Japanese Friendship Hospital, Beijing 100029, China
Yue-Wen Gong, Faculty of Pharmacy, University of Manitoba, Canada
Co-correspondents: Dr. Ping Li
Correspondence to: Dr. Hui-Juan Cui, Chinese-Japanese Friendship Hospital, Yinghua Dong Lu, Hepingli Chaoyang District, Beijing 100029, China. cuihj1963@sina.com
Telephone: 13911835018   **Fax:** +86-10-64206643
Received: 2003-09-15   **Accepted:** 2003-10-22

Abstract

AIM: To evaluate the hepatic function in patients with severe acute respiratory syndrome (SARS) and possible causes of hepatic disorder in these patients.

METHODS: One hundred and eighty-two patients with SARS were employed in a retrospective study that investigated hepatic dysfunction. Liver alanine aminotransferase (ALT), aspartate aminotransferase (AST) and lactic dehydrogenase (LDH) were analyzed in these patients. Patients with different hospital treatments were further investigated.

RESULTS: Of the 182 patients, 128(70.3%) had abnormal ALT activity, 57(31.3%) had abnormal AST activity and 87 (47.8%) had abnormal LDH activity. The peak of elevated hepatic enzyme activities occurred between the sixth day and the tenth day after the first day of reported fever. Of the 182 patients, 160(87.9%) had been treated with antibiotics, 137(75.2%) with Ribavirin, and 115(63.2%) with methylpredisolone. There was no statistically significant correlation between the duration of Ribavirin treatement and hepatic dysfunction.

CONCLUSION: Abnormal liver functions were common in patients with SARS and could be associated with virus replication in the liver.

INTRODUCTION

Severe acute respiratory syndrome (SARS) or so-called atypical pneumonia with unknown etiology started to appear in Guangdong Province, China in November 2002 and quickly spread to other parts of China and around the world[1,2-4]. A novel coronaviruses has been identified as the etiological agent of the syndrome[5-8]. Most coronaviruses may cause either a respiratory or an enteric change. During the outbreak of SARS,

abnormal hepatic enzyme activity was reported in patients of Toronto area, Canada[9]. The present study summarized the hepatic enzyme activities in patients with SARS who were treated at the China-Japan Friendship Hospital, Beijing, which started to receive patients with SARS in mid-March 2003, and was designated as one of the three hospitals in Beijing to treat patients with SARS in April 2003.

MATERIALS AND METHODS

Patients

Our study included all patients who received a diagnosis of SARS with no pre-existing live diseases and were treated at the China-Japan Friendship Hospital between March 10 and May 31, 2003, and excluded such patients with a history of liver disorders. According to the criteria for SARS that have been established by the Ministry of Health, China-Clinical Diagnostic Criteria for Severe Acute Respiratory Syndrome[10], our case definition was a fever (temperature >38 ℃), a chest radiograph of the thorax showing evidence of consolidation with or without respiratory symptoms and a history of close contact with a person to whom SARS had been diagnosed. The diagnosis was confirmed by an indirect immunofluorescence assay with fetal rhesus kidney cells that were infected with coronavirus and fixed in acetone to detect a serological response to the virus[3] or by a positive viral culture. Patients in the study included 103 male and 79 female with age ranging from 11 to 86. The age distribution is shown in Table 1.

Table 1 Age distribution of the patient

Age range (yr)	Case number (n)	%
Under 20	18	9.89
21-30	45	24.73
31-40	35	19.23
41-50	29	15.93
51-60	18	9.89
Above 60	37	20.33

Laboratory examination

Hepatic functions included alanine aminopeptidase (ALT), aspartate aminotransferase (AST) and lactic dehydrogenase (LDH). We studied these variables from the first day of admission to May 31, 2003. The normal values of these enzymes were 0-40 U/L for ALT, 0-42 U/L for AST and 100-250 U/L for LDH.

Data collection

We retrospectively analyzed data from 3 aspects. First, total incidence rate of abnormal liver enzyme activities were analyzed from 182 patients with SARS. Second, the time course of abnormal liver enzyme activities was dissected in 57 patients because these patients were admitted to China-Japan Friendship Hospital from beginning of the illness. The other large proportion of patients with SARS was transferred to China-Japan Friendship Hospital after the hospital was designated

specifically to treat patients with SARS on April 28, 2003. Third, analysis of ribavirin treatment for patients with SARS was performed in 84 cases, as well as their abnormal liver enzyme activities after ribavirin treatment.

Statistical analysis

We used univariate analysis to compare patients with normal and abnormal serum hepatic enzyme activities, and an unpaired Student's t test, χ^2 test, or Fisher's exact test, as appropriate. We then performed multiple logistic regression analysis with stepwise analysis to identify independent predictors of the abnormality[3]. A P value of less than 0.05 was considered to indicate statistical significance. All probabilities are two tailed. Statistical analysis software StatView 5.0 for Macintosh OS was employed and data were reported as mean±SD unless otherwise indicated.

RESULTS

Between March 10, and May 31, 2003, more than 100 of patients with SARS were admitted to the China-Japan Friendship Hospital; especially on May 8 a large number of patients with SARS were transferred to our hospital at severe stage and some patients were at convalescent stage. Serum samples were collected immediately after the patients were admitted to the hospital. The study included 103 male and 79 female patients from all ethnic background. The mean age was 40.42 years (range 15-78 years).

Incidence rate of abnormal liver enzyme activities in 182 patients

Transiently elevated ALT was observed in 128 (70.3%) patients with SARS. Of the 182 patients with SARS, 57 (31.3%) had elevated AST while 87 (47.8%) had abnormal LDH as indicated in Table 2.

Table 2 Incidence rate of abnormal-liver-function outcomes

	ALT	AST	LDH
Total cases (n)	182	182	139
Abnormal cases (n)	128	57	87
Ratio (%)	70.3	31.3	62.6

Time course of abnormal liver enzyme activities

The time course of abnormal liver enzyme activities was obtained from 57 patients with SARS who were admitted to our hospital at the beginning of illness. The earliest day of abnormal liver enzyme activities was the first day of illness. The peak of abnormal liver enzyme activities was between the sixth and the tenth d of illness. Liver function started to recover 15 d after onset. However, for some patients, abnormal liver enzyme activities could last for almost a month (Figure 1).
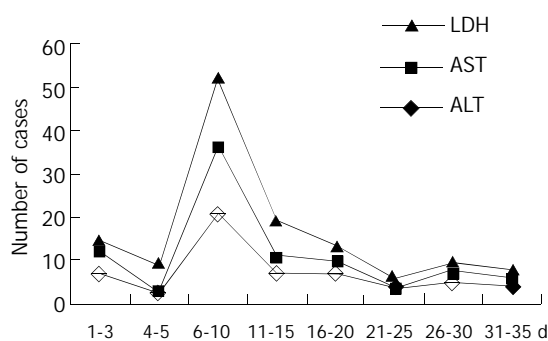

Figure 1 Abnormal-liver-function outcomes at different days.

Comparison of liver enzyme activities before and after hospital treatment

To explore whether hospital treatment could lead to abnormal liver enzyme activities in patients with SARS, we analyzed data of all patients who had normal or abnormal liver enzyme activities before and after hospital treatment. The deadline for entering analysis was June 15, 2003. Patients with hospital treatment less than 15 d were excluded from the study. As shown in Table 3, statistically significant difference was observed in AST and LDH ($P<0.01$) while no significant difference was obtained in ALT.

Table 3 Abnormal-liver-function outcomes before treatment *vs* after treatment

Cases (n)	ALT		AST		LDH	
	Before	After	Before	After	Before	After
Total	182	166	182	164	122	105
Normal	93	85	133	145	46	81
Abnormal	89	81	49	19	76	24

Hospital treatment in 182 patients with SARS

Most patients with SARS in our hospital received empirical treatment with antibiotics or ribavirin 400-500 mg, twice daily, or intravenous methylprednisolone at high dosage. As listed in Table 4, of the 182 patients with SARS, 160(87.9%) received antibiotics, 137(75.2%) received ribavirin and 115 (63.2%) received methylprednisolone. Since Ribavirin is a drug that inhibits viral replication, it has been widely used in patients with SARS after it was confirmed that coronavirus is etiological factor of SARS. We further analyzed the duration of Ribavirin treatment and its relation to abnormal liver enzyme activities in patients with SARS.

Table 4 Therapeutic drugs in 182 SARS patients

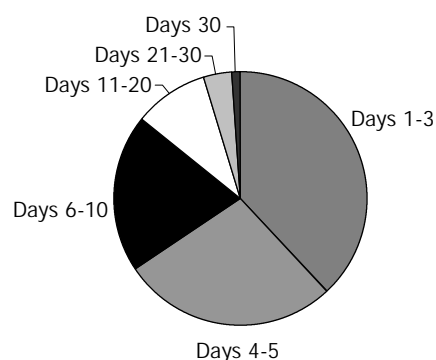|	Antibiotics	Ribavirin	Methylpredisolone
Cases (n)	160	137	115
Rate of usage (%)	87.9	75.2	63.2

Figure 2 The distribution of of ribavirin treatment in 84 SARS patients.

Distribution of ribavirin treatment in 84 patients with SARS

Although 137 patients with SARS were recorded of ribavirin treatment, only 84 patients were employed for analysis of ribavirin treatment. The reason for choosing these patients was that these patients had detailed record of receiving ribavirin in our hospital and the other 53 patients had already received ribavirin treatment before admitting to our hospital. As shown in Figure 2, 32(38.1%) patients with SARS received ribavirin treatment at d 1 to 3 after diagnosis of SARS, 23(27.4%) patients received ribavirin treatment at d 4 to 5, 17(20.2%)

patients received ribavirin treatment at days 6 to 10. A total of 55(65.5%) patients with SARS received ribavirin treatment within 5 d of the illness while a total of 72(85.7%) patients received ribavirin treatment within 10 d of the illness.

Correlation of ribavirin treatment and abnormal liver enzyme activities

Correlation of ribavirin treatment and abnormal liver enzyme activities was analyzed in 84 patients with SARS. The duration of ribavirin treatment was different among these patients. Twenty-six (29.8%) patients with SARS received ribavirin treatment for 1 to 7 d, 32(35.7%) patients for 8 to 14 d, 20(22.6%) patients for 15 to 21 d and 10(11.9%) patients for more than 22 d. However, as shown in Table 5, there was small increase in liver enzyme activities in patients with longer Ribavirin treatment, but it did not reach statistically significant.

Table 5 The distribution of ribavirin treatment in 84 SARS patients

Treatment	Days 1-3	Days 4-5	Days 6-10	Days 11-20	Days 21-30	Days 30
Cases number	32	23	17	8	3	1
%	38.1%	27.4%	20.2%	9.5%	3.6%	1.2%

DISCUSSION

Abnormal serum liver enzyme activities have been reported by different hospitals with inconsistent incident rates. It was reported that there were 44.7% patients with SARS having abnormal liver enzyme activities in Guangzhou Southern Hospital[11], And 53.3% was reported in the First Hospital of Beijing University[12]. Moreover, 40% patients with SARS having abnormal liver enzyme activities were reported in hospitals around great Toronto area[9]. In our study, we have found that 70% patients with SARS suffered from abnormal liver enzyme activities. The higher percentage of liver damage in our patients might be related to the fact that large number of patients with severe illness were transferred to our hospital.

The difference between these reports may also be associated with different treatment strategies between these areas, especially in the use of ribavirin. Ribavirin (1-b-D- ribofuranosyl- 1,2,4-triazole), a broad spectrum antiviral nucleoside, is one of the first antiviral drugs ever discovered. It was first approved in the United States in an aerosol form for the treatment of a severe lung infection in infants[13]. Recently, it has been employed as an anti-HIV treatment[14-17] and in combination with interferon for the treatment of hepatitis A, B, and C[18-21]. Compared with hospitals around great Toronto area (88%), the usage of ribavirin in our hospital (75%) was less. However there were a larger proportion of patients (70%) with abnormal liver enzyme activities in our hospital than that (40%) in hospital around Toronto area. This indicated that ribavirin could not be a contributing factor for abnormal liver enzyme activities observed in patients with SARS. Although there was an increased trend of elevated liver enzyme activities with duration of ribavirin treatment, there was no statistic significant correlation between abnormal liver enzyme activities and duration of ribavirin treatment.

Abnormal liver enzyme activities could also be caused by coronavirus induced liver damage. Although liver biopsy was not feasible in these patients, pathological evaluation of the fatal cases revealed that hepatocytes underwent fatty degeneration, cloudy swelling, focal hemorrhage, apoptosis and dot necrosis, Kupffer cell proliferation, portal infiltration of lymphocytes and dispersive eosinophilic body in the liver[22, 23]. There was an enlargement of the liver in 23 patients with SARS in our study observed by B-ultrasonic examination

(data reported in another study). Because of difficulty in clinical practice, it was not documented whether pathological impairments of liver function and structure were present in the early stage of the disease. However, we have used herbal medicines and liver protective drugs in these patients. These treatments did not alter the outcome of abnormal liver enzyme activities. Therefore, it is unlikely that hospital treatment contributes to the outcome of abnormal liver enzyme activities in patients with SARS.

Our conclusions are that abnormal liver enzyme activities are common in patients with SARS and coronaviruses that cause severe acute respiratory syndrome might affect the liver and induce liver damage in the course of infection.

REFERENCES

1   **Luo D.** SARS treatment: experience from a team in Guangdong, China. *Chin Med J* 20003; **116**: 838-839
2   **Chan YM,** Yu WC. Outbreak of severe acute respiratory syndrome in Hong Kong Special Administrative Region: case report. *Bmj* 2003; **326**: 850-852
3   **Lee N,** Hui D, Wu A, Chan P, Cameron P, Joynt GM, Ahuja A, Yung MY, Leung CB, To KF, Lui SF, Szeto CC, Chung S, Sung JJ. A major outbreak of severe acute respiratory syndrome in Hong Kong. *N Engl J Med* 2003; **348**: 1986-1994
4   **Poutanen SM,** Low DE, Henry B, Finkelstein S, Rose D, Green K, Tellier R, Draker R, Adachi D, Ayers M, Chan AK, Skowronski DM, Salit I, Simor AE, Slutsky AS, Doyle PW, Krajden M, Petric M, Brunham RC, McGeer AJ. Identification of severe acute respiratory syndrome in Canada. *N Engl J Med* 2003; **348**: 1995-2005
5   **Drosten C,** Gunther S, Preiser W, van der Werf S, Brodt HR, Becker S, Rabenau H, Panning M, Kolesnikova L, Fouchier RA, Berger A, Burguiere AM, Cinatl J, Eickmann M, Escriou N, Grywna K, Kramme S, Manuguerra JC, Muller S, Rickerts V, Sturmer M, Vieth S, Klenk HD, Osterhaus AD, Schmitz H, Doerr HW. Identification of a novel coronavirus in patients with severe acute respiratory syndrome. *N Engl J Med* 2003; **348**: 1967-1976
6   **Ksiazek TG,** Erdman D, Goldsmith CS, Zaki SR, Peret T, Emery S, Tong S, Urbani C, Comer JA, Lim W, Rollin PE, Dowell SF, Ling AE, Humphrey CD, Shieh WJ, Guarner J, Paddock CD, Rota P, Fields B, DeRisi J, Yang JY, Cox N, Hughes JM, LeDuc JW, Bellini WJ, Anderson LJ. A novel coronavirus associated with severe acute respiratory syndrome. *N Engl J Med* 2003; **348**: 1953-1966
7   **Peiris JS,** Lai ST, Poon LL, Guan Y, Yam LY, Lim W, Nicholls J, Yee WK, Yan WW, Cheung MT, Cheng VC, Chan KH, Tsang DN, Yung RW, Ng TK, Yuen KY. Coronavirus as a possible cause of severe acute respiratory syndrome. *Lancet* 2003; **361**: 1319-1325
8   **Kuiken T,** Fouchier RA, Schutten M, Rimmelzwaan GF, van Amerongen G, van Riel D, Laman JD, de Jong T, van Doornum G, Lim W, Ling AE, Chan PK, Tam JS, Zambon MC, Gopal R, Drosten C, van der Werf S, Escriou N, Manuguerra JC, Stohr K, Peiris JS, Osterhaus AD. Newly discovered coronavirus as the primary cause of severe acute respiratory syndrome. *Lancet* 2003; **362**: 263-270
9   **Booth CM,** Matukas LM, Tomlinson GA, Rachlis AR, Rose DB, Dwosh HA, Walmsley SL, Mazzulli T, Avendano M, Derkach P, Ephtimios IE, Kitai I, Mederski BD, Shadowitz SB, Gold WL, Hawryluck LA, Rea E, Chenkin JS, Cescon DW, Poutanen SM, Detsky AS. Clinical features and short-term outcomes of 144 patients with SARS in the greater Toronto area. *JAMA* 2003; **289**: 2801-2809
10 **Ministry of Health, PR China.** Clinical diagnostic criteria for Severe Acute Respiratory Syndrome (SARS) (On Trial). *http: wwwChinacdcNetcn/56/kong56-2htm#/* May 3, 2003:
11 **Peng J,** Hou JL, Guo YB, Feng YK, Cheng JJ, Liu DL, Zhu YY, Jiang RL, Chen YP. Clinical features of severe acute respiratory syndrome in the Guangzhou area. *Zhonghua Chuanranbing* 2003; **21**: 89
12 **Huo N,** Lu HY, Xu XY, Wang GF, Li HC, Wang GQ, Li JP, Wang J, Nie LG, Gao XM, Zhao ZH, Li J, Li YH, Zhuang H. The clinical characteristics and outcome of 45 early patients with SARS. *Beijing Daxue Xuebao* 2003; **35**(S1): 19-22

13   **Hall CB,** McBride JT, Walsh EE, Bell DM, Gala CL, Hildreth S, Ten Eyck LG, Hall WJ. Aerosolized Ribavirin treatment of infants with respiratory syncytial viral infection. A randomized double-blind study. *N Engl J Med* 1983; **308**: 1443-1447

14   **Japour AJ,** Lertora JJ, Meehan PM, Erice A, Connor JD, Griffith BP, Clax PA, Holden-Wiltse J, Hussey S, Walesky M, Cooney E, Pollard R, Timpone J, McLaren C, Johanneson N, Wood K, Booth D, Bassiakos Y, Crumpacker CS. A phase-I study of the safety, pharmacokinetics, and antiviral activity of combination didanosine and Ribavirin in patients with HIV-1 disease. AIDS Clinical Trials Group 231 Protocol Team. *J Acquir Immune Defic Syndr Hum Retrovirol* 1996; **13:** 235-246

15   **Vogt MW,** Hartshorn KL, Furman PA, Chou TC, Fyfe JA, Coleman LA, Crumpacker C, Schooley RT, Hirsch MS. Ribavirin antagonizes the effect of azidothymidine on HIV replication. *Science* 1987; **235**: 1376-1379

16   **Crotty S**, Andino R. Implications of high RNA virus mutation rates: lethal mutagenesis and the antiviral drug Ribavirin. *Microbes Infect* 2002; **4**: 1301-1307

17   **Meier V,** Burger E, Mihm S, Saile B, Ramadori G. Ribavirin inhibits DNA, RNA, and protein synthesis in PHA-stimulated human peripheral blood mononuclear cells: possible explanation for therapeutic efficacy in patients with chronic HCV infection. *J Med Virol* 2003; **69**: 50-58

18   **Saito Y,** Escuret V, Durantel D, Zoulim F, Schinazi RF, Agrofoglio LA. Synthesis of 1, 2, 3-triazolo-carbanucleoside analogues of Ribavirin targeting an HCV in replicon. *Bioorg Med Chem* 2003; **11**: 3633-3639

19   **Liu CJ,** Chen PJ, Lai MY, Kao JH, Jeng YM, Chen DS. Ribavirin and interferon is effective for hepatitis C virus clearance in hepatitis B and C dually infected patients. *Hepatology* 2003; **37**: 568-576

20   **Rakov NE.** Peginterferon alfa-2a plus Ribavirin for chronic hepatitis C. *N Engl J Med* 2003; **348**: 259-260

21   **Zhang H,** Yang G, Yang X. Prospective study of combination of interferon-alpha with Ribavirin for treatment of chronic hepatitis C in children. *Zhonghua Shiyan Helin Chuangbing Duxue Zazhi* 2001; **15**: 81-82

22   **Wang CE,** Qin ED, Gan YH, Li YC, Wu XH, Cao JT, Yu M, Si BY, Yan G, Li JF, Zhu QY. Pathological observation on sucking mice and Vero E6 cells inoculated with SARS samples. *Jifangjun Yuxue Zazhi* 2003; **28**: 383-384

23   **Hong T,** Wang JW, Sun YL, Duan SM, Chen LB, Qu JG, Ni AP, Liang GD, Ren LL, Yang RQ, Guo L, Zhou WM, Chen J, Li DX, Xu WB, Xu H, Guo YJ, Dai SL, Bi SL, Dong XP, Ruan L. Chlamydia-like and coronavirus-like agents found in dead cases of atypical pneumonia by electron microscopy. *Zhonghuan Yixue Zazhi* 2003; **83**: 632-636

Edited by Zhu LH **Proofread by** Xu FM

• BRIEF REPORTS •

Maastricht II treatment scheme and efficacy of different proton pump inhibitors in eradicating *Helicobacter pylori*

Engin Altintas, Orhan Sezgin, Oguz Ulu, Ozlem Aydin, Handan Camdeviren

Engin Altintas, Orhan Sezgin, Department of Gastroenterology, Mersin University, Faculty of Medicine, Mersin, Turkey
Oguz Ulu, Department of Internal Medicine, Mersin University, Faculty of Medicine, Mersin, Turkey
Ozlem Aydin, Department of Pathology, Mersin University, Faculty of Medicine, Mersin, Turkey
Handan Camdeviren, Department of Biostatistics, Mersin University, Faculty of Medicine, Mersin, Turkey
Correspondence to: Engin Altintas, MD, Asst. Professor Mersin Universitesi Tip Fakultesi Hastanesi, İç Hastalıkları A.D. Zeytinlibahce Caddesi, Eski Otogar Yani 33079 Mersin,
Turkey. enginaltintas@mersin.edu.tr
Telephone: +90-324-3374300   **Fax:** +90-324-3367117
Received: 2003-12-28   **Accepted:** 2004-01-09

Abstract

AIM: The Maastricht II criteria suggest the use of amoxicillin and clarithromycin in addition to a proton pump inhibitor over 7-10 d as a first line therapy in the eradication of *Helicobacter pylori (H pylori)*. For each proton pump inhibitor, various rates of eradication have been reported. The present study was to compare the efficacy of different proton pump inhibitors like omeprazole, lansoprazole and pantoprazole in combination with amoxicillin and clarithromycin in the first line eradication of *H pylori* and to investigate the success of *H pylori* eradication in our district.

METHODS: A total of 139 patients were included having a *Helicobacter pylori* (+) gastroduodenal disorders diagnosed by means of histology and urease test. Besides amoxicillin (1 000 mg twice a day) and clarithromycin (500 mg twice a day), they were randomized to take omeprazole (20 mg twice a day), or lansoprazole (30 mg twice a day), or pantoprozole (40 mg twice a day) for 14 d. Four weeks after the therapy, the eradication was assessed by means of histology and urease test. It was evaluated as eradicated if the *H pylori* was found negative in both. The complaints (pain in epigastrium, nocturnal pain, pyrosis and bloating) were graded in accordance with the Licert scale. The compliance of the patients was recorded.

RESULTS: The eradication was found to be 40.8% in the omeprazole group, 43.5% in the lansoprazole group and 47.4% in the pantoprazole group. Sixty-three out of 139 patients (45%) had eradication. No statistically significant difference was observed between the groups. Significant improvements were seen in terms of the impact on the symptom scores in each group.

CONCLUSION: There was no difference between omeprazole, lansoprazole and pantoprazole in *H pylori* eradication, and the rate of eradication was as low as 45%. Symptoms were improved independent of the eradication in each treatment group. The low eradication rates suggest that the antibiotic resistance or the genetic differences of the microorganism might be in effect. Further studies are required to verify these suggestions.

INTRODUCTION

So far, no ideal treatment exists although there have been plenty of treatment schemes in the eradication of *Helicobacter pylori* (*Hp*). Therefore, research on this subject has substantially increased. In order to achieve the optimal treatment regimen various combinations including antibiotics and antisecretory agents have been tested[1]. In 2000, use of amoxicillin and clarithromycin for a period of at least 1 wk in combination with a proton pump inhibitor (PPI) was suggested[2]. Diverse eradication rates have been reported with this specific treatment scheme[3-6]. Up to date, five diverse PPIs have been launched in our country. The outcomes obtained from studies related with those inhibitors have resulted in confusing eradication rates.

The present study aimed to investigate the efficacy of three different PPIs given in combination with antibiotics, which have been accepted to be standard in the eradication of Hp and the success of *Hp* eradication by this standard treatment.

MATERIALS AND METHODS

Between September 2001 and July 2002, 139 patients with gastritis, gastric ulcer and duodenal ulcer were enrolled in this study. All patients were positive in urease test and histopathological examination for *Hp*. Patients with a concomitant serious illness and a history of gastric surgery, pregnancy, patients taking antibiotics, H-2 receptor blockers or on PPI treatment within the last two months, being allergic to macrolides and having a previous eradication treatment were excluded. Their written informed consent was received. They were randomized to take omeprazole 2×20 mg/d (OAC), lansoprazole 2×30 mg/d (LAC) or pantoprazole 2×40 mg/d (PAC) plus amoxicillin 2×1 000 mg/d and clarithromycin 2×500 mg/d for 14 d. All of the eligible patients had standard laboratory tests, and their history, physical examination and concomitant treatment regimens were recorded. Their complaints (epigastric pain, bloating, nocturnal pain and pyrosis) were graded in accordance to the Licert scale (0=none, 1=mild, 2=moderate, 3=severe, 4=very severe). Two biopsies were taken from the antrum and corpus for pathology, and a biopsy from the antrum for urease test. The pathological assessment was based on the Sidney classification for gastritis. 4 wk after the therapy the side effects and alterations were re-evaluated, and a blinded gastroenterologist repeated the endoscopical examination. Negative *Hp* in both urease test and biopsy was accepted as eradication.

To understand the compliance, the patients were asked to report how many prescribed drugs they used (100%-forgotten for 0 d, 80-99%-forgotten only for 1 d, 60-79%-forgotten for 2 d and below 59%-forgotten more than 2 d). The side effects were recorded.

Statistical analysis

The definitive statistics were calculated (mean±SD, numbers and % values). For age comparison in three groups, simple analysis of variance was used while gender, smoking, NSAID use, alcohol consumption, eradication status and relationship between the three groups were determined by Pearson chi-square test, which was also used to determine the relation between the eradication status and antral gastritis and pangastritis plus smoking and histological activity in the antrum prior to eradication. The differences in the symptom score between the eradicated and non-eradicated were investigated by Wilcoxon test before and after the eradication. Furthermore, t-test was applied to compare the improvement rates in the separate symptom score between the eradicated and non-eradicated in relation to the difference between the rates in 3 groups.

RESULTS

Table 1 gives the demographical characteristics of the patients in the three groups. Of the patients, 73(58.3%) were women, and 66(41.7%) were men, and the average age was 47.9±11.8 years. The patient compliance was 95%. Two patients from each group discontinued the therapy for 8 d due to side effects (nausea, vomiting, and diarrhea). The endoscopical lesions are shown in Table 2. The eradication was found in 22 out of 49 patients (40.8%) in the omeprazole group, 20 out of 46 patients (43.5%) in the lansoprazole group, and 21 out of 44 patients (47.4%) in the pantoprazole group. There was no any differences between three groups ($P>0.05$). The overall eradication rate was 45%. Twenty-two out 62 patients (37%) with antral gastritis had eradication while 19 out of 34 patients (55%) with pangastritis had eradication ($P<0.05$). No correlation was found between eradication and smoking and histological activity in the antrum prior to eradication ($P>0.05$). Significant improvements were observed in the symptom score between the eradicated and non-eradicated compared to pre-eradication status ($P<0.05$), but no significant differences were found between the groups.

Table 1 Demographic features of study population

	OAC	LAC	PAC	*P*
Patient number	49	46	44	NS
Female/Male	26/23	23/23	24/20	NS
Year				
Mean	47.5±13.4	45.7±12.5	44.5±13.5	NS
Range	20-75	21-73	20-70	NS
Smoking	7 (14.2%)	6 (13%)	6 (13.6%)	NS
NSAID	9 (18.3%)	8 (17.3%)	8 (17.1%)	NS
Alcohol	(22.4%)	9 (19.5%)	10 (22.7%)	NS

Table 2 Endoscopic findings

Finding	Patient *n*, (%)
Antral gastritis	62 (44.5)
Pangastritis	34 (24.5)
Bulbitis	14 (10)
Bile reflux gastritis	12 (8.6)
Duodenal ulcer	7 (5.3)
Atrophic gastritis	6 (4.3)
Gastric ulcer	4 (2.8)

DISCUSSION

Recently, triple therapies including a PPI and two antibiotics have been found to be the most effective eradication regimens in the treatment of *Hp* eradication[7,8]. The most common antibiotics used in the triple therapies were amoxicillin, clarithromycin and metronidazole[7,8]. Treatment regimens including PPIs are now used at all stages of the *Hp* eradication. The highest eradication rates for *Hp* (80-95%) have been achieved by using antibiotics at least for one week[9]. However, even the highest doses of omeprazole or an increased treatment duration for 2 wk did not provide 100% eradication[10-13]. In the European consensus meeting, it suggested that PPI treatment for one week including amoxicillin and clarithromycin was the first line therapy[10].

Our study showed that triple therapy for 2 wk was safe and well tolerated. The patient compliance was 95%. However, the eradication rate was 45%. Similarly in a study from Adana (Southern Anatolia), a two-week usage of lansoprazole, amoxicillin and clarithromycin resulted in 59% eradication[14]. In Istanbul (North Western Anatolia) and Nigde (Central Anatolia) the eradication rates were found below 50% in two different studies[15,16].

Similarly, in Iran, the eradication rates with omeprazole, amoxicillin and clarithromycin were found to be below 70%[17]. Also, some European studies reported similar rates of eradication[12,13,18-20,22,23]. Rinaldi[21] studied 278 patients by using a treatment regimen similar to ours (omeprazole, lansoprazole and pantoprazole in combination with amoxicillin and clarithromycin for one week). The eradication rates were found to be 86%, 74% and 76% respectively, which were higher than our results, yet far beyond the acceptance levels[21].

Different eradication results obtained by similar treatment regimens suggest that resistance to antibiotics, virulent factors of *Hp* or type of gastroduodenal disorders of patients might have played a role in the outcomes. In some of the studies resulted in lower eradication rates, the resistance to clarithromycin was as high as 10%[24]. In a study carried out in Ankara (Central Anatolia), the resistance to clarithromycin was 11.4%[25]. An Italian study found the primary resistance to clarithromycin was 3.2%[26]. The primary resistance to macrolides was between 3-12% in Europe and 2-10% in the United States[27,28]. We did not investigate the resistance to antibiotics in the present study. However, we believe that the resistance to antibiotics might have played an important role in our results. Also the majority of the events were from the non-ulcer dyspepsia group, therefore this might have an effect on the result because a lower rate of eradication was reported in patients with non-ulcer dyspepsia compared to those with peptic ulcer[24,29]. Our results showed that patients with pangastritis had a better eradication than those with antral gastritis ($P<0.05$). This was in compliance with the correlation between the severity of gastritis and the rate of eradication[30,31].

In conclusion, our findings from Mersin (Southern Anatolia) with lower eradication rates obtained by similar treatment regimens compared to other districts in Turkey and in the World demonstrate that it is necessary to find out a treatment scheme specific to the district. The findings prove that standard treatment regimens might not be suitable and therefore establishment of a new treatment protocol in accordance with the results obtained locally is inevitable. We believe that the lower rates of eradication might have resulted from the resistance to antibiotics.

REFERENCES

1 **Fennerty MB.** What are the treatment goals for helicobacter pylori infection? *Gastroenterology* 1997; **113** (Suppl): S120-125

2 **Malfertheiner P,** Megraud F, O' Morain C, Hungin AP, Jones R, Axon A, Graham DY, Tytgat G. European *Helicobacter pylori* Study Group (EHPSG). Current concepts in the management of helicobacter pylori infection-The Maastricht 2-2 000 Consen-

sus report. *Aliment Pharmacol Ther* 2002; **16**: 167-180

3   **Herrerias JM,** Bujanda L, Pena D. Efficacy and cost study in Portugal and Spain of three different 7 day eradication regimens of *Helicobacter pylori. Gastroenterology* 1999; **116**: A186

4   **Spinzi GC,** Bortoli A, Corbellini A. One week therapy with omeprazole (PPÝ) or ranitidine bismuth citrate (RBC) and two antibiotics for the eradication of *Helicobacter pylori* in duodenal ulcer: a preliminary report. *Gastroenterolgy* 1998; **116**: A294

5   **Sung JY,** Leung WK, Ling TK, Yung MY, Chan FK, Lee YT, Cheng AF, Chung SC. One week use of ranitidine bismuth citrate, amoxicillin and claritromycin for the treatment of *Helicobacter pylori* related duodenal ulcer. *Aliment Pharmacol Ther* 1998; **12**: 723-730

6   **Susi D.** The best treatment for *Helicobacter pylori* infection among for different 7 day triple therapies. *Gut* 1998; **43** (Suppl 2): A80

7   **Peura DA.** The report of the digestive health initiative international update conference on *Helicobacter pylori. Gastroenterology* 1997; **113**: 4-8

8   **Chey WD.** Treating *Helicobacter pylori*: candidate and regimen selection. *Contemp* 1997; **9**: 52-61

9   **Pounder RE.** New developments in *H pylori* eradication therapy. *Scand J Gastroenterol* 1997; **32** (suppl): 43-45

10   **The European Helicobacter Pylori Study Group.** Current European concepts in the management of *Helicobacter pylori* infection. The Maastricht Consensus Report. Gut 1997; **41**: 8-13

11   F**orne M,** Viver JM, Esteve M, Fernandez-Banares F, Lite J, Quintana S, Salas A, Garau J. Randomized clinical trial comparing two one week triple therapy regimens for the eradication of *Helicobacter pylori* infection and duodenal ulcer healing. *Am J Gastroenterol* 1998; **93**: 35-38

12   **Delchier JC,** Elamine I, Goldfain D , Chaussade S, Barthelemy P, Idstrom JP. Omeprazole-amoxicillin versus omeprazole-amoxicillin-clarithtomycin in the eradication of *Helicobacter pylori. Aliment Pharmacol Ther* 1995; **10**: 263-268

13   **Scwartz H,** Krause R, Sahba B, Haber M, Weissfeld A, Rose P, Siepman N, Freston J. Triple versus dual therapy eradication of *Helicobacter pylori* and preventing ulcer recurrence: a randomized, double-blind, multicenter study of lansoprazole, clarithyromycin, and/or amoxicillin in different dosing regimens. *Am J Gastroenterol* 1998; **93**: 584-590

14   **Ergün Y,** Abaylı B, Öksüz M. Helikobakter pilori pozitif kronik aktif gastritli hastalarda degisik iki tedavi protokolünün etkinligi. *Turk J Gastroenterol* 2002; **13**(Suppl 1): 86

15   **Bölükbası F,** Kılıç H, Bölükbası C. *Helikobakter pilori* eradikasyonu sonrası reflü özefajit sıklıgı. *Turk J Gastroenterol* 2001; **12**(Suppl 1): 87

16   **Bölükbası F,** Kılıç H, Bölükbası C. *Helikobakter* pilori eradikasyon tedavisinde eradikasyon oranları ve tedavi süresinin bu oranlara etkisi. *Turk J Gastroenterol* 2001; **12**(Suppl 1): 88

17   **Sotoudehmanesh R,** Malekzadeh R, Vahedi H, Dariani NE, Asgari AA, Massarrat S. Second-line *Helicobacter pylori* eradication with a furazolidon-based regimen in patients who have failed a metranidazole-based regimen. *Digestion* 2001; **64**: 222-225

18   **Tursi A,** Cammarato G, Montalto M, Papa A, Veneto G, Cuoco L, Trua F, Branca G, Fedeli G, Gasbarrini G. Low-dose omeprazole plus clariythromycin and either tinidazole or amoxicillin for

Helicobacter pylori infection. *Aliment Pharmacol Ther* 1996; **10**: 285-288

19   **Spinzi GC,** Bierty L, Bortoli A, Colombo E, Fertitta AM, Lanzi GL, Venturelli R, Minoli G. Comparison of omeprazole and lansoprazole in short term triple therapy for *Helicobacter pylori* infection. *Aliment Pharmacol Ther* 1998; **12**: 433-438

20   **Catalano F,** Catanzaro R, Bentivegna C, Brogna A, Condorelli G, Cipolla R. Ranitidine bismuth citrate versus omeprazole triple therapy for *Helicobacter pylori* infection. *Aliment Pharmacol Ther* 1998; **12**: 59-62

21   **Rinaldi V,** Zullu A, De Francesco V, Hassan C, Winn S, Stoppino V, Faleo D, Attili AF. *H pylori* eradication with proton pomp inhibitor based triple therapies and re-treatment with ranitidine bismuth citrate based triple therapy. *Aliment Pharmacol Ther* 1999; **13**: 163-168

22   **Deltenre M,** Jonas C, van Gossum M, Buset M, Otero J, De Koster E. Omeprazole-based antimicrobial thérapies: results in 198 *H pylori* positive patients. *Eur J Gastroenterol Hepatol* 1995; **7**(Suppl 1): 39-44

23   **Labenz J,** Stolte M, Peitz U, Tillenburg B, Becker T, Borsch G. One-week triple therapy with omeprazole, amoxicillin and clarithromycin or metranidazole for cure of *Helicobacter pylori* infection. *Aliment Pharmacol Ther* 1996; **10**: 207-210

24   **Biggard MA,** Delchier JC, Riachi G, Thibault P, Barthelemy P. One week triple therapy using omeprazole, amoxicillin and clarithromycin for the eradication of *Helicobacter pylori* infection in patients with non-ulcer dyspepsia: influence of dosage of amoxicillin and clarithromycin. *Aliment Pharmacol Ther* 1998; **12**: 383-388

25   **Özaslan E,** Balaban G, Tatar H. *Helikobakter pilori* eradikasyonunda en yaygın kullanılan LAK protokolünün baþarısı azalıyor mu? *Turk J Gastroenterol* 2001; **12**(Suppl 1):93

26   **Bazzoli F,** Zagari M, Pozzato P, Varoli O, Fossi S, Ricciardiello L, Alampi G, Nicolini G, Sottili S, Simoni P, Roda A, Roda E. Evaluation of short term low dose triple therapy for the eradication of *Helicobacter pylori* by factorial design in a randomized, double-blind, controlled study. *Aliment Pharmacol Ther* 1998; **12**: 439-445

27   **Huang JQ,** Hunt RH. Treatment failure: the problem of non-responders. *Gut* 1999; **45**(Suppl): 140-144

28   **Tankowic J,** Lamarque D, Lascols C, Soussy CJ, Delchier JC. The impact of *Helicobacter pylori* resistance to clarithromycin on the efficacy of the omeprazole-amoxicillin-clarithromycin therapy. *Aliment Pharmacol Ther* 2001; **15**: 707-713

29   **Schimd CH,** Ross SD, Witing GW. Omeprazole plus antibiotics in the eradication of *Helicobacter pylori* infection: a meta regression. *Gut* 1996; **39**(Suppl 2): A37

30   **Kamada T,** Haruma K, Komoto K, Mihara M, Chen X, Yoshihara M, Sumii K, Kajiyama G, Tahara K, Kawamura Y. Effect of smoking and histological gastritis severity on the rate of *Helicobacter pylori* eradication with omeprazole, amoxicillin and clarithromycin. *Helicobacter* 1999; **4**: 204-210

31   **Georgopoulos SD,** Ladas SD, Karatapanis S, Mentis A, Spiliadi C, Artikis V, Raptis SA. Factors that may affect treatment outcome of triple *Helicobacter pylori* eradication therapy with omeprazole, amoxicillin, and clarithromycin. *Dig Dis Sci* 2000; **45**: 63-67

Edited by Wang XL **Proofread by** Xu FM

• BRIEF REPORTS •

Liver regional continuous chemotherapy: Use of femoral or subclavian artery for percutaneous implantation of catheter-port systems

An-Long Zhu, Lian-Xin Liu, Da-Xun Piao, Ya-Xin Lin, Jin-Peng Zhao, Hong-Chi Jiang

An-Long Zhu, Lian-Xin Liu, Da-Xun Piao, Jin-Peng Zhao, Hong-Chi Jiang, Department of General Surgery, First Clinical College, Harbin Medical University, Harbin, 150001, Heilongjiang Province, China
Ya-Xin Lin, Department of Neurology, Heilongjiang Province Hospital, Harbin 150036, Heilongjiang Province, China
Supported by National Natural Science Foundation of China, No. 30300339
Correspondence to: Lian-Xin Liu, Department of General surgery, First Clinical College, Harbin Medical University, Harbin, 150001, Heilongjiang Province, China. liulianxin@sohu.com
Telephone: +86-451-53658828   **Fax:** +86-451-53670428
Received: 2004-02-06   **Accepted:** 2004-02-18

Abstract

AIM: To evaluate the feasibility and safety of the intraarterial chemotherapy of the liver cancer by an interventional method, catheter-port system.

METHODS: Thirty-two catheter-port systems were implanted percutaneously via the femoral artery or subclavian artery. Chemotherapies were performed 0-5 d after the implantation of the catheter-port systems. The mean interval between two sequent chemotherapies was 4 wk. The occurrence of side effects of the implantation was examined clinically.

RESULTS: Implantation of the catheter-port was successful in all patients. Mean patency period was 210 d. One occlusion (3.1%) of the catheter was observed. Displacement of the catheter was observed in one case (3.1%). One patient rated a hematoma in the chest wall as important. Mild hematoma was reported in 8 cases (25%). In 3 of 32 cases (9.4%), mild pain was reported initially, and dysesthesia was reported in seven (21.9%). No patient rated overall discomfort as mild, severe, or important.

CONCLUSION: Percutaneous placement is feasible and safe for liver regional continuous chemotherapy. Compared with surgical placement, the overall complication rate is comparable or less.

INTRODUCTION

Systemic chemotherapy in cases of liver cancer and liver metastases of colorectal cancer has nearly been abandoned due to the high non-response rates. Regional continuously intraarterial chemotherapy has demonstrated better response rates than systemic chemotherapy[1-4]. Percutaneously implantable catheter-port systems have been developed for long-term use to facilitate the long-term administration of chemotherapeutic agents. These systems allow easy and repetitive puncture in infusion therapy without doing much harm to the vessels, and their use is comfortable for the patient. So far, the implantation of permanent intraarterial catheter systems in the gastroduodenal artery[1,5-9] or via the subclavian, axillary, or brachial arteries into the common hepatic artery[10-12] has been performed surgically with considerable complication rates. Moreover, the repair and replacement of malfunctioning port systems previously required surgery[9,13,15,16]. Thus far, percutaneous implantation of catheter-port systems for intraarterial use in various target organs, particularly in regional chemotherapy of the liver, has been successfully performed by radiologists[14,17-20].

MATERIALS AND METHODS

Patients

From December 1999 to July 2003, 32 percutaneously implantable catheter-port systems (B|BRAUN, Germany) were placed in 32 patients (23 men and 9 women; age range, 26-65 years; mean age, 56 years) with primary malignancies of the liver (26 cases) and metastasizes (6 cases). Three patients had Cholangioma within the 25 primary malignancies. In all patients, the catheter-port system implanted percutaneously with radiologic guidance was the first method used to administer intraarterial chemotherapy. One patient had been performed intervention for 2 times because the catheter-port systems failed to be implanted through the femoral arteries in the first performance of intervention. The catheter-ports were implanted percutaneously through subclavian arteries in the second time. We obtained informed consent from each patient prior to the procedure.

Catheter-port system

The standard catheter-port device consisted of a polysulphone port reservoir with a silicone septum at the puncture site and a lateral stem to slip the silicone catheter over. The connection between the silicone catheter and the polyurethane catheter was reinforced with a small plastic cannula. The port reservoir, polyurethane catheter, cannula, and suture material were commercially available as part of the standard catheter-port system.

Technical procedure

The angiographic catheter was advanced into the respective target vessel such as the common or proper hepatic artery with fluoroscopic guidance after the common femoral or subclavian artery was punctured with use of the Seldinger technique, and visceral arteriography was performed to assess variant arterial supply. The final position of the catheter tip, and thereby the region of perfusion, was chosen according to the anatomy of each patient and the location of the lesion at digital subtraction angiography. The catheter tip was placed into the right hepatic artery ($n=9$), the proper hepatic artery ($n=21$), and the common hepatic artery ($n=1$). The latter position was used in one patient

with variant common hepatic artery without the proper hepatic artery (Figure 1). In this patient, the gastroduodenal artery was occluded because of the variant arterial supplies (Figure 2). The correct position of the catheter was verified with digital subtraction angiography.
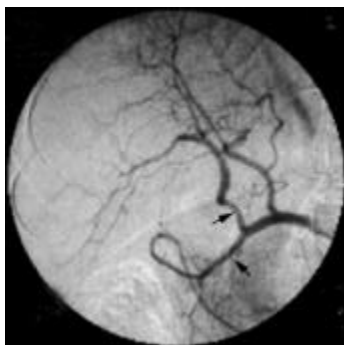

Figure 1 The gastroduodenal artery is the end of the branch of the common hepatic artery. The proper hepatic artery was absent. Gastroduodenal artery (white arrow), right hepatic artery (black arrow).
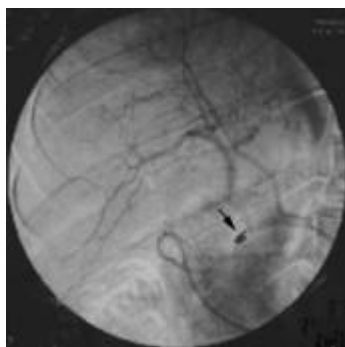

Figure 2 The gastroduodenal artery has been occluded by a fibered platinum coil (arrow).

The catheter-port systems were implanted percutaneously in inpatients. The antibiotic agent was given 20 min before operation and no conscious sedation treatment was administered.

To insert the catheter-port system, an incision approximately 3 cm long was made in the skin distally to the right groin at the anterior surface of the thigh or at the anterior surface of the left or right chest wall, starting from 3 cm distally to the cutaneous puncture site and leading downward along the femoral triangle or leading parallel to the dermatoglyph. A subcutaneous pocket was then formed wherein the port reservoir was to be placed. The end of the catheter was cut off distally to the puncture site, and then was connected tightly to the port reservoir.

Tunneling was made from the puncture site to the incision and the port reservoir was not fixed to the subcutaneous tissue with an extra suture (Figure 3). Final port angiography helped verify the integrity of the system and correct position of the catheter. When necessary, malposition or dysfunction was corrected before the subcutaneous pocket was closed. A compression bandage was applied in each patient for 24 h.

The patients were mobilized 24 h after the intervention. There were no restrictions on patient activity 24 h after the device was in place. Bed rest was not necessary. By choice, most patients stayed in hospital until the onset of chemotherapy, which was 0-5 d after implantation (mean, 2 d) because of the healing of the incisions or the amelioration of liver function. We regularly flushed the catheter system with 10 mL of heparin sodium (25 eIU/mL heparin) at the end of each chemotherapeutic cycle, and before final withdrawal of the port needle, but not between two chemotherapeutic cycles. Patients did not receive any anticoagulation therapy systemically or via the catheter system. At the end of the study, no patients were lost to follow-up. Correct functioning of each catheter-port system was verified with digital subtraction angiography prior to each chemotherapeutic treatment cycle. At each angiographic study, patients were examined clinically for the occurrence of negative side effects, such as peripheral embolization, occlusion. They were also asked to complete a questionnaire regarding their satisfaction with the percutaneously implanted catheter-port system and the presence of local complications, such as hematoma, infection, pain, restriction of motion, dysesthesia, and long-term discomfort. The patients rated these complications as absent, mild, or important. Mild hematoma was defined as discoloration of the skin without subcutaneous swelling or induration for a maximum of 1 wk. Important hematoma was defined as subcutaneous induration with palpable liquid collection around the device of more than 2 cm in diameter.

Figure 3 Fluoroscopic image depicts a catheter-port system in the right side of the groin in a 36-year-old male patient with hepatic carcinoma catheter (arrowheads), stem (large open arrow), and port reservoir (thin black arrow).

RESULTS

Implantation of the catheter-port was successful in all patients. Only 2 patients were performed for 2 times because of the failures of implantation through femoral arteries in the first operation. We changed to the subclavian artery and the implantation was successful in the second time. All implantation procedures were performed in the interventional radiology suite with a mean procedure time of 51 min (range, 30-145 min). No peri-interventional complications were noticed. The mean follow-up of the systems was 210 d (range, 36-680 d).

Complications occurred in 2(6.25%) of 32 cases. One occlusion (1 of 32 cases, 3%) of the catheter was observed on d 36. The occlusion was a result of misuse of heparin solution after the chemotherapy with a subsequent reflux of blood into the catheter. Because lytic therapy with 10 000 IU of urokinase in 2 mL of water solution was not successful in this patient, the catheter-port system was disused.

Displacement of the catheter was observed in one case (1 of 32 cases, 3%) at the third angiographic follow-up study. The catheter tip was dislocated into the abdominal artery and could be repositioned into the common hepatic artery by using an interventional maneuver. Since the patient did not want to continue chemotherapy, the port system was entirely disused, but was not removed by operation.

The overall disused rate was 6% (2 of 32 cases). All disused catheter-ports were not removed.

After implantation of a catheter-port system, one patient rated a hematoma in the chest wall as important, but this could not be verified at any clinical follow-up examination, and it did

not require surgical intervention. Immediately after implantation, mild hematoma was reported in 8 of 32 cases (25%), but no hemorrhage at the implantation or puncture site was found at the first follow-up examination in any of these cases. In 3 of 32 cases (9%), mild pain was reported initially, and dysesthesia was reported in 7(22%). No patient rated overall discomfort as mild, severe, or important.

Till July 2003, 145 port angiographic studies were performed as follow-up examinations at a mean interval of 4 wk between each study. The patients were examined clinically for the occurrence of side effects at the time of each angiographic examination. No patients showed signs of peripheral arterial embolization, occlusion, or embolic effects. At all follow-up examinations, we did not find infection, leakage, kinking, or disconnection of any catheter-port system. According to the patient questionnaires, all patients were entirely satisfied with the system. No patient reported restriction of motion or discomfort owing to the port reservoir in the groin or chest wall.

DISCUSSION

Continuous chemotherapeutic infusion has proved to be prior to the systemic chemotherapy in liver cancer. Permanent percutaneously implanted catheter-port systems are widely used method for it with the advantage for repeated external arterial or central venous access for regional or systemic chemotherapy and prolonged parenteral nutrition[2,6,16]. The majority of catheter-port devices developed for intraarterial regional chemotherapy have necessitated surgical implantation before the interventional method was applied clinically[7,11,21-23]. The common sites of surgical implantation are gastroduodenal, common or proper hepatic arteries for regional intraarterial chemotherapy of the liver.

It has been reported the implantation of an intraarterial catheter-port with fluoroscopic guidance in the interventional radiology suite without laparotomy[8]. The femoral arteries were used for minimally invasive catheter placement. Radiologic implantation is also associated with various complications, such as catheter dislocation, occlusion, and infection. Dislocation and occlusion of catheter are the severest complications, which lead to the termination of chemotherapy or another traumatic implantation procedure[10,12,16,23].

Thrombotic complications such as catheter occlusion and occlusion of the hepatic artery are also commonly associated with both surgically and radiologically implanted catheter-port systems[1,7,9,10,12,23]. Catheter placement via the brachial artery can also be accompanied by thrombosis or occlusion of the brachial artery[12,13]. In our patient group, one case of catheter occlusion was caused by blood reflux into the 4-F catheter. Catheters with small diameters have higher occlusion rates. Niederhuber *et al.*[20] also found that small-bore catheters had an inferior patency rate and drug infusion might be difficult owing to the higher resistance of small catheters. Some infusion pumps might stop at pressure levels that are too high. Therefore, on the basis of results in our study and the literature, we do not recommend the use of catheter below 4-F for permanent implantation in this context.

With regard to prevent catheter thrombosis, different authors have various ideas. Two methods have been recommended: administration of warfarin sodium and continuous catheter perfusion with heparin[18]. We believe that keeping blood from the lumen of catheter and perfusion with the end of each chemotherapy are the efficient methods. We do not consider systemic or other type of anticoagulation therapy necessary. Lytic therapy with tissue plasminogen activator, urokinase, or streptokinase has been reported to be useful in cases of catheter occlusion, but this method is successful only in a few cases[9,16]. In our study, lytic therapy was not effective.

But the permanent existence of the disused catheter-port system has no harm to the patient if there is no septic episode.

The frequency of dislocation appeared to be particularly high when the axillary or brachial artery was used[10,12]. It could be due to the too soft and flexible catheter material and the mobility of the upper limb. In our study, displacement occurred in one of our cases (3.1%), in which the port reservoir was implanted in the chest wall through right subclavian artery, into the abdominal artery. Retrospectively, we believe this displacement into the abdominal artery was probably due to too much tension on the indwelling catheter and the mobility of upper limb. Therefore, optimal catheter configuration and the approach are crucial. We recommend that the right femoral artery should be the best approach.

Infection is another complication in permanently implanted catheter systems that often makes removal of the device necessary[8,19,24,29,30]. Infection rates ranged from 0%[25-28] to 7.6%[11,17,23,24]. Infection and sepsis during chemotherapy can be caused by the use of inappropriate hygienic measures and can be treated successfully with antibiotic therapy. It has been noticed that after an infected catheter-port system was removed and replaced with a new one, however, infection recurred in some patients[14]. In our study patients, antibiotic agents were administered 20 min before operation for the aim of prophylaxis of infection, and infection was not observed. Infection rates after radiologic implantation are lower than those after surgical implantation. Therefore, interventional radiology suites and the antibiotic agent seem to provide sufficient hygienic conditions for this type of intervention.

The relatively low complication rate and pain increase patient acceptance of this procedure. Placement of the catheter-port system on the anterior surface of the thigh below the groin or chest wall seems to be well accepted, even in very active patients. Its superficial placement allows easy palpation and puncture, and provides little risk for dislocation or disconnection of the port needle from the reservoir during chemotherapy. But careful palpations are required in obese patients.

Radiologic implantation of catheter-port systems is a quick and simple procedure that does not require general anesthesia compared with surgical implantation. Patency rates are equal to or higher than those for surgically implanted systems. Radiologic placement is also possible in patients with anatomic vascular variations. In contrast to the surgical method, catheter-port systems placed radiologically cause less morbidity in the case of dysfunction, because the systems can be removed or repositioned more easily. Complicated surgical revisions or corrections requiring laparotomy can be avoided as proposed by Doughty *et al*[31]. Radiologic placement does not allow performance of preventive cholecystectomy to avoid cholecystitis, but this does not seem to be a crucial problem.

Our results indicate that percutaneous implantation of a catheter-port system via the femoral artery or subclavian artery is easy to perform, simplifies intraarterial chemotherapy of the liver with equal patency rates, and has fewer complications as compared with surgical placement, and is well accepted by patients.

REFERENCES

1   **de Takats PG,** Kerr DJ, Poole CJ, Warren HW, McArdle CS. Hepatic arterial chemotherapy for metastatic colorectal carcinoma. *Br J Cancer* 1994; **69:** 372-378

2   **Sterchi JM.** Hepatic artery infusion for metastatic neoplastic disease. *Surg Gynecol Obstet* 1985; **160:** 477-489

3   **Hohn DC,** Stagg RJ, Friedman MA, Hannigan JF Jr, Rayner A, Ignoffo RJ, Acord P, Lewis BJ. A randomized trial of continuous intravenous versus hepatic intraarterial floxuridine in patients with colorectal cancer metastatic to the liver: the Northern California Oncology Group trial. *J Clin Oncol* 1989; **7:** 1646-1654

4   **Chang AE,** Schneider PD, Sugarbaker PH, Simpson C, Culnane

M, Steinberg SM. A prospective randomized trial of regional versus systemic continuous 5-fluorodeoxyuridine chemotherapy in the treatment of colorectal liver metastases. *Ann Surg* 1987; **206:** 685-693

5   **Kemeny N,** Seiter K, Conti JA, Cohen A, Bertino JR, Sigurdson ER, Botet J, Chapman D, Mazumdar M, Budd AJ. Hepatic arterial floxuridine and leucovorin for unresectable liver metastases from colorectal carcinoma. New dose schedules and survival update. *Cancer* 1994; **73:** 1134-1142

6   **Link KH,** Sunelaitis E, Kornmann M, Schatz M, Gansauge F, Leder G, Formentini A, Staib L, Pillasch J, Beger HG. Regional chemotherapy of nonresectable colorectal liver metastases with mitoxantrone, 5-fluorouracil, folinic acid, and mitomycin C may prolong survival. *Cancer* 2001; **92:** 2746-2753

7   **Strecker EP,** Ostheim-Dzerowycz W, Boos IB. Intraarterial infusion therapy via a subcutaneous port for limb-threatening ischemia: a pilot study. *Cardiovasc Intervent Radiol* 1998; **21:** 109-115

8   **Oberfield RA,** McCaffrey JA, Polio J, Clouse ME, Hamilton T. Prolonged and continuous percutaneous intra-arterial hepatic infusion chemotherapy in advanced metastatic liver adenocarcinoma from colorectal primary. *Cancer* 1979; **44:** 414-423

9   **Ekberg H,** Tranberg KG, Lundstedt C, Hanff G, Ranstam J, Jeppsson B, Bengmark S. Determinants of survival after intraarterial infusion of 5-fluorouracil for liver metastases from colorectal cancer: a multivariate analysis. *J Surg Oncol* 1986; **31:** 246-254

10   **Okuyama K,** Tohnosu N, Koide Y, Awano T, Matsubara H, Sano T, Nakaichi H, Funami Y, Matsushita K, Kikuchi T. Complications and their management in intraarterial infusion chemotherapy. *Gan To Kagaku Ryoho* 1992; **19:** 1007-1013

11   **Allen-Mersh TG,** Earlam S, Fordy C, Abrams K, Houghton J. Quality of life and survival with continuous hepatic-artery floxuridine infusion for colorectal liver metastases. *Lancet* 1994; **344:** 1255-1260

12   **Laffer U,** Durig M, Bloch HR, Zuber M, Stoll HR. Implantable catheter systems. Experience with 205 patients. *Dtsch Med Wochenschr* 1989; **114:** 655-658

13   **Germer CT,** Boese-Landgraf J, Albrecht D, Wagner A, Wolf KJ, Buhr HJ. The fully implantable minimally invasive hepatic artery catheter for locoregional chemotherapy of nonresectable liver metastases in defective conventional implanted therapy catheters. *Chirurg* 1996; **67:** 458-462

14   **Kuroiwa T,** Honda H, Yoshimitsu K, Irie H, Aibe H, Shinozaki K, Nishie A, Nakayama T, Masuda K. A safe and simple method of percutaneous transfemoral implantation of a port-catheter access system for hepatic artery chemotherapy infusion. *Gan To Kagaku Ryoho* 2001; **28:** 1573-1577

15   **Pullyblank AM,** Carey PD, Pearce SZ, Tanner AG, Guillou PJ, Monson JR. Comparison between peripherally implanted ports and externally sited catheters for long-term venous access. *Ann R Coll Surg Engl* 1994; **76:** 33-38

16   **Harvey WH,** Pick TE, Reed K, Solenberger RI. A prospective evaluation of the Port-A-Cath implantable venous access system in chronically ill adults and children. *Surg Gynecol Obstet* 1989; **169:** 495-500

17   **Civalleri D,** Cafiero F, Cosimelli M, Craus W, Doci R, Repetto M, Simoni G. Regional arterial chemotherapy of liver tumours. I. Performance comparison between a totally implantable pump and a conventional access system. *Eur J Surg Oncol* 1986; **12:** 277-282

18   **Huk I,** Entscheff P, Prager M, Schulz F, Polterauer P, Funovics J. Patency rate of implantable devices during long-term intraarterial chemotherapy. *Angiology* 1990; **41:** 936-941

19   **Ross MN,** Haase GM, Poole MA, Burrington JD, Odom LF. Comparison of totally implanted reservoirs with external catheters as venous access devices in pediatric oncologic patients. *Surg Gynecol Obstet* 1988; **167:** 141-144

20   **Niederhuber JE,** Ensminger W, Gyves JW, Liepman M, Doan K, Cozzi E. Totally implanted venous and arterial access system to replace external catheters in cancer treatment. *Surgery* 1982; **92:** 706-712

21   **Wopfner F.** Treatment of inoperable liver metastases: preliminary results with intrahepatic chemotherapy via a new type of indwelling catheter (author' s transl). *Dtsch Med Wochenschr* 1981; **106:** 1099-1102

22   **Balch CM,** Urist MM, McGregor ML. Continuous regional chemotherapy for metastatic colorectal cancer using a totally implantable infusion pump. A feasibility study in 50 patients. *Am J Surg* 1983; **145:** 285-290

23   **Buchwald H,** Grage TB, Vassilopoulos PP, Rohde TD, Varco RL, Blackshear PJ. Intraarterial infusion chemotherapy for hepatic carcinoma using a totally implantable infusion pump. *Cancer* 1980; **45:** 866-869

24   **Dresing K,** Lottner C, Stock W. Port-catheter perforation into the duodenum and other early complications after port implantation before intra-arterial infusion therapy of the liver with chemotherapeutic drugs. *Med Klin* 1991; **86:** 245-250

25   **al-Hathal M,** Malmfors G, Garwicz S, Bekassy AN. Port-A-Cath in children during long-term chemotherapy: complications and outcome. *Pediatr Hematol Oncol* 1989; **6:** 17-22

26   **Hohn DC,** Rayner AA, Economou JS, Ignoffo RJ, Lewis BJ, Stagg RJ. Toxicities and complications of implanted pump hepatic arterial and intravenous floxuridine infusion. *Cancer* 1986; **57:** 465-470

27   **Strecker EP,** Boos IB, Ostheim-Dzerowycz W, Heber R, Vetter SC. Percutaneously implantable catheter-port system: preliminary technical results. *Radiology* 1997; **202:** 574-577

28   **Fuchs R,** Leimer L, Koch G, Westerhausen M. Clinical experience with bacterial contamination of Port-A-Cath systems in tumor patients. *Dtsch Med Wochenschr* 1987; **112:** 1615-1618

29   **Zanon C,** Grosso M, Zanon E, Veltri A, Alabiso O, Bazzan M, Chiappino I, Mussa A. Transaxillary access to perform hepatic artery infusion (HAI) for secondary or primitive hepatic tumors. *Minerva Chir* 1996; **51:** 755-758

30   **Bern MM,** Lokich JJ, Wallach SR, Bothe A Jr, Benotti PN, Arkin CF, Greco FA, Huberman M, Moore C. Very low doses of warfarin can prevent thrombosis in central venous catheters. A randomized prospective trial. *Ann Intern Med* 1990; **112:** 423-428

31   **Doughty JC,** Keogh G, McArdle CS. Methods of replacing blocked hepatic artery catheters. *Br J Surg* 1997; **84:** 618-619

Edited by Kumar M **Proofread by** Xu FM

• BRIEF REPORTS •

Expression of subtypes of somatostatin receptors in hepatic stellate cells

Sheng-Han Song, Xi-Sheng Leng, Tao Li, Zhi-Zhong Qin, Ji-Run Peng, Li Zhao, Yu-Hua Wei, Xin Yu

Sheng-Han Song, Xi-Sheng Leng, Tao Li, Zhi-Zhong Qin, Ji-Run Peng, Li Zhao, Yu-Hua Wei, Xin Yu, Department of Hepatobiliary Surgery, Peking University People's Hospital, Beijing 100044, China
Correspondence to: Xi-Sheng Leng, Professor, Department of Hepatobiliary Surgery, Peking University People's Hospital, Beijing 100044, China. lengxs2003@yahoo.com.cn
Telephone: +86-10-6868792703

Abstract

AIM: To elucidate the mechanism by which somatostatin and its analogue exert the influence on liver fibrosis, and to investigate the mRNA expression of somatostatin receptors subtypes (SSTRs) and the distribution of somatostatin analogue octreotide in rat hepatic stellate cells (HSCs).

METHODS: HSCs were isolated from Sprague Dawley (SD) rats by *in situ* perfusion and density gradient centrifugation. After several passages, the mRNA expression of 5 subtypes of SSTRs were assessed by reverse transcription-polymerase chain reaction (RT-PCR). HSCs were planted on coverslip and co-cultured with octreotide tagged by FITC. Then the distribution of FITC fluorescence was observed under laser scanning confocal microscope (LSCM) in 12-24 h.

RESULTS: There were mRNA expression of SSTR2, SSTR3 and SSTR5 but not SSTR1 and SSTR4 in SD rat HSCs. The mRNA expression level of SSTR2 was significantly higher than that of other subtypes ($P<0.01$). FITC fluorescence of octreotide was clearly observed on the surface and in the cytoplasm, but not in the nuclei of HSCs under LSCM.

CONCLUSION: The effect exerted by somatostatin and its analogues on HSCs may mainly depend on the expression of SSTR2, SSTR3 and SSTR5. Octreotide can perfectly combine with HSCs, and thereby exerts its biological activity on regulating the characters of active HSCs. This provides a potential prevention and management against liver fibrosis.

INTRODUCTION

In recent years, it has become clear that HSCs play an important role during occurence and progress of hepatic fibrosis and portal hypertension[1,2]. HSCs are located in a perisinusoidal orientation within the sinusoid and encircle vascular endothelial cells. They can also contract or relax in response to various vasoactive mediators. All of these suggest that these cells may have the capacity to modulate intrahepatic vascular resistance and blood flow at the sinusoidal level[3]. When HSCs are activated and proliferated abundantly, they can excrete many kinds of cytokine related to fibrosis to promote synthesis and deposition of extracellular matrix (ECM)[4,5]. Therefore, how to reduce and inhibit activation and proliferation of HSCs has become a hot spot in the area of liver fibrosis research[6].

Somatostatin and its analogues have comprehensive inhibitory actions on proliferation of many kinds of cells and the capacity to induce apoptosis, so they have been applied in cancer biotherapy at the present time[7,8]. The biological base by which somatostatin exerts its actions is the existence of somatostatin receptors (SSTRs). SSTRs belong to G-protein-coupled receptors family and are located on cell membrane. Only after somatostatin combines with SSTRs, could it exert the actions of anti-proliferation. Up to date, five different SSTR subtypes, termed SSTR1 to SSTR5, have been cloned and characterized[9].

In this research, we studied the mRNA expression and distribution of somatostatin receptors in hepatic stellate cells (HSCs) of rats to elucidate the mechanism by which somatostatin and its analogue exert the influence on liver fibrosis.

MATERIALS AND METHODS

Materials

Male Sprague Dawley rats, weighing (450±50) g, were purchased from Experimental Animal Center of the Chinese Academy of Medical Science, Beijing, China. Nycodenz, fluorescein isothiacyanate (FITC) and collagenase IV were purchased from Sigma Co., U.S.A. Fetal bovine serum (FBS), Dulbecco MEM (DMEM) culture medium, Trizol and superscript II reverse transcriptase were produced by Gibco Co., U.S.A. Taq DNA polymerase, dNTPs, Oligo (dT) and RNasin were products of Promega Co. Octreotide (0.1 g/mL) was provided by Novartis Co. Mouse anti-human desmin antibody and rabbit anti-cow glial fibrillary acidic protein (GFAP) antibody were purchased from Genetech Co. Primers were synthesized by Shanghai Sangon Co.

Isolation and culture of hepatic stellate cells (HSC)

Adult male Sprague Dawley rats (450±50 g) were treated in accordance with the institution's guidelines for the care and use of laboratory animals in research. All procedures were performed with animals under ether anesthesia. According to the method of Geerts and Weng *et al*[10,11], HSCs were isolated by *in situ* perfusion and density gradient centrifugation with nycodenz. Firstly, the trochar was inserted into the rat's portal vein and the liver was perfused with pre-perfusion liquid. Then the liver was removed from the body and continuously perfused with perfusion liquid containing collagenase IV to digest the extracellular matrix. After centrifugation with 150 g/L nycodenze, the cells located in the interface were extracted and cultured in DMEM containing 200 mL/L FBS. HSC were fully stick to the wall within 48 h. Then the culture medium was exchanged in every 2-3 d. The identification of HSC was performed by observation of ultraviolet-excited fluorescence of vitamine A

lipid droplet in HSC and immunocytochemical stain for desmin and GFAP.

Isolation of total RNA and semiquantitative RT-PCR

Total RNA was isolated from HSC with Trizol by phenol-chloroform extraction and isopropanol precipitation following manufacturer's instructions. Reverse transcription of total RNA was carried out according to the instructions of the RT kit. Design of specific primers against rat SSTRs sequences was refered to the references[12] and verified in NCBI Blast. They are shown in Table 1. The PCR system (total 25 μL) contained 40 pmol/L primers of SSTRs or β-actin, 0.5 μL of 10 mmol/L dNTPs, 1.5 μL of 50 mmol/L MgCl$_2$, 2 μL of cDNA, 2.5 μL of 10×PCR buffer, 2.5 μL of Taq DNA polymerase. The PCR conditions included an initial denaturation for 5 min at 94 ℃; 40 amplification cycles consisting of denaturation at 94 ℃ for 1 min, primer annealing at 60 ℃ for 1 min and elongation at 72 ℃ for 1 min; and a final extension at 72 ℃ for 7 min. The PCR products or DNA marker mixed with 2 μL of loading buffer were electrophoresed on a 15 g/L agarose gel and visualized under ultraviolet light excitation. Then the images were taken and anlaylized by Kodak digital camera and science software (Kodak, EDAS290, U.S.A). The expression of SSTRs was calculated by determining the ratio of SSTRs relative to β-actin.

Table 1 Primer sequence and expected PCR product length

Primer designation		Sequence	Product length
SSTR1	upstream	5'-CAC GCA CCG CAG CCA ACA-3'	390 bp
	downstream	5'-GGA AGC CGT AGA GTA TGG GGT T-3'	
SSTR2	upstream	5'-CCG GAG CAA CCA GTG GGG-3'	390 bp
	downstream	5'-GCG TAC AGG ATG GGG TTG GC-3'	
SSTR3	upstream	5'- CCC GGG GCA TGA GCA CGT-3'	415 bp
	downstream	5'-AAG CCG TAG AGG ATG GGG TTT GC-3'	
SSTR4	upstream	5'-TCG TGG GGG TGA GGC AGT AG-3'	365 bp
	downstream	5'-CAT AGA GAA TCG GGT TGG CAC AG-3'	
SSTR5	upstream	5'-ATG GAG CCC CTC TCT CTG G-3'	250 bp
	downstream	5'-CGT CAG CCA CGG CCA GGT T-3'	
β-actin	upstream	5'-TGG GAC GAT ATG GAG AAG AT–3'	522 bp
	downstream	5'-ATT GCC GAT AGT GAT GAC CT –3'	

The observation of combination of octreotide with HSC and distribution in HSC

After 3-4 passages, HSCs were planted on coverslip and culture medium was exchanged after sticking to the walls. Then octreotide tagged by FITC was added into the culture medium (10 μg/mL). After 24 h, the culture medium was removed and the coverslips were rinsed three times with PBS, whereafter the distribution of FITC fluorescence in live HSCs was observed by laser scanning confocal microscope (LSCM).

Statistical methods

The results of electrophoresis of PCR products were expressed as mean±SD and analyzed by t-test and analysis of variance.

RESULTS

Expression of mRNA of somatostatin receptor subtypes

The mRNA expression of SSTR2, SSTR3 and SSTR5 were observed, whereas those of SSTR1 and SSTR4 were not observed in rat HSCs. Moreover the mRNA expression level of SSTR2 was significantly higher than those of other subtypes (4 and 5.64 times higher than that of SSTR3 and SSTR5, respectively, $P<0.01$). There was no significant difference between the mRNA expression of SSTR3 and SSTR5 (Figures 1, 2, and 3, Table 2).

Table 2 Expression of SSTRs mRNA in quantity (mean±SD)

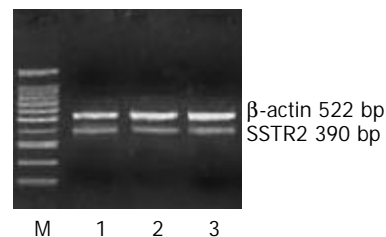| Subtypes	n	Expression of mRNA
SSTR2	3	0.8213±0.1210
SSTR3	3	0.2041±0.1662[b]
SSTR5	3	0.1457±0.1981[d]

[b]$P<0.01$ vs SSTR2, [d]$P<0.01$ vs SSTR2.

Figure 1 Expression of SSTR2 mRNA. M: 100 bp Marker; Lanes1-3: three groups of samples.
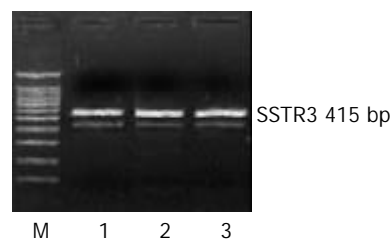

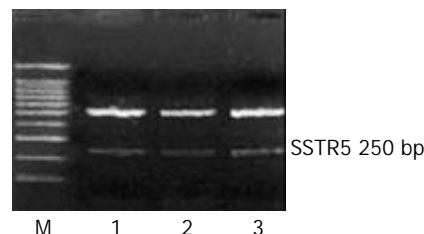**Figure 2** Expression of SSTR3 mRNA. M: 100 bp Marker; Lanes 1-3: three groups of samples.

Figure 3 Expression of SSTR5 mRNA. M: 100 bp Marker; Lanes 1-3: three groups of samples.

Distribution of octreotide in HSCs

The green fluorescence of FITC had an extensive distribution on the surface of HSCs and also in cytoplasm, but not in nucleus (Figure 4).
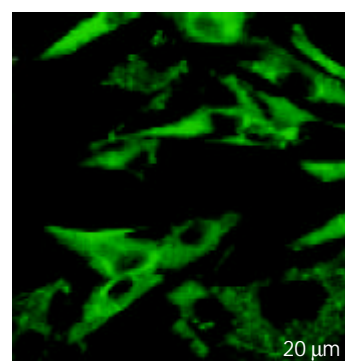

Figure 4 Distribution of the green fluorescence of octreotide tagged by FITC in live HSCs. FITC fluorescence of octreotide was clearly observed on the surface and in the cytoplasm, but not in the nuclei of HSCs under LSCM.

DISCUSSION

Several studies have demonstrated that somatostatin could restrain and decrease the process of hepatic fibrosis of rat liver cirrhosis models[14-16]. In addition, researchers studied the anti-fibrosis mechanisms of somatostatin. Reynaert *et al.*[13] proved that somatostatin could suppress rat hepatic stellate cell contraction induced by endothelin-1. Chatterjee *et al.*[17] found that in rat liver cirrhosis models of schistosomiasis, somatostatin might have the direct anti-fibrosis effects through modulating the synthesis and expression of collagen I, III and smooth muscle actin (SMA) of rat HSCs. All of these findings suggest that there are SSTRs on the surface of HSCs, thereby somatostatin could exert its actions on HSCs.

Whether SSTRs exist and what kind of SSTRs subtypes are expressed in rat HSCs? We observed mRNA expression of SSTR2, SSTR3 and SSTR5, but not of SSTR1 and SSTR4 in Sprague Dawley rat HSCs. Our results slightly differed from Reynaert *et al.*[13] that SSTR1, SSTR2 and SSTR3 were expressed, but not SSTR4 and SSTR5 in Wistar rat HSCs. Besides, we found that the mRNA level of SSTR2 was significantly higher than those of other subtypes in quantity. These results suggest that theoretically, somatostatin may be available to exert its inhibitive and pre-appoptosis actions on active HSCs by means of SSTRs (especially SSTR2) and consequently has the ability of anti-fibrotic action. Therefore, if the proper somatostatin analogues that have strong affinity to SSTR2, 3 and 5 are chosen, they will be able to exert better effect on active HSCs.

Taking advantage of the strong appetency by which somatostatin could combine with SSTRs, some researchers have applied the somatostatin analogues tagged by radioactive isotope to study the expression and distribution of SSTRs in cancer tissues and consequently the locational diagnosis of cancers. This kind of method has been proved to be satisfactory. Since our results showed that SSTR2, 3 and 5 were expressed and other studies reported that octreotide had the special affinity to SSTR2 and SSTR5[7,9], we treated HSCs with octreotide tagged by FITC. By means of the characteristics that hormones can specially bind to its receptors, we observed the green fluorescence on the surface of live HSCs, which reflected the distribution of SSTRs. This proves that octreotide has strong affinity with HSCs and thus the existence of SSTRs is supported. Meanwhile, we also observed the distribution of octreotide in the cytoplasm, but not in the nuclei of HSCs. In general, octreotide contains 8 peptides, so it can't pass through the cell membrane without other pathways were introduced. Thereby, we presume that the endocytosis conducted by the receptors may works. But whether octreotide in cytoplasm is able to exert its biological actions by a certain mechanism independent of SSTRs remains to be confirmed in the future.

In conclusion, we demonstrates that SSTR2, 3 and 5 are obviously expressed in SD rat HSCs. In addition, octreotide, a somatostatin analogue, is able to combine perfectly with HSCs and thereby exerts its biological actions on liver fibrosis in clinical practice.

REFERENCES

1   **Wu J**, Zern MA. Hepatic stellate cells: a target for the treatment of liver fibrosis. *J Gastroenterol* 2000; **35**: 665-672

2   **Pinzani M**, Gentilini P. Biology of hepatic stellate cells and their possible relevance in the pathogenesis of portal hypertension in cirrhosis. *Semin Liver Dis* 1999; **19**: 397-410

3   **Rockey DC**. Hepatic blood flow regulation by stellate cells in normal and injured liver. *Semin Liver Dis* 2001; **21**: 337-349

4   **Shen H**, Huang GJ, Gong YW. Effect of transforming growth factor beta and bone morphogenetic proteins on rat hepatic stellate cell proliferation and trans-differentiation. *World J Gastroenterol* 2003; **9**: 784-787

5   **Pinzani M**, Marra F. Cytokine receptors and signaling in hepatic stellate cells. *Semin Liver Dis* 2001; **21**: 397-416

6   **Liu XJ**, Yang L, Mao YQ, Wang Q, Huang MH, Wang YP, Wu HB. Effects of the tyrosine protein kinase inhibitor genistein on the proliferation, activation of cultured rat hepatic stellate cells. *World J Gastroenterol* 2002; **8**: 739-745

7   **Pawlikowski M**, Melen-Mucha G. Perspectives of new potential therapeutic applications of somatostatin analogs. *Neuroendocrinol Lett* 2003; **24**: 21-27

8   **Wang CH,** Tang CW, Liu CL, Tang LP. Inhibitory effect of octreotide on gastric cancer growth via MAPK pathway. *World J Gastroenterol* 2003; **9**: 1904-1908

9   **Patel YC**. Somatostatin and its receptor family. *Fron Neuroendocrinol* 1999; **20**: 157-198

10   **Geerts A**, Niki T, Hellemans K, De Crarmer D, Van Den Berg K, Lazou JM, Stange G, Van De Winkel M, De Bleser P. Purification of rat hepatic stellate cells by side scatter-activated celll sorting. *Hepatology* 1998; **27**: 590-598

11   **Weng SG**, Leng XS, Wei YH, Peng JR, Zheng ET, Cheng JH, Zham YB, Lu JF, Du RY. An improved method of isolating and identifying rat hepatic stellate cells. *Beijing Daxue Xuebao* 2001; **1**: 83-86

12   **Zhong ZH**, Zhu JY, Leng XS, Du RY. Study on mRNA expression of subtypes of somatostatin receptors in the liver tissue of liver cirrhosis rats. *Zhonghua Shiyan Waike Zazhi* 2000; **5**: 439-441

13   **Reynaert H,** Vaeyens F, Qin H, Hellemans K, Chatterjee N, Winand D, Quartier E, Schuit F, Urbain D, Kumar U, Patel YC, Geerts A. Somatostatin suppresses Endothelin1-induced rat hepatic stellate cell contraction via somatostatin receptor subtype 1. *Gastroenterology* 2001; **121**: 915-930

14   **Karalis K**, Mastorakos G, Chrousos GP, Tolis G. Somatostatin analogues suppress the inflammatory reaction *in vivo*. *J Clin Invest* 1994; **93**: 2000-2006

15   **Fort J**, Oberti F, Pilette C, Veal N, Gallois Y, Douay O, Rousselet MC, Rosenbaum J, Cales P. Antifibrotic and hemodynamic effects of the early and chronic administration of octreotide in two models of liver fibrosis in rats. *Hepatology* 1998; **28**: 1525-1531

16   **Wang J**, Gong H, Wang Y. Experimental study on the preventive effect of octreotide on liver fibrosis. *Zhonghua Gandan Waike Zazhi* 2003; **2**: 100-102

17   **Chatterjee S**, Van Marck E. The role of somatostatin in schistosomiasis: a basis for immunomodulation in host-parasite interactions? *Trop Med Int Health* 2001; **6**: 578-581

• BRIEF REPORTS •

Filamentous-actins in human hepatocarcinoma cells with CLSM

Xia Huo, Xi-Jin Xu, Yao-Wen Chen, Hai-Wei Yang, Zhong-Xian Piao

Xia Huo, Xi-Jin Xu, Yao-Wen Chen, Hai-Wei Yang, Zhong-Xian Piao, Central Laboratory, Shantou University Medical College, Shantou 515031, Guangdong Province, China
Supported by the Medical Research Fund of Guangdong Province, No. 2000004
Correspondence to: Dr. Xia Huo, Central Laboratory, Shantou University Medical College, 22 Xinlin Road, Shantou 515031, Guangdong Province, China. xhuo@stu.edu.cn
Telephone: +86-754-8900307   **Fax:** +86-754-8557562
Received: 2002-12-30   **Accepted:** 2003-02-17

Abstract

AIM: To establish a method for optical sections of HepG2 human hepatoblastoma cells with confocal laser scanning microscope (CLSM) and to study the spatial structure of filamentous actin (F-actin) in HepG2 cells.

METHODS: HepG2 cells were stained with FITC-phalloidin that specifically binds F-actin, with propidium iodide (PI) to the nucleus, and scanned with a CLSM to generate optically sectioned images. A series of optical sections taken successively at different focal levels in steps of 0.7 μm were reconstructed with the CLSM reconstruction program.

RESULTS: CLSM images showed that the FITC-stained F-actin was abundant microfilament bundles parallel or netted through the whole cell and its processes. Most F-actin microfilaments extended through the cell from one part toward the other or run through the process. Some microfilaments were attached to the plasma membrane, or formed a structural bridge connecting to the neighboring cells.

CONCLUSION: A method for double labeling HepG2 human hepatoblastoma cells and CLSM imaging F-actin microfilaments and nuclei by image thin optical sections and spatial structure was developed. It provides a very useful way to study the spatial structure of F-actin.

INTRODUCTION

Cytoskeleton, consisting of proteins, is the structural network in cells. It closely relates to the functions of cells, such as cell movement, cell morphology and transmenbrane signal conduction, etc. Observation and analysis of cell F-actin with CLSM are a precise, rapid, and simple method. This paper aimed at using CLSM in combination with double label for the observation and analysing of the three-dimensional structure of cytoskeleton system in HepG2 hepatocarcinoma cells.

MATERIALS AND METHODS

Cell culture

HepG2 cells were inoculated in improved Petri dish (normal Petri dishes with a center hole bottomed by quartz glass), with 100 mL/L BAS/RPMI-1640 as culture medium for 24-48 h in an incubator at 37 ℃ with a 950 mL/L air/50 mL/L CO_2 atmosphere. After the dish glass was covered fully with cells, the culture medium was poured out. The cells were rinsed with PBS twice, and then fixed in 40 g/L paraformaldehyde for 30 min at 4 ℃.

Specimen preparation

The above-mentioned specimens were rinsed with PBS twice, then permeabilized for 10 min in 2 g/L Triton X-100 at room temperature, and nonspecific background was blocked using 5 g/L BSA for a while. Specimens were then stained with 5 mg/L FITC-phalloidin (Sigma) at room temperature for 30 min. After that, the specimens were rinsed with PBS twice and stained with 5 mg/L PI (Sigma), and finally rinsed twice with PBS and a little PBS in dishes was reserved for observation. All procedures must be performed from light.

CLSM observation and examination

Specimens were examined with an ACAS Ultima 312 CLSM (Meridian Instruments, USA) equipped with an argon ion laser providing simultaneous excitation at 514.5 nm, 488 nm and 351-364 nm, an output power of 50 mW for the UV and 200 mW for the combined visible wavelengths, a high-precision mechanical scanning stage (0.1 μm in the X-Y plane and 0.1 μm in the Z axis), and an inverted microscope (Olympus), three photomultiplier tubes (PMT). The availability of a variety of excitation wavelengths on a single microscope setup offers the power and convenience of using combinations of fluorescent probes in a single specimen. In this experiment, the parameters were as follows: Objective: 100×1.30 oil, Pinhole: 255 μm, X points: 270, Y point: 290, Z step: 0.7 μm, Data model: Z image, Scan Type: Mirror, Step Size: 0.20 μm, Speed: 20 mm/s, Samples/pt: 15, Laser Power: 612 mw, Scan stress: 100%, PMT 1: 40%, PMT 2: 40%, Z point: 15. According to the above parameters, a series of images were collected sequentially from single optical sections at 0.7 μm intervals (15 planes per series) using the 488, 530 nm laser lines to excite FITC and PI, respectively. Randomly selected regions of specimens were scanned to image using Z-series program of CLSM. With the program the specimens could be scanned cross-sectionally along the X, Y, and Z axes, and serial optical sections of different layers could be obtained without injury. Firstly, the cell top was confirmed by prescanning, and then the specimen from top to bottom was scanned according to Z-step to obtain optical sections layer by layer, and each image was recorded. The images were electronically colored. The optical sections were reconstructed to stereoscopic images with CLSM reconstruction program.

RESULTS

The HepG2 cells stained with FITC-phalloidin and PI were successfully labeled. There were six serial optical sections of HepG2 cells as shown in Figure 1. The interval between two sections was fixed at 0.7 μm. The images shown on Figure 2-Figure 4 were all three-dimensional images obtained from sequential optical sections, which were reconstructed with the reconstruction program of CLSM. The HepG2 cells, having many primary and secondary processes, were irregular in shape. The FITC-stained F-actin filaments appeared in bundles,

which ran in parallel to the main cell axis or through cell processes. Some microfilaments were attached to the plasma membrane, or formed a structural bridge connecting to the neighboring cells. When detector 1 of CLSM for 488 nm line was on, only F-actin marked with FITC-phalloidin could be shown (Figure 1). When both of the two detectors of CLSM were turned on, F-actin marked with FITC-phalloidin and the nuclei marked with PI could be shown simultaneously (Figure 2). F-actin appeared green, the distinct nuclei appeared red, and the region around the nuclei was overlapped by green F-actin and red nuclei appeared yellow.

Figure 2 CLSM three-dimensional images of HepG2 cells by double labeling.

DISCUSSION

Cytoskeleton, composed largely of actin filaments, is the internal framework of a cell. It includes micro-tubes, microfilaments and middling fibers, and is the base structure for cell movement, cell morphology and transmembrane signal conduction. Microfilament mainly consists of actin participating in keeping cell pattern and tight junction between cells. It is also related to the adhesion of the ground substance outside the cells. Microfilament exists in the form of G-actin when it is dissociated or exists in the form of F-actin when it is polymerized. The change and balance of microfilament dissociation and polymerization in normal cells are the important regulatory factors for the movement, adhesion and fission cycle of cells[1,2]. Cell mutation involves cytoskeletal rearrangement and morphological alterations. As a sensitive norm in examining the development of tumor cells at the early stage, F-actin has been used in human mammary gland cancer and T-lymphocyte cancer[3-5]. Our result showed that F-actin microfilaments of HepG2 cells existed in the form of bunches of fibers that were thick, long and dense. F-actin filaments formed bundles running through the main cell axis or cellular processes. The relationship between the change of microfilament morphology and cancer occurrence in cells is still unknown. But when microfilament's component and distribution change, cells cannot receive normal regulation. And it leads to the loss of control of cell growth and propagation and to cancer occurrence. According to some researches, the change of microfilaments might reduce the gap junction in number and function, and the communication function of cells, which is the main reason why propagation ability of carcinoma cells rose up and the ability of adherence lowered, and easily fell off[6-9]. The mechanism underlying the morphological changes of microfilaments in the process of cancer cells is unclear.

In this experiment, F-actin was marked with FITC-phalliodin and the nuclei with PI, so the cytoskeleton and nuclei could be observed. This provides a very useful way to study the relationship between cytoskeleton and nucleus. Compared with other methods, such as immunohistochemistry, light microscopy or electrical microscopy[10-12], CLSM has several advantages[13-17]: Firstly, resolution obtained with a CLSM is better than that of conventional microscopy because of the combination of laser illuminator and detection pinhole. With conventional light microscopy, the fluorescence of the entire specimen interferes with the resolution, while CLSM allows examining the organization of fluorescent labeled cells and tissues by eliminating the "out-of-focus" flare of the specimen, thus providing sharp, high-contrast images of cells and subcellular structures within thick samples. Since images are obtained by scanning, excessive illumination of the specimen and quick decrease of the fluorescent signal are avoided. And light bleaching is minimized because exposure to light is restricted

Figure 1 CLSM images of HepG2 cells stained with FITC-phalloidin. (A: Serial optical sections (1-6) B: Three-dimensional images of Figure 1 serial optical sections. C: Three-dimensional images of HepG2 cells).

to the area of the preparation being examined. Secondly, this method of embedding and sectioning specimens, which are a time-consuming and a destructive procedure, can now be avoided. So it is quick and simple to make samples using CLSM. Under conventional microscopy, structures present in the tissues can be observed only after sectioning (microtome sections). With the CLSM it is possible to obtain a number of serial optical sections of quite thick specimens without physical sectioning. Furthermore, serial optical sections can be collected and displayed as digitalized images, and by using a computer, the digitalized images obtained may be reconstructed as a 3-dimensional structure. In addition, the procedure is not destructive for a living cell or tissue. In this experiment using CLSM, the images of the cytoskeleton marked by the double label technique and the stereoscopy of three-dimensional images were very clear. As the sectioning with CLSM is not done physically but optically, the procedure is not destructive for an intact cell, and the process of sectioning turns simpler and quicker and more reliable, and it can notably keep the normal morphology and function of the cell.

In summary, our results showed that in HepG2 cells F-actin microfilaments existed in the form of bunches of fibers that were thick, long and dense, and ran through the main cell axis or cellular processes. It is suggested that F-actin may play an important role in HepG2 cells.

REFERENCES

1   **Yang YL**. Polymerization of actins. *Biology* 1995; **18**: 13-14
2   **Shumilina EV**, Negulyaev YA, Morachevskaya EA, Hinssen H, Khaitlina SY. Regulation of sodium channel activity by capping of actin filaments. *Mol Biol Cell* 2003; **14**: 1709-1716
3   **Sugiura T**, Nakane S, Kishimoto S, Waku K, Yoshioka Y, Tokumura A. Lysophosphatidic acid, a growth factor-like lipid, in the saliva. *J Lipid Res* 2002; **43**: 2049-2055
4   **Shestakova EA**, Wyckoff J, Jones J, Singer RH, Condeelis J. Correlation of beta-actin messenger RNA localization with metastatic potential in rat adenocarcinoma cell lines. *Cancer Res* 1999; **59**: 1202-1205
5   **Williams JI**, Weitman S, Gonzalez CM, Jundt CH, Marty J, Str

6   **Autieri MV**, Carbone C, Mu A. Expression of allograft inflammatory factor-1 is a marker of activated human vascular smooth muscle cells and arterial injury. *Arterioscler Thromb Vasc Biol* 2000; **20**: 1737-1744
7   **Yamakita Y**, Oosawa F, Yamashiro S, Matsumura F. Caldesmon inhibits Arp2/3-mediated actin nucleation. *J Cell Biol* 2003; **278**: 17937-17944
8   **Yan H**, Rivkees SA. Hepatocyte growth factor stimulates the proliferation and migration of oligodendrocyte precursor cells. *J Neurosci Res* 2002; **69**: 597-606
9   **Fischer R**, Fritz-Six KL, Fowler VM. Pointed-end capping by tropomodulin3 negatively regulates endothelial cell motility. *J Cell Biol* 2003; **161**: 371-380
10   **Uchida M**, Hanai S, Uematsu N, Sawamoto K, Okano H, Miwa M, Uchida K. Overexpression of poly (ADP-ribose) polymerase disrupts organization of cytoskeletal F-actin and tissue polarity in Drosophila. *J Biol Chem* 2002; **277**: 6696-6702
11   **Lin H**, Bhatia R, Lal R. Amyloid beta protein forms ion channels: implications for Alzheimer's disease pathophysiology. *FASEB J* 2001; **15**: 2433-2444
12   **Fischer RS**, Lee A, Fowler VM. Tropomodulin and tropomyosin mediate lens cell actin cytoskeleton reorganization *in vitro*. *Invest Ophthalmol Vis Sci* 2000; **41**: 166-174
13   **Masuda T**, Fujimaki N, Ozawa E, Ishikawa H. Confocal laser microscopy of dystrophin localization in guinea pig skeletal muscle fibers. *J Cell Biol* 1992; **119**: 543-548
14   **Huo X**, Lu JX, Yang RD, Li ZZ, Wei WX, Zheng XH, Tu WX, Xiao ZX, Zhang FL. Comparison of laser scanning confocal microscope with light microscope. *Jiguang Shengwu Xuebao* 2001; **10**: 76-79
15   **Dailey M**, Marrs G, Satz J, Waite M. Concepts in imaging and microscopy. Exploring biological structure and function with confocal microscopy. *Biol Bull* 1999; **197**: 115-122
16   **Li J**, Jester JV, Cavanagh HD, Black TD, Petroll WM. On-line 3-Dimensional confocal imaging *in vivo*. *Invest Ophthalmol Vis Sci* 2000; **41**: 2945-2953
17   **Benbow U**, Orndorff KA, Brinckerhoff CE, Givan AL. Confocal assay for invasion: use of propidium iodide fluorescence and laser reflectance to quantify the rate of migration of cells through a matrix. *Cytometry* 2000; **40**: 253-259

SD, Holroyd KJ, Mclane MP, Chen Q, Zasloff M, Von Hoff DD. Squalamine treatment of human tumors in nu/nu mice enhances platinum-based chemotherapies. *Clin Cancer Res* 2001; **7**: 724-733

• BRIEF REPORTS •

Effect of intraoperative radiotherapy combined with external beam radiotherapy following internal drainage for advanced pancreatic carcinoma

Hong-Bing Ma, Zheng-Li Di, Xi-Jing Wang, Hua-Fen Kang, Huai-Ci Deng, Ming-Hua Bai

Hong-Bing Ma, Zheng-Li Di, Xi-Jing Wang, Hua-Fen Kang, Ming-Hua Bai, Department of Oncology, the Second Hospital of Xi' an Jiaotong University, Xi' an 710004, Shaanxi Province, China
Huai-Ci Deng, Department of Radiation Oncology, the First Hospital of Xi' an Jiaotong University, Xi' an 710068, Shaanxi Province, China
Supported by the Technology Project Entry Foundation of Shaanxi Province, No. 2002K10-G3
Correspondence to: Dr. Hong-Bing Ma, Department of Oncology, the Second Hospital of Xi' an Jiaotong University, Xi' an 710004, Shaanxi Province, China. m68d69@pub.xaonline.com
Telephone: +86-29-7679789
Received: 2003-07-04   **Accepted:** 2003-09-18

Abstract

AIM: To determine the survival of advanced pancreatic cancer patients treated with intraoperative radiotherapy (IORT) combined with external beam radiation therapy (EBRT) following internal drainage (cholecystojejunostomy or choledochojejunostomy).

METHODS: Eighty-one patients with advanced pancreatic cancer who received IORT combined with EBRT following internal drainage (ID) between 1996 and 2001 were retrospectively analyzed. Among the 81 patients, 18 underwent ID+IORT, 25 ID+IORT+EBRT (meanwhile, given 5-Fu 300 mg/m^2 iv drip, 2f/w), 16 EBRT, 22 had undergone simple internal drainage. The IORT dose was 15-25Gy in a single fraction. The usual EBRT dose was 30-40Gy with a daily fraction of 1.8-2.0 Gy.

RESULTS: The complete remission rate, partial remission rate of patients with backache and abdominal pain treated with ID+IORT were 55.5%, 33.3% respectively. Alleviation of pain was observed 2 or 3 wk after IORT. The median survival time (MST) of ID+IORT group was 10.7 mo. The pain remission rate of patients treated with ID+IORT+EBRT was 92%, and their MST was 12.2 mo. The MST of patients treated with EBRT and simple internal drainage was 5.1 mo and 7.0 mo, respectively. The survival curve of ID+IORT group and ID+IORT+EBRT group was significantly better than that of EBRT group ($P<0.05$). The difference between the ID+IORT+EBRT group and ID group was significant ($P<0.05$).

CONCLUSION: IORT combined with EBRT following internal drainage can alleviate pain, improve quality of life and prolong survival time of patients with advanced pancreatic cancer.

INTRODUCTION

During the past two decades, the incidence rate of pancreatic cancer has been increasing. Pancreatic cancer is extremely difficult to diagnose at early stage, and the prognosis is very poor. In spite of the developments in surgical and anesthetic techniques, the median survival time (MST) remains in the range of 7-11 mo, and only 3% of the patients were alive 5 years after diagnosis[1-6].

The local recurrence rate is extremely high even after curative resection. Evans *et al.*[7] reported that more than 50% of patients with post-operative relapse were due to local recurrence. Local recurrence is the most uncomfortable event for patients, and often produces various complications, and decreases the patients' quality of life. Thus, local control is an important issue for pancreatic cancer. IORT is one of the most potent local interventions. Saeki *et al.*[8] reported that IORT could reduce pain and improve quality of life in patients with unresectable pancreatic cancer. In the present study, we investigated the survival time of advanced pancreatic cancer patients treated with intraoperative radiotherapy (IORT) combined with external beam radiation therapy (EBRT) following internal drainage.

MATERIALS AND METHODS

Patient selection

From 1996 to 2001, 81 patients with advanced pancreatic cancer were treated at our hospital. The patients aged from 43 to 72 years with a median of 57 years. Fifty-nine patients were male and 22 were female. All the tumors had no interspace between the superior mesenteric vein and portal vein, and the blood vessel was wrapped by the tumor. All patients had jaundice, the blood total bilirubin ranged from 156 μmol/L to 402 μmol/L with a median of 304 μmol/L. Sixty-one (75.3%) 81 of the patients were given AP-237 or pethidine to relieve pain, and other 20 (24.7%) patients took oral acesodyne intermittently. No ascitic fluid and iver metastasis were noted. Among the 81 patients, 18 received ID+IORT, 25 received ID+IORT +EBRT (meanwhile, given 5-Fu 300 mg/m^2 iv drip, 2 f/w), 16 received simple EBRT and 22 received simple internal drainage.

Surgery

Under continuous epidural anesthesia, all patients underwent laparotomy and their tumors were found unresectable. Cholecystojejunostomy and choledochojejunostomy were performed for patients whose cystic ducts were obstructed and unobstructed after IORT.

IORT

IORT was administered using high-energy electron beams from a Varian Clinac linear accelerator for patients without distant metastases and severe cardiac and lung diseases. A cylinder of 5 cm×5 cm to 8 cm×8 cm, 5 to 8 cm in diameter, or an ellipse with an inclination angle of 10-30° degree was introduced into the patients to encompass the tumor bed and paraaortic lymph

node area. The IORT dose was 15-25 Gy with a median dose of 20 Gy in a single fraction.

EBRT

EBRT was administered mainly postoperatively by 6- or 15-MV photons from a linear accelerator, mostly using two portal veins from the anterior, left, right and/or posterior in directions. In the irradiated field, the paraaortic lymph node area and tumor or tumor bed were completely included with a margin of 3 cm. The usual median EBRT dose was 42 Gy (range, 30-45 Gy) with a daily fraction of 1.8-2.0 Gy, 5F/w. The patients, meanwhile, were given 5-Fu 300 mg/m^2, iv drip, 2f/w.

Statistic analysis

The cause-specific survival rate was calculated and plotted from the day of operation using the Kaplan-Meier method with significance compared by log-rank test.

RESULTS

Relief of pain and survival condition

The causes of death were local relapse and extensive metastasis. The MST of patients treated with ID+IORT, ID+IORT+EBRT, EBRT, ID, was 10.7, 12.2, 5.1 and 7 mo, respectively, which was significantly longer than the patients treated with EBRT (χ^2=10.5835, P<0.05; χ^2=17.8972, P<0.05). The difference of MST between ID+IORT+EBRT and ID was significant (χ^2=8.1361, P<0.05), and it was not significant while between ID+IORT and ID+IORT+EBRT, (P>0.05) (Figure 1). No significant differences in remission of pain and tumor were detected among ID+IORT, ID+IORT+EBRT, and EBRT (P>0.05) groups (Table 1).
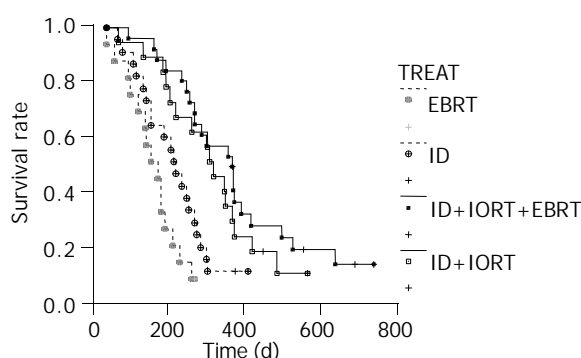

Figure 1 Survival curves for pancreatic cancer according to radiation modalities.

Complications

Three patients had the delayed gastric emptying after ID+IORT, and they recovered after given parenteral nutritional support for 4-5 wk. One patient died of liver and renal failure in the ID+IORT group. Intestinal perforation and digestive tract bleeding were unrelated to ID+IORT. Nausea, decreased appetite and frequent defecation were found early after ID+IORT+EBRT. One patient died of liver and renal failure after simple internal drainage, and 2 patients had delayed gastric emptying and 1 wound infection. No significant difference in the occurrence rate of complications was observed among different treatment methods (P>0.05).

DISCUSSION

The goal of IORT is used to enhance regional tumor control, and have been IORT is used in most modern protocol studies as a radiation boost component of multidisciplinary treatment approaches. More recently, clinical experiences have shown that IORT could improve local control and disease-free survival time, especially when it was used in adjuvant setting, combined with external beam irradiation in some neoplasms such as cancer of the stomach, pancreas, colorectum, and soft tissue sarcoma[9].

The use of IORT for unresectable pancreatic cancer has been reported by several groups. Many reports failed to prove its survival benefit[9,10]. Miyamatsu demonstrated that the MST to IORT group was 7.6 mo, compared to 3 mo for palliative therapy group, with no statistical significance[10]. Ouchi proposed that IORT was not beneficial to either survival or quality of life[11]. Shibamoto reported that among non-stage IV patients, the median survival of the EBRT+IORT group (8.5 mo) and the EBRT group (8 mo) was similar, while in stage IV patients, the prognosis was not influenced by the type of radiotherapy[12]. In contrast to these results, survival advantage with IORT was reported by several groups. Literature data suggested the use of schedules with IORT had a better local control and perhaps a better survival than surgery alone or the palliative treatment[13]. Tanada demonstrated a significant difference in the survival rate between IORT cases and no treatment cases (median survival of 212 d and 109 d, respectively)[14]. Dobelbower reported that the median survival time of patients treated with radical surgery alone was 6.5 mo. The median survival time for the surgery plus IORT group was 9 mo, and 33.3% (2 of 6) of these patients survived longer than 5 years. This survival pattern was significantly better than that for the surgery alone group. The surgery plus EBRT and the surgery plus IORT and EBRT groups had a median survival time of 14.5 and 17.5 mo, respectively. These were significantly better than that of the surgery alone group. The addition of radiation therapy did not increase the treatment complication rate[15].

Patients with advanced pancreatic cancer usually have symptoms such as obstructive jaundice, poor appetite, fatigue and weight loss. Therefore, relief of symptoms, especially relief of obstructive jaundice and improvement of liver function, is clinically beneficial to these patients. In the colligation treatment, internal drainage has been used for the extinction of obstructive jaundice, enhancement of appetite and improvement of liver

Table 1 Patient characteristics after treated with ID+IORT, ID+IORT+EBRT, ID, and EBRT

	IORT+ID		IORT+ERBT+ID		ID		ERBT	
	n	%	n	%	n	%	n	%
Pain								
Complete remission	10	55.5	15	60.0	/		5	31.3
Partial remission	6	33.3	8	32.0	/		7	43.7
Tumor								
Light diminution	4	22.2	8	32.0	/		2	12.5
Unchanged	14	77.7	17	68.0	22	100.0	14	87.5
Jaundice	extinction		extinction		extinction		extinction	

function, which was also beneficial to IORT and EBRT[16,17]. IORT has also been used in an attempt to increase the radiotherapy dose on the target without damaging surrounding normal tissues. A higher radiation dose could be given to the target tumor by combining IORT with EBRT[11,18]. Our studies showed that colligation treatment (ID+IORT+EBRT) could relieve jaundice, pain, improve quality of life, diminish tumor and prolong survival time in patients with unresectable pancreatic cancer.

Among the groups of ID+IORT, surgery, ID+IORT+EBRT, jaundice was improved quickly. However, it was not obviously improved in EBRT group. Pain was not relieved in surgery group, but obviously relieved in 75-92% of the patients in the other groups. So radiotherapy had a good and a long-term pain relieving effect. IORT relieved pain quickly and could kill the remnant tumor, better than drugs. The tumor was not reduced in size in surgery group, while in the other groups, the tumor size was decreased in varying degrees, with no statistical significance ($P > 0.05$).

In the present study, the MST was 5.1 mo for EBRT group, 7 mo for ID group, 10.7 mo for ID+IORT group and 12.2 mo for ID+IORT+EBRT group. The survival curves of the ID+IORT group and ID+IORT+EBRT group were significantly better than that of the EBRT group ($P < 0.05$). The difference between the ID+IORT+EBRT and the ID groups was significant ($P < 0.05$). Thus, ID+IORT+EBRT could relieve the pain and jaundice , improve survival and quality of life.

Complications resulting from surgery and radiotherapy occurred in 9.3% of patients (4/43) in both ID+IORT and ID+IORT+EBRT groups. No major side effects were noted during the course of treatment. Schwarz reported IORT was not related to a significantly increased risk of complications, hospital stay, or survival hazard[19]. Though a very small amount of normal tissues was exposed in IORT, complications often occurred if radiotherapy dose was too big. The safety level of a radiation dose for IORT alone is limited to 30 Gy[20]. The dose in IORT ranging from 20 Gy to 25 Gy combined with the dose in EBRT ranging from 40 Gy to 50 Gy was considered to contribute to the improvement of prognosis without causing serious side effects[21].

In conclusion, multimodal therapy can relieve jaundice, pain, improve quality of life, reduce tumor mass and prolong survival time of patients with advanced pancreatic cancer.

REFERENCES

1   **Reni M**, Panucci MG, Ferreri AJ, Balzano G, Passoni P, Cattaneo GM, Cordio S, Scaglietti U, Zerbi A, Ceresoli GL, Fiorino C, Calandrino R, Staudacher C, Villa E, Di Carlo V. Effect on local control and survival of electron beam intraoperative irradiation for resectable pancreatic adenocarcinoma. *Int J Radiat Oncol Biol Phys* 2001; **50**: 651-658

2   **Kokubo M**, Nishimura Y, Shibamoto Y, Sasai K, Kanamori S, Hosotani R, Imamura M, Hiraoka M. Analysis of the clinical benefit of intraoperative radiotherapy in patients undergoing macroscopically curative resection for pancreatic cancer. *Int J Radiat Oncol Biol Phys* 2000; **48**: 1081-1087

3   **Wang L,** Yang GH, Lu XH, Huang ZJ, Li H. Pancreatic cancer mortality in China (1991-2000). *World J Gastroenterol* 2003; **9**: 1819-1823

4   **Shankar A,** Russell RC. Recent advances in the surgical treatment of pancreatic cancer. *World J Gastroenterol* 2001; **7**: 622-626

5   **Liu MP,** Ma JY, Pan BR, Ma LS. Study of Chinese pancreatic cancer. *Shijie Huaren Xiaohua Zazhi* 2001; **9**: 1103-1109

6   **Wang ZQ,** Li JS, Lu GM, Zhang XH, Chen ZQ, Meng K. Correlation of CT enhancement, tumor angiogenesis and pathologic grading of pancreatic carcinoma. *World J Gastroenterol* 2003; **9**: 2100-2104

7   **Evans DB,** Abbruzzese JL, Rich TA. Cancer of the pancreas. In: Devita VT, Hellmann S, Rosenberg SA, eds. Cancer, principles and practice of oncology. 6th ed. *Philadelphia:Lippincott* **2001**: 1126-1161

8   **Saeki H**, Sugimasa Y, Yamada R, Akaike M, Takemiya S, Masaki T, Miyagawa K, Okawa S. Intraoperative radiotherapy (IORT) for unresectable stage IVb pancreatic cancer. *Gan To Kagaku Ryoho* 2002; **29**: 2221-2223

9   **Valentini V,** Balducci M, Tortoreto F, Morganti AG, De Giorgi U, Fiorentini G. Intraoperative radiotherapy: current thinking. *Eur J Surg Oncol* 2002; **28**: 180-185

10 **Miyamatsu A,** Morinaga S, Yukawa N, Akaike M, Sugimasa Y, Takemiya S. Intraoperative radiation therapy (IORT) for locally unresectable pancreatic cancer. *Gan To Kagaku Ryoho* 1999; **26**: 1846-1848

11 **Ouchi K,** Sugawara T, Ono H, Fujiya T, Kamiyama Y, Kakugawa Y, Mikuni J, Yamanami H. Palliative operation for cancer of the head of the pancreas: significance of pancreaticoduodenectomy and intraoperative radiation therapy for survival and quality of life. *World J Surg* 1998; **22**: 413-416

12 **Shibamoto Y,** Manabe T, Ohshio G, Sasai K, Nishimura Y, Imamura M, Takahashi M, Abe M. High-dose intraoperative radiotherapy for unresectable pancreatic cancer. *Int J Radiat Oncol Biol Phys* 1996; **34**: 57-63

13 **Fellin G,** Pani G, Tomio L, Tirone G, Eccher C. Intraoperative radiotherapy in the combined treatment of pancreatic cancers. *Tumori* 1999; **85**(1 Suppl): S33-S35

14 **Tanada M,** Takashima S, Endoh H, Hyoudou I, Jinno K, Kataoka M. Multimodal treatment including intraoperative irradiation for advanced pancreatic cancer with extended metastasis. *Gan To Kagaku Ryoho* 2001; **28**: 1681-1683

15 **Dobelbower RR,** Merrick HW, Khuder S, Battle JA, Herron LM, Pawlicki T. Adjuvant radiation therapy for pancreatic cancer: a 15-year experience. *Int J Radiat Oncol Biol Phys* 1997; **39**: 31-37

16 **Zhou ZH,** Song MZ. Current therapy of pancreatic carcinoma. *Shijie Huanren Xiaohua Zazhi* 2000; **8**: 214-215

17 **Ghaneh P,** Slavin J, Sutton R, Hartley M, Neoptolemos JP. Adjuvant therapy in pancreatic cancer. *World J Gastroenterol* 2001; **7**: 482-489

18 **Shibamoto Y,** Nishimura U, Abe M. Intraoperative radiotherapy and hyperthermia for unresectable pancreatic cancer. *Hepatogastroenterology* 1996; **43**: 326-332

19 **Schwarz RE,** Smith DD, Keny H, Ikle DN, Shibata SI, Chu DZ, Pezner RD. Impact of intraoperative radiation on postoperative and disease-specific outcome after pancreatoduodenectomy for adenocarcinoma: a propensity score analysis. *Am J Clin Oncol* 2003; **26**: 16-21

20 **Egawa S,** Tsukiyama I, Akine Y, Kajiura Y, Ogino T, Ozaki H, Kinoshita T, Kosuge T. Control of aftereffects due to intraoperative radiotherapy. *Gan No Rinsho* 1990; **36**: 815-820

21 **Tanaka Y,** Takeshita N, Niwa K, Matsuda T. Studies on treatment results and prognostic factors of intraoperative radiotherapy in pancreatic carcinoma. *Nippon Igaku Hoshasen Gakkai Zasshi* 1989; **49**: 614-621

Edited by Zhu LH and Wang XL **Proofread by** Xu FM

• BRIEF REPORTS •

Effects of *mu* and *kappa* opioid receptor agonists and antagonists on contraction of isolated colon strips of rats with cathartic colon

Bao-Hua Liu, Ping Mo, Sheng-Ben Zhang

Bao-Hua Liu, Ping Mo, Sheng-Ben Zhang, Department of General Surgery, Daping Hospital, Third Military Medical University, Chongqing 400042, China
Correspondence to: Dr. Bao-Hua Liu, Department of General Surgery, Daping Hospital, Third Military Medical University, Chongqing 400042, China. lbh57268@163.com
Telephone: +86-23-68757248

Abstract

AIM: To study the effects of *mu* and *kappa* opioid receptor agonists and antagonists on the isolated colon strips of rats with cathartic colon.

METHODS: Cathartic colon model was established by feeding rats with contact laxatives, and effects of *mu* and *kappa* opioid receptor agonists and antagonists on electricity-stimulated contraction of isolated colon strips of rats with cathartic colon were observed.

RESULTS: Compared with control group, exogenous *mu* and *kappa* agonists inhibited significantly electricity-stimulated contraction of strips of cathartic colon (8.50 ± 0.89 mm, 6.24 ± 0.91 mm, 3.35 ± 0.6 mm vs 11.40 ± 0.21 mm $P<0.01$; 8.98 ± 0.69 mm, 6.89 ± 0.71 mm, 4.43 ± 0.99 mm vs 11.40 ± 0.21 mm, $P<0.01$). In contrast, the exogenous *mu* antagonist significantly enhanced electricity-stimulated contraction of isolated colon strips (13.18 ± 0.93 mm, 15.87 ± 0.98 mm, 19.46 ± 1.79 mm vs 11.40 ± 0.21 mm, $P<0.01$), but *kappa* antagonist had no effect on the isolated colon strips of rats with cathartic colon.

CONCLUSION: *Mu* and *kappa* opioid receptors are involved in the regulation of colon motility of rats with cathartic colon.

INTRODUCTION

The cause and pathogenesis of slow-transit constipation (STC) still remain unknown now[1]. To study the mechanism of STC, more and more attention has been recently paid on the function of numerous neurotransmitters involved in the onset of STC[2-8]. With a rat model of cathartic colon[9,10], we investigated the effects of opioids, inhibitory neurotransmitters, on the electricity-stimulated contraction of isolated cathartic colon strips.

MATERIALS AND METHODS

Materials

Rhubarb and phenolphthalein powders were provided by

Chongqing Traditional Chinese Medicine Pharmaceutical Factory and Chongqing Dongfeng Reagent Factory, respectively. Mu and kappa opioid receptor antagonists (Naloxone, Norbni) and agonists (Damgo, U50488H) were purchased from Sigma Co USA.

Fifty Wistar rats of either sex, weighing 230 ± 70 g, were divided randomly into control group ($n=10$) and cathartic colon group treated with rhubarb ($n=20$) and phenolphthalein ($n=20$). Because both rhubarb and phenolphthalein belong to the same kind of contact cathartics, the two groups were considered as one cathartic colon group.

Rats were housed in cage, one per cage under standard laboratory conditions (room temperature, 18-28 ℃, relative humility, 40-80%). Control rats were given soft chows, while the rats in rhubarb group were given chows premixed with rhubarb powder. The initial rhubarb dosage was 200 mg/kg.d, and another 200 mg/kg was added every day until it reached 1000 mg/kg.d for several days until loose stool disappeared. Then, rhubarb was added 200 mg/k.d again until 2 400 mg/kg.d. for 3 mo. The rats in phenolphthalein group were fed chows premixed with an initial dosage of phenolphthalein 200 mg/kg. Its 50% for dosage diarrhea was 1 400 mg/kg.d and its final dosage was 3 200 mg/kg.d.

Method

Rats were killed by head-strike, the abdominal cavity was opened through a median incision, and a 5 cm colon in length far from the ileocecum was then quickly dissected and transferred to Krebs solution and rinsed. The Krebs solution contained NaCl, 112.8 mmol; KCl, 5.90 mmol; $CaCl_2$ mmol, 1.97; $MgCl_2$, 1.18 mmol; $NaHPO_4$, 1.22 mmoL; $NaHCO_3$, 25.0 mmol; Glu, 11.49 mmol (pH 7.2-7.4). Rinsed colon was scratched off serous membrane and cut into 2 cm×2 cm strips. One end of the strip was fixed on a supporting rod, and the another was fixed to the tension transducer. Each muscle strip was vertically placed in an organ bath filled with 10 mL Krebs solution maintained at 37 ℃ and gased with (950 mL/LO₂)/(50 mL/LCO₂). Muscle contraction was activated by electrical field stimulation with a pair of external platinum ring electrodes connected to a square wave stimulator. The electrodes were parallelly placed on each end of the strip, on which continuous electrical stimulations (4 ms in duration, 10 Hz and 70 V in electric pressure) were conducted. The strips were given 1 g initial tensions and equilibrated for 60 min. Isometric contraction was measured with a tension transducer connected to a physiological recorder, and the contraction amplitude was printed on standard chart paper. The direct effects of opioid receptor agonists and antagonists on the contractility of isolated muscle strips were studied by addition of opioid receptor agonists and antagonists to organ bath to make a required solution. The recorded data were depicted into concentration-response curves. To evaluate the response of muscle strips to electrical stimulation, the contraction amplitude was calculated and the average of amplitude was accounted.

Statistical Analysis

Results were expressed as mean±SE. Differences were

analyzed by Student t test. *P*<0.05 was considered statistically significant.

RESULTS

Electricity-stimulated contractile response of isolated colon strips

The contractile response of most colon strips (about 70%) showed a typical sinusoid curve, while about 30% strips demonstrated wild and irregular waves. In the cathartic colon group, the decrease of contraction amplitude was about 27.43% of that in control group.

Effect of mu opioid receptor agonists on electricity-stimulated contractile response of cathartic colon strips

The mu opioid receptor, agonist Damgo, caused a concentration-dependent inhibition of electricity-stimulated contraction of cathartic colon strips. Damgo solutions (0.05 μmol/L, 0.10 μmol/L, 1.00 μmol/L) could induce a significant inhibition of the contractile response, which showed that the amplitude of muscle strip contraction was significantly reduced (*P*<0.01) in the presence of Damgo (Table 1).

Table 1 Effect of Damgo on electricity-stimulated contractile response of cathartic colon strips (mean±SD)

Concentration (μmol/L)	Basic contraction amplitude without Dampo (mm)	Contraction amplitude with Dampo (mm)
0.05	11.40±0.21	8.50±0.89[b]
0.10	11.40±0.21	6.24±0.91[ab]
1.00	11.40±0.21	3.35±0.64[bd]

[a]*P*<0.05 *vs* 0.05 μmol/L, [b]*P*<0.01 *vs* without Dampo, [d]*P*<0.01 *vs* 0.05 μmol/L.

Effect of mu opioid receptor antagonists on electricity-stimulated contractile response of cathartic colon strips

The mu opioid receptor antagonist, naloxone, could induce a concentration-dependent elevation of electricity-stimulated contraction amplitude of cathartic colon strips. Each naloxone concentration (0.05 μmol/L, 0.10 μmol/L, 1.00 μmol/L) induced a significant elevation of the contractile response, which showed the contraction amplitude was significantly elevated (*P*<0.01) in the presence of naloxone (Table 2).

Table 2 Effect of naloxone on electricity-stimulated contractile response of cathartic colon strips(mean±SD)

Concentration (μmoL)	Basic contraction amplitude without naloxone(mm)	Contraction amplitude with naloxone(mm)
0.05	11.40±0.21	13.18±0.93[b]
0.10	11.40±0.21	15.87±0.98[ab]
1.00	11.40±0.21	19.46±1.79[bd]

[a]*P*<0.05 *vs* 0.05 μmol/L, [b]*P*<0.01 *vs* without Naloxone, [d]*P*<0.01 *vs* 0.05 μmol/L.

Table 3 Effects of U50488H on electricity-stimulated contractile response of cathartic colon strips (mean±SD)

Concentration (μmol/L)	Basic contraction amplitude before administration(mm)	Contraction amplitude after administration(mm)
0.05	11.40±0.21	8.98±0.69[b]
0.10	11.40±0.21	6.89±0.71[ab]
1.00	11.40±0.21	4.43±0.99[bd]

[a]*P*<0.05 *vs* 0.05 μmol/L, [b]*P*<0.01 *vs* before administration, [d]*P*<0.01 *vs* 0.05 μmol/L.

Effect of kappa opioid receptor agonists on electricity-stimulated contractile response of cathartic colon strips

U50488H, a highly-selective kappa opioid receptor agonist, could cause an evident suppression of the electricity stimulated contraction of colon strips of rats with cathartic colon. Each U50488H concentration (0.05 μmol/L, 0.10 μmol/L, 1.00 μmol/L) induced a significant inhibition of the contractile response (*P*<0.01) (Table 3).

Effect of kappa opioid receptor antagonists on electricity-stimulated contractile response of cathartic colon strips

Norbin is a highly-selective kappa opioid receptor antagonist, which did not show any evident effect on the electricity stimulated contraction of colon strips of rats with cathartic colon. No concentration of Norbin in our experiment could induce any effect on the contraction amplitude of muscle strips, even at the maximal concentration of Norbin (data not shown).

DISCUSSION

Opioids have extensive distributions and potent effects on the gastrointestinal tract[11,12]. Contractility studies also indicated that opioids, in combination with mu, kappa and delta opioid receptor agonists, could inhibit motor activity of the gastrointestinal tract by suppression of excitatory neurotransmitter release[13-15]. Our study manifested that exogenously added opioid receptor agonists (*mu*, *kappa*) inhibited the contractility of colon strips of rats with cathartic colon, which showed a significant reduction of contraction amplitude as compared to the basic contraction with no agonists. The inhibitory effects were negatively correlated with concentrations. In contrast, mu receptor antagonists elevated electricity stimulated contraction of cathartic colon in rats. However, kappa receptor antagonists had no effect. The results suggested that mu and kappa opioid receptor might play an important role in the regulation of gastrointestinal motility in rats. It also further approved that opioids could slow down the propulsive peristalsis performed by nerves and muscles in colon and played a very important role in the onset and pathologic process of STC.

Kreek hypothesized that the changes of opioids activity were the important etiological factor, and STC patients could be successfully treated with naloxone, a mu opioid receptor antagonists. The present study was designed to investigate the effects of opioid agonists and antagonists on isolated cathartic colon muscle strips, it provided a new fundamental theory on the STC treatment with opioid receptor antagonists. It also indicated that the studies on the subtype and binding site of opioid receptors, as well as the overall research in clinic, would provide new methods for STC therapies, and also benefit the clarification of the pathogenesis of STC. In conclusion, mu and kappa opioid receptors are involved in the regulation of colon motility of rats with cathartic colon.

REFERENCES

1   **Liu BH**, Mo P, Tong WT, Gong SG, Fu T, Fang SW. Diagnosis and Therapy of Constipation. *Beijing: Military Medical Science Publishing House* 2002: P174-182
2   **Hruby VJ**, Agnes RS. Conformation-activity relationships of opioid peptides with selective activities at opioid receptors. *Biopolymers* 1999; **51**: 391-410
3   **Sora I**. Opioid receptor knockout mice. *Nihon Shinkei Seishin Yakurigaku Zasshi* 1999; **19**: 239-249
4   **Camilleri M**. Management of the irritable bowel syndrome. *Gastroenterology* 2001; **120**: 652-668
5   **Callahan MJ**. Irritable bowel syndrome neuropharmacology. A review of approved and investigational compounds. *J Clin Gastroenterol* 2002; **35**(1 Suppl): S58-67

6   **Tong WD**, Zhang SB, Zhang LY, Cai WQ, Du WH, Mu JH. Iden-
     tification of interstitial cells of cajal in the myenteric plexus of
     colon of rats. *Chinese J Anatomy* 1999; **22**: 316-318
7   **Tong WD**, Zhang SB, Liu BH, Zhang LY, Huang XK, Gao F.
     Effect of long term application of rhubarb on colonic motility
     and enteric nervous system in rats. *World Chinese J Digestol* 2003;
     11: 665-667
8   **Tong WD**, Liu BH, Zhang SB, Zhang LY, Huang XK, Gao F. Ab-
     dominal colectomy as a treatment of obstinate slow transit
     constipation: clinical results and aetiological analysis. *Formos J
     Surg* 2003; **36**: 112-119
9   **Tong WD**, Zhang SB, Liu BH, Zhang LY, Huang XK. Effects of
     phenolphthalein on colonic motility and enteric nervous system
     in rats. *Chin J Dig Dis* 2003; **23**: 723-726
10   **Liu BH**, Zhang SB, Mo P. Effect of agonists, antagonists of mu,
     kappa receptors in mouse intestine transmission function. *J

Coloproctol Surg* 2002; **8**: 14-16
11   **Tan-No K**, Niijima F, Nakagawasai O, Sato T, Satoh S, Tadano
     T. Development of tolerance to the inhibitory effect of
     loperamide on gastrointestinal transit in mice. *Eur J Pharm Sci*
     2003; **20**: 357-363
12   **Sengupta JN**, Snider A, Su X, Gebhart GF. Effects of kappa opio-
     ids in the inflamed rat colon. *Pain* 1999; **79**: 175-185
13   **Bagnol D**, Henry M, Cupo A, Jule Y. Distribution of enkephalin-
     like immunoreactivity in the cat digestive tract. *J Auton Nerv Syst*
     1997; **64**: 1-11
14   **Kaufman PN**, Krevsky B, Malmud LS, Maurer AH, Somers MB,
     Siegel JA, Fiaher RS. Role of opiate receptors in the regulation of
     colonic transit. *Gastroenterology* 1988; **94**: 1351-1356
15   **Liu M**, Wittbrodt E. Low-dose oral naloxone reverses opioid-
     induced constipation and analgesia. *J Pain Symptom Manage*
     2002; **23**: 48-53

Edited by Ren SY and Wang XL **Proofread by** Xu FM

• BRIEF REPORTS •

Serum level of TSGF, CA242 and CA19-9 in pancreatic cancer

Jing-Ting Jiang, Chang-Ping Wu, Hai-Feng Deng, Ming-Yang Lu, Jun Wu, Hong-Yu Zhang, Wen-Hui Sun, Mei Ji

Jing-Ting Jiang, Chang-Ping Wu, Hai-Feng Deng, Ming-Yang Lu, Jun Wu, Hong-Yu Zhang, Wen-Hui Sun, Mei Ji, Department of Tumor Biological Treatment, the Third Affiliated Hospital of Suzhou University, Changzhou 213003, Jiangsu Province, China
Correspondence to: Dr. Jing-Ting Jiang, Department of Tumor Biological Treatment, the Third Affiliated Hospital of Suzhou University, Changzhou 213003, Jiangsu Province, China. jitnew@163.com
Telephone: +86-519-6180978   **Fax:** +86-519-6621235
Received: 2003-12-19   **Accepted:** 2004-02-01

Abstract

AIM: To establish a method to detect the expression of the tumor specific growth factor TSGF, CA242 and CA19-9 in serum and evaluate their value in diagnosis of pancreatic cancer.

METHODS: ELISA and Biochemical colorimetric assay were used to detect the serum content of TSGF, CA242 and CA19-9 in 200 normal cases, 52 pancreatitis patients and 96 pancreatic cancer patients.

RESULTS: The positive likelihood ratios of TSGF, CA242 and CA19-9 were 5.4, 12.6 and 6.3, respectively, and their negative likelihood ratios were 0.10, 0.19 and 0.17, respectively. With single tumor marker diagnosed pancreatic cancer, the highest sensitivity and specificity of TSGF were 91.6% and 93.5%. In combined test with 3 markers, when all of them were positive, the sensitivity changed to 77.0% and the specificity and the positive predictive value were 100%. The levels of TSGF and CA242 were significantly higher in the patients with pancreatic cancer of head than those in the patients with pancreatic cancer of body, tail and whole pancreas, but the expression of CA19-9 had no correlation with the positions of the pancreatic cancer. The sensitivity of TSGF, CA242 and CA19-9 was increased with the progress in stages of pancreatic cancer. In stage I, the sensitivity of TSGF was markedly higher than CA242 and CA19-9.

CONCLUSION: The combined use of TSGF, CA242 and CA19-9 expressions can elevate the specificity for pancreatic cancer diagnosis. And it shows that it plays an important role to differentiate positions and tissue typing. It is a forepart diagnosis for the pancreatic cancer by combination checking. There is very important correlation between the three markers and the pancreatic cancer.

INTRODUCTION

Early period of pancreatic cancer lacked the typical clinic performances[1,2], was high malignant and had a low survival time in five years[3-6]. And it was difficult to be diagnosed and made the patients lose the chances of radical cures. So it was very important to diagnose pancreatic cancer early[7-9]. But the sensitivity and specificity were not ideal in examining pancreatic cancer with a single method. We assayed the content of TSGF, CA242 and CA19-9 in serum of pancreatic cancer suffers and analyzed their expression in different positions and tissue typing in order to improve the level of early period of the pancreatic cancer diagnosis.

MATERIALS AND METHODS

Materials

To collect 200 normal people who had medical check-up in the hospital as normal group, including 112 males and 88 females with a mean age of 55.0±11.2 (range,22-68 years). To collect 52 pancreatitis suffers as pancreatitis group, including 29 males and 23 females with an average age of 66.0±8.0 (range, 60-74 years). To collect 96 pancreatic cancer suffers as pancreatic cancer group, including 61 males and 35 females with an average age of 67.6±6.7 (range, 60-88 years). There were 64 heads of pancreatic cancer, 18 body of pancreatic cancer and 10 tail of pancreatic cancer, which were all proved by pathology.

Methods

TSGF was assayed by colorimetric of biochemistry from Fujian New Continent Biochemical Technology Limited Company. CA242 and CA19-9 were assayed by ELISA from Sweden CanAg Company. All operations were followed by manuals. All data were showed as mean±SD and calculated by *t* test, and positive ratios were calculated by χ^2 test.

RESULTS

TSGF, CA242 and CA19-9 assay of three groups

Statistical significance of the contents of the three markers was found when pancreatic cancer group was compared with normal group and pancreatitis group (*P*<0.01). No statistical significance was found between normal group and pancreatitis group (*P*>0.05, Table 1).

Table 1 Laboratory parameters of the 3 tumor markers in pancreatic cancer group, pancreatitis group and normal group (mean±SD, ×10³U/L)

Group	No. of cases	TSGF	CA242	CA19-9
Critical value		>71	>20	>37
Pancreatic cancer	96	80.7±7.6[b]	90.2±10.9[b]	643.5±203.6[b]
Pancreatitis	52	61.4±6.7	21.1±10.5	30.9±5.9
Normal				
22-59 yr	113	54.3±5.1	17.5±8.3	14.5±5.0
60-68 yr	87	56.6±5.8	19.2±9.6	17.2±5.9

[b]*P*<0.01 *vs* normal group.

Evaluate the value of diagnosis in pancreatic cancer by a single tumor marker

When diagnosing pancreatic cancer by a single tumor marker, TSGF had the highest sensitivity of 91.6%, CA242 had the highest specificity of 93.5%; TSGF and CA19-9 had the exactly validity. The positive likelihood ratio of TSGF, CA242 and CA19-9 were 5.4, 12.6 and 6.3, and the negative likelihood ratio were 0.10, 0.19 and 0.17 (Table 2).

Table 2 Evaluation of the value of diagnosis in pancreatic cancer by a single tumor marker of 96 cases

Value of diagnosis	Sensitivity (%)	Specificity (%)	Positive likelihood ratio	Negative likelihood ratio
TSGF	91.6 (88)[a]	83.0	5.4	0.10
CA242	82.3 (79)	93.5[b]	12.6	0.19
CA19-9	85.4 (82)	86.5	6.3	0.17

( ), No. of cases; [a]$P<0.05$, [b]$P<0.01$ vs the other two indexes. sensitivity=truepositive/patients×100%=TP/(TP+FN)×100%, specificity=true negative/normal×100%=TN/(TN+FP)×100% positive likelihood ratio=true positive/false positive=sensitivity/ (1-specificity) negative likelihood ratio=(1-true positive)/(1-false positive)=(1-sensitivity)/specificity.

The different combinations of the 3 markers to the diagnosis in pancreatic cancer

When diagnosing pancreatic cancer by any of the 3 markers was over the critical value, the sensitivity, specificity and positive predictive value were 93.8%, 79.0% and 68.2%. When two of the 3 markers were over the critical value, the sensitivity, specificity and positive predictive value were 89.5%, 95.5% and 90.5%. When the 3 markers were all over the critical value, the sensitivity was 77.0% and the specificity and positive predictive value were both 100%. Therefore, the combination diagnosis in pancreatic cancer could increase the specificity of the diagnosis (Table 3).

Table 3 Analyses of The different combinations of the 3 markers to the diagnosis in pancreatic cancer (No. of cases)

Group	No. of cases	1 Item (+)	2 Item (+)	3 Item (+)
Pancreatic cancer	96	90 (93.8)	86 (89.5)	74 (77.0)
Normal	200	42 (21.0)	9 (4.5)	0 (100)
Positive likelihood rate (%)		68.2	90.5	100

( ), sensitivity (%).

The correlation between the different positions of pancreatic cancer and the levels of the 3 markers

International Union Against Cancer (UICC) divided pancreatic cancer into head, body, tail and whole of pancreatic cancer. Statistical significance was found that the levels of TSGF and CA242 in head of pancreatic cancer were extra better than those in the other three kinds of pancreatic cancer ($P<0.01$). But no statistical significance was found in the levels of the 3 markers in the other three kinds of pancreatic cancer ($P>0.05$). The levels of CA19-9 had no correlation with the positions of the pancreatic cancer ($P>0.05$). (Table 4).

Table 4 The content of the 3 markers in the different positions of pancreatic cancer (mean±SD, ×10³U/L)

Position of pancreatic cancer	No. of cases	TSGF	CA242	CA19-9
Head	64	88.5±9.0[b]	106.4±12.6[b]	653.7±217.8
Body	18	78.2±6.7	82.5±10.4	633.9±192.4
Tail	10	77.1±5.7	81.6±8.2	659.4±211.0
Whole	4	74.5±3.1	83.0±9.5	615.3±187.1

[b]$P<0.001$ vs body, tail and whole of pancreatic cancer.

To compare the sensitivity of the 3 tumor markers in different stages of pancreatic cancer

We analyzed the sensitivity of the 3 tumor markers in serum in different stages of pancreatic cancer (Table 5). The results showed that the sensitivity gradually strengthened by the progress of clinical stages. Statistical significance was found

between stage II, III, IV, and stage I ($P<0.01$). The sensitivity of CA19-9 was higher than that of CA242, but there was no statistical significance ($P>0.05$). The sensitivity of TSGF in stage I was significant better than that of CA242 and CA19-9 ($P<0.01$). So TSGF could be regarded as a tumor marker to filtrate pancreatic cancer in early stage.

Table 5 Analyses of the sensitivity of the 3 tumor markers in different stages of pancreatic cancer (No. of cases)

Clinical stages	No. of cases	TSGF	CA242	CA19-9
I	10	6 (60.0)[bd]	3 (30.0)[d]	4 (40.0)[d]
II	12	9 (75.0)	6 (50.0)	7 (58.3)
III	25	22 (88.0)	20 (80.0)	21 (84.0)
IV	49	46 (93.8)	40 (81.6)	42 (85.7)

Note: ( ), sensitivity (%); [d]$P<0.01$ vs the sensitivity of stage II, III, IV; [b]$P<0.01$ vs the sensitivity of CA242, CA19-9.

DISCUSSION

The incidence of pancreatic cancer is rising[10,11]. We want to diagnose pancreatic cancer in early stage by tumor markers[12]. First, we should find one tumor marker of good specificity[13,14]. TSGF was a gene that could promote the growth of tumor blood vessels. It could greatly hyperplasy in the tumor tissues and capillary vessels around. No correlation was found in the hyperplasia of non-tumor blood vessels. TSGF had good sensitivity to malignant tumors. CA19-9 belonged to the ramification of lactotetraose and was a kind of the ganglioside lipoprotein protein[15-17]. It was mucoprotein when in serum and its epipositions was pentaglucose determinant. Despite advances in preoperative radiologic imaging, a significant fraction of potentially resectable pancreatic cancers are found to be unresectable at laparotomy[18]. CA242 was a kind of sialic acid mucoprotein tumor associated antigen linked Mucin pyrenoid by –O-. It existed in the same molecule with CA19-9. But it belonged to the different antigen determinant with CA19-9. Therefore, there was no correlation between CA19-9 and CA242[19]. But they were complemental. They had good sensitivity in pancreatic cancer diagnosis. This result was exactly similar with the report of Ichihara et al[20]. This research also showed that 3 tumor markers in pancreatic cancer group were remarkably higher than that of normal group. And the levels of the 3 tumor markers in pancreatitis group were not high.

The research showed that the positive likelihood ratio of TSGF, CA242 and CA19-9 were 5.4, 12.6 and 6.3, and the negative likelihood ratio were 0.1, 0.19 and 0.17. So the three indexes were very important in clinical pancreatic cancer diagnosis. TSGF had good sensitivity in pancreatic cancer diagnosis as 91.6%. CA19-9 was very important to evaluate the curative effect of chemotherapy and to judge the survival time[21-26]. CA242 had good specificity as 93.5%. When diagnosing with the combination assay of the 3 indexes, the sensitivity was 77.0% and the specificity and positive predictive value were both 100%. Therefore, combination diagnosis should be used in pancreatic cancer diagnosis in order to improve the specificity[27-29].

The research of Metsuyama et al. proved that there was significant correlation in malignant tumors between the creation of blood vessels and blood transfer[30]. TSGF and CA242 had high levels. It was related to the rich blood supply of the head of pancreas. Pancreas had the priority and step artery pancreaticoduodenalis superior and the forward and back branches down pancereaticoduodenales inferiors. The arteries were connected by anastomosis at the head of pancreas to be arcuate arterial. The arcuate arterial gave out branches to supply the forward and back parts of the head of pancreas and duodenum. It accelerated the head of pancreas circulation. So

it made the carbohydrate antigen excreted by tumors to be a high level in serum. But there was no correlation between the expression of CA19-9 and the position of tumor. This needs further researches. TSGF was a new tumor marker related to the blood vessel hyperplasia of malignant tumors. It was also a result of the hyperplasia of the malignant tumors and the capillary vessels around. It was released to blood with the acceleration of blood circulation. In the different stage of pancreatic cancer, the sensitivity of the tumor markers TSGF, CA242 and CA19-9 increased with the progress in different stages. Statistical significance was found in the sensitivity of stage II, III, IV and stage I. This result disagreed that Frebourg *et al* reported that there was no correlation between the level of CA19-9 in serum and the stage of pancreatic cancer[31]. The sensitivity of CA19-9 was a little higher than that of CA242, but there was no statistical significance. In the stage I of pancreatic cancer, the sensitivity of TSGF was remarkably higher than that of CA242 and CA19-9. Therefore, TSGF can be regarded as a tumor marker to filtrate pancreatic cancer in early stage.

The research shows that there is very important correlation between the levels of TSGF, CA242 and CA19-9 and pancreatic cancer. The combined assay of the 3 indexes does help to diagnose pancreatic cancer in early stage. At the same time they are very important in analyzing the position of pancreatic cancer and the pathology typings. Therefore, the 3 indexes can be regarded as the tumor markers of pancreatic cancer diagnosis in early stage.

REFERENCES

1   **Barbe L,** Ponsot P, Vilgrain V, Terris B, Flejou JF, Sauvanet A, Belghiti J, Hammel P, Ruszniewski P, Bernades P. Intraductal papillary mucinous tumors of the pancreas. Clinical and morphological aspects in 30 patients. *Gastroenterol Clin Biol* 1997; **21:** 278-286

2   **Love L,** Fizzotti G, Damascelli B, Ceglia E, Garbagnati F, Milella M. Pancreatic tumor imaging by III generation CT, gray-scale ultrasound and improved angiography . *Tumori* 1980; **66:** 357-372

3   **Sahmoun AE,** D' Agostino RA Jr, Bell RA, Schwenke DC. International variation in pancreatic cancer mortality for the period 1955-1998. *Eur J Epidemiol* 2003; **18:** 801-816

4   **Burcharth F,** Trillingsgaard J, Olsen SD, Moesgaard F, Federspiel B, Struckmann JR. Resection of cancer of the body and tail of the pancreas. *Hepatogastroenterology* 2003; **50:** 563-566

5   **Soga J.** Primary endocrinomas (carcinoids and variant neoplasms) of the gallbladder. A statistical evaluation of 138 reported cases. *J Exp Clin Cancer Res* 2003; **22:** 5-15

6   **Pingpank JF Jr,** Hoffman JP, Sigurdson ER, Ross E, Sasson AR, Eisenberg BL. Pancreatic resection for locally advanced primary and metastatic nonpancreatic neoplasms. *Am Surg* 2002; **68:** 337-340

7   **Birk D,** Schoenberg MH, Gansauge F, Formentini A, Fortnagel G, Beger HG. Carcinoma of the head of the pancreas arising from the uncinate process. *Br J Surg* 1998; **85:** 498-501

8   **Standop J,** Schneider MB, Ulrich A, Pour PM. Experimental animal models in pancreatic carcinogenesis: lessons for human pancreatic cancer. *Dig Dis* 2001; **19:** 24-31

9   **Berberat P,** Friess H, Kashiwagi M, Beger HG, Buchler MW. Diagnosis and staging of pancreatic cancer by positron emission tomography. *World J Surg* 1999; **23:** 882-887

10 **Zalatnai A.** Pancreatic cancer - a continuing challenge in oncology. *Pathol Oncol Res* 2003; **9:** 252-263

11 **Shore S,** Raraty MG, Ghaneh P, Neoptolemos JP. Review article: chemotherapy for pancreatic cancer. *Aliment Pharmacol Ther* 2003; **18:** 1049-1069

12 **Otsuki M.** Chronic pancreatitis in Japan: epidemiology, prognosis, diagnostic criteria, and future problems. *J Gastroenterol* 2003; **38:** 315-326

13 **Laurent-Puig P,** Lubin R, Semhoun-Ducloux S, Pelletier G, Fourre C, Ducreux M, Briantais MJ, Buffet C, Soussi T. Antibodies against p53 protein in serum of patients with benign or ma-
lignant pancreatic and biliary diseases. *Gut* 1995; **36:** 455-458

14 **Abrams RA,** Grochow LB, Chakravarthy A, Sohn TA, Zahurak ML, Haulk TL, Ord S, Hruban RH, Lillemoe KD, Pitt HA, Cameron JL, Yeo CJ. Intensified adjuvant therapy for pancreatic and periampullary adenocarcinoma: survival results and observations regarding patterns of failure, radiotherapy dose and CA19-9 levels. *Int J Radiat Oncol Biol Phys* 1999; **44:** 1039-1046

15 **Vestergaard EM,** Wolf H, Orntoft TF. Increased concentrations of genotype-interpreted Ca 19-9 in urine of bladder cancer patients mark diffuse atypia of the urothelium. *Clin Chem* 1998; **44:** 197-204

16 **Ugorski M,** Laskowska A. Sialyl Lewis[a]: a tumor-associated carbohydrate antigen involved in adhesion and metastatic potential of cancer cells. *Acta Biochim Pol* 2002; **49:** 303-311

17 **Magnani JL,** Steplewski Z, Koprowski H, Ginsburg V. Identification of the gastrointestinal and pancreatic cancer-associated antigen detected by monoclonal antibody 19-9 in the sera of patients as a mucin. *Cancer Res* 1983; **43:** 5489-5492

18 Schlieman MG, Ho HS, Bold RJ. Utility of tumor markers in determining resectability of pancreatic cancer. *Arch Surg* 2003; **138:** 951-956

19 **Banfi G,** Zerbi A, Pastori S, Parolini D, Di Carlo V, Bonini P. Behavior of tumor markers CA19.9, CA195, CAM43, CA242 and TPS in the diagnosis and follow-up of pancreatic cancer. *Clin Chem* 1993; **39:** 420-423

20 **Ichihara T,** Nomoto S, Takeda S, Nagura H, Sakamoto J, Kondo K, Horisawa M, Nakao A. Clinical usefulness of the immunostaining of the tumor markers in pancreatic cancer. *Hepatogastroenterology* 2001; **48:** 939-943

21 **Frebourg T,** Bercoff E, Manchon N, Senant J, Basuyau JP, Breton P, Janvresse A, Brunelle P, Bourreille J. The evaluation of CA19-9 antigen level in the early detection of pancreatic cancer. A prospective study of 866 patients. *Cancer* 1988; **62:** 2287-2290

22 **Ziske C,** Schlie C, Gorschluter M, Glasmacher A, Mey U, Strehl J, Sauerbruch T, Schmidt-Wolf IG. Prognostic value of CA 19-9 levels in patients with inoperable adenocarcinoma of the pancreas treated with gemcitabine. *Br J Cancer* 2003; **89:** 1413-1417

23 **Halm U,** Schumann T, Schiefke I, Witzigmann H, Mossner J, Keim V. Decrease of CA 19-9 during chemotherapy with gemcitabine predicts survival time in patients with advanced pancreatic cancer. *Br J Cancer* 2000; **82:** 1013-1016

24 **Masaki T,** Ohkawa S, Hirokawa S, Miyakawa K, Tamai S, Tarao K. A case of advanced pancreatic cancer showing remarkable response to gemcitabine treatment. *Gan To Kagaku Ryoho* 2003; **30:** 1333-1336

25 **Kamisawa T,** Tu Y, Egawa N, Ishiwata J, Tsuruta K, Okamoto A, Hayashi Y, Koike M, Yamaguchi T. Ductal and acinar differentiation in pancreatic endocrine tumors. *Dig Dis Sci* 2002; **47:** 2254-2261

26 **Koopmann J,** Zhang Z, White N, Rosenzweig J, Fedarko N, Jagannath S, Canto MI, Yeo CJ, Chan DW, Goggins M. Serum diagnosis of pancreatic adenocarcinoma using surface-enhanced laser desorption and ionization mass spectrometry. *Clin Cancer Res* 2004; **10:** 860-868

27 **Schlieman MG,** Ho HS, Bold RJ. Utility of tumor markers in determining resectability of pancreatic cancer. *Arch Surg* 2003; **138:** 951-956

28 **Dianxu F,** Shengdao Z, Tianquan H, Yu J, Ruoqing L, Zurong Y, Xuezhi W. A prospective study of detection of pancreatic carcinoma by combined plasma K-ras mutations and serum CA19-9 analysis. *Pancreas* 2002; **25:** 336-341

29 **Mu DQ,** Wang GF, Peng SY. p53 protein expression and CA19.9 values in differential cytological diagnosis of pancreatic cancer complicated with chronic pancreatitis and chronic pancreatitis. *World J Gastroenterol* 2003; **9:** 1815-1818

30 **Metsuyama K,** Chiba Y, Sasaki M, Tanaka H, Muraoka R, Tanigawa N. Tumor angiogenesis as a prognostic marker in operable non-small cell lung cancer. *Ann Thorac Surg* 1998; **65:** 1405-1409

31 **Frebourg T,** Bercoff E, Mouchon N, Senant J, Basuyau JP, Breton P, Janvresse A, Brunelle P, Bourreille J. The evaluation CA19-9 antigen level in the early detection of pancreatic cancer. *Cancer* 1988; **62:** 2287-2290

• BRIEF REPORTS •

Liver biopsy in evaluation of complications following liver transplantation

Ying-Yan Yu, Jun Ji, Guang-Wen Zhou, Bai-Yong Shen, Hao Chen, Ji-Qi Yan, Cheng-Hong Peng, Hong-Wei Li

Ying-Yan Yu, Jun Ji, Guang-Wen Zhou, Bai-Yong Shen, Hao Chen, Ji-Qi Yan, Cheng-Hong Peng, Hong-Wei Li, Transplantation Center and Institute of Digestive Surgery, Ruijin Hospital, Shanghai Second Medical University, Shanghai 200025, China
Correspondence to: Ying-Yan Yu, Transplantation Center and Institute of Digestive Surgery, Ruijin Hospital, Shanghai Second Medical University, Shanghai 200025, China. yingyan3y@yahoo.com.cn
Telephone: +86-21-64370045-611018   **Fax:** +86-21-64370045
Received: 2003-10-10   **Accepted:** 2003-11-06

Abstract

AIM: To analyze the role of liver biopsies in differential diagnosis after liver transplantation.

METHODS: A total of 50 biopsies from 27 patients with liver dysfunction out of 52 liver transplantation cases were included. Biopsies were obtained 0-330 d after operation, in which, 44 were fine needle biopsies, another 6 were wedge biopsies during surgery. All tissues were stained with haemotoxylin-eosin. Histochemical or immunohistochemical stain was done.

RESULTS: The rate of acute rejection in detected cases and total transplantation cases was 48.2% and 25.0%, chronic rejection rate in detected cases and total transplantation cases was 14.8% and 7.7%, preservation-reperfusion injury in detected cases and total transplantation cases was 25.9% and 13.5%, hepatic artery thrombosis rate in detected cases and total transplantation cases was 11.1% and 5.8%, intrahepatic biliary injury rate in detected cases and total transplantation cases was 7.4 % and 3.8%, CMV infection rate in detected cases and total transplantation cases was 3.7% and 1.9%, hepatitis B recurrence rate in detected cases and total transplantation cases was 3.7% and 1.9%, the ratio of suspicious drug-induced hepatic injury in detected cases and total transplantation cases was 11.1% and 5.8%.

CONCLUSION: Acute rejection and preservation-reperfusion injury are the major factors in early liver dysfunction after liver transplantation. Hepatic artery thrombosis and prolonged cold preservation may result in intrahepatic biliary injury. Acute rejection and viral infection may involve in the pathogenesis of chronic rejection. Since there are no specific lesions in drug-induced hepatic injury, the diagnosis must closely combine clinical history and rule out other possible complications.

INTRODUCTION

Liver transplantation has been accepted as an effective therapeutic option for patients with acute or chronic end-stage liver diseases. However, the postoperative course of liver transplant recipients will face to rejection for alloantigens and a number of complications. Among which, hepatic artery thrombosis, intrahepatic biliary injury, preservation-reperfusion injury, opportunistic infection as well as immunosuppressive drug-induced hepatic injury are critically for allograft liver poor function. Clinically, the complications are short of specific symptoms and signs, although the supervision for blood biochemistry, Doppler-ultrasound and radiologic image has some value to the evaluation of graft liver dysfunction, the final diagnosis still relies on liver biopsy evaluation. Here is a pathological study on fifty allograft liver biopsies which have been collected in our transplantation center since June 2002. These biopsies covered a number of complications following liver transplantation.

MATERIALS AND METHODS

Collection of allograft liver biopsies
From June 2002 to September 2003, a total of 52 orthotopic liver transplantations (OLTs) were performed in Transplantation Center, Ruijin Hospital of Shanghai. Fifty liver biopsies were obtained from 27 patients with liver dysfunction 0-330 d after operation. In which, 44 were fine needle biopsies, another 6 were wedge biopsies during surgery. All tissues were fixed in 40 g/L buffered formaldehyde and embedded in paraffin.

Histopathologic evaluation of liver biopsies
Serial 3 μm thick sections were cut on all biopsies. One section was stained with hemotoxylin-eosin. Others were stained by histochemical or immunohistochemical methods whenever it was needed. For example, if cytomegalovirus (CMV) infection was suspicious, CMV antigen immunohistochemistry would be done. If chronic rejection was suspicious, CK19 or CA19-9 immunohistochemistry for bile duct detection would be done. Criteria for evaluating acute rejection were based on Banff Schema published in 1997[1,2]. Criteria for evaluating chronic rejection were based on Banff Schema published in 2000[3]. Acute rejection was characterized by predominant portal-based lesions, including a classical triad of mixed inflammatory cell infiltrates, venous endothelial inflammation and inflammatory infiltration of bile ducts. Chronic rejection was characterized by ductopenia and obliterative arteriopathy.

Evaluation of preservation-reperfusion injury was based on the criteria proposed by Starzl Transplantation Institute of Pittsburgh University as well as University of Birmingham[4]. The histological features included: sinusoidal neutrophilic infiltration without portal mixed inflammatory cell infiltration, hepatocyte ballooning, cholestasis, hepatocyte apoptosis and regenerative change. Macrovesicular steatosis was graded as follows: mild, fat present in less than 30% of hepatocyte; moderate, fat infiltration of 30-60%; and severe, fat infiltration greater than 60% of hepatocytes.

This clinical study was performed on archival pathological files, which were obtained as part of routine clinical practice.

RESULTS

In this group, the earliest biopsy was got at 5 h following the

re-vascularization during transplantation procedure, the latest biopsy was got 330 d after transplantation. Twenty-seven cases out of 52 liver transplantation patients with poor allograft function accepted 1 to 6 liver biopsy detections according to clinical requirement. The lesions revealed in biopsy tissues are summarized in Table 1.

Table 1 Classification of lesions in 50 allograft liver biopsies

Lesions	n	Rate in detected cases (%) (n=27)	Ratio in total transplantation cases(%) (n=52)
Acute rejection	13	48.2	25.0
Chronic rejection	4	14.8	7.7
CMV infection	1	3.7	1.9
Hepatic artery thrombosis	3	11.1	5.8
Intrahepatic biliary injury	2	7.4	3.8
Drug-induced hepatic injury	3	11.1	5.8
Preservation-reperfusion injury	7	25.9	13.5
Recurrent hepatitis	1	3.7	1.9

The occurring time of different complications was different. Preservation-reperfusion injury and hepatic artery thrombosis mainly occurred within 2 wk following operation. Acute rejection could happen at any time from 1 wk to 310 d, but often took place at the end of 1 wk to 30 d following operation. The poor graft liver function that occurred 60-90 d postoperation was closely related to intrahepatic biliary injury. Early chronic rejection could happen as early as 45 d after transplantation but mainly occurred from 90 to 330 d post-transplantation. Only one recurrent hepatitis B happened in this group, 300 d after transplantation. The occurring time features of different complications are shown in Figure 1.

Figure 1 Time features of different complications in allograft liver biopsy.
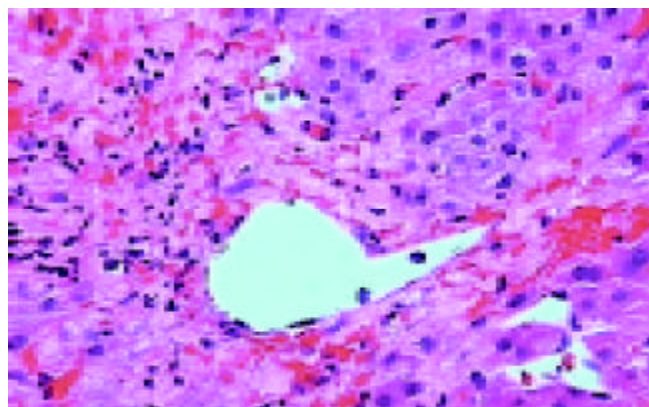

Figure 2 Hepatocytes necrosis and bleeding surrounding central vein caused by HAT 12 d after transplantation, HE ×200.
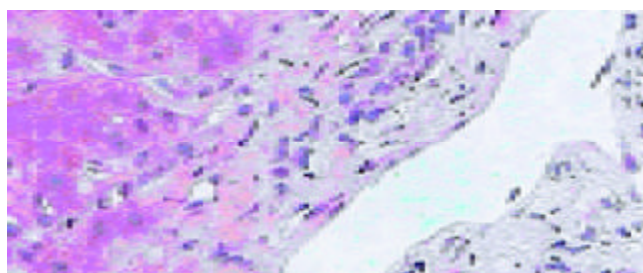

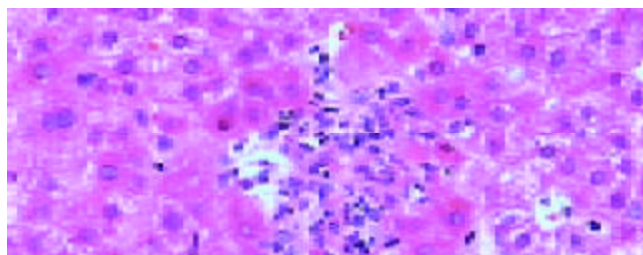**Figure 3** Bile duct damage with inflammation 80 d after transplantation. HE ×200.

Figure 4 CMV infection in peripheral blood and micro-abscess without inclusion bodies in liver cells 1 mo after transplantation. HE ×200.
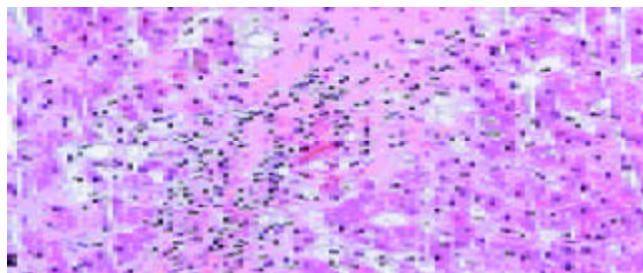

Figure 5 Bile duct loss in portal tract compatible with early chronic rejection 3 mo after transplantation. HE×200.
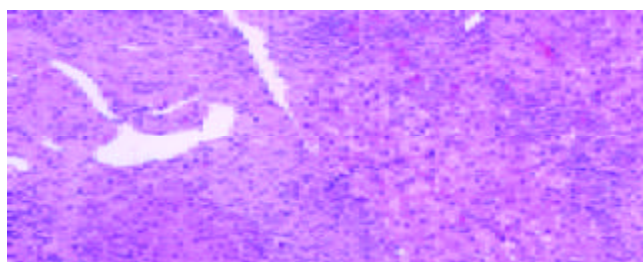

Figure 6 Fibrosis in portal area with lymphocyte infiltration and interface hepatitis in patient with recurrent hepatitis B 300 d post-transplantation, HE ×100.
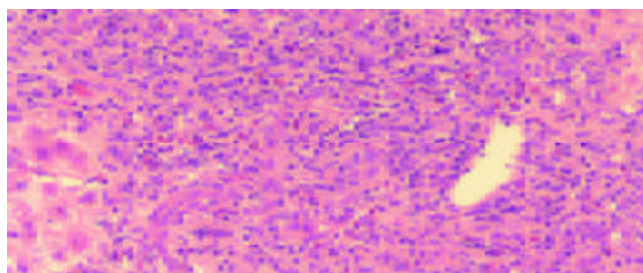

Figure 7 Acute rejection and mixed inflammatory cells in portal area with bile duct infiltration and venous endothelial inflammation 7 d post-transplantation. HE ×100.

The pathological examination on different biopsies from the same patient showed that one patient with hepatic artery thrombosis (HAT) 12 d postoperation (Figure 2) developed to intrahepatic biliary injury (IBI) 80 d following transplantation (Figure 3). Two cases in our group occurred IBI 2-3 mo after operation. One of which was secondary to HAT (the donor liver with warm ischemia for 5 min, cold storage time was 9 h), there was warm ischemia after 7 min, and cold storage time was 8 h for donor liver in another case with IBI. One case was diagnosed as chronic rejection (Figure 4) at 3 mo postoperation and disclosed persistent cytomegalovirus (CMV) infection at early stage following transplantation (Figure 5). Chronic rejection was occurred in another case due to recurrence of hepatitis B (Figure 6). Chronic rejection occurred in one case due to acute rejection (Figure 7), early chronic rejection occurred in one case at onset. If poor allograft liver function was persistent, liver biopsy showed hepatocyte ballooning, macrovesicular steatosis, cholestasis, and above-mentioned complications could not be confirmed, drug-induced hepatic injury was suspected.

DISCUSSION

In liver transplantation, liver biopsy is currently used to confirm the clinical diagnosis, to assess the degree of necroinflammatory injury or fibrosis, to evaluate a space-occupying lesion, and to evaluate the changes following therapeutic intervention. Since liver biopsy plays an important role in the diagnosis and management, a representative tissue sampling is needed. Ideally, a good biopsy sample should include at least 4 portal tracts. The subcapsular hepatic parenchyma is avoided in interpretation, as it often contains fibrous extensions from the capsule and has some injuries during peri-operative period[5].

The experience for evaluation of allograft liver biopsy in our transplantation center revealed that although acute rejection was still the major factor of liver dysfunction at the first few weeks following operation, there was referable international consensus evaluating criteria for acute rejection. All the cases with acute rejection were promptly diagnosed and cured by the close cooperation between the clinician and pathologist[2]. Chronic rejection is also called ductopenic allograft rejection and characterized by the presence of ductopenia and foamy cell arteriopathy. The overall occurrent rate of chronic rejection was 2-20%. The pathogenesis of chronic rejection was more complex than that in acute rejection. It involved in several factors such as cellular immunology, humoral immunology, ischemia and infection[6]. In our group, the chronic rejection rate in detected cases and total transplantation cases was 14.8% and 7.7% respectively, similar to those reported by other transplantation center. Chronic rejection occurred due to CMV infection and hepatitis B recurrence in two cases, due to acute rejection in one case, early chronic rejection occurred in one case 45 d post-transplantation. Therefore, the mechanisms of chronic rejection are multiple and complex. The above data confirmed that viral infection was the inducing factor of chronic rejection.

Preservation-reperfusion injury (PRI) refers to any injury during donor liver harvesting, cold storage as well as liver implantation. It is a major contributing factor to primary allograft failure after orthotopic liver transplantation. Clinically, it is characterized by high serum aspartate transaminase (AST) levels in the early postoperative period without technique problem, hepatic artery thrombosis and hyperacute rejection. To date, the pathogenesis of PRI is not very clear and there are no consistent histological evaluation criteria for PRI. A number of histological features have been observed in our group. For example, the predominant features of reperfusion especially at the first several hours after re-vascularization were sinusoidal endothelial cell impairment with neutrophilic cells infiltration;

hepatocyte injuries such as ballooning change, centrilobular cholestasis and apoptosis become predominance at late course of reperfusion. It is suggested that sinusoidal endothelial cells are more susceptible to PRI than hepatocytes themselves. Busquets et al.[7] found that there were 17% PRI out of 162 postreperfusion liver biopsy specimens in their retrospective analysis. They also disclosed that if cold storage time longer than 12 h, intrahepatic biliary complications resulted from PRI were increased. Another report revealed that storage time exceed 10 to 12 h, late posttransplantation biliary strictures occurred in more than 25% of liver transplant recipients, 30% of patients with graft dysfunction needed retransplantation within the first 3 mo after transplantation[8].

Hepatic artery thrombosis (HAT) occurred in 2-9% of adult transplantation recipients. It is the most frequent arterial complication in liver transplantation. Surgical technique, hemadynamic, immunologic factors, PRI and hypercoagulation have been suggested as the causes for HAT[9]. In Humboldt University Transplantation Center, among 1 192 liver transplantation cases, 30 HAT were observed, resulting in an incidence of 2.5%. Re-transplantation was necessary in 46.7% of patients with HAT in that group[10]. The histological features in HAT showed severe midzonal hepatocyte necrosis and bleeding, especially in centrolobular of allograft.

Intrahepatic biliary injury (IBI) is characterized by non anastomotic biliary strictures and is a relatively late complication, usually diagnosed between 1 and 4 mo after liver transplantation. The incidence of IBI was 2-10% of transplantation recipients. Clinically, there were repeated episodes of cholangitis and the necessity for re-transplantation was about 30-50%. Accumulating evidence has shown that IBI is associated with ischemia, secondary to HAT, ABO incompatible blood group donors, and chronic ductopenic rejection as well as prolonged warm ischemic time or cold ischemic time prior to implantation[11-14]. IBI occurred in 2 cases of our group 2-3 mo after operation. One of which was secondary to HAT (the donor liver with warm ischemia was 5 min, cold storage time was 9 h), another case of IBI showed warm ischemia for 7 min, cold storage time was 8 h for donor liver. It is suggested that improved hepatic artery supplying and the lowest total ischemia time may reduce the incidence of IBI.

Drug-induced hepatic injury (DIHI) is the "hot" but also troublesome problem in hepatic diseases. Therapeutic drugs such as corticosteroids, azathioprine and cyclosporine A in transplantation recipients could cause liver damage[15]. However, the report about DIHI after liver transplantation is rare. Recently, an introductory review about drug-induced hepatotoxicity progress was published in The New England Journal of Medicine[16]. The most frequent hepatotoxic drug reactions could lead to moderate to severe injuries to hepatocytes with a clinical symptom that resembles viral hepatitis, characterized by a rapid onset of jaundice in association with elevated aminotransferase levels. Acute liver failure may develop after weeks of onset, particularly if the patient has continued the drug. The histological characteristics of DIHI include ballooning degeneration or steatosis of hepatocytes with cholestasis, centrolobular or midzonal hepatocyte dropout or necrosis, portal tracts with severe bile duct damage surrounded by lymphocytes, plasma cells and eosinophils with or without granulomas, and lobular disarray with acidophilic bodies and sinusoidal chronic inflammation. Since many pathological changes in DIHI overlapped with the features observed at acute or chronic rejection, PRI or viral hepatitis recurrence, the diagnosis of DIHI in transplantation population is more difficult than in non-transplant population.

REFERENCES

1   **An International Panel**. Banff schema for grading liver allograft

rejection: an international consensus document. *Hepatology* 1997; **25**: 658-663

2   **Yu YY**, Shen BY, Zhou GW, Chen H, Yan JQ, Peng CH, Li HW. Application of Banff schema in grading acute rejection following transplantation. *Zhonghua Qiguan Yizhi Zazhi* 2003; **24**: 76-77

3   **Demetris A**, Adams D, Bellamy C, Blakolmer K, Clouston A, Dhillon AP, Fung J, Gouw A, Gustafsson B, Haga H, Harrison D, Hart J, Hubscher S, Jaffe R, Khettry U, Lassman C, Lewin K, Martinez O, Nakazawa Y, Neil D, Pappo O, Parizhakaya M, Randhawa P, Rasoul-Rockenschaub S, Reinholt F, Reynes M, Robert M, Tsamandas A, Wanless I, Wiesner R, Wernerson A, Wrba F, Wyatt J, Yamabe H. Update of the international Banff schema for liver allograft rejection: working recommendations for the histopathologic staging and reporting of chronic rejection. *Hepatology* 2000; **31**: 792-799

4   **Neil DA**, Hubscher SG. Are parenchymal changes in early post-transplant biopsies related to preservation-reperfusion injury or rejection? *Transplantation* 2001; **71**: 1566-1572

5   **Brunt EM**. Liver biopsy interpretation for the gastroenterologist. *Curr Gastroenterol Rep* 2000; **2**: 27-32

6   **Quaglia AF**, Del Vecchhio Blanco G, Greaves R, Burroughs AK, Dhillon AP. Development of ductopaenic liver allograft rejection includes a "hepatitic" phase prior to duct loss. *J Hepatol* 2000; **33**: 773-780

7   **Busquets J**, Figueras J, Serrano T, Torras J, Ramos E, Rafecas A, Fabregat J, Lama C, Xiol X, Baliellas C, Jaurrieta E. Postreperfusion biopsies are useful in predicting complications after liver transplantation. *Liver Transpl* 2001; **7**: 432-435

8   **Kukan M**, Haddad PS. Role of hepatocytes and bile duct cells in preservation –reperfusion injury of liver grafts. *Liver Transpl* 2001; **7**: 381-400

9   **Bramhall SR**, Minford E, Gunson B, Buckels JAC. Liver transplantation in the UK. *World J Gastroenterol* 2001; **7**: 602-611

10   **Stange BJ,** Glanemann M, Nuessler NC, Settmacher U, Steinmuller T, Neuhaus P. Hepatic artery thrombosis adult liver transplantation. *Liver Transpl* 2003; **9**: 612-620

11   **Rull R**, Garcia Valdecasas JC, Grande L, Fuster J, Lacy AM, Gonzalez FX, Rimola A, Navasa M, Iglesias C, Visa J. Intrahepatic biliary lesions after orthotopic liver transplantation. *Transplt Int* 2001; **14**: 129-134

12   **Huang XQ**, Huang ZQ, Duan WD, Zhou NX, Feng YQ. Severe biliary complications after hepatic artery embolization. *World J Gastroenterol* 2002; **8**: 119-123

13   **Abt P**, Crawford M, Desai N, Markmann J, Olthoff K, Shaked A. Liver transplantation from controlled non-heart-beating donors: an increased incidence of biliary complications. *Transplantation* 2003; **75**: 1659-1663

14   **Jagannath S**, Kalloo AN. Biliary Complications after liver transplantation. *Curr Treat Options Gastroenterol* 2002; **5**: 101-112

15   **Farrell GC.** Drugs and steatohepatitis. *Semin Liver Dis* 2002; **22**: 185-194

16   **Lee WM**. Drug-induced hepatotoxicity. *N Engl J Med* 2003; **349**: 474-485

• BRIEF REPORTS •

CDw75 is a significant histopathological marker for gastric carcinoma

Lei Shen, Hai-Xia Li, He-Sheng Luo, Zhi-Xiang Shen, Shi-Yun Tan, Jie Guo, Jun Sun

Lei Shen, Hai-Xia Li, He-Sheng Luo, Zhi-Xiang Shen, Shi-Yun Tan, Jie Guo, Jun Sun, Department of Gastroenterology, Renmin Hospital, Wuhan University, 238 Jie-fang Road, Wuhan 430060, Hubei Province, China
Correspondence to: Lei Shen, Department of Gastroenterology, Renmin Hospital, Wuhan University, 238 Jie-fang Road, Wuhan 430060, Hubei Province, China. mssquall@263.net
Telephone: +86-27-88041911-8571
Received: 2003-08-06   **Accepted:** 2003-09-18

Abstract

AIM: To study the expression of CDw75 in patients with gastric carcinoma and to correlate CDw75 expression with progression of the tumor.

METHODS: Immunohistochemical method was used to examine the expression of CDw75 in 72 cases of the gastric carcinoma and adjacent normal gastric mucosa, and the percentage of the cells positively stained with CDw75 was calculated using a computer-aided microscopic image analysis system.

RESULTS: CDw75 was not expressed in normal gastric mucosa but detected in 37 of the 72 neoplastic gastric lesions. The expression of CDw75 was associated with the tumor progression as indicated by its close correlation with the depth of the tumor infiltration (χ^2=18.415, P<0.01), TNM stage (χ^2=10.419, P<0.05) and lymph node metastasis (χ^2=6.675, P<0.01). The overall survival rate of the patients with positive CDw75 expression (32.4%) was significantly lower than that of the patients without CDw75 expression (71.4%) (P<0.01). There was no significant correlation between the expression of CDw75 and the sex and age and histological type of patients (P>0.05).

CONCLUSION: These findings suggest that the expression of CDw75 is a significant histopathological marker for more advanced stage of gastric carcinoma and indicates a poor prognosis for the patients.

INTRODUCTION

Invasiveness and metastasis are the most important characteristics of malignant tumor and mortality factors. Clinicopathological parameters are usually used for diagnosis and prognosis. Recent studies have shown that the expression of sialylated glycoconjugates is closely associated with the aggressiveness and metastatic potential of malignant cells. CDw75 epitope is a sialylated carbohydrate determinant generated by the β-galactosyl α-2,6-sialyltransferase, and it has been reported to be associated with the progression of gastric cancer[1]. Gastric cancer is one of the most common tumors of alimentary tract in China, and its mortality is high. In this study, we examined the expression of CDw75 in 72 cases of gastric carcinoma and adjacent normal gastric mucosa using immunohistochemical method to determine whether CDw75 is correlated with the invasiveness and metastasis of gastric carcinoma.

MATERIALS AND METHODS

Materials

Seventy-two patients with gastric cancer, who were diagnosed and treated at the Departments of Pathology and General Surgery, Renmin Hospital of Wuhan University, from 1995 to 1999, were randomly selected for this study. The patients had undergone subtotal or total gastrectomy combined with lymph node resection. Sections from the surgical specimens were fixed in 40 g/L formaldehyde and embedded in paraffin. The mean age of the patients was 59 years with a range from 35 to 74 years and a male-to-female ratio of 1.48. The patients were followed to determine clinical outcome and the median follow-up time at the end of the study was 45 mo (range, 3-64 mo). The other clinicopathological characteristics are listed in Table 1. The histological type of the tumor was defined by World Health Organization classification (tubular, papillary, mucinous, or signet ring[2], the degree of differentiation (well, moderate, or poor) was recorded on haematoxylin and eosin (H & E) stained tissues, and tumor stage was graded according to new PTNM criterion which was published by International Union Against Cancer (IUCC)[2].

Immunohistochemistry

Streptavidin-peroxidase (S-P) method was used to detect the expression of CDw75. The mouse monoclonal antibody against human CDw75 (LN1) was purchased from NeoMarkers Company, Wuhan, China, immunostaining S-P kit and DAB reagent were purchased from Fuzhou Maxim Biotechnical Company, Fuzhou, China. Sections from each primary tumor and adjacent mucosa were deparaffinized and heated in a microwave oven for 15 min to retrieve antigens. Endogenous peroxidase was blocked with 3 mL/L hydrogen peroxide methanol for 10 min at room temperature. After washing with phosphate-buffered saline (0.01 g/L, pH 7.4) for 3×5 min, the tumor sections were incubated with normal non-immune serum from bull for 15 min at room temperature to eliminate nonspecific staining. The sections were then incubated with the primary antibody against CDw75 (dilution 1/100) for 60 min at room temperature, washed with PBS for 3×5 min, and incubated with the secondary biotinylated antibody for 15 min followed by avidin-biotin-peroxidase for 15 min at room temperature. Finally, the slides were washed for 3×15 min with PBS, visualized with DAB reagent and counterstained with haematoxylin. Negative and positive controls were used simultaneously to ensure specificity and reliability of the staining process. The negative controls were performed by substituting the primary antibody with PBS, and a positive section supplied by manufacturer of the staining kit was taken as positive control.

Positive staining with CDw75 was defined as brown staining of cell membrane or cytoplasm. The degree of the CDw75 staining was calculated semiquantitatively with computer-aided analysis of four non-overlapping high power microscopic fields and classified as follows: –, negative staining; +, less than 25% tumor cells were CDw75 positive; ++, between 25% and 50% of

tumor cells were CDw75 positive; +++, between 51% and 75% of tumor cells were CDw75 positive; and ++++, more than 75% of tumor cells were CDw75 positive.

Statistical analysis

CDw75 expression in all patients with gastric carcinoma was analyzed against clinicopathological parameters. The correlation between CDw75 expression and selected clinicopathological parameters was analyzed with the Wilcoxon rank sum test and χ^2 test. Kaplam-meier curve was constructed to assess the survival. *P* value of less than 0.05 was considered to be statistically significant.

RESULTS

Immunohistochemical staining of CDw75

Normal gastric mucosa was consistently negative for CDw75 staining (Figure 1), while positive staining was observed in 37 of 72 (51.4%) gastric cancers. The staining intensity was as follows: -, 35 cases (48.6%); +, 9 cases (12.5%); ++,13 cases (18.1%); +++, 9 cases (12.5%); ++++, 6 cases (8.3%). The positive staining of CDw75 was localized predominantly in gastric cancer cells, and all the positive cases showed diffuse membrane staining, or cytoplasmic staining in some cases (Figure 2). The immunoreactive cells were either distributed unevenly throughout the tumor tissue or aggregated in focal clusters. In addition, positive staining was occasionally detected in lymphocytes or other inflammatory cells infiltrating the cancer nests (Figure 3).

Table 1 xClinicopathological parameters of gastric carcinoma and their association with CD75w expression.

	Expressing levels of CDw75			*P*
	Negative	Positive	Positive rate (%)	
Sex				
Male	43	24	19	44.19	2.217
Female	29	11	18	62.07	
Age (yr)				
<50	17	9	8	47.06	0.167
≥50	55	26	29	52.73	
Histologic type				
WD	12	8	4	33.33	3.445
MD	16	9	7	43.75	
PD	35	15	20	57.14	
Mucinous	5	2	3	60.00	
Signet ring	4	1	3	75.00	
Depth of invasion				
T1	8	7	1	12.50	18.415[b]
T2	17	13	4	23.53	
T3	32	13	19	59.38	
T4	15	2	13	86.67	
TNM stage				
I	24	17	7	29.17	10.419[a]
II	8	5	3	37.50	
III	20	8	12	60.00	
IV	20	5	15	75.00	
Lymph node metastasis				
Negative	32	21	11	34.38	6.675[b]
Positive	40	14	26	65.00	
Distant metastasis				
M0	56	30	26	46.43	2.482
M1	16	5	11	68.75	

[a]*P*<0.05, [b]*P*<0.01; WD: Well differentiation, MD: Moderate differentiation, PD: Poor differentiation.

Table 2 Survival time of patients with gastric carcinoma

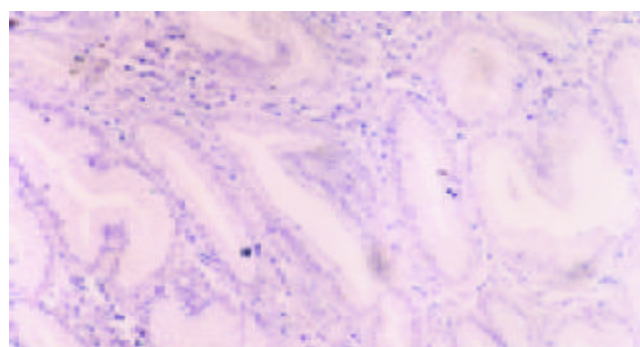| CDw75 expression	Death/survival	Median survival time
Negative (*n*=35)	10/25	53
Positive (*n*=37)	25/12	37

Figure 1 Expression of CDw75 in normal gastric mucosa. No gastric mucosa cell were brown-stained either on membrane or in cytoplasm. (SP×400).
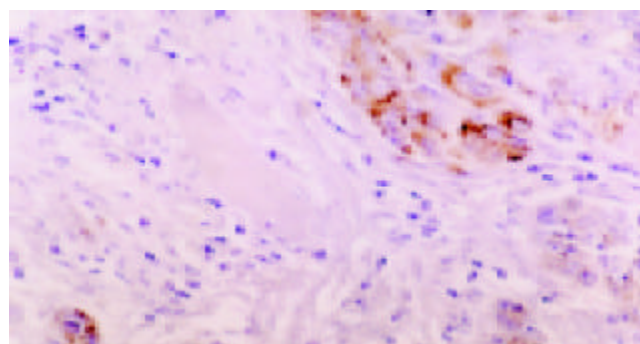

Figure 2 Weak staining of CDw75 in gastric cancer cells. There were a few gastric cancer cells brown-stained on membrane or in cytoplasm (SP×200).
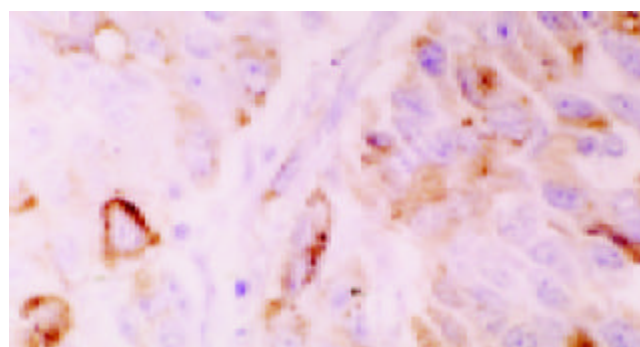

Figure 3 Strong staining of CDw75 in gastric cancer cells. There were many gastric cancer cells brown-stained on membrane or in cytoplasm (SP×200)

Correlation between CDw75 and the invasiveness or the metastasis of gastric carcinoma

The CDw75 expression in tumor tissues was related significantly to clinicopathologic factors, such as the depth of tumor invasion, TNM stageand lymph node metastasis (Table 1). The percentage of CDw75 expression in tumors which invaded serosal or deeper layers (T3 or T4) was significantly higher than that in tumors which were restricted within mucosa or muscular layers (T1 or T2) (*P*<0.01). When tumors were accompanied by lymph node metastasis, CDw75 expression was elevated significantly

compared with those without metastasis ($P<0.05$). The cases were also categorized by TNM staging. To compensate the error due to shortage of cases, stage I and stage II cases were combined into one group. CDw75 expression was found in 10 of 32 (31.3%)stage I+II cases, 12 of 20 (60.0%) stage III cases and 15 of 20 (75.0%) stage IV cases. The percentage of positive CDw75 staining in stage III and IV cases was significantly higher than that in stage I+II ($P<0.05$ and $P<0.01$, respectively), while there was no significant difference in those between stage III and stage IV ($P>0.05$).

No significant correlation was found between the expression of CDw75 antigen and the distant metastasis or the histological type of gastric cancer. Similarly, no significant difference was found between the cases with positive and negative CDw75 expression regarding the sex and age of patients.

Correlation between CDw75 expression and the survival of the patients with gastric carcinoma

At the end of the follow-up period, 37 of 72 patients (51.4%) were alive. The survival of patients with positive CDw75 expression was significantly shorter than those with negative CDw75 expression (Table 2). AS shown by the Kaplam-Meier curve, the overall survival rate of patients with CDw75 expression (32.4%) was significantly lower than that of patients without CDw75 expression (71.4%) ($P<0.01$, Figure 4).
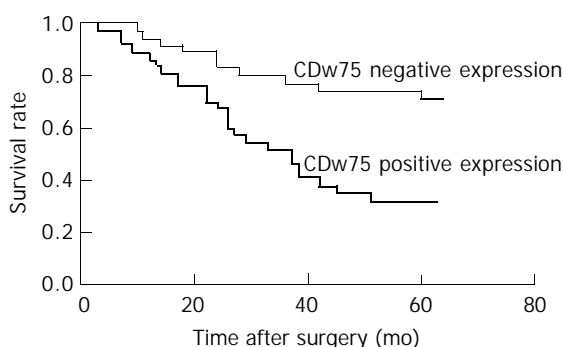

Figure 4 A Kaplan-Meier plot shows the survival rates after curative resection for gastric carcinoma patients with or without CDw75 expression.

DISSCUSSION

The infiltration and metastasis of gastric carcinoma is a multistage, complicated process, which could be influenced by many factors, such as the formation of neoplastic vessels, degradation of tissue membrane and matrix, mobility of tumor cells and quantity and activity of infiltrating leucocyte inside the tumor tissues. Recently, many tumor makers have been identified which are used not only for diagnosis but also for assessment of aggressiveness and prognosis of tumors[3-8]. Tumor markers are antigens or other biological products generated by tumor cells, which are present few or none in normal and nonneoplastic tissues. They usually indicate the change of genes associated with development of tumor and can be detected in tumor tissues or body humour or excretions of the patients[9,10]. CDw75 antigen is one plausible tumor marker that has been shown recently to be associated with the progression and metastasis of gastric carcinoma[1]. Consistent with previous finding[1], the present work demonstrated that CDw75 expression was constantly negative in normal gastric mucosa but positive in 37 of 72 (51.4%) gastric cancers.

CDw75 antigen is a cluster of differentiation antigen of human leucocyte designated at the fourth World Leucocyte-Type Conference in 1989[1]. It is a sialylated carbohydrate determinant generated bySia-T1[11] and has many different

isomers, which are specifically expressed in different tissues and can be recognized by corresponding monoclonal antibodies. There have been 4 monoclonal antibodies raised to react with CDw75 antigen, including EBU-141, OKB4, HH2 and LN1, etc.[1]. These CDw75 monoclonal antibodies are likely to identify spatially related structures since binding inhibition studies have shown that binding of each CDw75 monoclonal antibody blocks the binding of the other CDw75 monoclonal antibody. The epitopes recognized by HH2, LN1 and EBU-141 are completely destroyed when cells are treated with neuraminidase, suggesting that sialic acid is a part of these CDw75 determinants[1,12]. In contrast, when the epitope reacts with neuraminidase, the binding of OKB4 with CDw75 epitope is increased, indicating that the OKB4 epitope may be masked by sialic acid and can appear after treatment with the neuraminidase[1,12]. These results suggest that sialic acid may have determinant impact on the character of CDw75 antigen.

Furthermore, studies have shown that cell-surface glycoconjugates play an important role in cell proliferation, adhesion, metastasis and immungenicity. Only the subclone of primary tumor cells that express specific glycoconjugates has metastatic ability[1,12]. The composition and structure of cell surface glycoproteins change frequently during the neoplastic transformation, and most of these changes are the extensive sialyation of cell surface glycoproteins. Moreover, tumor-associated expression of sialylated glycoconjugates has been found to be closely associated with aggressive activity and increased metastatic potential of malignant cells[3]. There are several plausible mechanisms underlining such a correlation: sialic acid reduces the attachment of tumor cells to collagen type IV and fibronectin, masks antigen determinants, inhibits the action of natural killer cells, and induces immunologic tolerance through an increase of the serum half-life of glycoconjugates, etc[1,12]. In gastric carcinoma, various sialylated glycoconjugates, such as Lewis X (Le^x), Lewis A (CA-19-9) and sialosyl-Tn, etc, have become clinically important in the detection of aggressive behavior of tumor cells and prediction of disease prognosis[13-16].

CDw75, a Sia-T1-dependent sialylated glycoconjugate, is associated with the biological behaviors of tumors[12,17]. In patients with gastric carcinoma, David and Elpek et al.[1] found that there was no CDw75 expression in normal gastric mucosa (except a few isolated parietal cells in the body of the stomach), foveolar hyperplasia, intestinal metaplasia and the adjacent tissues to carcinoma. In contrast, the expression of CDw75 in primary tumor and the metastatic focus of gastric carcinoma was significantly increased. The CDw75 antigen could, therefore, be used as a marker of malignant transformation of gastric epithelium. Our study agreed with their findings. In addition, we found that the expression of CDw75 antigen is closely associated with the depth of the tumor invasion. Patients with serosal or deeper layer invasion of the tumor (T3 or T4) showed significantly higher expression of CDw75 than those with the tumor restricted within mucosa or muscular layers (T1 or T2), indicating that the gastric cancer cells with CDw75 high expression might have increased potential to invade into adjacent tissues. The most important feature of gastric carcinoma is its infiltrative growth and the earliest metastasis path is lymph node metastasis. We found that the positive expression rate of CDw75 (65%) in gastric cancer tissues with lymph node metastasis was significantly higher than that without lymph node metastasis (34%). With regard to TNM stage, CDw75 expression in stage I or stage II tumor tissues was not much higher than normal mucosa, but significantly higher in stage III and stage IV tumor tissues.. These findings suggested that CDw75 plays an important role in the progression of gastric cancer from localized lesion to metastasized neoplasia. As a result, overall survival rate of patients with CDw75

expression (32.4%) was lower than that of patients without CDw75 expression (71.4%), and the survival curve of patients with CDw75 expression was significantly poorer than that of patients without CDw75 expression by Kaplam Meier analysis.. In conclusion, CDw75 was not detected in normal gastric mucosa but expressed in gastric cancer tissues and the higher expression rate was seen in patients with deeper tumor invasion, higher TNM stage and in patients with lymph node metastasis. The survival time of patients with CDw75 expression was less than that of patients without CDw75 expression. Therefore, CDw75 appears to be a useful marker indicating more advanced stage of the malignancy and poor prognosis in patients with gastric carcinoma.

REFERENCES

1   **Elpek GO**, Gelen T, Karpuzoglu G, Karpuzoglu T, Keles N. Clinicopathologic evaluation of CDw75 antigen expression in patients with gastric carcinoma. *J Pathol* 2001; **193**: 169-174

2   **Luk GD**. Tumors of the stomach In: Mark Feldman, Brwe F. Gastrointestinal and Liver Disease. Volume I, 6th, Edition. Science Press, 2001, Beijing

3   **Zheng CX**, Zhan WH, Zhao JZ, Zheng D, Wang DP, He YL, Zheng ZQ. The prognostic value of preoperative serum levels of CEA, CA19-9 and CA72-4 in patients with colorectal cancer. *World J Gastroenterol* 2001; **7**: 431-434

4   **Duraker N**, Celik AN. The prognostic significance of preoperative serum CA 19-9 in patients with resectable gastric carcinoma: comparison with CEA. *J Surg Oncol* 2001; **76**: 266-271

5   **Marrelli D**, Roviello F, De Stefano A, Farnetani M, Garosi L, Messano A, Pinto E. Prognostic significance of CEA, CA 19-9 and CA 72-4 preoperative serum levels in gastric carcinoma. *Oncology* 1999; **57**: 55-62

6   **American Society of Clinical Oncology**. 1997 update of recommendations for the use of tumor markers in breast and colorectal cancer. *J Clin Oncol* 1998; **16**: 793-795

7   **Gartner F**, David L, Seruca R, Machado JC, Sobrinho-Simoes M. Establishment and characterization of two cell lines derived from human diffuse gastric carcinomas xenografted in nude mice. *Virchows Arch* 1996; **428**: 91-98

8   **Hammer RD**, Vnencak-Jones CL, Manning SS, Glick AD, Kinney MC. Microvillous lymphomas are B-cell neoplasms that frequently express CD56. *Mod Pathol* 1998; **11**: 239-246

9   **Huang CW**, Bai L. Clinical value of carbohydrate antigen 50 and carbohydrate antigen 242 in the diagnosis of colorectal carcinoma. *Diyi Junyi Daxue Xuebao* 2002; **22**: 1116-1118

10   **Zhang S**, Ma Y, Yang X. The diagnostic values of CA242 combining other tumor markers for lung cancer. *Zhonghua Jiehe Hehuxi Zazhi* 1999; **22**: 271-273

11   **Dall' Olio F**, Chiricolo M, Mariani E, Facchini A. Biosynthesis of the cancer-related sialyl-alpha 2,6-lactosaminyl epitope in colon cancer cell lines expressing beta-galactoside alpha 2,6-sialyltransferase under a constitutive promoter. *Eur J Biochem* 2001; **268**: 5876-5884

12   **Elpek GO**, Gelen T, Karpuzoglu G, Karpuzoglu T, Aksoy NH, Keles N. Clinicopathologic evaluation of CDw75 antigen expression in colorectal adenocarcinomas. *Pathol Oncol Res* 2002; **8**: 175-182

13   **Nakagoe T**, Sawai T, Tsuji T, Jibiki MA, Nanashima A, Yamaguchi H, Yasutake T, Ayabe H, Arisawa K, Ishikawa H. Difference in prognostic value between sialyl Lewis(a) and sialyl Lewis(x) antigen levels in the preoperative serum of gastric cancer patients. *J Clin Gastroenterol* 2002; **34**: 408-415

14   **Futamura N**, Nakamura S, Tatematsu M, Yamamura Y, Kannagi R, Hirose H. Clinicopathologic significance of sialyl Le (x) expression in advanced gastric carcinoma. *Br J Cancer* 2000; **83**: 1681-1687

15   **Nakagoe T**, Fukushima K, Sawai T, Tsuji T, Jibiki M, Nanashima A, Tanaka K, Yamaguchi H, Yasutake T, Ayabe H, Ishikawa H. Increased expression of sialyl Lewis(x) antigen in penetrating growth type A early gastric cancer. *J Exp Clin Cancer Res* 2002; **21**: 363-369

16   **Nakagoe T**, Sawai T, Tsuji T, Jibiki M, Nanashima A, Yamaguchi H, Yasutake T, Ayabe H, Arisawa K, Ishikawa H. Pre-operative serum levels of sialyl Tn antigen predict liver metastasis and poor prognosis in patients with gastric cancer. *Eur J Surg Oncol* 2001; **27**: 731-739

17   **Dunphy CH**, Polski JM, Lance Evans H, Gardner LJ. Paraffin immunoreactivity of CD10, CDw75, and Bcl-6 in follicle center cell lymphoma. *Leuk Lymphoma* 2001; **41**: 585-592

Edited by Liu HX and Xu FM

• CASE REPORT •

Fatal liver failure due to reactivation of lamivudine-resistant HBV mutant

Tatehiro Kagawa, Norihito Watanabe, Hisashi Kanouda, Ichiro Takayama, Tadahiko Shiba, Takashi Kanai, Kazuya Kawazoe, Shinji Takashimizu, Nobue Kumaki, Kazuo Shimamura, Shohei Matsuzaki, Tetsuya Mine

Tatehiro Kagawa, Norihito Watanabe, Hisashi Kanouda, Ichiro Takayama, Tadahiko Shiba, Takashi Kanai, Kazuya Kawazoe, Shinji Takashimizu, Shohei Matsuzaki, Tetsuya Mine, Department of Internal Medicine, Tokai University School of Medicine, Boseidai, Isehara, Kanagawa 259-1193, Japan
Nobue Kumaki, Kazuo Shimamura, Department of Pathology, Tokai University School of Medicine, Boseidai, Isehara, Kanagawa 259-1193, Japan
Correspondence to: Dr. Tatehiro Kagawa, Department of Internal Medicine, Tokai University School of Medicine, Boseidai, Isehara, Kanagawa 259-1193, Japan. kagawa@is.icc.u-tokai.ac.jp
Telephone: +81-463-931121
Received: 2003-11-17   **Accepted:** 2004-02-11

Abstract

We report a case of fatal liver failure due to reactivation of lamivudine-resistant HBV. A 53-year-old man was followed since 1998 for HBV-related chronic hepatitis. Serum HBV-DNA was 150 MEq/mL (branched DNA signal amplification assay) and ALT levels fluctuated between 50-200 IU/L with no clinical signs of liver cirrhosis. Lamivudine (100 mg/d) was started in May 2001 and serum HBV-DNA subsequently decreased below undetectable levels. In May 2002, serum HBV-DNA had increased to 410 MEq/mL, along with ALT flare (226 IU/L). The YMDD motif in the DNA polymerase gene had been replaced by YIDD. Lamivudine was continued and ALT spontaneously decreased to the former levels. On Oct 3 the patient presenting with general fatigue, nausea and jaundice was admitted to our hospital. The laboratory data revealed HBV reactivation and liver failure (ALT: 1828 IU/L, total bilirubin: 10 mg/dL, and prothrombin INR: 3.24). For religious reasons, the patient and his family refused blood transfusion, plasma exchange and liver transplantation. The patient died 10 d after admission. The autopsy revealed remarkable liver atrophy.

Kagawa T, Watanabe N, Kanouda H, Takayama I, Shiba T, Kanai T, Kawazoe K, Takashimizu S, Kumaki N, Shimamura K, Matsuzaki S, Mine T. Fatal liver failure due to reactivation of lamivudine-resistant HBV mutant. *World J Gastroenterol* 2004; 10(11): 1686-1687

http://www.wjgnet.com/1007-9327/10/1686.asp

INTRODUCTION

The emergence of lamivudine-resistant hepatitis B virus (HBV) mutant is relatively frequent after long-term lamivudine treatment. Liaw *et al.* reported acute exacerbation in 41% of lamivudine-treated patients who developed YMDD mutation, recovering mostly with HBeAg seroconversion[1]. Conversely, evolution toward acute liver failure is rare but possibly fatal as published in 2001 by Kim *et al*[2]. We report here a new case of fatal liver failure consecutive to the emergence of a lamivudine-resistant mutant HBV.

CASE REPORT

This 53-year-old man had been followed since 1998 for HBV-related chronic hepatitis. He was positive for HBs and HBe antigens. Serum HBV-DNA was 150 MEq/mL (branched DNA signal amplification assay)[3]. Alanine aminotransferase (ALT) fluctuated between 50-200 IU/L with no clinical signs of liver cirrhosis. Serum albumin and prothrombin time were normal. Lamivudine (100 mg/d) was started in May 2001 (Figure 1). Subsequently, serum HBV-DNA decreased below undetectable level (October 2001). In May 2002, serum HBV-DNA had increased to 410 MEq/mL, along with ALT flare (226 IU/L). Mini-sequencing[4] showed that the YMDD motif in the DNA polymerase gene had been replaced by YIDD, supporting reactivation was due to the emergence of a lamivudine-resistant HBV mutant. Lamivudine was continued and ALT spontaneously decreased to the former levels. To improve a pre-existing non-insulin dependent diabetes mellitus (serum HgbA1c: 6.5-7.6%) acarbose (300 mg/d) was initiated on Aug 20, 2002, but
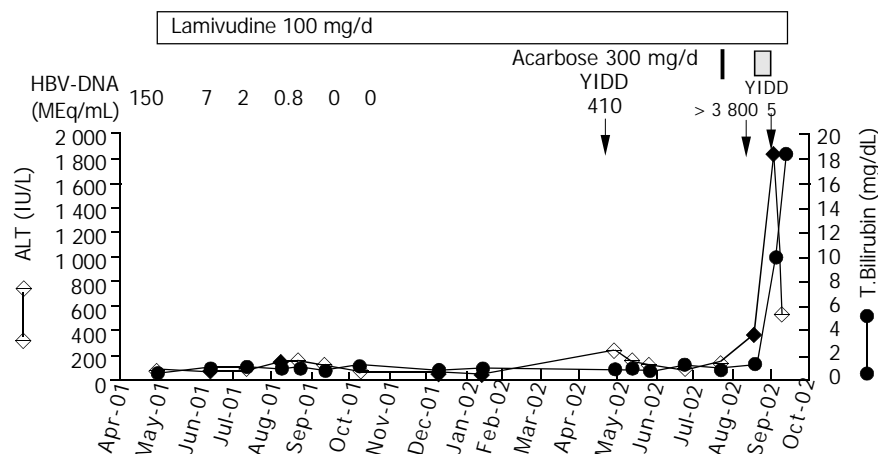

Figure 1 Serum ALT, total bilirubin and HBV-DNA levels.

discontinued after only 3 d due to flatulence. At the next outpatient clinic visit (Sept 17), the patient presented no clinical sign of liver disorder, so acarbose was restarted. In fact, laboratory investigations performed prior to restarting acarbose revealed that HBV-DNA had dramatically increased to 3 800 MEq/mL while ALT was 9 times that of the upper limit of normal (357 IU/L). On Oct 3, the patient presenting with general fatigue, nausea and jaundice was admitted to the hospital. ALT was 1 828 IU/L, total and direct bilirubin, 10 and 5.8 mg/dL, respectively, and prothrombin INR 3.24. Antinuclear and antismooth muscle antibodies as well as HIV tests were negative. Despite discontinuation of acarbose, liver failure developed and hepatic encephalopathy appeared. For religious reasons, the patient and his family refused blood transfusion, plasma exchange and liver transplantation. The patient died 10 d after admission. The autopsy revealed liver atrophy (620 g) and panlobular necrosis surrounded by extensive fibrosis consisting of immature collagen (Figure 2). Lymphoid cell infiltration was observed in the fibrosis.

Figure 2 Histological findings of liver autopsy specimens. Irregularly shaped parenchymal islands are surrounded by extensive fibrosis consisting of immature collagen. 75 x EVG staining.

DISCUSSION

The reactivation of HBV prior to any clinical sign and administration of acarbose supports that the liver failure reported here is consecutive to the rapid proliferation of lamivudine-resistant HBV (YIDD). Although rare, acute liver failure associated with lamivudine-resistant HBV is reported in the literature, including one successfully treated with liver transplant[5], one co-infected with HIV[6], two with advanced cirrhosis[7] and one immunocompetent patient[2]. The last case was a Korean male, who developed fatal liver failure after 20 mo of lamivudine therapy. The background is similar to our patient, indicating that Asian males might be susceptible to this type of mutants. Lamivudine-resistant HBV is sensitive to adefovir dipivoxil[8], a nucleotide analogue, shown to be effective for chronic HBV infection[9]. Adefovir dipivoxil, unavailable in Japan, could not be used in our case.

Acarbose is a pseudotetrasaccaride acting by competitive inhibition of intestinal alpha-glucosidases, indicated for the treatment of type II diabetes mellitus. The incidence of acarbose-related liver injury is low although a few severe cases were reported[10,11]. It is unclear whether acarbose might have aggravated the liver injury consecutive to the mutation-related relapse of viral activity. In any case, as stressed in the Summary of Product Characteristics for acarbose *"Glucobay is contraindicated in patients with hepatic impairment"*. The above medical history supports closely monitoring patients with lamivudine-resistant HBV even in immunocompetent patients and, once reactivation occurs, adefovir dipivoxil should be administered.

REFERENCES

1 **Liaw YF,** Chien RN, Yeh CT, Tsai SL, Chu CM. Acute exacerbation and hepatitis B virus clearance after emergence of YMDD motif mutation during lamivudine therapy. *Hepatology* 1999; **30**: 567-572

2 **Kim JW,** Lee HS, Woo GH, Yoon JH, Jang JJ, Chi JG, Kim CY. Fatal submassive hepatic necrosis associated with tyrosine-methionine-aspartate-aspartate-motif mutation of hepatitis B virus after long-term lamivudine therapy. *Clin Infect Dis 2001*; **33**: 403-405

3 **Hendricks DA,** Stowe BJ, Hoo BS, Kolberg J, Irvine BD, Neuwald PD, Urdea MS, Perrillo RP. Quantitation of HBV DNA in human serum using a branched DNA (bDNA) signal amplification assay. *Am J Clin Pathol* 1995; **104**: 537-546

4 **Kobayashi S,** Shimada K, Suzuki H, Tanikawa K, Sata M. Development of a new method for detecting a mutation in the gene encoding hepatitis B virus reverse transcriptase active site (YMDD motif). *Hepatol Res* 2000; **17**: 31-42

5 **de Man RA,** Bartholomeusz AI, Niesters HG, Zondervan PE, Locarnini SA. The sequential occurrence of viral mutations in a liver transplant recipient re-infected with hepatitis B: hepatitis B immune globulin escape, famciclovir non-response, followed by lamivudine resistance resulting in graft loss. *J Hepatol* 1998; **29**: 669-675

6 **Bonacini M,** Kurz A, Locarnini S, Ayres A, Gibbs C. Fulminant hepatitis B due to a lamivudine-resistant mutant of HBV in a patient coinfected with HIV. *Gastroenterology* 2002; **122**: 244-245

7 **Malik AH,** Lee WM. Hepatitis B therapy: the plot thickens. *Hepatology* 1999; **30**: 579-581

8 **Perrillo R,** Schiff E, Yoshida E, Statler A, Hirsch K, Wright T, Gutfreund K, Lamy P, Murray A. Adefovir dipivoxil for the treatment of lamivudine-resistant hepatitis B mutants. *Hepatology* 2000; **32**: 129-134

9 **Marcellin P,** Chang TT, Lim SG, Tong MJ, Sievert W, Shiffman ML, Jeffers L, Goodman Z, Wulfsohn MS, Xiong S, Fry J, Brosgart CL. Adefovir dipivoxil for the treatment of hepatitis B e antigen-positive chronic hepatitis B. *N Engl J Med* 2003; **348**: 808-816

10 **Fujimoto Y,** Ohhira M, Miyokawa N, Kitamori S, Kohgo Y. Acarbose-induced hepatic injury. *Lancet* 1998; **351**: 340

11 **Carrascosa M,** Pascual F, Aresti S. Acarbose-induced acute severe hepatotoxicity. *Lancet* 1997; **349**: 698-699

• CASE REPORT •

Brain metastasis of hepatocellular carcinoma: A case report and review of the literature

Bilge Tunc, Levent Filik, Irsel Tezer-Filik, Burhan Sahin

Bilge Tunc, Levent Filik, Burhan Sahin, Turkiye Yuksek Ihtisas Hospital, Gastroenterology Clinic, Ankara 06520, Turkey
Irsel Tezer-Filik, Hacettepe University, Department of Neurology, Ankara 06520, Turkey
Correspondence to: Dr. Levent Filik, Cemal Gursel Cad. Erk Apt: 52/2, Kurtulus, Ankara 06520, Turkey. leventfilik@yahoo.co.uk
Telephone: +90-536-4881179
Received: 2003-12-28   **Accepted:** 2004-02-11

INTRODUCTION

Hepatocellular carcinoma (HCC) is one of the most frequent malignancies in the world. It is more common in far eastern countries and relatively rare in the United States and western European countries where at autopsy it accounts for only 1-2% of malignant tumors. The disease is usually manifested in the the 6th and 7th decade of life. HCC is one of the highly malignant neoplasms. Extrahepatic metastases are seen in 64% of patients with HCC. The lungs, regional lymph nodes, kidney, bone marrow and adrenals are common sites of HCC metastasis[1-3]. But, metastasis to brain and skull is extremely rare. Table 1 shows some of the reported cases of HCC with brain metastasis. These case reports reaffirms the complex and multidisciplinary care of these patients[4-15].

The interval between diagnosis of primary cancer and detection of brain metastasis ranged from 2 to 54 mo. The mean survival period was only 3 mo after diagnosis of brain metastasis. The patients with HCC metastasized to brain died of neurologic causes rather than hepatic failure. Although no treatment is clearly defined to increase survival in patients with unresectable tumors, early diagnosis could improve the chance of curative surgical resection[9-12].

We describe a case of HCC presenting with the initial manifestations of an intracranial mass lesion without any symptoms or signs suggestive of the primary hepatic site of the tumor. The diagnosis could not be made until he was admitted to hospital with unilateral weakness and numbness.

CASE REPORT

The patient was a 55-year-old man admitted to our hospital due to numbness and weakness on his right side. The patient's medical history was significant for chronic HBV-related hepatitis and insulin dependent-diabetes mellitus. The patient was oriented and did not have pathologic reflexes. His initial laboratory examination revealed Hb: 12.6 g/dL, Hct: 36.8, white blood cell count 3 560/μL, plt: 54 000/μL, prothrombin time (INR): 1.9, erythrocyte sedimentation rate: 28 mm/h, blood glucose: 196 mg/dL, urea: 39 mg/dL, creatinine: 0.8 mg/dL, AST: 160 U/L, ALT: 88 U/L, GGT: 55 U/L, alkalene phospatase: 288 mg/dL, albumin: 2.59, globulin: 3.7, total bilirubin: 1.6 mg/dL. Serum electrolyte levels, urinalysis were within normal range.

Computed tomography (CT) of the patient's head revealed multiple intracranial masses and homogenous enhancement by post-contrast CT (Figure 1).
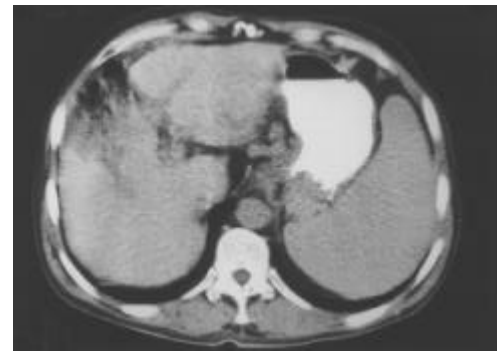

Figure 1 CT image of the lesion in the liver.

Abdominal sonography revealed findings consistent with chronic hepatitis. Thorax-abdomen-pelvic CT scan showed a hypodense mass lesion with irregular margins and 2.8 cm in diameter in the left lobe of the liver (Figure 2). Serum alpha-feto-protein level was higher than 400 U/L. Fine needle biopsy from the mass in the liver was performed. Pathological examination was consistent with the HCC.

He was given glucocorticoid therapy and referred to radiation oncology division for cranial radiotherapy.

Table 1 Some of the previous case presentations with HCC and brain metastasis in the literature

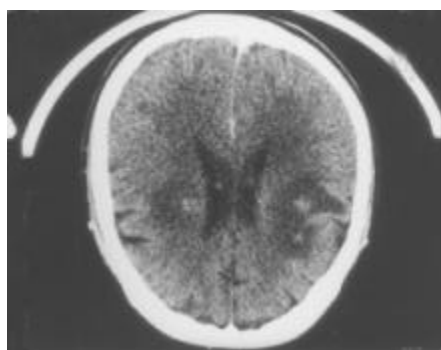| Author	Distinctive presentation
Moriya *et al.*	Brain metastasis seen in 1 year interval after hepatectomy for HCC
Endo *et al.*	Subgleal and epidural metastasis presenting as epidural hemorrhage and died from hepatic failure
Peres *et al.*	Cerebral metastasis presenting as initial finding of HCC
Tanabe *et al.*	15-year-old boy and the other case presenting as headache
Loo *et al.*	Two cases with cerebral metastasis presenting as initial finding of HCC
Salvati *et al.*	Cerebral metastasis with stroke-like presentation
Asahara *et al.*	Brain metastasis seen after hepatectomy for HCC in 5 cases
Kim *et al.*	Seven patients with brain metastasis
Yen *et al.*	Eighteen cases with brain metastasis
Shuangshoti *et al.*	Nine cases with brain metastasis
Friedman *et al.*	A rare case with no identifiable risk factor for primary liver cancer

Figure 2 CT image of the metastatic lesions in brain.

DISCUSSION

Although brain metastasis may arise from primary sites in various organs and tissues, they are frequently seen with bronchogenic, breast, and prostate cancers. HCC commonly metastasizes to the lung, regional lymph nodes, peritoneum, and adrenal glands, but rarely to brain. Shuangshoti *et al*. reported that the secondary intracranial hepatic carcinomas were 1.3-2.9% among intracranial metastatic tumors[14].

Most extrahepatic HCC occurs in patients at advanced intrahepatic tumor stage. Incidental extrahepatic lesions found at CT in patients having HCC of intrahepatic stage I or II are unlikely to represent metastatic HCC[2]. Our case had single nodule 2.8 cm in diameter. His bilirubin level was near normal. He did not have ascites. He had neither ascites nor history of hepatic encephalopathy. He had liver cirrhosis in Child A stage. If he had not had brain metastasis, he could have been candidate for curative hepatectomy. We believe that brain metastasis from HCC is relatively early in the disease progression.

Yen *et al*. reported a well documented group of 33 patients. Eighteen had brain parenchymal metastasis without skull involvement, the other 15 cases disclosed skull metastasis with brain invasion. The underlying HCC are mainly of expanding 39.4% and multifocal 39.4% types, and 54.5% had mental changes not related to hypoglycemia or hepatic encephalopathy. Nevertheless, our case had unifocal HCC[16].

Yen *et al*. reported that 90% of 15 cases had hyperdense mass lesion by non-contrast computed tomography scan and 17 cases showed homogenous enhancement (77.3%) by post-contrast CT images. In the non-skull involved group, 41.7% disclosed ring-shape enhancement and 87.5% had perifocal edema, and 24.2% presented as intracerebral hemorrhage. Our patient had perifocal edema in the brain but without hemorrhage[16].

Because no effective treatment for brain metastasis from HCC is available, further study is needed. Yen *et al*. reported 36.4% death of brain herniation[16].

Most of non-skull involved cases had simultaneous lung metastasis without bony metastasis, while the skull involved group (66.7%) disclosed extracranial bony metastasis without lung metastasis[15,16]. However, no other simultaneous metastasis site was found of our patient. HCC with intracranial metastasis is symptomatic and life threatening. Half the cases may come from pulmonary metastasis and the other half may be from bony metastasis even though our patient had neither of them. Surgery of the brain or skull metastasis is of no particular technical problem as long as they are located in accessible areas. Brain irradiation or surgery can prolong the survival. Radiotherapy seems to improve the quality and quantity of residual life, although the number of patients describes in the literature is not large enough

to draw any definite conclusion.

Loo *et al*. reported that light microscopic examination of the metastatic tumor from HCC revealed a trabecular HCC with focal hemorrhage and necrosis. Their immunohistochemical profile was identical to that described in primary HCC[12].

Salvati *et al*. suggested that the stroke-like presentation of the cerebral localization of the disease can be explained by both the important vascularization of the tumor and the frequent hemocoagulative alterations caused by the cirrhosis[9].

In conclusion, the rarity of this type of case gives the clinician the suspicion of such associations when confronted with a patient with liver dysfunction and neurologic findings.

REFERENCES

1   **Katyal S,** Oliver JH 3rd, Peterson MS, Ferris JV, Carr BS, Baron RL. Extrahepatic metastasis of hepatocellular carcinoma. *Radiology* 2000; **216**: 698-703
2   **Tang ZY.** Hepatocellular carcinoma- cause, treatment and metastasis. *World J Gastroenterol* 2001; **7**: 445-454
3   **Sithinamsuwan P,** Piratvisuth T, Tanomkiat W, Apakupakul N, Tongyoo S. Review of 336 patients with hepatocellular carcinoma at Songklanagarind Hospital. *World J Gastroenterol* 2000; **6**: 339-343
4   **Moriya H,** Ohtani Y, Tsukui M, Tanaka Y, Tajima T, Makuuchi H, Tanaka Y, Itou K. A case report: tumorectomy for brain metastasis of hepatocellular carcinoma. *Tokai J Exp Clin Med* 1999; **24**: 105-110
5   **Frati A,** Salvati M, Giarnieri E, Santoro A, Rocchi G, Frati L. Brain metastasis from hepatocellular carcinoma associated with hepatitis B virus. *J Exp Clin Cancer Res* 2002; **21**: 321-327
6   **Endo M,** Hamano M, Watanebe K, Wakai S. Combined chronic subdural and acute epidural hematoma secondary to metastatic hepatocellular cancer: case report. *No Shinkei Geka* 1999; **27**: 331-334
7   **Peres MF,** Forones NM, Malheiros SM, Ferraz HB, Stavale JN, Gabbai AA. Heomrrhagic cerebral metastasis as a first manifestation of a hepatocellular carcinoma. Case report. *Arq Neuropsiquiatr* 1998; **56**: 658-660
8   **Kim M,** Na DL, Park SH, Jeon BS, Roh JK. Nervous system involvement by metastatic hepatocellular carcinoma. *J Neurooncol* 1998; **36**: 85-90
9   **Salvati M,** Cimatti M, Frati A, Santoro A, Gagliardi FM. Brain metastasis from hepatocellular carcinoma. A case report. *J Neurosurg Sci* 2002; **462**: 77-80
10 **Asahara T,** Yano M, Fukuda S, Fukuda T, Nakahara H, Katayama K, Itamato T, Dohi K, Nakanishi T, Kitamoto M, Azuma K, Ito K, Moriwaki K, Yuge O, Shimamato F. Brain metastasis from hepatocellular carcinoma after radical hepatectomy. *Hiroshima J Med Sci* 1999; **48**: 91-94
11 **Tanabe H,** Kondo A, Kinuta Y, Matsuura N, Hasegawa K, Chin M, Saiki M. Unusual presentation of brain metastasis from hepatocellular carcinoma-two case reports. *Neurol Med Chir* 1994; **34**: 748-753
12 **Loo KT,** Tsui WM, Chung KH, Ho LC, Tang SK, Tse CH. Hepatocellular carcinoma metastasizing to the brain and orbit: report of three cases. *Pathology* 1994; **26**: 119-122
13 **Friedman HD.** Hepatocellular carcinoma with central nervous system metastasis: a case report and literature review. *Med Pediatr Oncol* 1991; **19**: 139-144
14 **Shuangshoti S,** Rungruxsirivorn S, Panyathanya R. Intracranial metastasis of hepatic carcinomas: a study of 9 cases within 28 years. *J Med Assoc Thai* 1989; **72**: 307-313
15 **Lee JP,** Lee ST. Hepatocellular carcinoma presenting as intracranial metastasis. *Surg Neurol* 1988; **30**: 316-320
16 **Yen FS,** Wu JC, Lai CR, Sheng WY, Kuo BI, Chen TZ, Tsay SH, Lee SD. Clinical and radiological pictures of hepatocellular carcinoma with intracranial metastasis. *J Gastroenterol Hepatol* 1995; **10**: 413-418